LEABHARLANN CHOLÁISTE NA TRÍONÓIDE, BAILE ÁTHA CLIATH | TRINITY COLLEGE LIBRARY DUBLIN
Ollscoil Átha Cliath | The University of Dublin

Terms and Conditions of Use of Digitised Theses from Trinity College Library Dublin

Copyright statement

All material supplied by Trinity College Library is protected by copyright (under the Copyright and Related Rights Act, 2000 as amended) and other relevant Intellectual Property Rights. By accessing and using a Digitised Thesis from Trinity College Library you acknowledge that all Intellectual Property Rights in any Works supplied are the sole and exclusive property of the copyright and/or other IPR holder. Specific copyright holders may not be explicitly identified. Use of materials from other sources within a thesis should not be construed as a claim over them.

A non-exclusive, non-transferable licence is hereby granted to those using or reproducing, in whole or in part, the material for valid purposes, providing the copyright owners are acknowledged using the normal conventions. Where specific permission to use material is required, this is identified and such permission must be sought from the copyright holder or agency cited.

Liability statement

By using a Digitised Thesis, I accept that Trinity College Dublin bears no legal responsibility for the accuracy, legality or comprehensiveness of materials contained within the thesis, and that Trinity College Dublin accepts no liability for indirect, consequential, or incidental, damages or losses arising from use of the thesis for whatever reason. Information located in a thesis may be subject to specific use constraints, details of which may not be explicitly described. It is the responsibility of potential and actual users to be aware of such constraints and to abide by them. By making use of material from a digitised thesis, you accept these copyright and disclaimer provisions. Where it is brought to the attention of Trinity College Library that there may be a breach of copyright or other restraint, it is the policy to withdraw or take down access to a thesis while the issue is being resolved.

Access Agreement

By using a Digitised Thesis from Trinity College Library you are bound by the following Terms & Conditions. Please read them carefully.

I have read and I understand the following statement: All material supplied via a Digitised Thesis from Trinity College Library is protected by copyright and other intellectual property rights, and duplication or sale of all or part of any of a thesis is not permitted, except that material may be duplicated by you for your research use or for educational purposes in electronic or print form providing the copyright owners are acknowledged using the normal conventions. You must obtain permission for any other use. Electronic or print copies may not be offered, whether for sale or otherwise to anyone. This copy has been supplied on the understanding that it is copyright material and that no quotation from the thesis may be published without proper acknowledgement.

An experimental study of the physical properties of lime mortar and their effect on lime-mortar masonry

by

Adrian Costigan

Thesis submitted to the University of Dublin, Trinity College

for the degree of

Doctor of Philosophy

in the subject of Engineering

March 2013

PhD in Engineering

TRINITY COLLEGE
1 9 JUN 2013
LIBRARY DUBLIN

Thesis 10459

DECLARATION

I declare that this thesis has not been submitted as an exercise for a degree at this or any other university and it is entirely my own work.

I agree to deposit this thesis in the University's open access institutional repository or allow the library to do so on my behalf, subject to Irish Copyright Legislation and Trinity College Library conditions of use and acknowledgement.

Signed: 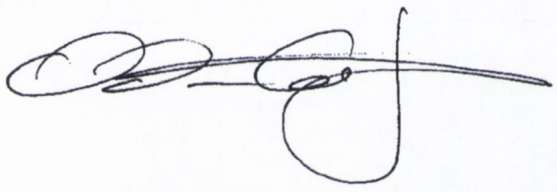 29/05/13

DECLARATION

I hereby declare that this thesis, in whole or in part, has not been submitted to this or any other University as an exercise for a degree. I confirm that this thesis is entirely my own work except where reference has been given in the text.

Furthermore, I hereby agree to deposit this thesis in the University's open access institutional repository or allow the library to do so on my behalf, subject to Irish Copyright Legislation and Trinity College Library conditions of use and acknowledgement.

Signed: _____ Date: _____

Adrian Costigan

ACKNOWLEDGMENT

I would like to warmly thank Dr. Sara Pavía for her direction, help and support throughout the past four years.

The Irish Office of Public Works generously provided funding for this project. I would like to extend a big thanks to Mr. Paul McMahon, Senior Conservation Architect, National Monuments, Architectural Heritage Division, for supporting and guiding this project.

All testing was undertaken in the Department of Civil, Structural and Environmental Engineering, Trinity College Dublin. I would like to thank Mr. Chris O'Donovan, Mr. Eoin Dunne, Dr. Kevin Ryan, and Mr. Dave McAuley for their assistance throughout this project. Their help is much appreciated.

I would also like to thank St. Astier Limes, France, The Traditional Lime Company, Ireland, Clogrenanne Lime Ltd. Ireland and Kingscourt Brick, Ireland for donating materials.

Finally, I would like to thank my family for their love and unconditional support and especially to my wife and best friend, Gretta, thank you.

ABSTRACT

The objective of this research is to provide new data in respect to the mechanical behaviour of lime mortar and masonry traditionally used in Ireland, especially the effect of water content and curing time and curing environment. To this end, highly porous bricks with low stiffness and cut and broken limestone, as well as sandstone units were selected. Cement-lime (M6), calcium lime (CL90-s) and natural hydraulic lime (NHL) mortars were manufactured to two flows (165 and 170 mm). The impact of the mortar's compressive and flexural strengths, and elastic modulus on the compressive and bond strengths of the respective masonry was investigated.

Water content was found to have a very significant effect on both mortar and masonry properties. Increasing the water content and therefore the workability of the mortar generally improved the compressive/flexural/bond strength and stiffness of the cement-lime and natural hydraulic lime masonry whereas it adversely affected these properties of calcium-lime masonry. This research evidences that the impact of varying the water content reduces as the hydraulic strength of the mortar increases and generally has a greater effect on the mechanical properties of masonry in the first 28 days of curing than it does at 6 months.

The compressive strength of brick masonry was found to tend towards a maximum of approximately 9 N/mm^2 (circa 75 % of the normalised compressive strength of the unit). For higher strength mortars, an increase of compressive/flexural strength and elastic modulus of mortar lead to a small compressive strength increase of masonry whereas, for the lower hydraulic strength mortar, small increases in mortar properties resulted in relatively large increases in masonry compressive strength. Clear relationships were established between (mortar compressive/flexural strength and stiffness) and masonry compressive strength and bond strength however, these relationships were found to be non-linear. Masonry compressive and bond strength are clearly influenced by the mechanical properties of the mortar, but the influence becomes progressively smaller as the compressive/bond strength of the masonry tend towards a maximum.

This research establishes a clear relationship between brick masonry bond and compressive strength, as both properties increase overtime and as the mortar hydraulic grade, mortar strength and water content increase. This study advances current knowledge and demonstrates that the relationship is non-linear. According to the results, masonry compressive strength reaches a maximum, after which, any further increases in bond are unlikely to cause additional gains in masonry compressive strength.

Regression analysis was applied to the experimentally obtained mortar and masonry characteristic compressive strength values and equations for the estimation of lime and cement-lime brick masonry compressive strength were proposed. The results were also compared with analytical values provided by standards and previous authors. According to the results, Eurocode 6 EN 1996-1-1 (2005) provided the best predictions, not only for cement-lime masonry, but also for the estimation of 28-day characteristic compressive strength of NHL 2, 3.5 and 5 brick masonry. Additionally, stress-strain curve estimation models proposed in literature were compared with lime and cement-lime masonry experimental stress-strain relationships. This research found good agreement using the model proposed by Kaushik *et al.* (2007) and poor predictions of stress-strain curves by other models, generally because they were unable to take the relatively large deformation associated with lime-mortar into consideration.

ABSTRACT

The objective of this research is to provide new data in respect to the mechanical behaviour of lime mortar and masonry traditionally used in Ireland, especially the effect of water content and curing time and curing environment. To this end, highly porous bricks with low stiffness and cut and broken limestone, as well as sandstone units were selected. Cement-lime (M6), calcium lime (CL90-s) and natural hydraulic lime (NHL) mortars were manufactured to two flows (165 and 170 mm). The impact of the mortar's compressive and flexural strengths, and elastic modulus on the compressive and bond strengths of the respective masonry was investigated.

Water content was found to have a very significant effect on both mortar and masonry properties. Increasing the water content and therefore the workability of the mortar generally improved the compressive/flexural/bond strength and stiffness of the cement-lime and natural hydraulic lime masonry whereas it adversely affected these properties of calcium-lime masonry. This research evidences that the impact of varying the water content reduces as the hydraulic strength of the mortar increases and generally has a greater effect on the mechanical properties of masonry in the first 28 days of curing than it does at 6 months.

The compressive strength of brick masonry was found to tend towards a maximum of approximately 9 N/mm^2 (circa 75 % of the normalised compressive strength of the unit). For higher strength mortars, an increase of compressive/flexural strength and elastic modulus of mortar lead to a small compressive strength increase of masonry whereas, for the lower hydraulic strength mortar, small increases in mortar properties resulted in relatively large increases in masonry compressive strength. Clear relationships were established between (mortar compressive/flexural strength and stiffness) and masonry compressive strength and bond strength however, these relationships were found to be non-linear. Masonry compressive and bond strength are clearly influenced by the mechanical properties of the mortar, but the influence becomes progressively smaller as the compressive/bond strength of the masonry tend towards a maximum.

This research establishes a clear relationship between brick masonry bond and compressive strength, as both properties increase overtime and as the mortar hydraulic grade, mortar strength and water content increase. This study advances current knowledge and demonstrates that the relationship is non-linear. According to the results, masonry compressive strength reaches a maximum, after which, any further increases in bond are unlikely to cause additional gains in masonry compressive strength.

Regression analysis was applied to the experimentally obtained mortar and masonry characteristic compressive strength values and equations for the estimation of lime and cement-lime brick masonry compressive strength were proposed. The results were also compared with analytical values provided by standards and previous authors. According to the results, Eurocode 6 EN 1996-1-1 (2005) provided the best predictions, not only for cement-lime masonry, but also for the estimation of 28-day characteristic compressive strength of NHL 2, 3.5 and 5 brick masonry. Additionally, stress-strain curve estimation models proposed in literature were compared with lime and cement-lime masonry experimental stress-strain relationships. This research found good agreement using the model proposed by Kaushik *et al.* (2007) and poor predictions of stress-strain curves by other models, generally because they were unable to take the relatively large deformation associated with lime-mortar into consideration.

TABLE OF CONTENTS

Declaration i
Acknowledgment ii
Abstract iii
Table of Contents iv
List of Figures viii
lIST of Tables xii

Chapter 1 Introduction and background research 1
1.1 Introduction 2
1.1.1 Scope of the problem 2
1.1.2 Aim of this research 3
1.2 Background research on lime mortar 4
1.2.1 Lime mortars 4
1.2.2 Mortar water content and workability 5
1.2.3 Mortar water retention 7
1.2.4 Mortar compressive strength 8
1.2.5 Influence of aggregate on mortar properties 11
1.2.6 Mortar flexural strength 12
1.2.7 Mortar elastic modulus 13
1.3 Background research on lime mortar 14
1.3.1 Bond strength 14
1.3.2 Flexural strength of masonry 23
1.3.3 Influence of bond strength on masonry compressive strength 24
1.3.4 Compressive strength and failure mechanics of masonry 25
1.3.5 Simple stress-strain relationship models 29
1.3.6 Estimation of masonry compressive strength 32
1.3.7 Effect of curing on mortar and masonry properties 36

Chapter 2 Materials and methods 38
2.1 Materials 40
2.1.1 Limes 40
2.1.2 Cement 40
2.1.3 Aggregate 40
2.2 Mortar preparation methods 42
2.2.1 Mixing 42
2.2.2 Moulding, curing and compaction 42

2.3 Plastic state mortar properties 43
2.3.1 Initial flow and statistical validation of initial flow 43
2.3.2 Water demand 45
2.3.3 Water retention 46
2.4 Hardened state mortar properties 48
2.4.1 Compressive strength 48
2.4.2 Flexural strength 48
2.4.3 Elastic modulus of mortar in compression 48
2.5 Masonry units 50
2.5.1 Types of masonry units 50
2.5.2 Masonry unit properties 51
2.5.3 Masonry unit testing methods 52
2.5.4 Results of masonry unit tests 55
2.6 Masonry preparation and testing 56
2.6.1 Masonry construction 56
2.6.2 Masonry curing 58
2.6.3 Compressive strength of masonry 59
2.6.4 Bond strength (bond wrench test) 61
2.6.5 Flexural bond strength (parallel to and perpendicular to bedding joints) 64

Chapter 3 Mortar results and discussion 68
3.1 Plastic state mortar results 70
3.1.1 Water demand, initial flow and workability 70
3.1.2 Statistical analysis of initial flow 73
3.2 Water retention results 76
3.2.1 Influence of water content on mortar water retention 77
3.3 Hardened state mortar results 79
3.3.1 Influence of water content on mechanical properties of mortar 82
3.3.2 Variations in mortar mechanical properties with curing age 86

Chapter 4 Brick masonry results and discussion 90
4.1 Influence of water content on the properties of brick masonry 95
4.1.1 Compressive strength and elastic modulus 95
4.1.2 Bond and flexural strength 96
4.2 Analysis of brick masonry strength development over time 101
4.2.1 Compressive strength and elastic modulus 101
4.2.2 Bond and flexural strength 104

4.3 Comparison between masonry bond and flexural strength testing 109

Chapter 5 Mortar and brick masonry relationships 112
5.1 Influence of mortar properties on the compressive strength of brick masonry 114
5.1.1 Impact of mortar compressive strength on the compressive strength of masonry 115
5.1.2 Influence of mortar flexural strength and stiffness on the compressive strength of brick-masonry 118
5.2 Influence of mortar mechanical properties on brick-masonry bond strength 121
5.3 Relationship between masonry bond and masonry compressive strength 126
5.4 Relationship between brick-masonry elastic modulus and compressive strength 129
5.5 Failure modes of brick masonry 132
5.5.1 Failure modes of brick masonry in compression 132
5.5.2 Failure modes of masonry in flexure 136
5.5.3 Bond strength failure modes (bond wrench test) 138

Chapter 6 Externally cured mortar and brick masonry results 140
6.1 Effect of outdoor curing on mortar properties 142
6.2 Effect of outdoor curing on masonry properties 146

Chapter 7 Stone masonry results and discussion 150
7.1 Mechanical properties of stone masonry 152
7.1.1 Limestone 152
7.1.2 Sandstone 153
7.1.3 Limestone vs. sandstone 154
7.2 Influence of water content on the properties of stone masonry 157
7.3 Stone masonry strength development over time 161
7.3.1 Compressive strength 161
7.3.2 Elastic modulus 162
7.3.3 Bond strength 163
7.4 Relationship between bond and compressive strength of stone masonry over time 166
7.5 Failure modes of stone masonry 168

Chapter 8 Theoretical vs. experimental evaluation 170
8.1 Estimation of masonry compressive strength 172
8.1.1 Estimating masonry strength by regression of experimental data 172
8.1.2 Estimating masonry strength using various analytical prediction models 179
8.2 Estimation of lime-masonry deformation characteristics 183
8.2.1 General stress-strain relationship 183

8.2.2 Fitness of simple analytical stress-strain models 184
8.2.3 Estimation of masonry elastic modulus 189
8.2.4 Estimation of peak strain 190

Chapter 9 Conclusions 194
9.1 Influence of mortar properties on the properties of masonry 196
9.2 Influence of curing on mortar and masonry properties 197
9.3 Mortar and masonry relationships 198
9.4 Masonry failure mechanisms 201
9.5 Estimation of masonry compressive strength 203
9.6 Estimation of lime-masonry deformation characteristics 204

Appendix A: Statistical analysis of mortar flow test 242

Appendix B: Mortar water retention test calculations 260

Appendix C: Mortar compressive strength & elastic modulus results and calculations 264

Appendix D: Mortar flexural strength results and calculations 282

Appendix E: Masonry compressive strength & elastic modulus results and calculations 294

Appendix F: Masonry bond strength results and calculations 324

Appendix G: Masonry flexural strength results and calculations (parallel and perpendicular to bedding joints) 418

Appendix H: Masonry unit test results and calculations 432

LIST OF FIGURES

Figure 1.1: The relationship between water:lime ratio and compressive strength (Allen *et al.* 2003) 9

Figure 1.2: Compressive strength vs. deformation (Arandigoyen and Alvarez, 2007) 11

Figure 1.3: The nature of stresses in the masonry unit and mortar in relation to their relative stiffness (Venkatarama and Vyas 2008) 27

Figure 1.4: Stress-strain curves for masonry prisms for different grades of mortar: stress is normalised with respect to prism compressive strength for each curve (Kaushik *et al.* (2007)). 30

Figure 1.5: Idealised stress-strain relationship Kaushik *et al.* (2007) 31

Figure 1.6: Stress-strain relationship for masonry in compression, EN 1996-1-1 (2005). 31

Figure 1.7: Comparison of past experimental results on masonry prisms with analytical predictions (Kaushik 2007). 35

Figure 2.1 Comparison of sand sieve analysis and standard upper and lower limits 41

Figure 2.2 (a) The flow table apparatus and (b) mortar specimen 44

Figure 2.3 Schematic of the water retention test for fresh mortar 46

Figure 2.4 Arrangement of loading of test specimen EN 12372 (2006) 54

Figure 2.5: Masonry test setup BS EN 1052-1 (1999) 59

Figure 2.6 Picture of masonry test setup 59

Figure 2.7 Schematic of mortar joint template. 61

Figure 2.8: Bond wrench test apparatus and setup (Hanley 2006) 62

Figure 2.9: Schematic of bond wrench test set-up, ... 62

Figure 2.10: Flexural bond strength test setup parallel to and perpendicular to bedding joints (EN 1052–2 1999). 64

Figure 2.11: Picture of flexural bond strength set-up. 65

Figure 3.1: Water demand of mortars at two different flows 71

Figure 3.2: Water:binder ratio of mortars at two different flows 71

Figure 3.3:Box plot of NHL 5 mortar flows 75

Figure 3.4: Box plot of NHL 3.5 mortar flows 75

Figure 3.5: Box plot of NHL 2 mortar flows 75

Figure 3.6: Box plot of CL90-s mortar flows 75

Figure 3.7: Box plot of mortar flows M6 at 1:½:4 75

Figure 3.8: Box plot of mortar flows NHL 3.5 at 0:1:2 75

Figure 3.9: Water retention of mortars of different hydraulic strengths at two flows 77

Figure 3.10: Comparison of NHL mortar water retention values with previous author, Hanley (2006) (RH values are estimated at 170 mm). 78

Figure 3.11: Effect of water content on the compressive strength of mortar 85

Figure 3.12: Effect of water content on the flexural strength of mortar 85

Figure 3.13: Effect of water content on the elastic modulus of mortar 85
Figure 3.14: Compressive strength development of lime mortar over time 86
Figure 3.15: Modulus of elasticity development of lime mortar over time 87
Figure 3.16: Flexural strength development of lime mortar over time 87
Figure 4.1: Effect of water increase on the compressive strength of masonry 99
Figure 4.2: Effect of water increase on the elastic modulus of masonry 99
Figure 4.3: Effect of water increase on the bond strength of masonry 99
Figure 4.4: Effect of water increase on the flexural strength of masonry (Type 1 - parallel to bedding joints) 100
Figure 4.5: Effect of water increase on the flexural strength of masonry (Type 2 - perpendicular to bedding joints) 100
Figure 4.6: Compressive strength development of brick masonry over time 103
Figure 4.7: Modulus of elasticity development of brick masonry over time 103
Figure 4.8: Bond strength development of brick masonry over time 107
Figure 4.9: Flexural strength development of brick masonry (Type 1 - parallel to bedding joints) 108
Figure 4.10: Flexural strength development of brick masonry (Type 2 - perpendicular to bedding joints) 108
Figure 4.11: Regression analysis of masonry bond and flexural strength 111
Figure 4.12: Regression analysis of masonry bond and flexural strength (lime masonry only) 111
Figure 5.1: Impact of mortar CS on the CS of masonry for mortar of different hydraulic strengths at increasing flow 115
Figure 5.2: Overall influence of mortar CS on the CS of brick masonry (includes different mortar hydraulic strengths, three curing ages and two flows) 115
Figure 5.3 Impact of mortar flexural strength on the CS of masonry for mortars of varying hydraulicity and increasing flow 119
Figure 5.4: Overall influence of mortar flexural strength on the CS of brick masonry (includes different mortar hydraulic strengths, three curing ages and two flows) 119
Figure 5.5: Impact of mortar elastic modulus on the CS of masonry for mortars of varying hydraulicity and increasing flow 120
Figure 5.6: Overall influence of mortar elastic modulus on the CS of brick masonry (includes different mortar hydraulic strengths, three curing ages and two flows) 120
Figure 5.7: Impact of mortar compressive strength on the BS of masonry for mortars of varying hydraulic strengths at increasing flow 123
Figure 5.8: Overall influence of mortar CS on the bond strength of brick masonry (includes different mortar hydraulic strengths, three curing ages and two flows) 123
Figure 5.9: Impact of mortar elastic modulus on the BS of masonry for mortars of varying hydraulic strengths at increasing flow 124

Figure 5.10: Overall influence of mortar elastic modulus on the bond strength of brick masonry (includes different mortar hydraulic strengths, three curing ages and two flows) 124

Figure 5.11: Impact of mortar flexural strength on the BS of masonry for mortars of varying hydraulic strengths at increasing flow 125

Figure 5.12: Overall influence of mortar flexural strength on the bond strength of brick masonry (includes different mortar hydraulic strengths, three curing ages and two flows) 125

Figure 5.13: Relationship between masonry bond strength and the CS of masonry over time for different mortar hydraulic strengths at two different flows. 128

Figure 5.14: Overall influence of bond strength on the CS of brick masonry during curing (includes different mortar hydraulic strengths, three curing ages and two flows) 128

Figure 5.15: Variation of masonry elastic modulus with the characteristic CS of masonry for mortars of different hydraulic strengths 130

Figure 5.16: Overall influence of elastic modulus on the CS of brick masonry during curing (includes different mortar hydraulic strengths, three curing ages and two flows) 131

Figure 5.17: Failure of NHL 5 brick masonry specimen in compression due to lateral tension (Mode I) 133

Figure 5.18: Failure of NHL 2 brick masonry in compression due to bond/mortar failure and bi-lateral tension (Mode II) 134

Figure 5.19 Failure of M6 masonry under compression due to diagonal shear 135

Figure 5.20: Flexural strength failure modes (Type 1 - parallel to bedding joints) 136

Figure 5.21: Flexural bond strength failure modes (Type 2 - perpendicular to bedding joints) 137

Figure 5.22: Bond strength failure modes, Annex A BS EN 1052-5 (2005) 138

Figure 6.1: Compressive strength development of externally cured mortars [a] 144

Figure 6.2: Flexural strength development of externally cured mortars [b] 144

Figure 6.3: Elastic modulus development of externally cured mortars [c, d] 144

Figure 6.4: Effect of curing conditions on the compressive strength of mortar 145

Figure 6.5: Effect of curing conditions on the flexural strength of mortar 145

Figure 6.6: Effect of curing conditions on the elastic modulus of mortar 145

Figure 6.7: Compressive strength development of externally-cured brick masonry [a] 147

Figure 6.8: Elastic modulus development of externally-cured brick masonry [b] 147

Figure 6.9: Bond strength development of externally-cured brick masonry [c, d] 147

Figure 6.10: Effect of curing conditions on the compressive strength of brick masonry 149

Figure 6.11: Effect of curing conditions on the elastic modulus of brick masonry 149

Figure 6.12: Effect of curing conditions on the bond strength of brick masonry 149

Figure 7.1: Compressive strength of broken-limestone masonry at varying hydraulic strength and flow 158

Figure 7.2: Elastic modulus of broken-limestone masonry at varying hydraulic strength and flow 158

Figure 7.3: Bond strength of broken-limestone masonry at varying hydraulic strength and flow 158

Figure 7.4: Compressive strength of cut-limestone masonry at varying hydraulic strength and flow 159

Figure 7.5 Elastic modulus of cut-limestone masonry at varying hydraulic strength and flow 159

Figure 7.6: Bond strength of cut-limestone masonry at varying hydraulic strength and flow 159

Figure 7.7 Compressive strength of broken-sandstone masonry at varying hydraulic strength and flow 160

Figure 7.8: Elastic modulus of broken-sandstone masonry at varying hydraulic strength and flow 160

Figure 7.9: Bond strength of broken-sandstone masonry at varying hydraulic strength and flow 160

Figure 7.10: Compressive strength development of stone masonry over time. 164

Figure 7.11: Elastic modulus development of stone masonry over time. 164

Figure 7.12: Bond strength development of stone masonry over time. 165

Figure 7.13: Correlation between the bond and compressive strength of stone masonry (during hardening) 167

Figure 8.1: Example of a stress-strain diagram with phases a, b, c and d 183

Figure 8.2: Normalized stress-strain diagram (Vermeltfoort, 2005) 185

Figure 8.3: Representative masonry stress-strain curves 185

Figure 8.4: Corrected masonry stress-strain curves 185

Figure 8.5: Comparison of experimental stress-strain curves for brick masonry (170 mm flow, 56 days curing) with curves estimated by analytical models proposed by other authors 187

LIST OF TABLES

Table 2.1: Particle size distribution of sands and CEN sand limits 41

Table 2.2: List of masonry unit properties tested 51

Table 2.3: Physical properties of masonry units 55

Table 2.4: Masonry testing schedule 57

Table 3.1: Summary of water demand and mortar flow 70

Table 3.2: Percentage increase in water content and water:binder ratio, for a 5 mm increase in initial flow 72

Table 3.3: Summary of mortar water retention test results 76

Table 3.4: Relative change in water retention due to an increase in the mortar flow 77

Table 3.5: Compressive strength of mortars cured in the laboratory (also presented in Figure 3.11) 81

Table 3.6: Flexural strength of mortars cured in the laboratory (also presented in Figure 3.12) 81

Table 3.7: Elastic modulus of mortars cured in the laboratory (also presented in Figure 3.13) 82

Table 3.8: Percentage increase in water content required to raise mortar flow from 165 to 170 mm 83

Table 3.9: Percentage change in the compressive strength of mortar due to the increase in initial flow 85

Table 3.10: Percentage change in the flexural strength of mortar due to the increase in initial flow 85

Table 3.11 Percentage change in the elastic modulus of mortar due to the increase in initial flow 85

Table 3.12: Percentage of strength and stiffness gained by the mortars at 28 and 56 days (as a percentage of the 6-month value). Laboratory-cured mortars. 88

Table 4.1: Compressive strength of masonry (also presented in Figure 4.1 and Table 4.6) 92

Table 4.2: Elastic modulus of masonry (also presented in Figure 4.2 and Table 4.7) 93

Table 4.3: Bond strength of masonry (also presented in Figure 4.3 and Table 4.8) 93

Table 4.4: Flexural strength of masonry (Type 1 - Parallel to bedding joints) Also presented in Figure 4.4 and Table 4.9 94

Table 4.5: Flexural strength of masonry (Type 2 - Perpendicular to bedding joints) Also presented in Figure 4.5 and Table 4.10. 94

Table 4.6: Percentage change in the compressive strength of masonry due to the increase in initial flow 99

Table 4.7: Percentage change in the elastic modulus of masonry due to the increase in initial flow 99

Table 4.8: Percentage change in the bond strength of masonry due to the increase in initial flow 99

Table 4.9: Percentage change in the flexural strength of masonry due to the increase in initial flow (Type 1 - parallel to bedding joints) 100

Table 4.10: Percentage change in the flexural strength of masonry due to the increase in initial flow (Type 2 - perpendicular to bedding joints) 100

Table 4.11: Percentage of strength and stiffness gained by the masonries at 28 and 56 days (as a percentage of the 6-month value). Laboratory-cured masonry. 107

Table 4.12: Comparison between bond wrench test and flexural strength test parallel to the bedding joints 109

Table 5.1: Percentage difference between the properties of NHL 3.5 and 5 mortar and masonry at 56 days and 6 months. 128

Table 5.2: Correlation between masonry elastic modulus and characteristic compressive strength 130

Table 6.1: Percentage change in compressive strength of mortar due to outdoor curing 145

Table 6.2: Percentage change in flexural strength of mortar due to outdoor curing 145

Table 6.3: Percentage change in elastic modulus of mortar due to outdoor curing 145

Table 6.4: Percentage change in the CS of brick-masonry due to outdoor curing 149

Table 6.5: Percentage change in the elastic modulus of brick-masonry due to outdoor curing 149

Table 6.6: Percentage change in the BS of brick-masonry due to outdoor curing 149

Table 7.1: Compressive strength results for stone masonry 155

Table 7.2: Elastic modulus results for stone masonry 155

Table 7.3: Bond strength results for stone masonry 156

Table 7.4: Percentage change in the CS of masonry due to the increase in initial flow 158

Table 7.5: Percentage change in the E-modulus of masonry due to the increase in initial flow 158

Table 7.6: Percentage change in the BS of masonry due to the increase in initial flow 158

Table 7.7: Percentage change in the CS of masonry due to the increase in initial flow 159

Table 7.8: Percentage change in the E-modulus of masonry due to the increase in initial flow 159

Table 7.9: Percentage change in the BS of masonry due to the increase in initial flow 159

Table 7.10: Percentage change in the CS of masonry due to the increase in initial flow 160

Table 7.11: Percentage change in the E-modulus of masonry due to the increase in initial flow 160

Table 7.12: Percentage change in the BS of masonry due to the increase in initial flow 160

Table 7.13: Development of stone masonry results, relative to 6-month value. 165

Table 8.1: Equations investigated for the estimation of lime-brick masonry strength 174

Table 8.2: Equations investigated for the estimation of cement-lime and stone masonry strength 175

Table 8.3: Comparison of experimental results in this thesis with analytical prediction models from various sources (all brick masonry) 176

Table 8.4: Comparison of experimental results of this thesis with analytical prediction models from various sources (cont. a) 177

Table 8.5: Comparison of experimental results in this thesis with analytical prediction models from various sources (all stone masonry) (cont. b) 178

Table 8.6: Summary of models for the estimation of masonry strength 181

Table 8.7: Summary of models by other authors for the estimation of masonry stress-strain curve 186

Table 8.8: Estimation of masonry elastic modulus (previously presented in Table 5.2) 189

Table 8.9: Summary of models by other authors for the estimation of masonry strain 190

Table 8.10: Comparison of experimental results with analytical prediction models from various sources. 193

Table 9.1: Summary of masonry failure modes in compression 201

Table 9.2: Summary of proposed equations for the estimation of lime-brick masonry strength 203

CHAPTER 1

INTRODUCTION AND BACKGROUND RESEARCH

1.1 INTRODUCTION

1.1.1 Scope of the problem

In the past, masonry mortars were lime based however, these were gradually replaced by cement mortars which were faster setting, harder and stronger. Nowadays, it is widely accepted that lime mortars should be used for repairs to traditional and historic masonry. In addition, they are increasingly specified in new building however, the wider uptake of lime mortars has been inhibited by a lack of design guidance and performance data.

In general, mortars play a crucial role in masonry structures. Among other functions, they enable good adhesion between masonry units, cushioning masonry joints to absorb stresses and prevent cracking, whilst simultaneously providing flexural strength to resist lateral load as well as eccentric vertical loads. While some relevant research on the properties of hydraulic and calcium-lime mortars has been completed, there is a research gap in the area of lime-mortar masonry. In particular, on the influence of lime-mortar properties on the resultant masonry.

Physical properties of lime mortar such as water content, water retention and workability affect the strength and deformation characteristics of lime mortar and masonry. However, no research to date has established to what extent this occurs. Additionally, no relationships have been established amongst important lime-mortar masonry properties such as compressive strength, flexural strength, bond strength and elastic modulus.

The general mechanics of masonry in compression are well defined however, previous research mainly focused on low strength cement mortars where lime was used as an additive to increase the workability of the mortar, rather than as the main binder. Furthermore, to date, models for the estimation of masonry strength, elastic modulus, peak strain and the prediction of the shape of stress-strain curves during compression (which are required for masonry design) have only been developed for CEMENT mortar masonry.

1.1.2 Aim of this research

This research studies how mortar properties affect the properties and behaviour of masonry. It investigates the role of influential properties such as water content, water retention and workability on lime mortar and lime-mortar masonry strength development over time. Additionally, the relationships between lime-mortar masonry properties (compressive, bond and flexural strength and stiffness) are examined for masonry built with different types of stone and brick units.

The aim of this research is to encourage and promote the appropriate use of lime mortars in new building and in the repair of historic structures. This study contributes to a better characterisation of natural hydraulic and calcium-lime mortars and masonry in order to enhance their use in new building and conservation.

Objectives are as follows:

- To determine the influence of mortar water content, curing time and the effect of outdoor curing on the mechanical properties of both lime mortar and masonry;
- To propose the optimum amounts of water for lime mortars of different hydraulic strengths which provide both good workability and mechanical performance;
- To establish relationships between bond strength, elastic modulus and the compressive and flexural strength of lime-mortar masonry;
- To investigate the influence of curing on the properties of lime mortar and lime-mortar masonry.
- To derive analytical estimation models for the characteristic compressive strength of brick and stone lime-masonry using obtained research data;
- To assess the ability of models proposed by Eurocode 6 EN 1996-1-1 (2005) and previous authors to predict the compressive strength/elastic modulus and peak strain of lime-mortared masonry and to evaluate stress-strain curve estimation models by comparing them with experimental stress-strain relationships.

1.2 BACKGROUND RESEARCH ON LIME MORTAR

1.2.1 Lime mortars

Traditionally, historic mortars were lime based, with additives sometimes included to enhance strength. Lime mortars began to be considered outdated and were replaced with the development of artificial cements. Artificial cements set, harden and develop strength faster than lime mortars. They are also mechanically stronger and more resistant to weather than lime mortars.

According to research and experience, artificial cements can have a detrimental effect on historical and traditional fabrics. Impermeable mortars increase moisture transport through masonry units thus enhancing pollutant deposition, mineral alteration, biological colonisation, salt crystallisation and frost damage. Many historic masonry buildings and structures in Ireland have been damaged due to repairs made using overly strong, inflexible, impermeable, salt-bearing artificial cement mortars (namely Portland cement) (Pavía and Bolton 2002). In contrast, mortars made with lime binders are usually porous, permeable and deformable. They do not contain elements capable of forming salts and are generally more compatible with historical and traditional fabrics.

To ensure the successful restoration of an historic structure, the choice of mortars is critical. It is well known and accepted that repair mortars need to be compatible with existing materials. Various recent Restoration Charters (Venice (1964) and Burra (1979) recommend the use of lime-based mortars for the restoration of ancient buildings and structures because of their compatibility with the original masonry mortars, renders, plasters and units. This compatibility can be separated into three main areas:

i. Chemical compatibility between the old materials (stone, brick and mortars) and the new mortars. Repair mortars must not react by forming salts, which can damage historic fabrics;

ii. Physical compatibility in relation to moisture transfer and solubility. A good mortar must be a conduit for moisture transfer within the masonry (Pavía 2006);

iii. Structural and mechanical compatibility, the strength and elasticity of the repair mortars must be similar to those of the historic one, so as not to place any new stresses on the structure.

1.2.2 Mortar water content and workability

Water content is the most important factor in mortar workability and directly governs its flow (measured by the initial flow test, EN 459-2 (2010)). BIA (2003) and Hanley and Pavía (2007) recommended that the water content should be the maximum amount of water that still renders a workable mortar to enhance strength. Davison (1974) stated that the maximum amount of water that still renders a workable mortar provides the best bond strength while still delivering a workable mortar with ample compressive strength. However, both BIA (2003) and Davison (1974) only considered cement mortars.

Hanley and Pavía (2007) found that more than one flow is required when trying to optimise the strength of natural hydraulic lime (NHL) mortar and that the flow diameter should depend on the hydraulic strength of the mortar. The authors investigated the properties of several mortars at three different flows (165, 185 and 195 mm) and concluded that an initial flow of 165 mm optimised the compressive strength of NHL 2 mortar whereas, 185 mm flow optimised NHL 3.5 and 5. However, they suggest that more testing is required to identify the ideal flow for each NHL strength classification.

The workability of a mortar largely depends on its water content, water retention and internal friction, and these properties are closely related to other factors such as porosity, size and shape of the aggregate, hydraulic strength of the binder and proportions of materials.

Low water content will result in a dry mix, thus increasing the risk of binder fracturing and a lack of internal adhesion between binder and aggregate. Subsequently, if additional water is lost due to suction from masonry units, a good bond may not develop. In addition, excessive water adversely affects mortar properties lowering mechanical strength and increasing the risk of failure due to shrinkage. Excessive water can also render a mortar too fluid to be workable and cause masonry units to 'float', thus weakening adhesion at the mortar-masonry interface and lowering bond strength.

Chemical processes such as lime leaching can also be related to an excess of water (Costigan and Pavía (2010); Hanley and Pavía (2007)).

Water content is one of the main factors that affect fresh and hardened mortar properties and therefore, the quality of the resultant masonry. Water content can have a greater influence on the properties of mortar and masonry than the type of binder or the nature of the aggregate (Army 2005). For example, it has been shown that mortar porosity, density and water absorption are more significantly affected by water content than by the aggregate quality (Pavía and Toomey 2008).

Despite the influence and great importance of water content, in practice, the mason often subjectively determines it by assessing the mortar's workability. This lack of explicit guidance on appropriate water content levels can lead to a lack of consistency in mortar properties and field performance. In addition, it adversely affects the large-scale uptake of lime mortars in new building and mainstream technology.

Hendrickx (1999) noted that masons on site are more concerned with workability than the mechanical properties of hardened masonry: "as long as they think the workability is good, they are happy". Therefore, Hendrickx (1999) concluded that water content is determined by the subjective feel of workability, rather than by strength or durability.

Water content cannot be universally specified for site works due to differences in the composition and nature of aggregates, binders and additions as well as differences in the material moisture content that depend on the environment and storage. As a result, adding the same amount of water to a 1:3 (lime:aggregate) calcium lime mortar in two different building sites can produce mortars with different properties, workability and performance. However, water content can be determined by making a mortar flow to a specific diameter on a flow table. This can ensure consistency in the amount of water added and the mortar's workability, avoiding the variation in mortar properties triggered by differences in water content and providing mortars with consistent properties and field performance. Therefore, all mortars in this research were mixed to specific flow diameters (Section 2.3.1)

1.2.3 Mortar water retention

Water retention is the ability of mortar to resist water loss. This property is important because water loss can negatively affect mortar workability and the mechanical behaviour of the resultant masonry (Army 2005). Lime mortars have great water retention characteristics. Values ranging between 84 % and 99 % have been consistently determined in literature (Bosiljkov (2001);Hanley and Pavía (2007); Pavía and Hanley (2010)

Mortars lose moisture in two ways; through evaporation when exposed to air and due to suction when mortars are in contact with absorbent masonry units. The suction of water from the mortar into the masonry units assists the bonding between the two. Suction carries the finer particles, particularly lime, into small voids in the masonry thereby improving the bond. If the suction is too great, then too much moisture is removed from the mortar at the interface. In hydraulic mortars, insufficient water will be available for the hydration process and this results in a reduction in the bond and compressive strength. In calcium lime mortars (CL90-s), a sudden loss of water due to suction can cause mortar fracturing and shrinkage. ASTM (2003b) and Groot (1993) agree that mortars which have stiffened due to water loss will have a poor bond and thus, water-permeable joints.

Good water retention allows the mortar to maintain sufficient moisture to enable proper curing by providing resistance to suction from dry or high suction masonry units. It also enables the mortar to retain its plasticity when in contact with absorptive masonry so that the mason can carefully align and level the units without breaking the bond (Pavía and Hanley (2010) citing MAC (2004)).

Less retentive mixes lead to moisture bleeding creating a thin layer of water between the mortar and the masonry unit. This causes the unit to float, resulting in a substantial decrease in masonry bond strength. In addition, an increased risk of failure due to shrinkage also exists in less retentive mortar mixes (Hanley (2006) citing MAC (2004)).

Hanley (2006) cited Army (2005) who carried out cement mortar and masonry research and concluded that the water retention of a mortar should be compatible with both the suction of the masonry units and the environmental conditions, so that adequate

workability is maintained. Palmer and Parsons (1934) suggested that the water retention of the mortar becomes more important as the absorption rate of the masonry increases or the temperature during installation rises. Therefore, to prevent excess water loss and reduced workability, masonry units with high suction should be bound using mortars with high water retention (Army (2005); Palmer and Parsons (1934)). MAC (2004) advised pre-wetting of high suction clay units, but noted that since these units tend to dry out quickly, the mortar used will be required to resist water loss.

Several authors agree that the addition of lime to cement mortar enhances its water retention (Francis *et al.* (1971): Groot (1993); Green *et al.* (1999); Sébaïbi *et al.* (2002)). Sébaïbi *et al.* (2002) explored the water-retention capacity of various limes and lime proportions in a cement-lime mortar. The authors concluded that, as the percentage of lime increased, the water retention initially decreased; however, after approximately 10-20 % lime content a minimum was reached and the water retention began to rise, reaching values of between 80 and 85 %. The strong water retention of lime was evidenced by Green *et al.* (1999). The authors demonstrated that cement and cement-lime mortars had similar water retention however, the calcium lime mortars were found have a considerably higher water retention.

1.2.4 Mortar compressive strength

Mortars are generally classified according to their compressive strength in design standards (e.g. EN 1996-1 (2005) and EN 1996-2 (2006)). The compressive strength of mortar is a universal property that is readily understood by designers and builders. The compressive strength of a mortar is an important property because it provides an indication of the overall quality of the mortar. Compressive strength is used as a comparative benchmark for mortars because compressive tests are relatively easy to perform and give clear, consistent results. However, since the masonry units carry the majority of the compressive load in masonry, the compressive strength of mortar may not be a critical property in masonry wall performance.

Testing mortar compressive strength usually involves crushing mortar cubes or prisms in a loading machine. The mortar prism strength is not directly related to the compressive strength of mortar in masonry joints because of several factors, such as the

state of stress, water content and dimensions of testing specimen's masonry unit suction and texture (Army (2005); Kjaer (1991)).

Kjaer (1991) showed that brick suction has a great influence on the strength of the hardened mortar in the masonry joints. The Author found that the compressive strength of mortar hardened in moulds was significantly lower than that of mortar in brick masonry joints. However, Army (2005) suggests that even though mortar prism and masonry joint strengths may differ, the compressive strength of the mortar prisms provides an excellent overall measure of mortar quality and hence its inclusion in this research.

Mortar compressive strength depends on many factors including aggregate/binder proportions, aggregate characteristics, mixing time and, most especially, water content. Several authors experimentally demonstrated that water content and thus mortar workability has a considerable impact on mortar compressive strength, increasing the water to lime ratio and the lime to aggregate ratio lowers strength as shown in Figure 1.1 (Allen *et al.* (2003); Hanley (2006); Arandigoyen and Alvarez (2007); Cosgrove and Pavía (2009)).

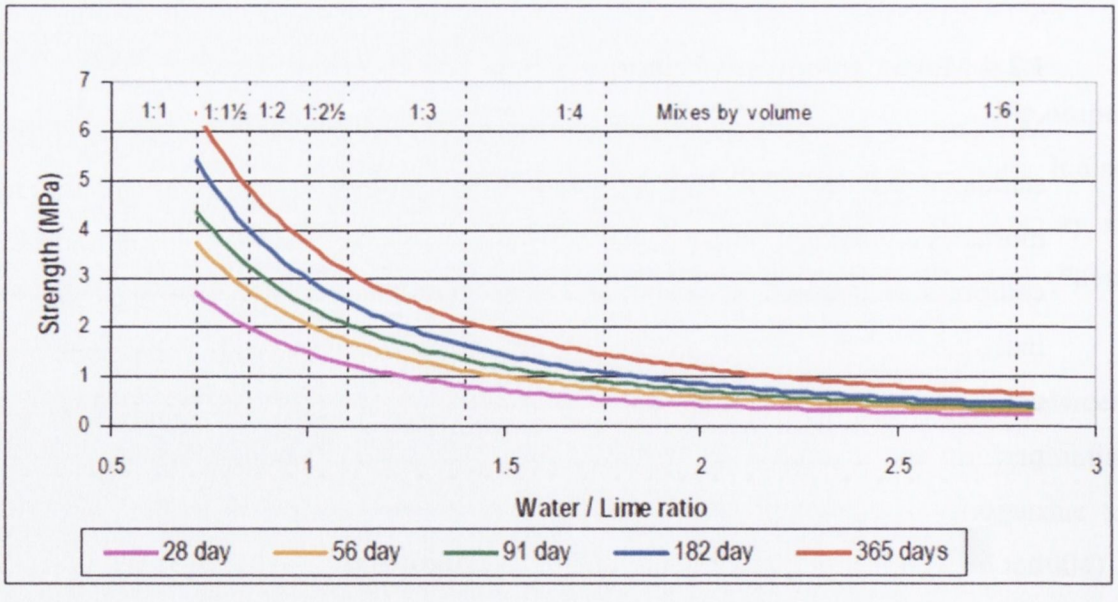

Figure 1.1: The relationship between water:lime ratio and compressive strength (Allen *et al.* 2003)

Zhou *et al.* (2008) contradicted previous authors by showing little variation in mortar compressive strength as a result of variations in the water:binder ratio. In addition, Zhou *et al.* (2008) suggested that the compressive strength of lime mortars may be less sensitive to changes in water content than that of cement-lime mortars.

A higher proportion of binder generally results in increased compressive strength while both increasing water content and adding too much aggregate result in a decrease in strength (BIA (2003); Allen *et al.* (2003); Lanas *et al.* (2004)).

The influence of water content/workability (measured as initial flow) on the flexural and compressive strength of natural hydraulic lime (NHL) mortar was studied by Hanley and Pavía (2007). The authors concluded that in order to optimise mortar strength, NHL 3.5 and 5 mortars should be mixed to attain a high (185 mm) flow whereas NHL 2 mixes require a significantly lower value (165 mm).

After investigating the mechanical and fluid transfer properties of a range of hydraulic and calcium lime mortars, Cosgrove and Pavía (2009) concluded that for higher water contents, lime mortars of greater hydraulicity attain higher mechanical strength and feebly hydraulic mortars (e.g. NHL 2 mortar) gain superior mechanical resistance when mixed to lower flow values. The authors suggested that one reason for this is that the binders with higher hydraulicity require more water for hydration.

Arandigoyen and Alvarez (2007) studied the pore structure and mechanical properties of cement-lime mortars. The authors considered compressive strength as a function of curing time, binder composition, and binder:aggregate ratio. The authors found that lime-rich mortars (cement:lime 0:1 and 1:8) continuously increased compressive strength over time. However, cement-rich binders did not show the same trend and increases in compressive strength were only observed until day seven. Thereafter, the compressive strength dropped before increasing again at 365 days.

Arandigoyen and Alvarez (2007) also investigated stress-strain relationships and Young's moduli for mortars in compression and concluded that, unlike cement-based mortars, cement-lime mortars present a large plastic region, which increases as the proportion of lime increases without changing the water/binder ratio, Figure 1.2.

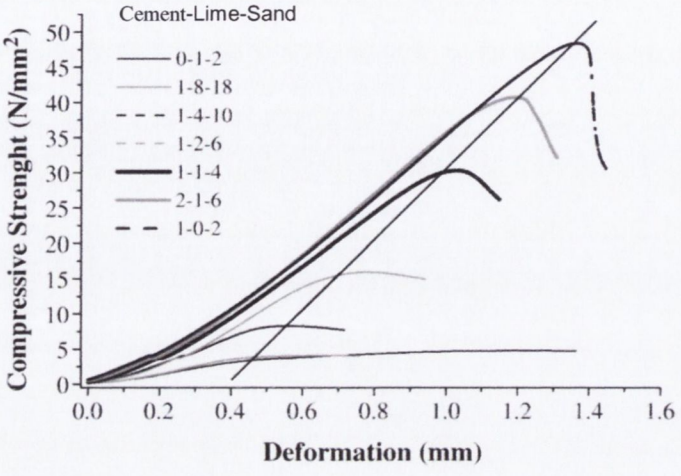

Figure 1.2: Compressive strength vs. deformation (Arandigoyen and Alvarez, 2007)

1.2.5 Influence of aggregate on mortar properties

In order to prepare a mortar with good strength, well-graded sand with a uniform distribution of particle sizes should be used (Holmes and Wingate 1997). The aggregate should be clean and free from silt and clay as they increase the water demand of the mortar, which subsequently reduces the compressive strength, flexural strength and permeability, whilst increasing the risk of cracking in the hardened mortar. It is vitally important to choose a suitable aggregate since the aggregate is responsible for the mortar structure (Allen *et al.* 2003).

According to Patterson and Pavía (2012), the aggregate characteristics that influence mortar strength are: particle size distribution; chemical composition; morphology (particle shape, surface roughness) and porosity, with particle size distribution being amongst the most important. It is well known that adequate grain size distribution including a wide range of particle sizes triggers a physical filler effect, whereby the smaller aggregate fills spaces between larger particles. This has the effect of enhancing packing, increasing density and lowering porosity, therefore leading to a greater strength and durability.

Previous studies have concluded that a good grading (i.e. a wide range of particle sizes) enhances strength and bulk density, whilst simultaneously lowering porosity, water

absorption and capillary suction (Lanas and Alvarez (2003); Cowper (1927); St. Astier/CESA (2001); Pavía and Bolton (2002); Allen *et al.* (2003); Pavía and Toomey (2008)) and that an aggregate with a lower average particle size also enhances strength (Lanas *et al.* (2004); Stefanidou and Papayiannai (2005)).

Venkatarama and Gupta (2006) conclude that when a fine sand is used in a mortar, 20-25% more water is required to keep the same consistency, and that mortar compressive strength and modulus decrease as the sand becomes finer. It is also widely accepted that an angular aggregate improves the mechanical strength and bulk density, therefore lowering porosity, water absorption and capillary suction (Lanas and Alvarez (2003); Cowper (1927); Pavía and Toomey (2008); Martin (1976); Eichholz and Pliny (1962); Hicky Morgan (1914); Plommer (1973); Holmes and Wingate (1997)).

As previously mentioned, the binder/aggregate ratio also affects strength. Natural hydraulic and calcium-lime mortars increase compressive and flexural strength with increasing binder content (Lanas and Alvarez (2003); Lanas *et al.* (2004)). Proportioning mortars by mass or by volume impacts strength because it affects the binder:aggregate ratio. Significantly more binder is used when prescribing proportions by volume because the aggregate is denser than the binder, therefore, when prescribing mortars by volume, the lower the density of the binder the higher the binder amount prescribed will be (Hanley and Pavía 2007).

1.2.6 Mortar flexural strength

Flexural strength is a significant mechanical property of mortar. It is a measure of the tensile strength of mortars, or the ability of unreinforced masonry to resist failure in bending. Flexural strength is generally 10-20 % of compressive strength; however, flexural tests are extremely sensitive to specimen preparation, handling and curing procedures (Hanley 2006). According to Patterson and Pavía (2012), flexural strength is also important because it indicates strength in tension e.g. that induced by expansion due to freeze-thaw or salt crystallisation and it also indicates how much movement the material will allow within the structure.

Arandigoyen and Alvarez (2007) also studied the flexural strength of cement-lime mortars as a function of curing time, binder composition, and binder:aggregate ratio. The authors found that lime-rich mortars (cement:lime 0:1 and 1:8) continuously increased flexural strength over time. However, in general, a reduction in the flexural strength of cement-rich binders (cement:lime 1:1 and 1:0.5) was found after 28 days of curing. This reduction in flexural strength shifted towards earlier curing times as the cement content was further increased.

1.2.7 Mortar elastic modulus

The Young's modulus, also known as elastic modulus characterises the stiffness and elasticity of a mortar. It also measures a mortar's ability to deform under an applied load. Young's modulus is important in the restoration of historic structures, especially where the accommodation of movement is a desirable attribute. Little research has been carried out on the elastic modulus of lime mortars to date, other than to generally state that lime-rich mortars present a plastic zone that allows them to absorb a high degree of deformation before breakage (Voss (1960); Hendry (2001); Mosquera *et al.* (2002); Arandigoyen and Alvarez (2007); Costigan and Pavía (2008, 2009, 2010)).

Research carried out by Voss (1960) found that cement-lime mortars with high lime content were slow hardening and remained deformable. Lime, therefore, enhanced the ability to accommodate stresses caused by building movement and cyclical changes without excessive cracking.

After studying cement block masonry constructed with cement mortar, Mohamad *et al.*(2006) concluded that that the mechanical properties of mortar governed the deformation behaviour of the masonry when the mortar was less stiff than masonry unit.

1.3 BACKGROUND RESEARCH ON LIME MORTAR

1.3.1 Bond strength

Bond strength is often considered the most important property of hardened mortar because it ensures the structural strength and integrity of masonry. Authors agree that a good bond between the units and the binding material is essential and determines how the masonry transfers and resists stresses from a variety of applied loads (Sinha (1967); Groot (1993); Grandet *et al* (1972) and Francis *et al.* (1971)). Furthermore, a bond that is complete, strong and durable is critical for the composite structural behaviour between mortar and masonry (MAC (2004); Venkatarama and Vyas (2008)). The majority of experimental bond strength research to date has concentrated on cement and cement-lime mortars.

The penetration of hydration products into voids and pores on the brick surface forms the bond between brick and mortar (Grandet *et al.* (1972); Groot (1993) and Lawrence and Cao (1988)). A defective bond can lead to water ingress causing subsequent damage to the structure. Structurally, masonry systems rely on the bond between the mortar and the masonry units to maintain the systems integrity under varying lateral loading conditions (PCA 1994). For example, during wind pressure or suction, masonry relies on the bond to transfer lateral stresses throughout the entire masonry segment. The mortar must develop sufficient bond strength in order to support the flexural tensile stresses. In addition, under static conditions, the bond between the mortar and the units is an integral part of the masonry system's mechanism to support compressive loads. Bond deterioration reduces the compressive strength of a wall and can destroy its tensile or shear strength (Colville *et al.* 1999).

The bond at the mortar-brick interface is responsible for a particular state of internal stress on load application, which initiates vertical splitting cracks in bricks and leads to a failure of the prisms (Mc Neary and Abrams (1985); Kaushik *et al.* (2007); Costigan and Pavía (2010)). The state of internal stress varies, depending on the relative stiffness of the mortar and unit. This is discussed in more detail in Section 1.2.10.

A systematic review of the literature in relation to bond mechanism reveals that the majority of previous studies concern aggregate to paste bond in cement mortar and concrete. Only a small number of studies are related to the interface between lime-mortar and masonry. It is well known that the bond between either, the aggregate and the binder or the mortar and masonry unit, is due to a combination of two mechanisms:

i. A chemical bond created by chemical reactions between the materials in contact along the interface. Adami and Vintzileou (2007) citing Farran (1956) and Lyubimova and Pinus (1962) showed that there is a difference between the paste surrounding aggregates and the bulk paste. The area of the matrix adjacent to the aggregate is one of the weakest areas of concrete and is generally referred to as the "interface transition zone" (ITZ). In the ITZ, large crystals of portlandite concentrate in a phenomenon known as the 'wall effect' (Maso 1980). The chemical bond is affected by factors such as the mineralogy of the substratum, the porosity and the presence of pozzolanic materials (Adami and Vintzileou 2007);

ii. A mechanical bond which is the most important part of the bond mechanism and depends on the substrate characteristics. The development of the brick-mortar bond is generally attributed to the mechanical inter-locking of cement hydration products with the surface pores of the bricks (Hendry and Khalaf (2001); Francis *et al.* (1971); Lawrence and Cao (1988) and Sinha (1967)).

1.3.1.1 Factors affecting masonry bond strength

Bond strength is a complex property that is influenced by mortar properties, masonry unit properties, aggregate characteristics, workmanship factors and curing time (Groot (1993); Hendry and Khalaf (2001)).

Mortar properties

Previous authors have investigated the relationships between the mechanical properties of mortar and the masonry bond strength. Sarangapani *et al.* (2005) referred to previous work by Samarasinghe and Lawrence (1992) and Venumadhava Rao *et al.* (1996) stating that the shear bond strength of masonry increases with mortar compressive strength, and that the masonry's flexural bond strength is enhanced by an increase of the mortar's strength irrespective of the type of masonry unit. The authors also refer to work by Grenley (1969) who suggested that the flexural and tensile bond strength of masonry, as well as its compressive strength, increases with the strength of the masonry units and the strength of the mortar.

A wide range of fresh mortar properties affect masonry bond including; water content, workability, flow, water retention and binder content. The water content of mortar determines its workability, which is measured by flow and influences the ability of the mortar to spread and cover the surface of masonry units. It is generally accepted that a complete contact between the mortar and unit is essential to develop the bond. Pavía and Hanley (2010) established relationships between masonry bond strength and mortar flow. The authors concluded that, for NHL 5 mortars, a high flow (185 mm) results in the strongest bond, simultaneously providing the best workability and highest water retention while, in contrast, for lower hydraulic strengths (NHL 2 and NHL 3.5 mortars), the flow that optimises workability (165 and 165-185 mm respectively) did not lead to the strongest bond.

Bond strength is largely governed by the mortar's water retention, as this property controls fluid transfer, which is essential for bond development (Groot 1993). Pavía and Hanley (2010) demonstrated that the strength of the bond is not determined by the hydraulic strength of the binder, but by the mortar's water retention. The authors concluded that the higher the water retention of the mortar the stronger the bond

strength. Water retention also measures the mortar's ability to resist water loss due to unit suction. Army (2005) suggests that bond strength is improved if mortars with high water retention values are used with masonry units of high suction.

Unit properties

The initial rate of absorption (IRA) of a brick indicates the amount of suction a brick will apply to a mortar. If the IRA is too low, the masonry unit could be prohibited from absorbing enough moisture from the mortar to allow satisfactory penetration of the mortar into the surface crevices and pores of the brick (Kayali 2005). It is generally accepted that a high IRA can result in rapid water loss and thus a weakened bond (Groot (1993); Army (2005)). To counteract the effect of too much suction, masonry units can be pre-wetted prior to use.

A number of authors have shown that a clear relationship exists between the moisture content of the brick unit at the time of laying and the bond strength of masonry (Sinha (1967); Gerard *et al.* (1985); Groot (1993); Venumadhava Rao *et al.* (1996); Walker (1999); Venkatarama and Gupta (2006)). Several of these authors determined that partially saturated masonry units with moisture content values in the range of 80-85% negated the suction effect of the units and facilitated optimisation of the bond strength. Furthermore, they concluded that any moisture within the unit, however small, enhanced bond strength.

It is generally accepted that the roughness, contact area and surface pore structure of the masonry units have a significant effect on masonry bond strength. Increasing either of these unit properties will enhance bond development (Thornton (1953); Kampf (1963); Sinha (1967); Grandet *et al.* (1972); Groot (1993); BIA (2003); Momayez *et al.* (2005); Ray *et al.* (2005); Sarangapani *et al.* (2005); Tate (2005); Adami and Vintzileou (2007); Venkatarama and Vyas (2008))

Aggregate

Several authors have concluded that sand grading has a significant influence on masonry bond strength. Groot (1993) cited Anderson and Held (1986) who investigated the influence of four sand gradings on the bond strength of cement-lime mortars with a

mix proportion of 1:1:6. The authors concluded that the grading of the sand had a significant influence on the mortar's properties and on the resultant bond strength, suggesting that increasing the fines content lowers bond strength. Several other authors (Wassermann *et al.* (2009) and Venkatarama and Gupta (2006)) agree that fine sands cause a reduction in the tensile bond strength of masonry. Groot (1993) citing Gerard *et al.* (1985) showed that no bond strength was obtained between clay bricks with a very high suction rate (IRA 10-12 $kg/m^2/min$) and cement mortars (300 kg/m^3 of sand) containing very fine sand. Groot (1993) offered the explanation that micro-structural effects at the interface might be causing the phenomenon. Gerard *et al.* (1985) also showed that the bond strength with very high-suction brick increased with coarser sand. In contrast, Sneck (1978) suggested that the additional initial water required by the fine sand was absorbed by the brick (when the mortar came into contact with the high IRA brick) and sufficient water still remained for the hydration process thus, increasing the bond.

Workmanship

Previous research showed that the workmanship factors that most affect bond strength are; time-lapse before application, amount of mortar used, pressure applied to the brick, movement of the bricks, tidiness of the joint edges and curing conditions (Groot (1993); Hendrickx (1999)).

The time-lapse between spreading the mortar and the placing of the unit affects bond strength because it alters initial flow and water content. BAI (2003) recommended that this time-lapse should be minimised to reduce the evaporation of the moisture required for hydration and bond development. The effect of time can be exacerbated when the mortar is spread on high-suction brick or when construction takes place during hot, dry weather. Literature shows that NHL lime mortars with higher flows generally give better bond strengths (Hanley 2006). Therefore, if the flow is reduced by the mechanisms mentioned above, it will result in reduced bond strength. This would be of particular importance if the mortar flow value was chosen to optimise masonry mechanical properties.

MAC (2004) advised that pressure should be applied to bricks when they are placed on the mortar bed to force the mortar into intimate contact with the brick surface. The unit should also be gently tapped to level it. This process was found to increase the bond strength by 50-100 % over hand pressure alone and has been taken into account in the European standard EN 1052-5 (2005). Once a unit has been placed on a bed of mortar and begins to harden by hydration, it is recommended that the masonry should not be disturbed. Any attempt to move the unit will break or seriously weaken the bond as the partially dried mortar will not have sufficient workability to re-adhere to the brick (BIA 2003). It should be noted that BIA (2003) referred to cement mortar whereas lime mortars have greater workability, water retention and setting times, therefore adverse workmanship should have less of a detrimental impact.

Curing time

Curing time (ageing) also has an influence on bond strength. Many authors have studied the effect of age on masonry bond strength, constructed with cement mortars (Kamimura *et al.* (1965); Baker (1979); Drysdale and Gazzola (1985); Neville and Brooks (1987); Sise *et al.* (1988); Lawrence and Cao (1988); Abrams (1995); Sugo *et al.* (2007)) however, little has been reported on lime mortar masonry.

It might be expected that since mortar and masonry compressive strength increase with time, bond strength would follow the same trend. However, a continuous increase in strength is not always observed. Most of the previously mentioned authors focused on the establishment of trends rather than on investigating the causes of bond variation. Generally, bond strength was found to increase consistently in the first seven days, followed by a significant period of variation. The frequency (or amount) of the variation reduced with time.

Baker (1979) noted a significant "up and down" variation in flexural bond strength over 28 days and concluded that no distinct relationship could be found between bond strength and curing time. The author suggests that the development of bond strength in masonry could be adversely affected by: (a) a poor degree of hydration; (b) shrinkage cracking due to early drying and (c) carbonation of the lime present in the mixture. However, the author does not make clear why bond strength is lost by carbonation.

After investigating the rate of flexural bond strength development of cement-lime masonry between 8 hours and 28 days, Matthys and Grimm (1979) found a consistent strength gain between 3 and 5 days. After 5 days an "up and down" period followed, with an overall gain in strength. The authors noted that in some cases, the variations were in the order of 40-50%. However, they found that the frequency of the variations reduced with time. Using statistical analysis, Drysdale and Gazzola (1985) found the behaviour to be inconsistent during the first 365 days. However, their work was only based on a small number of time intervals: 2, 28, 90 days and 365 days in some cases.

Sise *et al.* (1988) reported that the bond strength of cement-lime masonry continued to increase after 7 days, or declined slightly and then stabilised. In contrast, cement masonry showed a continuous decline in the bond strength after 7 days, with close to no strength reported at 365 days.

Lawrence and Cao (1988) endeavoured to explain the causes of variations in bond strength over time. The authors compared the microstructure of a 7-day-old cement mortar with mortar samples from a 4-year-old cement masonry wall. They found little difference in the degree of hydration between the two specimens and failed to offer an explanation for bond strength fluctuations over time.

Sugo *et al.* (2007) also attempted to identify the bond strength gain and loss mechanisms by correlating the tensile bond strength to the micro constituents formed within the mortar. The authors investigated clay brick and 1:1:6 cement-lime mortar specimens. The bond strengths were measured at ages ranging from 3 to 365 days. They recorded the maximum bond strength at 180 days, with minimums occurring at 90 and 365 days. Using statistical analysis (ANOVA) the authors established that increases in bond strength over time were "significant" and decreases were "marginally significant". The mortars constituents and hydration were studied using scanning electron microscopy and x-ray diffraction techniques. Increasing density of the paste was observed up to 28 days which showed a correlation with the initial increase in bond strength. However, the authors were unable to explain strength variations between 28 and 365 days.

1.3.1.2 Bond strength testing

As previously discussed, bond strength of masonry is affected by many variables such as mortar properties, masonry unit characteristics, curing time and workmanship. Because of the many factors involved, it has proven difficult to develop laboratory tests to measure bond and flexural strength that produce consistent results (Hanley 2006).

Bond strength testing in the laboratory does not precisely duplicate the conditions of exposure of masonry elements in-situ. PCA (1994) suggests that it is more difficult to build consistent masonry assemblies for bond testing than to build a structurally sound masonry wall. As a result, the variability associated with assembly testing is generally higher than that associated with testing masonry wall segments. However, correlations between assembly and wall segment tests can be established through parallel testing under controlled conditions that makes bond strength testing useful (PCA 1994).

Early bond strength tests performed by Anderegg (1932) consisted of treating masonry assemblies as simple beams and subjecting them to centre-point loading. A decade later, new testing techniques were developed consisting of two bonded bricks and an eccentric load applied to break the bond. This arrangement produced higher bond strengths (Anderegg 1940, 1942). Early work by Anderegg (1932) illustrated the importance of masonry preparation, curing, and testing procedures on the final bond strength of the assembly. Direct tensile tests were later conducted by Sinha and Hendry (1966) to determine bond strength. Their results, while suffering from a high degree of variability, demonstrated that bond strength tends to increase for wetter mortars until the mortars become saturated, at which point strength reduces rapidly.

In 1974, a bending test for masonry prisms examining bond strength was adopted by American testing standards (ASTM E 518 1974). The standard involves fabricating masonry prism assemblies and testing them horizontally as simple beams (ASTM 2003a). Load is applied using third-point or uniform loading, where the side opposite to the applied load is subjected to tension. Riddington and Jukes (1994) used direct tensile tests, bending tests, and bond wrench tests to determine and compare results of the masonry bond strength. The authors concluded that a direct tensile test is more likely to produce a representative value for bond strength than a bending or wrench test,

provided that a stress multiplication factor is applied to the average failure stress. The stress multiplication factor is calculated from a finite-element analysis of the particular loading arrangement (Jukes *et al.* 1997).

Several other direct tension test setups have been developed that have utilised various clamping methods (Jung (1988); Ritchie (1961)). Taylor-Firth and Taylor (1990) developed a different arrangement, which allowed the specimen to be tested in direct tension without the need for clamping devices. Another efficient test setup is the use of epoxy resin to glue the unit to steel plates. Due to its efficiency, a large number of authors have implemented this method (Chinwah (1972); Kuenning (1966); Sinha and Hendry (1975); Ghazali (1986); Van Der Pluijm (1993; 1999)). Recently, a test has been developed that uses specimens constructed from two units in a Z-shaped configuration, and failure is induced by bending the specimens under three-point loading (Khalaf 2005).

Crossed brick couplet tests have also been used to investigate bond strength. These tests involve bricks configured at right angles to each other. The brick units tend to bend when subjected to a tensile force and high stresses concentrate at the corners of the bond interface largely due to preparation mistakes in addition to early set and accompanying shrinkage. This results in non-uniform stresses over the mortar-brick interface. Hence, values for true direct tension are not attained (Held and Anderson (1983); ASTM (2000a; 2002a); BIA 2003).

Wall segment tests that investigate a portion of an entire masonry wall have been used to examine bond strength. ASTM E 72 (1947) was produced as a standard for examining the transverse strength of masonry wall segments (ASTM 2005). The test procedure involved applying a transverse load to a 1.2 m wide wall with a height equal to the typical height of the building element being examined. The test involves a wall segment roughly the size of the masonry elements used in construction, thus closely replicating the performance of a masonry wall in the field. However, the cost and difficulty in assembling such a specimen of this size makes this test impractical for most research endeavours.

In the European Standard EN 5628-2 (1999), wall segments are subjected to four-point loading during a test to determine flexural strength. However, the test does not give the direct tensile bond strength, which many engineers regard as being of practical importance in masonry design (Khalaf 2005). The main issues noted in literature in respect to this test are that the test specimens are quite large and the setup cumbersome. EN 5628 (2005) and EN 1996-2 (2006) provide tables from which the characteristic flexural bond strength can be determined using the wallette test data. They also specify that half of the flexural bond strength value can be conservatively used for direct tensile bond strength. However, the low strength classes required for most limes are not covered within these tables.

This research uses the bond wrench test referred to in EN 1052-5 (2005) (Section 2.6.5). This test is widely used in literature and is generally accepted as an efficient and accurate method of determining masonry bond strength.

1.3.2 Flexural strength of masonry

Flexural strength is another important property of masonry because it is a direct measure of the masonry's ability to resist or absorb lateral loadings due to wind pressures and eccentric vertical forces and it is a vital requirement in masonry design. The flexural strength of masonry is closely related to the masonry bond strength since it is the bond between the mortar and the masonry unit that resists moments due to flexural stresses. No previous literature was found where the flexural strength of masonry has been correlated to mortar properties however, relationships between mortar properties and masonry bond strength have been discussed in the previous section.

Almeida *et al.* (2002) concluded that low insight was available with respect to the relationship between the flexural bond strength and tensile bond strength of masonry. However, several authors have suggested that the results of the bond wrench test can be correlated with those obtained from masonry flexural bond strength testing (BRE (1991); Zhou *et al.* (2008)). BRE (1991) demonstrated this for high strength cement-lime masonry and Zhou *et al.* (2008) for a small number of lime masonry samples. This research investigates this correlation in order to validate the use of the less cumbersome, bond wrench test, for the determination of lime-masonry flexural strength (Chapter 4).

1.3.3 Influence of bond strength on masonry compressive strength

Previous research demonstrates that a distinct relationship exists between the bond strength and the compressive strength of masonry. However, authors conflict when considering the relative influence of bond strength on masonry compressive strength when other factors (unit and mortar strength) remain constant (Grenley (1969); Venkatarama *et al.* (1995); Sarangapani *et al.* (2005); Gumaste *et al.* (2006) Venkatarama *et al.* (2007); Venkatarama and Vyas (2008); Costigan and Pavía (2010)).

Sarangapani *et al.* (2005) carried out one of the first systematic studies to better understand the influence of brick-mortar bond strength on masonry compressive strength however, the authors only considered the situation where the brick elastic modulus (E_{unit}) was lower than that of the mortar (E_{mortar}). Sarangapani *et al.* (2005) found that an increase in bond strength, while keeping the mortar composition and strength constant, resulted in a significant improvement in the compressive strength of the masonry. A four-fold increase in flexural bond strength doubled the masonry compressive strength.

Attempts were also made by Venkatarama *et al.* (2007) to correlate bond strength with masonry compressive strength. However, in this case, the modulus of elasticity of the unit was in the same range as that of the mortar. The authors only observed marginal increases in compressive strength as bond strength increased. Venkatarama and Vyas (2008) concluded that masonry compressive strength is not sensitive to bond strength variations when the masonry unit is stiffer than the mortar.

Venumadhava Roa *et al.* (1995) also studied the relationship between mortar and masonry strengths, and concluded that bond strength and masonry compressive strength are not significantly impacted by the strength of the mortar. The authors also demonstrated that mortars with distinctly different compressive strengths but similar bond strength result in similar masonry compressive strengths.

Gumaste *et al.* (2006) conclude that rather than the strength of the bond, crushing of the weakest brick in a wallet specimen often determines the masonry strength and this masks the influence of mortar strength on masonry strength. The authors also conclude

that when using weak mortar, masonry failure is primarily due to loss of bond between mortar and brick.

Earlier research by Grenley (1969) considered the effect of various mortars on the mechanical properties of masonry. The author found a clear relationship between bond and masonry compressive strength, as both properties improved with increased unit and mortar strength. However, Grenley (1969) was unable to determine the relative influence of bond strength on masonry compressive strength since the mortar compressive strength was not kept constant during testing.

1.3.4 Compressive strength and failure mechanics of masonry

Several theories have been presented on the behaviour of masonry under compressive loads (Hilsdorf (1969); Khoo and Hendry (1969); Francis *et al.* (1971); Shrive and Jessop (1980); Atkinson and Noland (1983); Ohler (1986) and Venkatarama and Vyas (2008)). Hilsdorf (1969) proposed a theory whereby the strength of a stack-bonded masonry prism with a solid-unit is limited by the strength of the mortar irrespective of mortar and unit stiffness. Other researchers, Mc-Neary *et al.* (1985) citing Khoo and Hendry (1969), suggest that the failure of a stack-bonded prism is defined by the maximum lateral tensile strain of brick (obtained by testing brick couplets under the combined stresses of compression and tension). Their theory relates the unit lateral strain to a tri-axial stress condition in the mortar joints, which relies on the assumption of strain compatibility between unit and mortar.

Shrive and Jessop (1980) proposed an expression for the lateral stress in the unit as a function of the masonry prism compressive strength; however, poor correlation between experimental and predicted results was found. Mc-Neary *et al.* (1985) claim that the poor correlation was due to the fact that the authors had assumed linear elastic properties for both mortar and unit and did not consider the non-linear characteristics of the mortar and the bi-axial failure of the brick units.

Atkinson and Noland (1983) proposed an expression, Equation 1.1, which takes both the non-linear behaviour of the mortar and the linear-elastic properties of the units into account. Equation 1.1 relates an increment of lateral brick stress to an increment of

prism compressive stress, and the elastic and geometric properties of both the brick unit and the mortar.

$$\Delta\sigma_{xb} = \frac{\Delta\sigma_y \left[v_b - \frac{E_b}{E_m(\sigma_1,\sigma_2)} v_m(\sigma_1,\sigma_2) \right]}{\left[1 + \frac{E_b}{E_m(\sigma_1,\sigma_2)} \frac{t_b}{t_m} - v_b - \frac{E_b}{E_m(\sigma_1,\sigma_2)} \frac{t_b}{t_m} v_m(\sigma_1,\sigma_2) \right]} \qquad \textbf{Equation 1.1}$$

where: $\Delta\sigma_{xb}$ = increment in lateral stress in the brick; $\Delta\sigma_y$ = increment in vertical stress on prism; v_b = Poisson's ratio of the brick; E_b = Young's modulus of the brick; v_m = Poisson's ratio of the mortar as a function of principal stresses; E_m = Young's modulus of the mortar as a function of principal stresses; t_b = thickness (height) of brick unit; and t_m = thickness of mortar bed joint.

Mc-Neary *et al.* (1985) and Mc-Neary and Abrams (1985) compared experimental results to those calculated using Equation 1.1 and concluded that the model was able to adequately represent the mechanics of clay-brick masonry in compression. The predicted strengths obtained by Mc Neary and Abrams (1985) were approximately 25 % below the observed experimental values. The authors suggest that the additional experimental strength was associated with lateral compression preload induced in the masonry prism due to shrinkage of the mortar, and reserve strength in the masonry after initial cracking takes place. Authors generally agree that the elastic behaviour of masonry in compression is largely dependent on the nonlinear properties of the mortar. (Mc-Neary *et al.* (1985); Mc-Neary and Abrams (1985); Mohamad *et al.* (2006)). This is because the masonry units are usually stiffer than the bedding mortar. However, this may not always be the case.

Failure theories for masonry under compression have been presented by many researchers (Hilsdorf (1969); Khoo and Hendry (1969); Atkinson *et al.* (1982) and Mc-Neary *et al.* (1985)). These theories are based on two main assumptions:

1. That the brick and mortar are a under multi-axial stress state.
2. That a perfect bond between the brick and mortar remains until ultimate failure.

According to all of these theories, the state of stress developed in the unit (brick) and the mortar depends on their relative stiffness. Venkatarama and Vyas (2008) considered

the nature of stresses developed in brick masonry prisms and presented two cases for different ratios of E_{unit} / E_{mortar} (Figure 1.3).

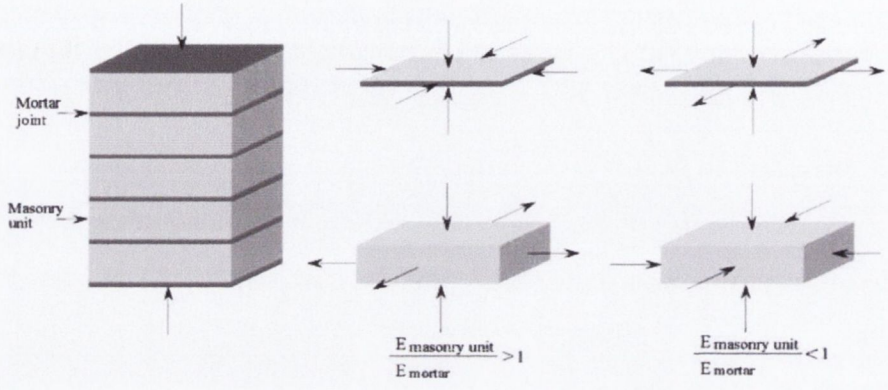

Figure 1.3: The nature of stresses in the masonry unit and mortar in relation to their relative stiffness (Venkatarama and Vyas 2008).

Case 1: ($E_{unit} > E_{mortar}$)

During compression, the mortar expands outwardly more than the bricks, due to its lesser stiffness; however, within the masonry the mortar is laterally confined, due to the bond. As a result, shear stresses at the interface result in an internal state of tri-axial compression in the mortar and bi-axial tension with uni-axial compression in the units. According to several authors (Drysdale *et al.* (1994); Atkinson and Noland (1983); Kaushik *et al.* (2007); Venkatarama and Vyas (2008); Sarangapani *et al.* (2005)) this state of stress initiates vertical splitting cracks in bricks that eventually spread to the mortar and lead to prism failure.

Sarangapani *et al.* (2005) investigated the influence of bond strength and the loss of bond on the ultimate strength of masonry prisms when the stiffness of the unit was greater than of the mortar. The authors found two modes of failure.

They concluded that when bond strengths are low, loss of bond is often associated with masonry failure in compression (Mode II), since the unit can be easily parted from the mortar. However when the bond strength increases, the bond does not detach (Mode I) and the masonry prism fails by way of diagonal shear cracks, much like the diagonal splitting pattern associated with concrete cylinders under compression.

Vasconcelos and Lourenco (2009) also studied masonry where the stiffness of the unit was greater than that of the mortar. The authors agree with Sarangapani *et al.* (2005) on that there are two main modes of failure at the unit-mortar joint:

- Mode I: shear failure (in which there is no bond loss). The shear failure is due to sliding of the units, lateral tension in the units and shear failure of the mortar joint.
- Mode II: tensile failure (where there is a loss of bond). The tensile failure is associated with stresses acting normal to the joint (horizontal tension).

According to Drysdale and Khattab (1995), the propensity for failure due to one mode or another or a combination of modes is closely related to both the orientation of the bed joint to the main stresses and the ratio of the main stresses.

Case 2: ($E_{unit} < E_{mortar}$)

In this case (see Figure 1.4) the mortar will be in bi-axial tension and uni-axial compression, while the masonry units will experience tri-axial compression. Venkatarama and Vyas (2008) explains the tri-axial compression in the masonry unit as resulting from the stiffer mortar pulling it inwards for strain compatibility. Horizontal shear stress at the unit-mortar interface causes the horizontal compression developed in the masonry unit. The authors propose that, if bond is lost at the interface, then the horizontal compression in the unit will vanish and the masonry will fail by lateral tension.

According to Venkatarama and Vyas (2008) and Gumaste *et al.* (2006), vertical splitting cracks first appear in the mortar because it is experiencing bi-axial tension. As the compressive load on the masonry prism increases, the vertical cracks propagate and spread to the unit, hence several splitting cracks can be seen before ultimate failure and collapse occurs.

Gumaste *et al.* (2006) further noted that if one of the bricks is very weak it can fail by crushing before the splitting failure of other bricks. The author also suggests that the vertical mortar joint in English bonded masonry walls can cause splitting failure in the brick below, since the stress in the mortar is much higher because of its greater stiffness.

Failure of English bonded masonry is therefore more likely to be by vertical splitting in the middle of the walls thickness.

1.3.5 Simple stress-strain relationship models

This section presents some simple stress-strain relationship models discussed in existing literature, with the aim of later comparing their predictive curves with actual brick-lime masonry stress-strain relationships, obtained in this research through experimentation.

Several authors have investigated the stress-strain relationship developed from uni-axial compression of masonry prisms and wallettes (Ewing and Kowalsky (2004); Priestley and Elder (1983); Paulay and Priestley (1992); Kaushik *et al.* (2007)). These relationships have been based on specimens constructed with cement or cement-lime masonry. All of the above mentioned authors elected to use the "modified" Kent-Park model (Kent and Park (1971); Priestley and Elder (1983)) in their investigations. The model consists of three portions: a parabolic rising curve, a linear falling branch and a final horizontal plateau of constant stress (20 % of masonry prism strength). They are defined by the following equations:

Rising curve

$$f_m = 1.067 f'_m \left[\frac{2\varepsilon_m}{0.002} - \left(\frac{\varepsilon_m}{0.002}\right)^2\right] \quad \text{for } 0 \leq \varepsilon_m \leq 0.0015 \qquad \textbf{Equation 1.2}$$

Descending curve

$$f_m = f'_m[1 - Z_m(\varepsilon_m - 0.0015)] \quad \text{Until } 0.2f'_m \qquad \textbf{Equation 1.3}$$

Final horizontal plateau

$$Z_m = \frac{0.5}{\left[\frac{3 + 0.29f_j}{145f_j - 1000}\right] - 0.002} \qquad \textbf{Equation 1.4}$$

where, f_m and ε_m = compressive stress and strain in masonry; f'_m = peak compressive strength of masonry; f_j = compressive strength of mortar; Z_m = final constant stress.

Both Ewing and Kowalsky (2004) and Paulay and Priestley (1992) concluded that the "modified" Kent-Park model could adequately predict the stress-strain curve of unconfined masonry. Ewing and Kowalsky (2004) also proposed four performance limit states. The performance limits correspond to 75 and 90 % of prism compressive

strength on the rising part of the stress-strain curve and 50 and 20 % of prism compressive strength on the falling branch. Based on the limit states proposed by Ewing and Kowalsky (2004) and experimental results, Kaushik *et al.* (2007) determined 6 control points, as shown in Table 1.1 and Figure 1.4. It should be noted, that the author only studied masonry where the units were stiffer than the mortar.

1.	0.33 f'_m	Stress-strain curves remain linear
2.	0.75 f'_m	Vertical splitting cracks appear in bricks; masonry still resists loads without much deterioration
3.	0.9 f'_m	Vertical splitting cracks propagate excessively
4.	f'_m	Ultimate stress level in masonry after which the load drops and strains increase excessively
5.	$0.5f'_m$	Proposed as maximum dependable compressive strength of masonry
6.	$0.2f'_m$	Residual compressive stress in masonry

Table 1.1: Stress-strain curve control points suggested by Kaushik *et al.* (2007)

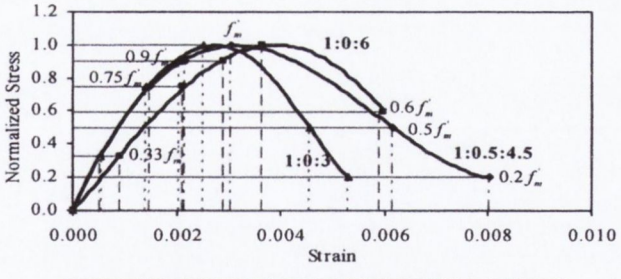

Stress in terms of f'_m	Strain in prism for mortar grades		
	1:0:6	1:0:3	1:0.5:4.5
0.00	0.0000	0.0000	0.0000
0.33	0.0009	0.0005	0.0005
0.75	0.0021	0.0014	0.0015
0.90	0.0029	0.0021	0.0021
1.00	0.0036	0.0025	0.0030
0.60	0.0059	-	-
0.50	-	0.0045	0.0062
0.20	-	0.0053	0.0080

Figure 1.4: Stress-strain curves for masonry prisms for different grades of mortar: stress is normalised with respect to prism compressive strength for each curve (Kaushik *et al.* (2007)).

Kaushik *et al.* (2007) also considered the parabolic variation of the ascending part of the masonry stress-strain curve previously verified by Priestly and Elder (1983); Sawko and Rouf (1984) and Paulay and Priestley (1992), and proposed a non-dimensional form of Equation 1.2 in terms of stress ratio and strain ratio (Equation 1.5) and an idealised stress-strain relationship as shown in Figure 1.4.

Rising curve $$\frac{f_m}{f'_m} = 2\frac{\varepsilon_m}{\varepsilon'_m} - \left(\frac{\varepsilon_m}{\varepsilon'_m}\right)^2$$ **Equation 1.5**

where, f_m and ε_m are the compressive stress and strain in masonry; f'_m and ε'_m are the peak compressive stress and strain of masonry.

Eurocode 6, EN 1996-1-1 (2005) acknowledges that the stress-strain relationship of masonry in compression is non-linear. The standard permits the stress-strain curve to be taken as linear (up to $\frac{1}{3}f'_m$) or as a parabolic rising curve (up to a strain of 0.002) and as a horizontal plateau up to 0.0035 of strain (Figure 1.6).

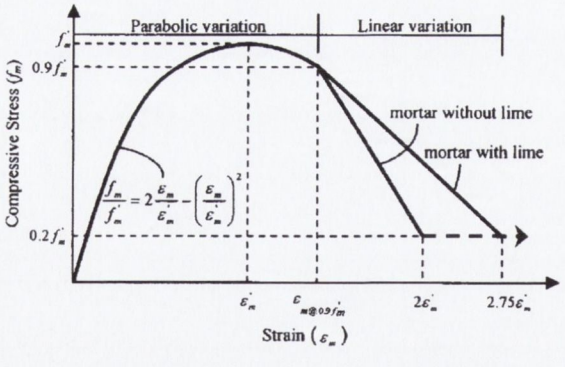

Figure 1.5: Idealised stress-strain relationship Kaushik *et al.* (2007)

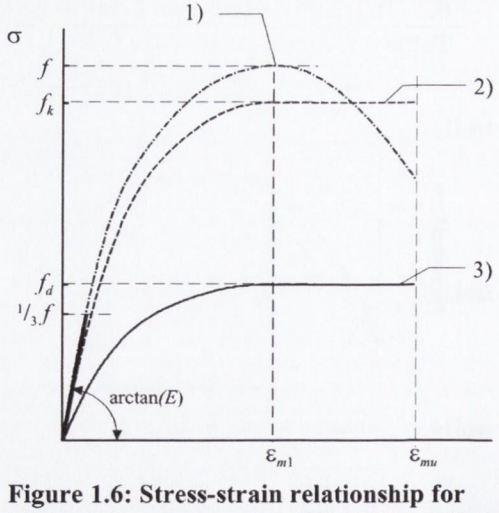

Figure 1.6: Stress-strain relationship for masonry in compression, EN 1996-1-1 (2005).
1: Typical

2: Idealised diagram (parabolic-rectangular)

3: Design diagram

Knutson (1993) evaluated stress-strain diagrams for brick masonry constructed with various cement mortars. The author showed that a relatively simple model (Equations 1.6 and 1.7) can represent them.

Ritter curve, if $\frac{f_m}{f'_m} \leq 0.75$ $$\varepsilon_m = -\frac{f'_m}{E_m} \, ln\left(1 - \frac{f_m}{f'_m}\right)$$ **Equation 1.6**

Ritter curve correction, if $\frac{f_m}{f'_m} > 0.75$ $$\varepsilon_m = -4\frac{f'_m}{E_m} \, ln\left(0.403 - \frac{f_m}{f'_m}\right)$$ **Equation 1.7**

Mohamad *et al.* (2006) found good agreement between the model proposed by Knutson (1993) and experimental results for stronger cement-lime mortars. However, the authors note that as the lime content increased, the non-linear behaviour of the masonry became more severe and the model was only useful up to 30 % of the ultimate compressive strength of the masonry.

Based on regression analysis of experimental results, Kaushik *et al.* (2007) proposed the following equation to estimate peak strain (ε'_m):

Peak strain $$\varepsilon'_m = \frac{0.27}{f_j^{0.25}}\left(\frac{f'_m}{E_m}\right)$$ **Equation 1.8**

1.3.6 Estimation of masonry compressive strength

The compressive strength of masonry (f'_m), is one of the most fundamental and important properties required for design of various masonry elements. Several analytical models for the prediction of compressive strength and deformation characteristics of masonry under uni-axial compression were proposed by previous researches (Grimm (1975); Priestley and Elder (1983); Binda *et al.* (1988); Paulay and Priestley (1992); Ewing and Kowalsky (2004)). Even though a significant number of studies have been carried out, few of these have been able to propose simple equations to determine the compressive strength and deformation characteristics of masonry. The majority of these equations are complicated and require a large amount of input data as well as the characteristics of the units, mortar and masonry in both compression and tension.

Furthermore, it is not always possible to carry out large series of experimental testing when f'_m is required. However, the values of mortar compressive strength (f_j) and unit compressive strength (f_b), are easily obtainable in design codes or from simple testing. This section introduces a number of simple models found in literature that relate these properties. They will then be compared with each other in Chapter 8, using the experimental data in this research; in order to identify which equation best estimates the compressive strength of lime and cement-lime masonry.

Bennett *et al.* (1997) carried out regression analysis on experimental data obtained from testing on structural clay bricks. They concluded that there was a linear relationship between the masonry prism strength and the compressive strength of the bricks. Stress-strain curves were compared for horizontal and vertical compressive testing. As a conclusion the authors proposed a relationship, Equation 1.9, to estimate the compressive strength of masonry as 0.3 times the brick compressive strength;

$$f'_m = 0.3 f_b \qquad \textbf{Equation 1.9}$$

where, f_b is equal to the compressive strength of the brick unit.

Masonry compressive strength (f'_m) could, however, be overestimated since the mortar strength is not taken into account. The authors also proposed a linear relationship between elastic modulus and the masonry prism compressive strength.

Eurocode 6 EN1996-1-1 (2005) relates the compressive strength of masonry with mortar and unit compressive strength as per the following equation:

$$f'_m = K {f_b}^{\alpha} {f_j}^{\beta} \qquad \textbf{Equation 1.10}$$

where, (K, α and β) are constants and the compressive strength of the brick is "normalised" as described in EN 711-1 (2003).

For general construction, where the stiffness of the brick is greater that than that of the mortar and the compressive strength of the mortar is not more than 20 N/mm^2, a greater portion of the masonry compressive strength is derived from the brick strength rather than from the mortar strength. Therefore, α will be a higher value than β. Eurocode 6 EN 1996-1-1 (2005) defines the values of α and β as 0.7 and 0.3, respectively, and

provides a range for K from 0.4-0.6. The K value depends on brick type and the brick-mortar joint characteristics.

Dayaratnam (1987) proposed Equation 1.11 with different K, α, and β values based on regression analysis of experimental data. As can be seen in Equation 1.11, equal weight was given to α and β. However, this is not realistic since in general, the units have more influence on masonry strength than the mortar.

$$f_m = 0.275 {f_b}^{0.5} {f_j}^{0.5} \qquad \textbf{Equation 1.11}$$

Kaushik *et al.* (2007) cited MSJC (2002) who proposed Equation 1.12 for the estimation of masonry compressive strength after carrying out regression analysis based on the testing of solid clay brick masonry.

$$f'_m = A(400 + Bf_b)\ (psi) \qquad \textbf{Equation 1.12}$$

where, A = 1.0 for inspected masonry and B ranges from 0.2-0.25 depending on mortar grade. MSJC (2002) notes that the units for f_b in Equation 1.12 are in pounds per square inch (psi), where 1 N/mm^2 = 145 psi.

Based on a series of experiments and subsequent regression analysis of the test data with, R^2 (Coefficient of Determination, see Section 8.11) and σ (Standard Deviation) values of 0.93 and 0.48 N/mm^2 respectively, Kaushik *et al.* (2007) proposed values of 0.63, 0.49 and 0.32 for K, α and β giving the following relationship:

$$f'_m = 0.63 {f_b}^{0.49} {f_j}^{0.32} \qquad \textbf{Equation 1.13}$$

Kaushik *et al.* (2007) investigated experimental results from various authors (Figure 1.6) and compared them to predicted compressive strength estimates based on Equation 1.13 and other equations by Eurocode 6 EN 1996-1-1 (2005); Dayaratnam (1987); Bennett *et al.* (1997) and MSJC (2002). They concluded that their equation generally gave a better prediction than the others for masonry prisms made with low and average strength bricks. They also noted that for brick with a compressive strength greater than approximately 25 N/mm^2, Equation 1.9 provided the best estimate of masonry compressive strength.

Research[a]	Experimental values (MPa)			Predicted values of f'_m (MPa)				
	f_b	f_j	f'_m	Present study Eq. (12)	Eurocode6 (CEN 1996)	Dayaratnam (1987)	Bennett et al. (1997)	MSJC (2002)
Sarangpani 1	8.2	3.1	2.3	2.5 {10.3}[b]	2.7 {17.6}	1.4 {65.9}	2.5 {7.0}	4.4 {91.2}
Tomaževič	10.0	0.5	2.0	1.6 {28.2}	2.3 {12.7}	0.6 {225.2}	3.0 {50.0}	4.8 {137.9}
Sarangpani 2	10.7	4.1	2.9	3.2 {9.0}	3.4 {18.9}	1.8 {59.2}	3.2 {10.7}	4.9 {68.9}
Sarangpani 2	10.7	10.6	3.2	4.3 {33.6}	4.4 {36.2}	2.9 {9.6}	3.2 {0.0}	4.9 {52.9}
Naraine	13.1	6.1	5.4	4.0 {36.2}	3.6 {49.2}	2.5 {119.7}	3.9 {37.4}	5.4 {0.4}
Tomaževič	15.0	2.5	2.5	3.2 {27.4}	4.4 {75.5}	1.7 {48.5}	4.5 {80.0}	5.8 {130.3}
Rai[c]	17.0	9.9	7.3	5.3 {38.8}	5.8 {25.7}	3.6 {104.6}	5.1 {43.1}	6.2 {18.5}
Present	20.8	3.1	4.1	4.0 {2.4}	5.0 {20.8}	2.2 {85.7}	6.2 {52.2}	6.9 {68.7}
Present	20.8	15.2	6.6	6.7 {0.9}	7.4 {11.6}	4.9 {35.0}	6.2 {5.8}	6.9 {4.8}
Present	20.8	20.6	7.5	7.3 {2.2}	—[d]	5.7 {31.8}	6.2 {20.2}	6.9 {8.4}
Hendry	25.5	15.2	9.3	7.4 {26.4}	7.0 {32.7}	5.4 {71.8}	7.7 {21.6}	7.9 {18.3}
Binda	26.9	12.7	14.5	7.1 {103.3}	6.7 {117.9}	5.1 {185.3}	8.1 {79.7}	8.1 {78.2}
Ewing	34.0	15.7	15.6	8.6 {82.3}	9.4 {66.4}	6.4 {145.5}	10.2 {52.9}	9.6 {63.2}
McNary	101.7	3.4	29.9	9.0 {232.2}	14.2 {110.3}	5.1 {484.7}	30.5 {2.0}	23.1 {29.4}
McNary	101.7	13.7	32.5	14.0 {131.8}	20.1 {61.4}	10.3 {216.6}	30.5 {6.5}	23.1 {40.7}
McNary	101.7	26.4	40.9	17.3 {136.5}	—[d]	14.2 {187.0}	30.5 {34.1}	23.1 {77.1}
McNary	101.7	52.6	48.2	21.6 {123.6}	—[d]	20.1 {139.6}	30.5 {58.0}	23.1 {108.7}

[a]Sarangpani 1=Sarangapani et al. (2002), Tomaževič=Tomaževič (1999), Sarangapni 2=Sarangapani et al. (2005), Naraine=Naraine and Sinha (1989), Rai=Rai and Goel (1996), Hendry=Hendry (1998), Binda=Binda et al. (1988), Ewing=Ewing and Kowalsky (2004), McNary=McNary and Abrams (1985).

[b]Figures in the { } bracket indicate the percent error between the experimental and predicted values.

[c]Reclaimed bricks from about 100 years old building in North America and 1:1:6 mortar were used in prisms.

[d]Eurocode6 (1996) is applicable only for masonry with mortar strength less than 20 MPa.

Figure 1.7: Comparison of past experimental results on masonry prisms with analytical predictions (Kaushik 2007).

In order to establish relationships between the compressive strength of masonry and the compressive strengths of mortar and units, Gumaste *et al.* (2006) brought together experimental results from a wide range of researchers (Varghese and Ashok (1965); Sridhar (1986); Dayaratnam *et al.* (1981); Matthana (1996); Raghunath (2003); Gumaste (2004); Sarangapani *et al.* (2005)). From these results, Gumaste *et al.* (2006) developed the following equation:

$$f'_m = 0.317 f_b^{0.866} f_j^{0.134} \qquad \textbf{Equation 1.14}$$

The authors then compared their proposed relationship with an empirical formula previously suggested by Hendry and Malek (1986), Equation 1.15 below.

$$f'_m = 0.317 f_b^{0.531} f_j^{0.208} \qquad \textbf{Equation 1.15}$$

In general, Gumaste *et al.* (2006) found that Equation 1.15 over-estimated the masonry compressive strength whereas Equation 1.14 tended to under-estimate the value. However, it should be noted that a large coefficient of variation in the brick (40 %) lead to a very wide range of different masonry compressive strengths.

García *et al.* (2012) recently presented results of a series of compressive strength tests on traditional stone masonry. The masonry was constructed with a weak cement-lime mortar. The authors compared the experimental results with a number of proposed equations and design codes (some of which are also considered in this research). They concluded that in the case of rough masonry, none of the consulted equations came close to experimental values and recommended that laboratory testing should be undertaken to accurately determine the compressive strength of traditional stone masonry, rather than relying on calculated values.

1.3.7 Effect of curing on mortar and masonry properties

A good understanding of masonry behaviour and masonry mechanical strength under different curing conditions is important for the correct specification of mortars. A small amount of research has been carried out in relation to the influence of mortar curing conditions on the physical properties of lime mortars (Lanas *et al.* (2006) and Maurenbrecher *et al.* (2005)). However, very little has been published on how curing conditions affect masonry bond and compressive strength. In this thesis both lime mortar prisms and masonry wallets are externally cured in order to simulate field conditions. The results of mechanical tests are then compared to those of laboratory-cured specimens.

Lanas *et al.* (2006) carried out a study on the mechanical behaviour of lime mortars (CL90 and HL 5) under different curing conditions. The authors found that in general, external exposure (5-15 ºC and RH 70-90 %) causes an increase in the mortar's compressive and flexural strength due to the higher degree of relative humidity while when cured indoors (20±5 ºC and RH 60±10 %), the authors found that lime mortars required longer curing times to improve strength.

It is well known that temperature, humidity and air movement influence mortar hydration and thus hardening. High temperatures and low humidity due to high winds or heavy insolation can cause sudden evaporation of moisture from the mortar or masonry. This leads to an overall reduction in mortar strength and thus masonry bond and compressive/flexural strength. Conversely, a lack of adequate insolation in colder conditions can also lead to an underdevelopment of the mortar strength or significant deterioration of strength due to freezing.

The importance of proper curing duration cannot be understated. Groot (1993) cites Isbener (1969), who studied mortar humidity in masonry at different depths over time and concluded that hydration stops at different depths depending on curing duration, leading to a strength differential across the joint that may result in shrinkage and a loss of the bond. Baker (1979) carried out limited laboratory testing on brick masonry and demonstrated that water-cured cement mortar-masonry gave better bond strength when compared to general ambient laboratory conditions. Research presented by Goodwin and Saunders (1988) on calcium silicate bricks concluded that covering for 28 days rather that 3 days resulted in significant increases in flexural bond strength. Therefore, this research investigates the effect of the aforementioned (laboratory and external) curing conditions on lime mortar prisms and masonry wallets at 28 days, 56 days and 6 months. Tests were also carried out after 1 year in certain instances.

CHAPTER 2

MATERIALS AND METHODS

2.1 MATERIALS

2.1.1 Limes

Several limes were studied during the course of this project, encompassing those most commonly used in conservation and new building in Ireland. They can be divided into two categories:

i. *Natural hydraulic lime (NHL)*

Three different types of this lime were used, NHL 2, 3.5 and 5. Their names are determined by their minimum 28 day hydraulic strengths of 2, 3.5 and 5 N/mm^2 respectively, for a standard mix. These limes were chosen because their resultant mortars provide a good range of hydraulic strengths. All three were produced by St. Astier in France.

ii. *Non-hydraulic, calcium lime (CL90-s).*

Non-hydraulic calcium lime is included due to its relatively low strength and low stiffness and because historically, it has been used extensively in Ireland. CL90-s lime was supplied by Clogrennan Lime, Co. Carlow Ireland, under the brand name "White Rino".

2.1.2 Cement

While cement is generally not recommended for use in conservation due to its incompatibility with historic fabrics, cement-lime mortars with a ratio of 1:½:4 (cement:lime:sand), amongst others, are referenced in several publications investigating masonry bond, compressive and flexural strength. It was therefore decided to include a reference cement-lime mortar for comparison purposes. Since EN 1996-1-1 (2005) also refers to the above mortar ratio, this study adopted 1:½:4 (mixed by volume) as a reference mortar (M6). The cement used in this project is Lagan Portland Limestone Cem II/ A-L, produced in Ireland.

2.1.3 Aggregate

Initially, it was proposed to use "normal" sand [EN196-1 (2005)]. However, this aggregate is expensive and not widely available. Since such large quantities of

aggregate were required for this project, its use was not feasible. Therefore, an alternative sand was sourced. Three aggregates were tested (Figure 2.1 and Table 2.1). The St. Astier sand (sable-001) was selected for this research as it best conformed to EN196-1 (2005), especially when considering fine particle content.

Sand Testing				CEN Sand Limits		
	(% Passing)				(% Passing)	
Sieve size (µm)	Cork 1	Cork 2	St Astier	Sieve size (µm)	Lower limit	Upper limit
4000	98	100	100	4000	100	100
2000	87	95	96	2000	100	100
1600	68	78	87	1600	88	98
100	45	56	66	1000	62	72
500	35	46	32	500	28	38
160	28	38	15	160	8	18
80	14	22	3	80	0	2
60	1	2	1	60	0	0

Table 2.1: Particle size distribution of sands and CEN sand limits

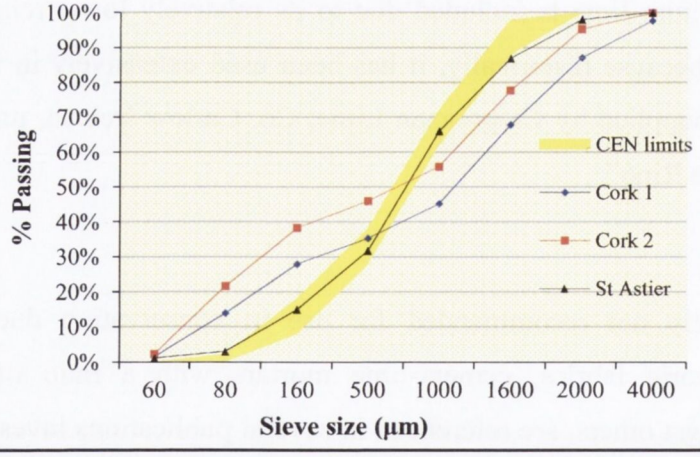

Figure 2.1 Comparison of sand sieve analysis and standard upper and lower limits

Even though the water content of aggregate is not required when mixing mortar to a specific flow (Section 2.2.1), for added consistency and increased reliability with test results, the sand was dried-out prior to use. This was achieved by spreading it over polythene sheeting on the laboratory floor in a thin layer 20 mm deep, for a period of 72 hours. The moisture content was then calculated, ensuring uniformity between each sand batch.

2.2 MORTAR PREPARATION METHODS

2.2.1 Mixing

The three natural hydraulic limes and the CL90-s lime were mixed in a lime:aggregate ratio of 1:3, by weight. A series of testing was also carried out on NHL 3.5 at a ratio of 1:2 by weight. EN 1996-1 (2005) refers to a cement-lime mortar for masonry designated as M6 (minimum compressive strength of 6 N/mm^2 at 28 days comparable to that of eminently hydraulic lime mortars). As previously mentioned, this was used as a reference mortar. The mix ratio for this mortar was 1:½:4 by volume (v) as specified by the standard. All mix ratios throughout this thesis are measured by weight unless otherwise denoted by (v).

An essential objective of this research is to study the effect of varying water content and initial flow of mortars on the resultant masonry. Previous research results on the factors that influence the workability and mechanical properties of lime mortar and masonry bond strength were discussed in Chapter 1. Based on these results, it was decided to manufacture the mortars to two specific initial flow values (165 $\pm$ 3 mm, and 170 $\pm$ 3 mm). All mortars were mixed in accordance with EN 459-2 (2001), which also refers to procedures set out in EN 196-1 (2005). The mortars were mixed with a 5 litre mixing mill and used within one hour. No remixing was undertaken.

2.2.2 Moulding, curing and compaction

Mortar prisms of each mortar type were made in accordance with EN 196-1 (2005). Standard 40x40x160 mm prism moulds were cleaned thoroughly of any surface dirt. The moulds were filled halfway with fresh mortar and compacted on a vibration table for five seconds. The remaining half of the mould was overfilled with mortar and compacted for another five seconds on the table. Any excess mortar was struck off the moulds by passing a steel float across the top surface using a sawing motion. The top surface was smoothened with a float tool.

After an initial curing period of eight hours, specimens were covered with a damp hessian material and polythene to restrict moisture loss in order to prevent fracturing

due to shrinkage. They were left for 24 hours to gain an initial set before being removed from the moulds and placed in storage.

The curing and storage of the mortar prisms was carried out according to EN 459-2 (2010). NHL 5 and NHL 3.5 mortars were placed in a humidity curing chamber with a relative humidity (r.h.) of 95±5 % and a temperature of 20±2 °C for 27 days. After this time they were either tested or placed into storage at 60±5 % r.h. and a temperature of 20±2 °C for a further 28 days. Prisms constructed from CL90-s mortar were stored at 60±5 % r.h. and a temperature of 20±2 °C until tested. The prisms made from cement-lime (M6) mortar were placed in a humidity curing chamber with a relative humidity (r.h.) of 95±5 % and a temperature of 20±2 °C until they were tested. Mortar specimens were also cured in external environmental conditions. They were cured in the same location and under the same exposure conditions as their corresponding masonry (see Section 2.6.2).

2.3 PLASTIC STATE MORTAR PROPERTIES

2.3.1 Initial flow and statistical validation of initial flow

Initial flow is a measurement of the outward flow of a fresh mortar and is an important indication of mortar workability. This was used to measure and keep consistent the water content of all mortar mixes in this research. Specifications for the preparation of mortars often prescribe exact proportions for the ingredients. These proportions are suitable when measuring dry ingredients such as binder and aggregate, but problems arise when specific water contents are prescribed. Mixing mortars with specific water contents does not take into account factors such as gradation of the aggregate, internal friction or environmental conditions including humidity and temperature. Additionally, if specific water contents are prescribed, all water in the mix needs to be accounted for including any moisture in the sand or mixing apparatus. Accounting for these various sources of water can be tedious and impractical and not possible on site.

The properties that influence mortar workability were previously discussed in Chapter 1. As stated, the water content is one of the main factors influencing workability and directly determines the initial flow of a mortar. Due to the complexity of factors affecting mortar workability, relating to the quality, type and amount of mortar

aggregates and binders, one reliable way to ensure that the correct amount of water that is added to a mortar is to specify an optimum initial flow. Specifying mortars by initial flow rather than water content allows the mason to ensure the final mix has the appropriate workability rather than a specific water content that may or may not correspond to a specific workability.

The flow table is the most widely accepted apparatus to measure the consistency of mortar (Figure 2.2). The flow table is referenced in both ASTM and European standards. Slight variations exist between the two standards which should be noted if comparisons are to be made between experiments in literature. For the purpose of this project, all flow table tests were carried out with reference to EN 459-2 (2010).

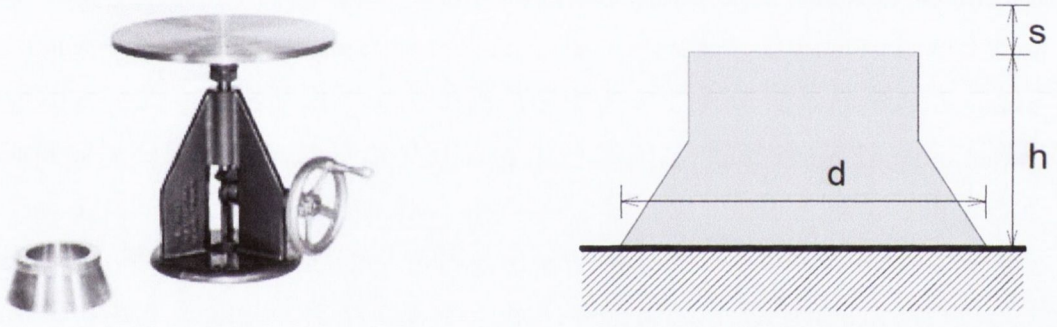

Figure 2.2 (a) The flow table apparatus and (b) mortar specimen

As shown in Figure 2.2, the flow table is a simple apparatus which consists of a circular plate, wheel and crank. Essentially, a fresh mortar sample is scooped into a conical frustum. This is done in two layers, each layer receiving ten tamps with the standard-sized tamping bar. The top of the specimen is then carefully levelled with a straight edge. The frustum is gently lifted, so that the material is allowed to deform under its own weight.

The basic theory behind the flow table test is that the shear stresses caused by gravity are higher than the yield stress of the material, therefore the lower part of the material deforms in shear flow (Figure 2.2 (b)). Equilibrium is reached when the stress causing deformation is equal to the yield stress. This is overcome by the dynamic effect of shocks (Pashias and Boger (1996); Roussel (2004); Roussel and Coussot (2005);

Hendrickx (2009)). The plate is lifted and then dropped fifteen times over a specified height by wheel and crank at a rate of once per second. Three separate measurements of the base diameter were taken with a large vernier callipers and the average was reported as the flow value for that particular sample. To ensure consistency between batches, three samples from each batch were tested.

Initial experimental work was carried out to determine the specific water contents required for each mortar to give an initial flow of 165 and 170 mm. The initial flow value of fresh mortar is found just after the mortar is first mixed. Many previous authors have noted that adding additional water to the mortar and remixing it will give a false flow result (Kampff (1961); Groot (1993); Hanley (2006); Hanley and Pavía (2007); Hendrickx (2009)). Therefore, to ensure accuracy, each time a mix did not reach the specified flow it was discarded and a new batch was made with the water content adjusted. The specific water content for a mortar mix was deemed in this research to be the amount of water that will give the required flow value from three samples from three consecutive batches. Statistical analysis was carried out to check the assumption that no statistically significant difference existed between batches, i.e. that the initial flows of the samples were consistent.

As mentioned previously, mortars were mixed to two flow values 165 and 170 mm. These flow values are very close to each other and the standard EN 459-2 (2010) allows for a variation of $\pm$ 3 mm which is quite large. Therefore, to test that there was a statistically significant difference between the two flow values, a series of tests were carried out for each mortar. Once a particular water content was determined to give a specific flow (165 or 170 mm) for a mortar, three batches of the mortar were mixed and 10 samples of each batch tested for initial flow. This provided 30 values for each mortar. ANOVA statistical analysis was then carried out. The results of the statistical analysis are presented in Section 3.1.2.

2.3.2 Water demand

The quantity of water required for the mortar to attain the specified flow diameter was determined in accordance with the requirements of EN 459-2 (2010). This water content is reported as a ratio of water to binder.

2.3.3 Water retention

The water retention of a mortar is defined as the mass of water retained after suction and expressed as a percentage of the original water content. The water retention of each mortar was measured as per EN 459-2 (2010). The apparatus used is shown in Figure 2.3.

As shown in Figure 2.3, a conical rigid mould ring (2), 140-150 mm internal diameter and 12 mm in depth, was placed upon a non-porous plate (1) and both the mould and the plate were weighed together. For each mortar type, a freshly mixed batch of mortar was placed into the mould and excess mortar was struck off the top with the straight edge. The bottom plate and mould with mortar were weighed. Then two pieces of white cotton gauze where placed over the mould. A filter paper plate (5), 190 x 190 x 2 mm, was then placed on the gauze and a non-porous plate was added on top. A 2 kg weight was placed on top of the top plate and the mould was allowed to sit for two minutes. Afterwards, the weight and top plate were removed and the filter paper weighed so as to determine the mass of water absorbed by the plate.

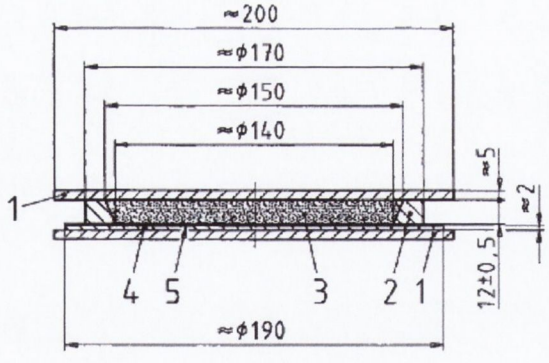

Figure 2.3 Schematic of the water retention test for fresh mortar

In order to calculate the water retention, the water fraction of the mortar batch was first found using the following equation:

$$W_1 = \frac{m_5}{m_5 + m_6}$$ **Equation 2.1**

where, W_1 is the water fraction of the mortar batch; m_5 is the total mass of water in the fresh mortar batch (g); m_6 is the mass of the dry mortar batch (g).

The water content of the mortar in the mould (W_2) is found with the following equation:

$$W_2 = m_7 \times W_1 \qquad \textbf{Equation 2.2}$$

$$m_7 = m_3 - m_2$$

where, W_2 is the water content of the mortar in the mould (g); m_7 is the mass of the mortar in the mould (g); m_2 is the mass of the mould and the bottom non-porous plate (g); m_3 is the mass of the bottom plate and the mould with mortar filling (g).

The mass of water absorbed by the filter plate (W_3) is calculated using the following equation:

$$W_3 = m_7 - m_1 \qquad \textbf{Equation 2.3}$$

where, W_3 is the mass of water absorbed by the filter plate (g); m_1 is the mass of the dry filter plate (g); m_7 is the mass of the soaked filter plate (g).

The relative loss of water from the mortar (W_4) was calculated using the following equation:

$$W_4 = \frac{W_3}{W_2} \times 100 \qquad \textbf{Equation 2.4}$$

where, W_4 is the percentage relative loss of water for the mortar. The water retention value (WRV) is calculated using the following equation:

$$WRV = 100 - W_4 \qquad \textbf{Equation 2.5}$$

Water retention is reported as a percentage and the average of three tests was recorded as the water retention for each mortar.

2.4 HARDENED STATE MORTAR PROPERTIES

2.4.1 Compressive strength

Mortar compressive strength tests were conducted according to EN196-1 (2005) with modifications from EN 459-2 (2010). The applied load was increased smoothly at a rate of 400 ± 40 N/s until failure occurred, as per EN 459-2 (2010). The Zwick test machine used is equipped with an internal load cell and a displacemeter recording the force applied, displacement and strain over time. The compressive strength was calculated using Equation 2.6:

$$R_c = \frac{F_c}{6400} \qquad \textbf{Equation 2.6}$$

where, R_c is the compressive strength, in N/mm^2; F_c is the maximum load at fracture in Newtons; 6400 is the area of the prism face in mm (160x40).

2.4.2 Flexural strength

The flexural strength of the mortar was determined using the three point flexural test in accordance with EN 196-1 (2005). The load was applied vertically at a smooth rate of 50 ± 10 N/s (as per the standard), utilising a Zwick test machine until failure. It was important that the orientation of the test specimen was such that loading was not carried out on the side which was exposed while the prism was in the mould. The flexural strength was calculated using Equation 2.7.

$$R_f = \frac{1.5 \times F_f \times l}{b^3} \qquad \textbf{Equation 2.7}$$

where, R_f is the flexural strength (N/mm^2); F_f is the load applied to the middle of the prism at fracture (in Newtons); b is the side of the square section of the prism, in millimetres; and l is the distance between the supports (in millimetres).

2.4.3 Elastic modulus of mortar in compression

The elastic modulus (E_b) was calculated for each mortar in compression and is the ratio of axial stress to axial strain in the range of stress in which Hook's Law holds. Due to the lack of guidance in mortar testing standards, authors use different mechanisms to determine E_b. Masonry testing standard EN 1052-1 (1999) recommends that elastic

modulus be calculated as the ratio of stress to strain at one third of the ultimate stress. This is the slope of, or tangent to the stress-strain curve at 33 % of the ultimate stress (σ_{ult}). However, EN 1052-1 (1999) is a standard for cement and cement-lime masonry and the point measured may not always be in the linear portion of the stress-strain curve of lime mortar. Therefore, for consistency and to improve accuracy, elastic modulus is determined as the slope of the linear portion of the stress-strain relationship between approximately 30-50 % of the ultimate stress.

Vertical displacement was recorded using the testing machine's internal meter. However, the machine had to travel a very short clearance distance prior to applying a load to the specimen. To take this into account, the displacement meter was zeroed at the point in time when the test machines internal load cell registered a reading. The strain was calculated by dividing the distance travelled by the original height of the specimen (40 mm). The following equations were used to calculate the modulus of elasticity in compression:

Stress $$\sigma = \frac{F_x}{A_i}$$ **Equation 2.8**

Strain $$\varepsilon = {}^{\Delta h}/_{h_0}$$ **Equation 2.9**

Modulus of elasticity $$E_b = \frac{\sigma_{50} - \sigma_{30}}{\varepsilon_{50} - \varepsilon_{30}}$$ **Equation 2.10**

where, E_b is the modulus of elasticity; σ and ε are the compressive stress and strain at any point on the stress-strain curve; F is the applied force; A_i is the loaded cross-sectional area; Δh is the change in height of the specimen, due to the applied force; h_0 is the original height of the specimen (40 mm).

2.5 MASONRY UNITS

2.5.1 Types of masonry units

The inclusion of different masonry units with a wide range of properties was deemed to be essential in this research. Therefore, four types of masonry units were chosen. These provided a good range of compressive strengths, surface textures, pore structure, porosity and suction properties. The four masonry units types were as follows:

i. *Winchester multi-stock brick.*

Machine-pressed, frogged, fired-clay bricks produced in Ireland were obtained from Kingcourt Brick, Co. Cavan, Ireland. Ten bales of bricks were needed and the bricks from these were mixed to limit variation due to batching. This particular type of brick was selected on account of its similarity with the range historically used in Ireland (high suction and relatively low strength and stiffness)

ii. *Kilkenny blue limestone*

This particular limestone has been used as a building material for centuries in Ireland and a large number of national monuments and listed buildings are either fully or part built with it. The stone required for this project was sourced from a quarry at Threecastles, Co. Kilkenny, Ireland. Records show that since its inception in 1831, the Office of Public Works (OPW) has consistently used limestone from this quarry for the construction and conservation of national monuments in Ireland.

Two forms of this stone were used to provide two different surface textures: cut stone and guillotined "broken" stone. The "cut" limestone was cut using diamond saws at the quarry factory into units of approximately the same dimensions as the brick (215x105x65 mm) featuring smooth surfaces. For the "broken" stone, a one square metre stone slab was cut into 100x100x1000 mm sections and then broken using a guillotine into approximately 65 mm lengths. The specimens had to be this particular size due to the mechanical restrictions of

the guillotine at the quarry. This provided units of rough surfaces with a large variation (± 3 mm) of height.

iii. Sandstone

Samples of sandstone relevant to national monuments were provided by the Office of Public Works . The samples were originally sourced from a quarry in Manorhamilton, Co Leitrim, Ireland. The sandstone units were all approximately 65 mm in height however they varied in length and width. They were placed into groups of approximately the same size in order to build masonry prisms.

2.5.2 Masonry unit properties

The physical properties of the masonry units were tested in the laboratory in order to classify them into three broad categories of mass structure, moisture transfer and mechanical strength (Table 2.2). These properties were selected because they were considered sufficient to characterize the masonry unit and they also provide information on the unit's interaction with the mortar.

Physical property	Parameter measured
Mass structure	Apparent density
	Open porosity
Moisture transfer	Capillary absorption (stone)
	Initial rate of absorption (brick)
Mechanical strength	Compressive strength
	Flexural strength
	Modulus of Elasticity

Table 2.2: List of masonry unit properties tested

The mass structure and moisture transfer properties have a considerable influence on how the masonry unit behaves when it comes in contact with a particular mortar. Therefore, they affect the mechanical behaviour of masonry, for example, the self-weight load applied to the fresh mortar; the amount of suction and moisture transfer

rate, have a significant influence on the compressive and flexural strength and, especially, on the elastic modulus.

2.5.3 Masonry unit testing methods

2.5.3.1 Determination of apparent density and open porosity of masonry units

The mass structure properties of apparent density and open porosity of the stone samples were determined in accordance with EN 1936 (1999). 6 samples of each stone masonry unit type were tested. The dimensions of all twelve edges of each specimen were measured to $\pm$ 0.1 mm, using callipers. The specimens were oven dried for a period of two to three hours after which time, they were allowed to cool, and then the dry mass (m_d) of each was measured to an accuracy of 0.1 g. They were then placed in a tray with approximately 2 mm of water and the capillary absorption was measured by taking a reading of time and mass, (t_i and m_i respectively). Both bedding orientations were considered for limestone and sandstone. On completion of this test, the specimens were immersed in water in a pressure vacuum for a period of at least 24 hours. Measurements of the hydrostatic and surface saturated masses, m_h and m_s, were made. The following equations were used:

Apparent density $$\rho_b = \frac{m_d}{(m_s - m_h) \times \rho_w} \quad (\text{Kg/m}^3)$$ **Equation 2.11**

Open porosity $$\rho_o = \frac{m_d}{(m_s - m_d) \times (m_s - m_h)} \times 100\ (\%)$$ **Equation 2.12**

2.5.3.2 Determination of the coefficient of water absorption for stone units

The coefficient of water absorption due to capillary action was determined in accordance with EN 772-11 (2011). Equation 2.13 was used in the calculation.

$$c_{w,s} = \frac{m_{so,s} - m_{dry,s}}{A_s\sqrt{t_{so}}} \left[\frac{g}{(m^2 \times s^{0.5})}\right]$$ **Equation 2.13**

where $c_{w,s}$ is the coefficient of water absorption due to capillary action; $m_{so,s}$ is the mass of the specimen in grams after soaking for time t (g); $m_{dry,s}$ is the mass of the specimen after drying (g); A_s is the gross area of the face of the specimen immersed in

water (mm^2) and t_{so} is the time for soaking (s). The graph of $\frac{m_{so,s} - m_{dry,s}}{A_s}$ is plotted against the square root of the time immersed, in seconds. $c_{w,s}$ is calculated as the gradient over the initial linear portion of the graph.

2.5.3.3 The initial rate of absorption (IRA) of the brick units

The initial rate of absorption (IRA) of the brick was found in accordance with EN 772-11 (2011). The following formula was used for its determination:

$$c_{w,i} = \frac{m_{so,s} - m_{dry,s}}{A_s t} \times 10^3 \; [kg/(m^2 \times min)] \qquad \textbf{Equation 2.14}$$

where, the time (t) is one minute.

2.5.3.4 Compressive strength of masonry units

The compressive strength of all masonry units was calculated as per EN 772-1 (2000). 6 specimens of each unit type were tested. The test faces of each of the stone unit samples were smoothened using a grinder/sander. The frogs of the brick units did not require capping with 3mm of capping mortar as per Section 7.2.5 in EN 772-1 (2000) because the net top load surface was greater than 35 % of the bed face. Strain gauges were attached to the faces of the specimens. Because of the presence of the strain gauges the specimens could not be conditioned by immersion however, section 7.3.2 EN 772-1 (2000) provides for such situations. Hence, test specimens were conditioned in the same laboratory environment at $\geq 15\,°C$ and relative humidity $\leq 65\,\%$ for a minimum of 14 days. The following formula was used to determine the compressive strength of the masonry units.

$$R_c = \frac{F_{c,max}}{A_i} \qquad \textbf{Equation 2.15}$$

where, $F_{c,max}$ is the maximum compressive force applied; A_i is the loaded cross-sectional area.

For design application, the compressive strength of masonry units must first be "normalized" (Chapter 8). In order to obtain the normalized compressive strength (f_b), the air-dried compressive strength of the masonry units are multiplied by a shape factor

given in EN 772-1 (2000). The shape factors applicable to the units in this research are all equal to 0.85.

2.5.3.5 Modulus of elasticity of masonry units

The modulus of elasticity of masonry units (E_c) was found from the linear portion of the stress-strain curve obtained during the compressive strength test. Equations 2.8, 2.9 and 2.10 were used. The displacement measurements were adjusted as per Section 2.4.3.

2.5.3.6 Flexural strength of masonry units

The flexural strength of the masonry units was determined in accordance with EN 12372 (2006). This standard for natural stone specifies a three point bending setup as in Figure 2.4 where 1 and 2 are the top and bottom loading rollers.

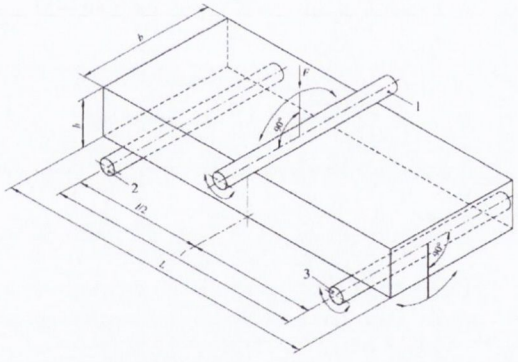

Figure 2.4 Arrangement of loading of test specimen EN 12372 (2006)

The surfaces of the unit specimens and rollers were cleaned and any loose grit or dirt was removed. The specimen is positioned centrally on the support rollers and roller 1 is cantered on the top face. The load (F_f) is applied uniformly at a rate of 0.25 $\pm$ 0.05 N until failure occurs. The machines internal loadcell and travelmeter recorded the applied force and the deflection of the specimen during the test. Equation 2.16 is used to calculate the flexural strength of the masonry units.

$$R_f = \frac{1.5 \times F_{f,max} \times l}{bh^2} \qquad \textbf{Equation 2.16}$$

where, $F_{f,max}$ is the load at failure (N); l is the distance between supports; b is the width of the specimen (mm) and h is the height of the specimen (mm).

2.5.4 Results of masonry unit tests

The properties of the masonry units are included in Table 2.3. Full calculations can be found in appendix H. As expected, the units provide a good range of physical properties. The bricks possess the highest porosity and are the most absorbent. They are also the most flexible and weakest in compression and flexion. The limestone behaves as expected, with high strength, stiffness and density and very low absorption values. The sandstone units were found to be much stronger and stiffer than the bricks, but not as strong or as stiff as the limestone. The sandstone has a relatively high absorption when compared to the limestone but as previously noted, the brick is significantly more absorbent than the limestone and sandstone both initially and over time.

Parameter measured	Brick		Sandstone		Limestone	
Unit size (mm)	215 x 102.5 x 65		≈ 250 x 110 x 65		Cut 215 x 102.5 x 65 Broken 100 x 100 x 65	
Apparent density (Kg/m^3)	1920		2325		2683	
Open porosity (%)	15		10.51		0.51	
Water absorption coefficient (stone only)	-		11.29 g/m^2/ s^{½}		0.2 g/m^2/ s^{½}	
Initial rate of absorption (brick only)	1 g/m^2/min		-		-	
Compressive strength (N/mm^2)	R_c	f_b	R_c	f_b	R_c	f_b
	15.02 {10}[a]	12.75	58.32 {8.31}	49.57	87.12 {5.87}	74.05
Flexural strength (N/mm^2)	R_f		R_f		R_f	
	2.63{4.33}		14.11{6.41}		18.60 {5.51}	
Modulus of Elasticity (N/mm^2)	E_c		E_c		E_c	
	1240 {7.52}		36,583 {10.27}		55,016 {7.83}	

[a] Values contained within { } refer to coefficient of variation (COV)

Table 2.3: Physical properties of masonry units

2.6 MASONRY PREPARATION AND TESTING

2.6.1 Masonry construction

Several masonry properties were selected for investigation; compressive strength, elastic modulus, flexural strength (both perpendicular and parallel to the bedding joints) and bond strength values (Table 2.4). These specific masonry properties were selected because they provide good overall information on the mechanical characteristics of masonry and because the results from these standard masonry tests can be compared with previous research on cement and cement-lime masonry. Each masonry test required a different size and a different number of masonry test wallettes. These were defined by the relevant standards and will be discussed in more detail in the subsequent sections.

The influence of unit type was studied by constructing masonry wallettes using four unit types (brick, broken sandstone and both cut and broken limestone). The effect of mortar binder and flow was investigated by using NHL, CL90-s and M6 mortars with two different workabilities (measured as initial flow). The influence of aggregate to binder ratio was investigated by varying the ratio of NHL 3.5 mortar from 0:1:3 to 0:1:2. The effect of external curing conditions was also studied because as previously discussed, little of no experimental data is available for outdoor cured lime-mortar masonry.

Lime and cement-lime mortar masonries develop strength over time. To examine this, masonry tests were carried out after 28 days, 56 days and 6 months of curing. A small series of testing was undertaken after 1 year. The 28 days test was chosen as it is a standard time to measure the properties of cement-lime masonry and thus enables comparison with previous research.

As aforementioned, due to their high IRA, the bricks were pre-wetted to approximately 80 % saturation prior to use. Stone masonry units were also pre-wetted however, this was more to reduce the effect of surface dust than that of suction. It should be noted that only the M6 cement mortar was mixed by volume to a ratio of 1:½:4 (v) (cement:lime;sand), all other mortars were mixed to specific ratios (0:1:3 and 0:1:2) by weight.

Unit type	Mix ratio	Flow (mm)	Binder	Curing	Tested Properties	Test dates
Brick	0:1:3	165 170	NHL 2, NHL 3.5 NHL 5 CL90-s	Lab	Compressive Strength Elastic Modulus Flexural strength (perpendicular to bedding joints) Flexural Strength (parallel to bedding joints) Bond Strength (Bond Wrench Test)	28 days 56 days 6 months 1 yr. (165 only)
Brick	1:½:4 (v)	165 170	M6	Lab	Compressive strength Elastic modulus Flexural strength (perpendicular to bedding joints) Flexural Strength (parallel to bedding joints) Bond Strength (Bond Wrench Test)	28 days 56 days 6 months
Brick	0:1:2	165	NHL3.5	Lab	Compressive Strength Elastic Modulus Flexural strength (perpendicular to bedding joints) Flexural Strength (parallel to bedding joints) Bond Strength (Bond Wrench Test)	28 days 56 days 6 months
Limestone (broken/ cut) Sandstone (broken)	0:1:3	165 170	NHL 2 CL90-s	Lab	Compressive Strength Elastic Modulus Bond Strength (Bond Wrench Test)	28 days 56 days 6 months
Brick	0:1:3	165 170	NHL2 CL90-s	Outdoor	Compressive Strength Elastic Modulus Bond Strength (Bond Wrench Test)	28 days 56 days 6 months
Brick	1:½:4 (v)	165 170	M6	Outdoor	Compressive Strength Elastic Modulus Bond Strength (Bond Wrench Test)	28 days 56 days 6 months

Table 2.4: Masonry testing schedule

2.6.2 Masonry curing

All masonry walls were cured in the same conditions as their corresponding mortar. Masonry wallettes and prisms were covered in damp hessian material and polythene to control moisture evaporation and excessive drying (which, might cause shrinkage, cracking or induced stresses in the wallettes) until sufficient strength was achieved to move the specimens.

NHL 5 and NHL 3.5 mortar wallettes were cured at relative humidity (r.h.) of 95±5 % and 20±2 °C temperature for 27 days, after which time they were either tested or placed into storage at 60±5 % r.h. and a temperature of 20±2 °C until tested. CL90-s mortar wallettes were cured at 60±5 % r.h. and a temperature of 20±2 °C until tested and M6 masonry was cured at 95±5 % r.h. and 20±2 °C temperature until tested.

In addition, mortars and masonry were exposed outdoors. An external storage area was sourced close to the Civil Engineering Building at Trinity College. The area was south facing and sheltered from harsh winds. Wallettes remained outdoors from September 2010 until March 2011, with temperatures ranging between -7 and 19 $°C$, with several rainy days and relative humidity ranging from 60-95 %.

Several freeze-thaw events occurred over the period, with the first taking place after 6 weeks of curing. Specimens were labelled and placed in the storage area once they had achieved sufficient strength to move. A heavy layer of wet hessian material was applied to all specimens and they were tested at 28 days, 56 days and 6 months.

2.6.3 Compressive strength of masonry

The compressive strength testing of the masonry wallettes was tested in accordance with EN 1052-1 (1999). Four lateral variable displacement transducers (L.V.D.Ts) were set-up on each wallette as shown in Figures 2.5 and 2.6 to record the strain values during compression on both sides of the test specimen. These were all connected to the data logger. The load was applied at a constant rate by the testing machine. The rate was adjusted so as to cause failure between 15 and 25 minutes as per above standard. The load was measured using a one hundred tonne load cell, which was connected to a data recorder and a computer. Three specimens were tested for each mortar type, unit type, flow, specimen age and curing condition.

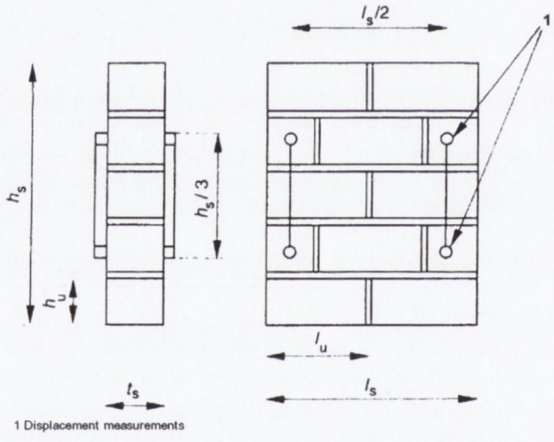

Figure 2.5: Masonry test setup BS EN 1052-1 (1999)

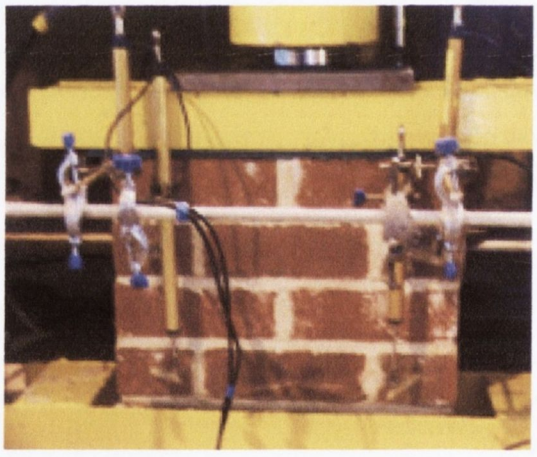

Figure 2.6 Picture of masonry test setup

Equation 2.17 was used to determine the compressive strength of each wallette:

$$f_i = \frac{F_{(i,\max)}}{A_i} \qquad \textbf{Equation 2.17}$$

where, f_i is the compressive strength of an individual masonry specimen (N/mm^2); $F_{i,max}$ is the maximum load reached on an individual masonry specimen (N); A_i is the loaded cross-section of and individual specimen (N/mm^2). The characteristic compressive strength was determined using Equation 2.18:

$$f_k = \frac{f}{1.2} \text{ or } f_k = f_{(i,min)} \text{ (N/mm}^2\text{), (whichever is smaller).} \qquad \textbf{Equation 2.18}$$

Adjustments were made to the specimen size referred to in EN 1052-1 (1999) for stone masonry. This was due to the weight of the material. Wallettes would have exceeded the safe lifting weight of 25 kg and would have required mechanical lifting, which was impractical in the tight laboratory environment. In addition, space was limited and curing chambers would not have been capable of withstanding such weights. It was decided to reduce the specimen size to one stone wide prisms. The height was kept the same at five units high. These stone masonry prisms were still quite heavy, but manageable. Due to limitations at the limestone quarry factory in Co. Kilkenny (see section 2.5.1) the unit dimensions of the broken limestone units were 100x100x100 mm. Constructing these units into five unit high prisms was impractical because the weight squeezed out fresh mortar in the lower joints and due to the risk of damage owing to specimen slenderness. Therefore it was decided that the broken limestone prisms should be three units in height.

Displacement measurements were then made by one lateral variable displacement transducer (LVDT), which measured the change in distance between the loading plates of the test machine. Displacement values were zeroed at the point when the specimen began carrying load as reported by the load cell and data logger. Strain was therefore a measure of the overall change in specimen height over the original specimen height.
Modulus of elasticity of masonry wallettes

As previously mentioned, EN 1052-1 (1999) recommends calculating the secant modulus of elasticity at one third the ultimate stress. Because of the non-linearity of the lime-masonry, it cannot be guaranteed that the point recommended will be in the linear portion of the stress-strain curve. Therefore, it was decided to calculate the modulus of elasticity of masonry (E_m) as the slope of the linear portion of the stress-strain curve obtained during the compressive strength test of the masonry wallettes. Equations 2.8, 2.9 and 2.10 were used. Strain values were calculated from the mean of the four displacement measurements (Figure 2.5). This was done to avoid the top and bottom of the prism where the testing surfaces of the machine would artificially confine the specimen. However, another problem arose whilst performing initial tests and analysing subsequent results. The average LVDT readings were not reliable due to the non-uniform strain distribution across the depth of the specimen. Other authors, Priestley

and Elder (1983) and Ewing and Kowalsky (2004) also experienced similar issues. Therefore, it was decided to add an additional LVDT to measure the overall change in the height of the wallette which was used to calculate the strain (figure 2.6).

2.6.4 Bond strength (bond wrench test)

Three masonry prisms were constructed for each mortar with 6 bricks per prism. Therefore a total of 15 joints were available for testing for each mortar. A minimum of ten test results is required by the standard EN 1052-5 (2005) to determine the mean bond strength. Pre-soaking of the masonry units prior to assembly was essential in order to reduce water loss from the mortar due to the absorbent masonry unit. Masonry units were immersed for three minutes.

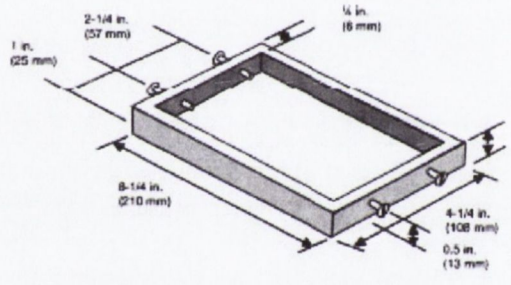

Figure 2.7 Schematic of mortar joint template.

During prism assembly, the first unit was placed on a plywood base slightly larger than the face of the unit. The pallet and the faces of the unit were aligned with levels in each direction. A mortar joint template (Figure 2.7) was also pre-wetted with a damp cloth prior to each use. This permitted its easy removal without disturbing the mortar. The template was placed on top of the masonry unit and filled with freshly prepared mortar. This template ensured a consistent mortar joint thickness of 12 mm before tamping. Excess mortar was struck off the template with a straight edge and the template was removed. The next masonry unit was immediately placed on top of the mortar bed and aligned vertically and horizontally with a spirit level. The brick was then tamped using a 1.0 kg hammer, dropped 6 times from a height of 40 mm as per the standard. The hammer was dropped so as to make contact with the brick at only one point. The hammer was dropped once at each corner of the unit and twice in the centre. After

tamping, excess mortar was struck off from the joints. This method of adding units to the prism was repeated until the prism reached 6 units.

The bond strength test set-up is shown in Figures 2.8 and 2.9. The masonry prism was placed in the test apparatus. It was levelled and positioned with the lower clamping device located in line with the middle of the second brick from the top. The prism was then clamped tightly in this position. While tightening this clamp, a level was used in order to ensure the prism was plumb. The upper clamping bracket was positioned on top of the prism so that the clamping bar was located vertically in line with the middle of the top brick. While tightening this clamp, the spirit level was again used to ensure that the clamping bracket remained horizontal. Care was taken when tightening the clamp on the top brick as the weakest bonded masonry could de-bond if jolted.

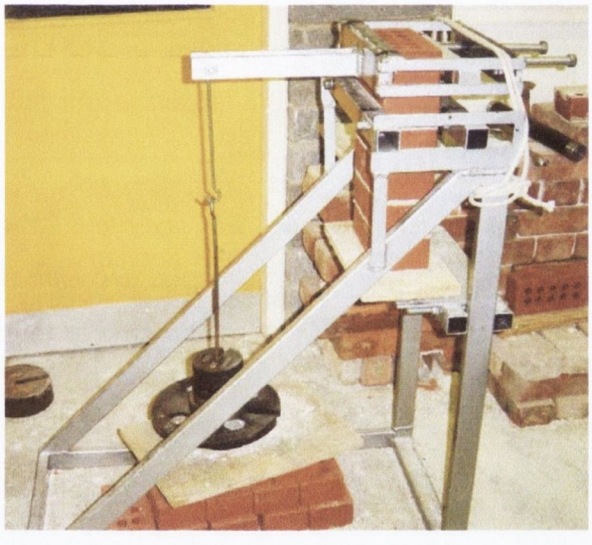

Figure 2.8: Bond wrench test apparatus and setup (Hanley 2006)

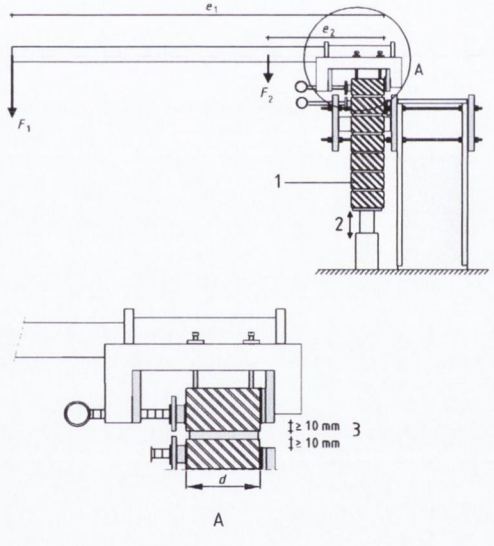

Figure 2.9: Schematic of bond wrench test set-up,
1 = specimen,
2 = adjustable height,
3 = enlargement area EN 1052-5 (2005).

After clamping the prism in position with the bracket, a bending moment is created in the unit-mortar joint by applying the load F_1 in Figure 2.9. The load is applied incrementally by adding weights to the extension arm attached to the loading arm. Weight was added slowly so as not to induce failure within the first minute. Depictions of failure modes encountered are presented in Section 4.3.

Once failure has taken place, the clamping brackets are loosened and the upper clamping bracket is removed. Without jolting, the prism was raised vertically and positioned within the apparatus in order to test the next mortar joint. The upper clamping bracket was reattached to the top brick and the test repeated. The flexural bond strength was calculated using the following equations:

$$f_{wi} = \frac{F_1 e_1 + F_2 e_2 - \frac{2}{3} d \left(F_1 + F_2 + \frac{W}{4}\right)}{Z} \quad \textbf{Equation 2.19}$$

$$Z = \frac{bd^2}{6} \quad \textbf{Equation 2.20}$$

where: b is the mean width of bed joint tested (mm); d is the mean depth of the specimen (mm); e_1 is the distance from the applied load to the tension face of the specimen (mm); e_2 is the distance from the centre of gravity of the lower and upper clamp from the tension face of the specimen (mm); F_1 is the applied load (N); F_2 is the weight of the bond wrench frame (N); W is the weight of the masonry unit pulled off the specimen and any adherent mortar.

The failure load was reported to the nearest kN and the mean flexural bond strength of ten joints (f_w) was then calculated to the nearest 0.1 N/mm^2. The characteristic flexural bond strength was calculated to the nearest 0.1 N/mm^2 using the following formula:

$$f_{wk} = antilog_{10}(Y_c) \quad \textbf{Equation 2.21}$$

$$Y_c = Y_{mean} - k.s \quad \textbf{Equation 2.22}$$

$$Y_i = log_{10} f_{wi} \quad \textbf{Equation 2.23}$$

$$Y_{mean} = \frac{\sum Y_{n-1}}{n} \quad \textbf{Equation 2.24}$$

where, s is the sample standard deviation of the n log values; k is 1.92 for 10 n; Y_i is $\log_{10}$ of the bond strength f_{wi}.

2.6.5 Flexural bond strength (parallel to and perpendicular to bedding joints)

The flexural strength was calculated for both planes of failure; parallel and perpendicular to the bed joints in accordance with EN 1052-2 (1999). Thus two different size masonry wallettes and two different testing rig set-ups were required. The standard EN 1052-2 (1999) specifies two set-ups depending on the unit size. The unit sizes used in this project were standard bricks 215x105x65 mm. Flexural bond strength specimens were constructed in accordance with Table 2, EN 1052-2 (1999). Due to the restricted laboratory manufacture, curing and storage space and the vast number of specimens required for this project, it was decided to use the smaller test set-up option.

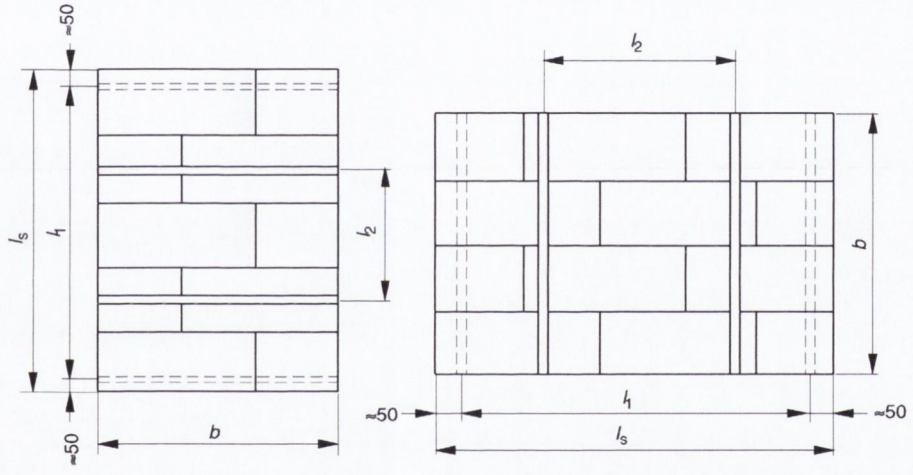

Figure 2.10: Flexural bond strength test setup parallel to and perpendicular to bedding joints (EN 1052–2 1999).

Five specimens were constructed for each mortar type and testing age. Each unit was conditioned prior to use by immersion in water for a period of three minutes. A joint template was used to consistently achieve the same joint size. A special joint template was constructed for the longer wallette, which contained in-built spirit levels in both horizontal x-y directions.

The masonry wallettes were constructed on a plywood base, which had a very small amount of shuttering oil applied to aid removal. A layer of mortar was placed on this and the first row of bricks laid, levelled and tamped. Vertical mortar joints were also kept consistent with the aid of a joint template. On completion of each wallette, a piece

of plywood was placed over the top and it was levelled and a weight applied so as to produce a uniformly distributed vertical stress on the specimen.

The curing of specimens was carried out as described in section 2.6.2. Wallettes were removed from the storage area and tested within one hour. Specimens were gently placed in the testing apparatus to avoid damage. The apparatus was constructed in such a way that both tests (parallel and perpendicular) could be performed. Changing between test set-ups only took ten minutes. The base of the specimens was insured to be free from frictional forces by placing two layers of polyurethane with grease between them and ball-bearing rollers under them.

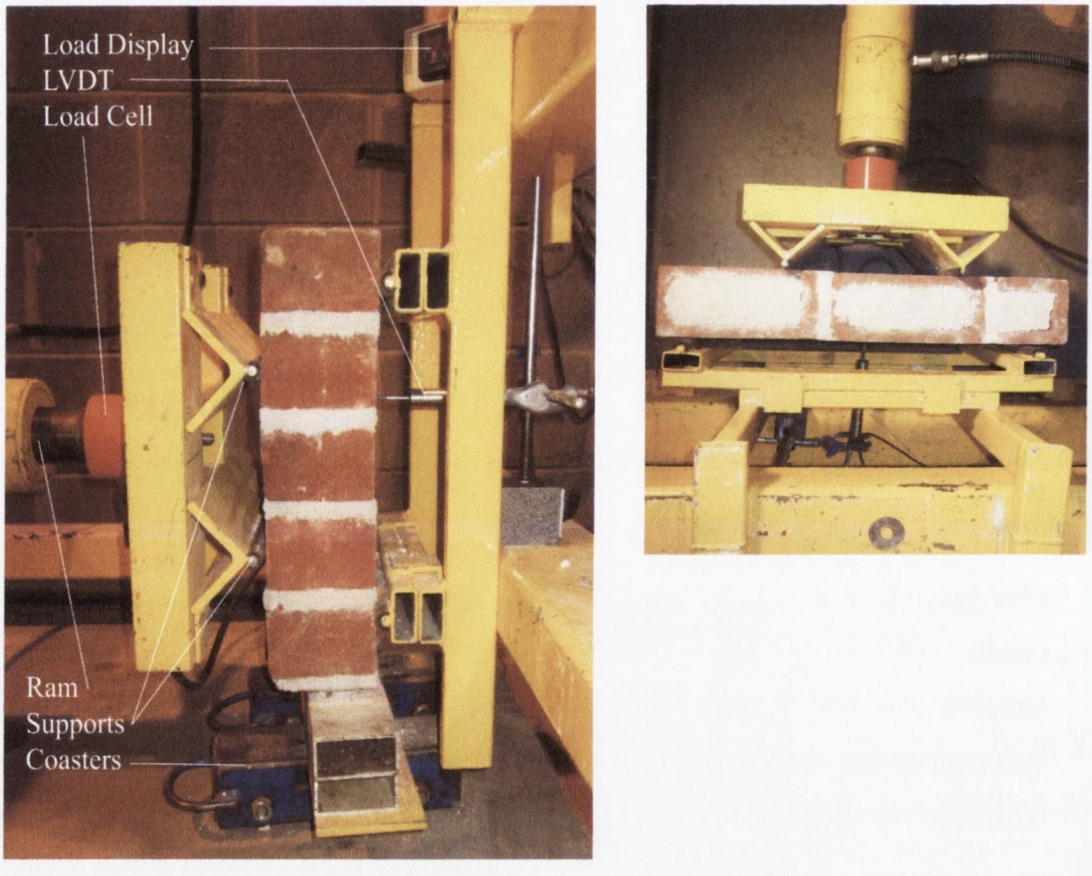

Figure 2.11: Picture of flexural bond strength set-up.
Left: parallel to bed joints. Right: perpendicular to bed joints.

A hydraulic jack connected to a small hand pump applied the load. The operator controlled the rate of load application, which was kept at a constant rate that would cause failure between five and ten minutes. The load was measured and recorded by a load-cell and data logger. An LVDT was placed behind the wallette and connected to the data logger to record the deflection at the centre due to the applied load. Equation 2.25 was used to calculate the flexural strength:

$$f_{xi} = \frac{3F_{i,\max}(l_1 - l_2)}{2bt_u^2} \qquad \textbf{Equation 2.25}$$

where, f_{ix} is the flexural strength of an individual masonry specimen (N/mm^2); $F_{i,max}$ is the maximum load reached on an individual masonry specimen (N); b is the height or width of a masonry specimen perpendicular to the direction of span, (mm); t_u is the width of a masonry unit (mm); l_1 and l_2 are the distance between outer and inner supports respectively (mm).

The characteristic flexural strength was calculated to the nearest 0.1 N/mm^2 from Equation 2.26.

$$f_{xk} = \frac{f_{mean}}{1.5} \qquad \textbf{Equation 2.26}$$

where, f_{mean} is the average of five specimen tests.

CHAPTER 3

MORTAR RESULTS AND DISCUSSION

3.1 PLASTIC STATE MORTAR RESULTS

3.1.1 Water demand, initial flow and workability

The specific amount of water required to produce the prescribed initial flows (165 and 170 mm) was determined for each mortar (Table 3.1). These initial flows (165 and 170 mm) provided adequate workability for all mortars. It should be noted that outside of these limits, the workability of the mortars was poor and either too stiff or too fluid for masonry construction. Figures 3.1 and 3.2 clearly show a relationship between water demand and hydraulicity. According to the results, at both flows, the water demand increases as hydraulic strength reduces; the non-hydraulic lime (CL90-s) requiring the greatest amount of water to achieve the prescribed flows.

Mortar Mix Id	Cement/ lime/sand	Cement	Lime	Sand	Water	Initial flow	COV	Water content	W:b[a] ratio
		(g)	(g)	(g)	(g)	(mm)	(%)	(%)	
NHL 5	0:1:3	0	4500	13500	2975	165	0.71	16.53	0.66
NHL 5	0:1:3	0	4500	13500	3150	170	1.28	17.50	0.70
NHL 3.5	0:1:3	0	4500	13500	3300	165	0.66	18.33	0.73
NHL 3.5	0:1:3	0	4500	13500	3400	170	1.01	18.89	0.76
NHL 2	0:1:3	0	4500	13500	3650	165	0.73	20.28	0.81
NHL 2	0:1:3	0	4500	13500	3890	170	0.90	21.61	0.86
CL90-s	0:1:3	0	4500	13500	4350	165	0.73	24.17	0.97
CL90-s	0:1:3	0	4500	13500	4500	170	0.88	25.00	1.00
NHL 3.5	0:1:2	0	6750	13500	3900	165	0.81	19.26	0.58
M6	1:½:4 (v)	2860	570	13840	2650	165	0.79	15.34	0.77
M6	1:½:4 (v)	2860	570	13840	2750	170	1.23	15.92	0.80

[a] W:b refers to water:binder ratio.

Table 3.1: Summary of water demand and mortar flow

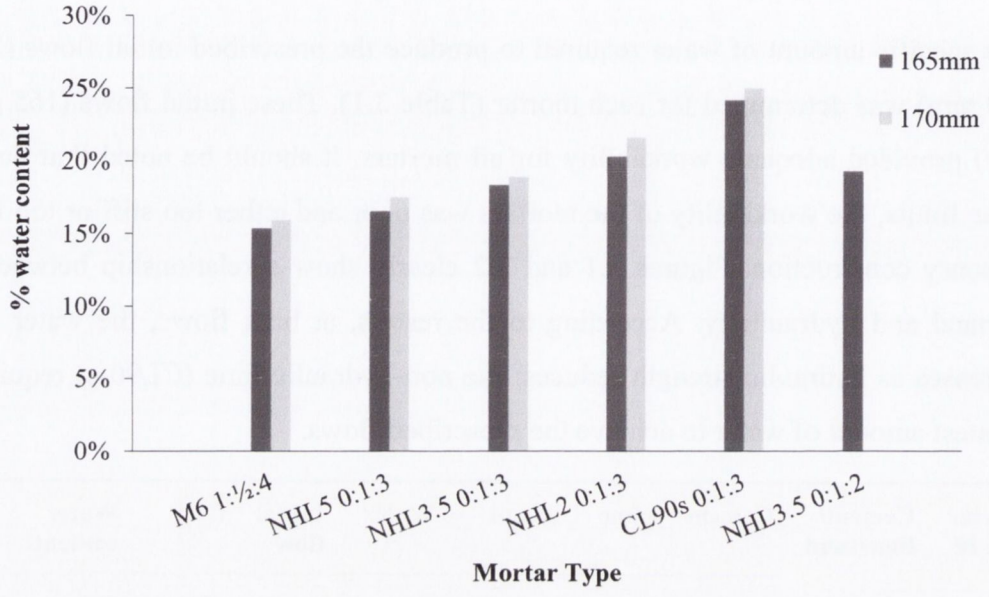

Figure 3.1: Water demand of mortars at two different flows

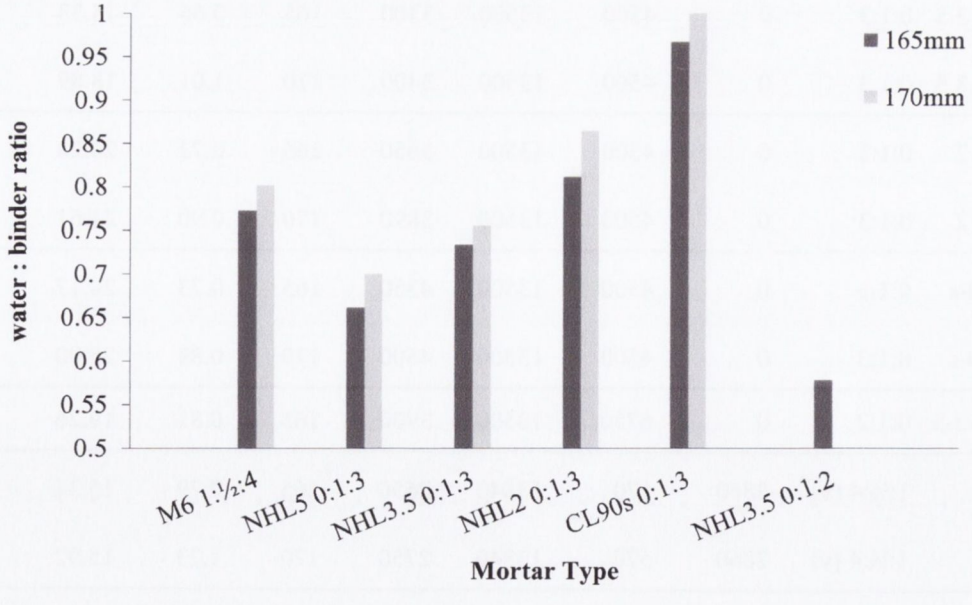

Figure 3.2: Water:binder ratio of mortars at two different flows

Mix Id	Mix ratio cement:lime:sand	Water content increase (%)	W:b increase (%)
NHL 5	0:1:3	0.97	6
NHL 3.5	0:1:3	0.56	3
NHL 2	0:1:3	1.33	7
CL90-s	0:1:3	0.83	3
M6	1:½:4 (v)	0.58	4

Table 3.2: Percentage increase in water content and water:binder ratio, for a 5 mm increase in initial flow

The CL90s mix has the greatest initial water demand however, it requires less additional water than most of the higher strength mixes in order to increase flow by 5mm.

According to the results obtained (Table 3.2), in general, a 3-7 % increase in water:binder ratio (i.e. a 0.6-1 % rise in water content) will increase the initial flow from 165 to 170 mm.

3.1.2 Statistical analysis of initial flow

European standard EN 459-2 (2010) provides guidance on initial flow value tolerances. These are given as $\pm$ 3 mm. Therefore, a 165 mm mortar can vary between 162 and 168 mm and a 170 mm mortar between 167 and 173 mm. Since such a large overlap is permitted by EN 459-2 (2010), statistical analysis on mortar initial flow testing was undertaken with the aim of: (a) establishing a statistical significant difference between mortars of different flows; and (b) demonstrating that a specific initial flow is consistent between batches. This statistical examination validates the comparison of testing results from mortars and masonry mixed to 165 and 170 mm initial flows.

Once the specific water contents required for each mortar to give either a 165 mm or 170 mm initial flow were found, three large batches of each mortar were mixed. Ten samples were then taken from each batch and the flow value was recorded for each sample as the average of three measurements of the flow diameter. It is important to note that initial flow testing was carried out directly after each mortar batch was mixed.

Statistical analysis tools assume that data is normally distributed. Therefore, prior to any variance analysis, the data was tested for normality. Two tests were used; the Shapiro-Wilk test (Shapiro and Wilk 1965) and the Kolmogorov-Smirnov test (Eadie *et al.* 1971). No evidence was found against normality for any of the data sets at a 5 % significance level.

T-tests were then carried out on the 10 samples of each individual batch to investigate if they differed significantly from their specific flow value (165 or 170 mm). After this, an analysis of variance (one-way ANOVA) was performed to ensure that there was no significant difference in flow value both within and between the three batches of a particular mortar. This analysis tool tests the hypothesis that the mean of two or more groups are equal. The ANOVA F–test (of the null-hypothesis that all treatments have exactly the same effect) is recommended as a practical test because of its robustness against many alternative distributions Moore and McCabe (2005).

Multiple analysis of variance (MANOVA) was then carried out to investigate whether there was any statistically significant difference between samples of a mortar with a 165 and a 170 mm initial flow. Flow testing and statistical analysis results are presented in

Appendix A. It was found, that in all cases, t-test P-values were much greater than 0.05. This indicates that, at 95 % confidence level, no statistically significant difference was found between the experimental flow values and the required flow values.

ANOVA analysis of each of the mortars at both flows found that the initial flow values were consistent between batches. MANOVA analysis indicated that there was a statistically significant difference between mortars with different specific flows. A visual representation of the flow data is summarised, for each mortar, in the flowing box plots in Figures 3.3-3.8. Box plots show the mean and interquartile range of each batch. The whisker lines denote the range of values obtained. Outliers are also noted.

In general, this analysis provides statistical evidence of consistency in the initial flow values both within and between mortar batches. Moreover, it also shows that there is a clear, statistically significant difference between mortars with initial flows of 165 and those with a 170 mm initial flow.

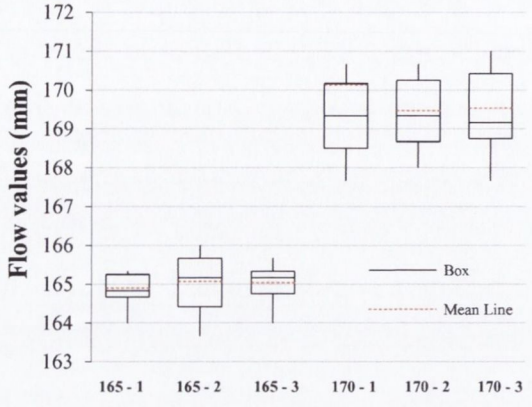

Figure 3.3:Box plot of NHL 5 mortar flows

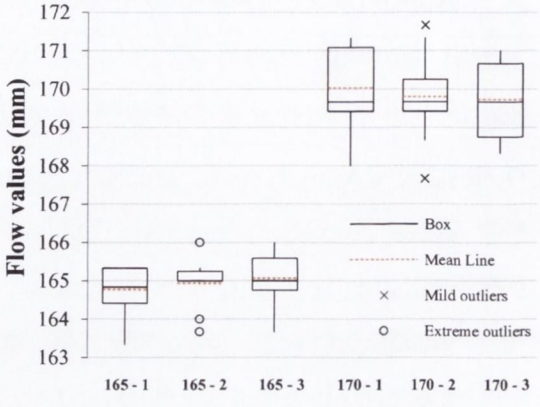

Figure 3.4: Box plot of NHL 3.5 mortar flows

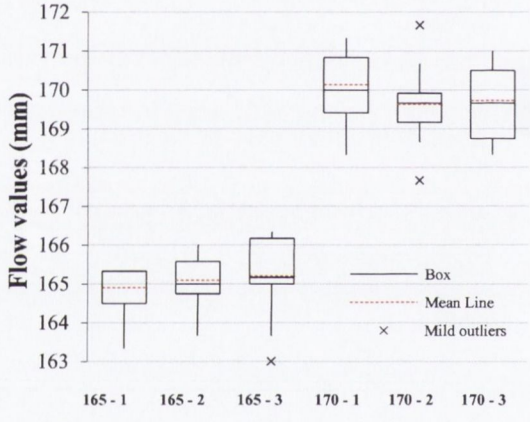

Figure 3.5: Box plot of NHL 2 mortar flows

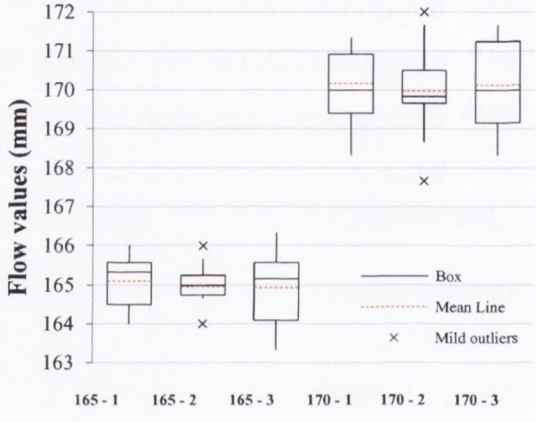

Figure 3.6: Box plot of CL90-s mortar flows

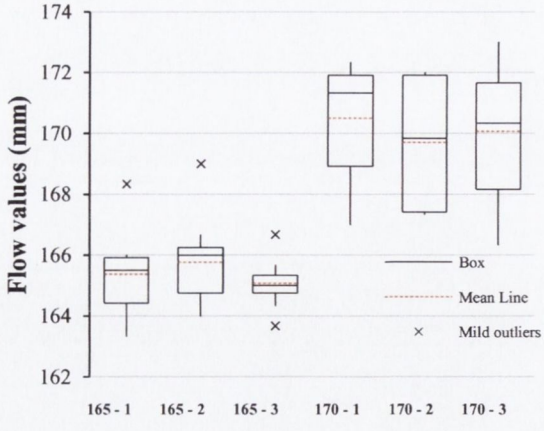

Figure 3.7: Box plot of mortar flows M6 at 1:½:4

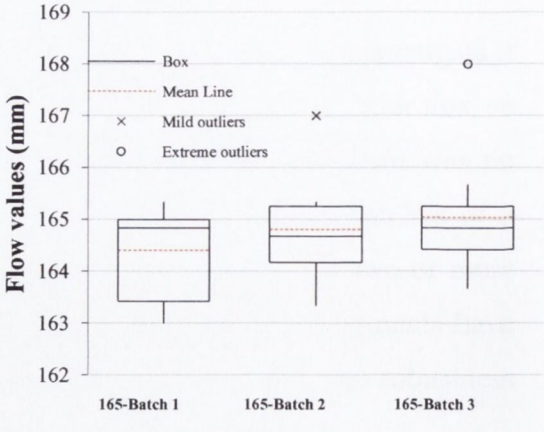

Figure 3.8: Box plot of mortar flows NHL 3.5 at 0:1:2

3.2 WATER RETENTION RESULTS

Water retention testing was carried out on all mortars as per Section 2.3.3. Calculations presented in Appendix B are summarised Table 3.3. Each value represents the mean of three individual batches. The coefficient of variation (COV) values are all relatively low indicating that the results are reliable. The results show that at both flows the water retention value (WRV) is inversely proportional to the hydraulicity of the lime mortar, i.e. the amount of free lime within the mortar. In this respect, the results agree with observations made by Pavía and Hanley (2010) and H. Schiffner (IKM Koln unpublished reports 2002-2006). CL90-s mortar displays the greatest capacity to retain water and cement-lime mortar (M6) the least. NHL 3.5 mortar with a mix ratio of 0:1:2 and an initial flow of 165 mm showed a water retention capacity similar to NHL 2 mortar with a mix ratio of 0:1:3 at the higher initial flow of 170 mm.

Mortar id	Mix ratio	165 mm initial flow		170 mm initial flow	
		Water retention (%)	COV (%)	Water retention (%)	COV (%)
M6	1:½:4 (v)	84.94 %	0.90	84.47 %	1.28
NHL 5	0:1:3	92.25 %	0.37	90.31 %	1.35
NHL 3.5	0:1:3	93.50 %	1.43	94.49 %	1.15
NHL 2	0:1:3	96.28 %	0.91	95.29 %	0.29
CL90-s	0:1:3	97.23 %	2.62	98.17 %	0.83
NHL 3.5	0:1:2	95.29 %	1.10	-	-

Table 3.3: Summary of mortar water retention test results

3.2.1 Influence of water content on mortar water retention

Table 3.4 summarises the water retention results calculated and presented in Appendix B. Increasing the initial flow value of the mortars from 165 to 170 mm only results in small variations in water retention values (WRV). M6, NHL 5 and NHL 2 mortars display a slight decrease in their water retention whilst NHL 3.5 and CL90-s mortars exhibit an increase of less than 1 %. According to Figure 3.9 and Table 3.4, the water retention of the cement-lime (M6) mortar is the least affected by changes in flow. The greatest change in WRV (-1.95 %) was associated with NHL 5 mortar.

Mix Id	Mix ratio cement:Lime:Sand	Relative change in water retention (%)
M6	1:½:4 (v)	-0.47 %
NHL 5	0:1:3	-1.95 %
NHL 3.5	0:1:3	0.99 %
NHL 2	0:1:3	-0.99 %
CL90-s	0:1:3	0.94 %

Table 3.4: Relative change in water retention due to an increase in the mortar flow

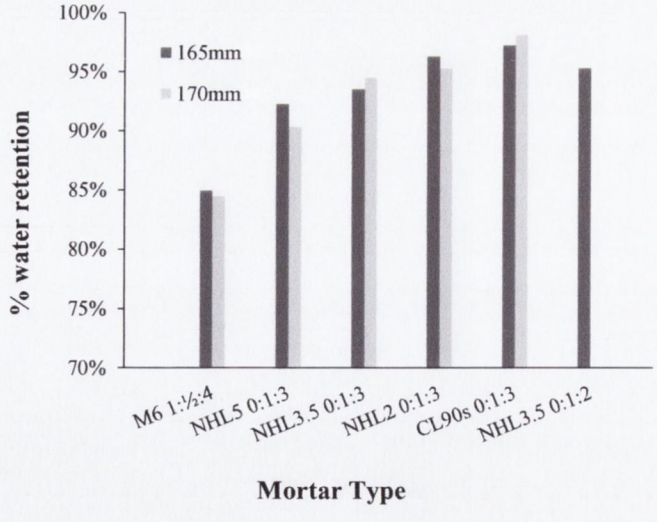

Figure 3.9: Water retention of mortars of different hydraulic strengths at two flows

The lack of research on the influence of water content on mortar's water retention was discussed in Chapter 1. The results in this research are comparable to those in Hanley (2006) as aggregate type, particle size, binder type and water content are similar (Figure 3.10). However, it should be noted that the mortar mix proportions tested by Hanley (2006) were 1:2.75 lime to sand ratio as compared to the 1:3 mix by mass used in the present study. Figure 3.10 demonstrates that, the water retention results obtained for natural hydraulic lime mortars in this research project are within the same range (90-98 %) of those by Hanley (2006) (RH). However, neither project displays a consistent trend with increasing flow. It should nevertheless be noted that the COV values for the water retention results are low, indicating substantial validity.

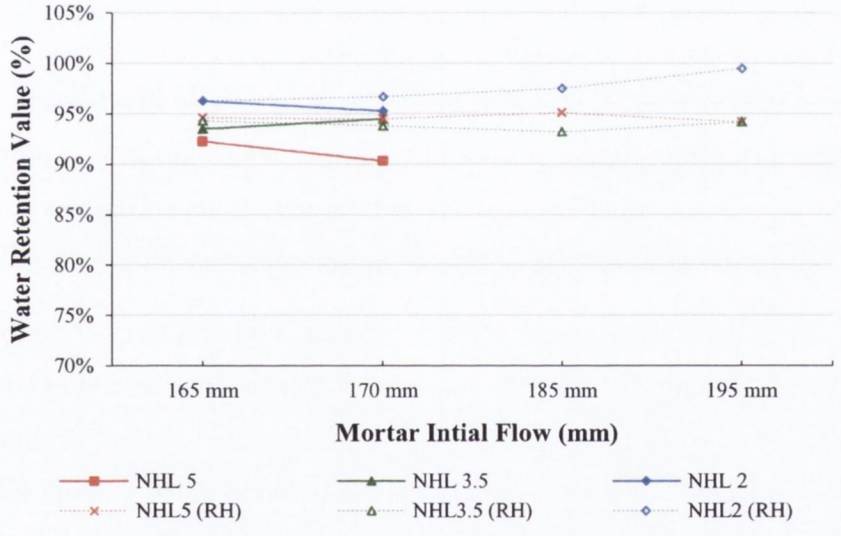

Figure 3.10: Comparison of NHL mortar water retention values with previous author, Hanley (2006) (RH values are estimated at 170 mm).

3.3 HARDENED STATE MORTAR RESULTS

Compressive, flexural strength and modulus of elasticity results are presented in Tables 3.5, 3.6 and 3.7 respectively. The values are a summary of the experimental data and calculations compiled in Appendices C and D, and are the mean of 3-6 specimens. Only laboratory-cured testing results are included in this chapter.

Coefficients of variation (COV) are also incorporated to provide information on the amount of variation for a particular mean value. Compressive strength results for each mortar were found to be greater than the minimum requirement of EN 459-2 (2010) (e.g. NHL 3.5 mortar should achieve in excess of 3.5 N/mm^2 after 28 days and it reached between 3.86 and 4.23 N/mm^2, Table 3.5).

Several high COV values were found, in particular some COV values for elastic modulus were in excess of 20 %. However, previous authors (Hanley (2006), Zhou *et al.* (2008) and Tate (2008)) reported similar findings with respect to lime mortar. These authors contend that the variability is due to the natural variability of lime as a material. Therefore, the high COVs found in the present study are not a cause for concern.

As expected, the mechanical properties of lime mortar (compressive strength, elastic modulus and flexural strength) generally increase with age, binder content and lime hydraulic strength. The results also indicate that the initial water content of lime mortar has a significant influence on its strength. This is discussed in further detail in Section 3.3.1.

As previously mentioned, EN 459-2 (2010) specifies strengths based on hydraulic grade. However, depending on water content, binder content and other factors, the strength of a particular mortar can be greater than that of a mortar including a higher hydraulic strength lime (i.e. a NHL 3.5 mortar can reach a compressive strength greater than 5 N/mm^2 and a NHL 2 mortar, a strength in excess of 3.5 N/mm^2). Nevertheless, within the flow range studied (165-170 mm), in most cases, no such overlap in strength or stiffness occurs between different hydraulic strength mortars as a result of the variation in water content (except for NHL 3.5 and 5 at 28 days). This lack of overlap was found even though varying the water content has a significant impact on a mortar's

mechanical properties and is demonstrated by comparing NHL 3.5 and 5 mortars at 56 days. The compressive strength of NHL 5 mortar varies between 6.33 and 7.02 N/mm^2, its flexural strength from 1.83 to 2.12 N/mm^2 and its elastic modulus from 501.05 to 525.15 N/mm^2, as a result of increasing water content. Whereas, the properties of NHL 3.5 mortar reach lower values, it's compressive strength ranges from 5.27 to 6.11 N/mm^2, its flexural strength from 0.71 to 0.98 N/mm^2 and its elasticity varies from 278.37 to 477.70 N/mm^2 (Tables 3.5, 3.6 and 3.7).

Similarly, no overlap in strength and stiffness due to changes in water content occurs between CL90-s and NHL 2 and between NHL 2 and NHL 3.5 (at 56 days). However, as aforementioned, an exception exists between NHL 3.5 and NHL 5 at 28 days where a large overlap exists. The compressive strength of both mortars is similar, however, the flexural strength and elastic modulus of NHL 5 mortar remain greater than those of NHL 3.5 (Tables 3.6 and 3.7). Therefore, NHL 3.5 can achieve a similar compressive strength as NHL 5 mortar during early curing (up to 28 days), while simultaneously remaining less stiff and more deformable.

With respect to mechanical properties, a clear pattern emerges whereby the mortars can be broadly broken down into three strength groups (Figures C.1, C.2 and D.1 in Appendices C and D). These groups appear to be independent of curing conditions or specimen age and consist of: cement-lime mortar, higher strength NHL mortars (3.5 and 5) and weaker mortars (CL90-s and NHL 2).

The strongest and stiffest mortar in all cases was found to be cement-lime (M6) mortar. Figures 3.11, 3.12 and 3.13 indicate that M6 mortars are over two times stronger and twice as stiff as NHL 5 mortars. According to the results, the M6 mortars (after 56 days) are stiffer than the brick units used in masonry construction (Table 2.2). Previous authors Sarangapani *et al.* (2005) suggest that the mechanical behaviour of the masonry is determined by the stiffness of the mortar with respect to the masonry unit. This is explored in more detail in Chapter 4.

Flow (mm)	Mortar type	Mix ratio	28 days (N/mm^2)	*COV (%)*	56 days (N/mm^2)	*COV (%)*	6 mts. (N/mm^2)	*COV (%)*	12 mts. (N/mm^2)	*COV (%)*
165	M6	1:½:4 (v)	11.22	*13.55*	18.00	*4.65*	22.20	*16.88*	23.03	*14.13*
	NHL 5	0:1:3	3.87	*2.77*	6.33	*3.46*	11.89	*4.21*	13.30	*2.28*
	NHL 3.5	0:1:3	3.86	*4.03*	5.27	*4.11*	8.95	*5.61*	10.00	*5.01*
	NHL 2	0:1:3	1.87	*8.32*	2.29	*3.76*	2.63	*13.09*	2.70	*6.10*
	CL90-s	0:1:3	0.62	*21.66*	0.89	*15.20*	1.39	*21.01*	1.40	*20.15*
	NHL 3.5	0:1:2	5.01	*27.36*	8.70	*10.52*	10.56	*4.40*	-	-
170	M6 @	1:½:4 (v)	14.28	*5.06*	19.23	*3.76*	21.45	*4.81*	-	-
	NHL 5	0:1:3	4.39	*2.21*	7.02	*5.41*	12.21	*2.04*	-	-
	NHL 3.5	0:1:3	4.23	*9.63*	6.11	*7.49*	9.30	*8.76*	-	-
	NHL 2	0:1:3	2.16	*6.23*	2.35	*1.49*	3.14	*12.58*	-	-
	CL90-s	0:1:3	1.29	*8.81*	1.52	*2.94*	2.00	*27.15*	-	-

Table 3.5: Compressive strength of mortars cured in the laboratory (also presented in Figure 3.11)

Flow (mm)	Mortar type	Mix ratio	28 days (N/mm^2)	*COV (%)*	56 days (N/mm^2)	*COV (%)*	6 mts. (N/mm^2)	*COV (%)*	12 mts. (N/mm^2)	*COV (%)*
165	M6	1:½:4 (v)	3.09	*4.31*	4.03	*9.73*	4.82	*9.76*	5.32	*5.19*
	NHL 5	0:1:3	1.20	*10.24*	1.83	*6.65*	2.53	*17.96*	2.88	*8.87*
	NHL 3.5	0:1:3	0.61	*12.38*	0.71	*9.24*	1.07	*36.06*	1.26	*8.36*
	NHL 2	0:1:3	0.32	*11.27*	0.37	*7.15*	0.48	*5.51*	0.57	*3.04*
	CL90-s	0:1:3	0.18	*10.18*	0.34	*1.79*	0.44	*12.65*	0.52	*3.33*
	NHL 3.5	0:1:2	1.24	*2.13*	1.96	*4.36*	2.49	*2.16*	-	-
170	M6	1:½:4 (v)	3.63	*7.46*	4.30	*23.73*	5.61	*4.92*	-	-
	NHL 5	0:1:3	1.26	*7.65*	2.12	*16.07*	2.83	*12.06*	-	-
	NHL 3.5	0:1:3	0.80	*6.61*	0.98	*5.40*	1.13	*15.66*	-	-
	NHL 2	0:1:3	0.23	*8.68*	0.34	*15.31*	0.40	*15.21*	-	-
	CL90-s	0:1:3	0.19	*7.86*	0.44	*7.12*	0.53	*4.99*	-	-

Table 3.6: Flexural strength of mortars cured in the laboratory (also presented in Figure 3.12)

Flow (mm)	Mortar type	Mix ratio	28 days (N/mm^2)	*COV* (%)	56 days (N/mm^2)	*COV* (%)	6 mts. (N/mm^2)	*COV* (%)	12 mts. (N/mm^2)	*COV* (%)
165	M6	1:½:4 (v)	926.45	5.86	1379.59	8.52	1586.95	15.01	1743.75	14.32
	NHL 5	0:1:3	277.65	10.81	501.05	15.22	660.70	23.52	683.25	17.82
	NHL 3.5	0:1:3	183.80	21.42	278.37	11.55	386.86	16.16	401.15	23.30
	NHL 2	0:1:3	129.75	6.81	187.05	6.15	165.35	7.61	197.20	13.07
	CL90-s	0:1:3	70.03	19.43	71.95	28.56	107.05	9.65	119.20	18.5
	NHL 3.5	0:1:2	320.40	15.19	556.65	23.42	811.50	13.58	-	-
170	M6 @	1:½:4 (v)	925.05	16.76	1352.25	12.57	1537.4	9.94	-	-
	NHL 5	0:1:3	307.00	16.15	525.15	6.07	693.48	18.80	-	-
	NHL 3.5	0:1:3	276.76	16.63	477.70	16.86	517.70	27.14	-	-
	NHL 2	0:1:3	114.85	31.84	146.25	11.03	161.90	3.39	-	-
	CL90-s	0:1:3	119.75	22.95	131.65	14.91	160.6	8.93	-	-

Table 3.7: Elastic modulus of mortars cured in the laboratory (also presented in Figure 3.13)

The following sections further investigate the mechanical behaviour of mortar, by isolating specific influencing factors. Firstly, the effect of water content is considered, and then an analysis of mechanical variations with age is carried out.

3.3.1 Influence of water content on mechanical properties of mortar

To gain a better understanding of the mechanical behaviour of lime mortars due to variations in water content, it is prudent to eliminate as many variables as possible. To this end, only controlled, laboratory-environment curing conditions are considered in this section. Two initial flows (165 and 170 mm) and three curing times (28 days, 56 days and 6 months) have been investigated for each mortar type.

In general, the results show that increasing the water content from 165 to 170 mm produces stronger, stiffer mortars.

Previous authors (Zhou *et al.* 2008) reported that variations in the water to binder ratio and thus the water content of hydraulic lime mortars did not overtly influence mortar compressive strength. However, the results in this research indicate that variations in water content have a significant effect on the compressive strength of all mortars. This

supports the findings of several authors (Allen *et al.* (2003); Hanley (2006); Arandigoyen and Alvarez (2007); Cosgrove and Pavía (2009)) who similarly concluded that water content significantly affects the compressive strength of mortar. Allen *et al.* (2003) and Tan (2003) noted that too much water renders a mortar unworkable (too fluid) and reduces its strength while, that too little water results in poor workability, insufficient moisture for the hydration process and thus reduced strength.

The influence of water content on the compressive strength of mortar shows a consistent trend for all mortars studied (Figure 3.11). All mortars display significant strength improvements due to the increase in flow. It is important to relate these changes in strength not only to the 5 mm increase in initial flow, but also to the percentage rise in water content required to increase the flow (measured in Section 3.1.1). This is included in Table 3.8 below.

Mortar Type	Mix Ratio	Relative increase in water content (%)
M6	1:½:4 (v)	0.58 %
NHL 5	0:1:3	0.97 %
NHL 3.5	0:1:3	0.56 %
NHL 2	0:1:3	1.33 %
CL90-s	0:1:3	0.8 3%

Same content as Table 3.2. Information is restated here for reader convenience

Table 3.8: Percentage increase in water content required to raise mortar flow from 165 to 170 mm

Table 3.9 provides an overall picture of the effect of increasing water content on the compressive strength of mortar. Green represents positive change and yellow is used when the change is less than or equal to 3%. Calcium lime mortar (CL90-s) displays the greatest percentage increase in compressive strength (from 0.62 to 1.29 N/mm^2), due to a 0.83 % rise in water content (Table 3.8). Even though there are large COV values (Table 3.5), CL90-s mortar shows a consistent trend. In addition, significant increases can be seen in both flexural strength and stiffness of CL90-s mortar as a result of increasing flow (Table 3.10 and 3.11).

The compressive and flexural strength of the cement-lime mortar (M6) improves by 27 % and 17 % respectively at 28 days (Table 3.9) as a result of a 0.58 % increase in water

content (Table 3.8). However, the stiffness of the cement-lime mortar does not appear to be significantly affected by variations in water content (Table 3.13).

Results for natural hydraulic lime mortars NHL 5 and 3.5 indicate gains in compressive strength of circa 10-13 %, in the first 28 days, resulting from a rise of less than 1 % in water content. Meanwhile, a 1.33 % increase in the water content of NHL 2 mortar leads to a significant 15 % improvement in compressive strength (Table 3.9).

The overall average influence of water content on compressive strength hydraulic lime mortars (a rise of 9-12 %) is consistent with observations made by Hanley (2006), where increasing the initial flow improves mortar strength. Hanley and Pavía (2007) reported an increase in the compressive strength of NHL 3.5 & 5 mortar (8-16 %), between 165 and 185 mm initial flow, which agrees with the present research.

With respect to all mortars, the influence of water content on the mortar's properties is greater during early curing and decreases over time (Tables 3.9-3.11). Increasing the water content of the mortars has a greater impact up to 56 days but this reduces over time, as hardening and stiffness develop. For example, the compressive strengths of NHL 3.5 and NHL 5 mortars increase by 10 % and 13 % respectively after 28 days, and by 11 % and 16 % after two months, but only by 3 and 4 % respectively after 6 months. Similarly, they display gains in stiffness of 51 % and 11 % at 28 days, which reduce to 34 % and 5 % at 6 months respectively.

The results demonstrate that gains in mortar compressive strength, due to water increases, are generally also accompanied by increases in flexural strength and stiffness (Tables 3.9-3.11). NHL 2 mortar is the only exception, increasing compressive strength but displaying losses in both flexural strength and elastic modulus. This does not agree with Hanley and Pavia (2007). These anomalous results coupled with the high COV values suggest some inconsistencies during testing of NHL 2 mortars.

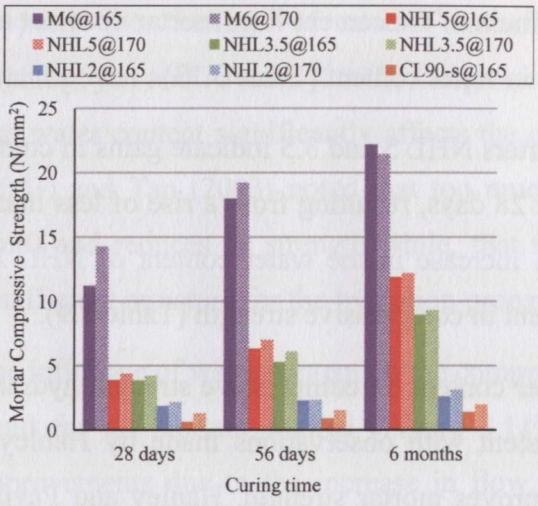

Figure 3.11: Effect of water content on the compressive strength of mortar

Mortar type	Mix ratio	Curing time			Avg.
		28 days	56 days	6 mts.	
M6	1:½:4^{v}	27 %	7 %	-3 %	10 %
NHL 5	0:1:3	13 %	11 %	3 %	9 %
NHL 3.5	0:1:3	10 %	16 %	4 %	10 %
NHL 2	0:1:3	15 %	3 %	19 %	12 %
CL90s	0:1:3	108 %	71 %	44 %	74 %

Table 3.9: Percentage change in the compressive strength of mortar due to the increase in initial flow

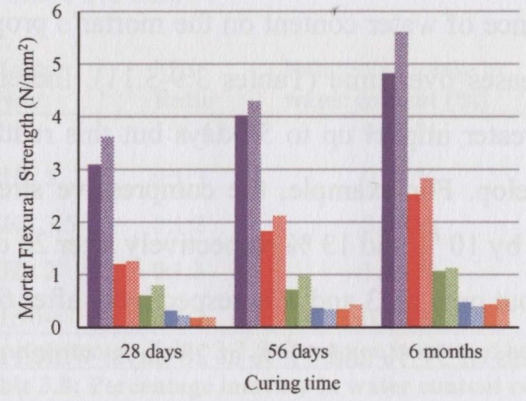

Figure 3.12: Effect of water content on the flexural strength of mortar

Mortar type	Mix ratio	Curing time			Avg.
		28 days	56 days	6 mts.	
M6	1:½:4^{v}	17 %	7 %	17 %	14 %
NHL 5	0:1:3	5 %	16 %	12 %	11 %
NHL 3.5	0:1:3	32 %	37 %	6 %	25 %
NHL 2	0:1:3	-27 %	-7 %	-17 %	-17 %
CL90s	0:1:3	6 %	27 %	21 %	18 %

Table 3.10: Percentage change in the flexural strength of mortar due to the increase in initial flow

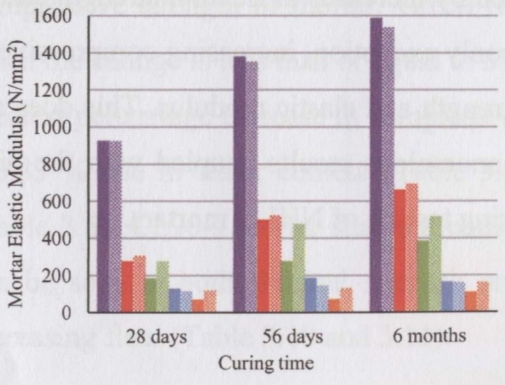

Figure 3.13: Effect of water content on the elastic modulus of mortar

Mortar type	Mix ratio	Curing time			Avg.
		28 days	56 days	6 mts.	
M6	1:½:4^{v}	0 %	-2 %	-3 %	-2 %
NHL 5	0:1:3	11 %	5 %	5 %	7 %
NHL 3.5	0:1:3	51 %	72 %	34 %	52 %
NHL 2	0:1:3	-11 %	-22 %	-2 %	17 %
CL90s	0:1:3	71 %	83 %	50 %	68 %

Table 3.11 Percentage change in the elastic modulus of mortar due to the increase in initial flow

3.3.2 Variations in mortar mechanical properties with curing age

In all cases, the compressive strength, flexural strength and elastic modulus of mortars cured in laboratory conditions increase with age (Figures 3.14-3.16). Strength development is due to both hydraulic set and the slower process of carbonation, which becomes more important as the hydraulicity of the mortar decreases.

The results show that the NHL 3.5 and 5 mortars develop compressive and flexural strength, and stiffness at a similar rate up to 28 days, after which NHL 5 performs significantly better. At 6 months, the compressive and flexural strength, and elastic modulus of NHL 5 mortar is approximately 30 % higher than that of the NHL 3.5 mortar. It should be noted that NHL 3.5 at a 2:1 Lime:Sand mix ratio and 165 mm flow generally performs similarly to NHL 5 mortars.

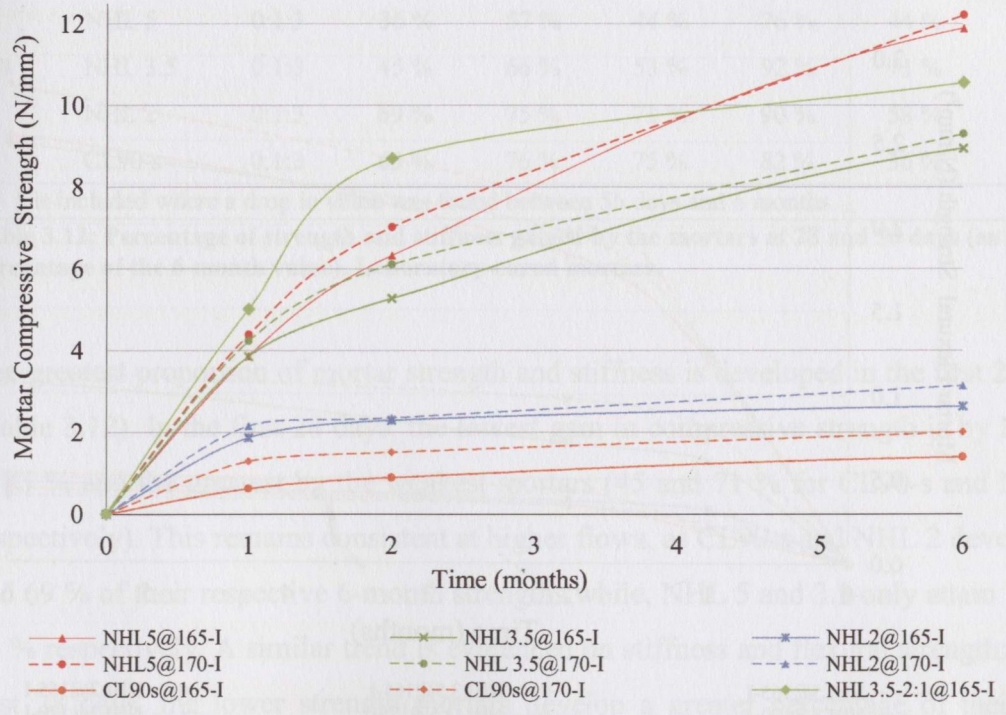

Figure 3.14: Compressive strength development of lime mortar over time

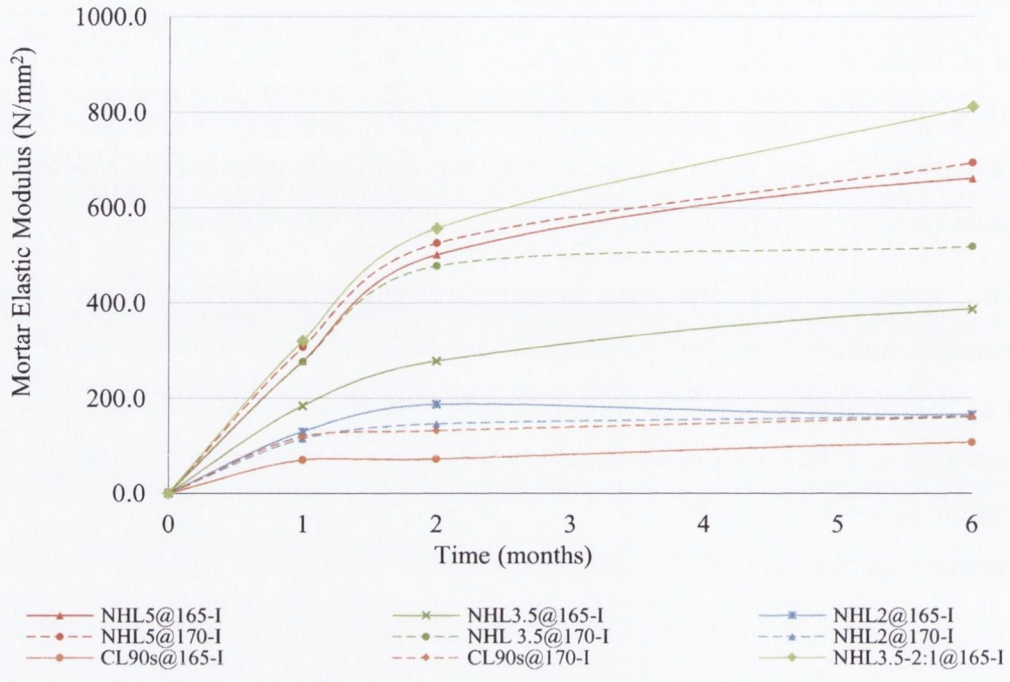

Figure 3.15: Modulus of elasticity development of lime mortar over time

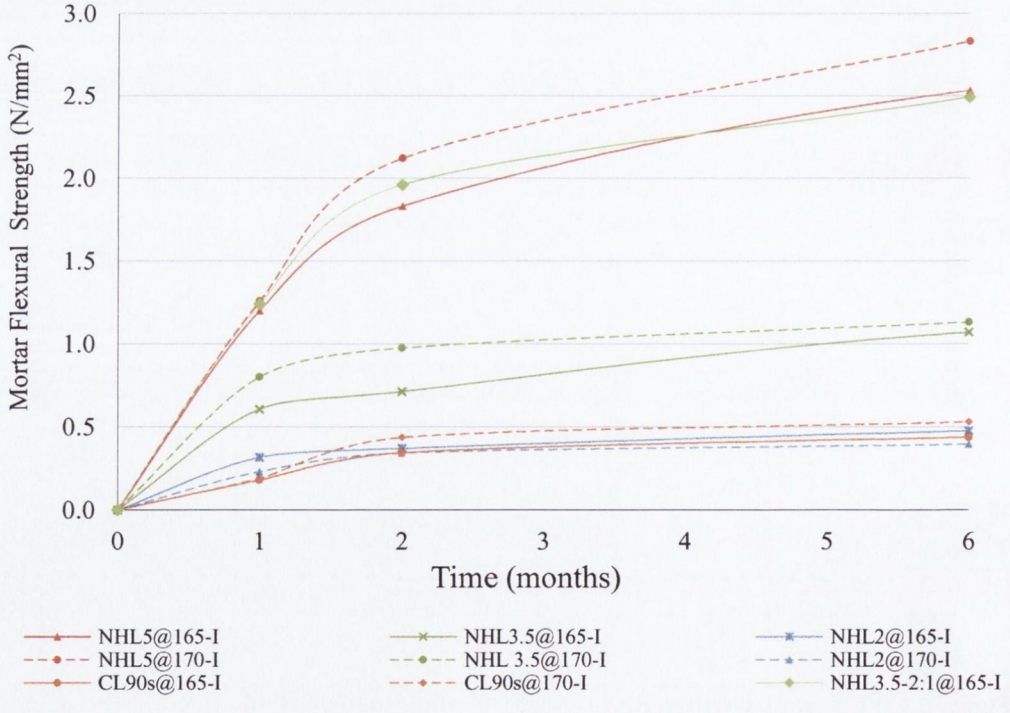

Figure 3.16: Flexural strength development of lime mortar over time

A considerable proportion of mortar strength and stiffness is achieved in the first 6 months of curing however, the mortar continues to gain significant strength and stiffness over time. The strength gains referred to in this section are presented as a percentage of 6-month results (Table 3.12) because comparable results are available for all tests carried out.

flow (mm)	Mortar type	Mix ratio	Percentage of 6-month results					
			Compressive strength (%)		Elastic modulus (%)		Flexural strength (%)	
			28 days	56 days	28 days	56 days	28 days	56 days
165	M6	1:½:4 (v)	51 %	81 %	58 %	87 %	64 %	84 %
	NHL 5	0:1:3	33 %	53 %	42 %	76 %	47 %	72 %
	NHL 3.5	0:1:3	43 %	59 %	48 %	72 %	57 %	67 %
	NHL 3.5	0:1:2	47 %	82 %	39 %	69 %	50 %	79 %
	NHL 2	0:1:3	71 %	87 %	78 %	{ - }[a]	67 %	78 %
	CL90-s	0:1:3	45 %	64 %	65 %	67 %	41 %	79 %
170	M6	1:½:4 (v)	67 %	90 %	60 %	88 %	65 %	77 %
	NHL 5	0:1:3	36 %	57 %	44 %	76 %	44 %	75 %
	NHL 3.5	0:1:3	45 %	66 %	53 %	92 %	71 %	86 %
	NHL 2	0:1:3	69 %	75 %	71 %	90 %	58 %	87 %
	CL90-s	0:1:3	65 %	76 %	75 %	82 %	36 %	82 %

[a]{ - } is included where a drop in value was found between 56 days and 6 months

Table 3.12: Percentage of strength and stiffness gained by the mortars at 28 and 56 days (as a percentage of the 6-month value). Laboratory-cured mortars.

The greatest proportion of mortar strength and stiffness is developed in the first 28 days (Table 3.12). In the first 28 days, the lowest gain in compressive strength is by NHL 5 at 33 % and the greatest by the weakest mortars (45 and 71 % for CL90-s and NHL 2 respectively). This remains consistent at higher flows, as CL90-s and NHL 2 develop 65 and 69 % of their respective 6-month strengths while, NHL 5 and 3.5 only attain 36 and 45 % respectively. A similar trend is evidenced on stiffness and flexural strength: in the first 28 days, the lower strength mortars develop a greater percentage of their total stiffness and flexural strength than the higher hydraulic strength ones (with the exception of the flexural strength of CL90-s). This is probably due to the water content

being too low slowing down hydration. The fact that the percentage strength gain by higher hydraulic strength mortars increases with the flow supports this observation.

According to the results (Table 3.12), when the flow is increased, the mortars gain a greater percentage of their ultimate strength and stiffness during early curing. As previously mentioned, increasing the water content of the mortars generally leads to increased strength and stiffness. Table 3.12 indicates that not only does the overall 6-month strength of the mortars increase, but also, a greater proportion of the compressive and flexural strength is achieved in the first 28 days. For instance, at 28 days, the compressive strength of NHL 5 (0:1:3) increases from 33 to 36 % and the flexural strength of NHL 3.5 (0:1:3) rises from 57 to 71 %, due to the increase in flow. The development of elastic modulus appears to follow a similar pattern with mortars gaining a greater percentage of ultimate stiffness during early curing, due to an increase in mortar flow. A consistent trend similar to compressive strength and elastic modulus cannot be seen for mortar flexural strength.

CHAPTER 4

BRICK MASONRY RESULTS AND DISCUSSION

Tables 4.1-4.4 constitute a concise summary of testing carried out on laboratory-cured brick-masonry specimens. Complete data results and calculations, including characteristic compressive and bond strengths can be found in Appendices E and F. Coefficients of variation (COV) are also included. Masonry compressive strength results generally show COV values under 10 % (Table 4.1) (CL90-s masonry is an exception, with several high COVs indicating some lack of reliability). However, COV's associated with modulus of elasticity, bond and flexural strengths vary considerably. This variability was expected, since masonry is a composite material constructed from naturally variable constituents. Previous authors (Sarangapani (2005); Hanley (2006); Pavía and Hanley (2007); Tate (2008) and Zhou *et al.* (2008)) experienced similar high COV values when studying the compressive strength and bond properties of lime and cement-lime mortared masonry. In the following sections, the results in Tables 4.1-4.4 are discussed with respect to water content and curing time.

Flow (mm)	Mortar type	Mix ratio	28 days (N/mm^2)	*COV (%)*	56 days (N/mm^2)	*COV (%)*	6 mts. (N/mm^2)	*COV (%)*	12 mts. (N/mm^2)	*COV (%)*
165	M6	1:½:4 (v)	6.90	*8.26*	7.72	*4.55*	9.74	*12.29*	-	-
	NHL 5	0:1:3	5.49	*7.11*	6.32	*14.29*	8.01	*6.30*	8.50	*8.85*
	NHL 3.5	0:1:3	5.07	*3.44*	5.89	*1.97*	7.71	*12.18*	8.90	*2.37*
	NHL 2	0:1:3	3.90	*3.53*	4.54	*13.40*	4.80	*8.44*	4.81	*8.18*
	CL90-s	0:1:3	0.89	*15.02*	1.53	*21.70*	3.94	*11.24*	4.30	*6.19*
	NHL 3.5	0:1:2	5.60	*7.33*	7.10	*3.17*	8.52	*0.71*	-	-
170	M6	1:½:4 (v)	6.90	*8.26*	7.53	*6.95*	10.63	*1.00*	-	-
	NHL 5	0:1:3	5.69	*7.90*	6.62	*4.77*	8.48	*19.02*	-	-
	NHL 3.5	0:1:3	5.52	*7.83*	6.41	*6.16*	8.46	*1.27*	-	-
	NHL 2	0:1:3	4.59	*14.30*	5.63	*4.20*	5.89	*3.45*	-	-
	CL90-s	0:1:3	0.88	*10.54*	2.62	*21.03*	3.34	*3.12*	-	-

Table 4.1: Compressive strength of masonry (also presented in Figure 4.1 and Table 4.6)

Flow (mm)	Mortar type	Mix ratio	28 days (N/mm^2)	*COV (%)*	56 days (N/mm^2)	*COV (%)*	6 mts. (N/mm^2)	*COV (%)*	12 mts. (N/mm^2)	*COV (%)*
165	M6	1:½:4 (v)	1435.74	*9.57*	1634.13	*5.73*	2270.10	*15.43*	-	-
	NHL 5	0:1:3	607.52	*12.07*	993.12	*11.37*	1409.04	*7.65*	1528.00	*3.81*
	NHL 3.5	0:1:3	384.68	*24.89*	567.96	*11.72*	841.96	*31.61*	970.00	*10.64*
	NHL 2	0:1:3	302.04	*9.01*	361.20	*17.22*	504.00	*15.43*	541.50	*24.43*
	CL90-s	0:1:3	196.00	*18.32*	244.00	*11.72*	295.86	*31.46*	317.48	*9.08*
	NHL 3.5	0:1:2	509.52	*15.86*	603.00	*7.63*	947.96	*6.87*	-	-
170	M6	1:½:4 (v)	1605.00	*35.68*	2036.70	*2.47*	2441.40	*15.21*	-	-
	NHL 5	0:1:3	670.00	*15.56*	1053.00	*6.16*	1440.00	*23.93*	-	-
	NHL 3.5	0:1:3	462.70	*23.96*	772.02	*14.65*	850.00	*22.10*	-	-
	NHL 2	0:1:3	323.34	*22.19*	430.11	*9.41*	537.60	*23.09*	-	-
	CL90-s	0:1:3	152.32	*25.59*	180.46	*7.05*	274.90	*31.86*	-	-

Table 4.2: Elastic modulus of masonry (also presented in Figure 4.2 and Table 4.7)

Flow (mm)	Mortar type	Mix ratio	28 days (N/mm^2)	*COV (%)*	56 days (N/mm^2)	*COV (%)*	6 mts. (N/mm^2)	*COV (%)*	12 mts. (N/mm^2)	*COV (%)*
165	M6	1:½:4 (v)	0.51	*21.98*	0.65	*24.22*	0.85	*27.21*	-	-
	NHL 5	0:1:3	0.211	*10.05*	0.28	*20.64*	0.4	*28.86*	0.48	*31.49*
	NHL 3.5	0:1:3	0.18	*28.76*	0.26	*16.64*	0.379	*31.11*	0.43	*28.13*
	NHL 2	0:1:3	0.11	*21.19*	0.15	*31.00*	0.19	*29.29*	0.2	*34.71*
	CL90-s	0:1:3	0.051	*41.70*	0.1	*19.77*	0.16	*26.63*	0.16	*27.73*
	NHL 3.5	0:1:2	0.32	*32.32*	0.37	*23.21*	0.415	*26.56*	-	-
170	M6	1:½:4	0.56	*22.05*	0.69	*14.55*	0.88	*14.20*	-	-
	NHL 5	0:1:3	0.28	*22.74*	0.383	*27.41*	0.434	*21.88*	-	-
	NHL 3.5	0:1:3	0.25	*25.49*	0.31	*30.60*	0.41	*29.54*	-	-
	NHL 2	0:1:3	0.13	*19.43*	0.2	*34.94*	0.21	*36.97*	-	-
	CL90-s	0:1:3	0.05	*26.10*	0.09	*19.58*	0.15	*33.13*	-	-

Table 4.3: Bond strength of masonry (also presented in Figure 4.3 and Table 4.8)

Flow (mm)	Mortar type	Mix ratio	28 days (N/mm^2)	*COV (%)*	56 days (N/mm^2)	*COV (%)*	6 mts. (N/mm^2)	*COV (%)*
165	M6	1:½:4 (v)	0.49	*12.79*	0.59	*5.99*	0.67	*10.33*
	NHL 5	0:1:3	0.22	*9.97*	0.32	*8.10*	0.43	*6.29*
	NHL 3.5	0:1:3	0.18	*8.83*	0.20	*7.62*	0.30	*6.75*
	NHL 2	0:1:3	0.08	*6.43*	0.14	*13.16*	0.19	*5.68*
	CL90-s	0:1:3	0.07	*26.76*	0.12	*13.03*	0.19	*4.81*
	NHL 3.5	0:1:2	0.30	*11.52*	0.39	*7.24*	0.45	*2.59*
170	M6	1:½:4 (v)	0.63	*7.13*	0.68	*12.54*	0.76	*8.02*
	NHL 5	0:1:3	0.24	*3.31*	0.35	*5.01*	0.51	*8.87*
	NHL 3.5	0:1:3	0.19	*4.81*	0.21	*4.60*	0.30	*5.63*
	NHL 2	0:1:3	0.09	*21.02*	0.18	*8.98*	0.21	*6.13*
	CL90-s	0:1:3	0.05	*15.43*	0.08	*8.93*	0.13	*10.83*

Table 4.4: Flexural strength of masonry (Type 1 - Parallel to bedding joints) Also presented in Figure 4.4 and Table 4.9

Flow (mm)	Mortar type	Mix ratio	28 days (N/mm^2)	*COV (%)*	56 days (N/mm^2)	*COV (%)*	6 mts. (N/mm^2)	*COV (%)*
165	M6	1:½:4 (v)	1.50	*2.95*	1.77	*2.62*	1.90	*2.78*
	NHL 5	0:1:3	1.05	*9.94*	1.18	*4.47*	1.32	*5.34*
	NHL 3.5	0:1:3	0.72	*6.21*	0.88	*6.76*	0.92	*3.96*
	NHL 2	0:1:3	0.45	*5.80*	0.47	*12.14*	0.57	*5.12*
	CL90-s	0:1:3	0.13	*12.04*	0.18	*6.25*	0.25	*16.00*
	NHL 3.5	0:1:2	0.87	*6.47*	1.32	*8.90*	1.43	*2.18*
170	M6	1:½:4 (v)	1.73	*3.22*	1.85	*14.90*	2.17	*3.01*
	NHL 5	0:1:3	1.08	*7.38*	1.23	*10.99*	1.54	*5.13*
	NHL 3.5	0:1:3	0.80	*8.55*	0.89	*7.17*	1.00	*13.08*
	NHL 2	0:1:3	0.46	*11.26*	0.56	*15.90*	0.61	*3.63*
	CL90-s	0:1:3	0.12	*11.26*	0.18	*15.90*	0.25	*3.63*

Table 4.5: Flexural strength of masonry (Type 2 - Perpendicular to bedding joints) Also presented in Figure 4.5 and Table 4.10.

4.1 INFLUENCE OF WATER CONTENT ON THE PROPERTIES OF BRICK MASONRY

The results indicate that varying mortar water content has a significant effect on the mechanical properties of brick masonry however, it affects stiffness, bond and flexural strength to a greater extent than compressive strength. With the exception of flexural strength, the variations of masonry properties as a result of increasing mortar water content, are significantly greater in the first two months of curing.

4.1.1 Compressive strength and elastic modulus

Increasing water content generally improves NHL mortar masonry strength and stiffness and lowers the strength and stiffness of CL mortar masonry. The results also show that the compressive strength of lime mortar masonry is more affected by changes in water content than that of cement-lime mortar masonry.

Increasing the mortar water content generally improves the performance of the cement-lime masonry. Although its early compressive strength does not appear to be significantly impacted by variations in flow (no change in compressive strength at 28 days and only a 2 % difference at 56 days), 6-month results indicate a 9 % improvement in strength (Table 4.6). There are also notable increases in cement-lime masonry stiffness, bond strength and flexural strength, due to increased flow (Tables 4.7-4.10).

According to the results, the compressive strength of NHL 5 masonry is only slightly greater (3-8 %) than that of NHL 3.5 masonry at both flows (over time) however, the NHL 5 masonry is significantly (over 30 %) stiffer than the NHL 3.5 masonry at all times and water contents.

The results also indicate that NHL 3.5 masonry, at the higher flow of 170 mm, is slightly stronger than NHL 5 masonry at a lower flow (165 mm). At 28 days, the compressive strength of NHL 3.5 at 170 mm initial flow is 5.52 N/mm^2 whereas that of NHL 5 at 165 mm is only 5.49 N/mm^2 (Figure 4.1). The results at 56 days and 6 months suggest that this trend remains consistent over time. These trends are not observed when other masonry types are compared.

As previously mentioned, a rise in compressive strength is experienced by NHL mortar masonry when the mortar's water content is raised. However, contrary to expectations, the rise becomes smaller as the hydraulic strength of the mortar increases (in terms of percentage change). For example, at 28 days, the compressive strength of NHL 2 masonry increases by 18 %, NHL 3.5 by 9 % and NHL 5 by only 4 % (Table 4.6). This inverse relationship remains consistent over time.

The results also demonstrate that water content has an effect on masonry stiffness. Masonry stiffness is an important property as it determines the masonry's ability to deform and accommodate movement. Table 4.7 indicates that the stiffness of cement-lime masonry is very sensitive to small changes in water content: a 0.58 % water rise (Table 3.8) results in a 12 % gain in masonry stiffness at 28 days and a 25 % increase at 56 days. NHL mortar masonry also displays significant improvements in elastic modulus (19-36 %) whereas, CL mortar masonry experiences a considerable drop (26 %) in stiffness due to a rise in flow.

Masonry stiffness is more sensitive to changes in mortar water content during early curing. For example, improvements in masonry stiffness are greater throughout the first 56 days of curing: NHL 5 and NHL 3.5 masonry gain 10 and 20 % respectively at 28 days however, by 6 months, the increase in stiffness is barely evident at 2 and 1 % (Figure 4.2 and Table 4.7)

4.1.2 Bond and flexural strength

Masonry types which gain compressive strength and elastic modulus with increasing mortar water content, also exhibit improved bond and flexural strength, while a reduction in compressive strength and elastic modulus is coupled to a reduction in bond and flexural strength.

The bond strengths of natural hydraulic lime and cement-lime masonry increase significantly with additional water content however, CL90-s masonry is negatively affected (Figure 4.3). NHL 5 and NHL 3.5 masonry display the greatest response at 28 days, gaining bond strength by 33 and 39 % respectively (Table 4.8), while CL90-s masonry shows a consistent drop in bond strength of 2-10 % over time.

Similarly to compressive strength and stiffness, masonry bond is more sensitive to changes in mortar water content during early curing (Table 4.8).

Given a constant flow, the bond strength of natural hydraulic lime masonry has been shown to generally rise with mortar hydraulicity. However, when the water content is varied within a range providing good workability (165-170 mm initial flow), some overlap occurs between the bond strengths of NHL 3.5 and NHL 5 masonry. The NHL 3.5 masonry at the higher flow possesses superior bond strength than the NHL 5 masonry at a lower flow. For example: at 56 days, the bond strength of NHL 3.5 masonry with an initial flow of 170 mm is 0.31 N/mm^2 which is 10 % greater than that of NHL 5 masonry (0.28 N/mm^2) at a lower flow (Figure 4.3). This relationship is maintained at all curing times and is consistent with observations previously made for masonry strength and stiffness. In contrast, no overlap is evident between the bond strengths of NHL 2 and NHL 3.5 or between NHL 2 and CL90-s.

The results indicate that the influence of water content on the flexural strength of masonry (both parallel and perpendicular to bedding joints) is comparable to the effect which increased water content has on bond and compressive strength: cement-lime and NHL mortar masonry generally improve while CL mortar masonry is adversely affected (Tables 4.9 and 4.10) and (Figures 4.4 and 4.5).

As expected, the flexural strength of masonry is greater when the load is applied perpendicular to the bedding joints as, in this case, the friction within the contra rotation portions of the masonry works together with the strength of the bond towards resisting the load applied (Hughes and Taylor 2005).

In contrast to bond and compressive strength results, no overlap in flexural strength, due to increased flow was found between masonry of different hydraulic strengths (NHL 3.5 and 5). Both flexural tests generally show a strength increase with increasing hydraulic strength, which agrees with compressive, bond and E modulus results (once flow is constant).

Furthermore, the flexural strength of masonry tends to be more sensitive to variations in water content during early curing (up to 56 days) (Tables 4.9 and 4.10). This is

consistent with previous observations for bond and compressive strength. This is important as it indicates that mortar flow can be increased within the workable range (165-170 mm) to improve early strength, bond and stiffness development. The rate of building can therefore increase, without adversely affecting the long-term strength, stiffness and durability of the masonry.

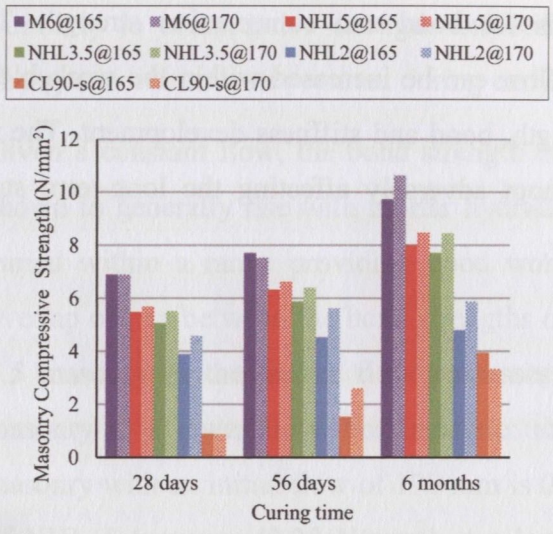

Figure 4.1: Effect of water increase on the compressive strength of masonry

Mortar type	Mix ratio	Curing time			
		28 days	56 days	6 mts.	Avg.
M6	1:½:4^{v}	0 %	-2 %	9 %	2 %
NHL 5	0:1:3	4 %	5 %	6 %	5 %
NHL 3.5	0:1:3	9 %	9 %	10 %	9 %
NHL 2	0:1:3	18 %	24 %	23 %	22 %
CL90s	0:1:3	-1 %	71 %	-15 %	18 %

Table 4.6: Percentage change in the compressive strength of masonry due to the increase in initial flow

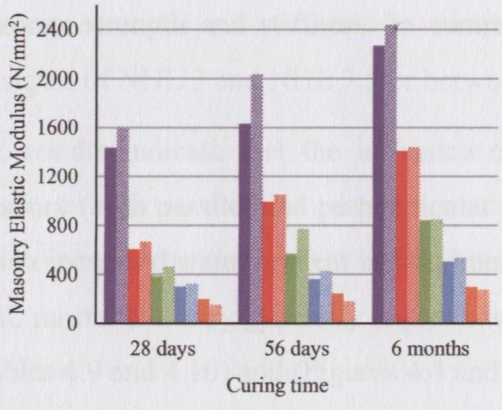

Figure 4.2: Effect of water increase on the elastic modulus of masonry

Mortar type	Mix ratio	Curing time			
		28 days	56 days	6 mts.	Avg.
M6	1:½:4^{v}	12 %	25 %	8 %	15 %
NHL 5	0:1:3	10 %	6 %	2 %	6 %
NHL 3.5	0:1:3	20 %	36 %	1 %	19 %
NHL 2	0:1:3	7 %	19 %	7 %	11 %
CL90s	0:1:3	-22 %	-26 %	-7 %	-18 %

Table 4.7: Percentage change in the elastic modulus of masonry due to the increase in initial flow

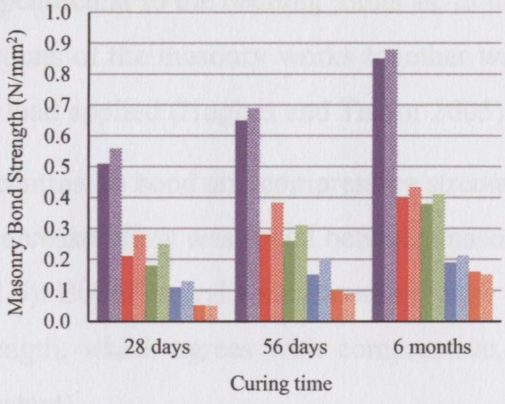

Figure 4.3: Effect of water increase on the bond strength of masonry

Mortar type	Mix ratio	Curing time			
		28 days	56 days	6 mts.	Avg.
M6	1:½:4^{v}	10 %	6 %	4 %	7 %
NHL 5	0:1:3	33 %	37 %	8 %	26 %
NHL 3.5	0:1:3	39 %	19 %	8 %	22 %
NHL 2	0:1:3	18 %	33 %	12 %	21 %
CL90s	0:1:3	-2 %	-10 %	-6 %	-6 %

Table 4.8: Percentage change in the bond strength of masonry due to the increase in initial flow

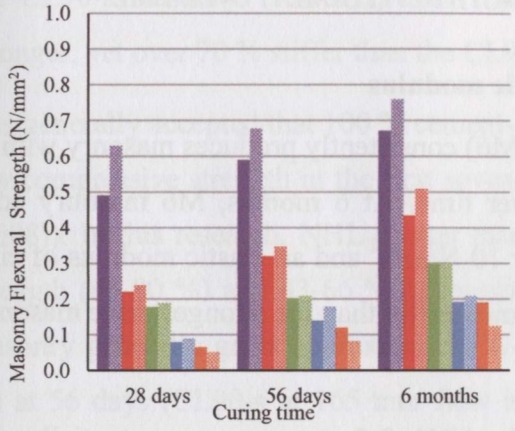

Figure 4.4: Effect of water increase on the flexural strength of masonry (Type 1 - parallel to bedding joints)

Mortar type	Mix ratio	Curing time			
		28 days	56 days	6 mts.	Avg.
M6	1:½:4^{v}	28 %	15 %	13 %	19 %
NHL 5	0:1:3	9 %	9 %	18 %	12 %
NHL 3.5	0:1:3	7 %	4 %	0 %	4 %
NHL 2	0:1:3	13 %	29 %	9 %	17 %
CL90s	0:1:3	-18 %	-31 %	-34 %	-28 %

Table 4.9: Percentage change in the flexural strength of masonry due to the increase in initial flow (Type 1 - parallel to bedding joints)

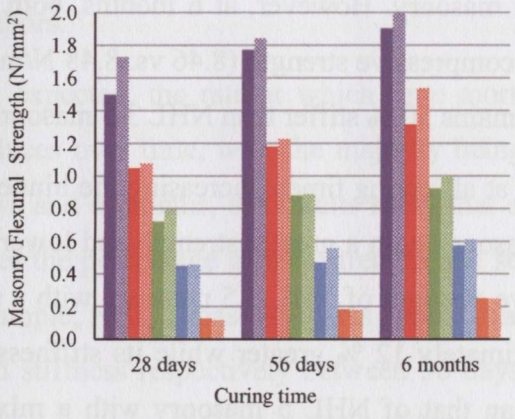

Figure 4.5: Effect of water increase on the flexural strength of masonry (Type 2 - perpendicular to bedding joints)

Mortar type	Mix ratio	Curing time			
		28 days	56 days	6 mts.	Avg.
M6	1:½:4^{v}	16 %	4 %	14 %	11 %
NHL 5	0:1:3	3 %	4 %	17 %	8 %
NHL 3.5	0:1:3	10 %	1 %	9 %	7 %
NHL 2	0:1:3	2 %	19 %	7 %	9 %
CL90s	0:1:3	-6 %	0 %	0 %	2 %

Table 4.10: Percentage change in the flexural strength of masonry due to the increase in initial flow (Type 2 - perpendicular to bedding joints)

4.2 ANALYSIS OF BRICK MASONRY STRENGTH DEVELOPMENT OVER TIME

4.2.1 Compressive strength and elastic modulus

As expected, the cement-lime mortar (M6) consistently produces masonry with superior compressive strength and stiffness over time. At 6 months, M6 masonry achieves a compressive strength of approximately 10 N/mm^2 and an elastic modulus of circa 2300 N/mm^2, being 22 % stronger and 1.5 times stiffer than the strongest lime masonry (NHL 5) (Figures 4.6 and 4.7).

Over time (greater than 6 months), the NHL 3.5 masonry can potentially provide a comparable compressive strength yet a greater flexibility than the NHL 5 masonry. As previously mentioned, at both 28 and 56 days, NHL 5 masonry is 3-8 % stronger and more than 30 % stiffer than NHL 3.5 masonry. However, at 6 months, both masonry types achieve approximately the same compressive strength (8.46 vs. 8.48 N/mm^2 at the higher flow), while NHL 5 masonry remains 30 % stiffer than NHL 3.5 masonry.

Furthermore, the results evidence that at all curing times, increasing the binder content of a NHL 3.5 mortar can provide a masonry with a greater strength and lower stiffness than a NHL 5 mortar. The compressive strength of NHL 3.5 masonry with a mix ratio of 0:1:2 (cement:lime:sand) is approximately 12 % greater while its stiffness remains significantly lower (circa16-33 %) than that of NHL 5 masonry with a mix ratio of (0:1:3).

At all curing times, NHL 3.5 masonry remains stronger than the NHL 2 masonry. Additionally, NHL 3.5 masonry gains strength and stiffness at a much faster rate than NHL 2 masonry (between 56 days and 6 months) thus becoming increasingly stronger and stiffer than the NHL 2 masonry over time. For example: at 56 days, NHL 3.5 masonry with a flow of 165 mm is only 5 % stronger than NHL 2 masonry at the higher flow, yet by 6 months the NHL 3.5 masonry is 30 % stronger. A similar pattern can be seen for the elastic modulus of the two masonries (Figures 4.6 and 4.7).

As expected, CL mortar masonry develops strength and stiffness at a much slower rate than NHL mortar brickwork. The results show that, during early curing, the NHL 2 masonry develops compressive strength and stiffness at a significantly faster rate than

the CL90-s masonry. However, after 6 months, the NHL 2 masonry is only 20 % stronger, yet over 70 % stiffer than the CL90-s masonry (Figures 4.6 and 4.7).

It is generally accepted that 100 % cement-mortar masonry develops two thirds of its 28 day compressive strength in the first seven days of curing (Tate (2008) and Zhou *et al.* (2008)). In this research, NHL mortar masonry gains approximately ⅔ of its 6 month strength (65-80 %) and 43-66 % of its elastic modulus at 28 days and CL90-s mortar masonry generally gains approximately ⅔ of its 6-month strength and stiffness (60-80 %) at 56 days (CL90-s at 165 mm flow is an exception) (Table 4.11). Therefore, the results suggest that the percentage of 6-month compressive strength gained by NHL mortar masonry at 28 days and CL90-s masonry at 56 days is equivalent to percentage pure cement mortar masonry's 28-day strength gained at 7 days, agreeing with previous authors.

As expected, the rate at which lime mortar masonry develops strength and stiffness reduces over time, with the majority being achieved in the first 28 days. Between 56 days and 6 months, the results show that as the mortar hydraulic strength increases so does the percentage gain in strength and stiffness of masonry at later curing times. For example, NHL 5 masonry gains approximately 28 % and 40 % in compressive strength and stiffness respectively between 56 days and 6 months compared to NHL 2, which only increases by approximately 5 % and 25 % respectively over the same time period (Figure 4.6 and 4.7).

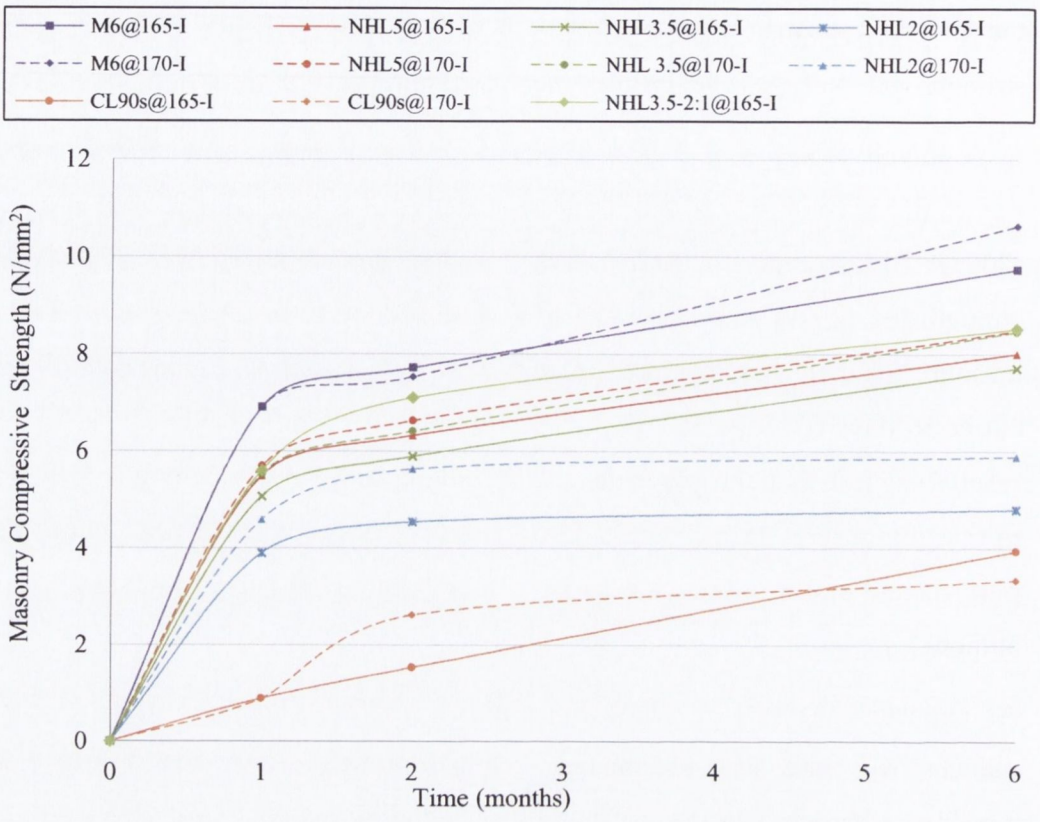

Figure 4.6: Compressive strength development of brick masonry over time

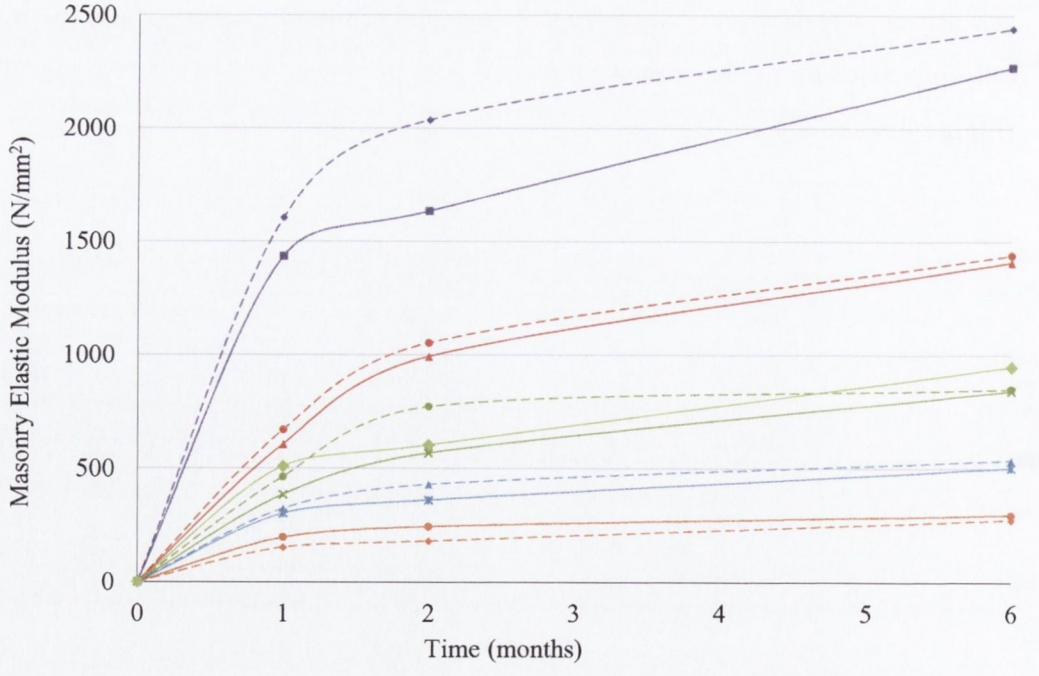

Figure 4.7: Modulus of elasticity development of brick masonry over time

4.2.2 Bond and flexural strength

Lime mortars develop most of their 6-month bond strength during the first two months of curing however, cement-lime mortars keep increasing bond strength significantly after 2 months (Figure 4.8). Table 4.11 illustrates how NHL mortar masonry gains a significant proportion of its 6-month bond strength during the first 28 days of curing (47-71 %). The results also indicate that, after 56 days, NHL mortar masonry has achieved 70-94 % of its 6-month bond strength. Calcium lime mortar has no hydraulic properties and therefore develops bond strength at a different rate. According to Table 4.11, CL90-s masonry only gains approximately 33 % of its 6-month bond strength by 28 days and circa 60 % after 56 days.

Cement-lime mortar (M6) provides a significantly greater bond strength than the lime mortars studied, developing bond strengths of between 0.85-0.88 N/mm^2 at 6 months, (over twice as strong as the nearest natural hydraulic lime masonry) (Table 4.3 and Figure 4.8). Furthermore, according to the results, cement-lime masonry (M6) possesses a significantly greater bond strength at 28 days (0.51 N/mm^2) than the NHL 5 masonry at 6 months (0.43 N/mm^2).

The bond strength of CL90-s masonry at 6 months (0.15 N/mm^2) is comparable to that of NHL 2 masonry at 28 days (0.13 N/mm^2). Similarly, 6-month results for NHL 2 masonry (0.19-0.21 N/mm^2) correspond well to 28 day NHL 3.5 values (0.18-0.25 N/mm^2) (Figure 4.8).

The bond of NHL 5, NHL 3.5, NHL 2 and CL90-s masonry at 165 mm flow was measured after 365 days. The results suggest that, in all masonry types, most of the bond strength is achieved in the first 6 months. Very little or no bond increase occurs between 6 months and 1 year.

As discussed in Chapter 1, previous authors who researched cement and cement-lime masonry found inconsistent bond strength development over time. In particular, they highlighted losses in strength at around 90 days and 365 days of curing (Kamimura *et al.* (1965); Baker (1979); Drysdale and Gazzola (1985); Neville and Brooks (1987); Sise *et al.* (1988); Lawrence and Cao (1988); Abrams (1995) and Sugo *et al.* (2007)). However, in this research, the results clearly show that bond strength consistently

increases with time for both lime and cement-lime masonry with no strength losses up to one year (Figure 4.8). This observation is irrespective of mortar water content. In all cases, 365-day bond strength results were found to be greater than 56-day and 6-month values (Table 4.3). Zhou *et al.* (2007), using similar materials and methods, support this observation, as they found that the bond strength of lime masonry increased over time.

Similarly to bond, most of the masonry flexural strength is achieved in the first two months. As expected, at all curing ages, flexural strength results from tests performed parallel to the bedding joints (Type 1) are significantly lower than results obtained perpendicular to the bedding joints (Type 2) (Figures 4.9 and 4.10). As aforementioned, this is due to differing mechanisms in each test resisting moments due to flexural stresses.

No overlap is evident on the flexural strength of different masonry types over time. Cement-lime masonry (M6) predictably develops significantly greater flexural strength than lime masonry in both test directions, for example: at 6 months, M6 masonry achieves flexural strengths of circa 0.7 N/mm^2 (Type 1) and approximately 2 N/mm^2 (Type 2), compared to 0.47 and 1.43 N/mm^2 for NHL 5. As previously mentioned, over time, NHL 5 masonry consistently out-performs NHL 3.5 masonry in flexure by approximately 50 % (Figures 4.9 and 4.10).

Similarly, the flexural strength of NHL 3.5 masonry is consistently higher than that of NHL 2 masonry and the flexural strength of NHL 2 is greater than that of the CL90-s masonry at all curing ages. For example: at 6 months, the Type 1 flexural strength of NHL 3.5 masonry is approximately 60 % greater and Type 2 50 % greater than those of NHL 2 masonry (Figures 4.9 and 4.10). The Type 1 flexural strength of NHL 2 masonry is only 25 % greater than CL90-s masonry at 6 months however, Type 2 flexural strength of NHL 2 is over twice as strong as CL90-s masonry.

Similar to compressive and bond strength, both cement-lime and lime masonry develop a significant proportion of their respective 6-month flexural strengths (approximately 34-83 %) during the first 28 days of hardening (Table 4.11). However, the results indicate that lime masonry develops Type 2 flexural strength at a faster rate than that of Type 1, for example: over the first 28 days, NHL 3.5 masonry gains 59 % of its (Type

1) 6-month flexural strength whereas, it gains 78 % of its Type 2 6-month flexural strength over the same period. This is due to the masonry having additional inherent flexural strength perpendicular to the bedding joints because of the different orientation of the applied loads and resultant stress-interactions. This trend is consistent for all lime masonry types. As aforementioned, additional forces and stress-interactions, such as the friction within the contra rotation portions of the masonry and bond of the vertical joints, are involved.

In contrast to the compressive and bond strength of masonry, clear differences can be seen between the flexural strength of different hydraulic strength masonries irrespective of the flexural test orientation, flow or specimen age (Figures 4.9 and 4.10).

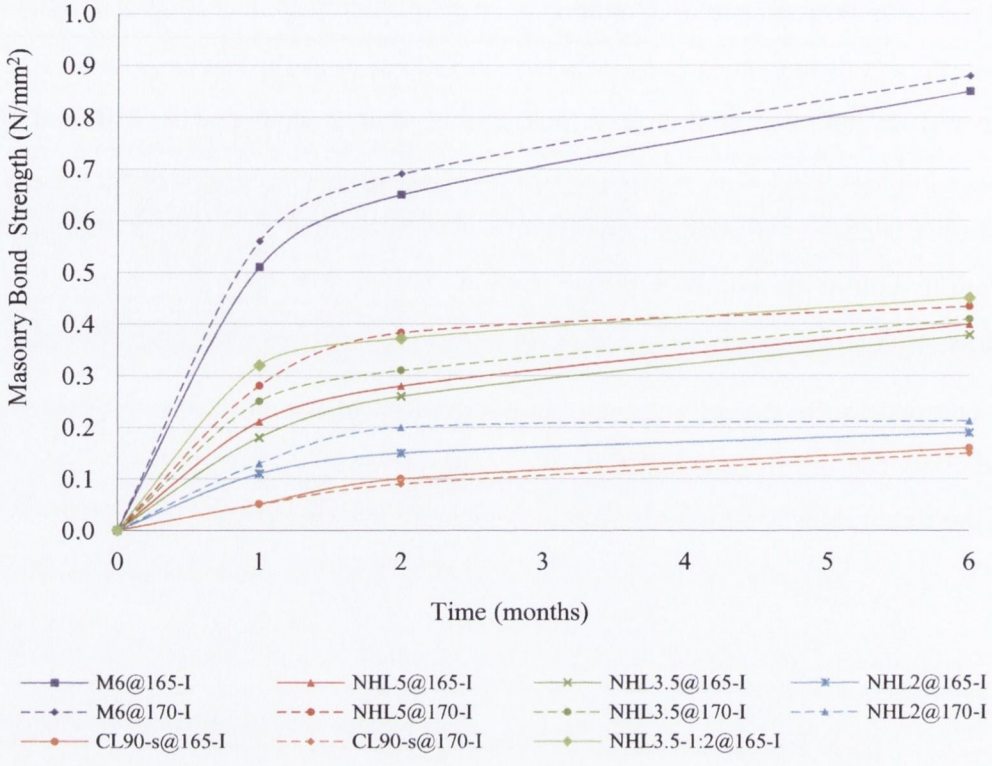

Figure 4.8: Bond strength development of brick masonry over time

Flow (mm)	Mortar type	Mix ratio	Compressive strength		Elastic modulus		Bond strength		Flexural strength (parallel)		Flexural strength (perpendicular)	
			28 days	56 days	28 days	56 days	28 days	56 days	28 days	56 days	28 days	56 days
165	M6	1:½:4 (v)	71	79	63	72	60	76	73	88	79	93
	NHL 5	0:1:3	69	79	43	70	53	70	51	74	80	90
	NHL 3.5	0:1:3	66	76	46	67	47	69	59	67	78	95
	NHL 3.5	0:1:2	66	83	54	64	71	82	66	86	61	92
	NHL 2	0:1:3	81	95	60	72	58	79	42	73	79	82
	CL90-s	0:1:3	23	39	66	82	32	63	34	63	50	72
170	M6	1:½:4 (v)	65	71	66	83	64	78	83	89	80	85
	NHL 5	0:1:3	67	78	47	73	65	88	47	68	70	80
	NHL 3.5	0:1:3	65	76	54	91	70	84	63	70	80	89
	NHL 2	0:1:3	78	96	60	80	61	94	43	86	75	92
	CL90-s	0:1:3	26	78	55	66	33	60	42	66	48	72

Table 4.11: Percentage of strength and stiffness gained by the masonries at 28 and 56 days (as a percentage of the 6-month value). Laboratory-cured masonry.

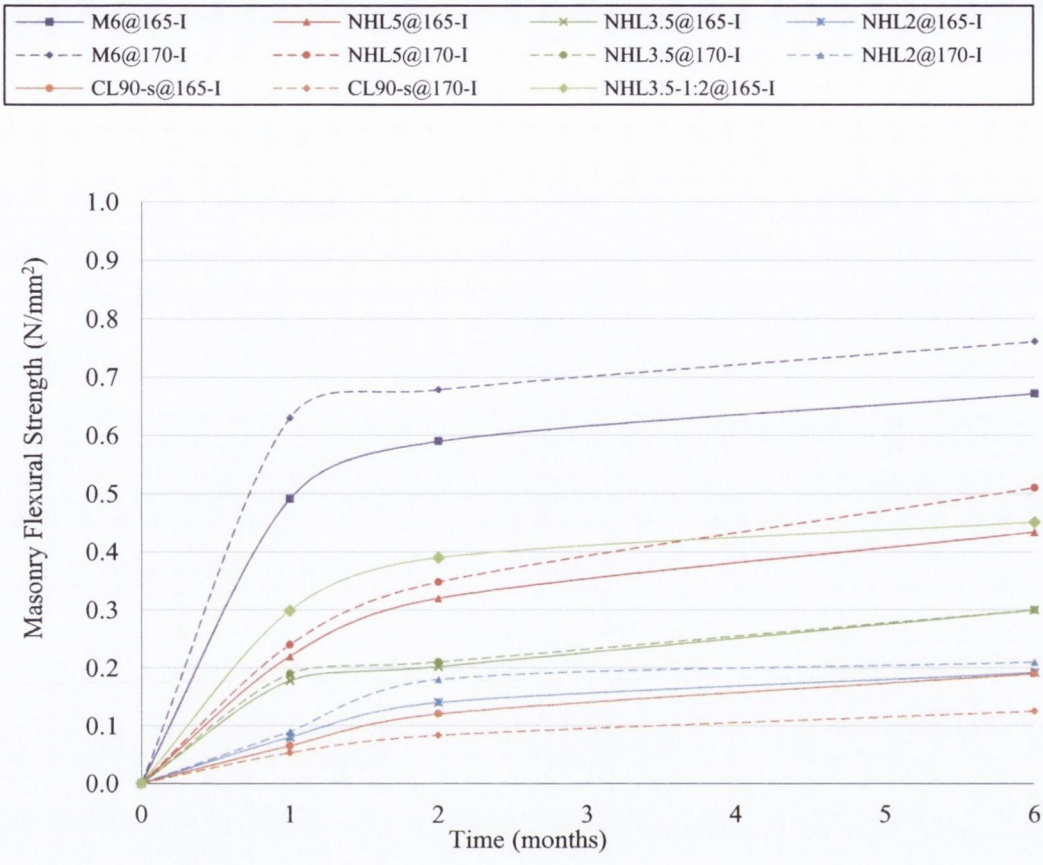

Figure 4.9: Flexural strength development of brick masonry (Type 1 - parallel to bedding joints)

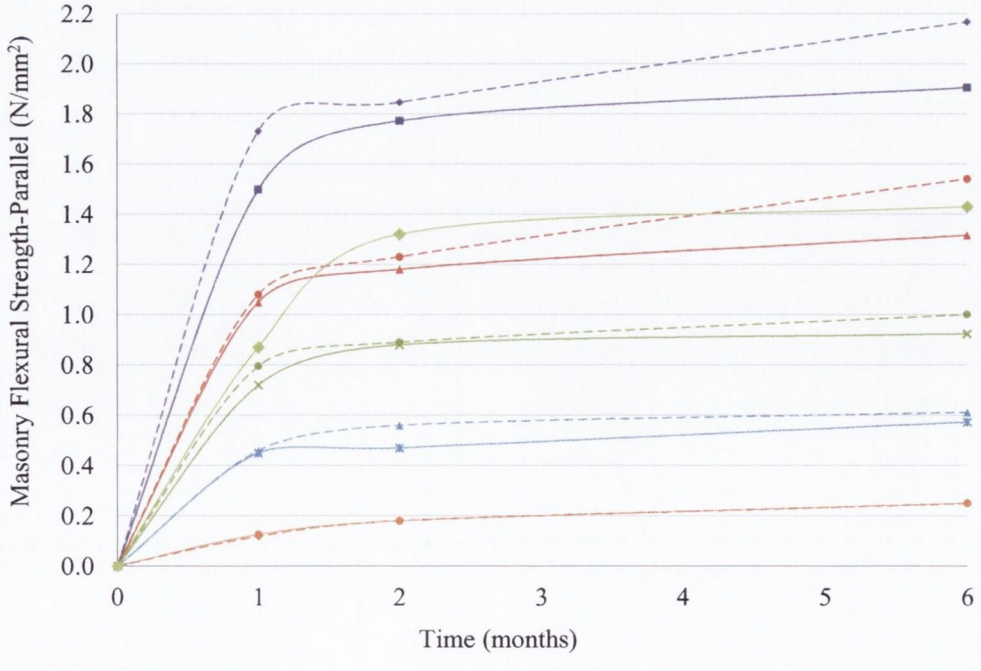

Figure 4.10: Flexural strength development of brick masonry (Type 2 - perpendicular to bedding joints)

4.3 COMPARISON BETWEEN MASONRY BOND AND FLEXURAL STRENGTH TESTING

As discussed in Chapter 1, some authors (BRE (1991) and Zhou *et al.* (2008)) previously suggested that the results of the bond wrench test can be correlated with masonry flexural strength (Type 1 – parallel to the bedding joints) values obtained in accordance with EN 1052-2 (1999). Almeida *et al.* (2002) reported that low insight was available with respect to the relationship between masonry flexural bond strength and tensile bond strength. The flexural strength of masonry is closely related to the masonry bond strength since it is the bond between the mortar and the masonry unit that mainly resists moments due to flexural stresses parallel to the bedding joints. Results from both the flexural (Type 1) and bond strength tests on laboratory-cured brick masonry have previously been presented in Tables 4.3 and 4.4.

Flow (mm)	Mortar type	Mix ratio	28 days (N/mm^2)			56 days (N/mm^2)			6 mts. (N/mm^2)			
			Bond	Flex.	*% Diff.*	Bond	Flex.	% Diff.	Bond	Flex.	*% Diff.*	Avg. Diff
165	**M6**	1:½:4 (v)	0.51	0.49	*3 %*	0.65	0.59	*9 %*	0.85	0.67	*21 %*	*11 %*
	NHL 5	0:1:3	0.211	0.22	*4 %*	0.28	0.32	*14 %*	0.4	0.43	*8 %*	*9 %*
	NHL 3.5	0:1:3	0.18	0.18	*0 %*	0.26	0.20	*30%*	0.379	0.30	*21 %*	*17 %*
	NHL 2	0:1:3	0.11	0.08	*18 %*	0.15	0.14	*7 %*	0.19	0.19	*0 %*	*8 %*
	CL90-s	0:1:3	0.051	0.07	*37 %*	0.1	0.12	*20 %*	0.16	0.19	*19 %*	*25 %*
	NHL 3.5	0:1:2	0.32	0.30	*6 %*	0.37	0.39	*5 %*	0.415	0.45	*8 %*	*6 %*
170	**M6**	1:½:4	0.56	0.63	*13 %*	0.69	0.68	*2 %*	0.88	0.76	*14 %*	*10 %*
	NHL 5	0:1:3	0.28	0.24	*14 %*	0.383	0.35	*9 %*	0.434	0.51	*18 %*	*14 %*
	NHL 3.5	0:1:3	0.25	0.19	*24 %*	0.31	0.21	*32 %*	0.41	0.30	*27 %*	*28 %*
	NHL 2	0:1:3	0.13	0.09	*31 %*	0.2	0.18	*10 %*	0.21	0.21	*0 %*	*14 %*
	CL90-s	0:1:3	0.05	0.05	*0 %*	0.09	0.08	*11 %*	0.15	0.13	*13 %*	*8 %*
Average Difference					*14 %*			*14%*			*14 %*	*14 %*

Table 4.12: Comparison between bond wrench test and flexural strength test parallel to the bedding joints

Table 4.12 displays the differences between the two tests. Average differences of 14 % are show for each masonry type. The overall average difference for all masonry types is 14 %. Linear regression analysis was also carried out on their data sets. Best-fit regression lines and their equations together with R^2 values, are included in Figure 4.11.

R^2 values of 0.94 were found (Figure 4.11), indicating a very good correlation between the two testing methods. This clear relationship can be seen irrespective of mortar flow. As discussed in Chapter 5, the equation of the linear regression line takes the form of $Y = b_0 + b_1X_1$, where b_0 is the Y-axis intercept and b_1 is the slope of the line. The Y-axis intercept was forced to zero. The nearer the slopes are to one the closer the lines are to 45 degrees. Therefore, at 0.93 and 0.98, the slopes of the lines in Figure 4.11 show a close connection between the two sets of test results. The bond wrench test proved to be relatively fast and accurate, and the stacked brick prisms required for the bond wrench test were vastly faster and easier to manufacture than the more complex wallettes required by EN 1052-2 (1999). Removing the cement-lime test results from the regression analysis (Figure 4.12), yields slightly reduced R^2 values of 0.86 and 0.88. However, the analysis still suggests a substantial correlation between the masonry bond strength and flexural strength results of lime-mortar masonry. Furthermore, the correlation found between the two testing methods is consistent with previous studies, including BRE (1991), who focused on higher strength cement-lime masonry and Zhou *et al.* (2008) who investigated lime masonry.

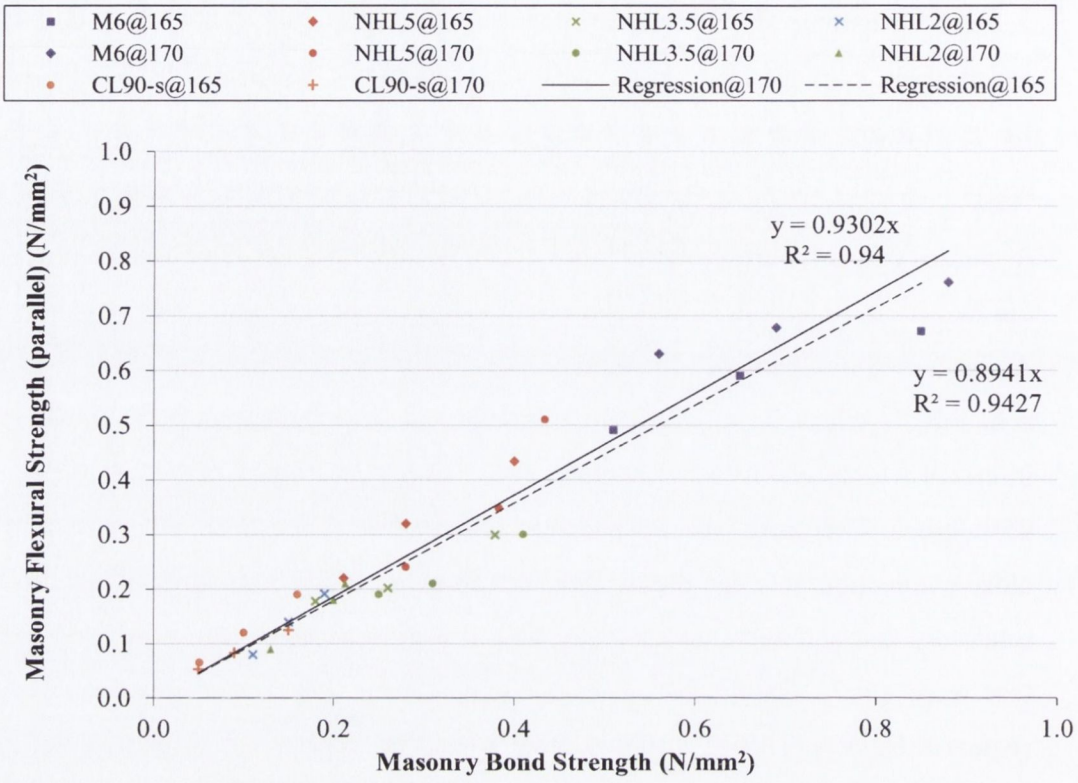

Figure 4.11: Regression analysis of masonry bond and flexural strength

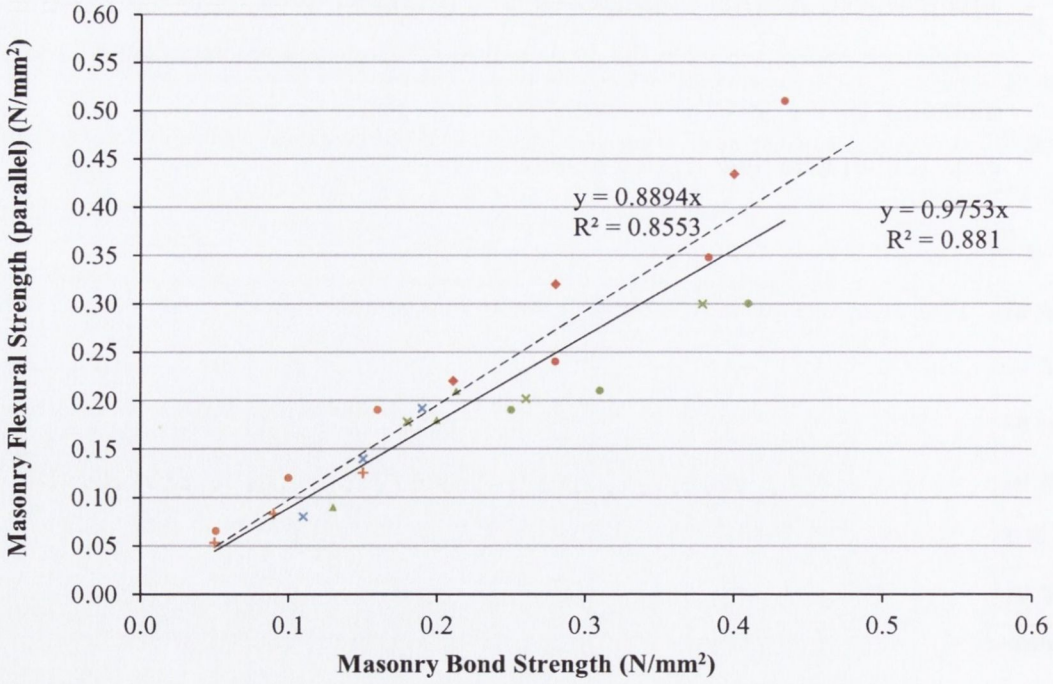

Figure 4.12: Regression analysis of masonry bond and flexural strength (lime masonry only)

CHAPTER 5

MORTAR AND BRICK MASONRY RELATIONSHIPS

This chapter examines the relationship between the mechanical characteristics of the mortar and those of the brick-masonry. It can be argued that, mortars harden and develop strength differently in masonry joints and in mortar specimens and therefore, the masonry and mortar results are not compatible. For instance, all 6 sides of the mortar prisms are in contact with the atmosphere whereas, in masonry, only a small proportion of the mortar is exposed at the joint surface. In addition, in masonry, other variables such as workmanship and unit suction, also affect mortar strength development and these are not accounted for in the mortar specimens.

In the present research, the influence of workmanship was significantly reduced by having all laboratory work carried out by the same person, namely the author. Furthermore, the effect of brick suction was mitigated by following suggestions made by previous authors, Gerard *et al.* (1985); Groot (1993); Sinha (1967) Venkatarama and Gupta (2006); Venumadhava Rao *et al.* (1996) and Walker (1999), who recommend the pre-wetting of high suction brick units to approximately 80 % saturation. Therefore, while the mortar prisms in this research are not a true characterisation of the mortars in the masonry joints, they provide a good representative indication of mechanical behaviour of the mortars in the masonry.

5.1 INFLUENCE OF MORTAR PROPERTIES ON THE COMPRESSIVE STRENGTH OF BRICK MASONRY

This section presents previously discussed mortar results obtained at 28 days, 56 days and 6 months, and plots them against the compressive strength results of masonry over time. Since the main specifying parameter of a mortar is its strength, the correlation between mortar compressive strength and masonry compressive strength is first considered. In principal, a clear relationship should exist, since both typically develop strength as they harden over time, as seen in Chapters 3 and 4. For example, in Figure 5.1, the first point on each trend line represents the 28-day mortar and masonry compressive strength results, the second point signifies the 56-day results, and the third point compares the 6-month values.

5.1.1 Impact of mortar compressive strength on the compressive strength of masonry

The results demonstrate that the hydraulic grade of the binder (and thus mortar strength) has a dramatic influence on the compressive strength (CS) development of both mortar and masonry, and hence it also affects their relationships.

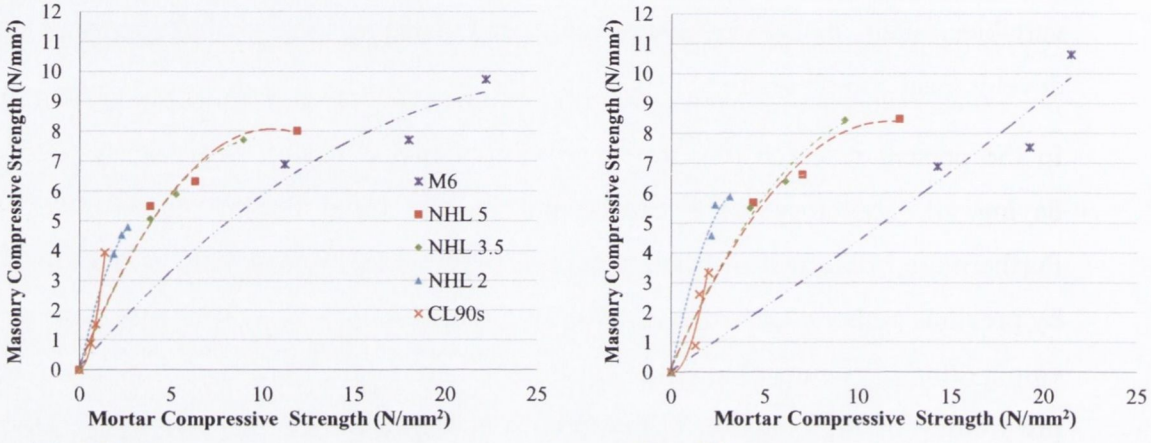

Figure 5.1: Impact of mortar CS on the CS of masonry for mortar of different hydraulic strengths at increasing flow

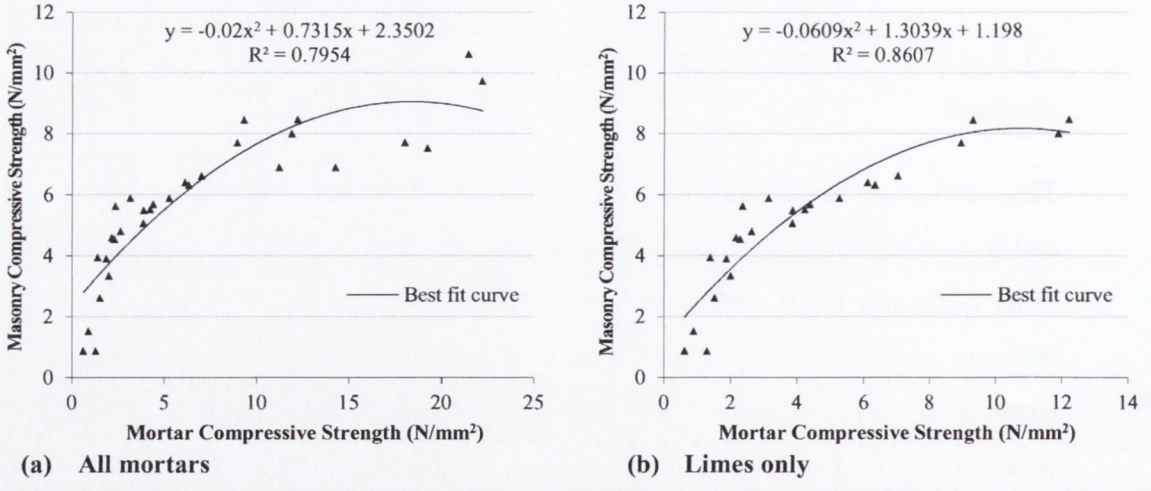

Figure 5.2: Overall influence of mortar CS on the CS of brick masonry (includes different mortar hydraulic strengths, three curing ages and two flows).

According to Figure 5.1 and Tables 3.5 and 4.1, mortars of higher hydraulic strength (M6, NHL 5 and 3.5) are stronger than their corresponding masonry. After 6 months,

M6 mortar at a 165 mm flow is over twice as strong as the corresponding masonry; NHL 5 mortar is also stronger in compression (11.89 N/mm^2) than its masonry (8.01 N/mm^2), and NHL 3.5 mortar follows a similar trend (8.95 N/mm^2 for mortar vs. 7.71 N/mm^2 for masonry). This observation remains consistent at the higher mortar flow.

In contrast, lower strength mortars, NHL 2 and CL90-s, show the opposite trend of being weaker than their masonry: the mortars have a 6-month compressive strength of 2.62 N/mm^2 and 1.39 N/mm^2 respectively, while the corresponding masonry strengths are much greater, at 4.8 N/mm^2 and 3.94 N/mm^2 respectively. This is consistent for both mortar flows.

Furthermore, Figure 5.1 demonstrates that, as the hydraulic grade of the binder increases, the slope of the relationship between mortar and masonry compressive strength (during curing) decreases. Therefore, the tendency for a mortar to be stronger than its corresponding masonry is closely related to the mortar's hydraulic strength grade, irrespective of mortar flow.

As previously mentioned, both mortar and masonry compressive strengths increase over time and are thus related. However, the results indicate that the influence of mortar strength on masonry strength is non-linear and it is related to the ratio of unit strength to mortar strength, i.e. the greater the strength of the mortar with respect to that of the unit; the smaller the influence of mortar strength variations on the masonry strength.

The results indicate that substantial increases in the compressive strength of higher strength natural hydraulic lime and cement-lime mortars during curing, do not lead to significant increases in masonry compressive strength over the same timeframe. As can be seen in Figure 5.1 and Tables 3.5 and 4.1, between 28 and 56 days (165 mm flow), the compressive strength of NHL 3.5 and NHL 5 mortar increases by 37 % and 64 % respectively however, the corresponding masonry only increases by 15 % and 16 %. The same relationship is maintained between 56 days and 6 months and at the higher mortar flow. In contrast, non-hydraulic (calcium lime) and feebly hydraulic lime (NHL 2) which are much weaker and less stiff than the brick units, show the opposite trend: small increases in mortar compressive strength are linked to relatively large gains in

brick-masonry compressive strength. This relationship is also consistent for both mortar flows.

The compressive strength of mortar and masonry has been shown to vary with water content (Chapters 3 and 4). Mortar and brick masonry compressive strength generally improve with increased flow (except for CL90-s masonry). However, percentage gains in mortar strength due to increased flow are much greater than those found for masonry. Furthermore, according to Chapter 4, the magnitude of the gain in masonry compressive strength (due to the variation in flow) reduces as the hydraulic strength of the mortar increases.

Figure 5.2 further illustrates the relationship between mortar and masonry compressive strength, where a best-fit curve is applied to the entire data set. The influence of mortar compressive strength on masonry compressive strength is shown to be non-linear with a strong R^2 of 0.795. The masonry strength tends towards a maximum of approximately 9 N/mm^2 as the mortar strength increases (Figure 5.2 (a)). This maximum is approximately 75 % of the normalised compressive strength of the masonry unit.

Since the compressive strength of M6 mortar is considerably greater than that of the lime mortars, this might have the effect of skewing the relationship between mortar and masonry compressive strength. Therefore, Figure 5.2 (b) is included to show that a non-linear relationship remains, irrespective of the stronger cement-lime results.

Previous authors (Venumadhava Rao *et al.* (1995) and Venkatarama and Vyas (2008)) suggested that masonry compressive strength is not significantly impacted by mortar strength. The authors based their conclusions on a small series of cement and cement-lime masonry tests. This research contradicts this and suggests that mortar compressive strength significantly influences masonry compressive strength, but that the impact becomes progressively smaller as the masonry strength moves towards its maximum (which is closely related to the unit lateral tensile and compressive strength).

5.1.2 Influence of mortar flexural strength and stiffness on the compressive strength of brick-masonry

Chapter 3 evidences that the flexural strength (f/s) and stiffness of mortars generally behave similarly to mortar compressive strength, increasing with mortar hydraulic grade, curing time and water content. Therefore, the influence of these mortar properties on the compressive strength of masonry (Figures 5.3 and 5.5) show similar patterns to mortar compressive strength in Figure 5.1. The slope of the relationship (between mortar f/s and elastic modulus, and the compressive strength of the masonry) generally becomes smaller as the hydraulic grade and strength of the mortar increases, irrespective of the mortar flow.

The results in Figures 5.3 and 5.5 indicate that substantial increases in the mortar flexural strength and elastic modulus of higher hydraulic grade NHL and cement-lime, do not lead to significant increases in masonry compressive strength over the same time period, irrespective of mortar flow. In contrast, the results also show that relatively small gains in the flexural strength and elastic modulus of CL90-s and NHL 2 mortars are related to significant improvements in masonry compressive strength, mainly occurring between 56 days and 6 months at both flows.

The non-linear best fit curves in Figures 5.4 and 5.6 support the previous observations and also indicate that masonry compressive strength is influenced by increases in mortar flexural strength and elastic modulus (due to ageing, water content and mortar hydraulic grade). However, as before, the influence becomes smaller as the compressive strength of the masonry moves towards its maximum load capacity.

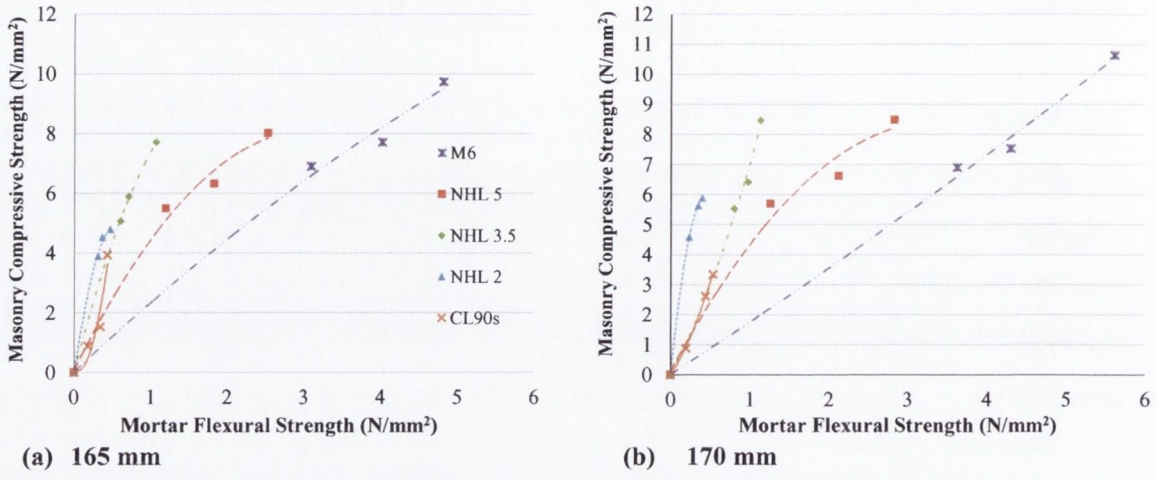

Figure 5.3 Impact of mortar flexural strength on the CS of masonry for mortars of varying hydraulicity and increasing flow

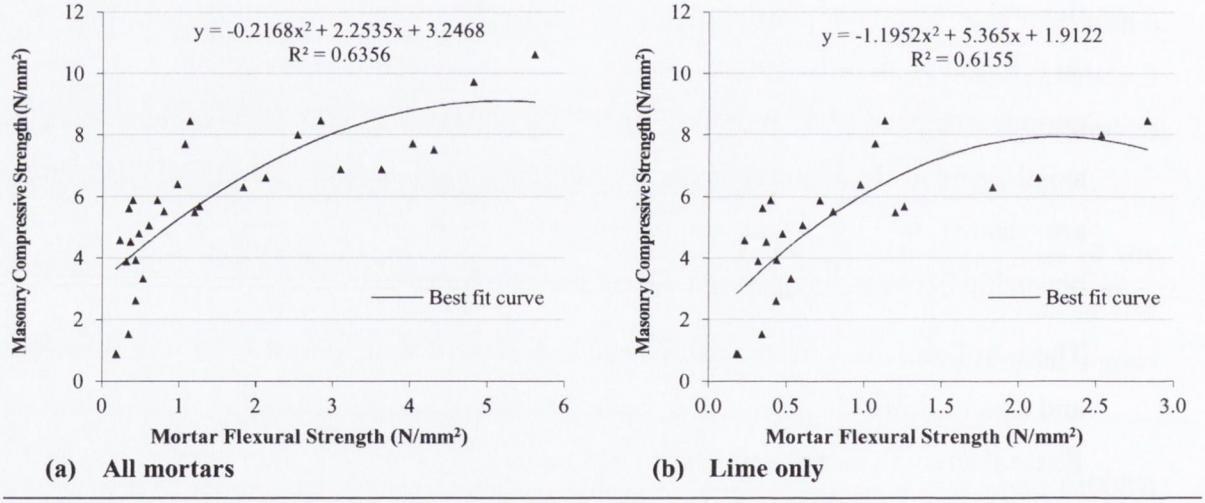

Figure 5.4: Overall influence of mortar flexural strength on the CS of brick masonry (includes different mortar hydraulic strengths, three curing ages and two flows)

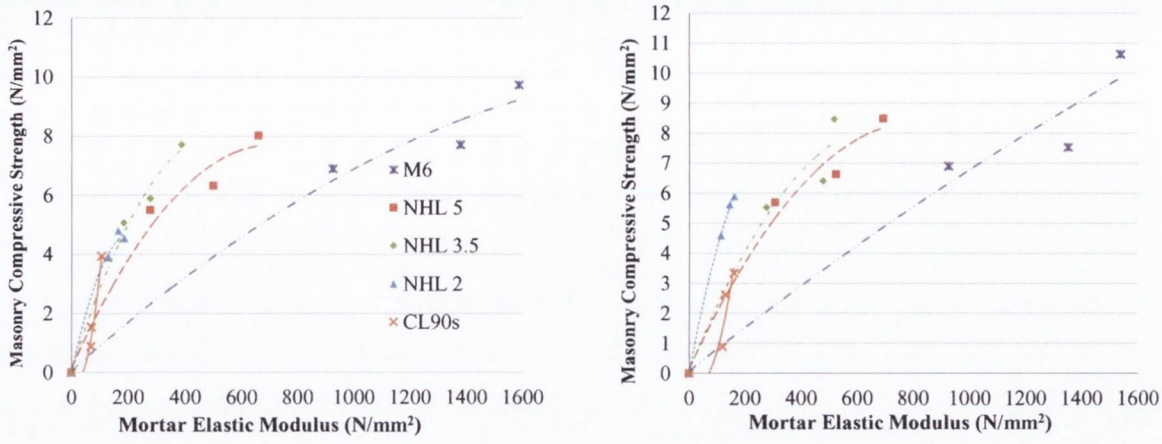

Figure 5.5: Impact of mortar elastic modulus on the CS of masonry for mortars of varying hydraulicity and increasing flow

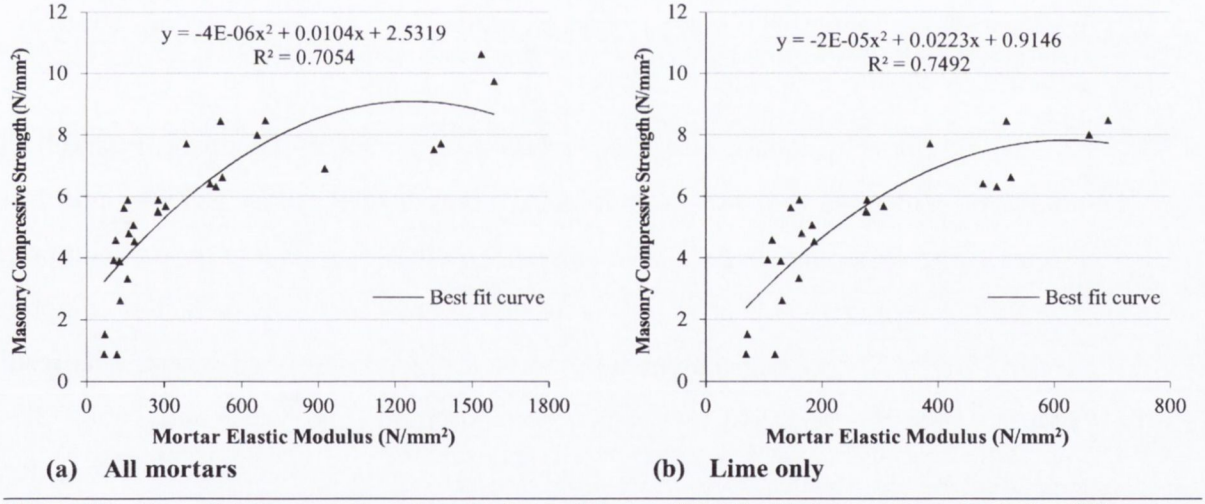

Figure 5.6: Overall influence of mortar elastic modulus on the CS of brick masonry (includes different mortar hydraulic strengths, three curing ages and two flows)

5.2 INFLUENCE OF MORTAR MECHANICAL PROPERTIES ON BRICK-MASONRY BOND STRENGTH

Results presented in Chapter 4 showed that masonry bond strength increases with the hydraulic strength of the binder. Bond also improves with increased water content (except for CL90-s masonry). The results in this section evidence relationships between mortar strength/stiffness and bond strength. According to the results, lower lime-grade masonry (CL90-s and NHL 2) develops bond strength at a faster rate (relative to the compressive strength, flexural strength and stiffness development of the constituent mortar) than higher lime grades (NHL 3.5 and 5). Additionally, the results show that large gains in the strength and elastic modulus of higher hydraulic lime mortars do not generally result in significant improvements in brick-mortar bond.

The results presented in Figures 5.7, 5.9 and 5.11 clearly show that, over time, masonry bond strength increases with increasing mortar compressive/flexural strength and stiffness, irrespective of water content.

According to the results, two distinct relationships, which depend on hydraulic lime grade are evident. The lower the hydraulic strength of the lime (CL90-s and NHL 2 mortars), the faster the rate of bond strength increase relative to mortar compressive strength development, for example: between 56 days and 6 months, the compressive strength of CL90-s mortar increases by 56 % (0.89-1.39 N/mm^2) whereas its resultant masonry gains 60 % (0.1-0.16 N/mm^2) bond strength (Figure 5.7 and Tables 3.5 and 4.3). In contrast, the compressive strength of NHL 5 mortar increases by a considerable 88 % (6.33-11.89 N/mm^2) however, its masonry bond strength only improves by 43 % (0.28-0.4 N/mm^2) over the same time period. This relationship is maintained at both flows for all mortars except for NHL 2, which behaves similarly to the higher strength mortars at the high flow.

Similarly, the mortar flexural strength and elastic modulus and the masonry bond strength (Figures 5.9 and 5.11) also show an inverse relationship with respect to the hydraulic grade of the binder. The lower hydraulic strengths display a greater slope. This indicates that the lower the mortar binder grade, the greater the influence that mortar flexural strength and stiffness will have on the bond strength of masonry: small

increases in elastic modulus result in relatively large gains in bond strength. The results suggest that this trend remains valid for both mortar flows studied.

The overall influence of the mortar mechanical properties (compressive strength, flexural strength and elastic modulus) on the bond strength of masonry was investigated with regression analysis (Figures 5.8, 5.10 and 5.12). The graphs include results for different hydraulic strength mortars, curing ages and mortar flows. Regression analysis indicates that the results fit well to polynomial curves. Relatively good R^2 values (0.93-0.97) represent a strong, non-linear relationship between mortar properties and masonry bond strength. According to these results, masonry bond strength displays a clear experimental link with the compressive/flexural strength and elastic modulus of mortar however, the magnitude of the influence becomes smaller as the masonry bond strength reaches higher values. As such, small increases in the mechanical properties of lower strength mortars (CL90-s/NHL 2) result in relatively large gains in masonry bond strength whereas, the higher bond strength masonries (those bond with higher strength mortars NHL 3.5, 5 and M6) are less affected by the mortar properties.

Since the mechanical properties of the mortars (compressive/flexural strength and elastic modulus) are inter-related and because they have not been isolated in this research, it is not possible to ascertain which of these properties most influences masonry bond strength.

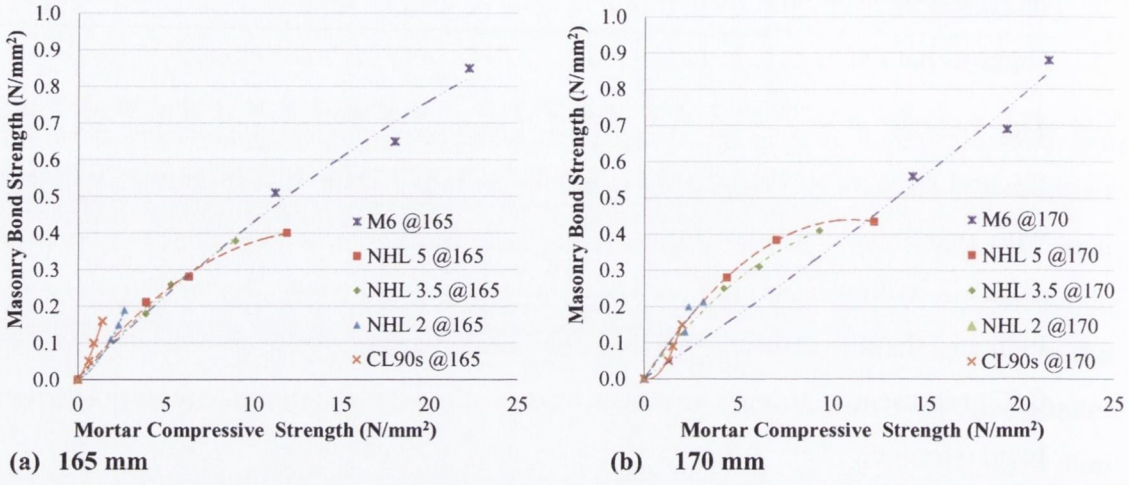

Figure 5.7: Impact of mortar compressive strength on the BS of masonry for mortars of varying hydraulic strengths at increasing flow

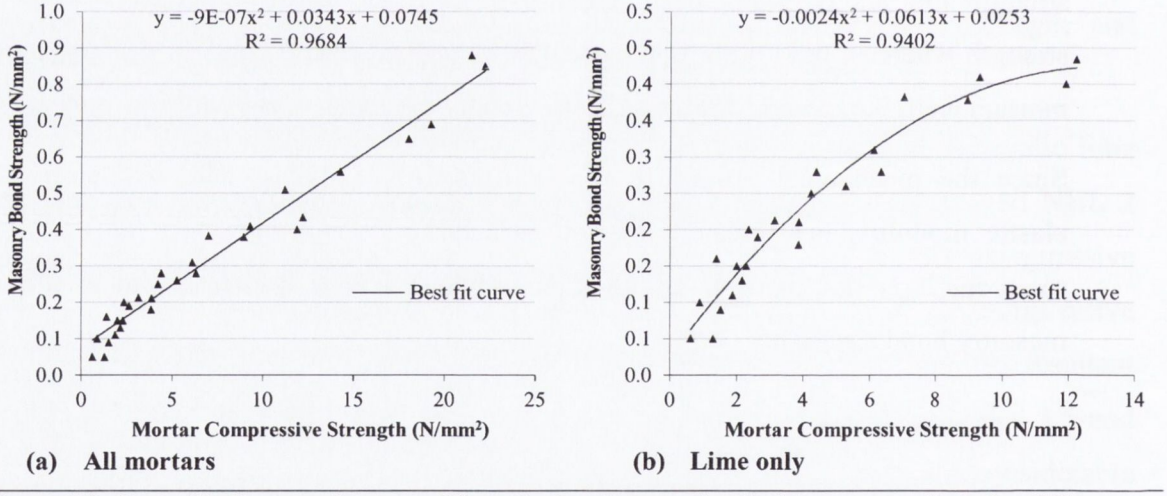

Figure 5.8: Overall influence of mortar CS on the bond strength of brick masonry (includes different mortar hydraulic strengths, three curing ages and two flows)

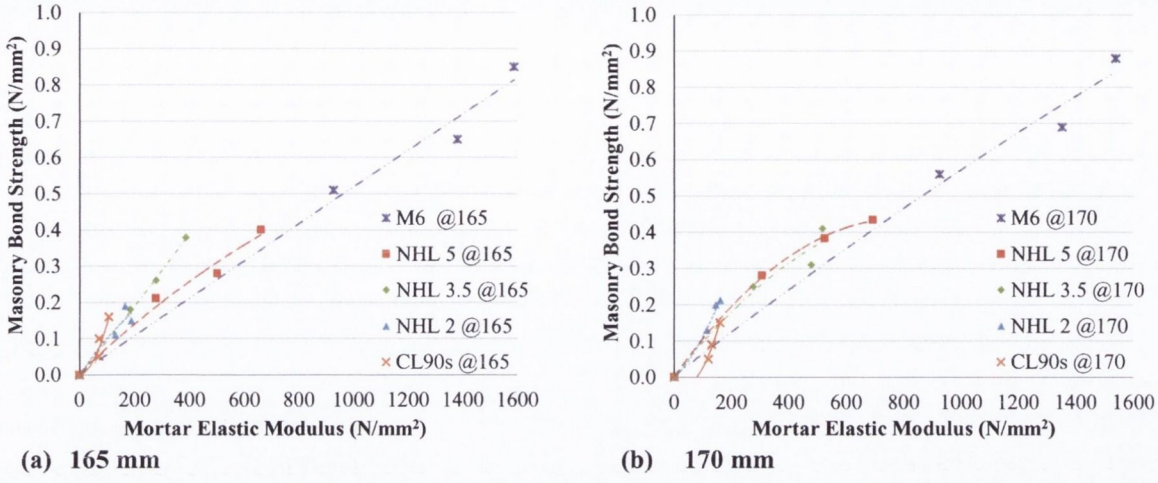

(a) 165 mm (b) 170 mm

Figure 5.9: Impact of mortar elastic modulus on the BS of masonry for mortars of varying hydraulic strengths at increasing flow

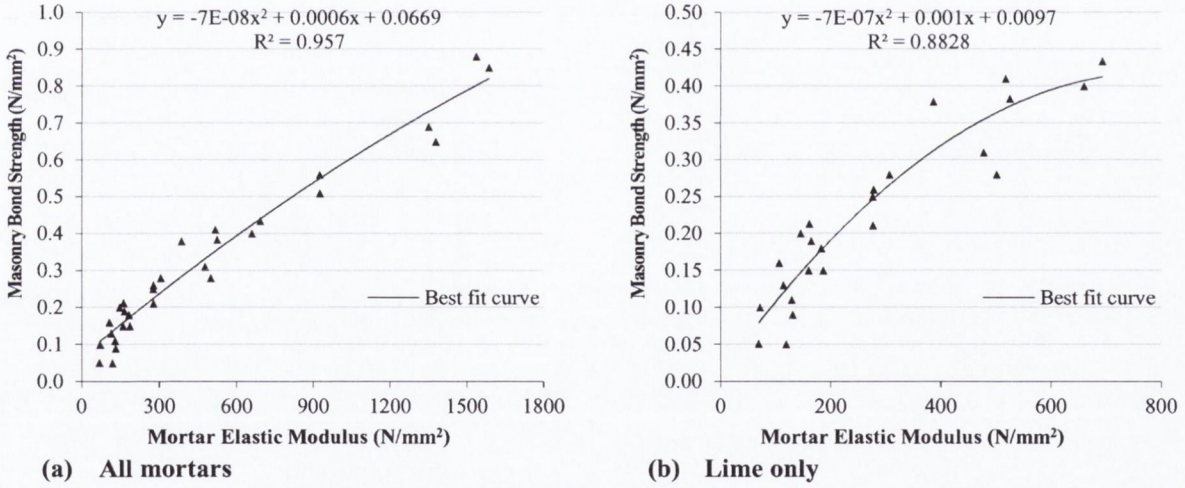

(a) All mortars (b) Lime only

Figure 5.10: Overall influence of mortar elastic modulus on the bond strength of brick masonry (includes different mortar hydraulic strengths, three curing ages and two flows)

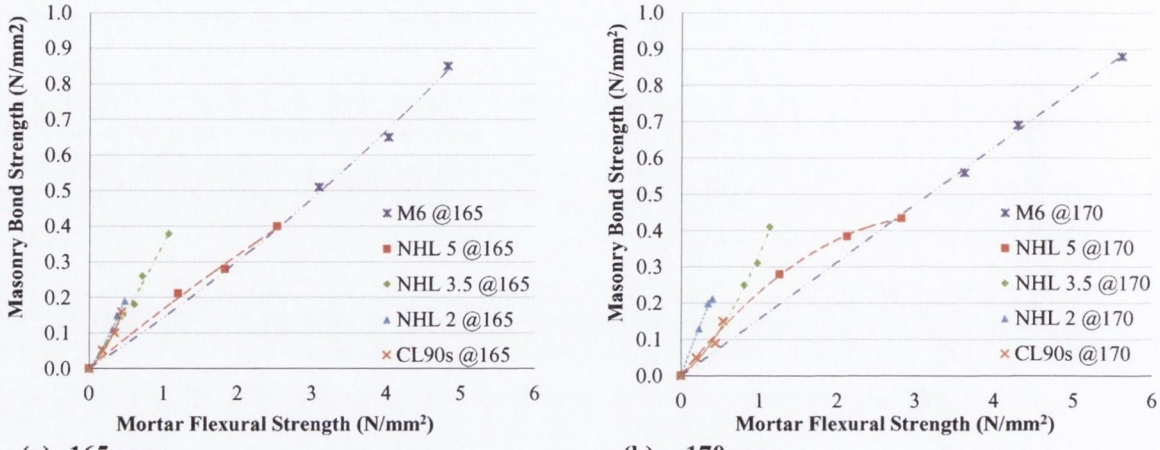

(a) 165 mm (b) 170 mm

Figure 5.11: Impact of mortar flexural strength on the BS of masonry for mortars of varying hydraulic strengths at increasing flow

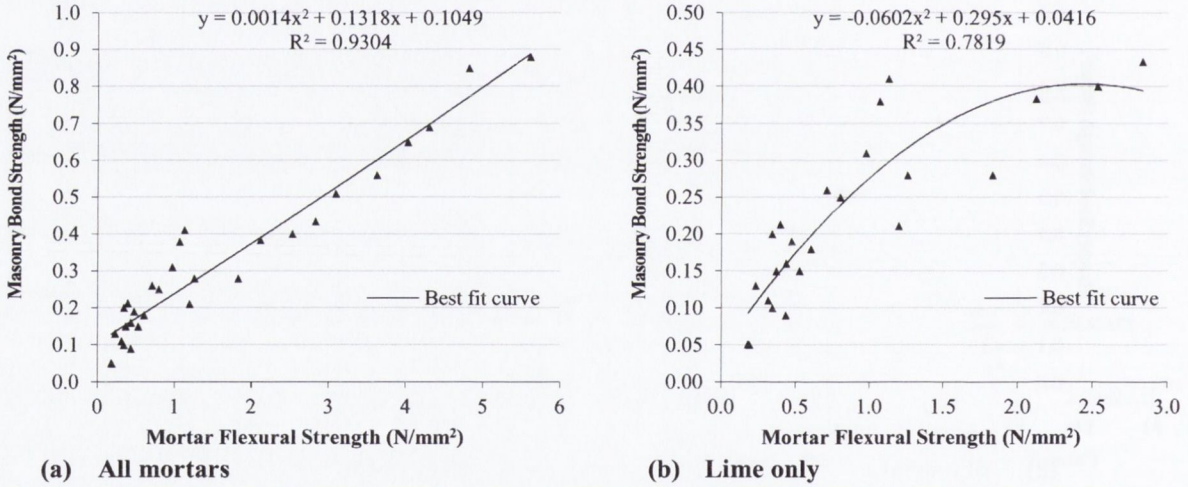

(a) All mortars (b) Lime only

Figure 5.12: Overall influence of mortar flexural strength on the bond strength of brick masonry (includes different mortar hydraulic strengths, three curing ages and two flows)

5.3 RELATIONSHIP BETWEEN MASONRY BOND AND MASONRY COMPRESSIVE STRENGTH

According to the results, a clear relationship exists between brick-bond and masonry compressive strength. As previously mentioned, both properties increase over time, and as hydraulic grade, mortar strength and water content increase. In addition, the relationships between masonry bond/compressive strength and mortar compressive strength were found to be non-linear. However, since the bond strength was not artificially altered while keeping the other properties (time, hydraulic grade and mortar strength) constant, the relative influence of mortar-brick bond on the compressive strength of masonry remains unclear. Grenley (1969) expressed similar concerns in relation to a study carried out on cement masonry.

Figure 5.13 plots the relationship between masonry bond and compressive strength over time for different mortar grades and flow. Chapter 4 demonstrated that both bond and masonry compressive strength consistently increase over time. However, Figure 5.13 indicates that masonry compressive strength increases at a faster rate than bond strength, except for cement-lime masonry, which shows a more or less linear relationship.

Figure 5.14 suggests an overall non-linear relationship between masonry bond and compressive strength, irrespective of flow, indicating (for this particular masonry unit) that, as the two properties increase, the masonry compressive strength reaches a maximum before the brick-bond does. This indicates that the masonry compressive strength reaches a maximum value, after which, any further increase in bond is unlikely to cause further gains in masonry compressive strength. This is likely due to the failure mechanisms associated with masonry when it is close to its maximum compressive strength. In such circumstances, failure is generally due to lateral tension in the bricks (causing them split) however, the bond is maintained (Section 1.2.12). Therefore, any further improvements in bond (due to hardening and strength development of the mortar) cease to affect the masonry compressive strength as it is limited by the lateral tensional capacity of the brick.

Chapter 4 evidenced that the masonry tends towards its maximum compressive strength value when the mortar stiffness is close to or greater than that of the unit (cement-lime masonry (M6)). Therefore, this research supports the cement-based masonry findings of Venkatarama *et al.* (2007) who reported only marginal improvements in masonry compressive strength as bond strength increased when the modulus of elasticity of the mortar was in the same range or greater than that of the masonry unit.

Other authors, Venumadhava Roa *et al.* (1995) reported that cement mortars with distinctly different compressive strengths but similar bond strengths resulted in comparable masonry compressive strengths. This research finds that only natural hydraulic lime (NHL 3.5 and NHL 5) mortar and masonry behave in such a manner. Relatively small differences between the brick-bond (6-14 %) and masonry compressive strength (3-8 %) of NHL 3.5 and NHL 5 were found whereas, large differences were associated with the compressive strength and elastic modulus of the mortars (15-31 % and 10-80 % respectively) (Table 5.1). However, similar relationships were not found between any of the other mortars or masonry studied. Therefore, this research does not support the conclusions of Venumadhava Roa *et al.* (1995). According to this research, lime and cement-lime mortars with significantly different compressive strength and stiffness, but similar bond strength, can, but do not necessarily result in masonry with comparable compressive strengths.

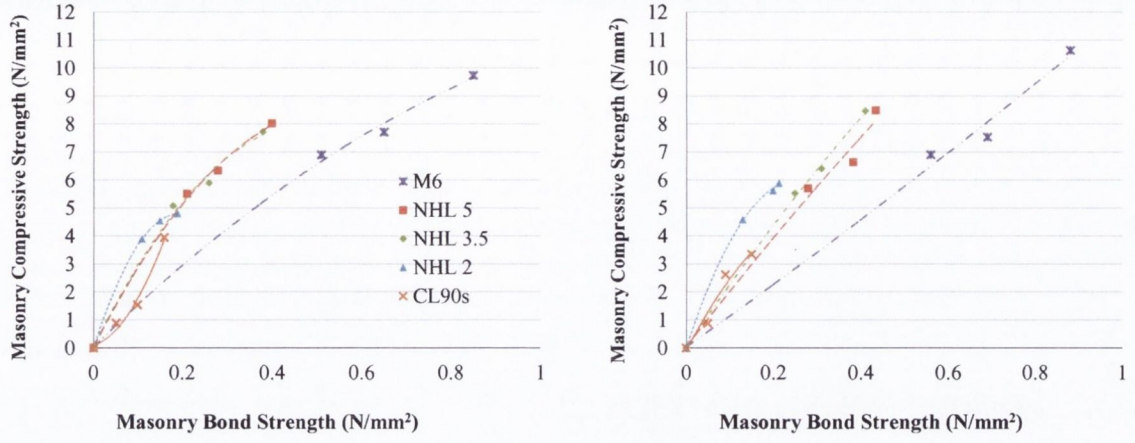

(a) 165mm (b) 170mm

Figure 5.13: Relationship between masonry bond strength and the CS of masonry over time for different mortar hydraulic strengths at two different flows.

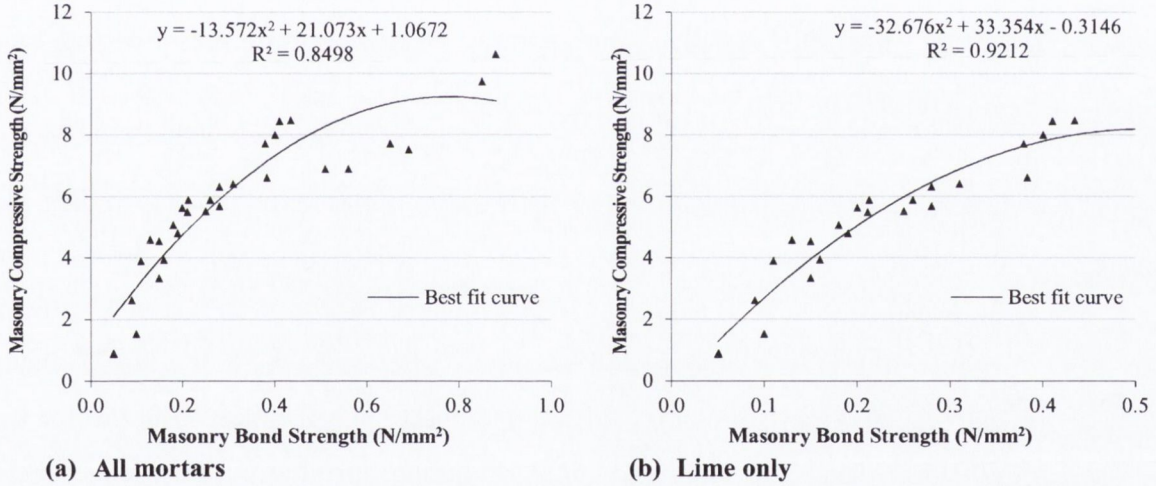

(a) All mortars (b) Lime only

Figure 5.14: Overall influence of bond strength on the CS of brick masonry during curing (includes different mortar hydraulic strengths, three curing ages and two flows)

	Mortar				Masonry					
	Compressive strength		Elastic modulus		Compressive strength		Bond strength		Elastic modulus	
Flow	*56 days*	*6 mts.*	*56 days*	*6 mts.*	*56 days*	*6 mts.*	*56 days*	*6 mts.*	*56 days*	*6 mts.*
165	20 %	33 %	80 %	71 %	7 %	4 %	8 %	6 %	75 %	67 %
170	15 %	31 %	10 %	34 %	3 %	0 %	14 %	6 %	36 %	69 %

Table 5.1: Percentage difference between the properties of NHL 3.5 and 5 mortar and masonry at 56 days and 6 months.

5.4 RELATIONSHIP BETWEEN BRICK-MASONRY ELASTIC MODULUS AND COMPRESSIVE STRENGTH

Masonry stiffness varies considerably with its compressive strength, as evidenced in the large number of studies on this relationship found in literature. Several authors (Paulay and Priestley (1992); Drysdale *et al.* (1994); Eurocode 6 EN 1996-1-1 (2005); MSJC (2002) and Vermeltfoort (2005) Mohamad *et al.* (2006) Kaushik *et al.* (2007)) assume a linear relationship between the elastic modulus (E'_m) and characteristic compressive strength of masonry (f'_m) as follows:

$$E'_m = k\, f'_m \qquad \textbf{Equation 5.1}$$

where, k is the slope of the linear regression line.

Kaushik *et al.* (2007) studied weak and strong cement-lime masonry and found (by linear regression) that the elastic modulus reached values between 250 and 1100 times the characteristic compressive strength of the masonry. By plotting elastic modulus and compressive strength results from a large number of past experimental studies, Drysdale *et al.* (1994) suggested a similar range (210-1670 times f'_m) to estimate masonry stiffness. Eurocode 6 EN 1996-1-1 (2005) suggests using a conservative k value of 1000 to estimate the elastic modulus of masonry. Other authors MSJC (2002); Paulay and Priestley (1992) and Vermeltfoort (2005) suggest approximately 700-750 for k. All of these authors studied cement and cement-lime masonry but no knowledge is available on the relationship between the elastic modulus and the characteristic compressive strength of lime-masonry. Due to the relatively low stiffness of lime materials, the k values obtained in the present study are significantly lower than those of the above authors.

Figure 5.15 plots the elastic modulus results of brick-lime masonry against the corresponding characteristic compressive strengths of the masonry. The characteristic compressive strength results are presented in Appendix E. Trend lines are drawn for each mortar hydraulic grade through the origin. Results of regression analysis are presented for each mortar grade in Table 5.2.

Table 5.2 shows that the elastic modulus of the masonry reaches values between 82 and 231 times its characteristic compressive strength. Relatively good R^2 values were found for stronger masonry (NHL 3.5, 5 and M6) while, for the lower strength masonry, R^2 was approximately 0.5. According to this research, three hydraulic strength groups are proposed for the estimation of masonry elastic modulus based on the masonry's characteristic compressive strength (Table 5.2): cement-lime masonry where $E'_m = 230f'_m$, higher hydraulic strength masonry where $E'_m = 130f'_m$ and low hydraulicity/calcium-lime masonry where $E'_m = 85f'_m$.

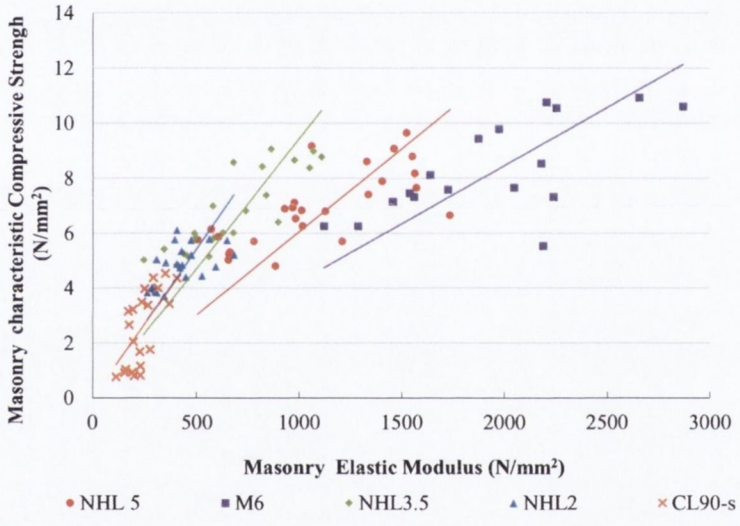

Figure 5.15: Variation of masonry elastic modulus with the characteristic CS of masonry for mortars of different hydraulic strengths

Masonry type	Relationship between E & f'_m	R^2	Proposed relationships
M6	$E = 231f'_m$	0.63	$E'_m = 230f'_m$
NHL 5	$E = 158f'_m$	0.51	$E'_m = 130f'_m$
NHL 3.5	$E = 102f'_m$	0.68	
NHL 2	$E = 88f'_m$	0.46	$E'_m = 85f'_m$
CL90-s	$E = 82f'_m$	0.48	

Table 5.2: Correlation between masonry elastic modulus and characteristic compressive strength

All of the above authors and existing design codes, assumed the relationship between masonry elastic modulus and compressive strength to be linear (Equation 5.1). However, this research evidences that this relationship is non-linear (Figures 5.15 and 5.16) which supports Mohamad *et al.* (2006), who also suggested that a polynomial curve best fitted the relationship. The results also show that as the hydraulic grade of the binder increases, the slope of the relationship between masonry elastic modulus and characteristic compressive strength decreases (Figure 5.15). Therefore, the influence of masonry stiffness (and thus mortar strength and stiffness) on the compressive strength of brick masonry becomes smaller as the hydraulic strength of the mortar increases. This supports the observations made in previous sections.

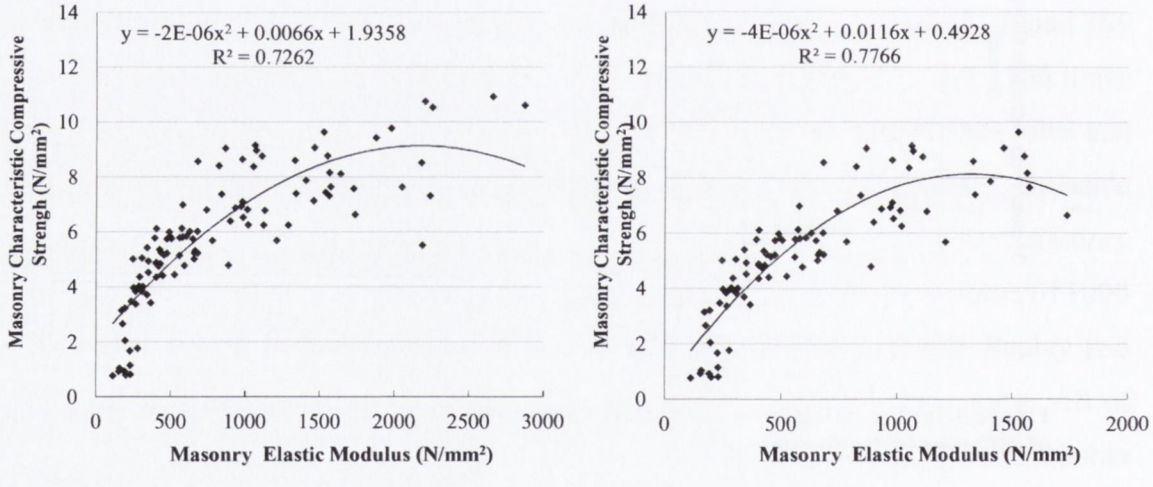

(a) All mortars **(b) Lime only**

Figure 5.16: Overall influence of elastic modulus on the CS of brick masonry during curing (includes different mortar hydraulic strengths, three curing ages and two flows)

5.5 FAILURE MODES OF BRICK MASONRY

5.5.1 Failure modes of brick masonry in compression

As previously discussed in Chapter 1, several authors, Venkatarama and Vyas (2008) and Kaushik *et al.* (2007), emphasised the influence of mortar and unit stiffness on the failure mode of masonry and related it to two situations: (a) $E_{unit} > E_{mortar}$ and (b) $E_{unit} < E_{mortar}$ (Figure 1.4). As previously mentioned, the elastic modulus in this research was measured from the linear portion of the stress-strain relationship in compression. Sarangapani *et al.* (2005) categorised masonry failure into two cases based on whether bond failure occurs or not. However, Gumaste *et al.* (2006) suggested that the failure of masonry constructed with weak mortar was primarily due to loss of the bond. Due to contradictory reports in literature, this research recognises that categorising the failure of masonry based on either mortar/unit stiffness or bond failure is insufficient and does not explain the mechanical behaviour of masonry. Furthermore, little or no previous detailed discussions on the failure modes of lime-mortar masonry have been found.

The elastic modulus of the brick used in this research is 1240 N/mm^2, as this research includes mortars of varying elastic moduli (70-1700 N/mm^2) and bond strength (0.05-0.88 N/mm^2), there are specimens available to observe the failure modes in the two situations aforementioned ($E_{unit} > E_{mortar}$ and $E_{unit} < E_{mortar}$).

(a) ($E_{unit} > E_{mortar}$)

Within this situation, two modes of failure were generally observed. Mode I, where the bond is largely maintained and failure is likely due to lateral tension in the masonry units and Mode II where failure may result from the breakdown of both the mortar and bond in combination with the lateral tensional failure of the brick. However, it should be noted that these explanations are based on generalised experimental observations in conjunction with mechanisms described by previous authors and are not definitive proof as to the failure mechanisms of masonry in compression. Furthermore, the steel plates at the top and bottom of the specimens have a restraining effect leading to uneven stress distributions. Bending of the steel plates and the theoretical 45 degree load application occurring within the specimen may also have caused uneven stress distributions. The

out-of-plane failure of the specimens may be due to the fact that they are less restrained in that direction.

- *Mode I* is generally associated with stronger/stiffer natural hydraulic lime masonry (NHL 3.5 and 5). Cracks in the masonry first appeared in the brick units at approximately 70 % of the peak load. Initially, the cracks were located on the front surface of the brick, near the vertical joints. This is because the joints are a weak point in the masonry. A small amount of mortar spalling along the horizontal joints also began to occur at this stage. As the applied force was increased, these cracks propagated up and down the height of the wallettes and final failure occurred with vertical splitting of the units. As seen in Figure 5.17, failure generally occurs without the bond between the mortar and the unit detaching.

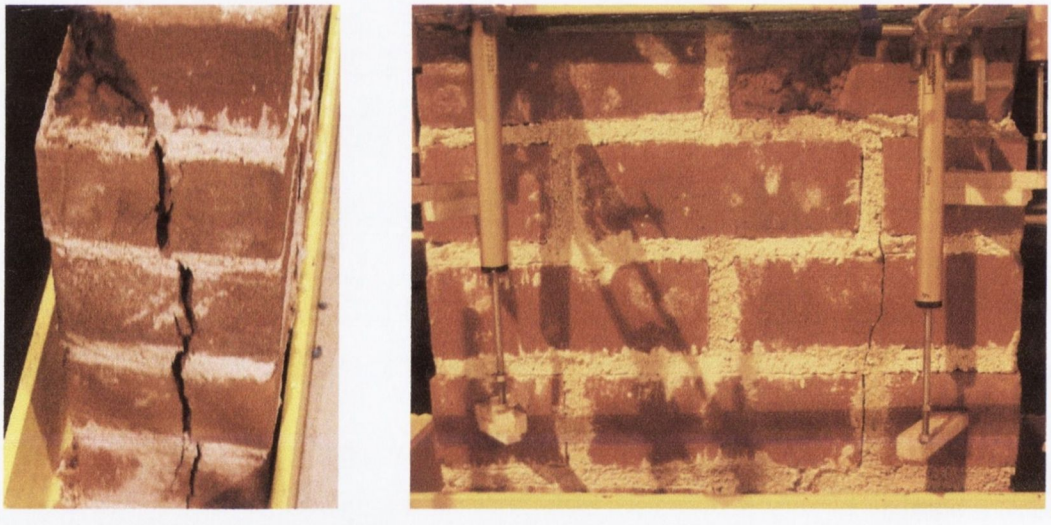

Figure 5.17: Failure of NHL 5 brick masonry specimen in compression due to lateral tension (Mode I)

The nature of the stresses involved and the failure mechanism might be explained as follows: When the masonry is initially compressed, the mortar tends to spread outwards since it is less stiff than the masonry units. However, the brick's frog and the bond at the brick-mortar interface confines the mortar laterally. This confinement leads to shear stress at the interface; therefore, the internal state of stress consists of tri-axial compression in the mortar and bi-lateral tension as well as uni-axial compression in the bricks. This state of stress

initiates vertical splitting cracks in the bricks as the masonry cannot alleviate stresses by straining alone. The specimens are less restrained in the longitudinal direction, therefore, they tend to split in the middle, due to lateral tension.

- *Mode II* generally relates to masonry constructed with more deformable mortars, NHL 2 and CL90-s. Spalling of the mortar begins earlier than in Mode I at approximately 50 % of the ultimate compressive strength. The spalling occurs because the mortar accommodates the majority of the strain experienced during early compression by spreading outwards. As the applied load continues to increase, vertical cracks are seen on all four faces of the wallette. Ultimate failure occurs due to the development of a large number of these cracks (Figure 5.18).

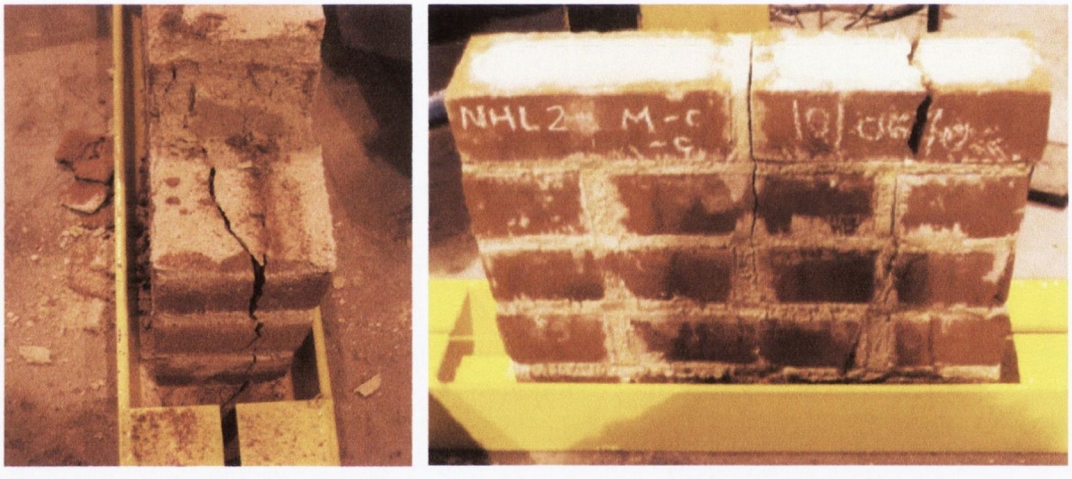

Figure 5.18: Failure of NHL 2 brick masonry in compression due to bond/mortar failure and bi-lateral tension (Mode II)

The disposal of the masonry after testing revealed that the bricks in Mode II had split vertically in both lateral directions and had become detached from the mortar. It was also noted that the mortar itself had failed turning into powder.

The nature of the stresses in the mortar and masonry units in Mode II is initially similar to those of Mode I: tri-axial compression in the mortar and bi-lateral tension combined with uni-axial compression in the bricks. However, as the masonry is further loaded, these less stiff, more deformable mortars demonstrate a greater ability to alleviate internal stresses. Nevertheless, previous authors

suggest (but have not demonstrated) that a point is reached at which the bond fails. Once this occurs, the lateral tension in the bricks increases and vertical cracks develop on both sides. Therefore, ultimate failure of the masonry may be due to a combination of bond failure and bi-lateral tensile failure of units in conjunction with the aforementioned uneven stress distributions within the specimen.

(b) $(E_{unit} < E_{mortar})$

Case b considers the situation where the elastic modulus of the mortar is greater than that of the masonry unit. This occurs for all cement-lime masonry (M6). As previously shown, increased mortar strength and stiffness results in greater bond strength. Therefore, the bond strength in this case is considerably greater than that in situation a. The application of a compressive load to this masonry induces compression and bi-axial tension in the mortar and tri-axial compression in the brick units. As the units are less stiff, they deflect outwards, however the strong bond at the brick-mortar interface confines them. Cracking is first seen in the masonry units at approximately 75 % of ultimate strength. The masonry wallette fails due to failure of the units with some diagonal shear due to the boundary confining (Figure 5.19). Upon failure, the bond at the mortar-unit interface remains intact.

Figure 5.19 Failure of M6 masonry under compression due to diagonal shear

5.5.2 Failure modes of masonry in flexure

5.5.2.1 Failure modes of flexural strength testing(Type 1 - parallel to bedding joints)

Under increasing load, the weakest of the two mortar joints within the constant moment zone eventually fractured (Figure 5.20). Two distinct modes of failure were found. Most fracture planes occurred along the interface between the bottom brick face and the bedding mortar (Mode I), although a combined failure along the joint interface and within the depth of the mortar joints was observed in a small number of the higher strength cement mortar masonry specimens (Mode II).

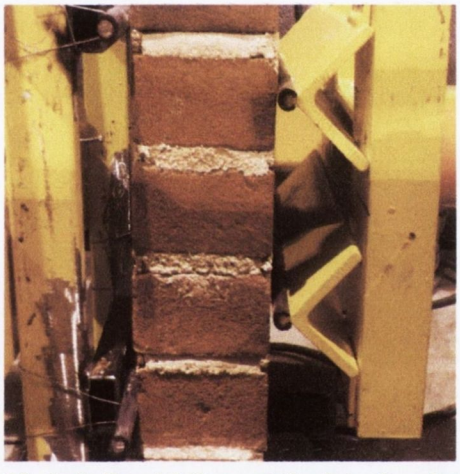

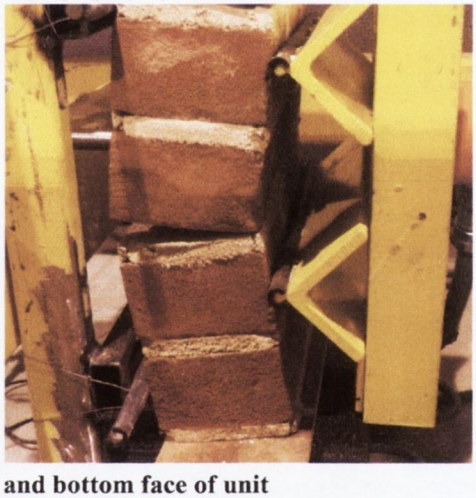

Mode I: Bond failure at the interface between bed mortar and bottom face of unit

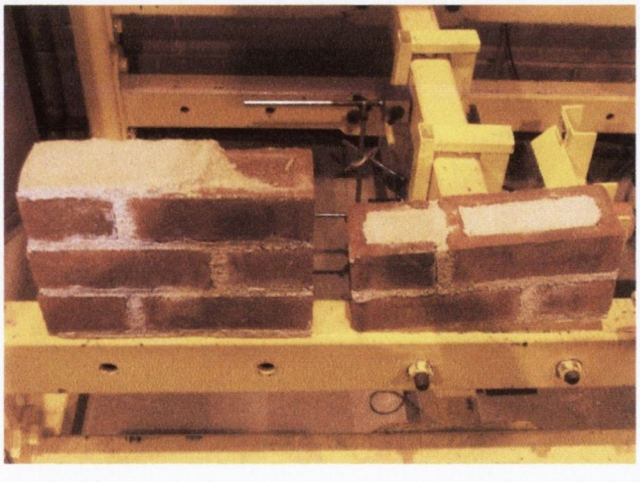

Mode II: Bond failure at the interface between bed mortar and both unit faces

Figure 5.20: Flexural strength failure modes (Type 1 - parallel to bedding joints)

5.5.2.2 Failure modes of flexural strength testing (Type 2 - perpendicular to bedding joint)

The Type 2 flexural strength tests develop tensile stresses perpendicular to the perpend joints and parallel to the bedding joints. At failure, fractures develop within the constant moment zone, from the top to the bottom of the horizontally spanning specimens. Three failure modes were identified as shown in Figure 5.21. In Mode I (lower strength mortars, CL90-s and NHL 2) the masonry fails by bond failure in the joints both parallel and perpendicular to the direction of load application, stepping up vertically and horizontally. As the bond strength of the masonry increases (NHL 2,3.5 and 5) failure is accompanied by vertical cracks passing through the units and bond failures of both the horizontal and vertical joints (Mode II). Mode III is the most common for all of the higher strength series (NHL 5 and M6). Failure in this case is due to the vertical cracking of the bricks close to vertical joints (perpends).

Mode I: Bond failure (CL90-s and NHL2)

Mode II: Combination of bond and unit failure (NHL 2, 3.5 and 5)

Mode III: Unit failure (NHL 5 and M6)

Figure 5.21: Flexural bond strength failure modes (Type 2 - perpendicular to bedding joints)

5.5.3 Bond strength failure modes (bond wrench test)

The mode of failure for each bond wrench test can be found in Appendix F. BS EN 1052-5 (2005) presents 6 modes of failure for this test. During testing this research found three distinctive modes (Figure 5.22):

- *Mode A1*: This was the most common failure mechanism. It was due to tensile fracture along the interface between the brick bed face and the adjacent mortar joint. This mode occurred for all masonry types and in approximately 95 % of tests. This is as expected, since the frog on the top face increases the contact surface area available for bond development compared to the flat bed face;
- *Mode A3*: This mode is a combination of interface and mortar joint failure and only occurred in a few occasions in the weak masonry (CL90-s and NHL 2). This is likely due to the natural variability of the materials and thus the bond generated;
- *Mode A6*: Failure at the mortar-frogface interface was noted on a small number of occasions for M6 masonry. This is likely due to a combination of the relatively high strength of the M6 mortar and a poor contact with the frog face.

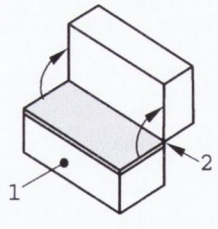

A1. Failure at the interface between mortar and upper unit face

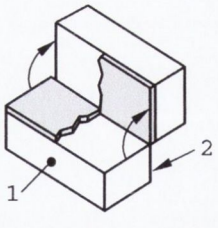

A3. Failure at the interface between mortar and both unit faces

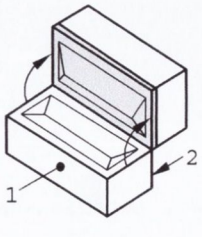

A6. Failure at the interface between mortar and frog face

Figure 5.22: Bond strength failure modes, Annex A BS EN 1052-5 (2005)

CHAPTER 6

EXTERNALLY CURED MORTAR AND BRICK MASONRY RESULTS

As mentioned in Section 2.6.2, outdoor temperatures ranged from between -7 and 19 $°C$. Several freeze-thaw events were recorded during the hardening process, the first of which occurred after 6 weeks of curing. Numerous rain showers also took place over the time period and the relative humidity varied between 60 and 95 %.

6.1 Effect of outdoor curing on mortar properties

The results indicate that outdoor curing conditions improved mortar strength and stiffness, up to 28 days (Figures 6.4-6.6). Lanas *et al.* (2006) made similar observations on both hydraulic and non-hydraulic lime mortars and suggested that strength gains were due to the higher relative humidity outdoors. However, the results show significant mortar strength losses between 28 and 56 days due to outdoor curing and the freezing weather conditions experienced. For example, NHL 5 mortar (at 165 mm flow) experiences a 25 % drop in compressive strength, while the strength of CL90-s reduces by 40 % (1.3-0.8 N/mm^2) (Figures 6.1-6.3).

In contrast, the cement-lime mortar continues to gain strength during the same time period. The drop in mortar strength and elastic modulus can generally be attributed to the freezing weather conditions experienced after 6 weeks of exposure.

Similarly to indoor curing, the compressive/flexural strength and stiffness of the cement-lime mortar (M6) were approximately twice those of the NHL mortars, irrespective of flow or curing duration. Predictably, the CL90-s mortar was the weakest and only developed an overall compressive strength between 1.3 and 1.51 N/mm^2 and an elastic modulus of 108-144 N/mm^2.

The effect of external curing was examined for two mortar water contents (165 and 170 mm flow). According to the results, the variation in mortar properties over time was generally consistent for both flows (Tables 6.1-6.3).

As previously mentioned, even though the mortar strength development over the first 28 days improves, when compared with the laboratory-cured specimens, dramatic reductions due to the freezing weather conditions were recorded between 28 and 56 days. However, in spite of these loses, the mortars continue to develop strength and stiffness between 56 days and 6 months. In particular, the compressive and flexural

strength of CL90-s mortar increased by 33-48 % and its stiffness by 25-41 %. Nevertheless, the 6-month compressive strength and elastic modulus results for outdoor curing remain substantially lower than those of laboratory-cured mortars, irrespective of mortar type or flow. The exact values are shown in Figures 6.1-6.3.

As expected, CL90-s mortars were the most damaged by freezing. In addition, the results demonstrate that the lime mortars with higher flows and thus greater water contents, tend to be more susceptible to degradation due to freezing conditions during hardening. For instance, the compressive strength of NHL 5 mortar shows a reduction of 43 % with a flow of 165 mm and 53 % when the flow is 170 mm, as a result of outdoor exposure, and the compressive strength of CL90-s mortar drops by 20 % at 165 mm flow vs. 45 % at the higher flow. The elastic modulus and flexural strength of both NHL 5 and CL90-s mortars display similar effects, with higher flow mortars losing considerably more strength and stiffness. In contrast, cement-lime mortars did not follow the same trend (increased deterioration in mechanical properties due to higher water contents) as lime mortars. Furthermore, the results do not indicate a particular mortar property is more damaged by freezing than another.

In general, when compared to laboratory mortars, all mortars (including CL90-s mortar) improve strength and stiffness up to 28 days when cured externally, but later suffer due to freezing. They recover some strength and stiffness but never achieve their full potential at 6 months compared to laboratory curing conditions.

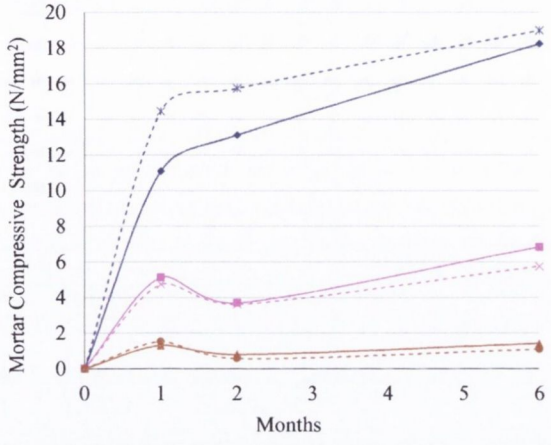

Figure 6.1: Compressive strength development of externally cured mortars [a]

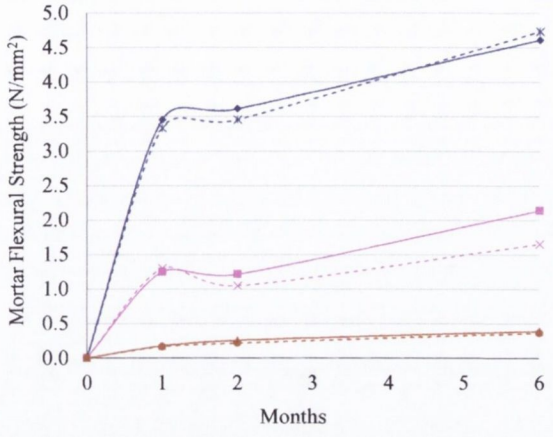

Figure 6.2: Flexural strength development of externally cured mortars [b]

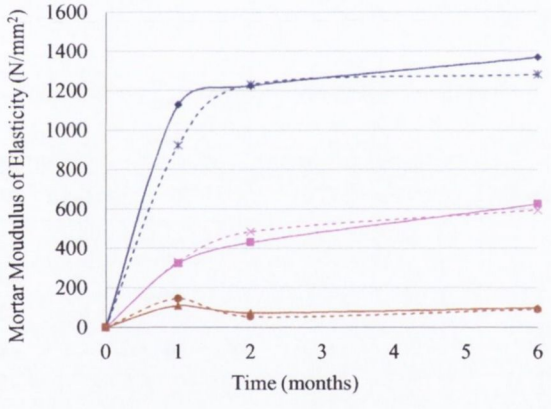

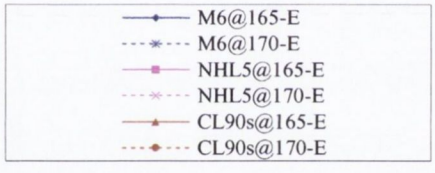

COV values were generally found to be low, except for:

[a] CL90-s@165 at 28 days

[b] CL90-s@165 at 28 and 56 days

[c] CL90-s@165 at 28 and 56 days

[d] CL90-s@170 at 28 days

Figure 6.3: Elastic modulus development of externally cured mortars [c, d]

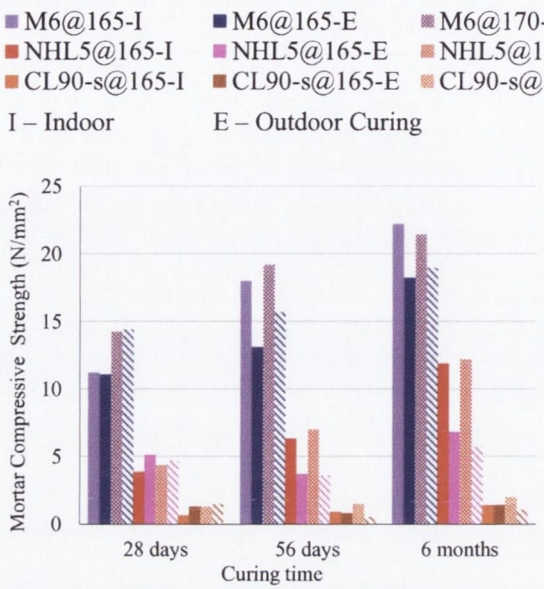

Figure 6.4: Effect of curing conditions on the compressive strength of mortar

Initial flow	Mortar type	Mix ratio	Curing Period		
			28 days	56 days	6 mts.
165	M6	1:½:4	-1 %	-27 %	-18 %
	NHL 5	0:1:3	32 %	-42 %	-43 %
	CL90-s	0:1:3	110 %	-10 %	2 %
170	M6	1:½:4	1 %	-18 %	-11 %
	NHL 5	0:1:3	8 %	-48 %	-53 %
	CL90-s	0:1:3	17 %	-63 %	-46 %

Table 6.1: Percentage change in compressive strength of mortar due to outdoor curing

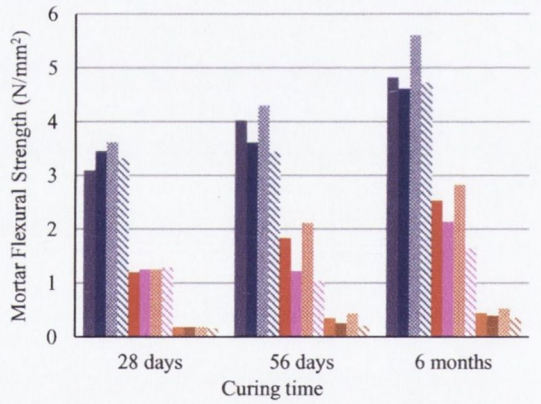

Figure 6.5: Effect of curing conditions on the flexural strength of mortar

Initial flow	Mortar type	Mix ratio	Curing Period		
			28 days	56 days	6 mts.
165	M6	1:½:4	12 %	-10 %	-4 %
	NHL 5	0:1:3	4 %	-34 %	-16 %
	CL90-s	0:1:3	-3 %	-25 %	-11 %
170	M6	1:½:4	4 %	-20 %	-16 %
	NHL 5	0:1:3	3 %	-51 %	-42 %
	CL90-s	0:1:3	-14 %	-51 %	-32 %

Table 6.2: Percentage change in flexural strength of mortar due to outdoor curing

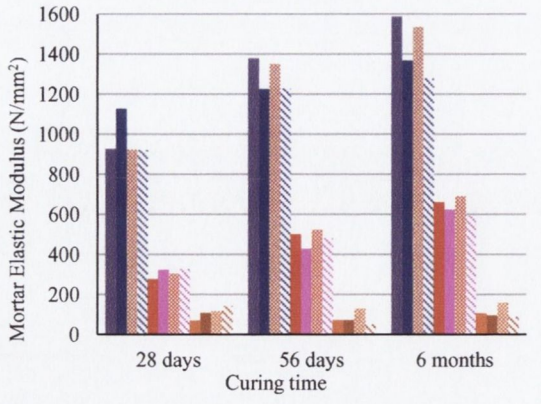

Figure 6.6: Effect of curing conditions on the elastic modulus of mortar

Initial flow	Mortar type	Mix ratio	Curing Period		
			28 days	56 days	6 mts.
165	M6	1:½:4	22 %	-11 %	-14 %
	NHL 5	0:1:3	17 %	-14 %	-5 %
	CL90-s	0:1:3	55 %	2 %	-9 %
170	M6	1:½:4	0 %	-9 %	-17 %
	NHL 5	0:1:3	8 %	-8 %	-14 %
	CL90-s	0:1:3	21 %	-60 %	-44 %

Table 6.3: Percentage change in elastic modulus of mortar due to outdoor curing

6.2 Effect of outdoor curing on masonry properties

Like the mortar specimens, the masonry wallettes were manufactured and cured in external conditions. As expected, cement-lime masonry (M6) displays the greatest strength and stiffness, followed by NHL 5 and then CL90-s masonry (Figures 6.7-6.9). Although M6 masonry far out-performs NHL 5 masonry during early curing, Figures 6.7 and 6.8 show that, over time, NHL 5 mortar can produce masonry that is almost as strong as M6 masonry in compression, whilst simultaneously remaining considerably more elastic and deformable. For example, according to the results at 6 months, M6 masonry with a compressive strength of 8.9 N/mm^2 is only 11 % stronger than NHL 5 masonry, yet NHL 5 masonry is over 30 % more deformable. It should be noted however, that the bond strength of NHL 5 masonry is significantly lower (approximately 60%) than that of the cement-lime masonry (Figure 6.9), indicating a reduced ability to resist lateral loads. This was also evidenced in the laboratory cured masonry.

As expected, the CL90-s mortar masonry was the weakest, however, it developed a significant compressive strength of 2.99 N/mm^2 despite the weather. The elastic modulus of CL90-s brick masonry ranges between 200 and 300 N/mm^2 when cured outdoors.

It is interesting to note that, in spite of the freezing weather conditions experienced after approximately 6 weeks, all of the masonries continued to gain significant strength and stiffness over time (unlike the respective mortars which, as seen in the previous section were adversely affected). This suggests the masonry units protect the mortar. It is especially remarkable for the weakest mortars (CL90-s), since they are generally considered highly susceptible to poor weather conditions. Between 56 days and 6 months, the compressive strength of CL90-s masonry increases by 14 %, the elastic modulus by 25 % and most interestingly, the bond strength rises by approximately 50 % (Figures 6.7-6.9).

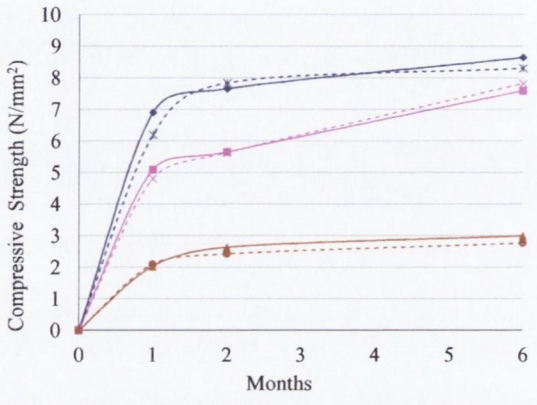

Figure 6.7: Compressive strength development of externally-cured brick masonry [a]

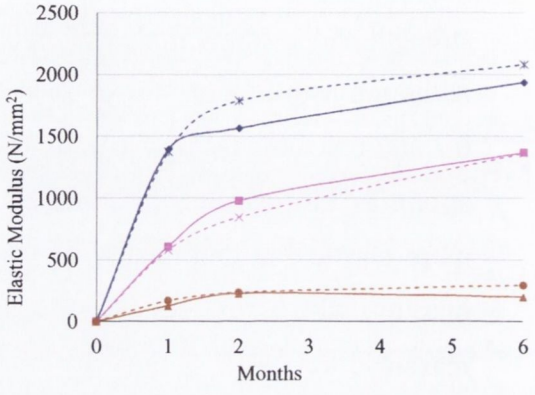

Figure 6.8: Elastic modulus development of externally-cured brick masonry [b]

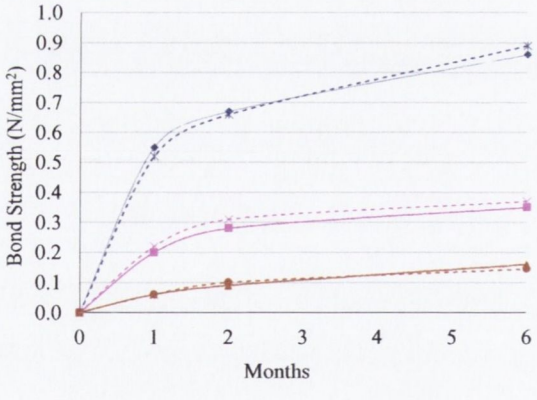

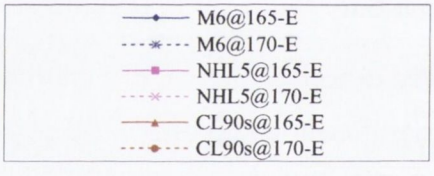

COV values were generally found to be low, except for:

[a] CL90-s @165 and 170 mm at 28 days

[b] All CL90-s results

[c] CL90-s @165 mm at 56 days

[d] CL90-s @170 mm at 56 days and 6 months

Figure 6.9: Bond strength development of externally-cured brick masonry [c, d]

Comparisons between laboratory (I) and outdoor cured (E) masonry results are presented in Figures 6.10-6.12. In contrast to outdoor cured mortars which increased in strength and stiffness during the first 28 days as a result of outdoor curing, cement-lime mortar masonry was not significantly affected and lime-mortar masonry showed a general decrease in strength and stiffness (inconsistencies in some CL90-s results can be associated to relatively high COV values. These are probably due to material variability and inconsistences in construction).

The results indicate that outdoor curing generally leads to a loss of the ultimate masonry compressive strength, elastic modulus and bond strength at 6 months. This is consistent with the effect of outdoor curing on mortars in the previous section. However, according to the results, the masonry is generally less affected by the curing environment that the mortar. The compressive strengths of mortars dropped by between 11 and 53 % whereas the masonry only reduced by 5-24 %. Similarly, the elastic modulus of the mortars dropped by approximately 5-44 % whereas the masonry by only reduced by 1-15 % due to outdoor curing conditions (Tables 6.4-6.6).

In contrast to the outdoor cured mortar results aforementioned, masonry specimens with higher flow mortar were not more adversely affected due to outdoor curing than those with lower flow.

The results do not show a particular masonry type being more affected by outdoor curing than any other. Furthermore, no consistent trend was found that might indicate that a particular masonry property is further damaged by freezing than others.

In general, all masonry types tend to loose strength and stiffness during curing as a results of outdoor exposure with the exception of CL mortar masonry which consistently improves stiffness and also improves compressive strength up to 28 days and bond strength up to 56 days. As previously mentioned, these inconsistencies are associated to high COV values, which are probably due to material variability and inconsistencies in construction.

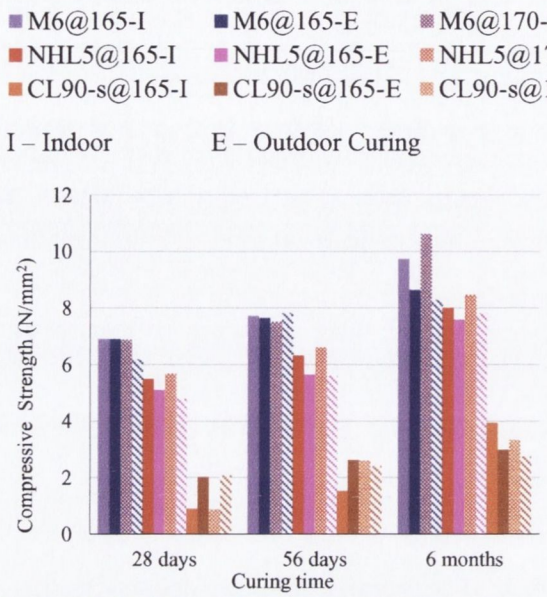

Figure 6.10: Effect of curing conditions on the compressive strength of brick masonry

Initial flow	Mortar type	Mix ratio	Curing Period		
			28 days	56 days	6 mts.
165	M6	1:½:4	0 %	-1 %	-11 %
	NHL 5	0:1:3	-11 %	-11 %	-5 %
	CL90-s	0:1:3	128 %	72 %	-24 %
170	M6	1:½:4	-10 %	4 %	-22 %
	NHL 5	0:1:3	-13 %	-15 %	-8 %
	CL90-s	0:1:3	138 %	-8 %	-17 %

Table 6.4: Percentage change in the CS of brick-masonry due to outdoor curing

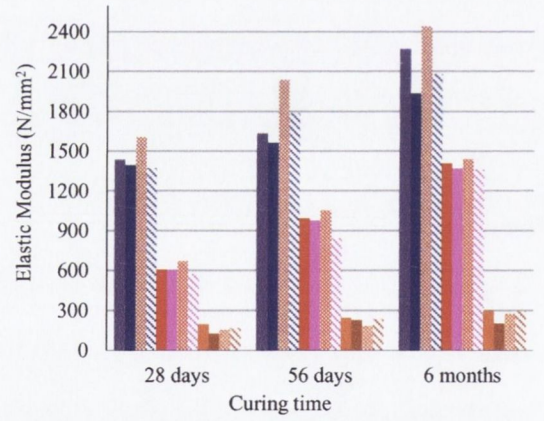

Figure 6.11: Effect of curing conditions on the elastic modulus of brick masonry

Initial flow	Mortar type	Mix ratio	Curing Period		
			28 day	56 days	6 mts.
165	M6	1:½:4	-3 %	-4 %	-15 %
	NHL 5	0:1:3	-10 %	-1 %	-3 %
	CL90-s	0:1:3	-36 %	-6 %	-33 %
170	M6	1:½:4	-14 %	-12 %	-15 %
	NHL 5	0:1:3	-5 %	-20 %	-5 %
	CL90-s	0:1:3	10 %	30 %	7 %

Table 6.5: Percentage change in the elastic modulus of brick-masonry due to outdoor curing

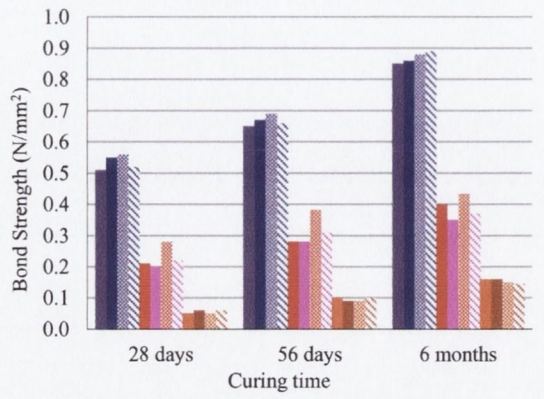

Figure 6.12: Effect of curing conditions on the bond strength of brick masonry

Initial flow	Mortar type	Mix ratio	Curing Period		
			28 day	56 days	6 mts.
165	M6	1:½:4	8 %	3 %	1 %
	NHL 5	0:1:3	-5 %	1 %	-12 %
	CL90-s	0:1:3	18 %	-10 %	0 %
170	M6	1:½:4	-7 %	-4 %	1 %
	NHL 5	0:1:3	-21 %	-19 %	-15 %
	CL90-s	0:1:3	22 %	6 %	-3 %

Table 6.6: Percentage change in the BS of brick-masonry due to outdoor curing

CHAPTER 7

STONE MASONRY RESULTS AND DISCUSSION

Only low-strength lime binders (CL90-s and NHL 2) were investigated in stone masonry because they are the most commonly used in Ireland for repairs to historic and traditional stone masonry. Due to inconsistencies in the results and the relatively small amount of stone masonry data, it was not feasible to investigate the influence of mortar mechanical properties on those of stone masonry in as much detail as for brick masonry in Chapter 5.

As previously mentioned, both cut and broken stone units were investigated in order to explore the influence of the surface characteristics on the strength and stiffness of masonry. This was deemed important due to the lack of agreement in previous studies aforementioned, especially in respect to the relationship between masonry bond and compressive strength.

7.1 MECHANICAL PROPERTIES OF STONE MASONRY

7.1.1 Limestone

Limestone masonry (both cut and broken) only achieves 15.58-23.96 N/mm^2 compressive strength at 28 days, which equates to approximately 30 % of the normalised limestone compressive strength (74.05 N/mm^2). According to research by previous authors, broken interfaces should increase bond strength as a result of the mechanical bond increase). Therefore, according to some authors, the compressive strength of broken limestone should be superior to that of cut limestone. However, the results indicate that it is the opposite at all curing ages. Irrespective of the mortar water content (flow), the compressive strength of the cut limestone is consistently superior to that of the broken limestone masonry, with the exception of NHL 2 at 28 days (Table 7.1). Nevertheless, the broken limestone masonry consistently produces a superior bond (Table 7.3). This disagrees with the brick masonry results, which demonstrated that the compressive strength of the masonry increases with the bond strength. This is likely due to micro cracking induced in the limestone when broken at the quarry and the rougher surface of the broken limestone units leading to point loading and thus a lower compressive strength.

Point loading and internal micro cracks may have caused premature failure of the broken limestone masonry under compression. The heights of the broken limestone units varied by ± 3 mm, therefore the top and bottom surfaces were not perfectly level in some instances. These dimensional inconsistencies caused variations in mortar thickness across the joint, which may have led to point-loading and premature failure due to induced stresses in the masonry. Furthermore, the geometry of the specimens affects the strength results and as noted in Chapter 2, the heights of the cut and broken masonry prisms and the number of units in each prism are different.

The elastic modulus of cut limestone masonry ranges (542.55-1636.58 N/mm^2) and broken limestone (798.3-1327 N/mm^2) demonstrating a significant overlap in the results. However, NHL 2 cut limestone masonry was found to be consistently stiffer than that of broken limestone masonry whereas the opposite can be seen for CL90-s masonry (Table 7.2). This is likely due to point loading, micro cracking and premature failure of the CL90-s broken limestone masonry and is examined in more detail in Section 7.3.1.

In both broken and cut limestone masonry, increasing the mortar water content significantly increases the compressive strength, stiffness and bond strength of the NHL 2 limestone masonry and generally lowers the compressive strength stiffness and bond strength of the CL90-s one. This is consistent with the brick masonry results discussed in Chapter 4. According to the results, the compressive strength of broken limestone was more influenced by a rise in flow than that of cut limestone however, no greater influence on bond or stiffness was found for one surface type over another.

7.1.2 Sandstone

As expected, the NHL 2 mortar consistently provides a stronger and stiffer sandstone masonry with a greater bond than that of CL90-s mortar, irrespective of flow or curing duration. For example, at six months and 170 mm flow, NHL 2 masonry reaches a compressive strength of 15.45 N/mm^2, elastic modulus of 1005.56 N/mm^2 and bond strength of 0.112 N/mm^2 whereas Cl90-s masonry only reaches values of 14.52, 635.3 and 0.058 N/mm^2 respectively at the same flow (Tables 7.1-7.3).

A rise in the mortar water content increases the strength of both the NHL 2 and CL90-s sandstone masonry however; the increases are more significant with the higher hydraulic strength masonry (NHL 2).

Sandstone masonry only reaches a fraction of the sandstone unit's compressive strength. At 6 months, sandstone masonry constructed with weak mortars (NHL 2/CL90-s) achieves a compressive strength of (14.41-15.45 N/mm^2), equating to approximately 30 % of the normalised compressive strength of the sandstone units (49.57 N/mm^2). This further demonstrates that the compressive strength of the unit plays a significant role in determining masonry compressive strength.

7.1.3 Limestone vs. sandstone

The sandstone masonry reaches a significantly lower compressive strength and stiffness than the limestone masonry at all ages, irrespective of the mortar water content and the lime hydraulic strength. As stated above, the sandstone reaches a compressive strength of (14.41-15.45 N/mm^2) and elastic modulus of (631.5-1005.56 N/mm^2) at six months while the limestone reaches (23.43-30.54 N/mm^2) and (669.9-1636.58 N/mm^2) respectively. This is probably due to the greater strength and stiffness of the limestone units.

The results indicate that when the units are significantly stronger than the mortar (as is the case for stone masonry in this research), the unit strength and not suction or bond strength, governs masonry compressive strength. According to previous results, masonry strength usually increases with the bond therefore the limestone masonry, with a greater strength and stiffness than the sandstone masonry, should have achieved a higher bond but this was not found to be the case. As previously mentioned, NHL 2 sandstone masonry exhibits the greatest bond strength (nearly two times greater than the corresponding broken-limestone prisms (Table 7.3)). Cut-limestone masonry incorporating CL90-s mortars performed the poorest (0.032-0.034 N/mm^2 at 56 days).

The variations in stone masonry compressive strength, elastic modulus and bond strength over time and in relation to water content as well as their associations are discussed in the following sections.

Unit type	Flow (mm)	Mortar type	28 days (N/mm^2)	*COV (%)*	56 days (N/mm^2)	*COV (%)*	6mts. (N/mm^2)	*COV (%)*
Broken Limestone	165	NHL 2	18.59	*3.11*	21.88	*8.93*	24.55	*17.16*
		CL90-s	15.58	*11.78*	20.68	*7.09*	25.26	*3.10*
	170	NHL 2	23.96	*15.44*	26.95	*1.55*	28.09	*2.44*
		CL90-s	10.67	*37.23*	19.13	*3.58*	23.43	*8.28*
Cut Limestone	165	NHL 2	19.04	*15.88*	28.11	*6.02*	30.54	*2.37*
		CL90-s	18.20	*25.49*	23.43	*1.44*	26.15	*2.40*
	170	NHL 2	20.43	*14.33*	29.60	*9.18*	32.38	*0.39*
		CL90-s	20.83	*3.46*	22.20	*3.94*	25.18	*5.38*
Broken Sandstone	165	NHL 2	12.54	*23.77*	13.91	*11.26*	14.87	*9.82*
		CL90-s	11.63	*12.84*	12.93	*6.35*	14.41	*4.44*
	170	NHL 2	15.01	*2.20*	15.29	*5.41*	15.45	*4.96*
		CL90-s	11.86	*9.64*	13.33	*11.86*	14.52	*8.26*

Table 7.1: Compressive strength results for stone masonry

Unit type	Flow (mm)	Mortar type	28 days (N/mm^2)	*COV (%)*	56 days (N/mm^2)	*COV (%)*	6mts. (N/mm^2)	*COV (%)*
Broken Limestone	165	NHL 2	868.58	*28.19*	957.59	*10.85*	1008.60	*11.14*
		CL90-s	877.58	*24.04*	894.34	*10.98*	976.99	*9.23*
	170	NHL 2	1068.80	*10.10*	1064.60	*22.43*	1327.00	*8.65*
		CL90-s	602.80	*46.56*	807.03	*4.94*	798.30	*11.24*
Cut Limestone	165	NHL 2	1157.80	*8.77*	1260.59	*6.78*	1465.87	*3.82*
		CL90-s	582.65	*14.95*	618.79	*31.26*	756.60	*18.23*
	170	NHL 2	1368.68	*11.73*	1712.00	*13.99*	1636.58	*2.27*
		CL90-s	542.55	*21.26*	612.64	*14.96*	669.90	*14.46*
Broken Sandstone	165	NHL 2	675.36	*17.11*	834.18	*19.81*	926.14	*9.91*
		CL90-s	506.76	*8.34*	586.8	*13.51*	631.5	*5.46*
	170	NHL 2	764.14	*9.18*	922.68	*2.57*	1005.56	*2.95*
		CL90-s	510.50	*4.49*	586.76	*9.91*	635.30	*22.02*

Table 7.2: Elastic modulus results for stone masonry

Unit type	Flow (mm)	Mortar type	28 days (N/mm^2)	*COV (%)*	56 days (N/mm^2)	*COV (%)*	6mts. (N/mm^2)	*COV (%)*
Broken Limestone	165	NHL 2	0.029	*28.83*	0.052	*25.94*	0.060	*18.88*
		CL90-s	0.028	*25.79*	0.041	*19.38*	0.048	*26.99*
	170	NHL 2	0.039	*24.09*	0.057	*26.73*	0.063	*21.32*
		CL90-s	0.027	*21.08*	0.039	*24.93*	0.043	*32.24*
Cut Limestone	165	NHL 2	0.028	*32.25*	0.045	*34.79*	0.051	*30.26*
		CL90-s	0.026	*33.31*	0.032	*62.11*	0.044	*32.56*
	170	NHL 2	0.034	*28.63*	0.050	*36.26*	0.059	*33.15*
		CL90-s	0.025	*32.68*	0.034	*28.70*	0.041	*28.78*
Broken Sandstone	165	NHL 2	0.061	*29.45*	0.082	*25.74*	0.103	*32.32*
		CL90-s	0.033	*38.78*	0.043	*26.37*	0.056	*27.80*
	170	NHL 2	0.068	*29.77*	0.093	*30.81*	0.112	*18.61*
		CL90-s	0.034	*25.06*	0.050	*47.06*	0.058	*38.86*

Table 7.3: Bond strength results for stone masonry

7.2 INFLUENCE OF WATER CONTENT ON THE PROPERTIES OF STONE MASONRY

The results clearly indicate that the water content of the mortar has a significant impact on the mechanical properties of the resultant masonry irrespective of unit type (Tables 7.4-7.12). All the NHL 2 masonry, as well as the CL90-s sandstone masonry, benefit from an increase in mortar flow, while CL90-s limestone masonry mainly experiences strength, stiffness and bond losses, due to an increase in mortar flow.

Many variables affect the influence of water content on masonry properties such as; strength, moisture transfer and surface roughness properties of the unit in addition to specimen size and shape and joint geometry etc. However, the gains in NHL 2 masonry are likely due to the hydraulic mortar hydrating better whereas CL90-s mortar does not benefit from this since extra water does not trigger hydration. Contrary to the CL90-s limestone masonry, the CL90-s sandstone masonry shows a significant enhancement in bond strength (4-16%) and marginal increases in compressive strength and stiffness (0-3%) as a result of increasing flow. This is probably due to the greater suction of the sandstone units removing a sufficient portion of the additional water in the CL90-s mortar to prevent a reduction in its strength and stiffness. The greater transfer of moisture between the mortar and the units (due to sandstone suction) may also account for the greater bond strength of the CL90-s sandstone masonry since, as previously discussed, this mechanism strengthens the bond.

The limestone masonry results agree with those of brick masonry in Chapter 4 (NHL2 masonry gaining strength and stiffness due to increased water content whereas CL90-s masonry is adversely affected). Furthermore, water content has a greater impact on stone masonry properties during the first 28 days of curing, also agreeing with the brick masonry results.

As in brick masonry, improvements in compressive strength, due to increased water content, are generally accompanied by gains in stiffness and bond strength while, compressive strength losses are coupled to losses in stiffness and bond strength.

According to the results, the broken limestone masonry is the most influenced by water content variations, generally experiencing the greatest changes in strength and stiffness.

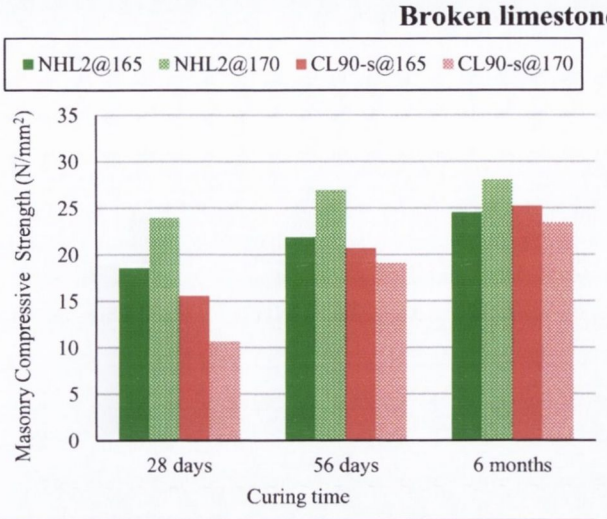

Figure 7.1: Compressive strength of broken-limestone masonry at varying hydraulic strength and flow

Mortar type	Mix ratio	Curing period		
		28 days	56 days	6 mts.
NHL 2	0:1:3	29 %	23 %	14 %
CL90-s	0:1:3	-31 %	-7 %	-7 %

Table 7.4: Percentage change in the CS of masonry due to the increase in initial flow

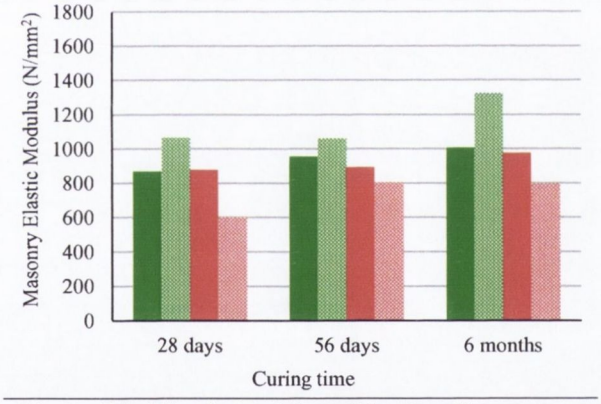

Figure 7.2: Elastic modulus of broken-limestone masonry at varying hydraulic strength and flow

Mortar type	Mix ratio	Curing period		
		28 days	56 days	6 mts.
NHL 2	0:1:3	19 %	10 %	24 %
CL90-s	0:1:3	-46 %	-11 %	-22 %

Table 7.5: Percentage change in the E-modulus of masonry due to the increase in initial flow

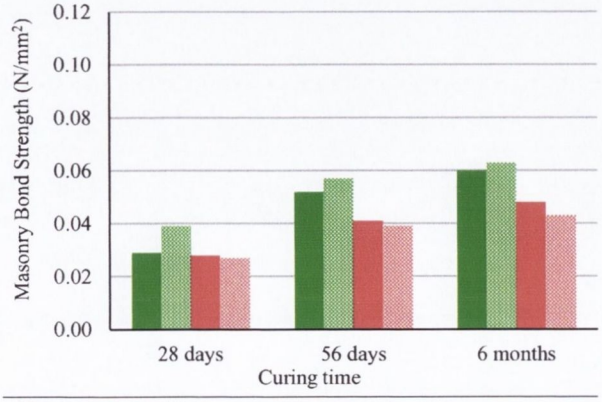

Figure 7.3: Bond strength of broken-limestone masonry at varying hydraulic strength and flow

Mortar type	Mix ratio	Curing period		
		28 days	56 days	6 mts.
NHL 2	0:1:3	34 %	10 %	5 %
CL90-s	0:1:3	-4 %	-5 %	-10 %

Table 7.6: Percentage change in the BS of masonry due to the increase in initial flow

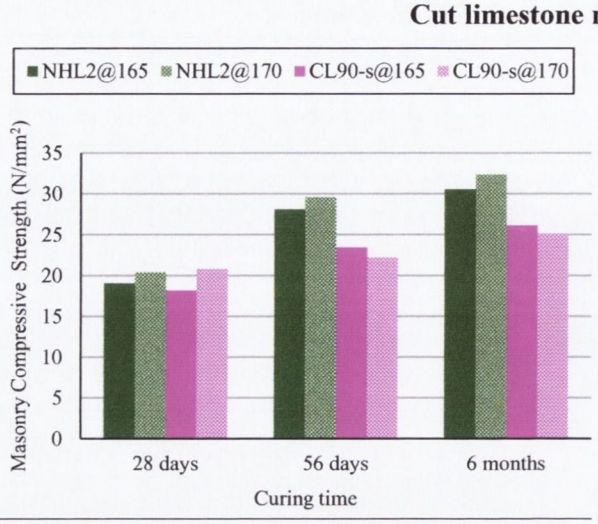

Figure 7.4: Compressive strength of cut-limestone masonry at varying hydraulic strength and flow

Mortar type	Mix ratio	Curing period		
		28 days	56 days	6 mts.
NHL 2	0:1:3	7 %	5 %	6 %
CL90-s	0:1:3	14 %	-5 %	-4 %

Table 7.7: Percentage change in the CS of masonry due to the increase in initial flow

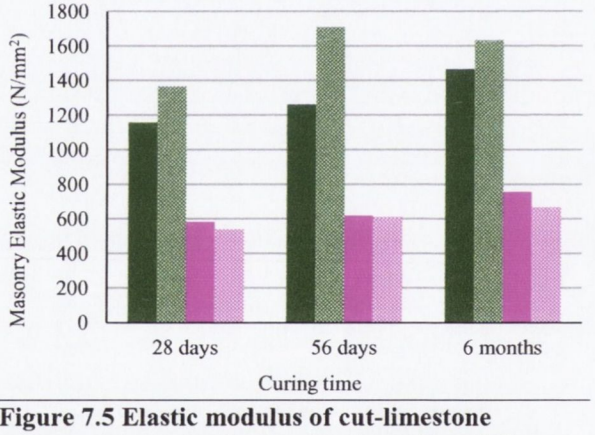

Figure 7.5 Elastic modulus of cut-limestone masonry at varying hydraulic strength and flow

Mortar type	Mix ratio	Curing period		
		28 days	56 days	6 mts.
NHL 2	0:1:3	18 %	36 %	12 %
CL90-s	0:1:3	-7 %	-1 %	-11 %

Table 7.8: Percentage change in the E-modulus of masonry due to the increase in initial flow

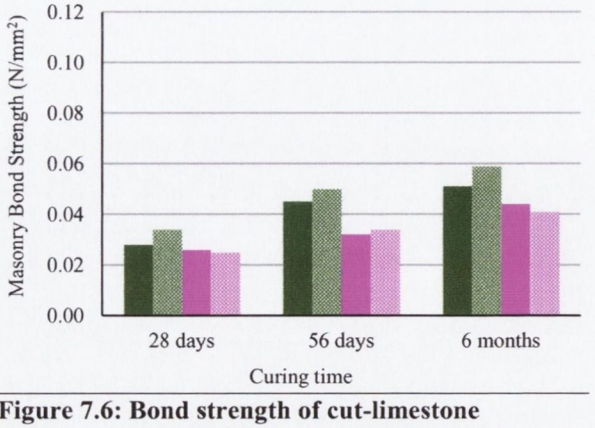

Figure 7.6: Bond strength of cut-limestone masonry at varying hydraulic strength and flow

Mortar type	Mix ratio	Curing period		
		28 days	56 days	6 mts.
NHL 2	0:1:3	21 %	11 %	16 %
CL90-s	0:1:3	-4 %	6 %	-7 %

Table 7.9: Percentage change in the BS of masonry due to the increase in initial flow

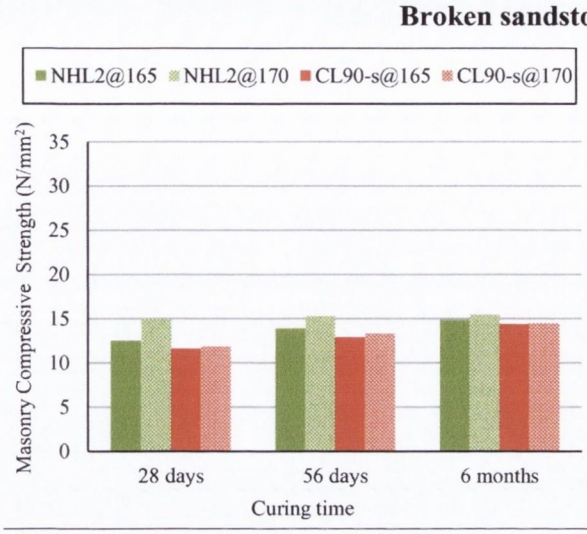

Figure 7.7 Compressive strength of broken-sandstone masonry at varying hydraulic strength and flow

Mortar type	Mix ratio	Curing period		
		28 days	56 days	6 mts.
NHL 2	0:1:3	20 %	10 %	4 %
CL90-s	0:1:3	2 %	3 %	1 %

Table 7.10: Percentage change in the CS of masonry due to the increase in initial flow

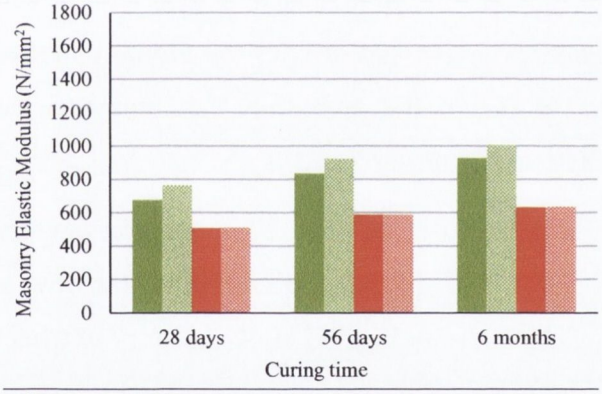

Figure 7.8: Elastic modulus of broken-sandstone masonry at varying hydraulic strength and flow

Mortar type	Mix ratio	Curing period		
		28 days	56 days	6 mts.
NHL 2	0:1:3	13 %	11 %	9 %
CL90-s	0:1:3	1 %	0 %	1 %

Table 7.11: Percentage change in the E-modulus of masonry due to the increase in initial flow

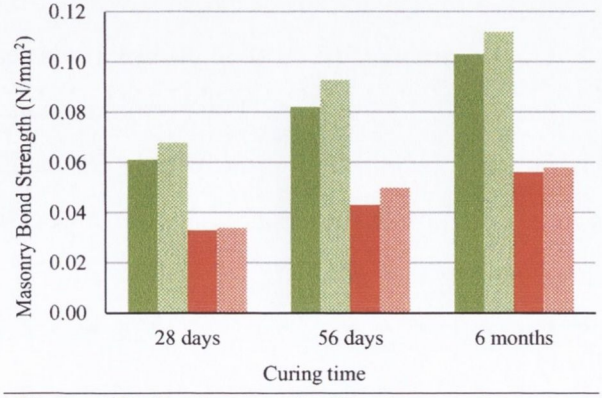

Figure 7.9: Bond strength of broken-sandstone masonry at varying hydraulic strength and flow

Mortar type	Mix ratio	Curing period		
		28 days	56 days	6 mts.
NHL 2	0:1:3	11 %	13 %	9 %
CL90-s	0:1:3	5 %	16 %	4 %

Table 7.12: Percentage change in the BS of masonry due to the increase in initial flow

7.3 STONE MASONRY STRENGTH DEVELOPMENT OVER TIME

7.3.1 Compressive strength

The results presented in Figures 7.10-7.12 show that all of the stone masonry types studied attained the largest proportion of their ultimate strength and stiffness during the first 28 days of curing, after which they continue to develop strength up to 6 months. This occurs regardless of mortar type (CL90-s/ NHL 2) and supports aforementioned brick masonry findings in respect to strength and stiffness development.

Irrespective of curing duration, the compressive strength of limestone and sandstone masonry is vastly greater than that of their constituent mortars. The maximum compressive strength achieved by NHL 2 limestone masonry at 6 months was 32.38 N/mm^2, whereas the mortar's strength was 2.35 N/mm^2. Similarly, the maximum compressive strength achieved by CL90-s limestone masonry was 26.15 vs. 1.52 N/mm^2 for the mortar (Tables 7.1 and 3.5). This agrees with the aforementioned fact that the strength of the masonry is determined by the strength of the units when the unit strength is significantly greater than that of the mortar.

According to Figure 7.10, stone masonry built with NHL 2 mortar consistently out-performs CL90-s mortar masonry at any curing age, irrespective of mortar flow or unit type. This observation is consistent with earlier findings on brick-masonry in Chapter 4.

Also similar to the brick-masonry constructed with the weakest mortars (CL90-s and NHL 2), relatively small increases in mortar compressive strength over time are coupled with significant gains in masonry strength. For example: between 28 and 56 days, CL90-s and NHL2 mortars increase by approximately (0.19-0.42 N/mm^2) whereas cut limestone for instance, generally gains 1.37-9.17 N/mm^2. This remains consistent irrespective of curing time, mortar flow or masonry unit type (Table 7.1 and 3.5). Therefore, as the compressive strength of the mortar increases, a greater proportion of the masonry unit strength is utilised for masonry strength.

In spite of the significant influence that variations in mortar strength have on the strength of stone masonry, the results show that the strongest masonry units produce the strongest masonry. The influence of the unit strength on the strength development of

masonry is consistent at all curing times, for example, at 56 days, the greatest compressive strengths (28.11-29.6 N/mm^2) were achieved by cut-limestone masonry, while broken-sandstone specimens (12.9-15.3 N/mm^2) were the weakest. This further indicates that the compressive strength of masonry is more dependent on the strength of the unit than on the mortar strength.

7.3.2 Elastic modulus

Stone masonry compressive strength and stiffness generally increase proportionally over time and usually the strongest masonry is also the stiffest. For example, according to the results, at 56 days, the weakest masonry (broken sandstone/CL90-s mortar) is also the most deformable with a mean elastic modulus of 586 N/mm^2, while the strongest masonry (cut limestone/NHL 2 mortar) is the stiffest, ranging from 1261-1712 N/mm^2. However, this relationship is not maintained for all of the stone masonry types studied. At 56 days, NHL 2 sandstone specimens are significantly stiffer but weaker than CL90-s cut-limestone ones (E: 824-922 vs. 615 N/mm^2 and CS: 13.9-15.2 vs. 22.2-23.4 N/mm^2) (Figures 7.10 and 7.11).

This indicates that the deformability/stiffness of the masonry is more related to the elastic modulus of the mortar than to the strength or stiffness of the unit, thus supporting observations by Mohamad *et al.* (2006) on cement/brick masonry. Mohamad *et al.* (2006) concluded that that the mechanical properties of mortar govern the non-linear deformation of cement mortar masonry.

Irrespective of curing time, NHL 2 mortars tend to produce considerably stiffer masonry than CL90-s mortars (NHL 2 sandstone masonry is approximately 50 % stiffer than CL90-s sandstone masonry). A similar trend exists for broken-limestone masonry at all curing times, which intensifies at higher flows. The superior stiffness that the NHL 2 mortar provides is magnified in the cut-stone masonry where the NHL 2 masonry is more than two times stiffer than the CL90-s masonry.

According to the results, the vast majority (over 70 %) of stone-masonry stiffness is developed during the first 28 days of curing. These results are consistent with the stone masonry compressive strength results and previous brick masonry and mortar results,

which show that mortars and brick masonry also attained significant values of strength and stiffness in the first 28 days of curing (Table 7.13).

7.3.3 Bond strength

Similarly to compressive strength and elastic modulus, the bond strength of stone-masonry consistently increases over time (Figure 7.12). At 56 days, the bond has generally reached 73-91 % of its 6-month value. In stone masonry, the bond takes longer to develop than the compressive strength and stiffness: after 28 days, bond strength has only reached 45-63 % of its 6-month value, while, as previously mentioned, the stone masonry compressive strength and elastic modulus have reached 62-85 % and 76-90 % of their 6-month value respectively (Table 7.13).

This is generally consistent with the CL90-s/NHL 2 brick masonry results where, at 28 days, the bond strength reaches 58-61 % (of its 6-month) compared to 78-81 % for the compressive strength and 55-66% for elastic modulus (Table 4.11). The only exception is CL90-s brick masonry compressive strength. This is likely due to several relatively high COV values at 28 days.

This suggests that once a small bond is achieved; confinement of the mortar in the joint takes place between the units during compression, thus increasing the masonry compressive strength, as previously discussed in chapter 5.

As expected, over time, the NHL 2 mortar generally provides greater bond strengths than the CL90-s mortar, irrespective of unit type and mortar water content (Figure 7.12).

Masonry constructed with sandstone consistently produces the strongest bond, irrespective of mortar type or curing duration (Table 7.3). Additionally, sandstone masonry gains a higher percentage of its 6-month bond strength at 28 days than limestone masonry. Therefore, not only does the greater suction of the sandstone result in greater bond strengths, it also plays a significant role in early bond strength development.

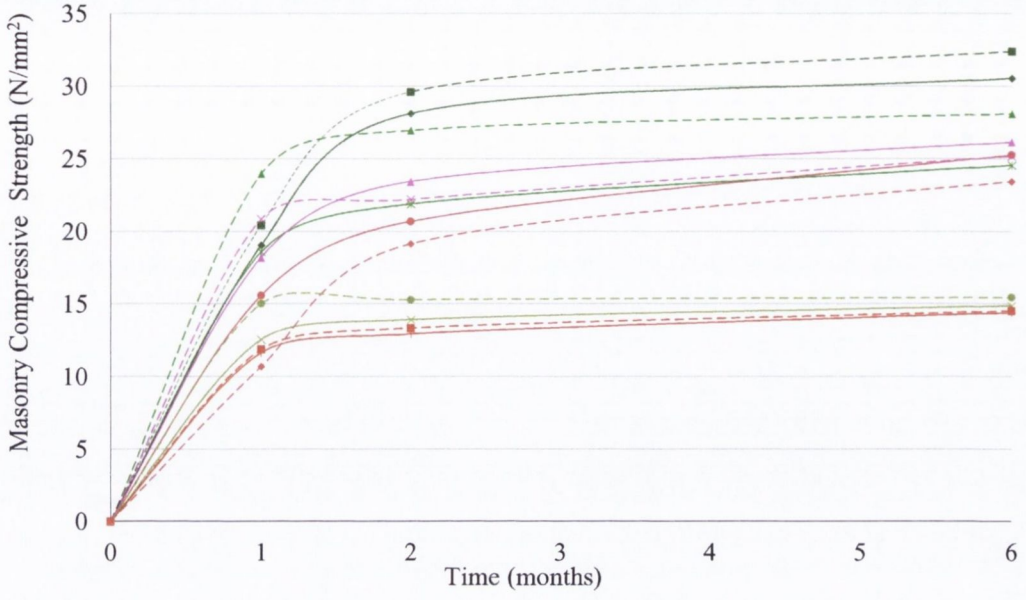

Figure 7.10: Compressive strength development of stone masonry over time.

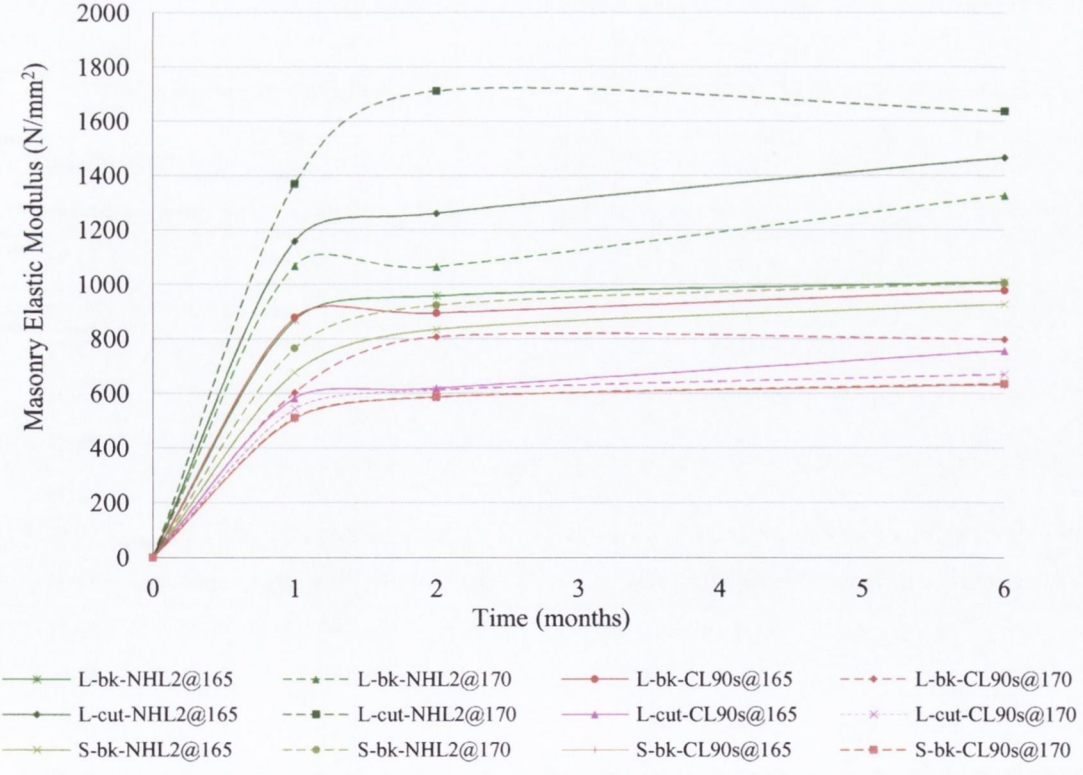

L-limestone; S-sandstone; bk-broken

Figure 7.11: Elastic modulus development of stone masonry over time.

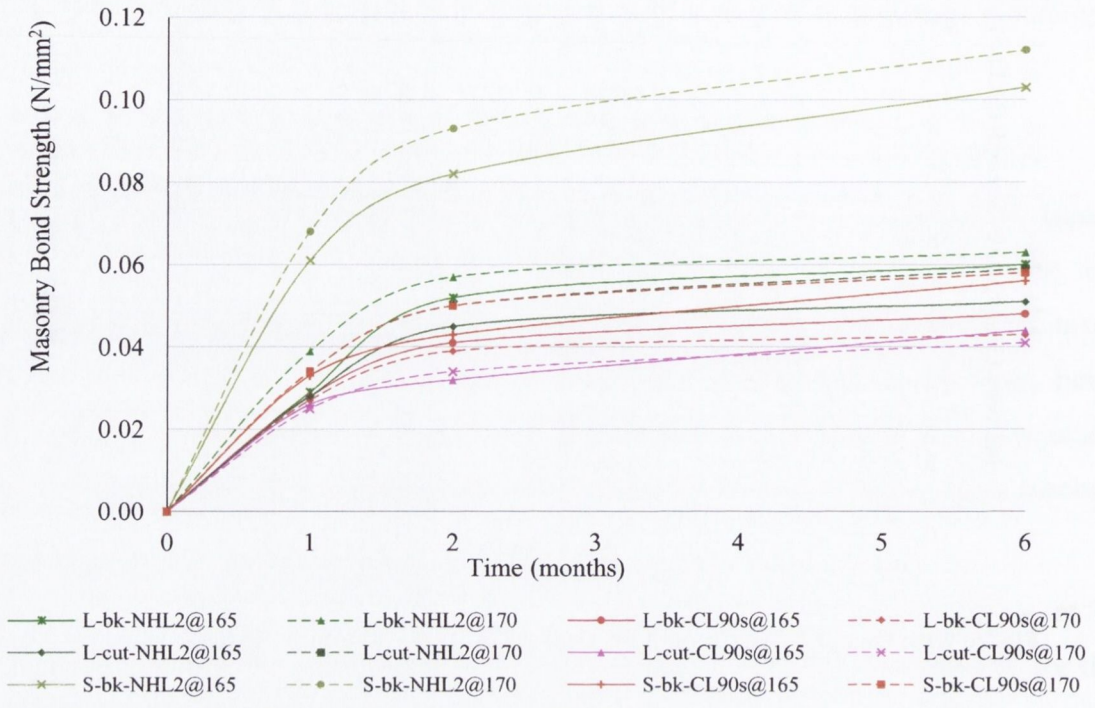

Figure 7.12: Bond strength development of stone masonry over time.

Unit type	Flow (mm)	Mortar type	Percentage of 6-month result					
			Compressive strength (%)		Elastic modulus (%)		Bond strength (%)	
			28 days	56 days	28 days	56 days	28 days	56 days
Broken Limestone	165	NHL 2	76 %	89 %	86 %	95 %	45 %	87 %
	170		85 %	96 %	81 %	{ - }[a]	62 %	90 %
	165	CL90-s	62 %	82 %	90 %	92 %	58 %	85 %
	170		46 %	82 %	76 %	{ - }[a]	63 %	91 %
Cut Limestone	165	NHL 2	83 %	88 %	81 %	91 %	55 %	88 %
	170		70 %	90 %	77 %	82 %	59 %	80 %
	165	CL90-s	63 %	91 %	84 %	{ - }[a]	59 %	73 %
	170		62 %	92 %	79 %	86 %	56 %	88 %
Broken Sandstone	165	NHL 2	84 %	94 %	73 %	90 %	59 %	80 %
	170		97 %	99 %	76 %	92 %	61 %	83 %
	165	CL90-s	81 %	90 %	80 %	93 %	59 %	77 %
	170		82 %	92 %	80 %	92 %	59 %	86 %

[a]{ - } is included where a drop in value was found between 56 days and 6 months

Table 7.13: Development of stone masonry results, relative to 6-month value.

7.4 RELATIONSHIP BETWEEN BOND AND COMPRESSIVE STRENGTH OF STONE MASONRY OVER TIME

While a clear relationship exists between stone-masonry bond and compressive strength (since both properties increase over time and with mortar hydraulic strength) (Figure 7.13), some of the results are inconsistent amongst the different stone masonry types and between stone and brick masonry.

This inconsistency can be explained by the vast difference between the compressive strength and stiffness of mortars and stone units in combination with very low unit-permeability, which generate relatively weak mortar-unit bond strength

The uneven contact surface and the variable mortar depth across the joints of the broken limestone leading to point loading, further explain the inconsistences in the relationship between the compressive and bond strength of stone masonry. In brick masonry built with weaker mortars (CL90-s and NHL 2), substantial increases in bond are coupled with significant gains in masonry compressive strength (Chapter 5) however, stone masonry does not show a similar consistent trend. For example, whilst the mortar hydraulic strength remains constant, the cut and broken limestone masonry compressive strength reduces substantially as the bond increases. This occurs for both NHL 2 and CL90-s mortars, irrespective of flow. Furthermore, relatively large increases in the bond strength of sandstone masonry do not necessarily equate to significant improvements in compressive strength, for example: between 56 days and 6 months, the bond strength of sandstone/NHL 2 mortar (165 mm flow) increases by 26 %, whereas the compressive strength only increases by 7 % (Figure 7.13).

These results suggest that, when the masonry consists of low suction units that are much stronger and stiffer than the mortars, masonry compressive strength is governed by unit strength rather than by the unit's properties (texture and initial rate of absorption) which influence bond strength. This supports the brick/stone masonry conclusions of previous sections.

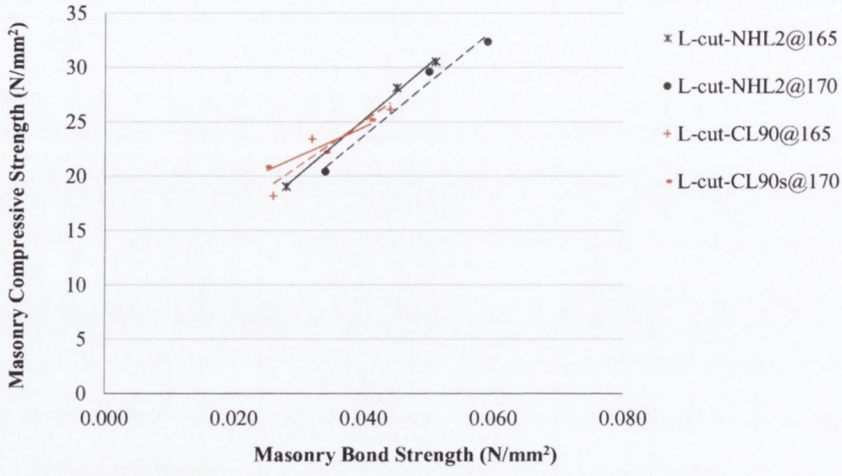

(a) Cut limestone

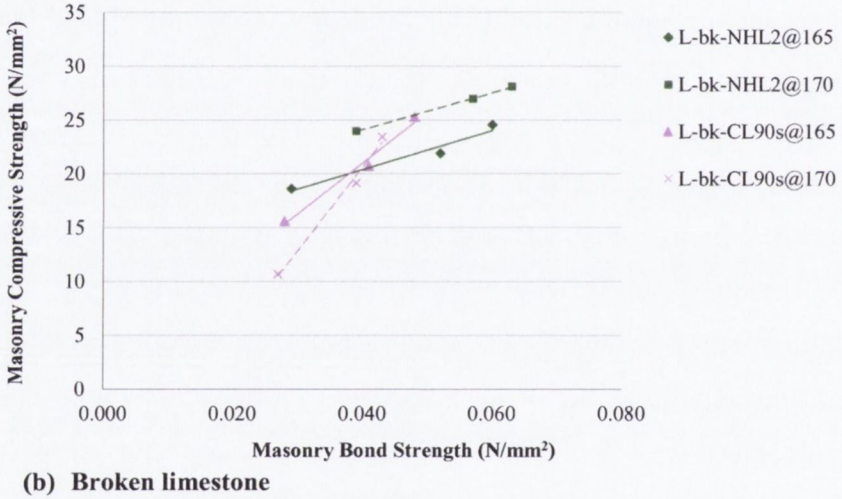

(b) Broken limestone

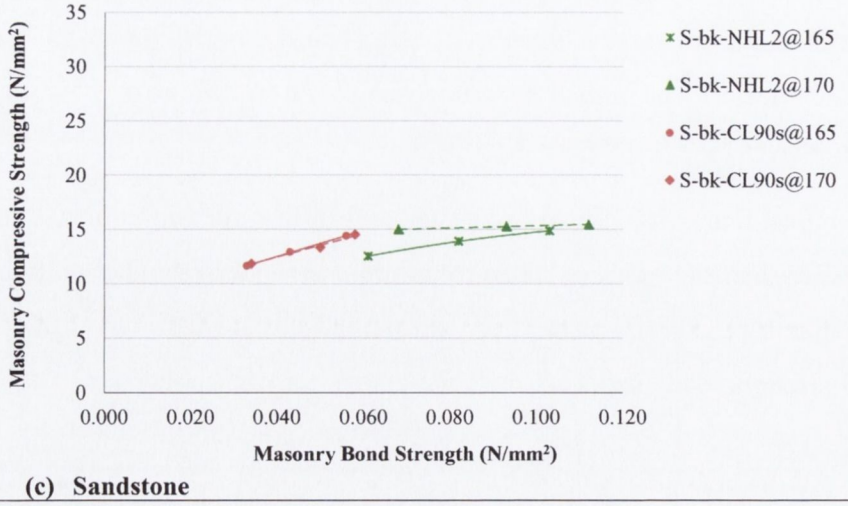

(c) Sandstone

Figure 7.13: Correlation between the bond and compressive strength of stone masonry (during hardening)

7.5 FAILURE MODES OF STONE MASONRY

The elastic modulus of the limestone and sandstone used in this research were 55,016 and 36,583 N/mm^2 respectively, and the elastic modulus of the CL90-s and NHL 2 mortar ranges from 70 to 162 N/mm^2. Therefore, situation a (Section 5.5) pertains to all of the stone masonry specimens investigated in this research where, $E_{unit} >> E_{mortar}$.

The failure of stone masonry constructed with strong, stiff units and weak mortars follows a similar pattern to brick masonry (Mode II, Section 5.5), where failure may due to a breakdown of both the mortar and the bond in combination with lateral tensional failure of the units. Spalling of the mortar begins at an early stage (approximately 25 % of the ultimate strength), as it accommodates all of the strain experienced during compression by spreading outwards. As the applied load continues to increase, vertical cracks are then seen on all four faces of the prism. Ultimate failure occurs due to the development of a large number of these cracks (Figure 7.14).

(a) Sandstone masonry (NHL 2 mortar)

(b) Cut limestone masonry (NHL 2 mortar)

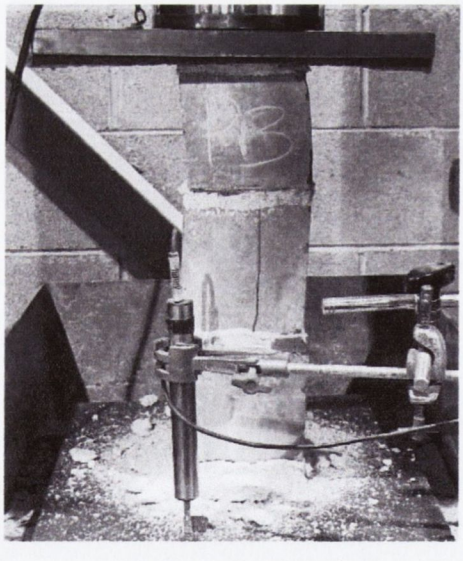

(c) Broken limestone masonry (CL90-s mortar)

Figure 7.14: Failure of stone masonry

CHAPTER 8

THEORETICAL VS. EXPERIMENTAL EVALUATION

8.1 ESTIMATION OF MASONRY COMPRESSIVE STRENGTH

The ability to predict the compressive strength of lime-mortar masonry is very important for promoting masonry design incorporating lime mortars. As previously noted, current standards (Eurocode 6) EN 1996-1-1 (2005) include equations for the estimation of masonry compressive strength however, these do not consider lime-mortar masonry. This section compares experimental results in this research with the most relevant analytical predictions of Eurocode 6 EN 1996-1-1 (2005) and various other authors. In addition, equations to predict the compressive strength of lime-mortar masonry are proposed.

8.1.1 Estimating masonry strength by regression of experimental data

A number of equations to estimate the compressive strength of masonry are investigated in this section for their fitness (Tables 8.1 and 8.2). These equations were established based on regression analysis of the experimental results in this research (Tables 8.3-8.5). Experimental results of this research for the normalized compressive strengths of brick units (f_b), average compressive strengths for a range of mortars (f_j) and the characteristic compressive strengths of masonry prism (f'_m) are also presented in Table 8.3. As previously mentioned, Eurocode 6 EN 1996-1-1 (2005) relates these three strengths in the form: $f'_m = K{f_b}^{\alpha} f_j^{\beta}$ where K, α and β are constants. This equation is rearranged to $f'_m - K{f_b}^{\alpha} f_j^{\beta} = 0$ and "least squares" regression analysis carried out whereby, K, α and β are systematically varied in order to minimize the sum of square errors (SSE)

$$SSE = \sum(f_i - f_{Ri})^2 \qquad \textbf{Equation 8.0}$$

where, f_i is the i^{th} experimental prism strength, f_{Ri} is the i^{th} regression estimate of masonry strength,

As previously discussed, two important parameters in regression analysis are R^2 and σ. R^2 is the coefficient of determination between experimentally obtained values and values acquired by the regression analysis. R^2 is defined as the ratio of the regression sum of squares (SSR) to the total sum of squares (SST). A R^2 value close to one

indicates a good fit while zero indicates a poor fit. Sigma (σ) represents the standard error of the estimate. A small σ value signifies a small scatter in the data about the regression estimate. R^2 and σ can be calculated using equations 8.1 and 8.2.

$$R^2 = 1 - \sqrt{\frac{\Sigma(f_i - f_{Ri})^2}{\Sigma(f_i - f_{mean})^2}} \qquad \textbf{Equation 8.1}$$

$$\sigma = \sqrt{\frac{\Sigma(f_i - f_{Ri})^2}{n - 3}} \qquad \textbf{Equation 8.2}$$

where, f_{mean} is the arithmetic average of experimentally obtained masonry strengths and n represents the number of data points investigated. Since three estimators K, α and β are desired, n-3 degrees of freedom are used in the calculation of σ, in order to achieve an unbiased estimate.

The equations listed in Table 8.1 are investigated for their fitness for the estimation of lime-brick masonry compressive strength at different curing times. These equations are based on regression analysis of the experimental results in Table 8.3. According to the results, Equation 8.3 provided good estimates of masonry compressive strength for natural hydraulic limes at 28 days however, poor predictions were found for CL mortar masonry (overestimated by 36-130 % at 28 days). The results suggest that this is mainly due to the large difference between the compressive strength of mortar and unit, since the estimates for CL90-s masonry strength become more accurate overtime, as the difference between the compressive strength of the mortar and unit becomes smaller. For example, at 6 months, Equation 8.3 only underestimates the strength of CL90-s masonry by 3 % (165 mm flow) and overestimates it by 32 % at 170 mm.

Due to the variability of the calcium lime mortar and masonry results, further regression analysis on the available experimental data was carried out treating the lower strength calcium lime and stronger hydraulic lime results separately. Table 8.1 indicates that removing CL90-s results from the model (Equation 8.4) improves the strength estimate of NHL brick-masonry to within 10 %. Equation 8.5 is investigated when calcium lime results are considered independently. Here, a R^2 value of 0.75 and a standard deviation

of 1.12 N/mm^2 indicate a wide variation within the results. Therefore, Equation 8.5 provides a poor estimate of the characteristic compressive strength of CL90-s masonry.

Time	Estimate equation	R^2	σ (N/mm^2)	
28 days All limes	$f'_m = 0.56 f_b^{0.53} f_j^{0.5}$	0.78	0.87	**Equation 8.3**
NHL's only	$f'_m = 0.69 f_b^{0.55} f_j^{0.37}$	**0.96**	**0.44**	**Equation 8.4**
CL90-s only	$f'_m = 0.55 f_b^{0.5} f_j^{0.5}$	0.75	1.12	**Equation 8.5**

Table 8.1: Equations investigated for the estimation of lime-brick masonry strength

Table 8.2 presents predictive models obtained by regression analysis of experimental results of cement-lime brick masonry and stone masonry. Equations 8.6 and 8.7 were set to estimate the characteristic compressive strength of the corresponding masonry, based on the experimental data in Tables 8.4 and 8.5. The results in Table 8.4 indicate that the proposed model for cement-lime brick masonry (Equation 8.6) provides a relatively good estimate of f'_m at 28 days (-4-8 % of the experimental value). However, Equation 8.6 does not perform as well at 56 days (over-estimating masonry compressive strengths by 5-15 %) and at 6 months (underestimating by 5-14 %). This is because overtime, the compressive strength of the mortar becomes much greater than that of the brick and this is not accounted for in the equation. It is noted that, for the calculation of f'_m at 6 months, the strength of the 6-month cement-lime mortar was assumed equal to 20 N/mm^2, which is the maximum strength permitted by EN 1996-1-1 (2005). However, the actual mortar strengths measured were 21.45-22.2 N/mm^2, which may explain why Equation 8.6 underestimates the strength by up to 14 % at 6 months.

For the stone masonry results (Tables 8.4 and 8.5), regression analysis revealed poor R^2 and standard deviation values evidencing large differences between estimated and actual experimental results. This is probably due to the large variation associated with the stone masonry experimental data for the reasons aforementioned including point loading, micro-cracking and great discrepancy in strength and stiffness between mortar and unit and differences in specimen geometry.

Masonry type	Estimate equation	R^2	σ (N/mm^2)	
Cement-lime/brick	$f'_m = 0.46 {f_b}^{0.5} {f_j}^{0.5}$	0.99	1.02	Equation 8.6
Weak Lime/Stone	$f'_m = 0.71 {f_b}^{0.74} {f_j}^{0.34}$	0.69	3.06	Equation 8.7

Table 8.2: Equations investigated for the estimation of cement-lime and stone masonry strength

The normalized compressive strength of the sandstone units used in this research is a third of that of the limestone units. The lower strength sandstone provides more consistent results than the higher strength limestone unit. This is likely due to the considerably smaller relative difference between mortar and masonry compressive strength and stiffness. Good R^2 and standard deviation values can be seen for regression analysis of sandstone masonry made with weak lime mortars in Table 8.2. Estimates for f'_m are also better for sandstone than for limestone masonry. According to Table 8.5, differences between experimental results for the characteristic compressive strength of sandstone masonry and those estimated by Equation 8.12 are generally under 10 %.

In general, Equation 8.7 is not reliable owing to the large number of inconsistent results associated with the low strength mortar/high strength stone unit masonry, previously discussed in Chapter 7. In addition, the stone masonry data sets were relatively small, compared to those of brick masonry.

Experimental results (N/mm^2)					Estimate of f_m (N/mm^2)		Predicted values of f_m by various authors (N/mm^2)						
Initial flow	Mortar Mix	Brick	Mortar	Masonry	Present study regression		Eurocode 6 (1996)	Bennett et al. (1997)	Dayaratnam (1987)	MSJC (2002)	kaushik (2007)	GVR (2006)	H & M (1986)
		f_b	f_j	f'_m	*Eq. 8.3*	*Eq. 8.4 NHL's*	*Eq. 8.8*	*Eq. 1.9*	*Eq. 1.11*	*Eq. 1.12*	*Eq. 1.13*	*Eq. 1.14*	*Eq. 1.15*
	28 days					[b] *Eq. 8.5 CL90-s*							
165	NHL5@ 0:1:3	12.75	3.87	4.57	4.25 {-7}[a]	4.62 {1}	4.46 {-2}	3.83{-16}	1.93 {-58}	2.78 {-39}	3.38 {-26}	3.44 {-25}	1.62 {-64}
	NHL3.5@ 0:1:3	12.75	3.86	4.23	4.24 {0}	4.61{9}	4.45 {5}	3.83 {-10}	1.93 {-54}	2.78 {-34}	3.38 {-20}	3.44 {-19}	1.62 {-62}
	NHL2@ 0:1:3	12.75	1.87	3.25	2.95 {-9}	3.35 {9}	3.58 10}	3.83 {18}	1.34 {-59}	2.78 {-15}	2.68 {-18}	3.13 {-4}	1.40 {-57}
	CL90s@ 0:1:3	12.75	0.62	0.74	1.70 {130}	1.55{109}[b]	2.57 {248}	3.83 {417}	0.77 {4}	2.78 {275}	1.88 {154}	2.7 {264}	1.11 {50}
	NHL 3.5@ 0:1:2	12.75	5.01	4.67	4.83 {3}	5.08 {9}	4.82 {3}	3.83 {-18}	2.20 {-53}	2.78 {-41}	3.67 {-21}	3.57 {-24}	1.71 {-63}
170	NHL5@ 0:1:3	12.75	4.39	4.74	4.52 {-5}	4.84 {2}	4.63 {-2}	3.83 {-19}	2.06 {-57}	2.78 {-41}	3.52 {-26}	3.5 {-26}	1.67 {-65}
	NHL3.5@ 0:1:3	12.75	4.23	4.60	4.44 {-4}	4.77 {4}	4.58 {0}	3.83 {-17}	2.02 {-56}	2.78 {-40}	3.48 {-24}	3.49 {-24}	1.65 {-64}
	NHL2@ 0:1:3	12.75	2.16	3.83	3.17 {-17}	3.72 {-3}	3.74 {-2}	3.83 {0}	1.44 {-62}	2.78 {-28}	2.81 {-27}	3.19 {-17}	1.44 {-62}
	CL90s@ 0:1:3	12.75	1.29	0.73	2.45 {236}	2.23{206}[b]	3.21 {339}	3.83 {424}	1.12 {53	2.78 {280}	2.38 {226}	2.97 {307}	1.29 {77}
	56 days												
165	NHL5@ 0:1:3	12.75	6.33	4.79	5.22 {9}	5.38 {12}	5.17 {8}	3.83 {-20}	2.47 {-48}	2.78 {-42}	3.96 {-17}	3.68 {-23}	1.80 {-62}
	NHL3.5@ 0:1:3	12.75	5.27	4.91	4.80 {-2}	4.95 {1}	4.89 {0}	3.83 {-22}	2.25 {-54}	2.78 {-43}	3.73 {-24}	3.59 {-27}	1.73 {-65}
	NHL2@ 0:1:3	12.75	2.29	3.78	3.27 {-13}	3.41 {-10}	3.81 {1}	3.83 {1}	1.49 {-61}	2.78 {-27}	2.86 {-24}	3.21 {-15}	1.46 {61}
	CL90s@ 0:1:3	12.75	0.89	1.15	2.12 {84}	1.55 {35}[b]	2.87 {149}	3.83 {233}	0.93 {-19}	2.78 {141}	2.11 {84}	2.83 {146}	1.20 {4}
	NHL 3.5@ 0:1:2	12.75	8.70	5.92	6.04 {2}	6.2 {5}	5.68 {-4}	3.83 {-35}	2.90 {-51}	2.78 {-53}	4.38 {-26}	3.84 {-35}	1.92 {-68}
170	NHL5@ 0:1:3	12.75	7.02	5.52	5.48 {-1}	5.63 {2}	5.33 {-3}	3.83 {-31}	2.60 {-53}	2.78 {-50}	4.09 {-26}	3.73 {-32}	1.84 {-67}
	NHL3.5@ 0:1:3	12.75	6.11	5.34	5.14 {-4}	5.29 {-1}	5.11 {-4}	3.83 {-28}	2.43 {-55}	2.78 {-48}	3.91 {-27}	3.66 {-31}	1.78 {-67}
	NHL2@ 0:1:3	12.75	2.35	4.69	3.31 {-29}	4.45 {-5}	3.84 {-18}	3.83 {-18}	1.51 {-68}	2.78 {-41}	2.88 {-39}	3.22 {-31}	1.46 {-69}
	CL90s@ 0:1:3	12.75	1.52	2.05	2.71 {32}	1.55 {-24}[b]	3.37 {64}	3.83 {87}	1.21 {-41}	2.78 {-35}	2.51 {22}	3.02 {-48}	1.34 {-35}
	Six months												
165	NHL5@ 0:1:3	12.75	11.89	6.68	7.07 {6}	7.14 {7}	6.24 {-7}	3.83 {-43}	3.39 {-49}	2.78 {-58}	4.48 {-28}	4.00 {-40}	2.05 {-69}
	NHL3.5@ 0:1:3	12.75	8.95	6.43	6.36 {-1}	6.28 {-2}	5.73 {-11}	3.83 {-41}	2.94 {-54}	2.78 {-57}	4.42 {-31}	3.85 {-40}	1.93 {-70}
	NHL2@ 0:1:3	12.75	2.63	4.00	4.04 {1}	3.62 {-9}	3.97 {-1}	3.83 {-4}	1.59 {-60}	2.78 {-31}	2.99 {-25}	3.27 {-18}	1.50 {-63}
	CL90s@ 0:1:3	12.75	1.39	3.28	3.2 {-3}	1.55 {-53}[b]	3.28 {0}	3.83 {17}	1.16 {-65}	2.78 {-15}	2.44 {-26}	3.00 {-8}	1.31 {-60}
	NHL 3.5@ 0:1:2	12.75	10.56	7.10	6.77 {-5}	6.77 {-5}	6.02 {-15}	3.83 {-46}	3.19 {-55}	2.78 {-61}	4.66 {-34}	3.94 {-44}	2.00 {-72}
170	NHL5@ 0:1:3	12.75	12.21	6.64	7.14 {8}	7.23 {9}	6.29 {-5}	3.83 {-42}	3.43 {-48}	2.78 {-58}	4.88 {-26}	4.02 {-39}	2.06 {-69}
	NHL3.5@ 0:1:3	12.75	9.30	7.05	6.46 {-8}	6.39 {-9}	5.8 {-18}	3.83 {-46}	2.99 {58}	2.78 {-61}	4.48 {-37}	3.87 {-45}	1.95 {-72}
	NHL2@ 0:1:3	12.75	3.14	4.91	4.32 {-12}	4.52 {-8}	4.19 {-15}	3.83 {-22}	1.74 {-65}	2.78 {-43}	3.16 {-36}	3.35 {-32}	1.55 {-68}
	CL90s@ 0:1:3	12.75	2.00	2.78	3.66 {32}	1.55 {-44}[b]	3.66 {32}	3.83 {38}	1.39 {-50}	2.78 {0}	2.74 {-2}	3.15 {13}	1.41 {-49}
	365 days												
165	NHL5@ 0:1:3	12.75	13.3	7.09	9.74 {37}	7.51 {6}	6.46 {-9}	3.83 {-46}	3.58 {-49}	2.78 {-61}	5.02 {-29}	4.06 {-43}	2.10 {-70}
	NHL3.5@ 0:1:3	12.75	10	7.42	8.57 {15}	6.61 {-11}	5.93 {-20}	3.83 {-48}	3.11 {-58}	2.78 {-63}	4.58 {-38}	3.91 {-47}	1.98 {-73}
	NHL2@ 0:1:3	12.75	2.7	4.01	4.75 {19}	3.67 {-9}	4 {0}	3.83 {-5}	1.61 {-60}	2.78 {-31}	3.01 {-25}	3.28 {-18}	1.51 {-62}
	CL90s@ 0:1:3	12.75	1.4	3.59	3.54 {-1}	1.55 {57}[b]	3.29 {-8}	3.83 {7}	1.16 {-68}	2.78 {-23}	2.44 {-32}	3.01 {-16}	1.31 {-63}
	Avg Absolute Error (All mortars)				{22}		{30}	{53}	{48}	{54}	{35}	{44}	{57}
	Avg Absolute Error (NHL mortars only)				{8}	{6}	{6}	{22}	{50}	{39}	{24}	{44}	{57}

[a] Values in { } represent the percentage error between estimated and actual experimental results

[b] Values in { }[b] represent the percentage error between estimated and actual experimental results of Eq 8.5 (CL90-s)

Table 8.3: Comparison of experimental results in this thesis with analytical prediction models from various sources (all brick masonry)

	Initial flow	Mortar Mix ID	Unit f_b	Mortar f_j	Masonry f'_m	Present study (regression) *Eq. 8.6*	Eurocode 6 (1996) *Eq. 8.8*	Bennett et al. (1997) *Eq. 1.9*	Dayaratnam (1987) *Eq. 1.11*	kaushik (2007) *Eq. 1.12*	MSJC (2002) *Eq. 1.13*	GVR (2006) *Eq. 1.14*	H & M (1986) *Eq. 1.15*
		Experimental results (N/mm^2)				Estimate of f'_m	Predicted values of f'_m from various sources (N/mm^2)						
Brick masonry		**28 days**											
	165	M6@1:½:4.5 (v)	12.75	11.22	5.75	5.50 {-4}[a]	6.13 {7}	3.83 {-34}	3.29 {-43}	2.78 {-52}	4.75 {-17}	3.97 {-31}	2.03 {-65}
	170	M6@1:½:4.5 (v)	12.75	14.28	5.75	6.21 {8}	6.59 {15}	3.83 {-34}	3.71 {-36}	2.78 {-52}	5.13 {-11}	4.10 {-29}	2.13 {-63}
		56 days											
	165	M6@1:½:4.5 (v)	12.75	18.00	6.43	6.97 {8}	7.07 {10}	3.83 {-41}	4.17 {-35}	2.78 {-57}	5.53 {-14}	4.23 {-34}	2.23 {-65}
	170	M6@1:½:4.5 (v)	12.75	19.23	6.28	7.20 {15}	7.21 {15}	3.83 {-39}	4.31 {-31}	2.78 {-56}	5.56 {-10}	4.27 {-32}	2.27 {-64}
		Six months											
	165	M6@1:½:4.5 (v)	12.75	22.20	8.12	7.74 {-5}[b]	7.30 {-10}[b]	3.83 {-53}	4.39 {-46}	2.78 {-66}	5.91 {-27}	4.35 {-46}	2.33 {-71}
	170	M6@1:½:4.5 (v)	12.75	21.45	8.86	7.61 {-14}[b]	7.30 {-18}[b]	3.83 {-57}	4.39 {-50}	2.78 {-69}	5.85 {-34}	4.33 {-51}	2.32 {-74}
Broken limestone masonry		**28 days**				*Eq. 8.7*	*Eq. 8.9*						
	165	NHL2@ 0:1:3	74.05	1.87	15.49	18.07 {17}	11.05 {-29}	22.22 {43}	3.24 {-79}	2.86 {-82}	6.34 {-59}	14.34 {-7}	3.55 {-77}
		CL90s@ 0:1:3	74.05	0.62	12.98	10.4 {-20}	7.94 {-39}	22.22 {71}	1.86 {-86}	2.86 {-78}	4.46 {-66}	12.37 {-5}	2.82 {-78}
	170	NHL2@ 0:1:3	74.05	2.16	19.70	19.42 {-1}	11.54 {-41}	22.22 {13}	3.48 {-82}	2.86 {-85}	6.64 {-66}	14.62 {-26}	3.66 {-81}
		CL90s@ 0:1:3	74.05	1.29	6.77	15.01 {122}	9.89 {46}	22.22 {228}	2.69 {-60}	2.86 {-58}	5.63 {-17}	13.64 {102}	3.29 {-51}
		56 days											
	165	NHL2@ 0:1:3	74.05	2.29	18.24	20.01 {10}	11.75 {-36}	22.22 {22}	3.58 {-80}	2.86 {-84}	6.77 {-63}	14.74 {-19}	3.70 {-80}
		CL90s@ 0:1:3	74.05	0.89	17.24	12.46 {-28}	8.84 {-49}	22.22 {29}	2.23 {-87}	2.86 {-83}	5.00 {-71}	12.98 {-25}	3.04 {-82}
	170	NHL2@ 0:1:3	74.05	2.35	22.46	20.27 {-10}	11.84 {-47}	22.22 {-1}	3.63 {-84}	2.86 {-87}	6.83 {-70}	14.79 {-34}	3.72 {-83}
		CL90s@ 0:1:3	74.05	1.52	15.95	16.29 {2}	10.39 {-35}	22.22 {39}	2.92 {-82}	2.86 {82}	5.94 {-63}	13.95 {-13]	3.40 {-79}
		Six months											
	165	NHL2@ 0:1:3	74.05	2.63	20.34	21.42 {5}	12.24 {-40}	22.22 {9}	3.84 {-81}	2.86 {-86}	7.07 {-65}	15.01 {-26}	3.81 {-81}
		CL90s@ 0:1:3	74.05	1.39	21.05	15.58 {-26}	10.11 {-52}	22.22 {6}	2.79 {-87}	2.86 {-86}	5.77 {-73}	13.78 {-35}	3.34 {-84}
	170	NHL2@ 0:1:3	74.05	3.14	23.41	23.41 {0}	12.91 {-45}	22.22 {-5}	4.19 {-82}	2.86 {-88}	7.49 {-68}	15.37 {-34}	3.95 {-83}
		CL90s@ 0:1:3	74.05	2.00	19.53	18.69 {-4}	11.28 {-42}	22.22 {14}	3.35 {-83}	2.86 {-85}	6.48 {-67}	14.47 {-26}	3.60 {-82}
		Avg Absolute Error (Cement-Brick Masonry)				{8}	{9}	{32}	{30}	{15}	{44}	{20}	{50}

[a] Values in { } represent the percentage error between estimated and actual experimental results

[b] Mortar strength assumed equal to 20 N/mm^2, since EN 1996-1-1 (2005) is only applicable for mortar strength less than this value

Table 8.4: Comparison of experimental results of this thesis with analytical prediction models from various sources (cont. a)

	Experimental results (N/mm^2)				Estimate of f_m	Predicted values of f_m from various sources (N/mm^2)						
	Initial flow	Mortar Mix	Unit f_b	Mortar f_j	Masonry f'_m	Present study (regression) *Eq. 8.7*	Eurocode 6 (1996) *Eq. 8.9*	Bennett et al. (1997) *Eq. 1.9*	Dayaratnam (1987) *Eq. 1.11*	kaushik (2007) *Eq. 1.12*	MSJC (2002) *Eq. 1.13*	GVR (2006) *Eq. 1.14*	H & M (1986) *Eq. 1.15*
Cut limestone masonry		**28 days**											
	165	NHL2@ 0:1:3	74.05	1.87	15.87	21.24 {34}[a]	11.05 {-30}	22.22 {40}	3.24 {-80}	2.86 {-82}	6.34 {-60}	14.34 {-10}	3.55 {-78}
		CL90s@ 0:1:3	74.05	0.62	14.12	14.59 {3}	7.94 {-44}	22.22 {57}	1.86 {-87}	2.86 {-80}	4.46 {-68}	12.37 {-12}	2.82 {-80}
	170	NHL2@ 0:1:3	74.05	2.16	17.03	22.30 {31}	11.54 {-32}	22.22 {30}	3.48 {-80}	2.86 {-83}	6.64 {-61}	14.62 {-14}	3.66 {-79}
		CL90s@ 0:1:3	74.05	1.29	17.36	18.72 {8}	9.89 {-43}	22.22 {28}	2.69 {-85}	2.86 {-84}	5.63 {-68}	13.64 {-21}	3.29 {-81}
		56 days											
	165	NHL2@ 0:1:3	74.05	2.29	23.43	22.76 {-3}	11.75 {-50}	22.22 {-5}	3.58 {-85}	2.86 {-88}	6.77 {-71}	14.74 {-37}	3.70 {-84}
		CL90s@ 0:1:3	74.05	0.89	19.53	16.5 {-15}	8.84 {-55}	22.22 {14}	2.23 {-89}	2.86 {-85}	5.00 {-74}	12.98 {-34}	3.04 {-84}
	170	NHL2@ 0:1:3	74.05	2.35	24.67	22.97 {-7}	11.84 {-52}	22.22 {-10}	3.63 {-85}	2.86 {-88}	6.83 {-72}	14.79 {-40}	3.72 {-85}
		CL90s@ 0:1:3	74.05	1.52	18.50	19.79 {7}	10.39 {-44}	22.22 {20}	2.92 {-84}	2.86 {-85}	5.94 {-68}	13 .95 {-25}	3.40 {-82}
		Six months											
	165	NHL2@ 0:1:3	74.05	2.63	25.45	23.85 {-6}	12.24 {-52}	22.22 {-13}	3.84 {-85}	2.86 {-89}	7.07 {-72}	15.01 {-41}	3.81 {-85}
		CL90s@ 0:1:3	74.05	1.39	21.79	19.2 {-12}	10.11 {-54}	22.22 {2}	2.79 {-87}	2.86 {-87}	5.77 {-74}	13.78 [-78]	3.34 {-85}
	170	NHL2@ 0:1:3	74.05	3.14	26.98	25.33 {-6}	12.91 {-52}	22.22 {-18}	4.19 {-84}	2.86 {-89}	7.49 {-72}	15.37 {-43}	3.95 {-85}
		CL90s@ 0:1:3	74.05	2.00	20.98	21.73 {4}	11.28 {-46}	22.22 {6}	3.35 {-84}	2.86 {-86}	6.48 {-69}	14.47 {-31}	3.60 {-83}
Sandstone masonry		**28 days**											
	165	NHL2@ 0:1:3	49.57	1.87	9.13	11.38 {25}	8.34 {-9}	14.87 {63}	*2.65 {-71}*	2.83 {-69}	5.21 {-43}	10.13 {11}	2.87 {-69}
		CL90s@ 0:1:3	49.57	0.62	9.69	9.54 {-2}	5.99 {-38}	14.87 {53}	1.52 {-84}	2.86 {-71}	3.66 {-62}	8.74 {-10}	2.28 {-76}
	170	NHL2@ 0:1:3	49.57	2.16	12.51	11.65 {-7}	8.71 {-30}	14.87 {19}	2.85 {-77}	2.86 {-77}	5.46 {-56}	10.33 {-17}	2.96 {-76}
		CL90s@ 0:1:3	49.57	1.29	9.88	10.73 {9}	7.47 {-24}	14.87 {50}	2.2 {-78}	2.86 {-71}	4.63 {-53}	9.64 {-2}	2.66 {-73}
		56 days											
	165	NHL2@ 0:1:3	49.57	2.29	11.59	11.76 {1}	8.87 {-23}	14.87 {28}	2.93 {-75}	2.86 {-76}	5.56 {-52}	10.41 {-10}	2.99 {-74}
		CL90s@ 0:1:3	49.57	0.89	10.78	10.11 {-6}	6.68 {-38}	14.87 {38}	1.83 {-83}	2.86 {-74}	4.11 {-62}	9.17 {-15}	2.46 {-77}
	170	NHL2@ 0:1:3	49.57	2.35	12.60	11.81 {-6}	8.94 {-29}	14.87{18}	2.97 {-76}	2.86 {-78}	5.61 {-55}	10.45 {-17}	3.01 {-76}
		CL90s@ 0:1:3	49.57	1.52	11.83	11.01 {-7}	7.84 {-34}	14.87 {26}	2.39 {-80}	2.86 {-76}	4.88 {-59}	9.85 {-17}	2.75 {-77}
		Six months											
	165	NHL2@ 0:1:3	49.57	2.63	12.39	12.02 {-3}	9.24 {-25}	14.87 {20}	3.14 {-75}	2.86 {-77}	5.81 {-53}	10.60 {-14}	3.08 {-75}
		CL90s@ 0:1:3	49.57	1.39	12.01	10.85 {-10}	7.63 {-36}	14.87 {24}	2.28 {-81}	2.86 {-76}	4.74 {-61}	9.73 {-19}	2.70 {-78}
	170	NHL2@ 0:1:3	49.57	3.14	12.88	12.37 {-4}	9.75 {-24}	14.87 {16}	3.43 {-73}	2.86 {-78}	6.15 {-52}	10.86 {-16}	3.20 {-75}
		CL90s@ 0:1:3	49.57	2.00	12.10	11.51 {-5}	8.51 {-30}	14.87 {23}	2.74 {-77}	2.86 {-77}	5.33 {-56}	10.22 {-16}	2.91 {-76}
		Avg Absolute Error (All Stone Masonry)				{13}	{39}	{31}	{81}	{62}	{81}	{24}	{79}
		Avg Absolute Error (NHL Stone Masonry)				{10}	{36}	{21}	{80}	{62}	{83}	{23}	{79}

[a]Values in { } represent the percentage error between estimated and actual experimental results

Table 8.5: Comparison of experimental results in this thesis with analytical prediction models from various sources (all stone masonry) (cont. b)

8.1.2 Estimating masonry strength using various analytical prediction models

As discussed in Chapter 1, several authors have proposed a range of models, which attempt to estimate the compressive strength of masonry (Equations 1.9-1.15 in Table 8.6). Investigations by these authors have focused on cement and cement-lime masonry. It is therefore interesting to study how closely these equations estimate the characteristic compressive strength of the masonry in this research. The objective of this section is to investigate whether these equations can be used to estimate the strength of lime-mortared masonry and if so, to highlight at which curing age and for what masonry type they perform best.

As previously mentioned, Tables 8.3 and 8.4 present lime mortar and masonry results at several curing ages. Eurocode 6, EN 1996-1-1 (2005) allows the characteristic compressive strength of brick masonry (at 28 days) to be determined using the following equation:

$$f'_m = 0.5 {f_b}^{0.7} {f_j}^{0.3} \qquad \textbf{Equation 8.8}$$

where, K = 0.5 (for group 1, clay units)

In general, Equation 8.8 produces good estimates of the characteristic compressive strength of natural hydraulic lime brick-masonry at 28 and 56 days (Table 8.3) (with the exception of higher flow NHL 2 masonry at 56 days). However, estimates of the characteristic compressive strength of CL90-s masonry are quite poor.

Cement-lime brick-masonry results are presented in Table 8.4. It can clearly be seen that Equation 8.8 provides reasonably good estimates of masonry compressive strength. The percentage error in compressive strength associated with these analytical predictions is < 15 % (at 28 and 56 days).

Eurocode 6 EN 1996-1-1 (2005) provides the best predictions of all those studied therefore, this research validates the use of this equation, not only for cement-lime but also for the estimation of Natural Hydraulic Lime brick-masonry characteristic compressive strength at 28 days.

As previously discussed, Eurocode 6 EN 1996-1-1 (2005) allows the use of the mortar strength classification to determine the compressive strength (f_j) when the specific compressive strength of the mortar is unknown. This can have the effect of vastly under estimating the potential strength of lime-masonry, since the compressive strength of lime mortar can vary greatly depending on water content (for example, a 13 % increase in NHL 5 resulting from a 1% rise in water content, as seen in Chapter 3). This research recommends using actual mortar strength values i.e. testing of site-made mortar prisms, to ascertain a better estimate of the strength of lime masonry.

Equation 8.9 below is also taken from Eurocode 6, EN 1996-1 (2005), where K is equal to 0.45 (natural stone units).

$$f'_m = 0.45 {f_b}^{0.7} {f_j}^{0.3} \qquad \textbf{Equation 8.9}$$

Eurocode 6, EN 1996-1 (2005) stipulates that the normalised compressive strength of the stone masonry unit be < 75 N/mm^2. Both sandstone (49.57 N/mm^2) and limestone (74.05 N/mm^2) units satisfy this criterion. In spite of this, Equation 8.14 severely underestimates the characteristic compressive strength of all stone masonry types considered in this research by approximately 20-50 % (Tables 8.4-8.5). This is likely due to large difference between the mortar and unit strength and inconsistencies in the results due to the natural variability of the material and discordant prism assembly. Equation 8.9 is therefore not a good predictor of stone masonry strength when strong stone units are coupled with feebly hydraulic and non-hydraulic lime mortars.

Source Reference	Model	
Bennett *et al.* (1997)	$f'_m = 0.3f_b$	**Equation 1.9**
Dayaratnam (1987)	$f_m = 0.275{f_b}^{0.5}{f_j}^{0.5}$	**Equation 1.11**
MSJC (2002)	$f'_m = (400 + 0.25f_b)/145$	**Equation 1.12**
Kaushik *et al.* (2007)	$f'_m = 0.63{f_b}^{0.49}{f_j}^{0.32}$	**Equation 1.13**
Gumaste and Venkatarama Reddy (2006)	$f'_m = 0.317{f_b}^{0.866}{f_j}^{0.134}$	**Equation 1.14**
Hendry and Malek (1986)	$f'_m = 0.317{f_b}^{0.531}{f_j}^{0.208}$	**Equation 1.15**

Table 8.6: Summary of models for the estimation of masonry strength

According to the results, at 28 days, all the authors in Table 8.6 significantly underestimate the compressive strength of NHL brick-masonry and vastly overestimate the strength of CL brick-masonry. Bennett *et al* (1997) provide the closest predictions for NHL masonry ($\leq$ 19 % error) while Kaushik *et al.* (2007) and Gumaste and Venkatarama (2006) underestimate the strength by 20-27 % and the other authors by 50-65 % (Table 8.3). According to the experimental results in this research, all of the equations presented in Table 8.6 are poor predictors of brick-lime masonry strength at 56 days and 6 months. They either, vastly overestimate or underestimate strength.

When the analytical models in Table 8.6 are applied to the experimental cement-lime mortar and masonry strength results in Table 8.4, Eurocode 6 is still the best at predicting masonry strength values. After this, Equation 1.13 by MSJC (2002) compares most accurately (within 17 % up to 56 days). The other equations generally underestimate the masonry strength by 30-65 %. Even though Equation 1.11 by Dayaratnam (1987) placed equal weight on the mortar and unit strength, similarly to Equation 8.9 (obtained by regression of the experimental results), the K value proposed by the author is too small to accurately predict f'_m.

In relation to the stone masonry, according to the results in Tables 8.4 and 8.5, all of the predictive models (Table 8.6) perform very poorly when considered to estimate the compressive strength of stone masonry constructed with weak limes. Equations (1.11-1.15) severely underestimate masonry strength by between 50 and 90 %. In contrast,

since Bennett *et al.* (2007) only takes the strength of the unit into account, Equation 1.9 tends to vastly over estimate masonry strength up to 56 days however, at 6 months Equation 1.9 performs the best and predicts the characteristic compressive strength of masonry as follows: broken limestone by $\leq$ 14 %, cut limestone $\leq$ 18 % and broken sandstone $\leq$ 24 %.

Considering all of the predictive models discussed in this section, only Eurocode 6, 1996-1-1 (2005) consistently provides the most accurate estimates of cement-lime and natural hydraulic lime brick masonry strength at 28 days. Due to the variability in the results of calcium lime mortar/masonry and the relatively large difference between mortar and unit strength, no model was found to predict the characteristic compressive strength of CL mortar masonry.

Furthermore, no simple model exists in literature to date that can consistently and accurately estimate characteristic compressive strength of stone masonry where the normalized compressive strength of the units is much greater than that of the constituent lime mortars.

Despite the fact that the models based on the present study and Eurocode 6 EN 1996-1 (2005) are accurate in the estimation of compressive strength of lime mortar masonry, they do not take into consideration the ability that lime masonry has to deform and accommodate movement. Therefore, to fully characterise lime mortar masonry and ensure a correct lime mortar specification, the estimation of elastic modulus, stress-strain behaviour, and peak strain is required.

8.2 ESTIMATION OF LIME-MASONRY DEFORMATION CHARACTERISTICS

8.2.1 General stress-strain relationship

An example of a typical lime masonry stress-strain curve is presented in Figure 8.1. The relationship between applied compressive load and deformation can generally be subdivided into four main areas.

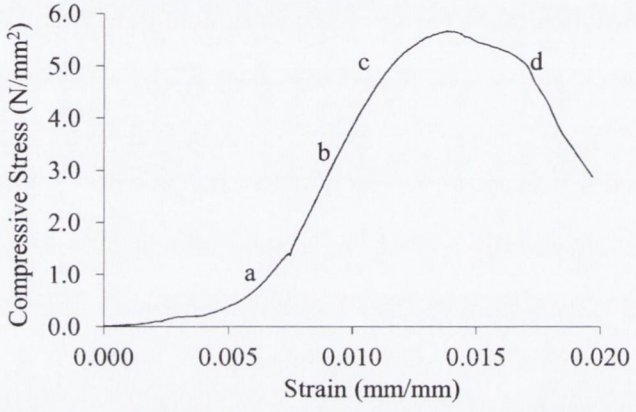

Figure 8.1: Example of a stress-strain diagram with phases a, b, c and d.

(a) Large deformations can be seen during early compression. The initial concave upwards shape of the stress-strain curve is due to closing of gaps, fissures and openings in conjunction with settling of the testing assembly.

(b) The initial upward concavity is followed by a more or less linear portion. For lime masonry, the linear part was generally found between 30 and 60 % of the ultimate stress. As previously discussed, this part of the curve was used to calculate the elastic modulus of masonry.

(c) Generally above 60 % of ultimate stress, the stress-strain relationship is non-linear as cracks propagate and material is lost.

(d) After the peak stress is reached, the deformation diagram changes considerably as the specimen fails to resist additional loading. In this research, the descending branch below $0.9f'_m$ was rarely recorded. This was because testing was usually stopped shortly after failure was deemed to have occurred in order to limit any potential damage to LVDTs, associated cables and equipment.

8.2.2 Fitness of simple analytical stress-strain models

For masonry design, a simple mathematical description of the stress-strain relationship is required. As aforementioned, several authors have proposed such models to represent the relationship between applied stress and strain deformation of masonry (Chapter 1). These equations are summarised in Table 8.7.

In order to compare these experimental curves from this study with curves predicted using previously mentioned analytical models, the initial part (a) of each experimental stress-strain curve requires correcting. A procedure described by Vermeltfoort (2005) was adopted. The stress-strain diagrams were first normalized by letting $\sigma_r = \sigma/\sigma_{max}$ and $\varepsilon_r = \varepsilon/\varepsilon_{r,90}$, where σ_{max} is the ultimate stress and $\varepsilon_{r,90}$ is the strain at 0.9 σ_{max} (see figure 8.2). Omitting the results in the concave portion of the stress-strain and using a best fit quadratic procedure, a curve is described with the general form of Equation 8.15 between approximate normalized stresses 0.3 and 0.9.

$$\sigma_r = A(\varepsilon_r) + B(\varepsilon)_r^2 \qquad \textbf{Equation 8.4}$$

The origin becomes the point where the parabolic curve crosses the strain axis. Part (a) of the stress-strain curve is then replaced by the lower portion of the parabolic curve and the corrected curve is rescaled by the ratio of $\varepsilon_{r,90}$ to $\varepsilon_{r,max}$.

For comparative analysis a representative sample of stress-stress diagrams obtained in this research were selected (Figure 8.3). One masonry specimen was chosen for each mortar grade. All were tested at the same age (56 days) and all had initial mortar flow of 170 mm. Corresponding corrected stress-strain curves are presented in Figure 8.4.

Figure 8.5 shows a comparison between the experimental stress-strain curves of brick masonry in this research, and those estimated by analytical models proposed by other authors. The input parameters of all modelled stress-strain curves were experimentally obtained (including peak strain).

Good agreement can be seen between the model proposed by Kaushik *et al.* (2007) (Equation 1.5) and the experimental curves. Equation 1.5 performs well, even when used to describe the stress-strain relationship of the highly elastic non-hydraulic lime masonry (CL90-s). Priestley and Elder (1983) (Equation 1.2) provides poor predictions

of stress-strain curves. Equation 1.2 is restricted and can only describe the rising curve up to a strain of 0.0015, and therefore cannot take the relatively large deformations associated with the lime masonry studied into consideration. Furthermore, the descending curve (Equation 1.3) is only applicable to mortars with compressive strength greater than approximately 7 N/mm^2 and hence no downward curvatures can be seen for lime masonry in Figure 8.5.

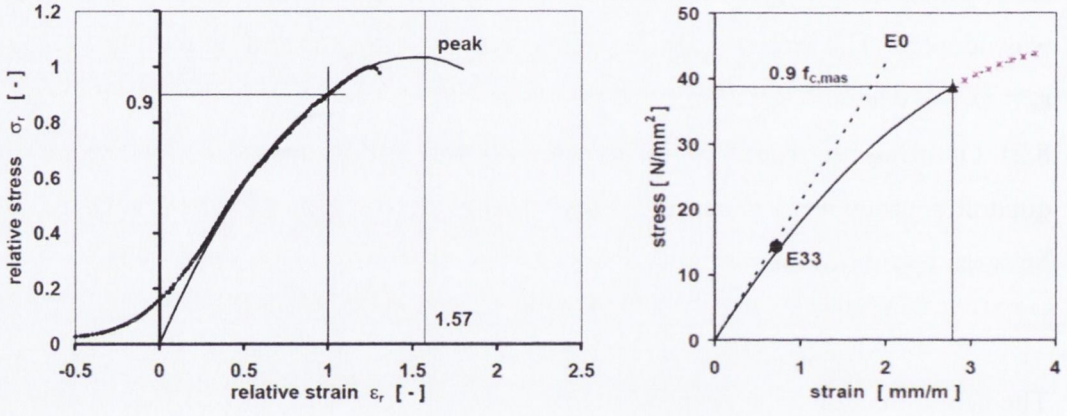

Figure 8.2: Normalized stress-strain diagram (Vermeltfoort, 2005)

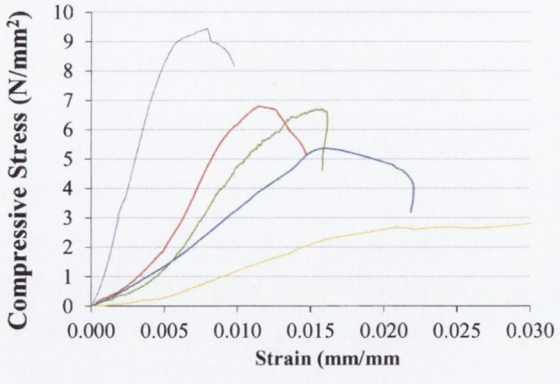

Figure 8.3: Representative masonry stress-strain curves

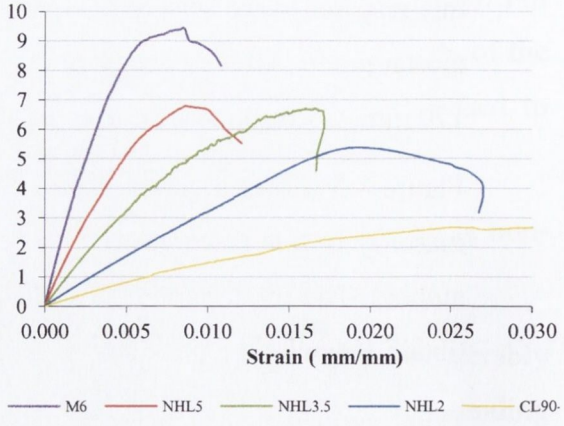

Figure 8.4: Corrected masonry stress-strain curves

Source Reference	Model	
Priestly and Elder (1983) Rising curve	$f_m = 1.067 f'_m \left[\frac{2\varepsilon_m}{0.002} - \left(\frac{\varepsilon_m}{0.002}\right)^2\right]$ for $0 \leq \varepsilon_m \leq 0.0015$	**Equation 1.2**
Descending curve	$f_m = f'_m[1 - Z_m(\varepsilon_m - 0.0015)]$ Until $0.2f'_m$	**Equation 1.3**
Final horizontal plateau	$Z_m = \frac{0.5}{\left[\frac{3 + 0.29 f_j}{145 f_j - 1000}\right] - 0.002}$	**Equation 1.4**
Kaushik *et al.* (2007)		
Rising curve	$\frac{f_m}{f'_m} = 2\frac{\varepsilon_m}{\varepsilon'_m} - \left(\frac{\varepsilon_m}{\varepsilon'_m}\right)^2$	**Equation 1.5**
Linear descending line	From $0.8\ f'_m$ until $0.2f'_m$ at $2.75\ \varepsilon'_m$	
Eurocode 6 EN 1996-1-1 (2005)	Equation 1.5, Kaushik *et al.* (2007) was also used to describe the parabolic rising curve (until a strain of 0.002) then a horizontal plateau until a 0.0035 of strain	
Knutson (1993)		
Ritter curve, if $\frac{f_m}{f'_m} \leq 0.75$	$\varepsilon_m = -\frac{f'_m}{E_m} ln\left(1 - \frac{f_m}{f'_m}\right)$	**Equation 1.6**
Ritter curve correction, if $\frac{f_m}{f'_m} > 0.75$	$\varepsilon_m = -4\frac{f'_m}{E_m} ln\left(0.403 - \frac{f_m}{f'_m}\right)$	**Equation 1.7**

Table 8.7: Summary of models by other authors for the estimation of masonry stress-strain curve

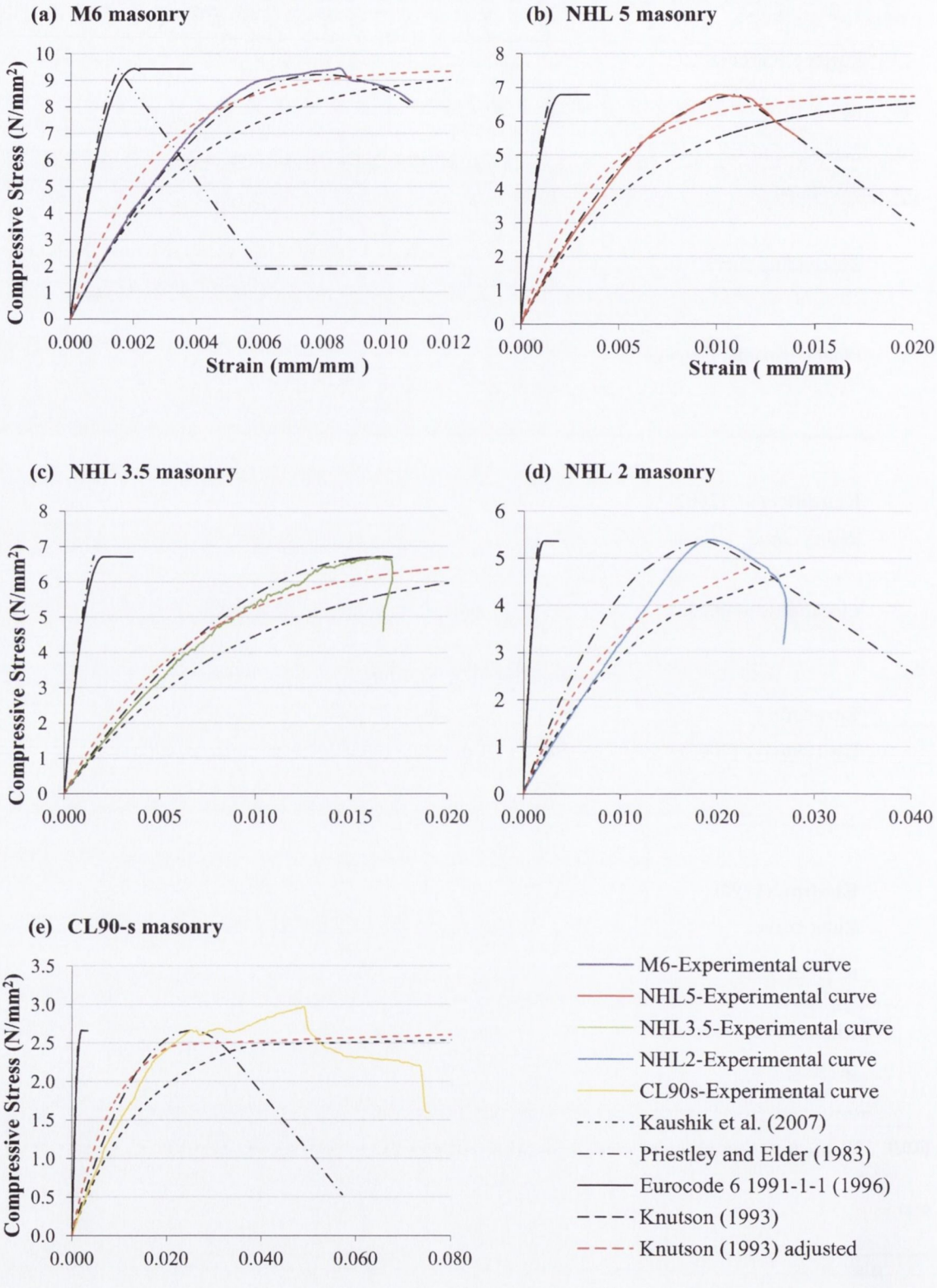

Figure 8.5: Comparison of experimental stress-strain curves for brick masonry (170 mm flow, 56 days curing) with curves estimated by analytical models proposed by other authors.

Eurocode 6 EN 1996-1-1 (2005) generates curves which are similar to Priestley and Elder (1983). This similarity is because Eurocode 6 EN 1996-1-1 (2005) also only allows for limited strains in the rising curve (0.002).

The final model (Equations 1.6 and 1.7) proposed by Kuntson (1993) performs reasonably well, but only up to approximately 30 % of the ultimate stress σ_{max}. As previously mentioned, Mohamad *et al.* (2006) found this divergence when considering the stress-strain curve of hollow block masonry constructed with flexible cement-lime mortars. The main issue associated with Kuntson (1993) is that the initial trajectory of the curve is too low. It is likely that the low trajectory is because the elastic modulus value used in Equation 1.6 was obtained from the linear portion of the experimental stress-strain diagram and not the initial tangent modulus (E_0).

Mohamad *et al.* (2006) used a hyperbolic method proposed by Kondner (1963) to obtain the initial tangent modulus and concluded that using it improved Equations 1.6 and 1.7. In the present study, the initial tangent modulus for each specimen was obtained from the corrected stress-strain curves (see Figure 8.2).

Adjusting the Kuntson (1993) equation by including E_0 generally improves the model's overall agreement with experimental curves (Figure 8.5). However, Equation 1.5 proposed by Kaushik *et al.* (2007) remains the most accurate estimate of the stress-strain curve of lime-masonry when the peak strain and elastic modulus is experimentally known.

8.2.3 Estimation of masonry elastic modulus

Three relationship groupings for the estimation of lime masonry elastic modulus have been proposed based on regression analysis of experimental data from this research: cement-lime, strong hydraulic and feebly hydraulic/non hydraulic (Section 5.4).

Masonry type	Grouping	Proposed relationships	
M6	Cement-lime	$E = 230 f'_m$	**Equation 8.5**
NHL 5 NHL 3.5	Strong hydraulic limes	$E = 130 f'_m$	**Equation 8.6**
NHL 2 CL90-s	Feebly hydraulic/ non hydraulic limes	$E = 85 f'_m$	**Equation 8.7**

Table 8.8: Estimation of masonry elastic modulus (previously presented in Table 5.2)

The above equations for the estimation of masonry elastic modulus were applied to the representative samples aforementioned (one specimen for each mortar grade at 56 days and with 170 mm initial flow). The results are presented in Table 8.10. As can be seen, three input values are used for f'_m, one experimental and two estimated values. Of the estimated values, one is based on regression analysis for present study data (Equations 8.7-8.9) and the other is based on Eurocode 6 EN 1996-1-1 (2005) (Equation 8.13).

The best estimates for the elastic modulus of cement-lime masonry are achieved when using the two predicted values of f'_m as inputs in Equation 8.16 (within 12 % of the experimental result). Using the experimental values of f'_m, generally overestimate the elastic modulus of CL90-s, NHL 2 and NHL 3.5 masonry but underestimate NHL 5 masonry. The predicted values of f'_m provide reasonable estimates of the elastic modulus for NHL 2 and NHL 3.5 masonry (within 7-20 % of the experimental result) and very poor estimates of CL90-s and NHL 5 masonry (within 25-63 %).

The results indicate that the reliable prediction of lime masonry elasticity can be difficult. Overall, the proposed equations do not consistently provide accurate estimations of elastic modulus. Therefore, further experimental research is required.

8.2.4 Estimation of peak strain

The ability to estimate the maximum strain (ε'_m) and therefore the amount to which a specimen will deform under an applied compressive load is very important to accurately predict the stress-strain relationship of masonry. The estimation of ε'_m becomes ever more critical when dealing with a deformable material such as lime.

Kaushik *et al.* (2007) proposed Equation 1.6 (Table 8.9) to ascertain peak strain based on regression analysis of a large body of cement masonry experimental data. It is generally accepted that the deformation characteristics of masonry are significantly influenced by the mortar, therefore Kaushik *et al.* (2007) includes the mortar compressive strength in Equation 1.6, even though it has already been taken into account in determining the masonry compressive strength component f'_m.

Source Reference	Model	
Kaushik *et al.* (2007)		
Peak strain	$\varepsilon'_m = \frac{0.27}{f_j^{0.25}}\left(\frac{f'_m}{E_m}\right)$	**Equation 1.6**
Regression analysis of experimental data		
Peak strain (Cement-lime and lime masonry)	$\varepsilon'_m = \frac{0.34}{f_j^{0.01}}\left(\frac{f'_m}{E_m}\right)$	**Equation 8.10**

Table 8.9: Summary of models by other authors for the estimation of masonry strain

Three different categories of input parameters are considered (Table 8.10):

a. All values obtained from the experimental data of the present study.

b. All f_j values are experimental, $f'_{m\text{-}1}$ and $E'_{m\text{-}1}$ values are predicted from equations proposed in this research (based on regression analysis)

c. All f_j values are experimental, f'_{m-2} values are predicted using Eurocode 6 (Equation 8.13) and E'_{m-2} values are predicted using the equations proposed for E'_m (with f'_{m-2} as an input).

According to the results, Equation 1.6 by Kaushik *et al.* (2007) is a poor predictor of peak strain (Table 8.10). In general, Equation 1.6 significantly underestimates the peak strain value of lime and cement-lime masonry, irrespective of which category of input parameter is used. Therefore, this equation should not be considered for use in the design of lime-mortared masonry.

As previously discussed, equation 1.6 by Kaushik *et al.* (2007) relates masonry strain to masonry characteristic compressive strength and stiffness, and mortar compressive strength in the form: $\varepsilon'_m = \frac{K}{f_j^{\alpha}}\left(\frac{f'_m}{E_m}\right)$ where K and α are constants. This equation is rearranged to $\varepsilon'_m - \frac{K}{f_j^{\alpha}}\left(\frac{f'_m}{E_m}\right) = 0$ and "least squares" regression analysis carried out whereby, K, and α are systematically varied in order to minimize the sum of square errors (SSE)

$$SSE = \sum(\varepsilon_i - \varepsilon_{Ri})^2 \qquad \textbf{Equation 8.11}$$

where, ε_i is the i^{th} experimental prism strength, ε_{Ri} is the i^{th} regression estimate of masonry strength,

R^2 and σ were calculated using equations 8.11 and 8.12.

$$R^2 = 1 - \sqrt{\frac{\sum(\varepsilon_i - \varepsilon_{Ri})^2}{\sum(\varepsilon_i - \varepsilon_{mean})^2}} \qquad \textbf{Equation 8.82}$$

$$\sigma = \sqrt{\frac{\sum(\varepsilon_i - \varepsilon_{Ri})^2}{n-2}} \qquad \textbf{Equation 8.13}$$

where, ε_{mean} is the arithmetic average of experimentally obtained masonry strains and n represents the number of data points investigated. Since two estimators K and α are desired, n-2 degrees of freedom are used in the calculation of σ, in order to achieve an unbiased estimate.

Equation 8.10 was established based on this regression analysis of cement-lime and lime mortar brick masonry experimental results in this research (Tables 8.3-8.5). R^2 and σ were found to be 0.93 and 0.0003 respectively, indicating good correlation. According to Table 8.10, equation 8.13 provides a more accurate estimate of masonry strain under a compressive load than that of Kaushik *et al.* (2007) however, it is still a poor predictor of strain and therefore should not be considered for use in the design of lime-mortared masonry.

	Experimental results [a]				Estimate of f'_m (N/mm^2)		Estimate of masonry elastic modulus (N/mm^2)				Estimate of Strain, Kaushik et al. (2007)			Estimate of Strain, Present Study (Eq. 8.10)		
Mix Type [b]	Masonry			Mortar	Present Study	Eurocode 6 (2005) Eq. 8.13	Equation	Using experimental f'_m	Using f'_{m-1}	Using f'_{m-2}	Using experimental f'_m & E_m	Using f'_{m-1} & E_{m-1}	Using f'_{m-2} & E_{m-2}	Using experimental f'_m & E_m	Using f'_{m-1} & E_{m-1}	Using f'_{m-2} & E_{m-2}
	f'_m (N/mm^2)	E_m (N/mm^2)	ε'_m	f_j (N/mm^2)	f'_{m-1}	f'_{m-2}		E_m	E_{m-1}	E_{m-2}	ε'_m	ε'_{m-1}	ε'_{m-2}	ε'_m	ε'_{m-1}	ε'_{m-2}
M6 (1:0.5:4)(v)	9.43	1874.01	0.0080	19.23	7.20 [d]	7.21	E_m=230f'_m	2168.9 {16} [c]	1656.00 {-12}	1658.30 {-12}	0.0006 {-92}	0.0007 {-91}	0.0007 {-91}	0.0017 {-79}	0.0014 {-82}	0.0014 {-82}
NHL5 (0:1:3)	6.79	1127.86	0.0114	7.02	5.63 [e]	5.33	E_m=130f'_m	882.7 {-22}	731.90 {-35}	692.90 {-39}	0.001 {-91}	0.0013 {-88}	0.0014 {-88}	0.002 {-82}	0.0026 {-77}	0.0026 {-77}
NHL3.5 (0:1:3)	6.70	738.52	0.0158	6.11	5.29 [e]	5.11		871 {18}	687.90 {-7}	664.30 {-10}	0.0016 {-90}	0.0014 {-91}	0.0014 {-91}	0.003 {-81}	0.0026 {-84}	0.0026 {-84}
NHL2 (0:1:3)	5.36	425.09	0.0159	2.35	4.55 [e]	3.84	E_m=85f'_m	455.6 {7}	386.70 {-7}	326.40 {-23}	0.0027 {-83}	0.0022 {-86}	0.0023 {-86}	0.0043 {-73}	0.0039 {-75}	0.0039 {-75}
CL90-s (0:1:3)	2.66	175.80	0.0200	1.52	1.55 [f]	3.37		226.1 {29}	131.75 {-25}	286.45 {63}	0.0037 {-82}	0.0028 {-86}	0.0023 {-88}	0.0051 {-74}	0.004 {-80}	0.004 {-80}

[a] Experimental results refer to selected representitive specimens

[b] All specimens of mortar and masonry were manufacured to 170 mm initial flow and tested at 56 days

[c] Values in { } represent the percentage error between estimated and actual experimental results

[d] Value estimated by Eq. 8.9

[e] Value estimated by Eq. 8.7

[f] Value estimated by Eq. 8.8

Table 8.10: Comparison of experimental results with analytical prediction models from various sources.

CHAPTER 9

CONCLUSIONS

9.1 INFLUENCE OF MORTAR PROPERTIES ON THE PROPERTIES OF MASONRY

The physical properties of lime mortar including water content, water retention and workability have a significant effect in the strength and deformation characteristics of lime mortar and masonry. Increasing the water content and therefore the workability of mortar generally improves the compressive/flexural/bond strength and stiffness of the cement-lime and natural hydraulic lime masonry whereas it adversely affects these properties of calcium lime masonry.

According to the results, the mortar water content influences the properties of lime-masonry to a greater extent than cement-lime masonry.

The results also demonstrate that varying water content affects brick masonry stiffness, bond and flexural strength to a greater extent than compressive strength; and that the impact of water content on masonry compressive/flexural/bond strength and stiffness reduces as the hydraulic strength of the mortars increases.

Furthermore, varying mortar water content within the same range producing an appropriate workability (165-170 mm initial flow) generally has a greater effect on the mechanical properties of masonry in the first 28 days of curing than it does at 6 months. This may indicate that the water content of mortar can be varied (within the above range) for workability, improved early strength development (28 days) and build rate, without significantly affecting the long-term strength and stiffness properties of masonry

Irrespective of mortar water content, this research finds that both brick and stone masonry constructed with NHL lime mortar develop the majority of their mechanical strength and stiffness in the first 28 days. The results suggest that the compressive strength gained by NHL mortar masonry at 28 days and CL mortar masonry at 56 days is equivalent to 7-day values of pure cement mortar masonry agreeing with previous authors (Tate (2008) and Zhou *et al.* (2008)).

Furthermore, the properties of lime-mortar and masonry (compressive/ flexural/ bond strength and stiffness) were found to consistently increase over time. This contradicts

observations on cement-mortar and masonry by previous authors who observed "up and down" variations over time.

This research also finds that the properties of lime mortar and masonry increase with the hydraulic strength of the mortar (except for NHL 3.5 and NHL 5 masonry). NHL 3.5 brick-masonry was shown to achieve comparable compressive strength to NHL 5 brick-masonry yet it remained significantly more deformable (30 %) which is a desirable characteristic in masonry conservation. In addition, the results suggest that increasing the binder content of NHL 3.5 mortar (from 0:1:3 to 0:1:2) provides masonry with significantly greater strength and superior deformability than NHL 5 mortar at 0:1:3.

9.2 Influence of curing on mortar and masonry properties

The curing environment has a significant influence on the development of both mortar and brick masonry properties. Lime-mortar masonry shows a general decrease in strength and stiffness whereas cement-lime mortar masonry was not significantly affected during the first 28 days of outdoor curing.

This research suggests that masonry units protect the joint mortar from adverse weather conditions, since all of the masonries continued to gain significant strength and stiffness over time despite the freezing conditions experienced at 6 weeks (unlike the respective mortars which were adversely affected). This is especially remarkable for CL-mortar masonry since it is generally considered highly susceptible to poor weather conditions.

In general, the results indicate that outdoor curing leads to a loss of the ultimate compressive strength, elastic modulus and bond strength of brick masonry at 6 months. However, according to this research, the masonry is generally less affected by the curing environment than the mortar. Furthermore, no consistent trends were found to indicate that a particular masonry type (CL90-s, NHL 2, M6) or masonry property (compressive strength, stiffness and bond strength) is more affected by outdoor curing than another.

9.3 MORTAR AND MASONRY RELATIONSHIPS

The compressive strength of brick masonry was found to tend towards a maximum of approximately 9 N/mm^2 (circa 75 % of the normalised compressive strength of the brick). This occurred for cement and higher strength hydraulic lime mortar masonry at the higher initial flow of 170 mm. Over 6 months of curing was required in all cases.

According to this study, the tendency of mortar to be stronger than its corresponding masonry, is closely related to the unit strength and the mortar hydraulic strength (M6, NHL 5, NHL 3.5 mortars are stronger than their masonry and NHL 2, CL90-s are weaker than their corresponding masonry.

For the higher hydraulic strength mortars, an increase of compressive/flexural strength and elastic modulus of mortar leads to a small compressive strength increase of masonry whereas, for the lower hydraulic strength mortar, small increases in mortar compressive/flexural strength and stiffness result in relatively large increases in masonry compressive strength.

An increase of mortar compressive strength increases masonry compressive strength, however this relationship is non-linear, therefore indicating that the stronger the mortar, the less sensitive the masonry is to increases in mortar strength.

The relationships between mortar flexural strength and stiffness, and brick-masonry compressive strength are also non-linear. This is as expected, since the flexural strength and stiffness of mortar and masonry compressive strength generally increase with mortar hydraulic grade, curing time and water content and since the masonry compressive strength tends towards a maximum as stated above.

This study contradicts previous authors (Venumadhava Rao *et al.* (1995) and Venkatarama and Vyas (2008)) who suggested that masonry compressive strength is not significantly impacted by mortar strength. According to this study, masonry compressive strength is clearly influenced by the mechanical properties of mortar, but the influence becomes progressively smaller as the compressive strength of the masonry moves towards its maximum load capacity (determined by the unit strength).

Brick masonry bond strength is similarly influenced by the mechanical properties of mortar and the overall relationships are also non-linear. Small enhancements of the mechanical properties of low strength mortars result in large bond gains whereas significant gains in the mechanical properties of higher strength mortars do not result in substantial bond improvement. This indicates that the magnitude of the influence of mortar properties on masonry bond strength becomes progressively smaller as the bond strength increases and tends towards a maximum.

This research establishes a clear relationship between brick masonry bond and compressive strength, since both properties increase over time and as mortar hydraulic grade, mortar strength and water content increase. Several Authors (Grenley (1969); Venkatarama *et al.* (1995); Sarangapani *et al.* (2005); Gumaste *et al.* (2006) Venkatarama *et al.* (2007) and Venkatarama and Vyas (2008)) also found a relationship between masonry bond and compressive strength however, this research advances current knowledge and demonstrates that the relationship is non-linear. According to the results, masonry compressive strength reaches a maximum value, after which, any further increase in bond is unlikely to cause further gains in masonry compressive strength. This is likely due to the failure mechanisms associated with masonry when it is close to its maximum compressive strength. In such circumstances, failure is generally due to lateral tension in the bricks (causing them split).

Furthermore, this research demonstrates that when masonry consists of low suction units that are significantly stronger and stiffer than the mortars, masonry compressive strength is more governed by the unit strength than the unit's properties (texture and IRA) which influence bond strength.

According to the results, the relationship between mortar and masonry stiffness has a significant influence on masonry compressive strength. Previous authors (Venkatarama *et al.* (2007)) found that increases in bond strength only result in marginal improvements in masonry compressive strength when the modulus of elasticity of the mortar is in the same range or greater than that of the masonry unit. This research agrees with (Venkatarama *et al.* (2007)) and suggests that masonry strength tends towards its maximum value when the mortar stiffness is close to or greater than that of the unit.

Other authors, Venumadhava Rao *et al.* (1995) reported that cement mortars with distinctly different compressive strengths but similar bond strengths resulted in comparable masonry compressive strengths. This research disagrees with Venumadhava Roa *et al.* (1995) since only natural hydraulic lime (NHL 3.5 and NHL 5) mortar and masonry behave in such a manner and therefore concludes that lime and cement-lime mortars with significantly different compressive strength and stiffness, but similar bond strength, do not necessarily result in masonry with comparable compressive strengths.

The relationship between masonry stiffness and masonry compressive strength is of great importance in the conservation of historic buildings and monuments. Strength is a key design parameter however, masonry stiffness and deformability must also be taken into consideration to ensure compatibility with historic materials. Repair mortars and masonry must be sympathetic to the existing materials, and deform and behave in a similar manner. Previous authors generally assumed a linear relationship between the elastic modulus and the characteristic compressive strength of masonry. They proposed a wide range of equations in the linear form: $E'_m = k\, f'_m$ (Equation 5.1) based on cement and cement-lime masonry research where k values vary considerably (210-1670). However, this research demonstrates that the overall relationship is non-linear. Therefore, the influence of masonry stiffness (and thus mortar strength and stiffness) on the compressive strength of brick masonry reduces as masonry strength tends towards a maximum. This is likely due to failure mechanisms associated with the lateral tensional capacity of the unit aforementioned.

9.4 MASONRY FAILURE MECHANISMS

Previous authors have emphasised the influence of mortar and unit stiffness on the failure mode of cement/lime masonry in compression (Venkatarama and Vyas (2008) and Kaushik *et al.* (2007); Gumaste *et al.* (2006); Sarangapani *et al.* (2005)). However, results from these studies are contradictory and none of the authors considered both situations (a) $E_{unit} > E_{mortar}$ and (b) $E_{unit} < E_{mortar}$ simultaneously. In addition, reports from previous literature tend to differ in terms of bond maintenance at failure. This research recognises that categorising the failure of masonry based on either mortar/unit stiffness or bond failure is insufficient and does not fully explain the mechanical behaviour of masonry. The present study considers a range of mortar elastic moduli (70-1700 N/mm^2) and bond strengths (0.05-0.88 N/mm^2) and since the brick elastic modulus was 1240 N/mm^2, both of the above situations with respect to E_{unit} and E_{mortar} are considered.

This research finds that the failure mechanics of lime and cement-lime masonry in compression do not depend on the ratio of mortar:masonry stiffness (Table 9.1) since similar failure patterns were observed for situations a and b.

Situation		Masonry type	Bond generally maintained	Description of Failure
(a) $E_{unit} > E_{mortar}$	Mode I	Stiffer/stronger NHL 3.5 and NHL 5 brick masonry	Yes	Cracking, crushing and lateral failure of the units
	Mode II	Weaker, more flexible brick and stone masonry made with CL90-s and NHL 2 mortar	No	Mortar failure, large amount of spalling, high strain values, bond failure, cracking and lateral failure of the units
(b) $E_{unit} < E_{mortar}$		Stronger cement-lime brick masonry	Yes	Cracking, crushing and lateral failure of the units/mortar with some diagonal shear failure of the composite masonry

Table 9.1: Summary of masonry failure observations in compression

Experimental observations and results suggest that maintenance (or loss) of the bond between the mortar and unit at failure, may influence the masonry failure mechanism and support previous authors suggested internal stress distributions and failure mechanics. However, the restraining effect of the steel plates at the top and bottom of the specimens, the steel plates bending under high loads and the theoretical 45 degree load application occurring within the specimen, may all have caused uneven stress distributions leading to the observed failure patterns. The out-of-plane failure of the masonry specimens may also be due to the fact that they are less restrained in that direction.

Flexural strength testing of masonry perpendicular to the bed joints reveals three failure patterns. The lower strength masonry (CL90-s and NHL 2) mainly experiences failure of the vertical and horizontal joints. Bond failure is accompanied by vertical splitting of some of the bricks units as the masonry strength and stiffness increases. For the higher strength series, failure is due to vertical cracking of the bricks close to vertical joints which also suffered bond failure. During testing of masonry parallel to the bedding joins, the weakest of the four mortar joints within the constant moment zone eventually fractures at failure. Most fracture planes occurred along the interface between the bottom brick face and the bedding mortar.

Bond wrench testing, evidences three distinctive failure modes. Similar to flexural strength parallel to the bedding joints, the vast majority of specimens failed at the interface between the bedding mortar and the brick bed.

9.5 ESTIMATION OF MASONRY COMPRESSIVE STRENGTH

The ability to predict the compressive strength of lime-masonry is very important for promoting masonry design incorporating lime mortars. This research uses regression analysis of experimental data to establish equations to estimate the characteristic compressive strength of masonry (f'_m).

When NHL masonry results are considered separately to those of calcium lime, the estimate for f'_m improves to within 10 % for 28 days (Equation 8.4). A sufficiently accurate predictive model has not been found for CL masonry, due to the relatively large variations associated with calcium lime mortar and masonry results.

Equation 8.6 (obtained by regression analysis of the results) provides a good estimate of the characteristic compressive strength of brick masonry constructed with cement-lime mortar (within 8 % of the experimental value at 28 days).

Origin	Estimate equation	
NHL's only	$f'_m = 0.69{f_b}^{0.55}{f_j}^{0.37}$	**Equation 8.4**
Cement-lime/brick	$f'_m = 0.46{f_b}^{0.5}{f_j}^{0.5}$	**Equation 8.6**
Eurocode 6	$f'_m = 0.5{f_b}^{0.7}{f_j}^{0.3}$	**Equation 8.8**

Table 9.2: Summary of proposed equations for the estimation of lime-brick masonry strength

This research finds that the estimation of stone-masonry strength is not reliable due inconsistencies in the experimental results associated with strong unit/weak mortar combination, the variable geometry of the specimens tested and variable joint width leading to point loading. Poor R^2 and standard deviation values evidenced during the regression analysis are accompanied by large differences between estimated and actual experimental results.

The characteristic compressive strengths of lime and cement-lime masonry were also estimated using various analytical prediction models from literature. This research validates the use of Eurocode 6 EN 1996-1-1 (2005) (Equation 8.8), not only for cement masonry, but also for the estimation of 28-day characteristic compressive strength of

NHL 2, 3.5 and 5 brick-lime masonry. Furthermore, this research recommends using the actual mortar strength (obtained by testing of site-made prisms) rather than the standard mortar strength classification to predict lime-masonry strength because the standard underestimates the potential strength of lime-masonry since the compressive strength of lime mortar can vary greatly depending on water content. It is also concluded that Eurocode 6 EN 1996-1-1 (2005) severely underestimates the characteristic compressive strength of stone masonry the unit strength is considerably greater than the mortar strength.

Additionally, this study establishes that no simple predictive model found in literature, can consistently and accurately estimate the characteristic compressive strength of brick or stone masonry, where the normalised compressive strength of the units is significantly greater than that of the constituent mortars. This is because the models were originally designed for cement-mortar masonry and large differences were not envisaged between mortar and masonry strengths.

9.6 Estimation of lime-masonry deformation characteristics

Lime mortars are less stiff and deform considerably more than cement mortars when loaded. Therefore, despite the fact that models based on the present study and Eurocode 6 afford good estimates of NHL masonry strength. These equations do not consider the strain and deformation behaviour of the masonry.

This research investigates three equations for the estimation of brick-masonry elastic modulus based on the hydraulic strength of mortar and obtained from regression analysis: E'_m=230f'_m for cement-lime masonry, E'_m=130f'_m for higher hydraulic strength masonry and E'_m=85f'_m for low hydraulicity/ calcium-lime masonry. Due to the deformability of lime materials, these values of k are low compared to other authors who studied cement masonry. Overall, this research concludes that these equations may not provide consistent and accurate estimates of lime-mortar masonry elastic modulus and therefore, they should be used with caution.

The ability to estimate the maximum strain (ε'_m) and therefore the amount to which a specimen will deform under an applied compressive load is very important to accurately predict the stress-strain relationship of masonry. The estimation of ε'_m becomes ever more critical when dealing with a very elastic materials such as lime.

The usefulness of the simple peak strain estimation model, proposed by Kaushik *et al.* (2007), was investigated for lime and cement-lime mortar-masonry. Despite incorporating the stiffness characteristics of the mortar, this equation performed poorly, generally underestimated the strain of lime-mortar masonry by 82-92 %. Following regression analysis of the results in this research, an equation was developed to estimate the peak strain of lime and cement-lime mortar masonry. The equation performed approximately 10 % better than that of Kaushik *et al.* (2007). However, this study concludes that both these equations should not be considered for use in the design of lime or cement-lime masonry due to low predictive accruacy.

Several authors have presented simple mathematical models to describe the relationship between applied stress and strain deformation of masonry in compression. These analytical models were compared with experimental curves by selecting a representative sample of stress-stress diagrams comprising one masonry specimen for each mortar grade. The input parameters for the modelled stress-strain curves were experimentally obtained. This research finds that Priestley and Elder (1983) and Eurocode 6 EN 1996-1-1 (2005) provide poor predictions of stress-strain curves because they were unable to take the relatively large deformations associated with the lime-mortar masonry into consideration, due to restrictions on strain parameters. Kuntson (1993) prediction performed well up to approximately 30 % of the ultimate stress. The model provides a poor prediction after 30% of the ultimate stress since the initial trajectory of the curve is too low. This is likely because the elastic modulus was determined from the linear portion of the experimental stress-strain curve. Adjusting the input parameters of the model by using the initial tangent modulus (E_0) rather than the elastic modulus determined from the linear portion of the stress-strain curve, improved the model's overall agreement with experimental curves. The model proposed by Kaushik *et al.* (2007) was found to be the most accurate model for estimating the shape of the stress-

strain curve of lime mortar and cement-mortar masonry. However, experimental input parameters were used for all of the above comparisons therefore Kaushik *et al.* (2007) should not be used to predict the stress-strain curve of lime mortar masonry until an accurate estimate of the masonry's peak strain can be determined.

LIST OF REFERENCES

Abrams, D P (1995). "Effect of mortar shrinkage on in-plane stresses in clay brickwork". TMS Journal 13: 77-84.

Adami, Chryssi-Elpida and Vintzileou, Elizabeth (2007). "Interventions to historic masonries: Investigation of the bond mechanism between stones or bricks and grouts". Materials and Structures 41: 255-267.

Adams, M A and Hobbs, D W (1994). "Bond strength of brickwork from crossed couplet and wallette tests: Some comparative results". Masonry International 8(1): 16-20.

Allen, G; Allen, J, Elton, N, Farey, M, Holmes, S, Livesey, H, Radonjic, M (2003). Hydraulic Lime Mortar for Stone, Brick and Block Masonry. Bristol, Donhead

Almeida, J C, Lourenco, P B and Barros, J A (2002). "Characterization of brick and brick-mortar interface under uniaxial tension". International Sessions on Structural Masonry for Developing Countries, Brazil, Editors A Santos *et al.* 67-76.

Anderegg, F O (1940). "Some Properties of Mortars in Masonry". Proceedings of the American Society for Testing Materials, Philadelphia, ASTM, 257-280.

Anderegg, F O (1942). "The effect of brick absorption characteristics upon mortar properties". Proceedings of the American Society for Testing Materials, Philadelphia, ASTM, 42:821.

Anderson, C and Held, L (1986). "The effect of sand grading on mortar properties and the tensile bond brickwork specimens". Proceedings of the British Masonry Society 1: 1-6.

Arandigoyen, M and Alvarez, J I (2007). "Pore structure and mechanical properties of cement-lime mortars". Cement and Concrete Research Journal 37: 767-775.

Army, U. S (2005). Masonry Structural Design for Buildings. Washington, DC, IN Joint Departments, U.S. Army, Navy and Air Force (Eds.).

AS3700 (1998). Australian Standards for Masonry Structures. Sydney, Australia.

ASTM (2000a). Standard test method for bond strength of chemical-resistant mortars. ASTM C 321. West Conshohocken, PA, ASTM International.

ASTM (2002a). Standard test method for bond strength of mortar to masonry units. ASTM C 952. West Conshohocken, PA, ASTM International.

ASTM (2003b). Standard test methods for sampling and testing brick and structural clay tile. ASTM C 67 West Conshohocken, PA, ASTM International.

ASTM (2005). Standard test methods of conducting strength tests of panels for building construction. ASTM E72. West Conshohocken, PA, ASTM International.

ASTM C1072a (2000). Standard test method for measurement of masonry flexural bond strength. West Conshohocken, PA. USA.

ASTM C1357 (2002). Standard test methods for evaluating masonry bond strength. West Conshohocken, PA. USA.

Atkinson, R H and Noland, J L (1983). "A proposed failure theory for brick masonry in compression". Procedings of the 3rd Canadian Masonry Symp. Edmonton, Alta., Canada: 510–517.

Atkinson, RH, Noland, JL and Abrams, DP (1982). "A deformation theory for stack bonded masonry prisms in compression". In: Proceedings 7th international brick masonry conference, Melbourne University, Melbourne, Australia, 565-567

Azeredo, G, Morel, J and Lamarque, C (2008). "Applicability of rheometers to characterizing earth mortar behavior. part i: experimental device and validation". Materials and structures 41: 1465-1472.

Baker, L R (1979). "Some factors affecting the bond strength of brickwork". Proceedings of the 5th International Brick Masonry Conference, Washington D C, The Brick Institute of America, Reston, VA. 62-72.

Banfill, P (1994). "Rheological methods for assessing the flow properties of mortar and related materials". Construction and Building Materials 8(1): 43–50.

Bennett, R M, Boyd, K A and Flanagan, R D (1997). "Compressive properties of structural clay tile prisms". Journal of Structural Engineering 123(7): 920-926.

BIA (2003). Mortars for Brick Masonry. Technical Notes on Brick Construction. Reston, VA, The Brick Industry Association.

Binda, L, Fontana, A and Frigerio, G (1988). "Mechanical behaviour of brick masonries derived from unit and mortar characteristics". Proceedings of the 8th Int. Brick and Block Masonry Conference, Dublin, Ireland, 1: 205-216.

Binda, L and Molina, C (1990). "Building materials durability". Journal of Materials in Civil Engineering 2(223-239).

Bosiljkov, BV (2001) "The use of industrial and traditional limes for lime mortars". Historical Constructions: 343-352. Lourenço, P.B. and Roca, P (Editors), Guimarães, Portugal.

Bosiljkov, V B (2001). "The use of lime mortars for sustainable restoration of ancient buildings". Proceedings of the 9th Canadian Masonry Symposium, University of New Brunswick. Canada.

Bosiljkov, V, Page, A, Bokan-bosiljkov, V and Zˇarnice, R. (2003). "Performance based studies of in-plane loaded unreinforced masonry walls". Mason International 16(2): 39-50.

BRE, British Research Estabishment (1991). "Testing bond strength of masonry". Digest 360, Garston, H K.

C952/76 (1976). Test of bond strength of mortar to masonry units, ASTM, American Society For Testing And Materials.

Carolinas Concrete Masonry Association (2010). "Carolinas Concrete Masonry Association ". from http:/ccmaon-line.com?NewPages/weather.

Casali, J and Prudencio, J (2008). "A new test method for the evaluation of the workability of concrete block masonry bedding mortars". In: Proceedings of the 14th International brick and block masonry conference, volume cd-rom. Masia, M, Totoev, Y, Page, A, and Sugo, H., editors, University of Newcastle, Sydney.

Chinwah, J C G (1972). Shear resistance masonry walls, University of London. Ph.D Thesis.

Christensen, G (1991). Modelling the flow of fresh concrete: the slump test, Princeton university. PhD Thesis.

Clayton, S, Grice, T and Boger, D (2003). "Analysis of the slump test for on-site yield stress measurement of mineral suspensions". International journal of mineral processing 70: 3–21.

Colville, J, Made, AM and Miltenberger, M (1999). "Tensile bond strength of polymer modified mortar". Material for Civil Engineering(11): 1-5.

Cosgrove, K and Pavia, S (2009). Mechanical and fluid transfer properties of some lime and Portland cement mortars. PROHITEC 09, Mazzolani editor. Rome, Taylor and Francis Group, London: 1603-1607.

Costigan, A and Pavía, S (2010). "The influence of mortar water content on the strength of lime-mortar masonry". Building limes forum journal 17: 43-45.

Costigan, A and Pavía, S (2010). "Mechanical properties of brick masonry bond with both hydrated and hydraulic limes". Proceedings of 8th International Masonry Conference. Dresden, 1102-1110.

Costigan, A and Pavía, S (2009). "Compressive, flexural and bond strength of brick/lime mortar masonry". Proceedings of PROHITEC 09 Rome, Taylor and Francis Group, London, 1609-1615

Cowper, AD (1927). Lime and Lime Mortars. Department of Scientific and Industrial Research. Building Research Special Report No. 9. His Majesty's Stationery Office. Reprinted Shaftesbury, Donhead 1998.

Davison, J (1974). "CBD-163 Masonry mortar". Canadian Building Digest.

Dayaratnam, P (1987). Brick and reinforced brick structures Oxford and IBH, New Delhi, India.

Dayaratnam, P, Ranganathan, R, Mukhopadhyay and Dasgupta, N (1981). "Experimental investigation on behaviour of brick and reinforced brickwork". Kanpur, India, Department of Civil Engineering, Indian Institute of Technology

De Vekey, R C, Edgell, G J and Dukes, R (1990). "The effect of sand grading on the performance and properties of masonry". In: Proceedings of The British Masonry Society, UK, 4: 152-159.

Drysdale, GR and Khattab, MM (1995). "In-plane behavior of grouted concrete masonry under biaxial tension–compression". ACI Struct J 92(6): 653-664.

Drysdale, R G and Gazzola, E A (1985). "Influence of mortar properties on the tensile bond strength of brick masonry". Proceedings of the 7th International Brick Masonry Conference, Melbourne, Australia Brick Development and Research Instiute and University of Melbourne, 927-937.

Drysdale, R G, Hamid, A A and Baker, L R (1994). "Masonry structures: Behaviour and design", Pretice Hall, Englewood Cliffs, New Jersey, USA.

Eadie, W T, Drijard, D, James, F E , Roos, M and Sadoulet, B (1971). First Edition, Statistical Methods in Experimental Physics, Amsterdam, North-Holland.

Eichholz and Pliny the Elder (1962). Natural History William Heinemann Ltd. London, Harvard University Press.

Elangonmani, C (1983). Compressive strength of brick masonry walls from prism tests. Department of Applied Mechanics and Structural Engineering, Annamalai University. M.E. Dissertation.

EN 196-9 (2010). "Methods of testing cement. Heat of hydration. Semi-adiabatic method". European Committee for Standardisation CEN, Brussels.

EN 196–1 (2005). "Method of testing cement. Part 1: Determination of strength". European Committee for Standardisation CEN, Brussels.

EN 459-2 (2010). "Building lime. Part 2: Test methods". European Committee for Standardisation CEN, Brussels.

EN 771–1 (2003). "Specification for masonry units. Part 1: Clay masonry units". European Committee for Standardisation CEN, Brussels.

EN 772-11 (2011). "Methods of test for masonry units. Part 11: Determination of water absorption of aggregate concrete, autoclaved aerated concrete, manufactured stone and

natural stone masonry units due to capillary action and the initial rate of water absorption of clay masonry units". European Committee for Standardisation CEN, Brussels.

EN 772–1 (2000). "Method to test masonry units. Part 1: Determination of compressive strength". European Committee for Standardisation CEN, Brussels.

EN 772–3 (2000). "Method to test masonry units. Part 1: Determination of net volume and % of voids of clay masonry units". European Committee for Standardisation CEN, Brussels.

EN 772–13 (2000). "Method to test masonry units. Part 1: Determination of net and gross dry density of masonry units". European Committee for Standardisation CEN, Brussels.

EN 1052–1 (1999). "Method of test masonry. Part 1: Determination of compressive strength". European Committee for Standardisation CEN, Brussels.

EN 1052–2 (1999). "Method of test masonry. Part 2: Determination of flexural strength". European Committee for Standardisation CEN, Brussels.

EN 1052–5 (2005). "Method of test masonry. Part 5: Determination of bond strength (Bond wrench method)". European Committee for Standardisation CEN, Brussels.

EN 1936 (1999). "Natural stone test methods. "Determination of real density and apparent density and of total and open porosity". European Committee for Standardisation CEN, Brussels.

EN 1996-1 (2005). Eurocode 6-Design of masonry structures. Part 1-1: "General rules for buildings—Reinforced and unreinforced masonry". ENV 1996-1-1. Brussels, Belgium. European Committee for Standardisation CEN, Brussels.

EN 1996-2 (2006). Eurocode 6-Design of masonry structures. Part 2: "Design considerations, selection of materials and execution of masonry". European Committee for Standardisation CEN, Brussels.

EN 5628-1 (2005). Code of practice for use of masonry Part 1: "Structural use of unreinforced masonry". European Committee for Standardisation CEN, Brussels.

EN 12372 (2006). "Natural stone test methods - Determination of flexural strength under concentrated load". Europeen Committee for Standardisation CEN, Brussels.

Ewing, Bryan D and Kowalsky, Mervyn J (2004). "Compressive behavior of unconfined and confined clay brick masonry", Journal of Structural Engineering (ASCW 2004).

Farran, J (1956). "Contribution mine´ralogique a` l'e´tude de l'adhe´rence entre les constituants hydrates des ci- ments et les mate´riaux enrobe´s". Revue des Mate´riaux de Construction et Travaux Publics 490-491:155-172.

Francis, A, Horman, C and Jerrems, L (1971). "T of joint thickness and other factors on compressive strength of brickwork". Proceedings of the 2nd international brick masonry conference, Stoke-on-Trent, pp 31–37.

García, D, San-José, J, Garmendia, L, San-Mateos, R, (2012). "Experimental study of traditional stone masonry under compressive load and comparision of results with design codes". Materials and Structures, 45: 995-1006

Gerard, R, Dugniolle, E and Kropp, J (1985). "Durabiliite des maconneries en briques liee a la compatabilite entre le mortier et la brique". C.S.T.C Bruxelles.

Ghazali, M Z (1986). "Shear strength of brick masonry joints", University of Sussex. D.Phil Thesis.

Godbey, R and Thomson, M (2002). "Emley plasticity testing: first steps to a precision and bias statement". In Throop, D. and Klingner, R, editors". Masonry: opportunities for the 21st century: 61–72.

Goodwin, J F and D, Saunders J (1988). "Investigation of bond between calcium silicate bricks and mortar". Proceedings of the 8th International Brick/Block Masonry Conference, Dublin, Editors: De Coursey J. 2: 987-994.

Grandet, J, Javelas, R, Perrin, B and Thenoz, B (1972). " Ro^le de l'ettringite dans la liaison de type me´canique entra la terre cuite et la pa^te de ciment-portland", Revue Terre Cuite 48: 21–28.

Green, K, Carter, M, Hoff, W and Wilson, M (1999). "The effects of lime and admixtures on the water-retaining properties of cement mortars", Cement and concrete research 29: 1743–1747.

Grenley, D G (1969). "Study of the effect of certain modified mortars on compressive and flexural strength of masonry". Designing, engineering, and constructing with masonry products, Gulf, Houston.

Grimm, C T (1975). "Strength and related properties of brick masonry". Journal Structural Division (1): 217-232.

Groot, Caspar JWS (1993). "Effects of water on mortar brick Bond", Delft, The Netherlands, University of Delft. PhD Thesis.

Gumaste, K S, Rao, KS, Venkatarama Reddy, B V and Jagadish, K S (2006). "Strength and elasticity of brick masonry prisms and wallettes under compression". Materials and Structures (2007) 29: 241-253.

Gumaste, KS (2004). "Studies on strength and elasticity of brick masonry walls", Department of Civil Engineering. Bangalore, India, Indian Institute of Science. PhD Thesis.

Hanley, R (2006). "The Relationship Between Workability and Bond Strength of Lime Mortars", Dept. of Civil, Structural and Environmental Engineering. Dublin, Trinity College. Masters.

Hanley, R and Pavia, S (2007). "A study of the workability of natural hydraulic lime mortars and it's influence on strength". Materials and Structures (RILEM 2007), 41: (2) 373-381.

Hedstrom, EG, Tarhini, KM and Thomas, RD (1991). "Flexural bond strength of concrete masonry prisms using cement and hydrated lime mortars". Masonry Society Journal 9(2): 8–23.

Heffler, L M, Stewart, M G, Masia, M J and Correa, M R S (2008). "Statistical Analysis and Spatial Correlation of Flectural Bond Strength for Masonry Walls". International masonry Society 21(2): 59-70.

Heirman, G, Hendrickx, R, Vandewalle, L, Van Gemert, D, Feys, D, De Schutter, G, Desmet, B and Vantomme, J (2009). "Integration approach of the couette inverse problem of powder type self-compacting concrete in a wide- gap concentric cylinder rheometer: Part ii. influence of mineral additions and chemical admixtures on the shear thickening flow behaviour". Cement and concrete research 39(3): 171-181.

Held, L and Anderson, C (1983). "The effect of sand grading on mortar properties and tensile bond". South Bank University London.

Hendrickx, R (2009). The adequate measurement of the workability of masonry mortar. Faculty of Engineering, Katholieke Universiteit Leuven. PhD Thesis.

Hendrickx, Roel (2009). Deformation hypothesis for free slump of a cylindrical volume of a yield stress material.

Hendry, A W and Khalaf, F M (2001). Masonry wall construction. London, E and FN Spon.

Hendry, AW and Malek, MH (1986). "Characteristic compressive strength of brickwork from collected test results". Masonry International 7: 15-24.

Hendry, E.A.W (2001). "Masonry walls: material and construction". Construction and Building materials 15: 323–330.

Hibbeler, R (2008). Mechanics of materials. Upper Saddle River, New Jersey.

Hicky Morgan, M (1914). Vitruvius: the ten books on architecture. Cambridge, Harvard University Press.

Hilsdorf, HK (1969). An investigation into the failure mechanism of brick masonry loaded in axial compression. In Johnson, FB (ed) Designing, engineering and constructing with masonry products, Gulf, Houston 34-41.

Holmes, S and Wingate, M (1997). "Building with Lime - A practical guide". Black Dog Press, UK; 3rd Revised edition (Dec 1997)

Hughes, John J and Taylor, Adrian K (2005). Compression and flexural strength testing of brick masonry panels con-structed with two contrasting traditionally produced lime mortars: Repair mortars for historic masonry. International workshop 2005, Faculty of Civil Engineering and Geos-ciences, Delft University of Technology, The Netherlands.

Isbener, A W (1969). Properties of masonry cement mortars. Designing, Engineering and Construction with Masonry Products. Houston, Texas, Ed F B Johnson Gulf Publishing.

Jukes, P, Bouzeghoub, M C. and Riddington, J R (1997). Measurement of tensile strain softening and its influence on bond tensile test results. Proceedings of the 4th International Symposium on Computer Methods in Struct. Masonry, Pande, G N, Middleton, J, Kralj, B ed, London, E and FN Spon, 1216-1221.

Jung, E (1988). The binding between mortar and brick. Proc. SIBMAC. Ed.J.W.de Courey. London, Elsevier Applied Science, Conference, Dublin, Ireland.

Kamimura, K, Serada, PJ and Swenson, EG (1965). "Changes in weight and dimensions in the drying and carbonation of Portland cement mortars". Magazine of Concrete Research(17): 5-14.

Kampf, L (1963). Factors affecting bond of mortar to brick. In: Proceedings of symposium on masonry testing. American Society for Testing and Materials, ASTM STP, 332-342.

Kampff, L (1961). "Workability of masonry mortars". Materials research and standards 1(1): 7-8.

Kaushik , HB, Rai, DC and Jain, SK (2007). "Stress-Strain Characteristics of Clay Brick Masonry under Uniaxial Compression". ASCE 19(9): 728-739.

Kayali, O (2005). High Performance Bricks from Fly Ash. World of Coal Ash Conference. University of Kentucky.

Khalaf, Fouad M (2005). "New Test for Determination of Masonry Tensile Bond Strength". Journal of materials in civil engineering (ACSE): 725-732.

Khoo, CL and Hendry, AW (1969). A failure criterion for brickwork in axial compression. In: Proceedings of 3rd international brick masonry conference, Stoke on Trent, UK, 141-145.

Knutson, H H (1993). "The stress-strain relationship for masonry " Masonry International 7(1): 31-33.

Kondner RL. Hyperbolic stress-strain response: cohesive soils. Journal of Soil Mechanics Foundation Division, ACSE 1963; 89(1):115-43

Kuenning, W H (1966). "Improved method testing tensile bond strength of masonry mortars". Journal of Materials 1(1): 180.

Lanas, J and Alvarez, J I (2003). "Masonry repair lime-based mortars: Factors affecting the mechanical behavior". Cement and concrete research 33: 1867-1876.

Lanas, J, Perez Bernal, J L, Bello, M A and Alvarez, J I (2004). "Mechanical properties of natural hydraulic lime-based mortars". Cement and concrete research 34: 2191-2201.

Lanas, J, Sirera, R and Alvarez, J I (2006). "Study of the mechanical behavior of masonry repair lime-based mortars cured and exposed under different conditions". Cement and concrete research 36: 961-970.

Lange, D, Deford, HD and Werner, AM (1999). "Micro- structural investigation of mortar/unit interaction". Journal of the Masonry Society 17(1): 31-42.

Lawrence, SJ and Cao, HT (1987). An experimental study of the interface between brick and mortar. Proceedings of the 4th International Masonry Conference, Dublin, Ireland. pp 194–204.

Lawrence, SJ and Cao, HT (1988). Microstructure of the interface between brick and mortar. Proceedings 8th International Brick/block Masonry Conference, Dublin, Ireland. pp 194–204.

Lourenço, PB (1996). Computational strategies for masonry structures. Delft, The Netherlands, Delft University of Technology. PhD Thesis ISBN: 90-407-1221-122.

Lyubimova, TYu and Pinus, ER (1962). "Crystallization structure in the contact zone between aggregate and cement in concrete". Colloid Journal USSR 24(5): 491-498.

MAC (2004). "Mortars" Masonry Technical Library. Park Ridge, Il, Masonry Advisory Council.

Malinowski, R (1979). "Concretes and mortars in ancient aqueducts". Concrete International: 66 – 76.

Martin, R (1976). "Palladius Traite´ D'Agriculture. Livre I. Societe´ D'Edition 'Les Belles Letres'".

Maso, JC (1980). The bond between aggregates and hydrated cement pastes. Proceedings of the 7th International Congress on the Chemistry of Cement: Septima Editions, Paris, 1211-1220.

Matthana, MHS (1996). Strength of brick masonry and masonry walls with openings. Department of Civil Engineering. Bangalore, India, Indian Institute of Science. Ph D Thesis.

Matthys, J H and Grimm, C T (1979). Flexural strength of non-reinforced brick masonry with age. Proceedings of the 5th Internaltional Brick Masonry Conference, Washingtion D C The Brick Institute of America, Reston, Virginia. USA., 114-121.

Maurenbrecher, A H P, Trischuk, K, Subercaseaux, M I and Suter, G T (2005). "Preliminary evaluation of the freeze-thaw resistance of hydraulic lime mortars". RILEM workshop on repair mortars for historic masonry, Delft University, the Netherlands.

Mc Neary, W S and Abrams, D P (1985). "Mechanics of masonry in compression". J. Struct. Eng. 111(4): 857-870.

Mc Neary, W S, Atkinson, R H, Abrams, D P and Noland, J L (1985). Basic Properties of Clay-Unit Masonry Stack-bond Prisms in Compression: http://www.iitk.ac.in/nicee/wcee/article/8_vol4_711.pdf.

Mohamad, G, Lourenco, P B and Humberto, R (2006). "Mechanics of hollow concrete block masonry prisms under compression: Review and prospects". Cement and Concrete Composites 29: 181-192.

Moore, D and McCabe, G (2005) "Introduction to practical statistics" W H Freeman and Co. UK; 5 Har/Cdr edition (June 2005)

Momayez, A, Ehsani, MR, Ramezanianpour, AA and Rajaie, H (2005). "Comparison of methods for evaluating bond strength between concrete substrate and repair materials". Cement and Concrte Restoration 35(4): 748-757.

Mosquera, M J, Benitez, D and Perry, H (2002). "Pore structure in mortars applied on restoration. Effect on properties relevant to decay of granite buildings". Cement and Concrete Restoration 32: 1883 – 1888.

Mosquera, M J, Benitez, D and Perry, S H (2002). "Pore structure in mortars applied on restoration: effects on properties relevant to decay ofgranite buildings". Cement and concrete research(32): 1883–1888.

MSJC, Masonry Standards Joint Committee (2002). "Building code requirements for masonry structures," ACI 530-02/ASCE 5-02/TMS 402-02, American Concrete Institute. Detroit., Structural Engineering Institute of the American Society of Civil Engineers, The Masonry Society.

Müller, M (2000). "Reducing the cost of lime cement plaster by selecting appropriate methylcellulose combinations". Technical Report an99072e-b, Anton Paar.

Murata, J (1984). "Flow and deformation of fresh concrete". Materials and structures 17: 117–129.

Neville, A M and Brooks, J J (1987). "Concrete Technology". Longman Scientific and Technical Harrow, UK.

Ohler, A (1986). "Zur berechnung der druckfestigeit von mauerwerk unter beruck-sichtigung der mehrachsigen spannungszustande in stein und mortel".Bautechnik 5.

Oliveira, D V (2006), Lourenco, P B, Roca, P. "Cyclic behaviour of stone and brick masonry under uniaxial compressive loading". Materials and Structures, 39: 247-257.

Olivito, R S and Stumpo, P (2001). "Fracture mechanics in the characterisation of brick masonry structures". Materials and Structures, 34: 217-223.

Palmer, L A and Parsons, D A (1934). "A study of the properties of mortars and bricks and their relation to bond". National Bureau of Standards, Journal of Research 12 (Research paper no. 683).

Pande, G N, Liang, J X and Middleton, J (1989). "Equivalent elastic moduli for brick masonry". Computers and Geotechnics 8(3): 243-265.

Pashias, N and Boger, D (1996). "A fifty cent rheometer for yield stress measurement". Journal of rheology 40(6): 1179–1189.

Patterson, R and Pavía, S (2012). "Influence of loading rate on lime mortar strength". In: Proceeding of Bridge and Concrete Research in Ireland, 511-517.

Paulay, T and Priestley, M J N (1992). "Seismic design of reinforced concrete and masonry buildings". Wiley-Interscience, New York.

Pavía, S (2006). "Repair mortars for masonry bridges". Bridge and Infrastructure Research in Ireland: Symposium 2006, Deptartment Of Civil, Structural and Environmental Engineering, Trinity College Dublin.

Pavía, S and Hanley, R (2010). "Flexural bond strength of natural hydraulic lime mortar and clay brick". Materials and Structures, 43: 913-926

Pavía, S and Bolton, J (2002). Stone, brick and mortar: historical use, decay and conservation of building materials in Ireland. Bray, Wordwell.

Pavía, S, Fitzgerald, B and Treacy, E (2006). "An assessment of lime mortars for masonry repair". Concrete research in ireland colloquium. Dublin, University College Dublin: 101-108.

Pavía, S and Toomey, B (2008). "Influence of the aggregate quality on the physical properties of natural feebly-hydraulic lime mortars". Materials and Structures 41: 559 – 569.

Pavía, S and Treacy, E (2006). "A comparative study of the durability and behaviour of fat lime and feebly-hydraulic lime mortars". Materials and Structures, 39: 359–365.

PCA (1994). Bond Strength Testing of Masonry. Masonry Information. Skokie, Illinois, Portland Cement Association.

Plommer, F (1973). "Vitruvius and later Roman building manuals". London, Cambridge University Press.

Priestley, M J N and Elder, D M (1983). "Stress-strain curves for unconfined and confined concrete masonry". American Concrete Institiute Journal 80(3): 192-201.

Raghunath, S (2003). "Static and dynamic behaviour of brick masonry with containment reinforcement". Department of Civil Engineering. Bangalore, India, Indian Institute of Science. Ph D Thesis.

Rassineux, F, Petit, J C and Meunier, A (1989). "Ancient analogues of modern cement: calcium hydrosilicates in mortars and concretes from Gallo- Roman thermal baths of Western France". Journal of American Ceramics Society 72(6): 1026-1032.

Ray, I, Davalos, J and Luo, S (2005). "Interface evaluations of overlay-concrete bi-layer composites by a direct shear test method". Cement and Concrete Composites 27(3): 339-347.

Reda, Taha MM and Shrive, NG (2001). "The use of pozzo- lans to improve bond and bond strength". Proceedings of the 9th Canadian Masonry Symposium, Canada.

Riddington, J R and Jukes, P (1994). "A masonry joint shear strength test method". ICE Journal 104: 267-274.

Ritchie, T A (1961). "Small-panel method for investigating moisture penetration and bond strength of brick masonry". Material Restoration at Stand. 1(5): 360.

Roussel, N (2004). "Three-dimensional numerical simulations of Slump tests". Annual Transactions of the Nordic Rheology Society 12.

Roussel, N and Coussot, P (2005). ""fifty-cent rheometer" for yield stress measurements: from slump to spreading flow". Journal of rheology 49(3):705–718.(3): 705–718.

Roussel, N and Le Roy, R (2005). "The marsh cone: a test or a rheological apparatus?". Cement and concrete research(35): 823–830.

Sabbioni, C, Bonaza, A and Zappia, G (2002). "Damage on hydraulic mortars: the Venice Arsenal". Journal of Cultural Herititage: 83–88.

Samarasinghe, W and Lawrence, S J (1992). "Effect of high suction rate in low strength bricks on brick mortar bond". Proceedings of the 4th International Seminar on Structural Masonry for Developing Countries, Madras, India, 435-442.

Sarangapani, G, Venkatarama, Reddy BV and Jagadish, KS (2005). "Brick–mortar bond and masonry compressive Strength". Journal of Material Civil Engineering (ASCE) 17(2):229–237.

Sawko, F and Rouf, M A (1984). "On the stiffness properties of masonry". Proceedings of the Institute of Civil Engineeing.

Schiffner, H. IKM Koln unpublished reports 2002-2006

Sébaïbi, Y, Dheilly, R M and Queneudec, M (2002). "Study of water-retention capacity of a lime-sand mortar: Influence of the physicochemical characteristics of the lime". Cement and concrete research 33: 689-696.

Shapiro, S S and Wilk, M B (1965). "An analysis of variance test for normality (complete samples)". Biometrika 52 (3-4): 591–611.

Shrive, N G and Jessop, E L (1980). "Anisotropy in extruded clay units and it's effect on masonry behavior". Proceedings or the 2nd Canadian Masonry Symposium, Ottawa, Canada, 1123-1131.

Sinha, B P and Hendry, A W (1966). "Further investigations of bond tension, bond shear and the effect of precompression on shear strength of model brick masonry couplets". Stoke-on-Trent, B. Ceram. R.A., TN80.

Sinha, B P and Hendry, A W (1975). "Tensile strength of brickwork specimens". Proc. British Ceramics Society, No.24, Ed. H.W.H. We Stoke-on-Trent.

Sinha, BP (1967). "Model studies related to load bearing brickwork". University of Edinburgh, UK. PhD Thesis.

Sise, A, Shrive, N G and Jessop, E L (1988). "Flexural bond strength of masonry stack prisms". Proceedings of the British Masonry Society No. 2.

Sneck, T (1978). "The influence of the suction on mortar in joint". Proceeding of RILEM/CIB Symposium, Moisture Problems in Buildings, Helsinki, 1322-1330.

Sridhar, Babu D (1986). "Strength of soil-cement block masonry". M.E. Project Report. Bangalore, India, Department of Civil Engineering, Indian Institute of Science.

St Astier/CESA (2001). "http://www.stastier.com/".

Stefanidou, M and Papayiannai, I (2005). "The role of aggregate on the structure and properties of lime mortars " Cement and Concrete Composites 27.

Sugo, H O , Page, A W and Lawrence, S J (2000). "The Development of Mortar/Unit Bond", Proceedings of the 9th Canadian Masonry Symposium, New Nrunswick, Canada, Editiors: Bischoff P.H. *et al.* 1044-1053.

Sugo, H O, Page, A W and Lawrence, S (2007). "Influence of age on masonry bond strength and mortar microstructure". Canadian Journal of Civil Engineering(34): 1433-1442.

Tan (2003). Technical advice note, "Preparation and use of lime mortars". The scottish lime centre, Technical conservation research and edcuation division.

Tate, Michael (2005). "The Most Important Property of Cement-Lime Mortar in Masonry is Bond Strength". International Building Lime Symposium 2005. Orlando, Florida.

Taylor-Firth, A and Taylor, I F (1990). "A bond tensile strength test for use in assessing the compatibility of brick/mortar interface". Constr. and Build. Mat. 4(2): 58-63.

The British Lime Association (2009). The Lime Cycle. http:// www.britishlime.org/edu lime01.php.

Thomson, M and Godbey, R (2000). "Plasticity, water retention, soundness and sand carrying capacity: what a mortar needs". International RILEM workshop on historic mortars: characterisation and tests: 163–172.

Thornton, JC (1953). "Relation between bond and surface physics of masonry units". Journal of the American Ceramic Society 36(4): 105–120.

Van Balen, K and Van Gemert, D (1991). Kalk in metselmortel. over het meten van verwerkbaarheid en hechting en over de invloed van luchtbelvormers en

superplastifieerders. Voorlopig rapport. Technical report, Katholieke universiteit Leuven.

Van Der Pluijm, R (1993). "Shear behavior of bed joints". Proceedings of the 6th North America Masonry Conference, Philadelphia, 156-164.

Van Der Pluijm, R (1999). "Out-of-plane Bending of Masonry Behavior and Strength" Eindhoven University of Technology. PhD Thesis.

Varghese, PC and Ashok, Kumar (1965). "Results of some tests on ultimate strength of brick piers made from hand moulded bricks". Journal of the Institute of Engineering (India) Civil Engineering Division 46(3 Part CI4): 381–390.

Vasconcelos, G and Lourenco, P B (2009). "Experimental characterization of stone masonry in shear and compression". Construction and Building Materials 23: 3337-3345.

Venkatarama Reddy, B V and Gupta, Ajay (2008). "Influence of sand grading on the characteristics of mortars and soil–cement block masonry". Construction and Building Materials 22: 1614-1623.

Venkatarama Reddy, B V and Vyas, Uday (2008). "Influence of shear bond strength on the compressive strength and stress-strain characteristics of masonry". Materials and Structures (2008) 41(1697-1712).

Venkatarama Reddy, BV and Gupta, A (2006). "Tensile bond strength of soil–cement block masonry couplets using cement–soil mortars". Journal of Material and Civil Engineering (ASCE) 18(1): 36-45.

Venkatarama Reddy, BV, Richardson, L and Nanjunda, Rao KS (2007). "Enhancing bond strength and characteristics of soil cement block masonry". Journal of Material and Civil Engineering (ASCE) 19(2): 164-172.

Venumadhava Rao, K, Venkatarama Reddy, B V and Jaga-dish, K S (1995). Influence of flexural bond strength on the compressive strength of masonry. Proceedings of the National Conference on Civil Engineering Materials and Structures Osmania University, Hyderabad, India, 103–108.

Venumadhava Rao, K, Venkatarama Reddy, B V and Jagadish, K S (1996). "Flexural bond strength of masonry using various blocks and mortars". Materials and Structures 29: 119-124.

Walker, PJ (1999). "Bond characteristics of earth block masonry". Journal of Material and Civil Engineering (ASCE) 11(3): 249-256.

Wallevik, J (2003). "Rheology of particle suspensions. fresh concrete, mortar and cement paste with various types of lignosulfonates". Norwegian University of Science and Technology. PhD Thesis.

Wassermann, R, Katz, A and Bentur, A (2009). "Minimum cement content requirements: a must of a myth". Materials and Structures 42: 973-982.

Westra, J (1973). Metselen: leer het zelf. Zomer en Keuning, Wageningen, 4th edition.

Yates, T and Ferguson, A (2008). "The use of lime-based mortars in new build," NHBC Foundation Amersham, UK.

Zhou, Z , Walker, P and D'Ayala, D (2008). "Strength characteristics of hydraulic lime mortared brickwork". Proceedings of the Institution of Civil Engineers - Construction Materials 161(CM4): 139–146.

Zhou, Z, Walker, P and D'Ayala, D (2007). "Flexural bond strength development of brickwork using natural hydraulic lime mortar". Department of Architecture and Civil Engineering, University of Bath, UK.

LIST OF SYMBOLS

A	Parameter for masonry compressive strength (Equation 1.12)	
A_o	Surface area	mm^2
A_s	Gross area of the face of the specimen immersed in water	mm^2
A_i	Loaded cross-sectional area	mm^2
ANOVA	Analysis of variance	
b	mean width of mortar bed joint tested	mm
b	Side of the square section of the mortar prism	mm
b	Height or width of a masonry specimen perpendicular to the direction of span (flexural strength test)	mm
b_0	Y-axis intercept of linear regression line	
b_1	Slope of linear regression line	
CS	Compressive strength	
$c_{w,s}$	Coefficient of water absorption due to capillary action	$\frac{g}{(m^2 \times s^{0.5})}$
$c_{w,i}$	Initial rate of absorption (1minute)	$\frac{kg}{(m^2 \times min)}$
COV	Coefficient of variation	%
d	mean depth of a mortar specimen	mm
e_1	distance from the applied load to the tension face of the specimen	mm
e_2	distance from the centre of gravity of the lower and upper clamp from the tension face of the specimen	mm
E	External	
E_b	Elastic modulus of mortar in compression	N/mm^2
E_m	Elastic modulus of masonry in compression	N/mm^2
E_c	Elastic modulus of a masonry unit in compression	N/mm^2
E_o	Initial tangent modulus	N/mm^2
E_{33}	Elastic modulus at 33 % of ultimate stress	N/mm^2
f_i	i^{th} experimental masonry prism strength	N/mm^2
f_{Ri}	i^{th} regression estimate of masonry prism strength	N/mm^2
f'_m	Characteristic compressive strength of masonry	N/mm^2
f_j	Compressive strength of mortar	N/mm^2
f_m	Compressive strength of masonry	N/mm^2
f'_m	Peak compressive stress in masonry	N/mm^2
f_b	Compressive strength of a masonry unit	N/mm^2
f_b	Normalized compressive strength of masonry unit	N/mm^2
f_k	Characteristic compressive strength	N/mm^2

$f_{i,min}$	Minimum compressive strength of a sample of masonry specimens	N/mm^2
f_{wi}	Bond strength of individual masonry specimen	N/mm^2
f_w	Mean bond strength of ten joints	N/mm^2
f_{wk}	Characteristic bond strength	N/mm^2
f_{mean}	Mean flexural strength of masonry	N/mm^2
f_{xk}	Characteristic flexural strength of masonry	N/mm^2
f_{ix}	Flexural strength of an individual masonry specimen	N/mm^2
$F_{i,max}$	Maximum load on an individual masonry specimen (flexural strength test)	N
$F_{i,max}$	Maximum load reached on an individual masonry specimen	N
$F_{c,max}$	Maximum applied force (masonry compression)	N
F_1	Applied load	N
F_2	Weight of the bond wrench frame	N
F_x	Applied force at point x	N
F_f	Peak load at fracture (mortar flexural test)	N
F_c	Peak load at fracture (mortar compression test)	N
h_0	Original height of the specimen	mm
IRA	Initial rate of absorption	
I	Indoor	
k	Parameter (characteristic flexural bond strength)	
K	Factor depending on brick and mortar properties	
l	Distance between the supports (mortar flexural test)	mm
l_1	Distance between outer supports (masonry flexural test)	mm
l_2	Distance between inner supports (masonry flexural test)	mm
LVDT	Lateral variable displacement transducer	
m_i	Mass	g
m_d	Dry mass	g
m_h	Hydrostatic saturated mass	g
m_s	Surface saturated mass	g
$m_{so,s}$	Mass of specimen after soaking for time t	g
$m_{dry,s}$	Mass of the specimen after drying	g
m_1	Mass of the dry filter plate	g
m_2	Mass of mould and bottom non-porous plate	g
m_3	Mass of the bottom plate and mould with mortar filling	g
m_4	mass of the soaked filter plate	g
m_5	Total mass of water	g
m_6	Mass of the dry mortar batch	g

m_7	Mass of mortar in the mould	g
M6	Cement-lime mortar/masonry specimen	
min	Minute	s
n	Sample size	
psi	Pounds per square inch	
P-value	Statistical result	
RH	Hanley (2006)	
R_c	Mortar compressive strength	N/mm^2
R_f	Mortar flexural strength	N/mm^2
R^2	Coefficient of Determination	
SSE	Sum of square errors	
SSR	Regression sum of squares	
SST	Total sum of squares	
s	Sample standard deviation of the n log values	
t_b	Thickness (height) of brick unit	mm
t_m	Thickness of mortar bed joint	mm
t_u	Width of a masonry unit	mm
t_i	Time	s
t_{so}	Time for soaking	s
t-test	Statistical test using t distribution	
W	Weight of the masonry unit pulled off the specimen and any adherent mortar	N
W_1	The water fraction of the mortar batch	g
W_2	Water content of the mortar in the mould	g
W_3	Mass of water absorbed by the filter plate	g
W_4	Percentage relative loss of water from the mortar	%
w/c	Water content	
WRV	Water retention value	%
Y_i	Log_{10} of the bond strength f_{wi}	
Z_m	Final constant stress (Equation 1.4)	N/mm^2
α, β	Parameters (Equation 1.10)	
ε_m	Compressive strain in masonry	N/mm^2
ε'_m	Peak compressive strain in masonry	N/mm^2
ε_r	Normalised strain	
ε_x	Compressive strain at point x on the stress-strain curve	
$\varepsilon_{r,90}$	Strain at 90 % of ultimate stress	
σ	Standard error of a regression estimate	

σ	Stress	N/mm^2
σ_x	Compressive stress at point x on the stress-strain curve	N/mm^2
σ_{ult}	Peak stress at fracture (mortar compression test)	N/mm^2
σ_{max}	Ultimate/maximum stress	N/mm^2
σ_r	Normalised stress	N/mm^2
ρ_w	Density of water	
v_b	Poisson's ratio of the brick	
v_m	Poisson's ratio of the mortar as a function of principal stresses	
Δh_x	Change in height of the specimen at point x	mm
$\Delta\sigma_{xb}$	Increment in lateral stress in the brick	N/mm^2
$\Delta\sigma_y$	Increment in vertical stress on prism	N/mm^2

APPENDICES

List of Figures (Appendices)

Figure C.1: Compressive strength development of mortar over time 265

Figure C.2: Elastic modulus development of mortar over time 266

Figure D.1: Flexural strength development of mortar over time 283

List of Tables (Appendices)

Table A.1: Initial flow results of NHL 5 mortar (165 mm) 243
Table A.2:Analysis of variance (one-way) of NHL 5 mortar (165 mm) 243
Table A.3: Initial flow results of NHL 5 mortar (170 mm) 244
Table A.4:Analysis of variance (one-way) of NHL 5 mortar (170 mm) 244
Table A.5: Initial flow results of NHL 3.5 mortar (165 mm) 245
Table A.6: Analysis of variance (one-way) of NHL 3. 5 mortar (165 mm) 245
Table A.7: Initial flow results of NHL 3.5 mortar (170 mm) 246
Table A.8: Analysis of variance (one-way) of NHL 3.5 mortar (170 mm) 246
Table A.9: Initial flow results of NHL 2 mortar (165 mm) 247
Table A.10: Analysis of variance (one-way) of NHL 2 mortar (165 mm) 247
Table A.11: Initial flow results of NHL 2 mortar (170 mm) 248
Table A.12: Analysis of variance (one-way) of NHL 2 mortar (170 mm) 248
Table A.13: Initial flow results of CL90-s mortar (165 mm)..... 249
Table A.14: Analysis of variance of CL90-s mortar (165 mm) 249
Table A.15: Initial flow results of CL90-s mortar (170 mm)..... 250
Table A.16: Analysis of variance (one-way) of CL90-s mortar (170 mm)..... 250
Table A.17: Initial flow results of M6 mortar (165 mm)..... 251
Table A.18: Analysis of variance (one-way) of M6 mortar (165 mm) 251
Table A.19: Initial flow results of M6 mortar (170 mm)..... 252
Table A.20: Analysis of variance of M6 (170 mm)..... 252
Table A.21: Initial flow results of NHL 2 mortar (165 mm) 253
Table A.22: Analysis of variance of NHL 2 mortar (165 mm)..... 253
Table A.23: Multiple analysis of variance of NHL 5 mortar (165 vs. 170 mm)..... 254
Table A.24: Multiple analysis of variance of NHL 3.5 mortar (165 vs. 170 mm)..... 255
Table A.25: Multiple analysis of variance of NHL 2 mortar (165 vs. 170 mm)..... 256
Table A.26: Multiple analysis of variance of CL90-s mortar (165 vs. 170 mm) 257
Table A.27: Multiple analysis of variance of M6 mortar (165 vs. 170 mm) 258
Table B.1: Calculation of mortar water retention (165 mm flow) 261
Table B.2: Calculation of mortar water retention (170 mm flow) 262
Table C.1: Compressive strength and elastic modulus results for NHL 5 mortar..... 267
Table C.2: Compressive strength and elastic modulus results for NHL 3.5 mortar (165 mm flow)..... 268
Table C.3: Compressive strength and elastic modulus results for NHL 3.5 mortar (170 mm flow)..... 269
Table C.4: Compressive strength and elastic modulus results for NHL 2 mortar..... 270
Table C.5: Compressive strength and elastic modulus results for CL90-s mortar..... 271
Table C.6: Compressive strength and elastic modulus results for M6 mortar (165 mm flow) 272
Table C.7: Compressive strength and elastic modulus results for M6 mortar (170 mm flow) 273
Table C.8: Compressive strength and elastic modulus results for NHL 3.5 mortar (165 mm flow and mix ratio 0:2:3)..... 274
Table C.9: Compressive strength and elastic modulus results for outdoor cured M6 mortar (165 mm flow) 275
Table C.10: Compressive strength and elastic modulus results for outdoor cured M6 mortar (170 mm flow) 276
Table C.11: Compressive strength and elastic modulus results for outdoor cured NHL 5 mortar (165 mm flow) 277
Table C.12: Compressive strength and elastic modulus results for outdoor cured NHL 5 mortar (170 mm flow) 278
Table C.13: Compressive strength and elastic modulus results for outdoor cured CL90-s mortar (165 mm flow) 279
Table C.14: Compressive strength and elastic modulus results for outdoor cured CL90-s mortar (170 mm flow) 280

Table D.1: M6 mortar flexural strength results and calculations 284
Table D.2: NHL 5 mortar flexural strength results and calculations 285
Table D.3: NHL 3.5 mortar flexural strength results and calculations 286
Table D.4: NHL 2 mortar flexural strength results and calculations 287
Table D.5: CL90-s mortar flexural strength results and calculations 288
Table D.6: NHL 3.5 mortar flexural strength results and calculations, mix ratio (0:2:3) 289
Table D.7: M6 mortar flexural strength results and calculations (outdoor curing) 290
Table D.8: NHL 5 mortar flexural strength results and calculations (outdoor curing) 291
Table D.9: CL90-s mortar flexural strength results and calculations (outdoor curing) 292
Table E.1: NHL 5 masonry compressive strength and elastic modulus results and calculations 295
Table E.2: NHL 5 masonry compressive strength and elastic modulus results and calculations (continued) 296
Table E.3: NHL 3.5 masonry compressive strength and elastic modulus results and calculations 297
Table E.4: NHL 3.5 masonry compressive strength and elastic modulus results and calculations (continued) 298
Table E.5: NHL 2 masonry compressive strength and elastic modulus results and calculations 299
Table E.6: NHL 2 masonry compressive strength and elastic modulus results and calculations (continued) 300
Table E.7: CL90-s masonry compressive strength and elastic modulus results and calculations 301
Table E.8: CL90-s masonry compressive strength and elastic modulus results and calculations (continued) 302
Table E.9: M6 masonry compressive strength and elastic modulus results and calculations 303
Table E.10: M6 masonry compressive strength and elastic modulus results and calculations (continued) 304
Table E.11: NHL 5 masonry compressive strength and elastic modulus results and calculations, outdoor curing 305
Table E.12: NHL 5 masonry compressive strength and elastic modulus results and calculations, outdoor curing (continued) 306
Table E.13: M6 masonry compressive strength and elastic modulus results and calculations, outdoor curing 307
Table E.14: M6 masonry compressive strength and elastic modulus results and calculations, outdoor curing (continued) 308
Table E.15: CL90-s masonry compressive strength and elastic modulus results and calculations, outdoor curing 309
Table E.16: CL90-s masonry compressive strength and elastic modulus results and calculations, outdoor curing (continued) 310
Table E.17: NHL 2-broken limestone masonry compressive strength and elastic modulus results and calculations 311
Table E.18: NHL 2-broken limestone masonry compressive strength and elastic modulus results and calculations (continued) 312
Table E.19: CL90-s-broken limestone masonry compressive strength and elastic modulus results and calculations 313
Table E.20: CL90-s-broken limestone masonry compressive strength and elastic modulus results and calculations (continued) 314
Table E.21: NHL 2-cut limestone masonry compressive strength and elastic modulus results and calculations 315
Table E.22: NHL 2-cut limestone masonry compressive strength and elastic modulus results and calculations (continued) 316
Table E.23: CL90-s-cut limestone masonry compressive strength and elastic modulus results and calculations 317
Table E.24: CL90-s-cut limestone masonry compressive strength and elastic modulus results and calculations (continued) 318
Table E.25: NHL 2-broken sandstone masonry compressive strength and elastic modulus results and calculations 319

Table E.26: NHL 2-broken sandstone masonry compressive strength and elastic modulus results and calculations (continued) 320
Table E.27: CL90-s-broken sandstone masonry compressive strength and elastic modulus results and calculations 321
Table E.28: CL90-s-broken sandstone masonry compressive strength and elastic modulus results and calculations (continued) 322
Table F.1: M6 brick masonry bond strength calculations, 165 mm flow (1 month) 325
Table F.2: M6 brick masonry bond strength calculations, 165 mm flow (2 months) 326
Table F.3: M6 brick masonry bond strength calculations, 165 mm flow (6 months) 327
Table F.4: NHL 5 brick masonry bond strength calculations, 165 mm flow (1 months) 328
Table F.5: NHL 5 brick masonry bond strength calculations, 165 mm flow (2 months) 329
Table F.6: NHL 5 brick masonry bond strength calculations, 165 mm flow (6 months) 330
Table F.7: NHL 5 brick masonry bond strength calculations, 165 mm flow (12 months) 331
Table F.8: NHL 3 5 brick masonry bond strength calculations, 165 mm flow (1 month) 332
Table F.9: NHL 3.5 brick masonry bond strength calculations, 165 mm flow (2 months) 333
Table F.10: NHL 3.5 brick masonry bond strength calculations, 165 mm flow (6 months) 334
Table F.11: NHL 3.5 brick masonry bond strength calculations, 165 mm flow (12 months) 335
Table F.12: NHL 2 brick masonry bond strength calculations, 165 mm flow (1 month) 336
Table F.13: NHL 2 brick masonry bond strength calculations, 165 mm flow (2 months) 337
Table F.14: NHL 2 brick masonry bond strength calculations, 165 mm flow (6 months) 338
Table F.15: NHL 2 brick masonry bond strength calculations, 165 mm flow (12 months) 339
Table F.16: CL90-s brick masonry bond strength calculations, 165 mm flow (1 month) 340
Table F.17: CL90-s brick masonry bond strength calculations, 165 mm flow (2 months) 341
Table F.18: CL90-s brick masonry bond strength calculations, 165 mm flow (6 months) 342
Table F.19: CL90-s brick masonry bond strength calculations, 165 mm flow (12 months) 343
Table F.20: NHL 3.5 brick masonry bond strength calculations, 165 mm flow (0:1:2) (1 month) 344
Table F.21: NHL 3.5 brick masonry bond strength calculations, 165 mm flow (0:1:2) (2 months) 345
Table F.22: NHL 3.5 brick masonry bond strength calculations, 165 mm flow (0:1:2) (6 months) 346
Table F.23: M6brick masonry bond strength calculations, 170 mm flow (1 month) 347
Table F.24: M6brick masonry bond strength calculations, 170 mm flow (2 months) 348
Table F.25: M6brick masonry bond strength calculations, 170 mm flow (6 months) 349
Table F.26: NHL 5 brick masonry bond strength calculations, 170 mm flow (1 month) 350
Table F.27: NHL 5 brick masonry bond strength calculations, 170 mm flow (2 months) 351
Table F.28: NHL 5 brick masonry bond strength calculations, 170 mm flow (6 months) 352
Table F.29: NHL3. 5 brick masonry bond strength calculations, 170 mm flow (1 month) 353
Table F.30: NHL3. 5 brick masonry bond strength calculations, 170 mm flow (2 months) 354
Table F.31: NHL3. 5 brick masonry bond strength calculations, 170 mm flow (6 months) 355
Table F.32: NHL2 brick masonry bond strength calculations, 170 mm flow (1 month) 356
Table F.33: NHL2 brick masonry bond strength calculations, 170 mm flow (2 months) 357
Table F.34: NHL2 brick masonry bond strength calculations, 170 mm flow (6 months) 358
Table F.35: CL90-s brick masonry bond strength calculations, 170 mm flow (1 month) 359
Table F.36: CL90-s brick masonry bond strength calculations, 170 mm flow (2 months) 360
Table F.37: CL90-s brick masonry bond strength calculations, 170 mm flow (6 months) 361
Table F.38: M6 brick masonry bond strength calculations, 165 mm flow, outdoor cured (1 month) 362
Table F.39: M6 brick masonry bond strength calculations, 165 mm flow, outdoor cured (2 months) 363
Table F.40: M6 brick masonry bond strength calculations, 165 mm flow, outdoor cured (6 months) 364
Table F.41: NHL 5 brick masonry bond strength calculations, 165 mm flow, outdoor cured (1 month) 365
Table F.42: NHL 5 brick masonry bond strength calculations, 165 mm flow, outdoor cured (2 months) 366
Table F.43: NHL 5 brick masonry bond strength calculations, 165 mm flow, outdoor cured (6 months) 367
Table F.44: NHL CL90-s brick masonry bond strength calculations, 165 mm flow, outdoor cured (1 month) 368
Table F.45: NHL 3.5 CL90-s brick masonry bond strength calculations, 165 mm flow, outdoor cured (2 months) 369

Table F.46: CL90-s brick masonry bond strength calculations, 165 mm flow, outdoor cured (6 months) 370
Table F.47: M6 brick masonry bond strength calculations, 165 mm flow, outdoor cured (1 month) 371
Table F.48: M6 brick masonry bond strength calculations, 165 mm flow, outdoor cured (2 months) 372
Table F.49: M6 brick masonry bond strength calculations, 165 mm flow, outdoor cured (6 months) 373
Table F.50: NHL 5 brick masonry bond strength calculations, 170 mm flow, outdoor cured (1 month) 374
Table F.51: NHL 5 brick masonry bond strength calculations, 170 mm flow, outdoor cured (2 months) 375
Table F.52: NHL 5 brick masonry bond strength calculations, 170 mm flow, outdoor cured (6 months) 376
Table F.53: CL90-s brick masonry bond strength calculations, 170 mm flow, outdoor cured (1 month) 377
Table F.54: CL90-s brick masonry bond strength calculations, 170 mm flow, outdoor cured (2 months) 378
Table F.55: CL90-s brick masonry bond strength calculations, 170 mm flow, outdoor cured (6 months) 379
Table F.56: CL90-s broken sandstone masonry bond strength calculations, 165 mm flow (1 month) 380
Table F.57: CL90-s broken sandstone masonry bond strength calculations, 165 mm flow (2 months) 381
Table F.58: CL90-s broken sandstone masonry bond strength calculations, 165 mm flow (6 months) 382
Table F.59: NHL 2 broken sandstone masonry bond strength calculations, 165 mm flow (1 month) 383
Table F.60: NHL 2 broken sandstone masonry bond strength calculations, 165 mm flow (2 months) 384
Table F.61: NHL 2 broken sandstone masonry bond strength calculations, 165 mm flow (6 months) 385
Table F.62: CL90-s broken sandstone masonry bond strength calculations, 170 mm flow (1 month) 386
Table F.63: CL90-s broken sandstone masonry bond strength calculations, 170 mm flow (2 months) 387
Table F.64: CL90-s broken sandstone masonry bond strength calculations, 170 mm flow (6 months) 388
Table F.65: NHL 2 broken sandstone masonry bond strength calculations, 170 mm flow (1 month) 389
Table F.66: NHL 2 broken sandstone masonry bond strength calculations, 170 mm flow (2 months) 390
Table F.67: NHL 2 broken sandstone masonry bond strength calculations, 170 mm flow (6 months) 391
Table F.68: CL90-s broken limestone masonry bond strength calculations, 165 mm flow (1 month) 392
Table F.69: CL90-s broken limestone masonry bond strength calculations, 165 mm flow (2 months) 393
Table F.70: CL90-s broken limestone masonry bond strength calculations, 165 mm flow (6 months) 394
Table F.71: NHL 2 broken limestone masonry bond strength calculations, 165 mm flow (1 month) 395
Table F.72: NHL 2 broken limestone masonry bond strength calculations, 165 mm flow (2 months) 396
Table F.73: NHL 2 broken limestone masonry bond strength calculations, 165 mm flow (6 months) 397
Table F.74: CL90-s broken limestone masonry bond strength calculations, 170 mm flow (1 month) 398
Table F.75: CL90-s broken limestone masonry bond strength calculations, 170 mm flow (2 months) 399
Table F.76: CL90-s broken limestone masonry bond strength calculations, 170 mm flow (6 months) 400
Table F.77: NHL 2 broken limestone masonry bond strength calculations, 170 mm flow (1 month) 401
Table F.78: NHL 2 broken limestone masonry bond strength calculations, 170 mm flow (2 months) 402
Table F.79: NHL 2 broken limestone masonry bond strength calculations, 170 mm flow (6 months) 403
Table F.80: CL90-s cut limestone masonry bond strength calculations, 165 mm flow (1 month) 404
Table F.81: CL90-s cut limestone masonry bond strength calculations, 165 mm flow (2 months) 405
Table F.82: CL90-s cut limestone masonry bond strength calculations, 165 mm flow (6 months) 406
Table F.83: NHL 2 cut limestone masonry bond strength calculations, 165 mm flow (1 month) 407
Table F.84: NHL 2 cut limestone masonry bond strength calculations, 165 mm flow (2 months) 408
Table F.85: NHL 2 cut limestone masonry bond strength calculations, 165 mm flow (6 months) 409
Table F.86: CL90-s cut limestone masonry bond strength calculations, 170 mm flow (1 month) 410
Table F.87: CL90-s cut limestone masonry bond strength calculations, 170 mm flow (2 months) 411
Table F.88: CL90-s cut limestone masonry bond strength calculations, 170 mm flow (6 months) 412
Table F.89: NHL 2 cut limestone masonry bond strength calculations, 170 mm flow (1 month) 413
Table F.90: NHL 2 cut limestone masonry bond strength calculations, 170 mm flow (2 months) 414
Table F.91: NHL 2 cut limestone masonry bond strength calculations, 170 mm flow (6 months) 415
Table G.1: M6 brick masonry flexural strength (parallel to bedding joints) 419
Table G.2: NHL 5 brick masonry flexural strength (parallel to bedding joints) 420
Table G.3: NHL3. 5 brick masonry flexural strength (parallel to bedding joints) 421

Table G.4: NHL3. 5 brick masonry flexural strength (parallel to bedding joints) (mix ratio 0:1:2)..... 422
Table G.5: NHL2 brick masonry flexural strength (parallel to bedding joints)..... 423
Table G.6: NHL3. 5 brick masonry flexural strength (parallel to bedding joints)..... 424
Table G.7: M6 brick masonry flexural strength (parallel to bedding joints) 425
Table G.8: NHL 5 brick masonry flexural strength (perpendicular to bedding joints)..... 426
Table G.9: NHL 3.5 brick masonry flexural strength (perpendicular to bedding joints)..... 427
Table G.10: NHL3. 5 brick masonry flexural strength (perpendicular to bedding joints) (mix ratio 0:1:2) 428
Table G.11: NHL 2 brick masonry flexural strength (perpendicular to bedding joints)..... 429
Table G.12: CL90-s brick masonry flexural strength (perpendicular to bedding joints) 430
Table H.1: Brick units compressive and flexural strength, and elastic modulus results and calculations..... 433
Table H.2: Limestone units compressive and flexural strength, and elastic modulus results and calculations..... 434
Table H.3: Sandstone units compressive and flexural strength, and elastic modulus results and calculations..... 435

APPENDIX A

STATISTICAL ANALYSIS OF MORTAR FLOW TEST

Mix ratio: 0:1:3

Sample	Dim. 1 (mm)	Dim. 2 (mm)	Dim. 3 (mm)	Mean (mm)	COV (%)	Batch Mean
1.a	164	165	165	164.67	0.35%	
1.b	165	166	163	164.67	0.93%	
1.c	166	167	165	166.00	0.60%	
1.d	164	165	166	165.00	0.61%	
1.e	166	164	164	164.67	0.70%	164.90
1.f	165	166	164	165.00	0.61%	
1.g	165	165	166	165.33	0.35%	
1.h	162	165	165	164.00	1.06%	
1.i	163	164	166	164.33	0.93%	
1.j	166	165	165	165.33	0.35%	
2.a	166	164	166	165.33	0.70%	
2.b	167	165	167	166.33	0.69%	
2.c	165	164	165	164.67	0.35%	
2.d	166	165	166	165.67	0.35%	
2.e	167	164	167	166.00	1.04%	165.07
2.f	168	163	164	165.00	1.60%	
2.g	166	165	166	165.67	0.35%	
2.h	165	162	164	163.67	0.93%	
2.i	165	163	165	164.33	0.70%	
2.j	164	165	163	164.00	0.61%	
3.a	163	164	165	164.00	0.61%	
3.b	165	166	166	165.67	0.35%	
3.c	167	165	164	165.33	0.92%	
3.d	164	165	166	165.00	0.61%	
3.e	166	164	164	164.67	0.70%	165.03
3.f	165	166	164	165.00	0.61%	
3.g	165	165	166	165.33	0.35%	
3.h	162	165	165	164.00	1.06%	
3.i	163	168	167	166.00	1.59%	
3.j	166	165	165	165.33	0.35%	

Table A.1: Initial flow results of NHL 5 mortar (165 mm)

Summary

Groups	*Sample size*	*Sum*	*Mean*	*Variance*
NHL5-165-batch 1	10	1,649.	164.9	0.3222
NHL5-165-batch 2	10	1,650.667	165.0666	0.7851
NHL5-165-batch 3	10	1,650.333	165.0333	0.4308

ANOVA

Source of Variation	*SS*	*df*	*MS*	*F*	*p-level*	*F crit*
Between Groups	0.1556	2	0.0778	0.1517	0.8599	3.3541
Within Groups	13.844	27	0.5127			
Total	14.	29				

Therefore we fail to reject the hypothesis since $F<F_{crit}$ and $P_{value}>0.05$

Table A.2: Analysis of variance (one-way) of NHL 5 mortar (165 mm)

Mix ratio: 0:1:3

Sample	Dim. 1 (mm)	Dim. 2 (mm)	Dim. 3 (mm)	Mean (mm)	COV (%)	Batch Mean
1.a	168	170	166	168.00	1.19%	
1.b	170	173	169	170.67	1.22%	
1.c	169	172	170	170.33	0.90%	
1.d	169	169	167	168.33	0.69%	
1.e	170	198	169	179.00	9.20%	170.13
1.f	167	170	166	167.67	1.24%	
1.g	168	170	169	169.00	0.59%	
1.h	169	170	170	169.67	0.34%	
1.i	170	169	170	169.67	0.34%	
1.j	170	168	169	169.00	0.59%	
2.a	168	170	169	169.00	0.59%	
2.b	169	170	170	169.67	0.34%	
2.c	173	170	172	171.67	0.89%	
2.d	169	168	169	168.67	0.34%	
2.e	168	169	167	168.00	0.60%	169.47
2.f	168	170	166	168.00	1.19%	
2.g	170	173	169	170.67	1.22%	
2.h	169	172	170	170.33	0.90%	
2.i	170	170	166	168.67	1.37%	
2.j	170	170	170	170.00	0.00%	
3.a	169	168	169	168.67	0.61%	
3.b	169	172	167	169.33	0.35%	
3.c	172	170	170	170.67	0.92%	
3.d	167	170	166	167.67	0.61%	
3.e	168	170	169	169.00	0.70%	169.53
3.f	169	170	170	169.67	0.61%	
3.g	173	170	170	171.00	0.35%	
3.h	170	167	170	169.00	1.06%	
3.i	169	168	169	168.67	1.59%	
3.j	170	172	173	171.67	0.35%	

Table A.3: Initial flow results of NHL 5 mortar (170 mm)

Summary

Groups	*Sample size*	*Sum*	*Mean*	*Variance*
NHL 5-170 batch 1	10	1,701.33	170.13	10.65
NHL 5-170 batch 2	10	1,694.67	169.47	1.46
NHL 5-170 batch 3	10	1,695.33	169.53	1.51

ANOVA

Source of Variation	*SS*	*df*	*MS*	*F*	*p-level*	*F crit*
Between Groups	2.696	2	1.348	0.29695	0.745	3.354
Within Groups	122.577	27	4.539			
Total	125.274	29				

Therefore we fail to reject the hypothesis since $F<F_{crit}$ and $P_{value}>0.05$

Table A.4: Analysis of variance (one-way) of NHL 5 mortar (170 mm)

Mix ratio: 0:1:3

Sample	Dim. 1 (mm)	Dim. 2 (mm)	Dim. 3 (mm)	Mean (mm)	COV (%)	Batch Mean
1.a	166	167	165	166.00	0.60%	
1.b	164	165	166	165.00	0.61%	
1.c	166	164	164	164.67	0.70%	
1.d	165	168	163	165.33	1.52%	
1.e	163	164	163	163.33	0.35%	164.77
1.f	163	164	164	163.67	0.35%	
1.g	164	166	166	165.33	0.70%	
1.h	164	165	165	164.67	0.35%	
1.i	163	164	166	164.33	0.93%	
1.j	166	165	165	165.33	0.35%	
2.a	166	164	165	165.00	0.61%	
2.b	165	166	164	165.00	0.61%	
2.c	165	165	166	165.33	0.35%	
2.d	168	163	167	166.00	1.59%	
2.e	164	163	164	163.67	0.35%	165.07
2.f	166	164	166	165.33	0.70%	
2.g	166	164	165	165.00	0.61%	
2.h	165	166	164	165.00	0.61%	
2.i	165	165	165	165.00	0.00%	
2.j	164	165	163	164.00	0.61%	
3.a	166	165	166	165.67	0.35%	
3.b	167	164	167	166.00	1.04%	
3.c	168	163	164	165.00	1.60%	
3.d	164	164	166	164.67	0.70%	
3.e	165	166	164	165.00	0.61%	165.03
3.f	163	164	164	163.67	0.35%	
3.g	163	164	166	164.33	0.93%	
3.h	164	166	165	165.00	0.61%	
3.i	163	168	167	166.00	1.59%	
3.j	166	165	165	165.33	0.35%	

Table A.5: Initial flow results of NHL 3.5 mortar (165 mm)

Summary

Groups	*Sample size*	*Sum*	*Mean*	*Variance*
NHL 3.5-165-batch 1	10	1,647.67	164.77	0.66
NHL 3.5-165-batch 2	10	1,649.33	164.93	0.43
NHL 3.5-165-batch 3	10	1,650.67	165.07	0.54

ANOVA

Source of Variation	*SS*	*df*	*MS*	*F*	*p-level*	*F crit*
Between Groups	0.45185	2	0.22593	0.41185	0.66651	3.35413
Within Groups	14.81111	27	0.54856			
Total	15.26296	29				

Therefore we fail to reject the hypothesis since $F<F_{crit}$ and $P_{value}>0.05$

Table A.6: Analysis of variance (one-way) of NHL 3. 5 mortar (165 mm)

Mix ratio: 0:1:3

Sample	Dim. 1 (mm)	Dim. 2 (mm)	Dim. 3 (mm)	Mean (mm)	COV (%)	Batch Mean
1.a	170	173	166	169.67	2.07%	
1.b	171	173	170	171.33	0.89%	
1.c	167	170	167	168.00	1.03%	
1.d	169	169	173	170.33	1.36%	
1.e	169	170	169	169.33	0.34%	170.03
1.f	171	172	171	171.33	0.34%	
1.g	170	169	170	169.67	0.34%	
1.h	173	170	173	172.00	1.01%	
1.i	168	169	172	169.67	1.23%	
1.j	170	168	169	169.00	0.59%	
2.a	173	171	170	171.33	0.89%	
2.b	173	170	172	171.67	0.89%	
2.c	168	170	170	169.33	0.68%	
2.d	169	173	169	170.33	1.36%	
2.e	170	169	167	168.67	0.91%	169.80
2.f	167	170	166	167.67	1.24%	
2.g	170	170	169	169.67	0.34%	
2.h	169	170	170	169.67	0.34%	
2.i	170	169	170	169.67	0.34%	
2.j	170	170	170	170.00	0.00%	
3.a	169	168	169	168.67	0.34%	
3.b	170	172	167	169.67	1.48%	
3.c	172	171	170	171.00	0.58%	
3.d	170	169	166	168.33	1.24%	
3.e	170	170	169	169.67	0.34%	169.73
3.f	169	170	170	169.67	0.34%	
3.g	173	170	170	171.00	1.01%	
3.h	170	167	170	169.00	1.02%	
3.i	169	168	169	168.67	0.34%	
3.j	170	172	173	171.67	0.89%	

Table A.7: Initial flow results of NHL 3.5 mortar (170 mm)

Summary

Groups	*Sample size*	*Sum*	*Mean*	*Variance*
NHL 3.5-170 batch 1	10	1,700.3	170.03	1.49
NHL 3.5-170 batch 2	10	1,698.33	169.8	1.36
NHL 3.5-170 batch 3	10	1,697.33	169.73	1.3

ANOVA

Source of Variation	*SS*	*df*	*MS*	*F*	*p-level*	*F crit*
Between Groups	0.493	2	0.24815	0.1798	0.831	3.3413
Within Groups	37.433	27	1.38642			
Total	37.923	29				

Therefore we fail to reject the hypothesis since $F<F_{crit}$ and $P_{value}>0.05$

Table A.8: Analysis of variance (one-way) of NHL 3.5 mortar (170 mm)

APPENDICES

List of Figures (Appendices)

Figure C.1: Compressive strength development of mortar over time 265

Figure C.2: Elastic modulus development of mortar over time 266

Figure D.1: Flexural strength development of mortar over time 283

List of Tables (Appendices)

Table A.1: Initial flow results of NHL 5 mortar (165 mm) 243
Table A.2:Analysis of variance (one-way) of NHL 5 mortar (165 mm) 243
Table A.3: Initial flow results of NHL 5 mortar (170 mm) 244
Table A.4:Analysis of variance (one-way) of NHL 5 mortar (170 mm) 244
Table A.5: Initial flow results of NHL 3.5 mortar (165 mm) 245
Table A.6: Analysis of variance (one-way) of NHL 3. 5 mortar (165 mm) 245
Table A.7: Initial flow results of NHL 3.5 mortar (170 mm) 246
Table A.8: Analysis of variance (one-way) of NHL 3.5 mortar (170 mm) 246
Table A.9: Initial flow results of NHL 2 mortar (165 mm) 247
Table A.10: Analysis of variance (one-way) of NHL 2 mortar (165 mm) 247
Table A.11: Initial flow results of NHL 2 mortar (170 mm) 248
Table A.12: Analysis of variance (one-way) of NHL 2 mortar (170 mm) 248
Table A.13: Initial flow results of CL90-s mortar (165 mm) 249
Table A.14: Analysis of variance of CL90-s mortar (165 mm) 249
Table A.15: Initial flow results of CL90-s mortar (170 mm) 250
Table A.16: Analysis of variance (one-way) of CL90-s mortar (170 mm) 250
Table A.17: Initial flow results of M6 mortar (165 mm) 251
Table A.18: Analysis of variance (one-way) of M6 mortar (165 mm) 251
Table A.19: Initial flow results of M6 mortar (170 mm) 252
Table A.20: Analysis of variance of M6 (170 mm) 252
Table A.21: Initial flow results of NHL 2 mortar (165 mm) 253
Table A.22: Analysis of variance of NHL 2 mortar (165 mm) 253
Table A.23: Multiple analysis of variance of NHL 5 mortar (165 vs. 170 mm) 254
Table A.24: Multiple analysis of variance of NHL 3.5 mortar (165 vs. 170 mm) 255
Table A.25: Multiple analysis of variance of NHL 2 mortar (165 vs. 170 mm) 256
Table A.26: Multiple analysis of variance of CL90-s mortar (165 vs. 170 mm) 257
Table A.27: Multiple analysis of variance of M6 mortar (165 vs. 170 mm) 258
Table B.1: Calculation of mortar water retention (165 mm flow) 261
Table B.2: Calculation of mortar water retention (170 mm flow) 262
Table C.1: Compressive strength and elastic modulus results for NHL 5 mortar 267
Table C.2: Compressive strength and elastic modulus results for NHL 3.5 mortar (165 mm flow) 268
Table C.3: Compressive strength and elastic modulus results for NHL 3.5 mortar (170 mm flow) 269
Table C.4: Compressive strength and elastic modulus results for NHL 2 mortar 270
Table C.5: Compressive strength and elastic modulus results for CL90-s mortar 271
Table C.6: Compressive strength and elastic modulus results for M6 mortar (165 mm flow) 272
Table C.7: Compressive strength and elastic modulus results for M6 mortar (170 mm flow) 273
Table C.8: Compressive strength and elastic modulus results for NHL 3.5 mortar (165 mm flow and mix ratio 0:2:3) 274
Table C.9: Compressive strength and elastic modulus results for outdoor cured M6 mortar (165 mm flow) 275
Table C.10: Compressive strength and elastic modulus results for outdoor cured M6 mortar (170 mm flow) 276
Table C.11: Compressive strength and elastic modulus results for outdoor cured NHL 5 mortar (165 mm flow) 277
Table C.12: Compressive strength and elastic modulus results for outdoor cured NHL 5 mortar (170 mm flow) 278
Table C.13: Compressive strength and elastic modulus results for outdoor cured CL90-s mortar (165 mm flow) 279
Table C.14: Compressive strength and elastic modulus results for outdoor cured CL90-s mortar (170 mm flow) 280

Table D.1: M6 mortar flexural strength results and calculations 284
Table D.2: NHL 5 mortar flexural strength results and calculations 285
Table D.3: NHL 3.5 mortar flexural strength results and calculations 286
Table D.4: NHL 2 mortar flexural strength results and calculations 287
Table D.5: CL90-s mortar flexural strength results and calculations 288
Table D.6: NHL 3.5 mortar flexural strength results and calculations, mix ratio (0:2:3) 289
Table D.7: M6 mortar flexural strength results and calculations (outdoor curing) 290
Table D.8: NHL 5 mortar flexural strength results and calculations (outdoor curing) 291
Table D.9: CL90-s mortar flexural strength results and calculations (outdoor curing) 292
Table E.1: NHL 5 masonry compressive strength and elastic modulus results and calculations 295
Table E.2: NHL 5 masonry compressive strength and elastic modulus results and calculations (continued) 296
Table E.3: NHL 3.5 masonry compressive strength and elastic modulus results and calculations 297
Table E.4: NHL 3.5 masonry compressive strength and elastic modulus results and calculations (continued) 298
Table E.5: NHL 2 masonry compressive strength and elastic modulus results and calculations 299
Table E.6: NHL 2 masonry compressive strength and elastic modulus results and calculations (continued) 300
Table E.7: CL90-s masonry compressive strength and elastic modulus results and calculations 301
Table E.8: CL90-s masonry compressive strength and elastic modulus results and calculations (continued) 302
Table E.9: M6 masonry compressive strength and elastic modulus results and calculations 303
Table E.10: M6 masonry compressive strength and elastic modulus results and calculations (continued) 304
Table E.11: NHL 5 masonry compressive strength and elastic modulus results and calculations, outdoor curing 305
Table E.12: NHL 5 masonry compressive strength and elastic modulus results and calculations, outdoor curing (continued) 306
Table E.13: M6 masonry compressive strength and elastic modulus results and calculations, outdoor curing 307
Table E.14: M6 masonry compressive strength and elastic modulus results and calculations, outdoor curing (continued) 308
Table E.15: CL90-s masonry compressive strength and elastic modulus results and calculations, outdoor curing 309
Table E.16: CL90-s masonry compressive strength and elastic modulus results and calculations, outdoor curing (continued) 310
Table E.17: NHL 2-broken limestone masonry compressive strength and elastic modulus results and calculations 311
Table E.18: NHL 2-broken limestone masonry compressive strength and elastic modulus results and calculations (continued) 312
Table E.19: CL90-s-broken limestone masonry compressive strength and elastic modulus results and calculations 313
Table E.20: CL90-s-broken limestone masonry compressive strength and elastic modulus results and calculations (continued) 314
Table E.21: NHL 2-cut limestone masonry compressive strength and elastic modulus results and calculations 315
Table E.22: NHL 2-cut limestone masonry compressive strength and elastic modulus results and calculations (continued) 316
Table E.23: CL90-s-cut limestone masonry compressive strength and elastic modulus results and calculations 317
Table E.24: CL90-s-cut limestone masonry compressive strength and elastic modulus results and calculations (continued) 318
Table E.25: NHL 2-broken sandstone masonry compressive strength and elastic modulus results and calculations 319

Table E.26: NHL 2-broken sandstone masonry compressive strength and elastic modulus results and calculations (continued) 320
Table E.27: CL90-s-broken sandstone masonry compressive strength and elastic modulus results and calculations 321
Table E.28: CL90-s-broken sandstone masonry compressive strength and elastic modulus results and calculations (continued) 322
Table F.1: M6 brick masonry bond strength calculations, 165 mm flow (1 month) 325
Table F.2: M6 brick masonry bond strength calculations, 165 mm flow (2 months) 326
Table F.3: M6 brick masonry bond strength calculations, 165 mm flow (6 months) 327
Table F.4: NHL 5 brick masonry bond strength calculations, 165 mm flow (1 months) 328
Table F.5: NHL 5 brick masonry bond strength calculations, 165 mm flow (2 months) 329
Table F.6: NHL 5 brick masonry bond strength calculations, 165 mm flow (6 months) 330
Table F.7: NHL 5 brick masonry bond strength calculations, 165 mm flow (12 months) 331
Table F.8: NHL 3 5 brick masonry bond strength calculations, 165 mm flow (1 month) 332
Table F.9: NHL 3.5 brick masonry bond strength calculations, 165 mm flow (2 months) 333
Table F.10: NHL 3.5 brick masonry bond strength calculations, 165 mm flow (6 months) 334
Table F.11: NHL 3.5 brick masonry bond strength calculations, 165 mm flow (12 months) 335
Table F.12: NHL 2 brick masonry bond strength calculations, 165 mm flow (1 month) 336
Table F.13: NHL 2 brick masonry bond strength calculations, 165 mm flow (2 months) 337
Table F.14: NHL 2 brick masonry bond strength calculations, 165 mm flow (6 months) 338
Table F.15: NHL 2 brick masonry bond strength calculations, 165 mm flow (12 months) 339
Table F.16: CL90-s brick masonry bond strength calculations, 165 mm flow (1 month) 340
Table F.17: CL90-s brick masonry bond strength calculations, 165 mm flow (2 months) 341
Table F.18: CL90-s brick masonry bond strength calculations, 165 mm flow (6 months) 342
Table F.19: CL90-s brick masonry bond strength calculations, 165 mm flow (12 months) 343
Table F.20: NHL 3.5 brick masonry bond strength calculations, 165 mm flow (0:1:2) (1 month) 344
Table F.21: NHL 3.5 brick masonry bond strength calculations, 165 mm flow (0:1:2) (2 months) 345
Table F.22: NHL 3.5 brick masonry bond strength calculations, 165 mm flow (0:1:2) (6 months) 346
Table F.23: M6brick masonry bond strength calculations, 170 mm flow (1 month) 347
Table F.24: M6brick masonry bond strength calculations, 170 mm flow (2 months) 348
Table F.25: M6brick masonry bond strength calculations, 170 mm flow (6 months) 349
Table F.26: NHL 5 brick masonry bond strength calculations, 170 mm flow (1 month) 350
Table F.27: NHL 5 brick masonry bond strength calculations, 170 mm flow (2 months) 351
Table F.28: NHL 5 brick masonry bond strength calculations, 170 mm flow (6 months) 352
Table F.29: NHL3. 5 brick masonry bond strength calculations, 170 mm flow (1 month) 353
Table F.30: NHL3. 5 brick masonry bond strength calculations, 170 mm flow (2 months) 354
Table F.31: NHL3. 5 brick masonry bond strength calculations, 170 mm flow (6 months) 355
Table F.32: NHL2 brick masonry bond strength calculations, 170 mm flow (1 month) 356
Table F.33: NHL2 brick masonry bond strength calculations, 170 mm flow (2 months) 357
Table F.34: NHL2 brick masonry bond strength calculations, 170 mm flow (6 months) 358
Table F.35: CL90-s brick masonry bond strength calculations, 170 mm flow (1 month) 359
Table F.36: CL90-s brick masonry bond strength calculations, 170 mm flow (2 months) 360
Table F.37: CL90-s brick masonry bond strength calculations, 170 mm flow (6 months) 361
Table F.38: M6 brick masonry bond strength calculations, 165 mm flow, outdoor cured (1 month) 362
Table F.39: M6 brick masonry bond strength calculations, 165 mm flow, outdoor cured (2 months) 363
Table F.40: M6 brick masonry bond strength calculations, 165 mm flow, outdoor cured (6 months) 364
Table F.41: NHL 5 brick masonry bond strength calculations, 165 mm flow, outdoor cured (1 month) 365
Table F.42: NHL 5 brick masonry bond strength calculations, 165 mm flow, outdoor cured (2 months) 366
Table F.43: NHL 5 brick masonry bond strength calculations, 165 mm flow, outdoor cured (6 months) 367
Table F.44: NHL CL90-s brick masonry bond strength calculations, 165 mm flow, outdoor cured (1 month) 368
Table F.45: NHL 3.5 CL90-s brick masonry bond strength calculations, 165 mm flow, outdoor cured (2 months) 369

Table F.46: CL90-s brick masonry bond strength calculations, 165 mm flow, outdoor cured (6 months) 370
Table F.47: M6 brick masonry bond strength calculations, 165 mm flow, outdoor cured (1 month) 371
Table F.48: M6 brick masonry bond strength calculations, 165 mm flow, outdoor cured (2 months) 372
Table F.49: M6 brick masonry bond strength calculations, 165 mm flow, outdoor cured (6 months) 373
Table F.50: NHL 5 brick masonry bond strength calculations, 170 mm flow, outdoor cured (1 month) 374
Table F.51: NHL 5 brick masonry bond strength calculations, 170 mm flow, outdoor cured (2 months) 375
Table F.52: NHL 5 brick masonry bond strength calculations, 170 mm flow, outdoor cured (6 months) 376
Table F.53: CL90-s brick masonry bond strength calculations, 170 mm flow, outdoor cured (1 month) 377
Table F.54: CL90-s brick masonry bond strength calculations, 170 mm flow, outdoor cured (2 months) 378
Table F.55: CL90-s brick masonry bond strength calculations, 170 mm flow, outdoor cured (6 months) 379
Table F.56: CL90-s broken sandstone masonry bond strength calculations, 165 mm flow (1 month) 380
Table F.57: CL90-s broken sandstone masonry bond strength calculations, 165 mm flow (2 months) 381
Table F.58: CL90-s broken sandstone masonry bond strength calculations, 165 mm flow (6 months) 382
Table F.59: NHL 2 broken sandstone masonry bond strength calculations, 165 mm flow (1 month) 383
Table F.60: NHL 2 broken sandstone masonry bond strength calculations, 165 mm flow (2 months) 384
Table F.61: NHL 2 broken sandstone masonry bond strength calculations, 165 mm flow (6 months) 385
Table F.62: CL90-s broken sandstone masonry bond strength calculations, 170 mm flow (1 month) 386
Table F.63: CL90-s broken sandstone masonry bond strength calculations, 170 mm flow (2 months) 387
Table F.64: CL90-s broken sandstone masonry bond strength calculations, 170 mm flow (6 months) 388
Table F.65: NHL 2 broken sandstone masonry bond strength calculations, 170 mm flow (1 month) 389
Table F.66: NHL 2 broken sandstone masonry bond strength calculations, 170 mm flow (2 months) 390
Table F.67: NHL 2 broken sandstone masonry bond strength calculations, 170 mm flow (6 months) 391
Table F.68: CL90-s broken limestone masonry bond strength calculations, 165 mm flow (1 month) 392
Table F.69: CL90-s broken limestone masonry bond strength calculations, 165 mm flow (2 months) 393
Table F.70: CL90-s broken limestone masonry bond strength calculations, 165 mm flow (6 months) 394
Table F.71: NHL 2 broken limestone masonry bond strength calculations, 165 mm flow (1 month) 395
Table F.72: NHL 2 broken limestone masonry bond strength calculations, 165 mm flow (2 months) 396
Table F.73: NHL 2 broken limestone masonry bond strength calculations, 165 mm flow (6 months) 397
Table F.74: CL90-s broken limestone masonry bond strength calculations, 170 mm flow (1 month) 398
Table F.75: CL90-s broken limestone masonry bond strength calculations, 170 mm flow (2 months) 399
Table F.76: CL90-s broken limestone masonry bond strength calculations, 170 mm flow (6 months) 400
Table F.77: NHL 2 broken limestone masonry bond strength calculations, 170 mm flow (1 month) 401
Table F.78: NHL 2 broken limestone masonry bond strength calculations, 170 mm flow (2 months) 402
Table F.79: NHL 2 broken limestone masonry bond strength calculations, 170 mm flow (6 months) 403
Table F.80: CL90-s cut limestone masonry bond strength calculations, 165 mm flow (1 month) 404
Table F.81: CL90-s cut limestone masonry bond strength calculations, 165 mm flow (2 months) 405
Table F.82: CL90-s cut limestone masonry bond strength calculations, 165 mm flow (6 months) 406
Table F.83: NHL 2 cut limestone masonry bond strength calculations, 165 mm flow (1 month) 407
Table F.84: NHL 2 cut limestone masonry bond strength calculations, 165 mm flow (2 months) 408
Table F.85: NHL 2 cut limestone masonry bond strength calculations, 165 mm flow (6 months) 409
Table F.86: CL90-s cut limestone masonry bond strength calculations, 170 mm flow (1 month) 410
Table F.87: CL90-s cut limestone masonry bond strength calculations, 170 mm flow (2 months) 411
Table F.88: CL90-s cut limestone masonry bond strength calculations, 170 mm flow (6 months) 412
Table F.89: NHL 2 cut limestone masonry bond strength calculations, 170 mm flow (1 month) 413
Table F.90: NHL 2 cut limestone masonry bond strength calculations, 170 mm flow (2 months) 414
Table F.91: NHL 2 cut limestone masonry bond strength calculations, 170 mm flow (6 months) 415
Table G.1: M6 brick masonry flexural strength (parallel to bedding joints) 419
Table G.2: NHL 5 brick masonry flexural strength (parallel to bedding joints) 420
Table G.3: NHL3. 5 brick masonry flexural strength (parallel to bedding joints) 421

Table G.4: NHL3. 5 brick masonry flexural strength (parallel to bedding joints) (mix ratio 0:1:2)..... 422
Table G.5: NHL2 brick masonry flexural strength (parallel to bedding joints)..... 423
Table G.6: NHL3. 5 brick masonry flexural strength (parallel to bedding joints)..... 424
Table G.7: M6 brick masonry flexural strength (parallel to bedding joints) 425
Table G.8: NHL 5 brick masonry flexural strength (perpendicular to bedding joints)..... 426
Table G.9: NHL 3.5 brick masonry flexural strength (perpendicular to bedding joints)..... 427
Table G.10: NHL3. 5 brick masonry flexural strength (perpendicular to bedding joints) (mix ratio 0:1:2) 428
Table G.11: NHL 2 brick masonry flexural strength (perpendicular to bedding joints)..... 429
Table G.12: CL90-s brick masonry flexural strength (perpendicular to bedding joints) 430
Table H.1: Brick units compressive and flexural strength, and elastic modulus results and calculations..... 433
Table H.2: Limestone units compressive and flexural strength, and elastic modulus results and calculations..... 434
Table H.3: Sandstone units compressive and flexural strength, and elastic modulus results and calculations..... 435

APPENDIX A

STATISTICAL ANALYSIS OF MORTAR FLOW TEST

Mix ratio: 0:1:3

Sample	Dim. 1 (mm)	Dim. 2 (mm)	Dim. 3 (mm)	Mean (mm)	COV (%)	Batch Mean
1.a	164	165	165	164.67	0.35%	
1.b	165	166	163	164.67	0.93%	
1.c	166	167	165	166.00	0.60%	
1.d	164	165	166	165.00	0.61%	
1.e	166	164	164	164.67	0.70%	164.90
1.f	165	166	164	165.00	0.61%	
1.g	165	165	166	165.33	0.35%	
1.h	162	165	165	164.00	1.06%	
1.i	163	164	166	164.33	0.93%	
1.j	166	165	165	165.33	0.35%	
2.a	166	164	166	165.33	0.70%	
2.b	167	165	167	166.33	0.69%	
2.c	165	164	165	164.67	0.35%	
2.d	166	165	166	165.67	0.35%	
2.e	167	164	167	166.00	1.04%	165.07
2.f	168	163	164	165.00	1.60%	
2.g	166	165	166	165.67	0.35%	
2.h	165	162	164	163.67	0.93%	
2.i	165	163	165	164.33	0.70%	
2.j	164	165	163	164.00	0.61%	
3.a	163	164	165	164.00	0.61%	
3.b	165	166	166	165.67	0.35%	
3.c	167	165	164	165.33	0.92%	
3.d	164	165	166	165.00	0.61%	
3.e	166	164	164	164.67	0.70%	165.03
3.f	165	166	164	165.00	0.61%	
3.g	165	165	166	165.33	0.35%	
3.h	162	165	165	164.00	1.06%	
3.i	163	168	167	166.00	1.59%	
3.j	166	165	165	165.33	0.35%	

Table A.1: Initial flow results of NHL 5 mortar (165 mm)

Summary

Groups	*Sample size*	*Sum*	*Mean*	*Variance*
NHL5-165-batch 1	10	1,649.	164.9	0.3222
NHL5-165-batch 2	10	1,650.667	165.0666	0.7851
NHL5-165-batch 3	10	1,650.333	165.0333	0.4308

ANOVA

Source of Variation	*SS*	*df*	*MS*	*F*	*p-level*	*F crit*
Between Groups	0.1556	2	0.0778	0.1517	0.8599	3.3541
Within Groups	13.844	27	0.5127			
Total	14.	29				

Therefore we fail to reject the hypothesis since $F<F_{crit}$ and $P_{value}>0.05$

Table A.2: Analysis of variance (one-way) of NHL 5 mortar (165 mm)

Mix ratio: 0:1:3

Sample	Dim. 1 (mm)	Dim. 2 (mm)	Dim. 3 (mm)	Mean (mm)	COV (%)	Batch Mean
1.a	168	170	166	168.00	1.19%	
1.b	170	173	169	170.67	1.22%	
1.c	169	172	170	170.33	0.90%	
1.d	169	169	167	168.33	0.69%	
1.e	170	198	169	179.00	9.20%	170.13
1.f	167	170	166	167.67	1.24%	
1.g	168	170	169	169.00	0.59%	
1.h	169	170	170	169.67	0.34%	
1.i	170	169	170	169.67	0.34%	
1.j	170	168	169	169.00	0.59%	
2.a	168	170	169	169.00	0.59%	
2.b	169	170	170	169.67	0.34%	
2.c	173	170	172	171.67	0.89%	
2.d	169	168	169	168.67	0.34%	
2.e	168	169	167	168.00	0.60%	169.47
2.f	168	170	166	168.00	1.19%	
2.g	170	173	169	170.67	1.22%	
2.h	169	172	170	170.33	0.90%	
2.i	170	170	166	168.67	1.37%	
2.j	170	170	170	170.00	0.00%	
3.a	169	168	169	168.67	0.61%	
3.b	169	172	167	169.33	0.35%	
3.c	172	170	170	170.67	0.92%	
3.d	167	170	166	167.67	0.61%	
3.e	168	170	169	169.00	0.70%	169.53
3.f	169	170	170	169.67	0.61%	
3.g	173	170	170	171.00	0.35%	
3.h	170	167	170	169.00	1.06%	
3.i	169	168	169	168.67	1.59%	
3.j	170	172	173	171.67	0.35%	

Table A.3: Initial flow results of NHL 5 mortar (170 mm)

Summary

Groups	*Sample size*	*Sum*	*Mean*	*Variance*
NHL 5-170 batch 1	10	1,701.33	170.13	10.65
NHL 5-170 batch 2	10	1,694.67	169.47	1.46
NHL 5-170 batch 3	10	1,695.33	169.53	1.51

ANOVA

Source of Variation	*SS*	*df*	*MS*	*F*	*p-level*	*F crit*
Between Groups	2.696	2	1.348	0.29695	0.745	3.354
Within Groups	122.577	27	4.539			
Total	125.274	29				

Therefore we fail to reject the hypothesis since $F<F_{crit}$ and $P_{value}>0.05$

Table A.4: Analysis of variance (one-way) of NHL 5 mortar (170 mm)

Mix ratio: 0:1:3

Sample	Dim. 1 (mm)	Dim. 2 (mm)	Dim. 3 (mm)	Mean (mm)	COV (%)	Batch Mean
1.a	166	167	165	166.00	0.60%	
1.b	164	165	166	165.00	0.61%	
1.c	166	164	164	164.67	0.70%	
1.d	165	168	163	165.33	1.52%	
1.e	163	164	163	163.33	0.35%	164.77
1.f	163	164	164	163.67	0.35%	
1.g	164	166	166	165.33	0.70%	
1.h	164	165	165	164.67	0.35%	
1.i	163	164	166	164.33	0.93%	
1.j	166	165	165	165.33	0.35%	
2.a	166	164	165	165.00	0.61%	
2.b	165	166	164	165.00	0.61%	
2.c	165	165	166	165.33	0.35%	
2.d	168	163	167	166.00	1.59%	
2.e	164	163	164	163.67	0.35%	165.07
2.f	166	164	166	165.33	0.70%	
2.g	166	164	165	165.00	0.61%	
2.h	165	166	164	165.00	0.61%	
2.i	165	165	165	165.00	0.00%	
2.j	164	165	163	164.00	0.61%	
3.a	166	165	166	165.67	0.35%	
3.b	167	164	167	166.00	1.04%	
3.c	168	163	164	165.00	1.60%	
3.d	164	164	166	164.67	0.70%	
3.e	165	166	164	165.00	0.61%	165.03
3.f	163	164	164	163.67	0.35%	
3.g	163	164	166	164.33	0.93%	
3.h	164	166	165	165.00	0.61%	
3.i	163	168	167	166.00	1.59%	
3.j	166	165	165	165.33	0.35%	

Table A.5: Initial flow results of NHL 3.5 mortar (165 mm)

Summary

Groups	*Sample size*	*Sum*	*Mean*	*Variance*
NHL 3.5-165-batch 1	10	1,647.67	164.77	0.66
NHL 3.5-165-batch 2	10	1,649.33	164.93	0.43
NHL 3.5-165-batch 3	10	1,650.67	165.07	0.54

ANOVA

Source of Variation	*SS*	*df*	*MS*	*F*	*p-level*	*F crit*
Between Groups	0.45185	2	0.22593	0.41185	0.66651	3.35413
Within Groups	14.81111	27	0.54856			
Total	15.26296	29				

Therefore we fail to reject the hypothesis since $F<F_{crit}$ and $P_{value}>0.05$

Table A.6: Analysis of variance (one-way) of NHL 3. 5 mortar (165 mm)

Mix ratio: 0:1:3

Sample	Dim. 1 (mm)	Dim. 2 (mm)	Dim. 3 (mm)	Mean (mm)	COV (%)	Batch Mean
1.a	170	173	166	169.67	2.07%	
1.b	171	173	170	171.33	0.89%	
1.c	167	170	167	168.00	1.03%	
1.d	169	169	173	170.33	1.36%	
1.e	169	170	169	169.33	0.34%	170.03
1.f	171	172	171	171.33	0.34%	
1.g	170	169	170	169.67	0.34%	
1.h	173	170	173	172.00	1.01%	
1.i	168	169	172	169.67	1.23%	
1.j	170	168	169	169.00	0.59%	
2.a	173	171	170	171.33	0.89%	
2.b	173	170	172	171.67	0.89%	
2.c	168	170	170	169.33	0.68%	
2.d	169	173	169	170.33	1.36%	
2.e	170	169	167	168.67	0.91%	169.80
2.f	167	170	166	167.67	1.24%	
2.g	170	170	169	169.67	0.34%	
2.h	169	170	170	169.67	0.34%	
2.i	170	169	170	169.67	0.34%	
2.j	170	170	170	170.00	0.00%	
3.a	169	168	169	168.67	0.34%	
3.b	170	172	167	169.67	1.48%	
3.c	172	171	170	171.00	0.58%	
3.d	170	169	166	168.33	1.24%	
3.e	170	170	169	169.67	0.34%	169.73
3.f	169	170	170	169.67	0.34%	
3.g	173	170	170	171.00	1.01%	
3.h	170	167	170	169.00	1.02%	
3.i	169	168	169	168.67	0.34%	
3.j	170	172	173	171.67	0.89%	

Table A.7: Initial flow results of NHL 3.5 mortar (170 mm)

Summary

Groups	*Sample size*	*Sum*	*Mean*	*Variance*
NHL 3.5-170 batch 1	10	1,700.3	170.03	1.49
NHL 3.5-170 batch 2	10	1,698.33	169.8	1.36
NHL 3.5-170 batch 3	10	1,697.33	169.73	1.3

ANOVA

Source of Variation	*SS*	*df*	*MS*	*F*	*p-level*	*F crit*
Between Groups	0.493	2	0.24815	0.1798	0.831	3.3413
Within Groups	37.433	27	1.38642			
Total	37.923	29				

Therefore we fail to reject the hypothesis since $F<F_{crit}$ and $P_{value}>0.05$

Table A.8: Analysis of variance (one-way) of NHL 3.5 mortar (170 mm)

Mix ratio: 0:1:3

Sample	Dim. 1 (mm)	Dim. 2 (mm)	Dim. 3 (mm)	Mean (mm)	COV (%)	Batch Mean
1.a	167	163	165	165.00	1.21%	
1.b	165	165	166	165.33	0.35%	
1.c	164	162	164	163.33	0.71%	
1.d	165	168	163	165.33	1.52%	
1.e	163	170	163	165.33	2.44%	164.90
1.f	163	164	164	163.67	0.35%	
1.g	164	166	166	165.33	0.70%	
1.h	164	165	169	166.00	1.59%	
1.i	163	164	166	164.33	0.93%	
1.j	166	165	165	165.33	0.35%	
2.a	166	167	164	165.67	0.92%	
2.b	165	168	163	165.33	1.52%	
2.c	169	165	166	166.67	1.25%	
2.d	168	163	167	166.00	1.59%	
2.e	164	163	164	163.67	0.35%	165.10
2.f	166	162	166	164.67	1.40%	
2.g	166	164	165	165.00	0.61%	
2.h	165	166	164	165.00	0.61%	
2.i	165	165	165	165.00	0.00%	
2.j	164	165	163	164.00	0.61%	
3.a	166	166	167	166.33	0.35%	
3.b	167	165	168	166.67	0.92%	
3.c	168	163	164	165.00	1.60%	
3.d	164	169	166	166.33	1.51%	
3.e	165	166	164	165.00	0.61%	165.20
3.f	163	164	164	163.67	0.35%	
3.g	163	164	162	163.00	0.61%	
3.h	164	166	165	165.00	0.61%	
3.i	162	168	167	165.67	1.94%	
3.j	166	165	165	165.33	0.35%	

Table A.9: Initial flow results of NHL 2 mortar (165 mm)

Summary

Groups	*Sample size*	*Sum*	*Mean*	*Variance*
NHL 2-165-batch 1	10	1,649.	164.9	0.71728
NHL 2-165-batch 2	10	1,651.	165.1	0.79136
NHL 2-165-batch 3	10	1,652.	165.2	1.36296

ANOVA

Source of Variation	*SS*	*df*	*MS*	*F*	*p-level*	*F crit*
Between Groups	0.46667	2	0.23333	0.24377	0.78538	3.35413
Within Groups	25.84444	27	0.9572			
Total	26.31111	29				

Therefore we fail to reject the hypothesis since $F < F_{crit}$ and $P_{value} > 0.05$

Table A.10: Analysis of variance (one-way) of NHL 2 mortar (165 mm)

Mix ratio: 0:1:3

Sample	Dim. 1 (mm)	Dim. 2 (mm)	Dim. 3 (mm)	Mean (mm)	COV (%)	Batch Mean
1.a	168	168	169	168.33	0.34%	
1.b	170	169	172	170.33	0.90%	
1.c	171	172	170	171.00	0.58%	
1.d	169	169	173	170.33	1.36%	
1.e	169	170	169	169.33	0.34%	170.13
1.f	171	172	171	171.33	0.34%	
1.g	170	169	170	169.67	0.34%	
1.h	173	170	174	172.33	1.21%	
1.i	168	169	172	169.67	1.23%	
1.j	170	168	169	169.00	0.59%	
2.a	168	170	169	169.00	0.59%	
2.b	169	168	172	169.67	1.23%	
2.c	173	170	172	171.67	0.89%	
2.d	169	174	169	170.67	1.69%	
2.e	170	169	167	168.67	0.91%	169.63
2.f	167	170	166	167.67	1.24%	
2.g	170	170	169	169.67	0.34%	
2.h	169	170	170	169.67	0.34%	
2.i	170	169	170	169.67	0.34%	
2.j	170	170	170	170.00	0.00%	
3.a	169	168	169	168.67	0.34%	
3.b	173	170	167	170.00	1.76%	
3.c	170	171	171	170.67	0.34%	
3.d	170	169	166	168.33	1.24%	
3.e	170	170	169	169.67	0.34%	169.73
3.f	169	170	170	169.67	0.34%	
3.g	173	170	170	171.00	1.01%	
3.h	170	167	170	169.00	1.02%	
3.i	169	168	169	168.67	0.34%	
3.j	170	172	173	171.67	0.89%	

Table A.11: Initial flow results of NHL 2 mortar (170 mm)

Summary						
Groups	*Sample size*	*Sum*	*Mean*	*Variance*		
NHL 2-170 batch 1	10	1,701.33	170.13	1.41		
NHL 2-170 batch 2	10	1,696.33	169.63	1.17		
NHL 2-170 batch 3	10	1,697.33	169.73	1.23		
ANOVA						
Source of Variation	*SS*	*df*	*MS*	*F*	*p-level*	*F crit*
Between Groups	1.4	2	0.7	0.56	0.59	3.35
Within Groups	34.32	27	1.28			
Total	35.72	29				

Therefore we fail to reject the hypothesis since $F<F_{crit}$ and $P_{value}>0.05$

Table A.12: Analysis of variance (one-way) of NHL 2 mortar (170 mm)

Mix ratio: 0:1:3

Sample	Dim. 1 (mm)	Dim. 2 (mm)	Dim. 3 (mm)	Mean (mm)	COV (%)	Batch Mean
1.a	168	165	165	166.00	1.04%	
1.b	166	166	165	165.67	0.35%	
1.c	169	164	164	165.67	1.74%	
1.d	165	164	165	164.67	0.35%	
1.e	163	170	165	166.00	2.17%	165.37
1.f	164	164	165	164.33	0.35%	
1.g	165	162	163	163.33	0.94%	
1.h	168	168	169	168.33	0.34%	
1.i	163	164	166	164.33	0.93%	
1.j	166	165	165	165.33	0.35%	
2.a	166	167	165	166.00	0.60%	
2.b	163	164	165	164.00	0.61%	
2.c	165	164	165	164.67	0.35%	
2.d	168	164	163	165.00	1.60%	
2.e	170	168	169	169.00	0.59%	165.77
2.f	162	168	169	166.33	2.28%	
2.g	169	164	165	166.00	1.59%	
2.h	168	166	164	166.00	1.20%	
2.i	165	169	166	166.67	1.25%	
2.j	164	165	163	164.00	0.61%	
3.a	165	168	167	166.67	0.92%	
3.b	167	164	164	165.00	1.05%	
3.c	164	165	166	165.00	0.61%	
3.d	164	162	168	164.67	1.86%	
3.e	165	166	164	165.00	0.61%	165.07
3.f	162	164	165	163.67	0.93%	
3.g	164	164	165	164.33	0.35%	
3.h	165	166	165	165.33	0.35%	
3.i	162	168	167	165.67	1.94%	
3.j	166	165	165	165.33	0.35%	

Table A.13: Initial flow results of CL90-s mortar (165 mm)

Summary

Groups	*Sample size*	*Sum*	*Mean*	*Variance*
CL90-s-*165 batch 1*	10	1,651.	165.1	0.57
CL90-s-*165 batch 2*	10	1,649.67	164.97	0.407
CL90-s-*165 batch 3*	10	1,649.33	164.93	1.131

ANOVA

Source of Variation	*SS*	*df*	*MS*	*F*	*p-level*	*F crit*
Between Groups	0.16	2	0.078	0.11	0.895	3.35
Within Groups	18.96	27	0.716			
Total	19.11	29				

Therefore we fail to reject the hypothesis since $F<F_{crit}$ and $P_{value}>0.05$

Table A.14: Analysis of variance of CL90-s mortar (165 mm)

Mix ratio: 0:1:3

Sample	Dim. 1 (mm)	Dim. 2 (mm)	Dim. 3 (mm)	Mean (mm)	COV (%)	Batch Mean
1.a	168	168	169	168.33	0.34%	
1.b	170	170	172	170.67	0.68%	
1.c	171	172	170	171.00	0.58%	
1.d	169	169	173	170.33	1.36%	
1.e	169	170	169	169.33	0.34%	170.17
1.f	171	172	171	171.33	0.34%	
1.g	170	169	170	169.67	0.34%	
1.h	173	170	174	172.33	1.21%	
1.i	168	169	172	169.67	1.23%	
1.j	170	168	169	169.00	0.59%	
2.a	171	170	169	170.00	0.59%	
2.b	174	172	170	172.00	1.16%	
2.c	173	170	172	171.67	0.89%	
2.d	169	174	169	170.67	1.69%	
2.e	170	169	167	168.67	0.91%	169.97
2.f	167	170	166	167.67	1.24%	
2.g	170	170	169	169.67	0.34%	
2.h	169	170	170	169.67	0.34%	
2.i	170	169	170	169.67	0.34%	
2.j	170	170	170	170.00	0.00%	
3.a	173	172	169	171.33	1.21%	
3.b	174	170	167	170.33	2.06%	
3.c	171	171	173	171.67	0.67%	
3.d	170	169	166	168.33	1.24%	
3.e	170	170	169	169.67	0.34%	170.13
3.f	169	170	170	169.67	0.34%	
3.g	173	170	170	171.00	1.01%	
3.h	170	167	170	169.00	1.02%	
3.i	169	168	169	168.67	0.34%	
3.j	170	172	173	171.67	0.89%	

Table A.15: Initial flow results of CL90-s mortar (170 mm)

Summary				
Groups	***Sample size***	***Sum***	***Mean***	***Variance***
CL90-s-*170 batch 1*	10	1,701.67	170.167	1.44
CL90-s-*170 batch 2*	10	1,699.67	169.97	1.64
CL90-s-*170 batch 3*	10	1,701.33	170.13	1.56

ANOVA						
Source of Variation	***SS***	***df***	***MS***	***F***	***p-level***	***F crit***
Between Groups	0.229	2	0.114	0.074	0.929	3.354
Within Groups	41.76	27	1.546			
Total	41.986	29				

Therefore we fail to reject the hypothesis since $F<F_{crit}$ and $P_{value}>0.05$

Table A.16: Analysis of variance (one-way) of CL90-s mortar (170 mm)

Mix ratio: 1:½:4.5

Sample	Dim. 1 (mm)	Dim. 2 (mm)	Dim. 3 (mm)	Mean (mm)	COV (%)	Batch Mean
1.a	168	165	165	166.00	1.04%	
1.b	166	166	165	165.67	0.35%	
1.c	169	164	164	165.67	1.74%	
1.d	165	164	165	164.67	0.35%	
1.e	163	170	165	166.00	2.17%	165.37
1.f	164	164	165	164.33	0.35%	
1.g	165	162	163	163.33	0.94%	
1.h	168	168	169	168.33	0.34%	
1.i	163	164	166	164.33	0.93%	
1.j	166	165	165	165.33	0.35%	
2.a	166	167	165	166.00	0.60%	
2.b	163	164	165	164.00	0.61%	
2.c	165	164	165	164.67	0.35%	
2.d	168	164	163	165.00	1.60%	
2.e	170	168	169	169.00	0.59%	165.77
2.f	162	168	169	166.33	2.28%	
2.g	169	164	165	166.00	1.59%	
2.h	168	166	164	166.00	1.20%	
2.i	165	169	166	166.67	1.25%	
2.j	164	165	163	164.00	0.61%	
3.a	165	168	167	166.67	0.92%	
3.b	167	164	164	165.00	1.05%	
3.c	164	165	166	165.00	0.61%	
3.d	164	162	168	164.67	1.86%	
3.e	165	166	164	165.00	0.61%	165.07
3.f	162	164	165	163.67	0.93%	
3.g	164	164	165	164.33	0.35%	
3.h	165	166	165	165.33	0.35%	
3.i	162	168	167	165.67	1.94%	
3.j	166	165	165	165.33	0.35%	

Table A.17: Initial flow results of M6 mortar (165 mm)

Summary

Groups	*Sample size*	*Sum*	*Mean*	*Variance*
M6-*165 batch 1*	10	1,653.67	165.37	1.84
M6-*165 batch 2*	10	1,657.67	165.77	2.19
M6-*165 batch 3*	10	1,650.67	165.07	0.64

ANOVA

Source of Variation	*SS*	*df*	*MS*	*F*	*p-level*	*F crit*
Between Groups	2.467	2	1.233	0.79	0.47	3.35
Within Groups	42.067	27	1.558			
Total	44.533	29				

Therefore we fail to reject the hypothesis since $F < F_{crit}$ and $P_{value} > 0.05$

Table A.18: Analysis of variance (one-way) of M6 mortar (165 mm)

Mix ratio: 1:½:4.5

Sample	Dim. 1 (mm)	Dim. 2 (mm)	Dim. 3 (mm)	Mean (mm)	COV (%)	Batch Mean
1.a	168	168	169	168.33	0.34%	
1.b	172	174	172	172.67	0.67%	
1.c	172	172	170	171.33	0.67%	
1.d	166	167	173	168.67	2.24%	
1.e	174	172	169	171.67	1.47%	170.50
1.f	171	172	171	171.33	0.34%	
1.g	170	169	170	169.67	0.34%	
1.h	173	170	174	172.33	1.21%	
1.i	168	166	167	167.00	0.60%	
1.j	170	174	172	172.00	1.16%	
2.a	166	167	169	167.33	0.91%	
2.b	174	172	170	172.00	1.16%	
2.c	173	170	172	171.67	0.89%	
2.d	169	166	167	167.33	0.91%	
2.e	170	174	172	172.00	1.16%	169.70
2.f	167	170	166	167.67	1.24%	
2.g	166	167	169	167.33	0.91%	
2.h	174	172	170	172.00	1.16%	
2.i	170	169	170	169.67	0.34%	
2.j	170	170	170	170.00	0.00%	
3.a	173	172	169	171.33	1.21%	
3.b	166	168	170	168.00	1.19%	
3.c	174	172	173	173.00	0.58%	
3.d	166	167	166	166.33	0.35%	
3.e	174	172	169	171.67	1.47%	170.07
3.f	169	166	167	167.33	0.91%	
3.g	174	174	172	173.33	0.67%	
3.h	171	167	170	169.33	1.23%	
3.i	169	168	169	168.67	0.34%	
3.j	170	172	173	171.67	0.89%	

Table A.19: Initial flow results of M6 mortar (170 mm)

Summary

Groups	*Sample size*	*Sum*	*Mean*	*Variance*
M6-*170 batch 1*	10	1,705.00	170.50	3.784
M6-*170 batch 2*	10	1,697.00	169.70	4.529
M6-*170 batch 3*	10	1,700.67	170.07	6.0197

ANOVA

Source of Variation	*SS*	*df*	*MS*	*F*	*p-level*	*F crit*
Between Groups	3.21	2	1.60	0.36	0.717	3.352
Within Groups	129.00	27	4.78			
Total	132.21	29				

Therefore we fail to reject the hypothesis since $F<F_{crit}$ and $P_{value}>0.05$

Table A.20: Analysis of variance of M6 (170 mm)

Mix ratio: 0:2:3

Sample	Dim. 1 (mm)	Dim. 2 (mm)	Dim. 3 (mm)	Mean (mm)	COV (%)	Batch Mean
1.a	165	163	162	163.33	0.94%	
1.b	164	165	166	165.00	0.61%	
1.c	166	165	164	165.00	0.61%	
1.d	165	164	165	164.67	0.35%	
1.e	163	163	163	163.00	0.00%	164.40
1.f	163	164	164	163.67	0.35%	
1.g	164	166	165	165.00	0.61%	
1.h	164	165	168	165.67	1.26%	
1.i	163	163	164	163.33	0.35%	
1.j	166	165	165	165.33	0.35%	
2.a	166	164	164	164.67	0.70%	
2.b	163	166	163	164.00	1.06%	
2.c	168	167	166	167.00	0.60%	
2.d	164	165	167	165.33	0.92%	
2.e	163	163	164	163.33	0.35%	164.80
2.f	166	164	166	165.33	0.70%	
2.g	164	165	165	164.67	0.35%	
2.h	166	164	164	164.67	0.70%	
2.i	165	165	165	165.00	0.00%	
2.j	164	165	163	164.00	0.61%	
3.a	163	165	166	164.67	0.93%	
3.b	169	168	167	168.00	0.60%	
3.c	168	163	165	165.33	1.52%	
3.d	164	165	166	165.00	0.61%	
3.e	166	164	164	164.67	0.70%	165.03
3.f	163	164	164	163.67	0.35%	
3.g	163	164	166	164.33	0.93%	
3.h	164	166	165	165.00	0.61%	
3.i	163	164	165	164.00	0.61%	
3.j	167	166	164	165.67	0.92%	

Table A.21: Initial flow results of NHL 2 mortar (165 mm)

Summary

Groups	*Sample size*	*Sum*	*Mean*	*Variance*
NHL 2-165-batch 1	10	1,644.0	164.4	0.93
NHL 2-165-batch 2	10	1,648.0	164.8	0.99
NHL 2-165-batch 3	10	1,650.33	165.03	1.44

ANOVA

Source of Variation	*SS*	*df*	*MS*	*F*	*p-level*	*F crit*
Between Groups	2.05	2	1.023	0.91	0.413	3.35
Within Groups	30.32	27	1.123			
Total	32.37	29				

Therefore we fail to reject the hypothesis since $F<F_{crit}$ and $P_{value}>0.05$

Table A.22: Analysis of variance of NHL 2 mortar (165 mm)

SUMMARY	Batch 1	Batch 2	Batch 3	Total
165 flow				
Count	10	10	10	30
Sum	1649	1650.67	1650.33	4950
Average	164.9	165.067	165.033	165
Variance	0.321489	0.784157	0.430401	0.482076
170 flow				
Count	10	10	10	30
Sum	1701.34	1694.68	1695.35	5091.37
Average	170.134	169.468	169.535	169.7123
Variance	10.64598	1.462573	1.511117	4.319536
Total				
Count	20	20	20	
Sum	3350.34	3345.35	3345.68	
Average	167.517	167.2675	167.284	
Variance	12.40426	6.161293	6.253352	

ANOVA						
Source of Variation	*SS*	*df*	*MS*	*F*	*P-value*	*F crit*
Sample	333.0913	1	333.0913	131.8676	4.09E-16	4.019541
Columns	0.778743	2	0.389372	0.154148	0.857521	3.168246
Interaction	2.066523	2	1.033262	0.409058	0.666317	3.168246
Within	136.4015	54	2.525953			
Total	472.338	59				

Table A.23: Multiple analysis of variance of NHL 5 mortar (165 vs. 170 mm)

Therefore, we reject the null hypothesis that all treatments have exactly the same effect since $F < F_{crit}$ and $P_{value} > 0.05$ and conclude that there is a statistically significant difference between the two mortar flows.

SUMMARY	Batch 1	Batch 2	Batch 3	Total
165 flow				
Count	10	10	10	30
Sum	1647.66	1649.33	1650.67	4947.66
Average	164.766	164.933	165.067	164.922
Variance	0.667071	0.437979	0.537734	0.525513
170 flow				
Count	10	10	10	30
Sum	1700.33	1698.01	1697.35	5095.69
Average	170.033	169.801	169.735	169.8563
Variance	1.490157	1.360454	1.30445	1.306396
Total				
Count	20	20	20	
Sum	3347.99	3347.34	3348.02	
Average	167.3995	167.367	167.401	
Variance	8.322184	7.088054	6.606883	

ANOVA						
Source of Variation	*SS*	*df*	*MS*	*F*	*P-value*	*F crit*
Sample	365.2147	1	365.2147	377.9487	4.78E-26	4.019541
Columns	0.014763	2	0.007382	0.007639	0.992391	3.168246
Interaction	0.930003	2	0.465002	0.481215	0.620657	3.168246
Within	52.18061	54	0.966308			
Total	418.3401	59				

Table A.24: Multiple analysis of variance of NHL 3.5 mortar (165 vs. 170 mm)

Therefore, we reject the null hypothesis that all treatments have exactly the same effect since $F < F_{crit}$ and $P_{value} > 0.05$ and conclude that there is a statistically significant difference between the two mortar flows.

SUMMARY	Batch 1	Batch 2	Batch 3	Total
165 flow				
Count	10	10	10	30
Sum	1648.98	1651.01	1652	4951.99
Average	164.898	165.101	165.2	165.0663
Variance	0.716351	0.791388	1.361489	0.906796
170 flow				
Count	10	10	10	30
Sum	1701.32	1696.36	1697.35	5095.03
Average	170.132	169.636	169.735	169.8343
Variance	1.410773	1.171804	1.231117	1.231081
Total				
Count	20	20	20	
Sum	3350.3	3347.37	3349.35	
Average	167.515	167.3685	167.4675	
Variance	8.216732	6.342098	6.640241	

ANOVA

Source of Variation	*SS*	*df*	*MS*	*F*	*P-value*	*F crit*
Sample	341.0074	1	341.0074	306.1601	6.56E-24	4.019541
Columns	0.223463	2	0.111732	0.100314	0.904722	3.168246
Interaction	1.62867	2	0.814335	0.731119	0.486074	3.168246
Within	60.1463	54	1.11382			
Total	403.0058	59				

Table A.25: Multiple analysis of variance of NHL 2 mortar (165 vs. 170 mm)

Therefore, we reject the null hypothesis that all treatments have exactly the same effect since $F < F_{crit}$ and $P_{value} > 0.05$ and conclude that there is a statistically significant difference between the two mortar flows.

SUMMARY	Batch 1	Batch 2	Batch 3	Total
165 flow				
Count	10	10	10	30
Sum	1653.66	1657.67	1650.67	4962
Average	165.366	165.767	165.067	165.4
Variance	1.839071	2.198201	0.63749	1.535869
170 flow				
Count	10	10	10	30
Sum	1701.66	1699.69	1701.34	5102.69
Average	170.166	169.969	170.134	170.0897
Variance	1.437293	1.639188	1.561293	1.447017
Total				
Count	20	20	20	
Sum	3355.32	3357.36	3352.01	
Average	167.766	167.868	167.6005	
Variance	7.61512	6.464238	7.797973	

ANOVA

Source of Variation	*SS*	*df*	*MS*	*F*	*P-value*	*F crit*
Sample	329.8946	1	329.8946	212.5487	2.29E-20	4.019541
Columns	0.729003	2	0.364502	0.234846	0.791496	3.168246
Interaction	1.961863	2	0.980932	0.632007	0.535409	3.168246
Within	83.81283	54	1.552089			
Total	416.3983	59				

Table A.26: Multiple analysis of variance of CL90-s mortar (165 vs. 170 mm)

Therefore, we reject the null hypothesis that all treatments have exactly the same effect since $F < F_{crit}$ and $P_{value} > 0.05$ and conclude that there is a statistically significant difference between the two mortar flows.

SUMMARY	Batch 1	Batch 2	Batch 3	Total
165 flow				
Count	10	10	10	30
Sum	1653.66	1657.67	1650.67	4962
Average	165.366	165.767	165.067	165.4
Variance	1.839071	2.198201	0.63749	1.535869
170 flow				
Count	10	10	10	30
Sum	1705	1697	1700.66	5102.66
Average	170.5	169.7	170.066	170.0887
Variance	3.783467	4.534822	6.023071	4.561377
Total				
Count	20	20	20	
Sum	3358.66	3354.67	3351.33	
Average	167.933	167.7335	167.5665	
Variance	9.599612	7.259982	9.731319	

ANOVA

Source of Variation	*SS*	*df*	*MS*	*F*	*P-value*	*F crit*
Sample	329.7539	1	329.7539	104.0445	3.37E-14	4.019541
Columns	1.346743	2	0.673372	0.212463	0.809263	3.168246
Interaction	4.328303	2	2.164152	0.682837	0.50949	3.168246
Within	171.1451	54	3.169354			
Total	506.5741	59				

Table A.27: Multiple analysis of variance of M6 mortar (165 vs. 170 mm)

Therefore, we reject the null hypothesis that all treatments have exactly the same effect since $F < F_{crit}$ and $P_{value} > 0.05$ and conclude that there is a statistically significant difference between the two mortar flows.

APPENDIX B

MORTAR WATER RETENTION TEST CALCULATIONS

Test no	Mortar ID	PC:Lime: Sand	Initial flow (mm)	Sample	Mass of mould and bottom non-porous plate (g) m_2	Mass of the bottom plate and mould with mortar filling (g) m_3	Mass of mortar in the mould (g) $m_7 = m_3 - m_2$	Water Fraction (W_1)	Water content of the mortar in the mould (g) $W_2 = W_1 \times m_7$	Mass of the bottom plate and dry filter plate (g) m_1	Mass of the bottom plate and soaked filter plate (g) m_7	Mass of water absorbed by the filter plate (g) $W_3 = m_7 - m_1$	Water retention (%) $(W_2-W_3)/W_2$	Mean water retention value (WRV) (%)	COV (%)
1	NHL 5	0:1:3	165	A	741.92	1138.16	396.24	0.17	65.49	655.76	660.55	4.79	92.68%		
2				B	742.39	1156.37	413.98		65.49	655.31	661.01	5.70	91.30%	92.25%	0.90
3				C	745.4	1150.58	405.18		66.97	655.64	660.48	4.84	92.78%		
4	NHL 3.5	0:1:3	165	A	745.87	1131.68	385.81	0.183	70.60	656.87	661.22	4.35	93.84%		
5				B	746.34	1138.68	392.34		71.80	657.38	662.04	4.66	93.51%	93.50%	0.37
6				C	745.23	1134.03	388.80		71.15	655.82	660.69	4.87	93.15%		
7	NHL 2	0:1:3	165	A	746.43	1126.48	380.05	0.203	77.15	660.74	662.58	1.84	97.62%		
8				B	745.34	1135.39	390.05		79.18	659.95	662.81	2.86	96.39%	96.28%	1.45
9				C	745.58	1115.77	370.19		75.15	656.78	660.66	3.88	94.84%		
10	CL90s	0:1:3	165	A	744.54	1084.63	340.09	0.242	82.30	660.12	662.96	2.84	96.55%		
11				B	744.58	1069.41	324.83		78.61	659.88	662.31	2.43	96.91%	97.23%	0.91
12				C	745.53	1097.35	351.82		85.14	658.45	659.96	1.51	98.23%		
13	M6	1:½:4	165	A	745.72	1157.95	412.23	0.153	63.07	655.79	666.87	11.08	82.43%		
14				B	745.24	1159.39	414.15		63.36	657.83	666.87	9.04	85.73%	84.94%	2.62
15				C	746.97	1160.36	413.39		63.25	659.34	667.78	8.44	86.66%		
16	NHL 3.5	0:1:2	165	A	745.73	1135.47	389.74	0.193	75.22	658.39	661.04	2.65	96.48%		
17				B	747.82	1145.39	397.57		76.73	660.36	664.56	4.20	94.52%	95.29%	1.10
18				C	745.19	1143.89	398.70		76.95	659.48	663.44	3.96	94.86%		

Table B.1: Calculation of mortar water retention (165 mm flow)

Test no	Mortar ID	PC:Lime: Sand	Initial flow (mm)	Sample	Mass of mould and bottom non-porous plate (g) m_2	Mass of the bottom plate and mould with mortar filling (g) m_3	Mass of mortar in the mould (g) $m_7 = m_3 - m_2$	Water Fraction (W_1)	Water content of the mortar in the mould (g) $W_2 = W_1 \times m_7$	Mass of the bottom plate and dry filter plate (g) m_1	Mass of the bottom plate and soaked filter plate (g) m_7	Mass of water absorbed by the filter plate (g) $W_3 = m_7 - m_1$	Water retention (%) $(W_2-W_3)/W_2$	Mean water retention value (WRV) (%)	COV (%)
19	NHL 5	0:1:3	170	A	745.79	1155.39	409.60	0.18	71.68	655.85	662.92	7.07	90.13%		
20				B	746.21	1160.32	414.11		72.47	657.42	665.21	7.79	89.25%	90.31%	1.28
21				C	745.88	1151.43	405.55		70.97	658.55	664.55	6.00	91.54%		
22	NHL 3.5	0:1:3	170	A	745.49	1139.53	394.04	0.189	74.47	657.11	660.14	3.03	95.93%		
23				B	746.2	1143.19	396.99		75.03	655.39	660.26	4.87	93.51%	94.49%	1.35
24				C	745.91	1135.33	389.42		73.60	656.98	661.37	4.39	94.03%		
25	NHL 2	0:1:3	170	A	745.35	1130.25	384.90	0.216	83.14	658.41	661.29	2.88	96.53%		
26				B	756.42	1129.49	373.07		80.58	656.80	661.31	4.51	94.40%	95.29%	1.16
27				C	745.55	1123.48	377.93		81.63	656.36	660.49	4.13	94.94%		
28	CL90s	0:1:3	170	A	745.8	1103.52	357.72	0.25	89.43	658.13	659.68	1.55	98.27%		
29				B	746.9	1090.43	343.53		85.88	671.44	673.29	1.85	97.85%	98.17%	0.29
30				C	747.36	1084.54	337.18		84.30	655.93	657.29	1.36	98.39%		
31	M6	1:½:4	170	A	745.03	1163.72	418.69	0.159	66.57	656.48	667.05	10.57	84.12%		
32				B	746.22	1168.18	421.96		67.09	655.15	665.03	9.88	85.28%	84.47%	0.83
33				C	747.28	1158.93	411.65		65.45	656.37	666.84	10.47	84.01%		

Table B.2: Calculation of mortar water retention (170 mm flow)

APPENDIX C

MORTAR COMPRESSIVE STRENGTH & ELASTIC MODULUS RESULTS AND CALCULATIONS

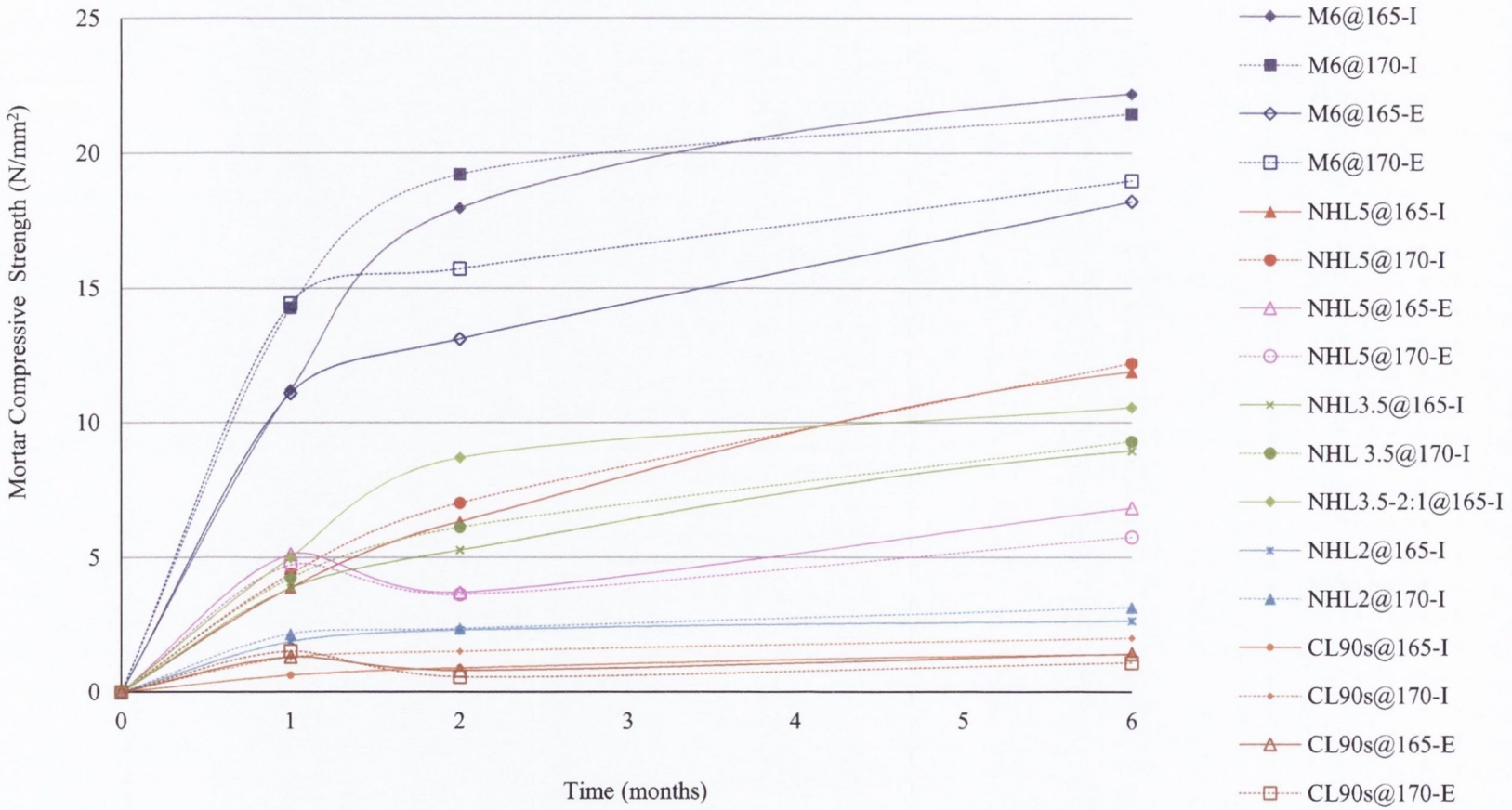

Figure C.1: Compressive strength development of mortar over time

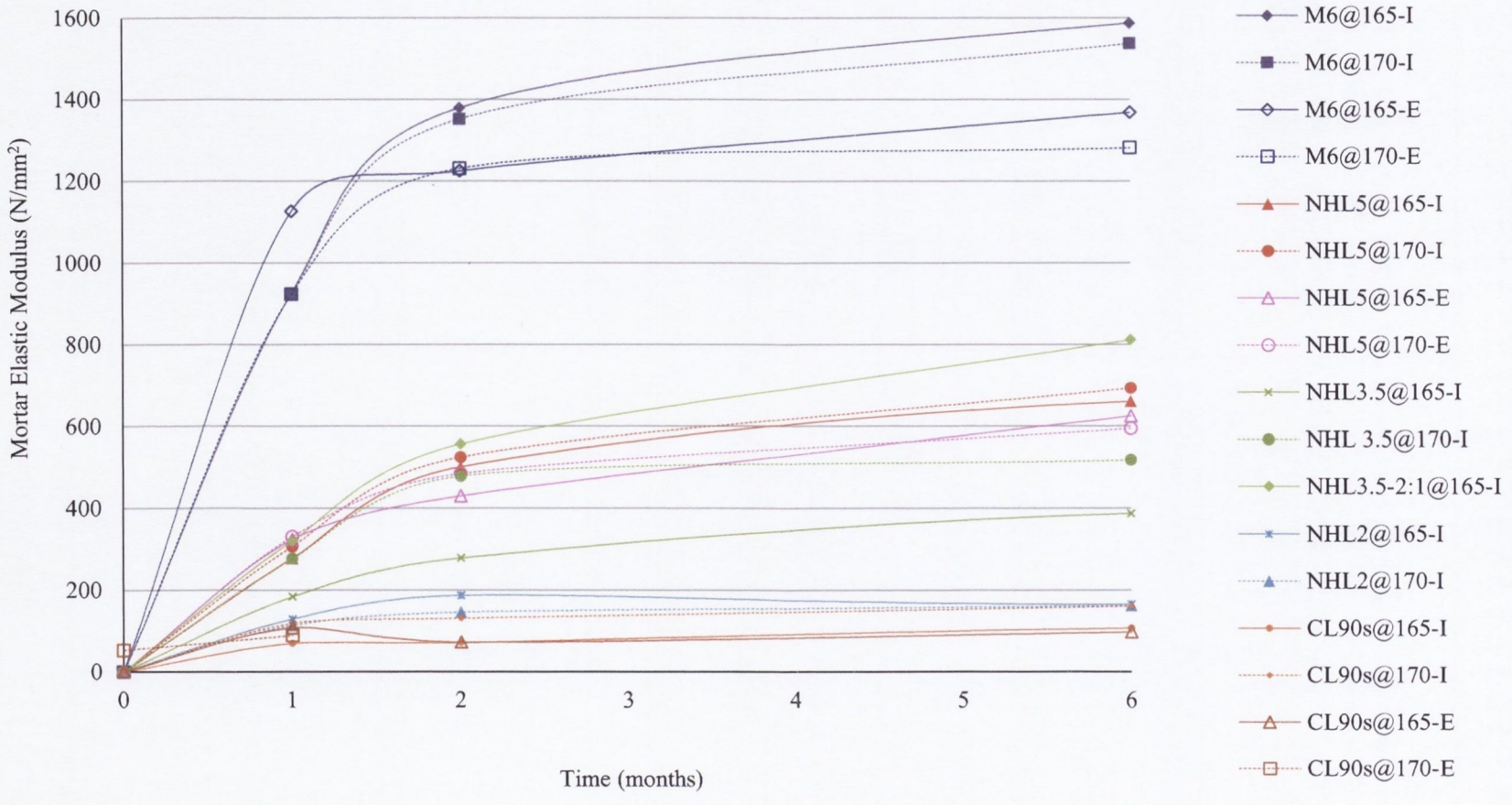

Figure C.2: Elastic modulus development of mortar over time

Test No.	Mortar ID		Mix Ratio PC/lime/ sand	Initial flow (mm)	Curing	Test Age (mts.)	Cross sectional area (mm^2)	Applied load, F_c (kN)	Compressive strength, R_i (N/mm^2)	Mean compressive strength, R_c (N/mm^2)	COV (%)	Elastic modulus E_i (N/mm^2)	Mean Elastic modulus (N/mm^2)	COV (%)
1	M-NHL5-1m-C	A	0:1:3	165	lab	1	6400	25.47	3.98	3.87	2.77	256.60	277.67	10.81
		B					6400	24.26	3.79			312.05		
		C					6400	24.32	3.80			264.35		
2	M-NHL5-2m-C	A	0:1:3	165	lab	2	6400	40.06	6.26	6.33	3.46	451.73	501.07	15.22
		B					6400	42.11	6.58			588.88		
		C					6400	39.42	6.16			462.60		
3	M-NHL5-6m-C	A	0:1:3	165	lab	6	6400	76.61	11.97	11.89	4.21	840.15	660.70	23.52
		B					6400	78.98	12.34			569.20		
		C					6400	72.64	11.35			572.75		
4	M-NHL5-1yr-C	A	0:1:3	165	lab	12	6400	86.85	13.57	13.30	2.28	765.60	683.27	17.82
		B					6400	83.01	12.97			543.40		
		C					6400	85.44	13.35			740.80		
5	M-NHL5-1m-C	A	0:1:3	170	lab	1	6400	27.97	4.37	4.39	2.21	255.10	307.00	16.15
		B					6400	27.58	4.31			312.05		
		C					6400	28.80	4.50			353.85		
6	M-NHL5-2m-C	A	0:1:3	170	lab	2	6400	46.78	7.31	7.02	5.41	560.19	525.15	6.07
		B					6400	42.18	6.59			497.78		
		C					6400	45.82	7.16			517.50		
7	M-NHL5-6m-C	A	0:1:3	170	lab	12	6400	77.12	12.05	12.21	2.04	840.15	693.50	18.80
		B					6400	77.38	12.09			649.70		
		C					6400	80.00	12.50			590.65		

Table C.1: Compressive strength and elastic modulus results for NHL 5 mortar

Test No.	Mortar ID		Mix Ratio PC/lime/ sand	Initial flow (mm)	Curing	Test Age (mts.)	Cross sectional area (mm^2)	Applied load, F_c (kN)	Compressive strength, R_i (N/mm^2)	Mean compressive strength, R_c (N/mm^2)	COV (%)	Elastic modulus E_i (N/mm^2)	Mean Elastic modulus (N/mm^2)	COV (%)
8	M-NHL3.5-1m-C	A	0:1:3	165	lab	1	1600	5.99	3.74	3.86	4.03	171.95	183.82	21.42
		B					1600	6.07	3.79			218.65		
		C					1600	6.58	4.11			191.80		
		D					1600	6.32	3.95			121.95		
		E					1600	5.89	3.68			214.75		
		F					1600	6.17	3.86			376.00		
9	M-NHL3.5-2m-C	A	0:1:3	165	lab	2	1600	8.24	5.15	5.27	4.11	330.25	278.37	11.55
		B					1600	8.88	5.55			247.95		
		C					1600	8.36	5.23			278.60		
		D					1600	8.73	5.46			267.85		
		E					1600	8.47	5.30			299.00		
		F					1600	7.92	4.95			246.55		
10	M-NHL3.5-6m-C	A	0:1:3	165	lab	6	1600	14.38	8.99	8.95	5.61	355.25	386.86	16.16
		B					1600	15.72	9.82			464.45		
		C					1600	14.72	9.20			315.65		
		D					1600	13.68	8.55			377.15		
		E					1600	13.76	8.60			462.45		
		F					1600	13.70	8.56			346.20		
11	M-NHL3.5-1yr-C	A	0:1:3	165	lab	12	6400	62.72	9.80	10.00	5.10	441.70	401.13	23.30
		B					6400	67.71	10.58			467.45		
		C					6400	61.57	9.62			294.25		

Table C.2: Compressive strength and elastic modulus results for NHL 3.5 mortar (165 mm flow)

Test No.	Mortar ID		Mix Ratio PC/lime/ sand	Initial flow (mm)	Curing	Test Age (mts.)	Cross Sectional area (mm^2)	Applied load, F_c (kN)	Compressive strength, R_i (N/mm^2)	Mean compressive strength, R_c (N/mm^2)	COV (%)	Elastic modulus E_i (N/mm^2)	Mean Elastic modulus (N/mm^2)	COV (%)
12	M-NHL3.5_1m-C	A	0:1:3	170	lab	1	1600	6.96	4.35	4.23	9.63	321.95	276.76	16.63
		B					1600	7.54	4.71			318.65		
		C					1600	7.02	4.39			274.70		
		D					1600	5.81	3.63			257.25		
		E					1600	6.48	4.05			211.25		
13	M-NHL3.5-2m-C	A	0:1:3	170	lab	2	6400	40.96	6.40	6.11	7.49	452.25	477.70	16.86
		B					6400	35.71	5.58			412.95		
		C					6400	40.58	6.34			567.90		
14	M-NHL3.5-6m-C	A	0:1:3	170	lab	6	6400	59.46	9.29	9.30	8.76	368.55	511.87	27.14
		B					6400	54.34	8.49			521.15		
		C					6400	64.77	10.12			645.90		

Table C.3: Compressive strength and elastic modulus results for NHL 3.5 mortar (170 mm flow)

Test No.	Mortar ID		Mix Ratio PC/lime/ sand	Initial flow (mm)	Curing	Test Age (mts.)	Cross sectional area (mm^2)	Applied load, F_c (kN)	Compressive strength, R_i (N/mm^2)	Mean compressive strength, R_c (N/mm^2)	COV (%)	Elastic modulus E_i (N/mm^2)	Mean Elastic modulus (N/mm^2)	COV (%)	Notes
15	M-NHL2-1m-C	A	0:1:3	165	lab	1	6400	12.67	1.98	1.87	8.32	136.00	129.75	6.81	
		B					6400	11.26	1.76			123.50			
		C					6400	-	-			-			damaged
16	M-NHL2-2m-C	A	0:1:3	165	lab	2	6400	14.08	2.20	2.29	3.76	198.55	187.05	6.43	
		B					6400	15.17	2.37			174.55			
		C					6400	14.78	2.31			188.05			
17	M-NHL2-6m-C	A	0:1:3	165	lab	6	6400	14.90	2.33	2.63	13.09	160.97	165.20	7.61	
		B					6400	16.35	2.55			179.34			
		C					6400	19.23	3.00			155.30			
18	M-NHL2-1yr-C	A	0:1:3	165	lab	12	6400	16.26	2.54	2.70	6.10	226.72	197.20	13.07	
		B					6400	18.37	2.87			185.73			
		C					6400	17.28	2.70			179.16			
19	M-NHL2-1m-C	A	0:1:3	170	lab	1	1600	3.59	2.24	2.16	6.23	88.15	114.87	31.84	
		B					1600	3.17	1.98			73.00			
		C					1600	3.60	2.25			128.40			
		D					1600	3.34	2.09			169.70			
		E					1600	3.31	2.07			92.25			
		F					1600	3.73	2.33			137.70			
20	M-NHL2-2m-C	A	0:1:3	170	lab	2	6400	14.91	2.39	2.35	1.49	131.75	146.20	11.03	
		B					6400	14.78	2.31			143.25			
		C					6400	15.10	2.36			163.60			
21	M-NHL2-6m-C	A	0:1:3	170	lab	6	6400	22.98	3.59	3.14	12.58	158.05	161.92	3.39	
		B					6400	18.24	2.85			159.50			
		C					6400	19.07	2.98			168.20			

Table C.4: Compressive strength and elastic modulus results for NHL 2 mortar

Test No.	Mortar ID		Mix Ratio PC/lime/ sand	Initial flow (mm)	Curing	Test Age (mts.)	Cross sectional area (mm^2)	Applied load, F_c (kN)	Compressive strength, R_i (N/mm^2)	Mean compressive strength, R_c (N/mm^2)	COV (%)	Elastic modulus E_i (N/mm^2)	Mean Elastic modulus (N/mm^2)	COV (%)
22	M-CL90s-1m-C	A	0:1:3	165	lab	1	6400	4.86	0.76	0.62	21.66	55.90	70.03	19.40
		B					6400	3.14	0.49			83.00		
		C					6400	3.97	0.62			71.20		
23	M-CL90s-2m-C	A	0:1:3	165	lab	2	6400	4.80	0.75	0.89	15.20	50.35	71.95	28.56
		B					6400	5.76	0.90			74.25		
		C					6400	6.53	1.02			91.25		
24	M-CL90s-6m-C	A	0:1:3	165	lab	6	6400	10.62	1.66	1.39	21.01	111.80	107.05	9.65
		B					6400	9.15	1.43			114.15		
		C					6400	6.91	1.08			95.20		
25	M-CL90s-1yr-C	A	0:1:3	165	lab	12	6400	10.62	1.66	1.40	20.15	133.94	119.20	18.50
		B					6400	9.22	1.44			129.81		
		C					6400	7.04	1.10			93.86		
26	M-CL90s-1m-C	A	0:1:3	170	lab	1	1600	1.74	1.09	1.29	8.81	94.35	119.75	22.95
		B					1600	2.18	1.37			133.65		
		C					1600	2.16	1.35			139.85		
		D					1600	2.24	1.40			111.20		
		E					1600	2.00	1.25			84.65		
		F					1600	2.03	1.27			154.80		
27	M-CL90s-2m-C	A	0:1:3	170	lab	2	6400	9.86	1.54	1.52	2.94	153.34	131.64	14.91
		B					6400	9.76	1.52			115.16		
		C					6400	9.32	1.46			126.42		
28	M-CL90s-6m-C	A	0:1:3	170	lab	6	6400	11.26	1.76	2.00	27.15	177.15	160.60	8.93
		B					6400	14.91	2.33			152.00		
		C					6400	13.38	2.09			152.65		

Table C.5: Compressive strength and elastic modulus results for CL90-s mortar

Test No.	Mortar ID		Mix Ratio PC/lime/ sand	Initial flow (mm)	Curing	Test Age (mts.)	Cross Sectional area (mm^2)	Applied load, F_c (kN)	Compressive strength, R_i (N/mm^2)	Mean compressive strength, R_c (N/mm^2)	COV (%)	Elastic modulus E_i (N/mm^2)	Mean Elastic modulus (N/mm^2)	COV (%)
29	M-M6-1m-C	A	0:1:3	165	lab	1	1600	19.09	11.93	11.22	13.55	954.50	926.45	5.860
		B					1600	20.06	12.54			1002.15		
		C					1600	19.22	12.02			952.65		
		D					1600	18.18	11.36			915.75		
		E					1600	17.89	11.18			854.85		
		F					1600	13.25	8.28			878.80		
30	M-M6-2m-C	A	0:1:3	165	lab	2	1600	28.38	17.74	18.00	4.65	1286.75	1379.59	8.52
		B					1600	30.93	19.33			1550.35		
		C					1600	27.96	17.48			1419.30		
		D					1600	29.71	18.57			1412.80		
		E					1600	27.15	16.97			1211.35		
		F					1600	28.69	17.93			1397.00		
31	M-M6-6m-C	A	0:1:3	165	lab	6	1600	40.57	25.36	22.20	16.89	1739.70	1586.97	15.01
		B					1600	39.80	24.88			1539.15		
		C					1600	29.44	18.40			1557.30		
		D					1600	40.79	25.50			1924.20		
		E					1600	35.48	22.18			1551.35		
		F					1600	27.08	16.92			1210.10		
32	M-M6-1yr-C	A	0:1:3	165	lab	12	1600	40.57	25.36	23.03	14.13	1739.70	1743.75	14.32
		B					1600	39.78	24.86			1539.15		
		C					1600	37.41	23.38			1557.30		
		D					1600	40.79	25.50			1924.20		
		E					1600	35.48	22.18			1551.35		
		F					1600	27.08	16.92			2150.80		

Table C.6: Compressive strength and elastic modulus results for M6 mortar (165 mm flow)

Test No.	Mortar ID		Mix Ratio PC/lime/ sand	Initial flow (mm)	Curing	Test Age (mts.)	Cross Sectional area (mm^2)	Applied load, F_c (kN)	Compressive strength, R_i (N/mm^2)	Mean compressive strength, R_c (N/mm^2)	COV (%)	Elastic modulus E_i (N/mm^2)	Mean Elastic modulus (N/mm^2)	COV (%)
33	M-M6-1m-C	A	0:1:3	170	lab	1	1600	24.18	15.11	14.28	5.06	1200.00	925.05	16.76
		B					1600	21.04	13.15			988.45		
		C					1600	22.08	13.80			750.00		
		D					1600	23.26	14.54			879.90		
		E					1600	22.77	14.23			887.00		
		F					1600	23.79	14.87			844.95		
34	M-M6-2m-C	A	0:1:3	170	lab	2	1600	29.68	18.55	19.23	3.76	1250.70	1352.25	12.57
		B					1600	30.88	19.30			1334.60		
		C					1600	31.09	19.43			1368.75		
		D					1600	32.86	20.54			1263.95		
		E					1600	30.05	18.78			1215.85		
		F					1600	30.08	18.80			1679.65		
35	M-M6-6m-C	A	0:1:3	170	lab	6	1600	31.44	19.65	21.45	4.81	1445.25	1537.40	9.94
		B					1600	35.71	22.32			1299.40		
		C					1600	33.76	21.10			1593.75		
		D					1600	34.30	21.44			1581.85		
		E					1600	36.04	22.53			1752.25		
		F					1600	34.67	21.67			1551.90		

Table C.7: Compressive strength and elastic modulus results for M6 mortar (170 mm flow)

Test No.	Mortar ID		Mix Ratio PC/lime/ sand	Initial flow (mm)	Curing	Test Age (mts.)	Cross Sectional area (mm^2)	Applied load, F_c (kN)	Compressive strength, R_i (N/mm^2)	Mean compressive strength, R_c (N/mm^2)	COV (%)	Elastic modulus E_i (N/mm^2)	Mean Elastic modulus (N/mm^2)	COV (%)
36	M-NHL3.5-1m-C	A	0:1:2	165	lab	1	1600	9.22	5.76	5.01	27.36	303.90	320.38	15.19
		B					1600	11.04	6.90			357.10		
		C					1600	9.47	5.92			373.70		
		D					1600	5.66	3.54			243.90		
		E					1600	6.51	4.07			349.50		
		F					1600	6.14	3.84			294.20		
37	M-NHL3.5-2m-C	A	0:1:2	165	lab	2	1600	11.98	7.49	8.70	10.52	503.90	556.65	23.42
		B					1600	14.54	9.09			457.30		
		C					1600	12.53	7.83			473.58		
		D					1600	16.03	10.02			543.50		
		E					1600	14.30	8.94			549.60		
		F					1600	14.10	8.81			812.00		
38	M-NHL3.5-6m-C	A	0:1:2	165	lab	6	6400	70.53	11.02	10.56	4.40	832.45	811.50	13.58
		B					6400	64.58	10.09			692.30		
		C					6400	67.71	10.58			909.75		

Table C.8: Compressive strength and elastic modulus results for NHL 3.5 mortar (165 mm flow and mix ratio 0:2:3)

Test No.	Mortar ID		Mix Ratio PC/lime/ sand	Initial flow (mm)	Curing	Test Age (mts.)	Cross Sectional area (mm^2)	Applied load, F_c (kN)	Compressive strength, R_i (N/mm^2)	Mean compressive strength, R_c (N/mm^2)	COV (%)	Elastic modulus E_i (N/mm^2)	Mean Elastic modulus (N/mm^2)	COV (%)	Notes
39	M-M6-1m-C	A	0:1:3	165	external	1	1600	15.49	9.68	11.09	12.29	1054.25	1127.42	9.65	
		B					1600	18.49	11.56			1153.10			
		C					1600	20.75	12.97			1307.70			
		D					1600	18.24	11.40			1060.05			
		E					1600	15.72	9.83			1062.00			
		F					1600	-	-			-			damaged
40	M-M6-2m-C	A	0:1:3	165	external	2	1600	16.55	10.35	13.12	17.88	890.20	1225.18	26.84	
		B					1600	19.71	12.32			962.25			
		C					1600	26.81	16.76			1436.00			
		D					1600	21.65	13.53			1675.40			
		E					1600	20.20	12.62			1162.05			
		F					1600	-	-			-			damaged
41	M-M6-6m-C	A	0:1:3	165	external	6	1600	25.05	15.66	18.24	14.11	1043.65	1368.42	23.97	
		B					1600	26.01	16.26			1178.40			
		C					1600	35.51	22.19			1903.90			
		D					1600	29.98	18.74			1328.00			
		E					1600	29.33	18.33			1388.15			
		F					1600	-	-			-			damaged

Table C.9: Compressive strength and elastic modulus results for outdoor cured M6 mortar (165 mm flow)

Test No.	Mortar ID		Mix Ratio PC/lime/ sand	Initial flow (mm)	Curing	Test Age (mts.)	Cross Sectional area (mm^2)	Applied load, F_c (kN)	Compressive strength, R_i (N/mm^2)	Mean compressive strength, R_c (N/mm^2)	COV (%)	Elastic modulus E_i (N/mm^2)	Mean Elastic modulus (N/mm^2)	COV (%)
42	M-M6-1m-C	A	0:1:3	170	external	1	1600	24.55	15.34	14.44	10.27	1200.00	923.58	16.89
		B					1600	18.41	11.51			988.45		
		C					1600	23.15	14.47			750.00		
		D					1600	24.73	15.46			879.90		
		E					1600	23.61	14.75			887.00		
		F					1600	24.19	15.12			836.10		
43	M-M6-2m-C	A	0:1:3	170	external	2	1600	25.62	16.01	15.74	6.71	1250.70	1231.21	8.30
		B					1600	24.56	15.35			1234.60		
		C					1600	27.20	17.00			1368.75		
		D					1600	26.04	16.27			1263.95		
		E					1600	25.45	15.91			1215.85		
		F					1600	22.21	13.88			1053.40		
44	M-M6-6m-C	A	0:1:3	170	external	6	1600	31.72	19.82	18.99	15.01	1345.25	1281.20	12.47
		B					1600	28.84	18.02			1299.40		
		C					1600	26.67	16.67			1093.75		
		D					1600	24.41	15.26			1081.85		
		E					1600	36.04	22.53			1402.25		
		F					1600	34.67	21.67			1464.70		

Table C.10: Compressive strength and elastic modulus results for outdoor cured M6 mortar (170 mm flow)

Test No.	Mortar ID		Mix Ratio PC/lime/ sand	Initial flow (mm)	Curing	Test Age (mts.)	Cross Sectional area (mm^2)	Applied load, F_c (kN)	Compressive strength, R_i (N/mm^2)	Mean compressive strength, R_c (N/mm^2)	COV (%)	Elastic modulus E_i (N/mm^2)	Mean Elastic modulus (N/mm^2)	COV (%)
45	M-NHL5-1m-C	A	0:1:3	165	external	1	6400	29.06	4.54	5.12	5.49	221.80	323.92	27.32
		B					6400	35.90	5.61			378.15		
		C					6400	33.34	5.21			371.80		
46	M-NHL5-2m-C	A	0:1:3	165	external	2	1600	6.39	4.00	3.70	5.96	468.90	429.76	13.22
		B					1600	5.40	3.37			362.90		
		C					1600	5.90	3.69			434.75		
		D					1600	5.77	3.61			360.65		
		E					1600	5.81	3.63			499.45		
		F					1600	6.22	3.89			451.90		
47	M-NHL5-6m-C	A	0:1:3	165	external	6	1600	10.10	6.32	6.83	6.38	603.60	625.06	9.18
		B					1600	10.44	6.53			573.55		
		C					1600	11.50	7.19			647.00		
		D					1600	10.35	6.47			558.90		
		E					1600	11.50	7.19			712.05		
		F					1600	11.65	7.28			655.25		

Table C.11: Compressive strength and elastic modulus results for outdoor cured NHL 5 mortar (165 mm flow)

Test No.	Mortar ID		Mix Ratio PC/lime/ sand	Initial flow (mm)	Curing	Test Age (mts.)	Cross Sectional area (mm^2)	Applied load, F_c (kN)	Compressive strength, R_i (N/mm^2)	Mean compressive strength, R_c (N/mm^2)	COV (%)	Elastic modulus E_i (N/mm^2)	Mean Elastic modulus (N/mm^2)	COV (%)
48	M-NHL5-1m-C	A	0:1:3	170	external	1	6400	32.00	5.00	4.72	7.88	287.55	330.58	12.17
		B					6400	31.17	4.87			367.25		
		C					6400	27.52	4.30			336.95		
49	M-NHL5-2m-C	A	0:1:3	170	external	2	1600	5.86	3.66	3.62	6.33	528.35	484.21	6.67
		B					1600	5.95	3.72			445.15		
		C					1600	5.18	3.24			518.05		
		D					1600	5.78	3.61			469.65		
		E					1600	6.30	3.94			478.55		
		F					1600	5.66	3.54			465.50		
50	M-NHL5-6m-C	A	0:1:3	170	external	6	1600	9.36	5.85	5.75	10.43	602.40	594.48	7.05
		B					1600	9.12	5.70			558.15		
		C					1600	7.57	4.73			630.60		
		D					1600	9.80	6.12			645.60		
		E					1600	10.42	6.51			594.60		
		F					1600	8.92	5.58			535.55		

Table C.12: Compressive strength and elastic modulus results for outdoor cured NHL 5 mortar (170 mm flow)

Test No.	Mortar ID		Mix Ratio PC/lime/ sand	Initial flow (mm)	Curing	Test Age (mts.)	Cross Sectional area (mm^2)	Applied load, F_c (kN)	Compressive strength, R_i (N/mm^2)	Mean compressive strength, R_c (N/mm^2)	COV (%)	Elastic modulus E_i (N/mm^2)	Mean Elastic modulus (N/mm^2)	COV (%)
51	M-CL90s-1m-C	A	0:1:3	165	external	1	6400	5.13	0.80	1.30	29.69	142.80	108.30	24.13
		B					6400	8.66	1.35			106.10		
		C					6400	11.17	1.75			79.25		
		D					6400	8.45	1.32			105.05		
52	M-CL90s-2m-C	A	0:1:3	165	external	2	1600	1.45	0.90	0.80	21.05	75.05	73.12	32.59
		B					1600	1.45	0.91			84.35		
		C					1600	1.63	1.02			106.50		
		D					1600	1.09	0.68			81.70		
		E					1600	1.05	0.66			44.55		
		F					1600	0.98	0.61			46.55		
53	M-CL90s-6m-C	A	0:1:3	165	external	6	1600	2.38	1.49	1.41	10.33	101.20	97.51	9.33
		B					1600	2.03	1.27			105.80		
		C					1600	2.00	1.25			89.35		
		D					1600	2.21	1.38			84.30		
		E					1600	2.33	1.46			97.40		

Table C.13: Compressive strength and elastic modulus results for outdoor cured CL90-s mortar (165 mm flow)

Test No.	Mortar ID		Mix Ratio PC/lime/ sand	Initial flow (mm)	Curing	Test Age (mts.)	Cross Sectional area (mm^2)	Applied load, F_c (kN)	Compressive strength, R_i (N/mm^2)	Mean compressive strength, R_c (N/mm^2)	COV (%)	Elastic modulus E_i (N/mm^2)	Mean Elastic modulus (N/mm^2)	COV (%)
54	M-CL90s-1m-C	A	0:1:3	170	external	1	6400	9.86	1.54	1.51	3.05	153.35	144.37	10.78
		B					6400	9.86	1.54			153.35		
		C					6400	9.34	1.46			126.40		
55	M-CL90s-2m-C	A	0:1:3	170	external	2	1600	0.79	0.49	0.57	11.82	39.75	53.05	15.77
		B					1600	0.97	0.61			58.60		
		C					1600	0.75	0.47			54.35		
		D					1600	0.97	0.61			58.60		
		E					1600	0.99	0.62			60.90		
		F					1600	0.97	0.61			46.10		
56	M-CL90s-6m-C	A	0:1:3	170	external	6	1600	1.56	0.97	1.09	10.17	84.35	89.80	13.68
		B					1600	1.93	1.20			95.60		
		C					1600	1.94	1.21			111.65		
		D					1600	1.53	0.96			87.95		
		E					1600	1.71	1.07			80.95		
		F					1600	1.77	1.11			78.30		

Table C.14: Compressive strength and elastic modulus results for outdoor cured CL90-s mortar (170 mm flow)

APPENDIX D

MORTAR FLEXURAL STRENGTH RESULTS AND CALCULATIONS

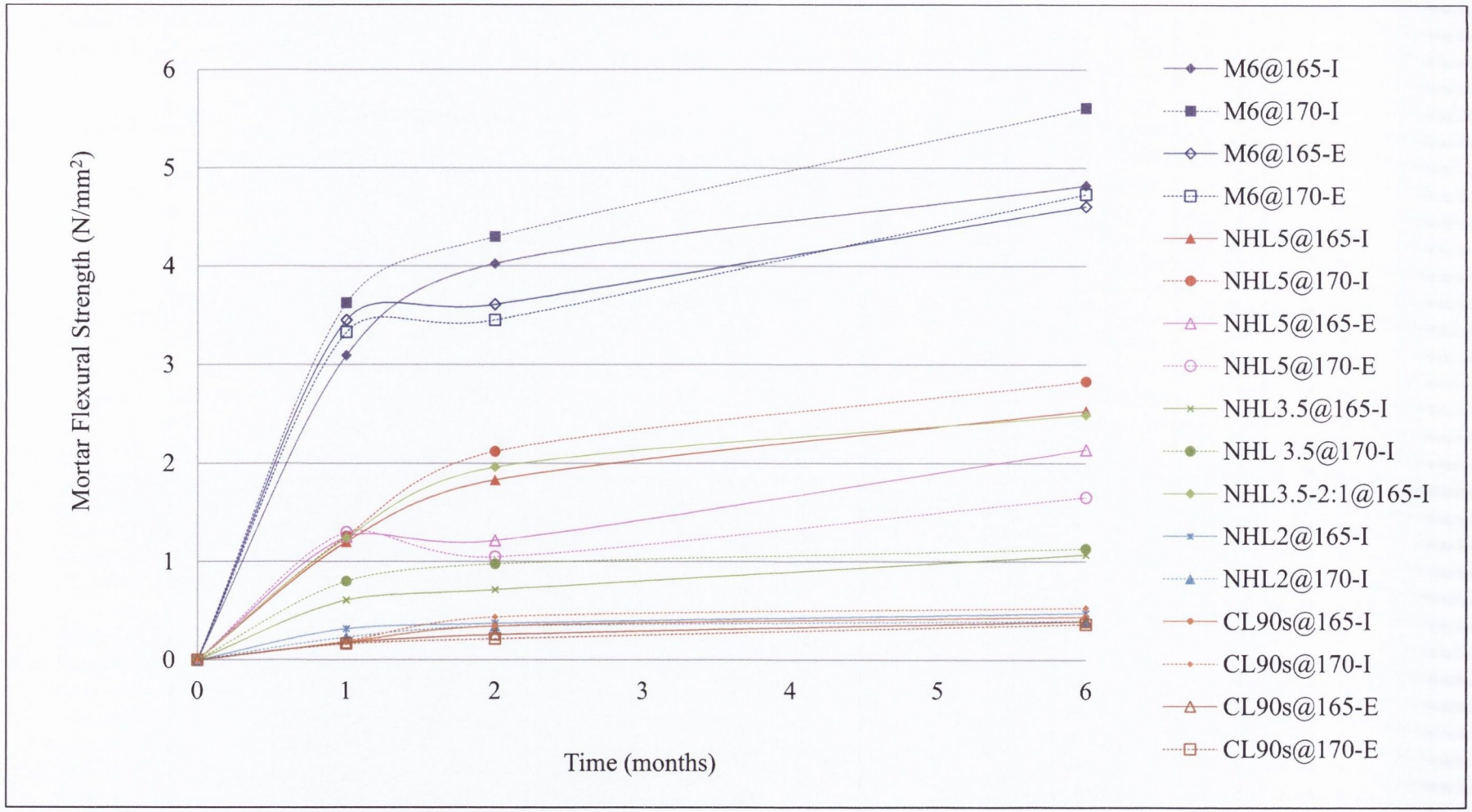

Figure D.1: Flexural strength development of mortar over time

Test No.	Series No.	Mortar ID	Specimen	Mix Ratio Cement/lime/ sand	Initial flow (mm)	Curing	Test age	Length (mm)	width (mm)	Applied load, F_f (kN)	Flexural strength, R_i (N/mm^2)	Mean R_f (N/mm^2)	COV (%)
1	1	M-M6-1m-F	A	0:1:3	165	lab	28 days	160	40	828.00	3.11	3.09	4.31%
2			B					160	40	786.67	2.95		
3			C					160	40	857.33	3.22		
4	2	M-M6-2m-F	A	0:1:3	165	lab	56 days	160	40	1122.67	4.21	4.03	9.73%
5			B					160	40	1146.67	4.30		
6			C					160	40	954.67	3.58		
7	3	M-M6-6m-F	A	0:1:3	165	lab	6 mts.	160	40	1162.67	4.36	4.82	9.76%
8			B					160	40	1280.00	4.80		
9			C					160	40	1413.33	5.30		
10	4	M-M6-6m-F	A	0:1:3	165	lab	365 days	160	40	1426.67	5.35	5.32	5.19%
11			B					160	40	1488.00	5.58		
12			C					160	40	1341.33	5.03		
13	5	M-M6-1m-F	A	0:1:3	170	lab	28 days	160	40	936.00	3.51	3.63	7.46%
14			B					160	40	917.33	3.44		
15			C					160	40	1050.67	3.94		
16	6	M-M6-2m-F	A	0:1:3	170	lab	56 days	160	40	869.33	3.26	4.30	23.73%
17			B					160	40	1157.33	4.34		
18			C					160	40	1413.33	5.30		
19	7	M-M6-6m-F	A	0:1:3	170	lab	6 mts.	160	40	1426.67	5.35	5.61	4.92%
20			B					160	40	1488.00	5.58		
21			C					160	40	1573.33	5.90		

Table D.1: M6 mortar flexural strength results and calculations

Test No.	Series No.	Mortar ID	Specimen	Mix Ratio Cement/lime/ sand	Initial flow (mm)	Curing	Test age	Length (mm)	width (mm)	Applied load, F_f (kN)	Flexural strength, R_i(N/mm^2)	Mean R_f (N/mm^2)	COV (%)
22	8	M-NHL5-1m-F	A	0:1:3	165	lab	28 days	160	40	333.33	1.25	1.20	10.24%
23			B					160	40	282.67	1.06		
24			C					160	40	344.00	1.29		
25	9	M-NHL5-2m-F	A	0:1:3	165	lab	56 days	160	40	466.67	1.75	1.83	6.65%
26			B					160	40	525.33	1.97		
27			C					160	40	472.00	1.77		
28	10	M-NHL5-6m-F	A	0:1:3	165	lab	6 mts.	160	40	621.33	2.33	2.53	17.96%
29			B					160	40	813.33	3.05		
30			C					160	40	589.33	2.21		
31	11	M-NHL5-12m-F	A	0:1:3	165	lab	365 days	160	40	709.33	2.66	2.88	8.87%
32			B					160	40	752.00	2.82		
33			C					160	40	842.67	3.16		
34	12	M-NHL5-1m-F	A	0:1:3	170	lab	28 days	160	40	317.33	1.19	1.26	7.65%
35			B					160	40	365.33	1.37		
36			C					160	40	325.33	1.22		
37	13	M-NHL5-2m-F	A	0:1:3	170	lab	56 days	160	40	501.33	1.88	2.12	16.07%
38			B					160	40	669.33	2.51		
39			C					160	40	525.33	1.97		
40	14	M-NHL5-6m-F	A	0:1:3	170	lab	6 mts.	160	40	856.00	3.21	2.83	12.06%
41			B					160	40	680.00	2.55		
42			C					160	40	728.00	2.73		

Table D.2: NHL 5 mortar flexural strength results and calculations

Test No.	Series No.	Mortar ID	Specimen	Mix Ratio Cement/lime/ sand	Initial flow (mm)	Curing	Test age	Length (mm)	width (mm)	Applied load, F_f (kN)	Flexural strength, R_i(N/mm^2)	Mean R_f (N/mm^2)	COV (%)
43	15	M-NHL3.5-1m-F	A	0:1:3	165	lab	28 days	160	40	144.00	0.54	0.61	12.38%
44			B					160	40	184.00	0.69		
45			C					160	40	160.00	0.60		
46	16	M-NHL3.5-2m-F	A	0:1:3	165	lab	56 days	160	40	208.00	0.78	0.71	9.24%
47			B					160	40	186.67	0.70		
48			C					160	40	173.33	0.65		
49	17	M-NHL3.5-6m-F	A	0:1:3	165	lab	6 mts.	160	40	384.00	1.44	1.07	36.06%
50			B					160	40	293.33	1.10		
51			C					160	40	178.67	0.67		
52	18	M-NHL3.5-12m-F	A	0:1:3	165	lab	365 days	160	40	365.33	1.37	1.26	8.36%
53			B					160	40	333.33	1.25		
54			C					160	40	309.33	1.16		
55	19	M-NHL3.5-1m-F	A	0:1:3	170	lab	28 days	160	40	218.67	0.82	0.80	6.61%
56			B					160	40	224.00	0.84		
57			C					160	40	197.33	0.74		
58	20	M-NHL3.5-2m-F	A	0:1:3	170	lab	56 days	160	40	272.00	1.02	0.98	5.40%
59			B					160	40	245.33	0.92		
60			C					160	40	266.67	1.00		
61	21	M-NHL3.5-6m-F	A	0:1:3	170	lab	6 mts.	160	40	344.00	1.29	1.13	15.66%
62			B					160	40	309.33	1.16		
63			C					160	40	250.67	0.94		

Table D.3: NHL 3.5 mortar flexural strength results and calculations

Test No.	Series No.	Mortar ID	Specimen	Mix Ratio Cement/lime/ sand	Initial flow (mm)	Curing	Test age	Length (mm)	width (mm)	Applied load, F_f (kN)	Flexural strength, R_i(N/mm^2)	Mean R_f (N/mm^2)	COV (%)
64	22	M-NHL2-1m-F	A	0:1:3	165	lab	28 days	160	40	93.33	0.35	0.32	11.27%
65			B					160	40	88.00	0.33		
66			C					160	40	74.67	0.28		
67	23	M-NHL2-2m-F	A	0:1:3	165	lab	56 days	160	40	106.67	0.40	0.37	7.15%
68			B					160	40	96.00	0.36		
69			C					160	40	93.33	0.35		
70	24	M-NHL2-6m-F	A	0:1:3	165	lab	6 mts.	160	40	136.00	0.51	0.48	5.51%
71			B					160	40	125.33	0.47		
72			C					160	40	122.67	0.46		
73	25	M-NHL2-12m-F	A	0:1:3	165	lab	365 days	160	40	149.33	0.56	0.57	3.04%
74			B					160	40	149.33	0.56		
75			C					160	40	157.33	0.59		
76	26	M-NHL3.5-1m-F	A	0:1:3	170	lab	28 days	160	40	58.67	0.22	0.23	8.68%
77			B					160	40	57.87	0.22		
78			C					160	40	67.47	0.25		
79	27	M-NHL2-2m-F	A	0:1:3	170	lab	56 days	160	40	74.67	0.28	0.34	15.31%
80			B					160	40	97.87	0.37		
81			C					160	40	99.47	0.37		
82	28	M-NHL2-6m-F	A	0:1:3	170	lab	6 mts.	160	40	114.67	0.43	0.40	15.21%
83			B					160	40	88.00	0.33		
84			C					160	40	117.33	0.44		

Table D.4: NHL 2 mortar flexural strength results and calculations

Test No.	Series No.	Mortar ID	Specimen	Mix Ratio Cement/lime/ sand	Initial flow (mm)	Curing	Test age	Length (mm)	width (mm)	Applied load, F_f (kN)	Flexural strength, R_f(N/mm^2)	Mean R_f (N/mm^2)	COV (%)
85	29	M-CL90-s-1m-F	A	0:1:3	165	lab	28 days	160	40	46.93	0.18	0.18	10.18%
86			B					160	40	43.73	0.16		
87			C					160	40	53.33	0.20		
88	30	M-CL90-s-2m-F	A	0:1:3	165	lab	56 days	160	40	89.60	0.34	0.34	1.79%
89			B					160	40	92.53	0.35		
90			C					160	40	89.87	0.34		
91	31	M-CL90-s-6m-F	A	0:1:3	165	lab	6 mts.	160	40	130.67	0.49	0.44	12.65%
92			B					160	40	120.00	0.45		
93			C					160	40	101.33	0.38		
94	32	M-CL90-s-12m-F	A	0:1:3	165	lab	365 days	160	40	136.00	0.51	0.52	3.33%
95			B					160	40	144.00	0.54		
96			C					160	40	136.00	0.51		
97	33	M-CL90-s-1m-F	A	0:1:3	170	lab	28 days	160	40	47.73	0.18	0.19	7.86%
98			B					160	40	49.07	0.18		
99			C					160	40	55.20	0.21		
100	34	M-CL90-s-2m-F	A	0:1:3	170	lab	56 days	160	40	113.33	0.43	0.44	7.12%
101			B					160	40	111.73	0.42		
102			C					160	40	126.93	0.48		
103	35	M-CL90-s-6m-F	A	0:1:3	170	lab	6 mts.	160	40	146.67	0.55	0.53	4.99%
104			B					160	40	144.00	0.54		
105			C					160	40	133.33	0.50		

Table D.5: CL90-s mortar flexural strength results and calculations

Test No.	Series No.	Mortar ID	Specimen	Mix Ratio Cement/lime/ sand	Initial flow (mm)	Curing	Test age	Length (mm)	width (mm)	Applied load, F_f (kN)	Flexural strength, R_i(N/mm^2)	Mean R_f (N/mm^2)	COV (%)
106	36	M-NHL3.5-1m-F	A	0:2:3	165	lab	28 days	160	40	333.33	1.25	1.24	2.13%
107			B					160	40	336.00	1.26		
108			C					160	40	322.67	1.21		
109	37	M-NHL3.5-2m-F	A	0:2:3	165	lab	56 days	160	40	546.67	2.05	1.96	4.36%
110			B					160	40	520.00	1.95		
111			C					160	40	501.33	1.88		
112	38	M-NHL3.5-6m-F	A	0:2:3	165	lab	6 months	160	40	662.13	2.48	2.49	2.16%
113			B					160	40	650.67	2.44		
114			C					160	40	679.20	2.55		

Table D.6: NHL 3.5 mortar flexural strength results and calculations, mix ratio (0:2:3)

Test No.	Series No.	Mortar ID	Specimen	Mix Ratio Cement/lime/ sand	Initial flow (mm)	Curing	Test age	Length (mm)	width (mm)	Applied load, F_f (kN)	Flexural strength, R_i(N/mm^2)	Mean R_f (N/mm^2)	COV (%)
115	39	M-M6-1m-F	A	0:1:3	165	external	28 days	160	40	904.00	3.39	3.45	2.77%
116			B					160	40	906.67	3.40		
117			C					160	40	949.33	3.56		
118	40	M-M6-2m-F	A	0:1:3	165	external	56 days	160	40	970.13	3.64	3.61	0.78%
119			B					160	40	962.67	3.61		
120			C					160	40	955.20	3.58		
121	41	M-M6-6m-F	A	0:1:3	165	external	6 mts.	160	40	1269.33	4.76	4.61	8.22%
122			B					160	40	1304.27	4.89		
123			C					160	40	1114.40	4.18		
124	42	M-M6-1m-F	A	0:1:3	170	external	28 days	160	40	877.33	3.29	3.33	1.83%
125			B					160	40	880.00	3.30		
126			C					160	40	906.67	3.40		
127	43	M-M6-2m-F	A	0:1:3	170	external	56 days	160	40	933.33	3.50	3.45	3.83%
128			B					160	40	880.00	3.30		
129			C					160	40	946.67	3.55		
130	44	M-M6-6m-F	A	0:1:3	170	external	6 mts.	160	40	1304.27	4.89	4.73	5.04%
131			B					160	40	1291.47	4.84		
131			C					160	40	1188.27	4.46		

Table D.7: M6 mortar flexural strength results and calculations (outdoor curing)

Test No.	Series No.	Mortar ID	Specimen	Mix Ratio Cement/lime/ sand	Initial flow (mm)	Curing	Test age	Length (mm)	width (mm)	Applied load, F_f (kN)	Flexural strength, R_i(N/mm^2)	Mean R_f (N/mm^2)	COV (%)
132	45	M-NHL5-1m-F	A	0:1:3	165	external	28 days	160	40	332.80	1.25	1.25	3.28%
133			B					160	40	322.67	1.21		
134			C					160	40	344.53	1.29		
135	46	M-NHL5-2m-F	A	0:1:3	165	external	56 days	160	40	314.13	1.18	1.21	5.09%
136			B					160	40	312.27	1.17		
137			C					160	40	341.60	1.28		
138	47	M-NHL5-6m-F	A	0:1:3	165	external	6 mts.	160	40	539.47	2.02	2.14	5.35%
139			B					160	40	600.53	2.25		
140			C					160	40	572.00	2.15		
141	48	M-NHL5-1m-F	A	0:1:3	170	external	28 days	160	40	363.73	1.36	1.30	4.33%
142			B					160	40	335.47	1.26		
143			C					160	40	340.80	1.28		
144	49	M-NHL5-2m-F	A	0:1:3	170	external	56 days	160	40	326.40	1.22	1.05	14.90%
145			B					160	40	268.00	1.01		
146			C					160	40	245.60	0.92		
147	50	M-NHL5-6m-F	A	0:1:3	170	external	6 mts.	160	40	444.00	1.67	1.65	3.87%
148			B					160	40	421.33	1.58		
149			C					160	40	454.67	1.71		

Table D.8: NHL 5 mortar flexural strength results and calculations (outdoor curing)

Test No.	Series No.	Mortar ID	Specimen	Mix Ratio Cement/lime/ sand	Initial flow (mm)	Curing	Test age	Length (mm)	width (mm)	Applied load, F_f (kN)	Flexural strength, R_i(N/mm^2)	Mean R_f (N/mm^2)	COV (%)
150	51	M-CL90-s-1m-F	A	0:1:3	165	external	28 days	160	40	41.60	0.16	0.18	19.37%
151			B					160	40	43.73	0.16		
152			C					160	40	58.67	0.22		
153	52	M-CL90-s-2m-F	A	0:1:3	165	external	56 days	160	40	62.13	0.23	0.26	13.03%
154			B					160	40	66.40	0.25		
155			C					160	40	79.47	0.30		
156	53	M-CL90-s-6m-F	A	0:1:3	165	external	6 mts.	160	40	103.47	0.39	0.39	2.86%
157			B					160	40	107.20	0.40		
158			C					160	40	101.33	0.38		
159	54	M-CL90-s-1m-F	A	0:1:3	170	external	28 days	160	40	53.07	0.20	0.16	26.08%
160			B					160	40	44.00	0.17		
161			C					160	40	30.93	0.12		
162	55	M-CL90-s-2m-F	A	0:1:3	170	external	56 days	160	40	69.33	0.26	0.22	30.71%
163			B					160	40	68.80	0.26		
164			C					160	40	37.87	0.14		
165	56	M-CL90-s-6m-F	A	0:1:3	170	external	6 mts.	160	40	89.33	0.34	0.36	7.91%
166			B					160	40	94.40	0.35		
167			C					160	40	104.27	0.39		

Table D.9: CL90-s mortar flexural strength results and calculations (outdoor curing)

APPENDIX E

MASONRY COMPRESSIVE STRENGTH & ELASTIC MODULUS RESULTS AND CALCULATIONS

Test no	Masonry ID	Specimen	Unit Type	Cement/ lime/ sand ratio	Initial flow (mm)	Curing	Test age	Length (mm)	Width (mm)	Height (mm)	Cross sectional area (mm^2)	Applied load, F_c (kN)	Compressive strength, R_i (N/mm^2)	Mean compressive strength, R_c (N/mm^2)	COV (%)
1	B_NHL5_165_1m_C	A	Brick	0:1:3	165	lab	1	450	102.5	375	46125.00	265.680	5.76	**5.49**	**7.11%**
2		B						450	102.5	375	46125.00	269.831	5.85		
3		C						450	102.5	375	46125.00	244.924	5.31		
4		D						450	102.5	375	46125.00	231.548	5.02		
5	B_NHL5_165_2m_C	A	Brick	0:1:3	165	lab	2	450	102.5	375	46125.00	220.943	4.79	**6.32**	**14.29%**
6		B						450	102.5	375	46125.00	319.655	6.93		
7		C						450	102.5	375	46125.00	317.142	6.88		
8		D						450	102.5	375	46125.00	301.242	6.53		
9		E						450	102.5	375	46125.00	262.451	5.69		
10		F						450	102.5	375	46125.00	327.746	7.11		
11	B_NHL5_165_6m_C	A	Brick	0:1:3	165	lab	6	450	102.5	375	46125.00	397.076	8.61	**8.01**	**6.30%**
12		B						450	102.5	375	46125.00	376.638	8.17		
13		C						450	102.5	375	46125.00	363.460	7.88		
14		D						450	102.5	375	46125.00	341.560	7.41		
15	B_NHL5_170_1yr_C	A	Brick	0:1:3	165	lab	12	450	102.5	375	46125.00	405.111	8.78	**8.50**	**8.85%**
16		B						450	102.5	375	46125.00	418.538	9.07		
17		C						450	102.5	375	46125.00	352.856	7.65		
18	B_NHL5_170_1m_C	A	Brick	0:1:3	170	lab	1	450	102.5	375	46125.00	283.065	6.14	**5.69**	**7.90%**
19		B						450	102.5	375	46125.00	241.603	5.24		
20		C						450	102.5	375	46125.00	262.686	5.70		
21	B_NHL5_170_2m_C	A	Brick	0:1:3	170	lab	2	450	102.5	375	46125.00	314.752	6.82	**6.62**	**4.77%**
22		B						450	102.5	375	46125.00	313.018	6.79		
23		C						450	102.5	375	46125.00	288.683	6.26		
24	B_NHL5_170_6m_C	A	Brick	0:1:3	170	lab	6	450	102.5	375	46125.00	422.505	9.16	**8.48**	**19.02%**
25		B						450	102.5	375	46125.00	306.164	6.64		
26		C						450	102.5	375	46125.00	444.645	9.64		

Table E.1: NHL 5 masonry compressive strength and elastic modulus results and calculations

Masonry ID	Specimen	Min compressive strength	Compressive strength/1.2	Characteristic compressive strength f_k (N/mm^2)	Change in Stress Δδ N/mm^2	Change in Strain Δε	Elastic modulus, E_i (N/mm^2)	Mean elastic Modulus, E (N/mm^2)	COV (%)	Notes
B_NHL5_165_1m_C	A	5.02	4.57	**4.57**	1.92	0.0038	504.32	**607.52**	**12.07%**	
	B				1.95	0.0032	606.29			
	C				1.77	0.0027	663.56			
	D				1.67	0.0026	655.91			
B_NHL5_165_2m_C	A	4.79	5.27	**4.79**	1.60	0.0018	886.32	**993.12**	**11.37%**	
	B				2.31	0.0024	969.40			
	C				2.29	0.0025	930.75			
	D				2.18	0.0022	983.83			
	E				1.90	0.0016	1211.26			
	F				2.37	0.0024	977.16			
B_NHL5_165_6m_C	A	7.41	6.68	**6.68**	2.87	0.0022	1330.61	**1409.04**	**7.65%**	
	B				2.72	0.0017	1562.9			
	C				2.63	0.0019	1404.38			
	D				2.47	0.0018	1338.27			
B_NHL5_170_1yr_C	A	7.65	7.09	**7.09**	2.93	0.0019	1550.5	**1528.00**	**3.81%**	
	B				3.02	0.0021	1461.88			
	C				2.55	0.0016	1571.62			
B_NHL5_170_1m_C	A	5.24	4.74	**4.74**	2.05	0.0036	572.050	**670.00**	**15.56%**	
	B				1.75	0.0027	658.373			
	C				1.90	0.0024	779.577			
B_NHL5_170_2m_C	A	6.26	5.52	**5.52**	2.27	0.0022	1012.66	**1053.00**	**6.16%**	
	B				2.26	0.0020	1127.86			
	C				2.09	0.0020	1018.48			
B_NHL5_170_6m_C	A	6.64	7.07	**6.64**	3.05	0.0029	1061.33	**1440.00**	**23.93%**	
	B				2.21	0.0013	1734.99			
	C				3.21	0.0021	1523.68			

Table E.2: NHL 5 masonry compressive strength and elastic modulus results and calculations (continued)

Test no	Masonry ID	Specimen	Unit Type	PC/ lime/ sand ratio	Initial flow (mm)	Curing	Test age	Length (mm)	Width (mm)	Height (mm)	Cross sectional area (mm^2)	Applied load, F_c (kN)	Compressive strength, R_i (N/mm^2)	Mean compressive strength, R_c (N/mm^2)	COV (%)
27	B_NHL3.5_165_1m_C	A	Brick	0:1:3	165	lab	1	450	102.5	375	46125.00	238.005	5.16	**5.07**	**3.44%**
28		B						450	102.5	375	46125.00	242.156	5.25		
29		C						450	102.5	375	46125.00	223.706	4.85		
30		D						450	102.5	375	46125.00	231.548	5.02		
31	B_NHL3.5_165_2m_C	A	Brick	0:1:3	165	lab	2	450	102.5	375	46125.00	267.986	5.81	**5.89**	**1.97%**
32		B						450	102.5	375	46125.00	277.673	6.02		
33		C						450	102.5	375	46125.00	268.909	5.83		
34		D						450	102.5	375	46125.00				
35	B_NHL3.5_165_6m_C	A	Brick	0:1:3	165	lab	6	450	102.5	375	46125.00	404.793	8.78	**7.71**	**12.18%**
36		B						450	102.5	375	46125.00	340.375	7.38		
37		C						450	102.5	375	46125.00	322.354	6.99		
38	B_NHL3.5_165_1yr_C	A	Brick	0:1:3	165	lab	12	450	102.5	375	46125.00	414.064	8.98	**8.90**	**2.37%**
39		B						450	102.5	375	46125.00	399.443	8.66		
40		C						450	102.5	375	46125.00	417.893	9.06		
41	B_NHL3.5_170_1m_C	A	Brick	0:1:3	170	lab	1	450	102.5	375	46125.00	276.423	5.99	**5.52**	**7.83%**
42		B						450	102.5	375	46125.00	237.327	5.15		
43		C						450	102.5	375	46125.00	250.081	5.42		
44	B_NHL3.5_170_2m_C	A	Brick	0:1:3	170	lab	2	450	102.5	375	46125.00	314.111	6.81	**6.41**	**6.16%**
45		B						450	102.5	375	46125.00	277.673	6.02		
46		C						450	102.5	375	46125.00	295.200	6.40		
47	B_NHL3.5_170_6m_C	A	Brick	0:1:3	170	lab	6	450	102.5	375	46125.00	386.491	8.38	**8.46**	**1.27%**
48		B						450	102.5	375	46125.00	395.845	8.58		
49		C						450	102.5	375	46125.00	388.234	8.42		
41	B_NHL3.5_165_1m_C	A	Brick	0:1:2	170	lab	1	450	102.5	375	46125.00	269.504	5.84	**5.60**	**7.73%**
42		B						450	102.5	375	46125.00	235.238	5.10		
43		C						450	102.5	375	46125.00	270.159	5.86		
44	B_NHL3.5_165_2m_C	A	Brick	0:1:2	170	lab	2	450	102.5	375	46125.00	337.635	7.32	**7.10**	**3.17%**
45		B						450	102.5	375	46125.00	316.879	6.87		
46		C						450	102.5	375	46125.00	327.949	7.11		
47	B_NHL3.5_165_6m_C	A	Brick	0:1:2	170	lab	6	450	102.5	375	46125.00	390.181	8.46	**8.52**	**0.72%**
48		B						450	102.5	375	46125.00	395.845	8.58		
49		C						450	102.5	375	46125.00	392.930	8.52		

Table E.3: NHL 3.5 masonry compressive strength and elastic modulus results and calculations

Masonry ID	Specimen	Min compressive strength	Compressive strength/1.2	Characteristic compressive strength f_k (N/mm^2)	Change in Stress Δδ N/mm^2	Change in Strain Δε	Elastic modulus, E_i (N/mm^2)	Mean elastic Modulus, E (N/mm^2)	COV (%)	Notes
B_NHL3.5_165_1m_C	A	4.85	4.23	**4.23**	1.72	0.0038	454.76	**384.68**	**24.89%**	
	B				1.75	0.0040	436.11			
	C				1.62	0.0040	403.18			
	D				1.67	0.0068	244.67			
B_NHL3.5_165_2m_C	A	5.81	4.91	**4.91**	1.94	0.0033	580.43	**567.96**	**11.72%**	
	B				2.01	0.0032	627.40			
	C				1.94	0.0039	496.05			
	D				-	-	-			damaged
B_NHL3.5_165_6m_C	A	6.99	6.43	**6.43**	2.93	0.0026	1109.71	**841.96**	**31.61%**	
	B				2.46	0.0029	838.76			
	C				2.33	0.0040	577.41			
B_NHL3.5_165_1yr_C	A	8.66	7.42	**7.42**	2.99	0.0028	1069.25	**970.00**	**10.64%**	
	B				2.89	0.0030	977.5			
	C				3.02	0.0035	863.25			
B_NHL3.5_170_1m_C	A	5.15	4.60	**4.60**	2.00	0.0041	488.500	**462.70**	**23.96%**	
	B				1.72	0.0031	558.410			
	C				1.81	0.0053	341.190			
B_NHL3.5_170_2m_C	A	6.02	5.34	**5.34**	2.27	0.0031	738.52	**772.02**	**14.65%**	
	B				2.01	0.0030	679.44			
	C				2.13	0.0024	898.10			
B_NHL3.5_170_6m_C	A	8.38	7.05	**7.05**	2.79	0.0027	1050.92	**850.00**	**22.10%**	
	B				2.86	0.0042	678.65			
	C				2.81	0.0034	820.43			
B_NHL3.5_170_1m_C	A	5.10	4.67	**4.67**	1.95	0.0034	576.000	**509.52**	**15.86%**	
	B				1.70	0.0032	533.000			
	C				1.95	0.0047	419.560			
B_NHL3.5_170_2m_C	A	6.87	5.92	**5.92**	2.44	0.0038	638.52	**603.00**	**7.63%**	
	B				2.29	0.0037	619.44			
	C				2.37	0.0043	551.04			
B_NHL3.5_170_6m_C	A	8.46	7.10	**7.10**	2.82	0.0031	903.55	**947.96**	**6.87%**	
	B				2.86	0.0028	1022.76			
	C				2.84	0.0031	917.57			

Table E.4: NHL 3.5 masonry compressive strength and elastic modulus results and calculations (continued)

Test no	Masonry ID	Specimen	Unit Type	PC/ lime/ sand ratio	Initial flow (mm)	Curing	Test age	Length (mm)	Width (mm)	Height (mm)	Cross sectional area (mm^2)	Applied load, F_c (kN)	Compressive strength, R_i (N/mm^2)	Mean compressive strength, R_c (N/mm^2)	COV (%)
50	B_NHL2_165_1m_C	A	Brick	0:1:3	165	lab	28 days	450	102.5	375	46125.00	171.124	3.71	**3.90**	**3.53%**
51		B						450	102.5	375	46125.00	179.426	3.89		
52		C						450	102.5	375	46125.00	183.578	3.98		
53		D						450	102.5	375	46125.00	185.423	4.02		
54	B_NHL2_165_2m_C	A	Brick	0:1:3	165	lab	56 days	450	102.5	375	46125.00	177.120	3.84	**4.54**	**13.40%**
55		B						450	102.5	375	46125.00	223.245	4.84		
56		C						450	102.5	375	46125.00	227.858	4.94		
57	B_NHL2_165_6m_C	A	Brick	0:1:3	165	lab	6 mts.	450	102.5	375	46125.00	240.773	5.22	**4.80**	**8.44%**
58		B						450	102.5	375	46125.00	220.478	4.78		
59		C						450	102.5	375	46125.00	203.411	4.41		
60	B_NHL2_165_1yr_C	A	Brick	0:1:3	165	lab	365 days	450	102.5	375	46125.00	219.094	4.75	**4.81**	**8.18%**
61		B						450	102.5	375	46125.00	241.234	5.23		
62		C						450	102.5	375	46125.00	205.256	4.45		
63	B_NHL2_170_1m_C	A	Brick	0:1:3	170	lab	28 days	450	102.5	375	46125.00	232.931	5.05	**4.59**	**14.30%**
64		B						450	102.5	375	46125.00	225.551	4.89		
65		C						450	102.5	375	46125.00	177.166	3.84		
66	B_NHL2_170_2m_C	A	Brick	0:1:3	170	lab	56 days	450	102.5	375	46125.00	265.062	5.75	**5.63**	**4.20%**
67		B						450	102.5	375	46125.00	246.999	5.36		
68		C						450	102.5	375	46125.00	266.593	5.78		
69	B_NHL2_170_6m_C	A	Brick	0:1:3	170	lab	6 mts.	450	102.5	375	46125.00	282.285	6.12	**5.89**	**3.45%**
70		B						450	102.5	375	46125.00	265.219	5.75		
71		C						450	102.5	375	46125.00	267.064	5.79		

Table E.5: NHL 2 masonry compressive strength and elastic modulus results and calculations

Masonry ID	Specimen	Min compressive strength	Compressive strength/1.2	Characteristic compressive strength f_k (N/mm^2)	Change in Stress Δδ N/mm^2	Change in Strain Δε	Elastic modulus, E_i (N/mm^2)	Mean elastic Modulus, E (N/mm^2)	COV (%)	Notes
B_NHL2_165_1m_C	A	3.71	3.25	**3.25**	1.24	0.0036	340.88	**302.04**	**9.01%**	
	B				1.30	0.0043	300.62			
	C				1.33	0.0047	281.06			
	D				1.34	0.0047	285.6			
B_NHL2_165_2m_C	A	3.84	3.78	**3.78**	1.28	0.0042	305.76	**361.20**	**17.22%**	
	B				1.61	0.0038	428.48			
	C				1.65	0.0047	349.35			
B_NHL2_165_6m_C	A	4.41	4.00	**4.00**	1.74	0.0037	473.34	**504.00**	**15.43%**	
	B				1.59	0.0027	592.395			
	C				1.47	0.0033	446.25			
B_NHL2_165_1yr_C	A	4.45	4.01	**4.01**	1.58	0.0038	418.26	**541.50**	**24.43%**	
	B				1.74	0.0026	681.3			
	C				1.48	0.0028	524.94			
B_NHL2_170_1m_C	A	3.84	3.83	**3.83**	1.68	0.0055	305.070	**323.34**	**22.19%**	
	B				1.63	0.0041	402.450			
	C				1.28	0.0049	262.500			
B_NHL2_170_2m_C	A	5.36	4.69	**4.69**	1.92	0.0041	472.85	**430.11**	**9.41%**	
	B				1.79	0.0042	425.09			
	C				1.93	0.0049	392.40			
B_NHL2_170_6m_C	A	5.75	4.91	**4.91**	2.04	0.0051	403.47	**537.60**	**23.09%**	
	B				1.92	0.0030	648.45			
	C				1.93	0.0034	560.88			

Table E.6: NHL 2 masonry compressive strength and elastic modulus results and calculations (continued)

Test no	Masonry ID	Specimen	Unit Type	PC/ lime/ sand ratio	Initial flow (mm)	Curing	Test age	Length (mm)	Width (mm)	Height (mm)	Cross sectional area (mm^2)	Applied load, F_c (kN)	Compressive strength, R_i (N/mm^2)	Mean compressive strength, R_c (N/mm^2)	COV (%)
72	B_CL90s_165_1m_C	A	Brick	0:1:3	165	lab	28 days	450	102.5	375	46125.00	37.823	0.82	**0.89**	**15.02%**
73		B						450	102.5	375	46125.00	47.970	1.04		
74		C						450	102.5	375	46125.00	36.900	0.80		
75	B_CL90s_165_2m_C	A	Brick	0:1:3	165	lab	56 days	450	102.5	375	46125.00	81.401	1.76	**1.53**	**21.70%**
76		B						450	102.5	375	46125.00	53.053	1.15		
77		C						450	102.5	375	46125.00	77.259	1.68		
78	B_CL90s_165_6m_C	A	Brick	0:1:3	165	lab	6 mts.	450	102.5	375	46125.00	183.199	3.97	**3.94**	**11.24%**
79		B						450	102.5	375	46125.00	201.105	4.36		
80		C						450	102.5	375	46125.00	160.377	3.48		
81	B_CL90s_165_1yr_C	A	Brick	0:1:3	165	lab	365 days	450	102.5	375	46125.00	208.946	4.53	**4.30**	**6.19%**
82		B						450	102.5	375	46125.00	201.566	4.37		
83		C						450	102.5	375	46125.00	184.961	4.01		
84	B_CL90s_170_1m_C	A	Brick	0:1:3	170	lab	28 days	450	102.5	375	46125.00	42.896	0.93	**0.88**	**10.54%**
85		B						450	102.5	375	46125.00	35.516	0.77		
86		C						450	102.5	375	46125.00	42.896	0.93		
87	B_CL90s_170_2m_C	A	Brick	0:1:3	170	lab	56 days	450	102.5	375	46125.00	94.556	2.05	**2.62**	**21.03%**
88		B						450	102.5	375	46125.00	145.294	3.15		
89		C						450	102.5	375	46125.00	122.693	2.66		
90	B_CL90s_170_6m_C	A	Brick	0:1:3	170	lab	6 mts.	450	102.5	375	46125.00	157.748	3.42	**3.34**	**3.12%**
91		B						450	102.5	375	46125.00	155.441	3.37		
92		C						450	102.5	375	46125.00	148.523	3.22		

Table E.7: CL90-s masonry compressive strength and elastic modulus results and calculations

Masonry ID	Specimen	Min compressive strength	Compressive strength/1.2	Characteristic compressive strength f_k (N/mm^2)	Change in Stress Δδ N/mm^2	Change in Strain Δε	Elastic modulus, E_i (N/mm^2)	Mean elastic Modulus, E (N/mm^2)	COV (%)	Notes
B_CL90s_165_1m_C	A	0.80	0.74	**0.74**	0.27	0.0012	229.84	**196.00**	**18.32%**	
	B				0.35	0.0022	158.34			
	C				0.27	0.0013	199.82			
B_CL90s_165_2m_C	A	1.15	1.28	**1.15**	0.59	0.0021	276.97	**244.00**	**11.72%**	
	B				0.38	0.0017	229.20			
	C				0.56	0.0025	225.82			
B_CL90s_165_6m_C	A	3.48	3.28	**3.28**	1.32	0.0053	249.2	**295.86**	**31.46%**	
	B				1.45	0.0036	403.04			
	C				1.16	0.0049	235.34			
B_CL90s_165_1yr_C	A	4.01	3.59	**3.59**	1.51	0.0043	348.48	**317.49**	**9.08%**	
	B				1.46	0.0050	291.46			
	C				1.34	0.0043	312.52			
B_CL90s_170_1m_C	A	0.77	0.73	**0.73**	0.31	0.0016	190.80	**152.32**	**25.59%**	
	B				0.26	0.0023	112.85			
	C				0.31	0.0020	153.32			
B_CL90s_170_2m_C	A	2.05	2.18	**2.05**	0.68	0.0035	194.86	**180.46**	**7.05%**	
	B				1.05	0.0062	170.71			
	C				0.89	0.0050	175.80			
B_CL90s_170_6m_C	A	3.22	2.78	**2.78**	1.14	0.0031	366.8	**274.90**	**31.86%**	
	B				1.12	0.0042	265.54			
	C				1.07	0.0056	192.36			

Table E.8: CL90-s masonry compressive strength and elastic modulus results and calculations (continued)

Test no	Masonry ID	Specimen	Unit Type	PC/ lime/ sand ratio	Initial flow (mm)	Curing	Test age	Length (mm)	Width (mm)	Height (mm)	Cross sectional area (mm^2)	Applied load, F_c (kN)	Compressive strength, R_i (N/mm^2)	Mean compressive strength, R_c (N/mm^2)	COV (%)
93	B_M6_165_1m_C	A	Brick	1:½:4	165	lab	28 days	450	102.5	375	46125.00	337.515	7.32	**6.90**	**8.26%**
94		B						450	102.5	375	46125.00	329.503	7.14		
95		C						450	102.5	375	46125.00	288.457	6.25		
96	B_M6_165_2m_C	A	Brick	1:½:4	165	lab	56 days	450	102.5	375	46125.00	374.314	8.12	**7.72**	**4.55%**
97		B						450	102.5	375	46125.00	343.747	7.45		
98		C						450	102.5	375	46125.00	349.692	7.58		
99	B_M6_165_6m_C	A	Brick	1:½:4	165	lab	6 mts.	450	102.5	375	46125.00	503.810	10.92	**9.74**	**12.29%**
100		B						450	102.5	375	46125.00	393.377	8.53		
101		C						450	102.5	375	46125.00	451.103	9.78		
102	B_M6_170_1m_C	A	Brick	1:½:4	170	lab	28 days	450	102.5	375	46125.00	337.515	7.32	**6.90**	**8.26%**
103		B						450	102.5	375	46125.00	329.503	7.14		
104		C						450	102.5	375	46125.00	288.457	6.25		
105	B_M6_170_2m_C	A	Brick	1:½:4	170	lab	56 days	450	102.5	375	46125.00	254.610	5.52	**7.53**	**6.95%**
106		B						450	102.5	375	46125.00	434.959	9.43		
107		C						450	102.5	375	46125.00	352.395	7.64		
108	B_M6_170_6m_C	A	Brick	1:½:4	170	lab	6 mts.	450	102.5	375	46125.00	486.319	10.54	**10.63**	**1.00%**
109		B						450	102.5	375	46125.00	495.862	10.75		
110		C						450	102.5	375	46125.00	489.100	10.60		

Table E.9: M6 masonry compressive strength and elastic modulus results and calculations

Masonry ID	Specimen	Min compressive strength	Compressive strength/1.2	Characteristic compressive strength f_k (N/mm^2)	Change in Stress Δδ N/mm^2	Change in Strain Δε	Elastic modulus, E_i (N/mm^2)	Mean elastic Modulus, E (N/mm^2)	COV (%)	Notes
B_M6_165_1m_C	A	6.25	5.75	**5.75**	2.44	0.0016	1560.75	**1435.74**	**9.57%**	
	B				2.38	0.0016	1457.88			
	C				2.08	0.0016	1288.58			
B_M6_165_2m_C	A	7.45	6.43	**6.43**	2.71	0.0017	1638.17	**1634.13**	**5.73%**	
	B				2.48	0.0016	1538.58			
	C				2.53	0.0015	1725.63			
B_M6_165_6m_C	A	8.53	8.12	**8.12**	3.64	0.0014	2656.89	**2270.10**	**15.43%**	
	B				2.84	0.0013	2178.95			
	C				3.26	0.0017	1974.45			
B_M6_170_1m_C	A	6.25	5.75	**5.75**	2.44	0.0011	2237.52	**1605.00**	**35.68%**	
	B				2.38	0.0016	1455.92			
	C				2.08	0.0019	1121.55			
B_M6_170_2m_C	A	5.52	6.28	**5.52**	1.84	0.0008	2188.35	**2036.70**	**2.47%**	
	B				3.14	0.0017	1874.01			
	C				2.55	0.0012	2047.74			
B_M6_170_6m_C	A	10.54	8.86	**8.86**	3.51	0.0016	2251.64	**2441.40**	**15.21%**	
	B				3.58	0.0016	2203.35			
	C				3.53	0.0012	2869.2			

Table E.10: M6 masonry compressive strength and elastic modulus results and calculations (continued)

Test no	Masonry ID	Specimen	Unit Type	PC/ lime/ sand ratio	Initial flow (mm)	Curing	Test age	Length (mm)	Width (mm)	Height (mm)	Cross sectional area (mm^2)	Applied load, F_c (kN)	Compressive strength, R_i (N/mm^2)	Mean compressive strength, R_c (N/mm^2)	COV (%)
111	B_NHL5_165_1m_C	A	Brick	0:1:3	165	External	28 days	450	102.5	375	46125.00	225.791	4.90	**5.09**	**4.69%**
112		B						450	102.5	375	46125.00	246.981	5.35		
113		C						450	102.5	375	46125.00	231.206	5.01		
114	B_NHL5_165_2m_C	A	Brick	0:1:3	165	External	56 days	450	102.5	375	46125.00	238.397	5.17	**5.65**	**7.87%**
115		B						450	102.5	375	46125.00	278.936	6.05		
116		C						450	102.5	375	46125.00	263.978	5.72		
117	B_NHL5_165_6m_C	A	Brick	0:1:3	165	External	6 mts.	450	102.5	375	46125.00	364.710	7.91	**7.59**	**9.79%**
118		B						450	102.5	375	46125.00	374.784	8.13		
119		C						450	102.5	375	46125.00	311.016	6.74		
120	B_NHL5_170_1m_C	A	Brick	0:1:3	170	External	28 days	450	102.5	375	46125.00	232.023	5.03	**4.81**	**5.28%**
121		B						450	102.5	375	46125.00	224.177	4.86		
122		C						450	102.5	375	46125.00	209.002	4.53		
123	B_NHL5_170_2m_C	A	Brick	0:1:3	170	External	56 days	450	102.5	375	46125.00	261.077	5.66	**5.63**	**4.53%**
124		B						450	102.5	375	46125.00	246.981	5.35		
125		C						450	102.5	375	46125.00	270.316	5.86		
126	B_NHL5_170_6m_C	A	Brick	0:1:3	170	External	6 mts.	450	102.5	375	46125.00	356.334	7.73	**7.82**	**4.34%**
127		B						450	102.5	375	46125.00	347.773	7.54		
128		C						450	102.5	375	46125.00	378.151	8.20		

Table E.11: NHL 5 masonry compressive strength and elastic modulus results and calculations, outdoor curing

Masonry ID	Specimen	Min compressive strength	Compressive strength/1.2	Characteristic compressive strength f_k (N/mm^2)	Change in Stress Δδ N/mm^2	Change in Strain Δε	Elastic modulus, E_i (N/mm^2)	Mean elastic Modulus, E (N/mm^2)	COV (%)	Notes
B_NHL5_165_1m_C	A	4.90	4.24	**4.24**	1.63	0.0023	707.22	**605.28**	**14.65%**	
	B				1.78	0.0032	562.50			
	C				1.67	0.0031	546.12			
B_NHL5_165_2m_C	A	5.17	4.71	**4.71**	1.72	0.0016	1073.35	**978.68**	**8.44%**	
	B				2.02	0.0022	921.55			
	C				1.91	0.0020	941.14			
B_NHL5_165_6m_C	A	6.74	6.33	**6.33**	2.64	0.0019	1365.74	**1368.00**	**3.14%**	
	B				2.71	0.0020	1326.23			
	C				2.25	0.0016	1412.03			
B_NHL5_170_1m_C	A	4.53	4.01	**4.01**	1.68	0.0031	540.960	**577.42**	**6.07%**	
	B				1.62	0.0027	610.890			
	C				1.51	0.0026	580.410			
B_NHL5_170_2m_C	A	5.35	4.69	**4.69**	1.89	0.0020	934.52	**845.06**	**12.84%**	
	B				1.78	0.0020	876.29			
	C				1.95	0.0027	724.37			
B_NHL5_170_6m_C	A	7.54	6.52	**6.52**	2.58	0.0016	1568.6	**1362.86**	**13.29%**	
	B				2.51	0.0020	1227.33			
	C				2.73	0.0021	1292.65			

Table E.12: NHL 5 masonry compressive strength and elastic modulus results and calculations, outdoor curing (continued)

Test no	Masonry ID	Specimen	Unit Type	PC/ lime/ sand ratio	Initial flow (mm)	Curing	Test age	Length (mm)	Width (mm)	Height (mm)	Cross sectional area (mm^2)	Applied load, F_c (kN)	Compressive strength, R_i (N/mm^2)	Mean compressive strength, R_c (N/mm^2)	COV (%)
129	B_M6_165_1m_C	A	Brick	1:½:4	165	External	28 days	450	102.5	375	46125.00	331.925	7.20	**6.90**	**13.26%**
130		B						450	102.5	375	46125.00	352.224	7.64		
131		C						450	102.5	375	46125.00	271.109	5.88		
132	B_M6_165_2m_C	A	Brick	1:½:4	165	External	56 days	450	102.5	375	46125.00	355.149	7.70	**7.66**	**4.69%**
133		B						450	102.5	375	46125.00	335.642	7.28		
134		C						450	102.5	375	46125.00	368.571	7.99		
135	B_M6_165_6m_C	A	Brick	1:½:4	165	External	6 mts.	450	102.5	375	46125.00	-	-	**8.64**	**7.72%**
136		B						450	102.5	375	46125.00	420.323	9.11		
137		C						450	102.5	375	46125.00	376.827	8.17		
138	B_M6_170_1m_C	A	Brick	1:½:4	170	External	28 days	450	102.5	375	46125.00	291.685	6.32	**6.20**	**2.91%**
139		B						450	102.5	375	46125.00	-	-		
140		C						450	102.5	375	46125.00	279.919	6.07		
141	B_M6_170_2m_C	A	Brick	1:½:4	170	External	56 days	450	102.5	375	46125.00	434.954	9.43	**7.84**	**18.40%**
142		B						450	102.5	375	46125.00	344.766	7.47		
143		C						450	102.5	375	46125.00	305.149	6.62		
144	B_M6_170_6m_C	A	Brick	1:½:4	170	External	6 mts.	450	102.5	375	46125.00	376.827	8.17	**8.30**	**1.61%**
145		B						450	102.5	375	46125.00	389.189	8.44		
146		C						450	102.5	375	46125.00	382.838	8.30		

Table E.13: M6 masonry compressive strength and elastic modulus results and calculations, outdoor curing

Masonry ID	Specimen	Min compressive strength	Compressive strength/1.2	Characteristic compressive strength f_k (N/mm^2)	Change in Stress Δδ N/mm^2	Change in Strain Δε	Elastic modulus, E_i (N/mm^2)	Mean elastic Modulus, E (N/mm^2)	COV (%)	Notes
B_M6_165_1m_C	A	5.88	5.75	**5.75**	2.40	0.0015	1570.29	**1395.00**	**11.06%**	
	B				2.55	0.0019	1335.24			
	C				1.96	0.0015	1279.47			
B_M6_165_2m_C	A	7.28	6.38	**6.38**	2.57	0.0017	1534.59	**1565.22**	**2.66%**	
	B				2.43	0.0015	1612.63			
	C				2.66	0.0017	1548.45			
B_M6_165_6m_C	A	8.17	7.20	**7.20**	-	-	-	**1937.19**	**2.96%**	damaged
	B				3.04	0.0015	1977.72			
	C				2.72	0.0014	1896.66			
B_M6_170_1m_C	A	6.07	5.16	**5.16**	2.11	0.0015	1401.900	**1373.58**	**2.92%**	
	B				-	-	-			damaged
	C				2.02	0.0015	1345.260			
B_M6_170_2m_C	A	6.62	6.53	**6.53**	3.14	0.0017	1874.97	**1788.00**	**4.22%**	
	B				2.49	0.0014	1740.02			
	C				2.21	0.0013	1749.00			
B_M6_170_6m_C	A	8.17	6.92	**6.92**	2.72	0.0015	1860.03	**2082.00**	**9.53%**	
	B				2.81	0.0013	2110.8			
	C				2.77	0.0012	2275.17			

Table E.14: M6 masonry compressive strength and elastic modulus results and calculations, outdoor curing (continued)

Test no	Masonry ID	Specimen	Unit Type	PC/ lime/ sand ratio	Initial flow (mm)	Curing	Test age	Length (mm)	Width (mm)	Height (mm)	Cross sectional area (mm^2)	Applied load, F_c (kN)	Compressive strength, R_i (N/mm^2)	Mean compressive strength, R_c (N/mm^2)	COV (%)
147	B_CL90s_165_1m_C	A	Brick	0:1:3	165	External	28 days	450	102.5	375	46125.00	90.391	1.96	**2.03**	**18.90%**
148		B						450	102.5	375	46125.00	77.753	1.69		
149		C						450	102.5	375	46125.00	112.702	2.44		
150	B_CL90s_165_2m_C	A	Brick	0:1:3	165	External	56 days	450	102.5	375	46125.00	131.848	2.86	**2.63**	**7.54%**
151		B						450	102.5	375	46125.00	117.812	2.55		
152		C						450	102.5	375	46125.00	114.644	2.49		
153	B_CL90s_165_6m_C	A	Brick	0:1:3	165	External	6 mts.	450	102.5	375	46125.00	143.555	3.11	**2.99**	**3.52%**
154		B						450	102.5	375	46125.00	134.274	2.91		
155		C						450	102.5	375	46125.00	136.442	2.96		
156	B_CL90s_170_1m_C	A	Brick	0:1:3	170	External	28 days	450	102.5	375	46125.00	92.435	2.00	**2.10**	**11.58%**
157		B						450	102.5	375	46125.00	109.538	2.37		
158		C						450	102.5	375	46125.00	88.431	1.92		
159	B_CL90s_170_2m_C	A	Brick	0:1:3	170	External	56 days	450	102.5	375	46125.00	121.590	2.64	**2.42**	**8.69%**
160		B						450	102.5	375	46125.00	111.433	2.42		
161		C						450	102.5	375	46125.00	102.181	2.22		
162	B_CL90s_170_6m_C	A	Brick	0:1:3	170	External	6 mts.	450	102.5	375	46125.00	128.947	2.80	**2.76**	**5.03%**
163		B						450	102.5	375	46125.00	132.826	2.88		
164		C						450	102.5	375	46125.00	120.322	2.61		

Table E.15: CL90-s masonry compressive strength and elastic modulus results and calculations, outdoor curing

Masonry ID	Specimen	Min compressive strength	Compressive strength/1.2	Characteristic compressive strength f_k (N/mm^2)	Change in Stress Δδ N/mm^2	Change in Strain Δε	Elastic modulus, E_i (N/mm^2)	Mean elastic Modulus, E (N/mm^2)	COV (%)	Notes
B_CL90s_165_1m_C	A	1.69	1.69	**1.69**	0.65	0.0053	123.69	**126.20**	**9.40%**	
	B				0.56	0.0049	115.80			
	C				0.81	0.0059	139.12			
B_CL90s_165_2m_C	A	2.49	2.19	**2.19**	0.95	0.0053	178.59	**228.21**	**19.25%**	
	B				0.85	0.0032	262.14			
	C				0.83	0.0034	243.92			
B_CL90s_165_6m_C	A	2.91	2.49	**2.49**	1.04	0.0050	206.79	**199.69**	**6.73%**	
	B				0.97	0.0047	208.08			
	C				0.99	0.0054	184.19			
B_CL90s_170_1m_C	A	1.92	1.75	**1.75**	0.67	0.0060	112.02	**167.47**	**37.58%**	
	B				0.79	0.0034	235.88			
	C				0.64	0.0041	154.52			
B_CL90s_170_2m_C	A	2.22	2.02	**2.02**	0.88	0.0062	142.05	**234.85**	**39.31%**	
	B				0.81	0.0034	235.82			
	C				0.74	0.0023	326.70			
B_CL90s_170_6m_C	A	2.61	2.30	**2.30**	0.93	0.0043	215.91	**294.40**	**27.16%**	
	B				0.96	0.0033	291.54			
	C				0.87	0.0023	375.77			

Table E.16: CL90-s masonry compressive strength and elastic modulus results and calculations, outdoor curing (continued)

Test no	Masonry ID	Specimen	Unit Type	PC/ lime/ sand ratio	Initial flow (mm)	Curing	Test age	Length (mm)	Width (mm)	Height (mm)	Cross sectional area (mm^2)	Applied load, F_c (kN)	Compressive strength, R_i (N/mm^2)	Mean compressive strength, R_c (N/mm^2)	COV (%)
165	L_bk_NHL2_165_1m_C	A	Broken Limestone	0:1:3	165	lab	28 days	100	100	352	10000.00	180.090	18.01	**18.59**	**3.11%**
166		B						100	100	350	10000.00	191.650	19.17		
167		C						100	100	352	10000.00	185.960	18.60		
168	L_bk_NHL2_165_2m_C	A	Broken Limestone	0:1:3	165	lab	56 days	100	100	352	10000.00	200.140	20.01	**21.88**	**8.93%**
169		B						100	100	352	10000.00	217.210	21.72		
170		C						100	100	351	10000.00	239.111	23.91		
171	L_bk_NHL2_165_6m_C	A	Broken Limestone	0:1:3	165	lab	6 mts.	100	100	353	10000.00	287.620	28.76	**24.55**	**17.16%**
172		B						100	100	354	10000.00	203.350	20.34		
173		C						100	100	352	10000.00	245.500	24.55		
174	L_bk_NHL2_170_1m_C	A	Broken Limestone	0:1:3	170	lab	28 days	100	100	352	10000.00	196.950	19.70	**23.96**	**15.44%**
175		B						100	100	352	10000.00	259.250	25.93		
176		C						100	100	353	10000.00	262.680	26.27		
177	L_bk_NHL2_170_2m_C	A	Broken Limestone	0:1:3	170	lab	56 days	100	100	354	10000.00	265.580	26.56	**26.95**	**1.55%**
178		B						100	100	352	10000.00	269.000	26.90		
179		C						100	100	352	10000.00	273.920	27.39		
180	L_bk_NHL2_170_6m_C	A	Broken Limestone	0:1:3	170	lab	6 mts.	100	100	353	10000.00	274.020	27.40	**28.09**	**2.44%**
181		B						100	100	250	10000.00	287.720	28.77		
182		C						100	100	352	10000.00	280.900	28.09		

Table E.17: NHL 2-broken limestone masonry compressive strength and elastic modulus results and calculations

Masonry ID	Specimen	Min compressive strength	Compressive strength/1.2	Characteristic compressive strength f_k (N/mm^2)	Change in Stress Δδ N/mm^2	Change in Strain Δε	Elastic modulus, E_i (N/mm^2)	Mean elastic Modulus, E (N/mm^2)	COV (%)	Notes
L_bk_NHL2_165_1m_C	A	18.01	15.49	**15.49**	6.00	0.0062	970.52	**868.58**	**28.19%**	
	B				6.39	0.0061	1046.00			
	C				6.20	0.0105	589.23			
L_bk_NHL2_165_2m_C	A	20.01	18.24	**18.24**	6.67	0.0079	844.84	**957.59**	**10.85%**	
	B				7.24	0.0074	978.54			
	C				7.97	0.0076	1049.40			
L_bk_NHL2_165_6m_C	A	20.34	20.46	**20.34**	9.59	0.0085	1125.43	**1008.60**	**11.14%**	
	B				6.78	0.0075	901.36			
	C				8.18	0.0082	999.01			
L_bk_NHL2_170_1m_C	A	19.70	19.97	**19.70**	6.57	0.0065	1006.02	**1068.80**	**10.10%**	
	B				8.64	0.0086	1006.94			
	C				8.76	0.0073	1193.44			
L_bk_NHL2_170_2m_C	A	26.56	22.46	**22.46**	8.85	0.0081	1096.82	**1064.60**	**22.43%**	
	B				8.97	0.0111	811.32			
	C				9.13	0.0071	1285.66			
L_bk_NHL2_170_6m_C	A	27.40	23.41	**23.41**	9.13	0.0076	1194.57	**1327.00**	**8.65%**	
	B				9.59	0.0069	1387.51			
	C				9.36	0.0067	1398.92			

Table E.18: NHL 2-broken limestone masonry compressive strength and elastic modulus results and calculations (continued)

Test no	Masonry ID	Specimen	Unit Type	PC/ lime/ sand ratio	Initial flow (mm)	Curing	Test age	Length (mm)	Width (mm)	Height (mm)	Cross sectional area (mm^2)	Applied load, F_c (kN)	Compressive strength, R_i (N/mm^2)	Mean compressive strength, R_c (N/mm^2)	COV (%)
183	L_bk_CL90s_165_1m_C	A	Broken Limestone	0:1:3	165	lab	28 days	100	100	352	10000.00	157.620	15.76	**15.58**	**11.78%**
184		B						100	100	353	10000.00	136.570	13.66		
185		C						100	100	352	10000.00	173.130	17.31		
186	L_bk_CL90s_165_2m_C	A	Broken Limestone	0:1:3	165	lab	56 days	100	100	350	10000.00	198.040	19.80	**20.68**	**7.09%**
187		B						100	100	353	10000.00	223.760	22.38		
188		C						100	100	352	10000.00	198.680	19.87		
189	L_bk_CL90s_165_6m_C	A	Broken Limestone	0:1:3	165	lab	6 mts.	100	100	351	10000.00	244.170	24.42	**25.26**	**3.10%**
190		B						100	100	353	10000.00	259.650	25.97		
191		C						100	100	351	10000.00	253.920	25.39		
192	L_bk_CL90s_170_1m_C	A	Broken Limestone	0:1:3	170	lab	28 days	100	100	354	10000.00	105.450	10.55	**10.67**	**37.23%**
193		B						100	100	352	10000.00	67.670	6.77		
194		C						100	100	351	10000.00	147.120	14.71		
195	L_bk_CL90s_170_2m_C	A	Broken Limestone	0:1:3	170	lab	56 days	100	100	350	10000.00	186.500	18.65	**19.13**	**3.58%**
196		B						100	100	354	10000.00	196.190	19.62		
197		C						100	100	353	10000.00	-	-		
198	L_bk_CL90s_170_6m_C	A	Broken Limestone	0:1:3	170	lab	6 mts.	100	100	353	10000.00	223.830	22.38	**23.43**	**8.28%**
199		B						100	100	352	10000.00	256.720	25.67		
200		C						100	100	352	10000.00	222.470	22.25		

Table E.19: CL90-s-broken limestone masonry compressive strength and elastic modulus results and calculations

Masonry ID	Specimen	Min compressive strength	Compressive strength/1.2	Characteristic compressive strength f_k (N/mm^2)	Change in Stress Δδ N/mm^2	Change in Strain Δε	Elastic modulus, E_i (N/mm^2)	Mean elastic Modulus, E (N/mm^2)	COV (%)	Notes
L_bk_CL90s_165_1m_C	A	13.66	12.98	**12.98**	5.25	0.0057	919.08	**877.58**	**24.04%**	
	B				4.55	0.0070	648.98			
	C				5.77	0.0054	1064.68			
L_bk_CL90s_165_2m_C	A	19.80	17.24	**17.24**	6.60	0.0082	809.49	**894.34**	**10.98%**	
	B				7.46	0.0074	1001.84			
	C				6.62	0.0076	871.68			
L_bk_CL90s_165_6m_C	A	24.42	21.05	**21.05**	8.14	0.0087	936.59	**976.99**	**9.32%**	
	B				8.66	0.0080	1081.24			
	C				8.46	0.0093	913.14			
L_bk_CL90s_170_1m_C	A	6.77	8.90	**6.77**	3.52	0.0063	561.65	**602.80**	**46.56%**	
	B				2.26	0.0065	345.01			
	C				4.90	0.0054	901.74			
L_bk_CL90s_170_2m_C	A	18.65	15.95	**15.95**	6.22	0.0080	778.86	**807.03**	**4.94%**	
	B				6.54	0.0078	835.21			
	C				-	-	-			damaged
L_bk_CL90s_170_6m_C	A	22.25	19.53	**19.53**	7.46	0.0107	696.80	**798.30**	**11.24%**	
	B				8.56	0.0099	867.04			
	C				7.42	0.0089	831.06			

Table E.20: CL90-s-broken limestone masonry compressive strength and elastic modulus results and calculations (continued)

Test no	Masonry ID	Specimen	Unit Type	PC/ lime/ sand ratio	Initial flow (mm)	Curing	Test age	Length (mm)	Width (mm)	Height (mm)	Cross sectional area (mm^2)	Applied load, F_c (kN)	Compressive strength, R_i (N/mm^2)	Mean compressive strength, R_c (N/mm^2)	COV (%)
183	L_cut_NHL2_165_1m_C	A	Cut Limestone	0:1:3	165	lab	28 days	215	102.5	385	22037.50	384.554	17.45	**19.04**	**15.88%**
184		B						215	102.5	385	22037.50	496.505	22.53		
185		C						215	102.5	385	22037.50	377.943	17.15		
186	L_cut_NHL2_165_2m_C	A	Cut Limestone	0:1:3	165	lab	56 days	215	102.5	385	22037.50	615.391	27.92	**28.11**	**6.02%**
187		B						215	102.5	385	22037.50	658.763	29.89		
188		C						215	102.5	385	22037.50	584.523	26.52		
189	L_cut_NHL2_165_6m_C	A	Cut Limestone	0:1:3	165	lab	6 mts.	215	102.5	385	22037.50	681.126	30.91	**30.54**	**2.37%**
190		B						215	102.5	385	22037.50	654.571	29.70		
191		C						215	102.5	385	22037.50	683.079	31.00		
192	L_cut_NHL2_170_1m_C	A	Cut Limestone	0:1:3	170	lab	28 days	215	102.5	385	22037.50	523.391	23.75	**20.43**	**14.33%**
193		B						215	102.5	385	22037.50	425.765	19.32		
194		C						215	102.5	385	22037.50	401.523	18.22		
195	L_cut_NHL2_170_2m_C	A	Cut Limestone	0:1:3	170	lab	56 days	215	102.5	385	22037.50	583.284	26.47	**29.60**	**9.18%**
196		B						215	102.5	385	22037.50	690.538	31.33		
197		C						215	102.5	385	22037.50	683.030	30.99		
198	L_cut_NHL2_170_6m_C	A	Cut Limestone	0:1:3	170	lab	6 mts.	215	102.5	385	22037.50	712.902	32.35	**32.38**	**0.39%**
199		B						215	102.5	385	22037.50	711.106	32.27		
200		C						215	102.5	385	22037.50	716.514	32.51		

Table E.21: NHL 2-cut limestone masonry compressive strength and elastic modulus results and calculations

Masonry ID	Specimen	Min compressive strength	Compressive strength/1.2	Characteristic compressive strength f_k (N/mm^2)	Change in Stress Δδ N/mm^2	Change in Strain Δε	Elastic modulus, E_i (N/mm^2)	Mean elastic Modulus, E (N/mm^2)	COV (%)	Notes
L_cut_NHL2_165_1m_C	A	17.15	15.87	**15.87**	5.82	0.0055	1064.22	**1157.80**	**8.77%**	
	B				7.51	0.0059	1265.69			
	C				5.72	0.0050	1143.49			
L_cut_NHL2_165_2m_C	A	26.52	23.43	**23.43**	9.31	0.0079	1172.99	**1260.59**	**6.78%**	
	B				9.96	0.0074	1343.71			
	C				8.84	0.0070	1265.06			
L_cut_NHL2_165_6m_C	A	29.70	25.45	**25.45**	10.30	0.0069	1486.55	**1465.87**	**3.82%**	
	B				9.90	0.0071	1402.48			
	C				10.33	0.0068	1508.58			
L_cut_NHL2_170_1m_C	A	18.22	17.03	**17.03**	7.92	0.0055	1452.12	**1368.68**	**11.73%**	
	B				6.44	0.0044	1470.39			
	C				6.07	0.0051	1183.53			
L_cut_NHL2_170_2m_C	A	26.47	24.67	**24.67**	8.82	0.0061	1435.58	**1712.00**	**13.99%**	
	B				10.44	0.0057	1845.64			
	C				10.33	0.0056	1854.79			
L_cut_NHL2_170_6m_C	A	32.27	26.98	**26.98**	10.78	0.0066	1643.35	**1636.58**	**2.27%**	
	B				10.76	0.0067	1596.48			
	C				10.84	0.0065	1669.91			

Table E.22: NHL 2-cut limestone masonry compressive strength and elastic modulus results and calculations (continued)

Test no	Masonry ID	Specimen	Unit Type	PC/ lime/ sand ratio	Initial flow (mm)	Curing	Test age	Length (mm)	Width (mm)	Height (mm)	Cross sectional area (mm^2)	Applied load, F_c (kN)	Compressive strength, R_i (N/mm^2)	Mean compressive strength, R_c (N/mm^2)	COV (%)
183	L_cut_CL90s_165_1m_C	A	Cut Limestone	0:1:3	165	lab	28 days	215	102.5	385	22037.50	311.170	14.12	**18.20**	**25.49%**
184		B						215	102.5	385	22037.50	379.927	17.24		
185		C						215	102.5	385	22037.50	512.372	23.25		
186	L_cut_CL90s_165_2m_C	A	Cut Limestone	0:1:3	165	lab	56 days	215	102.5	385	22037.50	523.818	23.77	**23.43**	**1.44%**
187		B						215	102.5	385	22037.50	508.980	23.10		
188		C						215	102.5	385	22037.50	516.339	23.43		
189	L_cut_CL90s_165_6m_C	A	Cut Limestone	0:1:3	165	lab	6 mts.	215	102.5	385	22037.50	560.235	25.42	**26.15**	**2.40%**
190		B						215	102.5	385	22037.50	583.773	26.49		
191		C						215	102.5	385	22037.50	584.611	26.53		
192	L_cut_CL90s_170_1m_C	A	Cut Limestone	0:1:3	170	lab	28 days	215	102.5	385	22037.50	477.368	21.66	**20.83**	**3.46%**
193		B						215	102.5	385	22037.50	450.283	20.43		
194		C						215	102.5	385	22037.50	449.517	20.40		
195	L_cut_CL90s_170_2m_C	A	Cut Limestone	0:1:3	170	lab	56 days	215	102.5	385	22037.50	501.917	22.78	**22.20**	**3.94%**
196		B						215	102.5	385	22037.50	467.058	21.19		
197		C						215	102.5	385	22037.50	498.687	22.63		
198	L_cut_CL90s_170_6m_C	A	Cut Limestone	0:1:3	170	lab	6 mts.	215	102.5	385	22037.50	521.872	23.68	**25.18**	**5.38%**
199		B						215	102.5	385	22037.50	562.609	25.53		
200		C						215	102.5	385	22037.50	580.034	26.32		

Table E.23: CL90-s-cut limestone masonry compressive strength and elastic modulus results and calculations

Masonry ID	Specimen	Min compressive strength	Compressive strength/1.2	Characteristic compressive strength f_k (N/mm^2)	Change in Stress Δδ N/mm^2	Change in Strain Δε	Elastic modulus, E_i (N/mm^2)	Mean elastic Modulus, E (N/mm^2)	COV (%)	Notes
L_cut_CL90s_165_1m_C	A	14.12	15.17	**14.12**	4.71	0.0080	590.82	**582.65**	**14.95%**	
	B				5.75	0.0117	491.74			
	C				7.75	0.0116	665.38			
L_cut_CL90s_165_2m_C	A	23.10	19.53	**19.53**	7.92	0.0112	705.65	**618.79**	**31.26%**	
	B				7.70	0.0194	397.12			
	C				7.81	0.0104	753.60			
L_cut_CL90s_165_6m_C	A	25.42	21.79	**21.79**	8.47	0.0139	609.24	**756.60**	**18.23%**	
	B				8.83	0.0113	778.02			
	C				8.84	0.0100	882.54			
L_cut_CL90s_170_1m_C	A	20.40	17.36	**17.36**	7.22	0.0109	664.58	**542.55**	**21.26%**	
	B				6.81	0.0129	527.76			
	C				6.80	0.0156	435.31			
L_cut_CL90s_170_2m_C	A	21.19	18.50	**18.50**	7.59	0.0126	601.74	**612.64**	**14.96%**	
	B				7.06	0.0134	526.9			
	C				7.54	0.0106	709.27			
L_cut_CL90s_170_6m_C	A	23.68	20.98	**20.98**	7.89	0.0136	580.81	**669.90**	**14.46%**	
	B				8.51	0.0130	655.88			
	C				8.77	0.0113	773.00			

Table E.24: CL90-s-cut limestone masonry compressive strength and elastic modulus results and calculations (continued)

Test no	Masonry ID	Specimen	Unit Type	PC/ lime/ sand ratio	Initial flow (mm)	Curing	Test age	Length (mm)	Width (mm)	Height (mm)	Cross sectional area (mm^2)	Applied load, F_c (kN)	Compressive strength, R_i (N/mm^2)	Mean compressive strength, R_c (N/mm^2)	COV (%)
201	S_bk_NHL2_165_1m_C	A	Broken Sandstone	0:1:3	165	lab	28 days	221.83	113.22	348.22	25115.59	347.600	13.84	**12.54**	**23.77%**
202		B						204.23	102.49	355.44	20931.53	191.105	9.13		
203		C						235.73	123.51	350.22	29115.01	426.535	14.65		
204	S_bk_NHL2_165_2m_C	A	Broken Sandstone	0:1:3	165	lab	56 days	215.35	115.84	345.23	24946.14	302.098	12.11	**13.91**	**11.26%**
205		B						226.42	110.28	348.89	24969.60	373.545	14.96		
206		C						214.4	126.34	355.36	27087.30	397.100	14.66		
207	S_bk_NHL2_165_6m_C	A	Broken Sandstone	0:1:3	165	lab	6 mts.	236.32	118.66	351.32	28041.73	432.964	15.44	**14.87**	**9.82%**
208		B						201.36	128.35	343.64	25844.56	341.407	13.21		
209		C						225.41	106.12	347.54	23920.51	381.771	15.96		
210	S_bk_NHL2_170_1m_C	A	Broken Sandstone	0:1:3	170	lab	28 days	228.49	115.59	352.56	26411.16	387.716	14.68	**15.01**	**2.20%**
211		B						211.25	122.76	356.44	25933.05	389.255	15.01		
212		C						209.44	114.91	351.29	24066.75	369.184	15.34		
213	S_bk_NHL2_170_2m_C	A	Broken Sandstone	0:1:3	170	lab	56 days	236.33	103.55	356.46	24471.97	374.666	15.31	**15.12**	**5.41%**
214		B						216.25	98.49	354.68	21298.46	336.942	15.82		
215		C						229.3	116.98	350.42	26823.51	381.430	14.22		
216	S_bk_NHL2_170_6m_C	A	Broken Sandstone	0:1:3	170	lab	6 mts.	237.11	128.54	344.56	30478.12	452.295	14.84	**15.45**	**4.96%**
217		B						231.65	123.54	348.51	28618.04	434.994	15.20		
218		C						229.83	119.27	354.83	27411.82	447.087	16.31		

Table E.25: NHL 2-broken sandstone masonry compressive strength and elastic modulus results and calculations

Masonry ID	Specimen	Min compressive strength	Compressive strength/1.2	Characteristic compressive strength f_k (N/mm^2)	Change in Stress Δδ N/mm^2	Change in Strain Δε	Elastic modulus, E_i (N/mm^2)	Mean elastic Modulus, E (N/mm^2)	COV (%)	Notes
S_bk_NHL2_165_1m_C	A	9.13	10.45	**9.13**	4.61	0.0060	770.52	**675.36**	**17.11%**	
	B				3.04	0.0056	546.80			
	C				4.88	0.0069	708.76			
S_bk_NHL2_165_2m_C	A	12.11	11.59	**11.59**	4.04	0.0063	644.84	**834.18**	**19.81%**	
	B				4.99	0.0053	949.34			
	C				4.89	0.0054	908.36			
S_bk_NHL2_165_6m_C	A	13.21	12.39	**12.39**	5.15	0.0056	920.40	**926.14**	**9.91%**	
	B				4.40	0.0053	837.33			
	C				5.32	0.0052	1020.69			
S_bk_NHL2_170_1m_C	A	14.68	12.51	**12.51**	4.89	0.0072	683.44	**764.14**	**9.18%**	
	B				5.00	0.0063	798.19			
	C				5.11	0.0063	810.79			
S_bk_NHL2_170_2m_C	A	14.22	12.60	**12.60**	5.10	0.0057	896.82	**922.68**	**2.57%**	
	B				5.27	0.0057	927.90			
	C				4.74	0.0050	943.32			
S_bk_NHL2_170_6m_C	A	14.84	12.88	**12.88**	4.95	0.0048	1029.20	**1005.56**	**2.95%**	
	B				5.07	0.0050	1015.20			
	C				5.44	0.0056	972.28			

Table E.26: NHL 2-broken sandstone masonry compressive strength and elastic modulus results and calculations (continued)

Test no	Masonry ID	Specimen	Unit Type	PC/ lime/ sand ratio	Initial flow (mm)	Curing	Test age	Length (mm)	Width (mm)	Height (mm)	Cross sectional area (mm^2)	Applied load, F_c (kN)	Compressive strength, R_i (N/mm^2)	Mean compressive strength, R_c (N/mm^2)	COV (%)
219	S_bk_CL90s_165_1m_C	A	Broken Sandstone	0:1:3	165	lab	28 days	213.48	94.83	348.24	20244.31	260.949	12.89	**11.63**	**12.84%**
220		B						234.35	105.43	352.53	24707.52	296.984	12.02		
221		C						225.46	124.26	355.4	28015.66	279.596	9.98		
222	S_bk_CL90s_165_2m_C	A	Broken Sandstone	0:1:3	165	lab	56 days	223.43	122.94	324.59	27468.48	335.665	12.22	**12.93**	**6.35%**
223		B						238.54	107.43	338.53	25626.35	326.480	12.74		
224		C						254.22	114.67	346.87	29151.41	403.164	13.83		
225	S_bk_CL90s_165_6m_C	A	Broken Sandstone	0:1:3	165	lab	6 mts.	224.49	118.42	348.03	26584.11	368.987	13.88	**14.41**	**4.44%**
226		B						231.84	112.43	354.63	26065.77	370.916	14.23		
227		C						225.16	101.35	358.64	22819.97	345.038	15.12		
228	S_bk_CL90s_170_1m_C	A	Broken Sandstone	0:1:3	170	lab	28 days	226.42	114.63	344.93	25954.52	274.599	10.58	**11.86**	**9.64%**
229		B						215.89	132.52	354.33	28609.74	365.633	12.78		
230		C						237.41	125.49	352.22	29792.58	364.065	12.22		
231	S_bk_CL90s_170_2m_C	A	Broken Sandstone	0:1:3	170	lab	56 days	231.69	112.43	358.15	26048.91	355.828	13.66	**14.19**	**11.86%**
232		B						221.63	113.42	351.11	25137.27	370.021	14.72		
233		C						218.35	102.58	345.93	22398.34	-	-		
234	S_bk_CL90s_170_6m_C	A	Broken Sandstone	0:1:3	170	lab	6 mts.	220.18	106.72	348.51	23497.61	331.551	14.11	**14.52**	**8.26%**
235		B						234.84	111.5	350.59	26184.66	355.588	13.58		
236		C						238.54	121.54	351.98	28992.15	460.105	15.87		

Table E.27: CL90-s-broken sandstone masonry compressive strength and elastic modulus results and calculations

Masonry ID	Specimen	Min compressive strength	Compressive strength/1.2	Characteristic compressive strength f_k (N/mm^2)	Change in Stress Δδ N/mm^2	Change in Strain Δε	Elastic modulus, E_i (N/mm^2)	Mean elastic Modulus, E (N/mm^2)	COV (%)	Notes
S_bk_CL90s_165_1m_C	A	9.98	9.69	**9.69**	4.30	0.0079	543.75	**506.76**	**8.34%**	
	B				4.01	0.0078	515.87			
	C				3.33	0.0072	460.66			
S_bk_CL90s_165_2m_C	A	12.22	10.78	**10.78**	4.07	0.0077	530.36	**586.80**	**13.51%**	
	B				4.25	0.0077	552.64			
	C				4.61	0.0068	677.40			
S_bk_CL90s_165_6m_C	A	13.88	12.01	**12.01**	4.63	0.0077	602.48	**631.50**	**5.46%**	
	B				4.74	0.0076	622.36			
	C				5.04	0.0075	669.66			
S_bk_CL90s_170_1m_C	A	10.58	9.88	**9.88**	3.53	0.0072	488.65	**510.50**	**4.49%**	
	B				4.26	0.0080	534.33			
	C				4.07	0.0080	508.52			
S_bk_CL90s_170_2m_C	A	13.66	11.83	**11.83**	4.55	0.0083	545.63	**586.76**	**9.91%**	
	B				4.91	0.0078	627.89			
	C				-	-	-			damaged
S_bk_CL90s_170_6m_C	A	13.58	12.10	**12.10**	4.70	0.0077	607.04	**635.30**	**22.02%**	
	B				4.53	0.0088	511.70			
	C				5.29	0.0067	787.16			

Table E.28: CL90-s-broken sandstone masonry compressive strength and elastic modulus results and calculations (continued)

APPENDIX F

MASONRY BOND STRENGTH RESULTS AND CALCULATIONS

Test No.	Mortar ID	Unit Type	PC/lime / sand Ratio	Curing	Sample No.	Joint No.	Applied Load (g)	Weight of Top Unit (g)	Applied Load, F_1 (N)	Weight of Top Unit, W (N)	Failure Mode	Bond Strength, f_{wi} (N/mm^2)	Notes	$\log_{10}$ of bond strength (Y_i)
1	B_M6_165_1m_T	Brick	1:½:4	Lab	1	1	76453	2447.52	750.00	24.01	A1	0.650		-0.19
						2	77778	2431.52	763.00	23.85	A1	0.661		-0.18
						3	57085	2556.21	560.00	25.08	A1	0.484		-0.32
						4	59633	2545.82	585.00	24.97	A1	0.505		-0.30
						5	50765	2431.52	498.00	23.85	A1	0.429		-0.37
					2	6	37717	2545.82	370.00	24.97	A1	0.317		-0.50
						7	55046	2556.21	540.00	25.08	A1	0.466		-0.33
						8	65240	2483.48	640.00	24.36	A1	0.554		-0.26
						9	59633	2327.61	585.00	22.83	A1	0.505		-0.30
						10	48930	2473.08	480.00	24.26	A1	0.414		-0.38
					3	11							damaged	
						12	76453	2525.04	750.00	24.77	A1	0.650		-0.19
						13	80530	2441.91	790.00	23.96	A1	0.685		-0.16
						14	46381	2452.30	455.00	24.06	A1	0.392		-0.41
						15	55556	2441.91	545.00	23.96	A1	0.470		-0.33
					Sample Mean							**0.513**		**-0.30**
					Sample Standard Deviation							**0.113**		**0.10**
					Coefficient of Variation							**0.220**		**-0.33**
					Y_c									**-0.49**
					Characteristic bond strength, f_{wk} (N/mm^2)									**0.33**

Table F.1: M6 brick masonry bond strength calculations, 165 mm flow (1 month)

Test No.	Mortar ID	Unit Type	PC/lime / sand Ratio	Curing	Sample No.	Joint No.	Applied Load (g)	Weight of Top Unit (g)	Applied Load, F_1 (N)	Weight of Top Unit, W (N)	Failure Mode	Bond Strength, f_{wi} (N/mm^2)	Notes	$\log_{10}$ of bond strength (Y_i)
2	B_M6_165_2m_T	Brick	1:½:4	Lab	1	1	88991	2431.52	873.00	23.85	A1	0.757		-0.12
						2	66667	2452.30	654.00	24.06	A1	0.566		-0.25
						3	56575	2483.48	555.00	24.36	A1	0.479		-0.32
						4	59531	2545.82	584.00	24.97	A1	0.505		-0.30
						5	78287	2525.04	768.00	24.77	A1	0.665		-0.18
					2	6	97859	2493.87	960.00	24.46	A1	0.833		-0.08
						7							damaged	
						8	87054	2441.91	854.00	23.96	A1	0.741		-0.13
						9	55556	2431.52	545.00	23.85	A1	0.470		-0.33
						10	50459	2441.91	495.00	23.96	A1	0.427		-0.37
					3	11	56677	2452.30	556.00	24.06	A1	0.480		-0.32
						12	95005	2473.08	932.00	24.26	A1	0.809		-0.09
						13	79511	2504.26	780.00	24.57	A1	0.676		-0.17
						14	89195	2379.56	875.00	23.34	A1	0.759		-0.12
						15	104995	2441.91	1030.00	23.96	A1	0.895		-0.05
					Sample Mean							**0.647**		**-0.20**
					Sample Standard Deviation							**0.157**		**0.11**
					Coefficient of Variation							**0.242**		**-0.54**
					Y_c									**-0.41**
					Characteristic bond strength, f_{wk} (N/mm^2)									**0.39**

Table F.2: M6 brick masonry bond strength calculations, 165 mm flow (2 months)

Test No.	Mortar ID	Unit Type	PC/lime / sand Ratio	Curing	Sample No.	Joint No.	Applied Load (g)	Weight of Top Unit (g)	Applied Load, F_1 (N)	Weight of Top Unit, W (N)	Failure Mode	Bond Strength, f_{wi} (N/mm^2)	Notes	$\log_{10}$ of bond strength (Y_i)
3	B_M6_165_6m_T	Brick	1:½:4	Lab	1	1	103976	2441.91	1020.00	23.96	A1	0.750		-0.12
						2	136595	2457.50	1340.00	24.11	A1	1.166		0.07
						3							damaged	
						4	79409	2525.04	779.00	24.77	A1	0.675		-0.17
						5	127421	2431.52	1250.00	23.85	A1	1.087		0.04
					2	6	90724	2441.91	890.00	23.96	A1	0.772		-0.11
						7	77064	2441.91	756.00	23.96	A1	0.655		-0.18
						8	112334	2338.00	1102.00	22.94	A1	0.958		-0.02
						9	70133	2462.69	688.00	24.16	A1	0.595		-0.23
						10	43119	2483.48	423.00	24.36	A1	0.364		-0.44
					3	11	134862	2369.17	1323.00	23.24	A1	1.151		0.06
						12	126707	2483.48	1243.00	24.36	A1	1.081		0.03
						13	90724	2431.52	890.00	23.85	A1	0.772		-0.11
						14	108767	2545.82	1067.00	24.97	A1	0.927		-0.03
						15	115189	2338.00	1130.00	22.94	A1	0.982		-0.01
					Sample Mean							**0.852**		**-0.09**
					Sample Standard Deviation							**0.236**		**0.14**
					Coefficient of Variation							**0.277**		**-1.58**
					Y_c									**-0.35**
					Characteristic bond strength, f_{wk} (N/mm^2)									**0.44**

Table F.3: M6 brick masonry bond strength calculations, 165 mm flow (6 months)

Test No.	Mortar ID	Unit Type	PC/lime / sand Ratio	Curing	Sample No.	Joint No.	Applied Load (g)	Weight of Top Unit (g)	Applied Load, F_1 (N)	Weight of Top Unit, W (N)	Failure Mode	Bond Strength, f_{wi} (N/mm^2)	Notes	$\log_{10}$ of bond strength (Y_i)
4	B_NHL5_165_1m_T	Brick	0:1:3	Lab	1	1	25831	2415.93	253.40	23.70	A1	0.216		-0.67
						2	20724	2394.11	203.30	23.49	A1	0.172		-0.77
						3	23827	2527.12	233.74	24.79	A1	0.198		-0.70
						4							damaged	
						5	30805	2385.80	302.20	23.40	A1	0.258		-0.59
					2	6	25923	2399.00	254.30	23.53	A1	0.216		-0.66
						7	22773	2402.74	223.40	23.57	A1	0.189		-0.72
						8	24801	2446.38	243.30	24.00	A1	0.207		-0.68
						9							damaged	
						10	25788	2456.46	252.98	24.10	A1	0.215		-0.67
					3	11	27054	2426.95	265.40	23.81	A1	0.226		-0.65
						12	24759	2507.58	242.89	24.60	A1	0.206		-0.69
						13	27054	2548.94	265.40	25.01	A1	0.226		-0.65
						14	25861	2452.09	253.70	24.06	A1	0.216		-0.67
						15	23007	2466.85	225.70	24.20	A1	0.191		-0.72
					Sample Mean							**0.211**		**-0.68**
					Sample Standard Deviation							**0.021**		**0.04**
					Coefficient of Variation							**0.100**		**-0.06**
					Y_c									**-0.76**
					Characteristic bond strength, f_{wk} (N/mm^2)									**0.17**

Table F.4: NHL 5 brick masonry bond strength calculations, 165 mm flow (1 months)

Test No.	Mortar ID	Unit Type	PC/lime / sand Ratio	Curing	Sample No.	Joint No.	Applied Load (g)	Weight of Top Unit (g)	Applied Load, F_1 (N)	Weight of Top Unit, W (N)	Failure Mode	Bond Strength, f_{wi} (N/mm^2)	Notes	$\log_{10}$ of bond strength (Y_i)
5	B_NHL5_165_2m_T	Brick	0:1:3	Lab	1	1	35311	2506.54	346.40	24.59	A1	0.297		-0.53
						2	18400	2441.91	180.50	23.96	A1	0.152		-0.82
						3	28175	2528.16	276.40	24.80	A1	0.236		-0.63
						4	39521	2456.46	387.70	24.10	A1	0.333		-0.48
						5	37574	2435.68	368.60	23.89	A1	0.316		-0.50
					2	6	25545	2582.19	250.60	25.33	A1	0.213		-0.67
						7	36147	2455.42	354.60	24.09	A1	0.304		-0.52
						8	38685	2487.63	379.50	24.40	A1	0.326		-0.49
						9	25015	2405.54	245.40	23.60	A1	0.209		-0.68
						10	27054	2445.03	265.40	23.99	A1	0.226		-0.65
					3	11	40826	2579.07	400.50	25.30	A1	0.344		-0.46
						12	31040	2467.89	304.50	24.21	A1	0.260		-0.58
						13	36116	2477.24	354.30	24.30	A1	0.304		-0.52
						14	38186	2437.75	374.60	23.91	A1	0.321		-0.49
						15	37251	2489.71	365.43	24.42	A1	0.313		-0.50
					Sample Mean							**0.277**		**-0.57**
					Sample Standard Deviation							**0.057**		**0.10**
					Coefficient of Variation							**0.206**		**-0.18**
					Y_c									**-0.76**
					Characteristic bond strength, f_{wk} (N/mm^2)									**0.17**

Table F.5: NHL 5 brick masonry bond strength calculations, 165 mm flow (2 months)

Test No.	Mortar ID	Unit Type	PC/lime / sand Ratio	Curing	Sample No.	Joint No.	Applied Load (g)	Weight of Top Unit (g)	Applied Load, F_1 (N)	Weight of Top Unit, W (N)	Failure Mode	Bond Strength, f_{wi} (N/mm^2)	Notes	$\log_{10}$ of bond strength (Y_i)
6	B_NHL5_165_6m_T	Brick	0:1:3	Lab	1	1	49674	2437.75	487.30	23.91	A1	0.420		-0.38
						2	49256	2446.07	483.20	24.00	A1	0.416		-0.38
						3	50795	2389.96	498.30	23.45	A1	0.430		-0.37
						4	44771	2363.46	439.20	23.19	A1	0.378		-0.42
						5	23772	2342.16	233.20	22.98	A1	0.198		-0.70
					2	6	57737	2324.49	566.40	22.80	A1	0.489		-0.31
						7	69664	2466.85	683.40	24.20	A6	0.591		-0.23
						8	61004	2438.79	598.45	23.92	A1	0.517		-0.29
						9	49908	2421.13	489.60	23.75	A1	0.422		-0.37
						10	60958	2440.87	598.00	23.94	A1	0.517		-0.29
					3	11	49684	2441.91	487.40	23.96	A1	0.420		-0.38
						12	36330	2525.04	356.40	24.77	A1	0.306		-0.51
						13	38369	2507.38	376.40	24.60	A1	0.323		-0.49
						14	34190	2456.46	335.40	24.10	A1	0.287		-0.54
						15	24424	2489.71	239.60	24.42	A1	0.203		-0.69
					Sample Mean							**0.395**		**-0.42**
					Sample Standard Deviation							**0.114**		**0.14**
					Coefficient of Variation							**0.289**		**-0.33**
					Y_c									**-0.69**
					Characteristic bond strength, f_{wk} (N/mm^2)									**0.20**

Table F.6: NHL 5 brick masonry bond strength calculations, 165 mm flow (6 months)

Test No.	Mortar ID	Unit Type	PC/lime / sand Ratio	Curing	Sample No.	Joint No.	Applied Load (g)	Weight of Top Unit (g)	Applied Load, F_1 (N)	Weight of Top Unit, W (N)	Failure Mode	Bond Strength, f_{wi} (N/mm^2)	Notes	$\log_{10}$ of bond strength (Y_i)
7	B_NHL5_165_1yr_T	Brick	0:1:3	Lab	1	1	35311	2434.64	346.40	23.88	A1	0.297		-0.53
						2	60041	2467.89	589.00	24.21	A1	0.509		-0.29
						3	86075	2535.43	844.40	24.87	A1	0.732		-0.14
						4	76952	2560.37	754.90	25.12	A1	0.654		-0.18
						5	58542	2435.68	574.30	23.89	A1	0.496		-0.30
					2	6	55586	2477.24	545.30	24.30	A1	0.471		-0.33
						7	36147	2530.24	354.60	24.82	A1	0.304		-0.52
						8	39195	2375.41	384.50	23.30	A1	0.330		-0.48
						9	40194	2639.34	394.30	25.89	A1	0.339		-0.47
						10	49694	2513.61	487.50	24.66	A1	0.420		-0.38
					3	11	40826	2467.89	400.50	24.21	A1	0.344		-0.46
						12	60581	2451.26	594.30	24.05	A1	0.514		-0.29
						13	50795	2446.07	498.30	24.00	A1	0.430		-0.37
						14	80061	2525.04	785.40	24.77	A1	0.681		-0.17
						15	83976	2437.75	823.80	23.91	A1	0.714		-0.15
					Sample Mean							**0.482**		**-0.34**
					Sample Standard Deviation							**0.152**		**0.14**
					Coefficient of Variation							**0.315**		**-0.40**
					Y_c									**-0.60**
					Characteristic bond strength, f_{wk} (N/mm^2)									**0.25**

Table F.7: NHL 5 brick masonry bond strength calculations, 165 mm flow (12 months)

Test No.	Mortar ID	Unit Type	PC/lime / sand Ratio	Curing	Sample No.	Joint No.	Applied Load (g)	Weight of Top Unit (g)	Applied Load, F_1 (N)	Weight of Top Unit, W (N)	Failure Mode	Bond Strength, f_{wi} (N/mm^2)	Notes	$\log_{10}$ of bond strength (Y_i)
8	B_NHL3.5_165_1M_T	Brick	0:1:3	Lab	1	1	17635	2311.93	173.00	22.68	A1	0.145		-0.84
						2	29052	2390.42	285.00	23.45	A1	0.243		-0.61
						3							damaged	
						4	13660	2399.59	134.00	23.54	A1	0.111		-0.95
						5							damaged	
					2	6	8155	2546.38	80.00	24.98	A1	0.064		-1.19
						7	19266	2589.19	189.00	25.40	A1	0.159		-0.80
						8	21713	2394.50	213.00	23.49	A1	0.180		-0.74
						9	24873	2430.17	244.00	23.84	A1	0.207		-0.68
						10	24098	2388.38	236.40	23.43	A1	0.201		-0.70
					3	11	22426	2589.19	220.00	25.40	A1	0.186		-0.73
						12	25790	2334.35	253.00	22.90	A1	0.215		-0.67
						13							damaged	
						14	23955	2515.80	235.00	24.68	A1	0.199		-0.70
						15	27217	2392.46	267.00	23.47	A1	0.227		-0.64
					Sample Mean							**0.178**		**-0.77**
					Sample Standard Deviation							**0.051**		**0.16**
					Coefficient of Variation							**0.288**		**-0.21**
					Y_c									**-1.08**
					Characteristic bond strength, f_{wk} (N/mm^2)									**0.08**

Table F.8: NHL 3 5 brick masonry bond strength calculations, 165 mm flow (1 month)

Test No.	Mortar ID	Unit Type	PC/lime / sand Ratio	Curing	Sample No.	Joint No.	Applied Load (g)	Weight of Top Unit (g)	Applied Load, F_1 (N)	Weight of Top Unit, W (N)	Failure Mode	Bond Strength, f_{wi} (N/mm^2)	Notes	$\log_{10}$ of bond strength (Y_i)
9	B_NHL3.5_165_2M_T	Brick	0:1:3	Lab	1	1							damaged	
						2	33945	2405.71	333.00	23.60	A1	0.285		-0.54
						3							damaged	
						4	24771	2388.38	243.00	23.43	A1	0.206		-0.69
						5	36086	2426.10	354.00	23.80	A1	0.303		-0.52
					2	6	23853	2399.59	234.00	23.54	A1	0.199		-0.70
						7	29460	2440.37	289.00	23.94	A1	0.247		-0.61
						8	29052	2487.26	285.00	24.40	A1	0.243		-0.61
						9							damaged	
						10	32824	2548.42	322.00	25.00	A1	0.275		-0.56
					3	11							damaged	
						12	40163	2533.13	394.00	24.85	A1	0.338		-0.47
						13	28033	2476.04	275.00	24.29	A1	0.234		-0.63
						14	27013	2426.10	265.00	23.80	A1	0.226		-0.65
						15	34047	2583.08	334.00	25.34	A1	0.286		-0.54
					Sample Mean							**0.258**		**-0.59**
					Sample Standard Deviation							**0.043**		**0.07**
					Coefficient of Variation							**0.166**		**-0.12**
					Y_c									**-0.73**
					Characteristic bond strength, f_{wk} (N/mm^2)									**0.19**

Table F.9: NHL 3.5 brick masonry bond strength calculations, 165 mm flow (2 months)

Test No.	Mortar ID	Unit Type	PC/lime / sand Ratio	Curing	Sample No.	Joint No.	Applied Load (g)	Weight of Top Unit (g)	Applied Load, F_1 (N)	Weight of Top Unit, W (N)	Failure Mode	Bond Strength, f_{wi} (N/mm^2)	Notes	$\log_{10}$ of bond strength (Y_i)
10	B_NHL3.5_165_6M_T	Brick	0:1:3	Lab	1	1	32620	2531.09	320.00	24.83	A1	0.274		-0.56
						2	55352	2433.23	543.00	23.87	A1	0.469		-0.33
						3	39144	2441.39	384.00	23.95	A1	0.330		-0.48
						4	41794	2379.20	410.00	23.34	A1	0.352		-0.45
						5	24363	2579.00	239.00	25.30	A1	0.203		-0.69
					2	6	25892	2640.16	254.00	25.90	A1	0.216		-0.67
						7	35678	2386.34	350.00	23.41	A1	0.300		-0.52
						8	48420	2444.44	475.00	23.98	A1	0.409		-0.39
						9	35270	2477.06	346.00	24.30	A1	0.296		-0.53
						10	47401	2436.29	465.00	23.90	A1	0.401		-0.40
					3	11	41794	2425.08	410.00	23.79	A1	0.352		-0.45
						12	58410	2523.96	573.00	24.76	A1	0.495		-0.31
						13	66769	2579.00	655.00	25.30	A1	0.567		-0.25
						14	50459	2388.38	495.00	23.43	A1	0.427		-0.37
						15	70744	2399.59	694.00	23.54	A1	0.601		-0.22
					Sample Mean							**0.379**		**-0.44**
					Sample Standard Deviation							**0.118**		**0.14**
					Coefficient of Variation							**0.311**		**-0.32**
					Y_c									**-0.71**
					Characteristic bond strength, f_{wk} (N/mm^2)									**0.20**

Table F.10: NHL 3.5 brick masonry bond strength calculations, 165 mm flow (6 months)

Test No.	Mortar ID	Unit Type	PC/lime / sand Ratio	Curing	Sample No.	Joint No.	Applied Load (g)	Weight of Top Unit (g)	Applied Load, F_1 (N)	Weight of Top Unit, W (N)	Failure Mode	Bond Strength, f_{wi} (N/mm^2)	Notes	$\log_{10}$ of bond strength (Y_i)
11	B_NHL3.5_165_1YR_T	Brick	0:1:3	Lab	1	1	0	0.00					damaged	
						2	56473	2441.91	554.00	23.96	A1	0.478		-0.32
						3	50765	2457.50	498.00	24.11	A1	0.429		-0.37
						4	40571	2462.69	398.00	24.16	A3	0.342		-0.47
						5	39348	2514.65	386.00	24.67	A1	0.331		-0.48
					2	6	50255	2525.04	493.00	24.77	A1	0.425		-0.37
						7	61570	2531.27	604.00	24.83	A1	0.522		-0.28
						8							damaged	
						9							damaged	
						10	70846	2479.84	695.00	24.33	A1	0.602		-0.22
					3	11	47401	2446.79	465.00	24.00	A1	0.401		-0.40
						12	36391	2431.52	357.00	23.85	A1	0.306		-0.51
						13	27829	2456.46	273.00	24.10	A1	0.233		-0.63
						14	55963	2489.71	549.00	24.42	A1	0.474		-0.32
						15	76453	2456.77	750.00	24.10	A1	0.650		-0.19
					Sample Mean							**0.433**		**-0.38**
					Sample Standard Deviation							**0.122**		**0.13**
					Coefficient of Variation							**0.281**		**-0.34**
					Y_c									**-0.63**
					Characteristic bond strength, f_{wk} (N/mm^2)									**0.24**

Table F.11: NHL 3.5 brick masonry bond strength calculations, 165 mm flow (12 months)

Test No.	Mortar ID	Unit Type	PC/lime / sand Ratio	Curing	Sample No.	Joint No.	Applied Load (g)	Weight of Top Unit (g)	Applied Load, F_1 (N)	Weight of Top Unit, W (N)	Failure Mode	Bond Strength, f_{wi} (N/mm^2)	Notes	$\log_{10}$ of bond strength (Y_i)
12	B_NHL2_165_1M_T	Brick	0:1:3	Lab	1	1	17023	2385.32	167.00	23.40	A1	0.140		-0.85
						2							damaged	
						3	16514	2525.04	162.00	24.77	A1	0.136		-0.87
						4	13456	2431.52	132.00	23.85	A1	0.109		-0.96
						5	13150	2441.91	129.00	23.96	A1	0.107		-0.97
					2	6	9888	2452.30	97.00	24.06	A1	0.079		-1.10
						7							damaged	
						8	19572	2452.30	192.00	24.06	A1	0.162		-0.79
						9							damaged	
						10	10601	2421.13	104.00	23.75	A1	0.085		-1.07
					3	11	13863	2431.52	136.00	23.85	A1	0.113		-0.95
						12							damaged	
						13	12232	2421.13	120.00	23.75	A6	0.099		-1.00
						14	13456	2441.91	132.00	23.96	A1	0.109		-0.96
						15	14781	2441.91	145.00	23.96	A1	0.121		-0.92
					Sample Mean							**0.114**		**-0.95**
					Sample Standard Deviation							**0.024**		**0.09**
					Coefficient of Variation							**0.212**		**-0.10**
					Y_c									**-1.13**
					Characteristic bond strength, f_{wk} (N/mm^2)									**0.07**

Table F.12: NHL 2 brick masonry bond strength calculations, 165 mm flow (1 month)

Test No.	Mortar ID	Unit Type	PC/lime / sand Ratio	Curing	Sample No.	Joint No.	Applied Load (g)	Weight of Top Unit (g)	Applied Load, F_1 (N)	Weight of Top Unit, W (N)	Failure Mode	Bond Strength, f_{wi} (N/mm^2)	Notes	$\log_{10}$ of bond strength (Y_i)
13	B_NHL2_165_2M_T	Brick	0:1:3	Lab	1	1	8155	2431.52	80.00	23.85	A1	0.064		-1.19
						2	15902	2525.04	156.00	24.77	A1	0.130		-0.89
						3	18858	2473.08	185.00	24.26	A1	0.156		-0.81
						4	19674	2535.43	193.00	24.87	A1	0.163		-0.79
						5							damaged	
					2	6							damaged	
						7	13761	2441.91	135.00	23.96	A1	0.112		-0.95
						8	15698	2487.63	154.00	24.40	A1	0.129		-0.89
						9	17941	2514.65	176.00	24.67	A1	0.148		-0.83
						10							damaged	
					3	11	25892	2441.91	254.00	23.96	A1	0.216		-0.67
						12							damaged	
													damaged	
						14	16718	2509.87	164.00	24.62	A1	0.137		-0.86
						15	25892	2483.48	254.00	24.36	A1	0.216		-0.67
					Sample Mean							**0.147**		**-0.85**
					Sample Standard Deviation							**0.046**		**0.15**
					Coefficient of Variation							**0.310**		**-0.18**
					Y_c									**-1.14**
					Characteristic bond strength, f_{wk} (N/mm^2)									**0.07**

Table F.13: NHL 2 brick masonry bond strength calculations, 165 mm flow (2 months)

Test No.	Mortar ID	Unit Type	PC/lime / sand Ratio	Curing	Sample No.	Joint No.	Applied Load (g)	Weight of Top Unit (g)	Applied Load, F_1 (N)	Weight of Top Unit, W (N)	Failure Mode	Bond Strength, f_{wi} (N/mm^2)	Notes	$\log_{10}$ of bond strength (Y_i)
14	B_NHL2_165_6M_T	Brick	0:1:3	Lab	1	1	9174	2421.13	90.00	23.75	A1	0.073		-1.14
						2	16820	2525.04	165.00	24.77	A1	0.138		-0.86
						3							damaged	
						4	19368	2441.91	190.00	23.96	A1	0.160		-0.80
						5							damaged	
					2	6	32824	2431.52	322.00	23.85	A1	0.275		-0.56
						7	25790	2441.91	253.00	23.96	A1	0.215		-0.67
						8	20183	2608.17	198.00	25.59	A1	0.167		-0.78
						9							damaged	
						10	26096	2525.04	256.00	24.77	A1	0.218		-0.66
					3	11							damaged	
						12	25892	2441.91	254.00	23.96	A1	0.216		-0.67
						13	24975	2545.82	245.00	24.97	A1	0.208		-0.68
						14	27013	2452.30	265.00	24.06	A1	0.226		-0.65
						15	18960	2618.56	186.00	25.69	A1	0.157		-0.81
					Sample Mean							**0.187**		**-0.75**
					Sample Standard Deviation							**0.055**		**0.16**
					Coefficient of Variation							**0.293**		**-0.21**
					Y_c									**-1.05**
					Characteristic bond strength, f_{wk} (N/mm^2)									**0.09**

Table F.14: NHL 2 brick masonry bond strength calculations, 165 mm flow (6 months)

Test No.	Mortar ID	Unit Type	PC/lime / sand Ratio	Curing	Sample No.	Joint No.	Applied Load (g)	Weight of Top Unit (g)	Applied Load, F_1 (N)	Weight of Top Unit, W (N)	Failure Mode	Bond Strength, f_{wi} (N/mm^2)	Notes	$\log_{10}$ of bond strength (Y_i)
15	B_NHL2_165_1YR_T	Brick	0:1:3	Lab	1	1	33028	2556.21	324.00	25.08	A1	0.277		-0.56
						2	23853	2431.52	234.00	23.85	A1	0.199		-0.70
						3	25892	2441.91	254.00	23.96	A1	0.216		-0.67
						4							damaged	
						5	32620	2504.26	320.00	24.57	A1	0.274		-0.56
					2	6	23547	2753.64	231.00	27.01	A1	0.196		-0.71
						7	8869	2639.34	87.00	25.89	A1	0.070		-1.16
						8	10398	2441.91	102.00	23.96	A1	0.083		-1.08
						9	32722	2452.30	321.00	24.06	A1	0.275		-0.56
						10							damaged	
					3	11	19368	2462.69	190.00	24.16	A1	0.160		-0.80
						12	35168	2441.91	345.00	23.96	A1	0.296		-0.53
						13	28135	2452.30	276.00	24.06	A1	0.235		-0.63
						14	20591	2639.34	202.00	25.89	A1	0.170		-0.77
						15	24975	2545.82	245.00	24.97	A1	0.208		-0.68
					Sample Mean							**0.205**		**-0.72**
					Sample Standard Deviation							**0.071**		**0.19**
					Coefficient of Variation							**0.347**		**-0.27**
					Y_c									**-1.10**
					Characteristic bond strength, f_{wk} (N/mm^2)									**0.08**

Table F.15: NHL 2 brick masonry bond strength calculations, 165 mm flow (12 months)

Test No.	Mortar ID	Unit Type	PC/lime / sand Ratio	Curing	Sample No.	Joint No.	Applied Load (g)	Weight of Top Unit (g)	Applied Load, F_1 (N)	Weight of Top Unit, W (N)	Failure Mode	Bond Strength, f_{wi} (N/mm^2)	Notes	$\log_{10}$ of bond strength (Y_i)
16	B_CL90s_165_1M_T	Brick	0:1:3	Lab	1	1	8869	2421.13	87.00	23.75	A1	0.070		-1.15
						2	3466	2441.91	34.00	23.96	A1	0.024		-1.63
						3							damaged	
						4	9990	2545.82	98.00	24.97	A1	0.080		-1.10
						5	6626	2525.04	65.00	24.77	A1	0.051		-1.29
					2	6	6830	2452.30	67.00	24.06	A1	0.053		-1.28
						7	7645	2431.52	75.00	23.85	A1	0.060		-1.23
						8							damaged	
						9	8155	2462.69	80.00	24.16	A1	0.064		-1.19
						10	7951	2628.95	78.00	25.79	A1	0.062		-1.21
					3	11							damaged	
						12	4383	2441.91	43.00	23.96	A1	0.032		-1.50
						13							damaged	
						14	2345	2473.08	23.00	24.26	A1	0.014		-1.85
						15							damaged	
					Sample Mean							**0.051**		**-1.34**
					Sample Standard Deviation							**0.021**		**0.24**
					Coefficient of Variation							**0.417**		**-0.18**
					Y_c									**-1.80**
					Characteristic bond strength, f_{wk} (N/mm^2)									**0.02**

Table F.16: CL90-s brick masonry bond strength calculations, 165 mm flow (1 month)

Test No.	Mortar ID	Unit Type	PC/lime / sand Ratio	Curing	Sample No.	Joint No.	Applied Load (g)	Weight of Top Unit (g)	Applied Load, F_1 (N)	Weight of Top Unit, W (N)	Failure Mode	Bond Strength, f_{wi} (N/mm^2)	Notes	$\log_{10}$ of bond strength (Y_i)
17	B_CL90s_165_2M_T	Brick	0:1:3	Lab	1	1	14577	2452.30	143.00	24.06	A1	0.119		-0.92
						2							damaged	
						3							damaged	
						4	13761	2535.43	135.00	24.87	A1	0.112		-0.95
						5	9684	2551.02	95.00	25.03	A1	0.077		-1.11
					2	6	13456	2431.52	132.00	23.85	A1	0.109		-0.96
						7	14577	2436.20	143.00	23.90	A1	0.119		-0.92
						8	12742	2379.56	125.00	23.34	A1	0.103		-0.99
						9							damaged	
						10	10499	2639.34	103.00	25.89	A1	0.084		-1.08
					3	11	8869	2421.13	87.00	23.75	A1	0.070		-1.15
						12	13660	2452.30	134.00	24.06	A1	0.111		-0.95
						13	8665	2545.82	85.00	24.97	A1	0.068		-1.17
						14							damaged	
						15	12232	2431.52	120.00	23.85	A1	0.099		-1.00
					Sample Mean							**0.097**		**-1.02**
					Sample Standard Deviation							**0.019**		**0.09**
					Coefficient of Variation							**0.198**		**-0.09**
					Y_c									**-1.20**
					Characteristic bond strength, f_{wk} (N/mm^2)									**0.06**

Table F.17: CL90-s brick masonry bond strength calculations, 165 mm flow (2 months)

Test No.	Mortar ID	Unit Type	PC/lime / sand Ratio	Curing	Sample No.	Joint No.	Applied Load (g)	Weight of Top Unit (g)	Applied Load, F_1 (N)	Weight of Top Unit, W (N)	Failure Mode	Bond Strength, f_{wi} (N/mm^2)	Notes	$\log_{10}$ of bond strength (Y_i)
18	B_CL90s_165_6M_T	Brick	0:1:3	Lab	1	1	8563	2431.52	84.00	23.85	A1	0.067		-1.17
						2	15596	2441.91	153.00	23.96	A1	0.128		-0.89
						3	17023	2441.91	167.00	23.96	A1	0.140		-0.85
						4								
						5	18858	2628.95	185.00	25.79	A1	0.156		-0.81
					2	6								
						7	16310	2441.91	160.00	23.96	A6	0.134		-0.87
						8								
						9	19368	2431.52	190.00	23.85	A1	0.160		-0.80
						10	18756	2338.00	184.00	22.94	A1	0.155		-0.81
					1	11								
						12	20489	2545.82	201.00	24.97	A1	0.170		-0.77
						13	24975	2452.30	245.00	24.06	A1	0.208		-0.68
						14	23445	2462.69	230.00	24.16	A1	0.195		-0.71
						15	25994	2628.95	255.00	25.79	A1	0.217		-0.66
					Sample Mean							**0.157**		**-0.82**
					Sample Standard Deviation							**0.042**		**0.14**
					Coefficient of Variation							**0.266**		**-0.17**
					Y_c									**-1.09**
					Characteristic bond strength, f_{wk} (N/mm^2)									**0.08**

Table F.18: CL90-s brick masonry bond strength calculations, 165 mm flow (6 months)

Test No.	Mortar ID	Unit Type	PC/lime / sand Ratio	Curing	Sample No.	Joint No.	Applied Load (g)	Weight of Top Unit (g)	Applied Load, F_1 (N)	Weight of Top Unit, W (N)	Failure Mode	Bond Strength, f_{wi} (N/mm^2)	Notes	$\log_{10}$ of bond strength (Y_i)
19	B_CL90s_165_1YR_T	Brick	0:1:3	Lab	1	1	14271	2431.52	140.00	23.85	A1	0.116		-0.93
						2	24771	2441.91	243.00	23.96	A1	0.206		-0.69
						3	19266	2431.52	189.00	23.85	A1	0.159		-0.80
						4	25892	2446.38	254.00	24.00	A1	0.216		-0.67
						5	12232	2525.04	120.00	24.77	A1	0.099		-1.01
					2	6	15698	2431.52	154.00	23.85	A1	0.129		-0.89
						7	23853	2639.34	234.00	25.89	A1	0.198		-0.70
						8	16208	2431.52	159.00	23.85	A1	0.133		-0.88
						9	9786	2452.30	96.00	24.06	A1	0.078		-1.11
						10	17329	2452.30	170.00	24.06	A6	0.143		-0.85
					3	11	27013	2448.67	265.00	24.02	A1	0.226		-0.65
						12	20183	2504.26	198.00	24.57	A1	0.167		-0.78
						13	22426	2556.21	220.00	25.08	A1	0.186		-0.73
						14	23955	2473.08	235.00	24.26	A1	0.199		-0.70
						15	18756	2379.56	184.00	23.34	A1	0.155		-0.81
					Sample Mean							**0.161**		**-0.81**
					Sample Standard Deviation							**0.045**		**0.13**
					Coefficient of Variation							**0.277**		**-0.16**
					Y_c									**-1.07**
					Characteristic bond strength, f_{wk} (N/mm^2)									**0.09**

Table F.19: CL90-s brick masonry bond strength calculations, 165 mm flow (12 months)

Test No.	Mortar ID	Unit Type	PC/lime / sand Ratio	Curing	Sample No.	Joint No.	Applied Load (g)	Weight of Top Unit (g)	Applied Load, F_1 (N)	Weight of Top Unit, W (N)	Failure Mode	Bond Strength, f_{wi} (N/mm^2)	Notes	$\log_{10}$ of bond strength (Y_i)
20	B_NHL3.5_165_1M_T	Brick	0:1:2	Lab	1	1	41998	2421.13	412.00	23.75	A1	0.354		-0.45
						2	15698	2441.91	154.00	23.96	A1	0.129		-0.89
						3	33639	2431.52	330.00	23.85	A1	0.282		-0.55
						4							damaged	
						5	34862	2545.82	342.00	24.97	A1	0.293		-0.53
					2	6	47401	2379.56	465.00	23.34	A1	0.401		-0.40
						7							damaged	
						8	45362	2441.91	445.00	23.96	A1	0.383		-0.42
						9	19878	2431.52	195.00	23.85	A1	0.164		-0.78
						10	33537	2441.91	329.00	23.96	A1	0.282		-0.55
					3	11	45362	2431.52	445.00	23.85	A1	0.383		-0.42
						12	35474	2473.08	348.00	24.26	A1	0.298		-0.53
						13	55352	2483.48	543.00	24.36	A1	0.469		-0.33
						14	34047	2525.04	334.00	24.77	A1	0.286		-0.54
						15	57492	2525.04	564.00	24.77	A1	0.487		-0.31
					Sample Mean							**0.324**		**-0.52**
					Sample Standard Deviation							**0.105**		**0.17**
					Coefficient of Variation							**0.323**		**-0.32**
					Y_c									**-0.83**
					Characteristic bond strength, f_{wk} (N/mm^2)									**0.15**

Table F.20: NHL 3.5 brick masonry bond strength calculations, 165 mm flow (0:1:2) (1 month)

Test No.	Mortar ID	Unit Type	PC/lime / sand Ratio	Curing	Sample No.	Joint No.	Applied Load (g)	Weight of Top Unit (g)	Applied Load, F_1 (N)	Weight of Top Unit, W (N)	Failure Mode	Bond Strength, f_{wi} (N/mm^2)	Notes	$\log_{10}$ of bond strength (Y_i)
21	B_NHL3.5_165_2M_T	Brick	0:1:2	Lab	1	1	32620	2431.52	320.00	23.85	A1	0.274		-0.56
						2							damaged	
						3	47910	2441.91	470.00	23.96	A1	0.405		-0.39
						4	25892	2462.69	254.00	24.16	A1	0.216		-0.67
						5	44343	2431.52	435.00	23.85	A1	0.374		-0.43
					2	6	35678	2452.30	350.00	24.06	A1	0.300		-0.52
						7	53109	2441.91	521.00	23.96	A1	0.449		-0.35
						8	37615	2525.04	369.00	24.77	A1	0.317		-0.50
						9							damaged	
						10	44139	2483.48	433.00	24.36	A1	0.373		-0.43
					3	11	35168	2504.26	345.00	24.57	A1	0.296		-0.53
						12	44037	2587.39	432.00	25.38	A1	0.372		-0.43
						13	59837	2296.44	587.00	22.53	A1	0.507		-0.29
						14	57492	2431.52	564.00	23.85	A1	0.487		-0.31
						15	46483	2441.91	456.00	23.96	A1	0.393		-0.41
					Sample Mean							**0.366**		**-0.45**
					Sample Standard Deviation							**0.085**		**0.11**
					Coefficient of Variation							**0.232**		**-0.24**
					Y_c									**-0.65**
					Characteristic bond strength, f_{wk} (N/mm^2)									**0.22**

Table F.21: NHL 3.5 brick masonry bond strength calculations, 165 mm flow (0:1:2) (2 months)

Test No.	Mortar ID	Unit Type	PC/lime / sand Ratio	Curing	Sample No.	Joint No.	Applied Load (g)	Weight of Top Unit (g)	Applied Load, F_1 (N)	Weight of Top Unit, W (N)	Failure Mode	Bond Strength, f_{wi} (N/mm^2)	Notes	$\log_{10}$ of bond strength (Y_i)
22	B_NHL3.5_165_6M_T	Brick	0:1:2	Lab	1	1	35678	2441.91	350.00	23.96	A1	0.300		-0.52
						2	59633	2431.52	585.00	23.85	A1	0.505		-0.30
						3	35168	2431.52	345.00	23.85	A1	0.296		-0.53
						4	58919	2441.91	578.00	23.96	A1	0.499		-0.30
						5	44343	2639.34	435.00	25.89	A1	0.374		-0.43
					2	6	32722	2525.04	321.00	24.77	A1	0.275		-0.56
						7	32620	2338.00	320.00	22.94	A1	0.274		-0.56
						8	38736	2441.91	380.00	23.96	A1	0.326		-0.49
						9	59123	2452.30	580.00	24.06	A1	0.501		-0.30
						10	55454	2473.08	544.00	24.26	A1	0.470		-0.33
					3	11	44037	2441.91	432.00	23.96	A1	0.372		-0.43
						12	55352	2441.91	543.00	23.96	A1	0.469		-0.33
						13	72579	2431.52	712.00	23.85	A1	0.616		-0.21
						14	45872	2473.08	450.00	24.26	A1	0.387		-0.41
						15	66259	2504.26	650.00	24.57	A1	0.562		-0.25
					Sample Mean							**0.415**		**-0.40**
					Sample Standard Deviation							**0.110**		**0.12**
					Coefficient of Variation							**0.266**		**-0.30**
					Y_c									**-0.62**
					Characteristic bond strength, f_{wk} (N/mm^2)									**0.24**

Table F.22: NHL 3.5 brick masonry bond strength calculations, 165 mm flow (0:1:2) (6 months)

Test No.	Mortar ID	Unit Type	PC/lime / sand Ratio	Curing	Sample No.	Joint No.	Applied Load (g)	Weight of Top Unit (g)	Applied Load, F_1 (N)	Weight of Top Unit, W (N)	Failure Mode	Bond Strength, f_{wi} (N/mm^2)	Notes	$\log_{10}$ of bond strength (Y_i)
23	B_M6_170_1m_T	Brick	1:½:4	Lab	1	1	76962	2431.52	755.00	23.85	A1	0.654		-0.18
						2	77472	2441.91	760.00	23.96	A1	0.658		-0.18
						3	57900	2441.91	568.00	23.96	A1	0.491		-0.31
						4	86137	2525.04	845.00	24.77	A1	0.733		-0.14
						5	51376	2441.91	504.00	23.96	A1	0.435		-0.36
					2	6	39144	2483.48	384.00	24.36	A1	0.330		-0.48
						7	56473	2608.17	554.00	25.59	A1	0.478		-0.32
						8							damaged	
						9	62080	2525.04	609.00	24.77	A1	0.526		-0.28
						10	60550	2431.52	594.00	23.85	A1	0.513		-0.29
					3	11	59531	2441.91	584.00	23.96	A1	0.505		-0.30
						12	77982	2431.52	765.00	23.85	A1	0.663		-0.18
						13	81346	2379.56	798.00	23.34	A1	0.692		-0.16
						14	85933	2452.30	843.00	24.06	A1	0.731		-0.14
						15	55556	2483.48	545.00	24.36	A1	0.470		-0.33
					Sample Mean							**0.563**		**-0.26**
					Sample Standard Deviation							**0.124**		**0.10**
					Coefficient of Variation							**0.220**		**-0.39**
					Y_c									**-0.45**
					Characteristic bond strength, f_{wk} (N/mm^2)									**0.35**

Table F.23: M6brick masonry bond strength calculations, 170 mm flow (1 month)

Test No.	Mortar ID	Unit Type	PC/lime / sand Ratio	Curing	Sample No.	Joint No.	Applied Load (g)	Weight of Top Unit (g)	Applied Load, F_1 (N)	Weight of Top Unit, W (N)	Failure Mode	Bond Strength, f_{wi} (N/mm^2)	Notes	$\log_{10}$ of bond strength (Y_i)
24	B_M6_170_2m_T	Brick	1:½:4	Lab	1	1	86646	2504.26	850.00	24.57	A1	0.737		-0.13
						2	70031	2431.52	687.00	23.85	A1	0.595		-0.23
						3	84811	2431.52	832.00	23.85	A1	0.721		-0.14
						4	59531	2441.91	584.00	23.96	A1	0.505		-0.30
						5	89195	2452.30	875.00	24.06	A1	0.759		-0.12
					2	6	97859	2514.65	960.00	24.67	A1	0.833		-0.08
						7	82773	2628.95	812.00	25.79	A1	0.704		-0.15
						8	87054	2441.91	854.00	23.96	A1	0.741		-0.13
						9	55556	2452.30	545.00	24.06	A1	0.470		-0.33
						10	84811	2483.48	832.00	24.36	A1	0.721		-0.14
					3	11	83894	2379.56	823.00	23.34	A1	0.714		-0.15
						12							damaged	
						13	79511	2431.52	780.00	23.85	A1	0.676		-0.17
						14	89195	2441.91	875.00	23.96	A1	0.759		-0.12
						15	85933	2473.08	843.00	24.26	A1	0.731		-0.14
					Sample Mean							**0.690**		**-0.17**
					Sample Standard Deviation							**0.100**		**0.07**
					Coefficient of Variation							**0.145**		**-0.42**
					Y_c									**-0.30**
					Characteristic bond strength, f_{wk} (N/mm^2)									**0.50**

Table F.24: M6brick masonry bond strength calculations, 170 mm flow (2 months)

Test No.	Mortar ID	Unit Type	PC/lime / sand Ratio	Curing	Sample No.	Joint No.	Applied Load (g)	Weight of Top Unit (g)	Applied Load, F_1 (N)	Weight of Top Unit, W (N)	Failure Mode	Bond Strength, f_{wi} (N/mm^2)	Notes	$\log_{10}$ of bond strength (Y_i)
25	B_M6_170_6m_T	Brick	1:½:4	Lab	1	1	103976	2431.52	1020.00	23.85	A1	0.886		-0.05
						2	104077	2441.91	1021.00	23.96	A1	0.887		-0.05
						3	124465	2462.69	1221.00	24.16	A1	1.062		0.03
						4	79409	2504.26	779.00	24.57	A1	0.675		-0.17
						5	127421	2431.52	1250.00	23.85	A1	1.087		0.04
					2	6	90724	2462.69	890.00	24.16	A1	0.772		-0.11
						7	100612	2441.91	987.00	23.96	A1	0.857		-0.07
						8	112334	2431.52	1102.00	23.85	A1	0.957		-0.02
						9	89297	2421.13	876.00	23.75	A1	0.760		-0.12
						10	98573	2628.95	967.00	25.79	A1	0.839		-0.08
					3	11	111927	2608.17	1098.00	25.59	A1	0.954		-0.02
						12	126707	2566.60	1243.00	25.18	A1	1.081		0.03
						13	90724	2587.39	890.00	25.38	A1	0.772		-0.11
						14	92966	2431.52	912.00	23.85	A1	0.791		-0.10
						15	98369	2441.91	965.00	23.96	A1	0.838		-0.08
					Sample Mean							**0.881**		**-0.06**
					Sample Standard Deviation							**0.125**		**0.06**
					Coefficient of Variation							**0.142**		**-1.04**
					Y_c									**-0.18**
					Characteristic bond strength, f_{wk} (N/mm^2)									**0.67**

Table F.25: M6brick masonry bond strength calculations, 170 mm flow (6 months)

Test No.	Mortar ID	Unit Type	PC/lime / sand Ratio	Curing	Sample No.	Joint No.	Applied Load (g)	Weight of Top Unit (g)	Applied Load, F_1 (N)	Weight of Top Unit, W (N)	Failure Mode	Bond Strength, f_{wi} (N/mm^2)	Notes	$\log_{10}$ of bond strength (Y_i)
26	B_NHL5_170_1m_T	Brick	0:1:3	Lab	1	1	25484	2441.91	250.00	23.96	A1	0.213		-0.67
						2							damaged	
						3	23955	2431.52	235.00	23.85	A1	0.199		-0.70
						4	43119	2545.82	423.00	24.97	A1	0.364		-0.44
						5	32824	2577.00	322.00	25.28	A1	0.275		-0.56
					2	6	39144	2483.48	384.00	24.36	A1	0.330		-0.48
						7	32620	2379.56	320.00	23.34	A1	0.274		-0.56
						8	33028	2431.52	324.00	23.85	A1	0.277		-0.56
						9	48930	2441.91	480.00	23.96	A1	0.414		-0.38
						10	37105	2639.34	364.00	25.89	A1	0.312		-0.51
					3	11	29256	2441.91	287.00	23.96	A1	0.245		-0.61
						12	29766	2441.91	292.00	23.96	A1	0.249		-0.60
						13	35576	2452.30	349.00	24.06	A1	0.299		-0.52
						14	26911	2525.04	264.00	24.77	A1	0.225		-0.65
						15	23955	3605.72	235.00	35.37	A1	0.199		-0.70
					Sample Mean							**0.277**		**-0.57**
					Sample Standard Deviation							**0.063**		**0.10**
					Coefficient of Variation							**0.227**		**-0.17**
					Y_c									**-0.75**
					Characteristic bond strength, f_{wk} (N/mm^2)									**0.18**

Table F.26: NHL 5 brick masonry bond strength calculations, 170 mm flow (1 month)

Test No.	Mortar ID	Unit Type	PC/lime / sand Ratio	Curing	Sample No.	Joint No.	Applied Load (g)	Weight of Top Unit (g)	Applied Load, F_1 (N)	Weight of Top Unit, W (N)	Failure Mode	Bond Strength, f_{wi} (N/mm^2)	Notes	$\log_{10}$ of bond strength (Y_i)
27	B_NHL5_170_2m_T	Brick	0:1:3	Lab	1	1	35311	2431.52	346.40	23.85	A1	0.297		-0.53
						2	44037	2441.91	432.00	23.96	A1	0.372		-0.43
						3	59531	2441.91	584.00	23.96	A1	0.505		-0.30
						4							damaged	
						5							damaged	
					2	6	27217	2473.08	267.00	24.26	A1	0.227		-0.64
						7	33537	2431.52	329.00	23.85	A1	0.282		-0.55
						8	40979	2431.52	402.00	23.85	A1	0.345		-0.46
						9	32926	2441.91	323.00	23.96	A1	0.276		-0.56
						10	43833	2431.52	430.00	23.85	A1	0.370		-0.43
					3	11							damaged	
						12	44139	2452.30	433.00	24.06	A1	0.373		-0.43
						13	55352	2483.48	543.00	24.36	A1	0.469		-0.33
						14	57492	2545.82	564.00	24.97	A1	0.487		-0.31
						15	66055	2452.30	648.00	24.06	A1	0.561		-0.25
					Sample Mean							**0.380**		**-0.44**
					Sample Standard Deviation							**0.104**		**0.12**
					Coefficient of Variation							**0.274**		**-0.28**
					Y_c									**-0.67**
					Characteristic bond strength, f_{wk} (N/mm^2)									**0.22**

Table F.27: NHL 5 brick masonry bond strength calculations, 170 mm flow (2 months)

Test No.	Mortar ID	Unit Type	PC/lime / sand Ratio	Curing	Sample No.	Joint No.	Applied Load (g)	Weight of Top Unit (g)	Applied Load, F_1 (N)	Weight of Top Unit, W (N)	Failure Mode	Bond Strength, f_{wi} (N/mm^2)	Notes	$\log_{10}$ of bond strength (Y_i)
28	B_NHL5_170_6m_T	Brick	0:1:3	Lab	1	1	51478	2388.38	505.00	23.43	A1	0.436		-0.36
						2	41081	2399.59	403.00	23.54	A1	0.346		-0.46
						3	51988	2477.06	510.00	24.30	A1	0.440		-0.36
						4	43119	2548.42	423.00	25.00	A1	0.364		-0.44
						5	25892	2742.10	254.00	26.90	A1	0.216		-0.67
					2	6	55963	3113.15	549.00	30.54	A1	0.474		-0.32
						7	69317	2399.59	680.00	23.54	A1	0.589		-0.23
						8	55352	2385.32	543.00	23.40	A1	0.469		-0.33
						9							damaged	
						10	55454	2497.45	544.00	24.50	A1	0.470		-0.33
					3	11	44241	2592.25	434.00	25.43	A1	0.373		-0.43
						12							damaged	
						13	59837	2399.59	587.00	23.54	A1	0.507		-0.29
						14	63507	2439.35	623.00	23.93	A1	0.539		-0.27
						15	49949	2479.10	490.00	24.32	A1	0.422		-0.37
					Sample Mean							**0.434**		**-0.37**
					Sample Standard Deviation							**0.095**		**0.11**
					Coefficient of Variation							**0.219**		**-0.29**
					Y_c									**-0.58**
					Characteristic bond strength, f_{wk} (N/mm^2)									**0.26**

Table F.28: NHL 5 brick masonry bond strength calculations, 170 mm flow (6 months)

Test No.	Mortar ID	Unit Type	PC/lime / sand Ratio	Curing	Sample No.	Joint No.	Applied Load (g)	Weight of Top Unit (g)	Applied Load, F_1 (N)	Weight of Top Unit, W (N)	Failure Mode	Bond Strength, f_{wi} (N/mm^2)	Notes	$\log_{10}$ of bond strength (Y_i)
29	B_NHL3.5_170_1M_T	Brick	0:1:3	Lab	1	1	32926	2434.64	323.00	23.88	A1	0.276		-0.56
						2	19286	2639.34	189.20	25.89	A1	0.159		-0.80
						3	29052	2528.16	285.00	24.80	A1	0.243		-0.61
						4	23649	3546.49	232.00	34.79	A1	0.196		-0.71
						5	24985	2420.09	245.10	23.74	A1	0.208		-0.68
					2	6	46004	2452.30	451.30	24.06	A1	0.389		-0.41
						7	36188	2375.41	355.00	23.30	A1	0.304		-0.52
						8	33598	2437.75	329.60	23.91	A1	0.282		-0.55
						9	20224	2479.32	198.40	24.32	A1	0.167		-0.78
						10	24098	2525.04	236.40	24.77	A1	0.201		-0.70
					3	11	32620	2553.10	320.00	25.05	A1	0.274		-0.56
						12	35474	2639.34	348.00	25.89	A1	0.298		-0.53
						13	29211	2525.04	286.56	24.77	A1	0.244		-0.61
						14	20856	2491.79	204.60	24.44	A1	0.173		-0.76
						15	31131	2441.91	305.40	23.96	A1	0.261		-0.58
					Sample Mean							**0.245**		**-0.62**
					Sample Standard Deviation							**0.062**		**0.11**
					Coefficient of Variation							**0.255**		**-0.18**
					Y_c									**-0.84**
					Characteristic bond strength, f_{wk} (N/mm^2)									**0.15**

Table F.29: NHL3. 5 brick masonry bond strength calculations, 170 mm flow (1 month)

Test No.	Mortar ID	Unit Type	PC/lime / sand Ratio	Curing	Sample No.	Joint No.	Applied Load (g)	Weight of Top Unit (g)	Applied Load, F_1 (N)	Weight of Top Unit, W (N)	Failure Mode	Bond Strength, f_{wi} (N/mm^2)	Notes	$\log_{10}$ of bond strength (Y_i)
30	B_NHL3.5_170_2M_T	Brick	0:1:3	Lab	1	1	33221	2431.52	325.90	23.85	A1	0.279		-0.55
						2	56024	2456.46	549.60	24.10	A1	0.474		-0.32
						3	47482	2525.04	465.80	24.77	A1	0.401		-0.40
						4	25234	2639.34	247.55	25.89	A1	0.210		-0.68
						5	55250	2452.30	542.00	24.06	A1	0.468		-0.33
					2	6	35817	2670.52	351.36	26.20	A1	0.301		-0.52
						7							damaged	
						8	25892	2438.79	254.00	23.92	A1	0.216		-0.67
						9	37207	2545.82	365.00	24.97	A1	0.313		-0.50
						10	23904	2457.50	234.50	24.11	A1	0.199		-0.70
					3	11	46335	2519.84	454.55	24.72	A1	0.391		-0.41
						12							damaged	
						13	27385	2449.18	268.65	24.03	A1	0.229		-0.64
						14	29515	2437.75	289.54	23.91	A1	0.247		-0.61
						15	42029	3517.81	412.30	34.51	A1	0.354		-0.45
					Sample Mean							**0.314**		**-0.52**
					Sample Standard Deviation							**0.096**		**0.13**
					Coefficient of Variation							**0.307**		**-0.25**
					Y_c									**-0.78**
					Characteristic bond strength, f_{wk} (N/mm^2)									**0.17**

Table F.30: NHL3. 5 brick masonry bond strength calculations, 170 mm flow (2 months)

Test No.	Mortar ID	Unit Type	PC/lime / sand Ratio	Curing	Sample No.	Joint No.	Applied Load (g)	Weight of Top Unit (g)	Applied Load, F_1 (N)	Weight of Top Unit, W (N)	Failure Mode	Bond Strength, f_{wi} (N/mm^2)	Notes	$\log_{10}$ of bond strength (Y_i)
31	B_NHL3.5_170_6M_T	Brick	0:1:3	Lab	1	1	36157	2431.52	354.70	23.85	A1	0.304		-0.52
						2	58512	2425.29	574.00	23.79	A1	0.496		-0.30
						3	34964	2441.91	343.00	23.96	A1	0.294		-0.53
						4	58002	2462.69	569.00	24.16	A1	0.491		-0.31
						5							damaged	
					2	6	30377	2521.40	298.00	24.73	A1	0.254		-0.59
						7	37513	2431.52	368.00	23.85	A1	0.316		-0.50
						8	39144	2548.94	384.00	25.01	A1	0.330		-0.48
						9	39653	2639.34	389.00	25.89	A1	0.334		-0.48
						10	47401	2548.94	465.00	25.01	A1	0.400		-0.40
					3	11	41794	2441.91	410.00	23.96	A1	0.352		-0.45
						12	58410	2468.30	573.00	24.21	A6	0.495		-0.31
						13	73394	2441.91	720.00	23.96	A1	0.623		-0.21
						14							damaged	
						15	69623	2441.91	683.00	23.96	A1	0.591		-0.23
					Sample Mean							**0.406**		**-0.41**
					Sample Standard Deviation							**0.120**		**0.12**
					Coefficient of Variation							**0.295**		**-0.31**
					Y_c									**-0.65**
					Characteristic bond strength, f_{wk} (N/mm^2)									**0.22**

Table F.31: NHL3. 5 brick masonry bond strength calculations, 170 mm flow (6 months)

Test No.	Mortar ID	Unit Type	PC/lime / sand Ratio	Curing	Sample No.	Joint No.	Applied Load (g)	Weight of Top Unit (g)	Applied Load, F_1 (N)	Weight of Top Unit, W (N)	Failure Mode	Bond Strength, f_{wi} (N/mm^2)	Notes	$\log_{10}$ of bond strength (Y_i)
32	B_NHL2_170_1M_T	Brick	0:1:3	Lab	1	1	18145	2479.10	178.00	24.32	A1	0.150		-0.83
						2	15291	2395.51	150.00	23.50	A1	0.125		-0.90
						3							damaged	
						4	19368	2374.11	190.00	23.29	A1	0.160		-0.80
						5	16004	2477.06	157.00	24.30	A1	0.131		-0.88
					2	6	9888	2589.19	97.00	25.40	A1	0.079		-1.10
						7							damaged	
						8							damaged	
						9	12232	2440.37	120.00	23.94	A6	0.099		-1.00
						10	12436	2424.06	122.00	23.78	A1	0.101		-1.00
					3	11	15698	2477.06	154.00	24.30	A1	0.129		-0.89
						12	14781	2501.53	145.00	24.54	A1	0.121		-0.92
						13							damaged	
						14	17941	2438.33	176.00	23.92	A1	0.148		-0.83
						15	15698	2387.36	154.00	23.42	A1	0.129		-0.89
					Sample Mean							**0.125**		**-0.91**
					Sample Standard Deviation							**0.024**		**0.09**
					Coefficient of Variation							**0.194**		**-0.10**
					Y_c									**-1.09**
					Characteristic bond strength, f_{wk} (N/mm^2)									**0.08**

Table F.32: NHL2 brick masonry bond strength calculations, 170 mm flow (1 month)

Test No.	Mortar ID	Unit Type	PC/lime / sand Ratio	Curing	Sample No.	Joint No.	Applied Load (g)	Weight of Top Unit (g)	Applied Load, F_1 (N)	Weight of Top Unit, W (N)	Failure Mode	Bond Strength, f_{wi} (N/mm^2)	Notes	$\log_{10}$ of bond strength (Y_i)
33	B_NHL2_170_2M_T	Brick	0:1:3	Lab	1	1	14679	2400.61	144.00	23.55	A1	0.120		-0.92
						2	24363	2535.17	239.00	24.87	A1	0.203		-0.69
						3	21509	2388.38	211.00	23.43	A1	0.178		-0.75
						4	37717	2395.51	370.00	23.50	A1	0.317		-0.50
						5	38940	2444.44	382.00	23.98	A1	0.328		-0.48
					2	6	19368	2604.49	190.00	25.55	A1	0.160		-0.80
						7	13456	2465.85	132.00	24.19	A1	0.109		-0.96
						8	24975	2282.36	245.00	22.39	A1	0.208		-0.68
						9	19164	2436.29	188.00	23.90	A1	0.158		-0.80
						10	21407	2399.59	210.00	23.54	A1	0.178		-0.75
					3	11							damaged	
						12	21407	2399.59	210.00	23.54	A1	0.178		-0.75
						13	35066	2477.06	344.00	24.30	A1	0.295		-0.53
						14	16718	2533.13	164.00	24.85	A1	0.137		-0.86
						15	25892	2354.74	254.00	23.10	A1	0.216		-0.67
					Sample Mean							**0.199**		**-0.72**
					Sample Standard Deviation							**0.070**		**0.15**
					Coefficient of Variation							**0.349**		**-0.20**
					Y_c									**-1.01**
					Characteristic bond strength, f_{wk} (N/mm^2)									**0.10**

Table F.33: NHL2 brick masonry bond strength calculations, 170 mm flow (2 months)

Test No.	Mortar ID	Unit Type	PC/lime / sand Ratio	Curing	Sample No.	Joint No.	Applied Load (g)	Weight of Top Unit (g)	Applied Load, F_1 (N)	Weight of Top Unit, W (N)	Failure Mode	Bond Strength, f_{wi} (N/mm^2)	Notes	$\log_{10}$ of bond strength (Y_i)
34	B_NHL2_170_6M_T	Brick	0:1:3	Lab	1	1	13456	2384.30	132.00	23.39	A1	0.109		-0.96
						2	17329	2390.42	170.00	23.45	A1	0.143		-0.85
						3	17125	2477.06	168.00	24.30	A1	0.141		-0.38
						4	23445	2503.57	230.00	24.56	A1	0.195		-0.71
						5	36086	2477.06	354.00	24.30	A1	0.303		-0.38
					2	6							damaged	
						7	25994	2598.37	255.00	25.49	A1	0.217		-0.66
						8	36290	2414.88	356.00	23.69	A1	0.305		-0.52
						9	12538	2399.59	123.00	23.54	A1	0.102		-0.38
						10	26096	2422.02	256.00	23.76	A1	0.218		-0.66
					3	11	39653	2436.29	389.00	23.90	A1	0.334		-0.38
						12	29052	2342.51	285.00	22.98	A1	0.243		-0.61
						13	32824	2579.00	322.00	25.30	A1	0.275		-0.56
						14							damaged	
						15	18960	2431.19	186.00	23.85	A1	0.157		-0.81
					Sample Mean							**0.211**		**-0.60**
					Sample Standard Deviation							**0.078**		**0.19**
					Coefficient of Variation							**0.370**		**-0.32**
					Y_c									**-0.98**
					Characteristic bond strength, f_{wk} (N/mm^2)									**0.11**

Table F.34: NHL2 brick masonry bond strength calculations, 170 mm flow (6 months)

Test No.	Mortar ID	Unit Type	PC/lime / sand Ratio	Curing	Sample No.	Joint No.	Applied Load (g)	Weight of Top Unit (g)	Applied Load, F_1 (N)	Weight of Top Unit, W (N)	Failure Mode	Bond Strength, f_{wi} (N/mm^2)	Notes	$\log_{10}$ of bond strength (Y_i)
35	B_CL90s_170_1M_T	Brick	0:1:3	Lab	1	1	7136	2422.02	70.00	23.76	A1	0.055		-1.26
						2	4485	2400.61	44.00	23.55	A1	0.032		-1.49
						3	6422	2538.23	63.00	24.90	A1	0.049		-1.31
						4							damaged	
						5	6014	2477.06	59.00	24.30	A1	0.046		-1.34
					2	6							damaged	
						7							damaged	
						8	7951	2412.84	78.00	23.67	A1	0.062		-1.21
						9	6626	2444.44	65.00	23.98	A1	0.051		-1.29
						10	4485	2385.32	44.00	23.40	A1	0.032		-1.49
					3	11	9786	2482.16	96.00	24.35	A1	0.078		-1.11
						12							damaged	
						13	7136	2547.40	70.00	24.99	A1	0.055		-1.26
						14							damaged	
						15	6626	2399.59	65.00	23.54	A1	0.051		-1.29
					Sample Mean							**0.051**		**-1.30**
					Sample Standard Deviation							**0.013**		**0.12**
					Coefficient of Variation							**0.261**		**-0.09**
					Y_c									**-1.53**
					Characteristic bond strength, f_{wk} (N/mm^2)									**0.03**

Table F.35: CL90-s brick masonry bond strength calculations, 170 mm flow (1 month)

Test No.	Mortar ID	Unit Type	PC/lime / sand Ratio	Curing	Sample No.	Joint No.	Applied Load (g)	Weight of Top Unit (g)	Applied Load, F_1 (N)	Weight of Top Unit, W (N)	Failure Mode	Bond Strength, f_{wi} (N/mm^2)	Notes	$\log_{10}$ of bond strength (Y_i)
36	B_CL90s_170_2M_T	Brick	0:1:3	Lab	1	1	12232	2422.02	120.00	23.76	A1	0.099		-1.00
						2	7034	2440.37	69.00	23.94	A1	0.054		-1.27
						3							damaged	
						4	12538	2347.60	123.00	23.03	A1	0.102		-0.99
						5	10398	2458.72	102.00	24.12	A1	0.083		-1.08
					2	6	10194	2465.85	100.00	24.19	A1	0.081		-1.09
						7	12232	2390.42	120.00	23.45	A1	0.099		-1.00
						8	9480	2434.25	93.00	23.88	A1	0.075		-1.12
						9	8665	2357.80	85.00	23.13	A1	0.068		-1.17
						10							damaged	
					3	11							damaged	
						12							damaged	
						13	9684	2430.17	95.00	23.84	A1	0.077		-1.11
						14	13252	2436.29	130.00	23.90	A1	0.108		-0.97
						15	12640	2477.06	124.00	24.30	A1	0.102		-0.99
					Sample Mean							**0.086**		**-1.07**
					Sample Standard Deviation							**0.017**		**0.09**
					Coefficient of Variation							**0.196**		**-0.09**
					Y_c									**-1.25**
					Characteristic bond strength, f_{wk} (N/mm^2)									**0.06**

Table F.36: CL90-s brick masonry bond strength calculations, 170 mm flow (2 months)

Test No.	Mortar ID	Unit Type	PC/lime / sand Ratio	Curing	Sample No.	Joint No.	Applied Load (g)	Weight of Top Unit (g)	Applied Load, F_1 (N)	Weight of Top Unit, W (N)	Failure Mode	Bond Strength, f_{wi} (N/mm^2)	Notes	$\log_{10}$ of bond strength (Y_i)
37	B_CL90s_170_6M_T	Brick	0:1:3	Lab	1	1	11213	2479.10	110.00	24.32	A1	0.090		-1.05
						2	12334	2504.59	121.00	24.57	A1	0.100		-1.00
						3	15698	2367.99	154.00	23.23	A1	0.129		-0.89
						4							damaged	
						5	19368	2444.44	190.00	23.98	A1	0.160		-0.80
					2	6	14985	2440.37	147.00	23.94	A1	0.122		-0.91
						7							damaged	
						8	8563	2501.53	84.00	24.54	A1	0.067		-1.17
						9	19062	2515.80	187.00	24.68	A1	0.157		-0.80
						10	17023	2354.74	167.00	23.10	A1	0.140		-0.85
					1	11	22834	2436.29	224.00	23.90	A1	0.190		-0.72
						12							damaged	
						13	25790	2482.16	253.00	24.35	A1	0.215		-0.67
						14	22936	2528.03	225.00	24.80	A1	0.191		-0.72
						15	26198	2538.23	257.00	24.90	A1	0.219		-0.66
					Sample Mean							**0.148**		**-0.85**
					Sample Standard Deviation							**0.049**		**0.16**
					Coefficient of Variation							**0.331**		**-0.19**
					Y_c									**-1.16**
					Characteristic bond strength, f_{wk} (N/mm^2)									**0.07**

Table F.37: CL90-s brick masonry bond strength calculations, 170 mm flow (6 months)

Test No.	Mortar ID	Unit Type	PC/lime / sand Ratio	Curing	Sample No.	Joint No.	Applied Load (g)	Weight of Top Unit (g)	Applied Load, F_1 (N)	Weight of Top Unit, W (N)	Failure Mode	Bond Strength, f_{wi} (N/mm^2)	Notes	$\log_{10}$ of bond strength (Y_i)
38	B_M6_165_1m_T	Brick	1:½:4	External	1	1	30581	2388.38	300.00	23.43	A1	0.256		-0.59
						2	80428	2412.84	789.00	23.67	A1	0.684		-0.17
						3	76860	2465.85	754.00	24.19	A1	0.653		-0.18
						4	58716	2509.68	576.00	24.62	A1	0.498		-0.30
						5	49847	2395.51	489.00	23.50	A1	0.422		-0.38
					2	6	31804	2618.76	312.00	25.69	A1	0.267		-0.57
						7	89093	2487.26	874.00	24.40	A1	0.758		-0.12
						8							damaged	
						9	81753	2385.32	802.00	23.40	A1	0.695		-0.16
						10	55352	2548.42	543.00	25.00	A1	0.469		-0.33
					3	11	57085	2416.92	560.00	23.71	A1	0.484		-0.32
						12	80122	2397.55	786.00	23.52	A1	0.681		-0.17
						13	73700	2502.55	723.00	24.55	A1	0.626		-0.20
						14	53313	2637.10	523.00	25.87	A1	0.451		-0.35
						15	91131	2392.46	894.00	23.47	A1	0.776		-0.11
					Sample Mean							**0.551**		**-0.28**
					Sample Standard Deviation							**0.169**		**0.15**
					Coefficient of Variation							**0.307**		**-0.55**
					Y_c									**-0.58**
					Characteristic bond strength, f_{wk} (N/mm^2)									**0.26**

Table F.38: M6 brick masonry bond strength calculations, 165 mm flow, outdoor cured (1 month)

Test No.	Mortar ID	Unit Type	PC/lime / sand Ratio	Curing	Sample No.	Joint No.	Applied Load (g)	Weight of Top Unit (g)	Applied Load, F_1 (N)	Weight of Top Unit, W (N)	Failure Mode	Bond Strength, f_{wi} (N/mm^2)	Notes	$\log_{10}$ of bond strength (Y_i)
39	B_M6_165_2m_T	Brick	1:½:4	External	1	1	86137	2480.12	845.00	24.33	A1	0.733		-0.14
						2	84811	2396.53	832.00	23.51	A1	0.721		-0.14
						3	53007	2402.65	520.00	23.57	A1	0.449		-0.35
						4	55963	2619.78	549.00	25.70	A1	0.474		-0.32
						5	80224	2691.13	787.00	26.40	A1	0.682		-0.17
					2	6	97248	2694.19	954.00	26.43	A1	0.828		-0.08
						7	50459	2385.32	495.00	23.40	A1	0.427		-0.37
						8	88991	2497.45	873.00	24.50	A1	0.757		-0.12
						9	58002	2395.51	569.00	23.50	A1	0.491		-0.31
						10	88583	2431.19	869.00	23.85	A1	0.754		-0.12
					3	11	67176	2489.30	659.00	24.42	A1	0.570		-0.24
						12	97248	2405.71	954.00	23.60	A1	0.828		-0.08
						13	81957	2395.51	804.00	23.50	A1	0.697		-0.16
						14	89704	2595.31	880.00	25.46	A1	0.763		-0.12
						15	104077	2436.29	1021.00	23.90	A1	0.887		-0.05
					Sample Mean							**0.671**		**-0.18**
					Sample Standard Deviation							**0.150**		**0.11**
					Coefficient of Variation							**0.224**		**-0.57**
					Y_c									**-0.39**
					Characteristic bond strength, f_{wk} (N/mm^2)									**0.41**

Table F.39: M6 brick masonry bond strength calculations, 165 mm flow, outdoor cured (2 months)

Test No.	Mortar ID	Unit Type	PC/lime / sand Ratio	Curing	Sample No.	Joint No.	Applied Load (g)	Weight of Top Unit (g)	Applied Load, F_1 (N)	Weight of Top Unit, W (N)	Failure Mode	Bond Strength, f_{wi} (N/mm^2)	Notes	$\log_{10}$ of bond strength (Y_i)
40	B_M6_165_6m_T	Brick	1:½:4	External	1	1	99898	2512.74	980.00	24.65	A1	0.851		-0.07
						2	134760	2389.40	1322.00	23.44	A1	1.150		0.06
						3	132416	2435.27	1299.00	23.89	A1	1.130		0.05
						4	83894	2412.84	823.00	23.67	A1	0.714		-0.15
						5	89602	2456.68	879.00	24.10	A1	0.762		-0.12
					2	6	95107	2476.04	933.00	24.29	A1	0.810		-0.09
						7	79511	2401.63	780.00	23.56	A1	0.676		-0.17
						8							damaged	
						9	76249	2513.76	748.00	24.66	A1	0.648		-0.19
						10	43323	2527.01	425.00	24.79	A1	0.366		-0.44
					3	11	132518	2399.59	1300.00	23.54	A1	1.131		0.05
						12	127829	2322.12	1254.00	22.78	A1	1.090		0.04
						13	91233	2401.63	895.00	23.56	A1	0.777		-0.11
						14	116106	2430.17	1139.00	23.84	A1	0.990		0.00
						15	115189	2441.39	1130.00	23.95	A1	0.982		-0.01
					Sample Mean							**0.862**		**-0.08**
					Sample Standard Deviation							**0.228**		**0.13**
					Coefficient of Variation							**0.265**		**-1.65**
					Y_c									**-0.34**
					Characteristic bond strength, f_{wk} (N/mm^2)									**0.46**

Table F.40: M6 brick masonry bond strength calculations, 165 mm flow, outdoor cured (6 months)

Test No.	Mortar ID	Unit Type	PC/lime / sand Ratio	Curing	Sample No.	Joint No.	Applied Load (g)	Weight of Top Unit (g)	Applied Load, F_1 (N)	Weight of Top Unit, W (N)	Failure Mode	Bond Strength, f_{wi} (N/mm^2)	Notes	$\log_{10}$ of bond strength (Y_i)
41	B_NHL5_165_1m_T	Brick	0:1:3	External	1	1	23445	2512.74	230.00	24.65	A1	0.195		-0.71
						2	23955	2536.19	235.00	24.88	A1	0.199		-0.70
						3	21407	2543.32	210.00	24.95	A1	0.178		-0.75
						4	36188	2390.42	355.00	23.45	A1	0.304		-0.52
						5	31906	2441.39	313.00	23.95	A1	0.268		-0.57
					2	6							damaged	
						7	23955	2356.78	235.00	23.12	A1	0.199		-0.70
						8	24465	2359.84	240.00	23.15	A1	0.204		-0.69
						9	18858	2401.63	185.00	23.56	A1	0.156		-0.81
						10							damaged	
					3	11	25280	2546.38	248.00	24.98	A1	0.211		-0.68
						12	24465	2482.16	240.00	24.35	A1	0.204		-0.69
						13	22426	2396.53	220.00	23.51	A1	0.186		-0.73
						14	19266	2395.51	189.00	23.50	A1	0.159		-0.80
						15	19878	2354.74	195.00	23.10	A1	0.164		-0.78
					Sample Mean							**0.202**		**-0.70**
					Sample Standard Deviation							**0.042**		**0.08**
					Coefficient of Variation							**0.208**		**-0.12**
					Y_c									**-0.86**
					Characteristic bond strength, f_{wk} (N/mm^2)									**0.14**

Table F.41: NHL 5 brick masonry bond strength calculations, 165 mm flow, outdoor cured (1 month)

Test No.	Mortar ID	Unit Type	PC/lime / sand Ratio	Curing	Sample No.	Joint No.	Applied Load (g)	Weight of Top Unit (g)	Applied Load, F_1 (N)	Weight of Top Unit, W (N)	Failure Mode	Bond Strength, f_{wi} (N/mm^2)	Notes	$\log_{10}$ of bond strength (Y_i)
42	B_NHL5_165_2m_T	Brick	0:1:3	External	1	1	29358	2331.29	288.00	22.87	A1	0.246		-0.61
						2	19878	2400.61	195.00	23.55	A1	0.164		-0.78
						3	39450	2396.53	387.00	23.51	A1	0.332		-0.48
						4							damaged	
						5	24975	2360.86	245.00	23.16	A1	0.208		-0.68
					2	6	39755	2497.45	390.00	24.50	A1	0.335		-0.48
						7	37105	2514.78	364.00	24.67	A1	0.312		-0.51
						8	39042	2485.22	383.00	24.38	A1	0.329		-0.48
						9	25892	2401.63	254.00	23.56	A1	0.216		-0.67
						10	27523	2352.70	270.00	23.08	A1	0.230		-0.64
					3	11	41794	2589.19	410.00	25.40	A1	0.352		-0.45
						12	31600	2505.61	310.00	24.58	A1	0.265		-0.58
						13							damaged	
						14	38736	2430.17	380.00	23.84	A1	0.326		-0.49
						15					A1			
					Sample Mean							**0.276**		**-0.57**
					Sample Standard Deviation							**0.062**		**0.11**
					Coefficient of Variation							**0.226**		**-0.19**
					Y_c									**-0.77**
					Characteristic bond strength, f_{wk} (N/mm^2)									**0.17**

Table F.42: NHL 5 brick masonry bond strength calculations, 165 mm flow, outdoor cured (2 months)

Test No.	Mortar ID	Unit Type	PC/lime / sand Ratio	Curing	Sample No.	Joint No.	Applied Load (g)	Weight of Top Unit (g)	Applied Load, F_1 (N)	Weight of Top Unit, W (N)	Failure Mode	Bond Strength, f_{wi} (N/mm^2)	Notes	$\log_{10}$ of bond strength (Y_i)
43	B_NHL5_165_6m_T	Brick	0:1:3	External	1	1	33129	2424.06	325.00	23.78	A1	0.278		-0.56
						2	45362	2528.03	445.00	24.80	A1	0.383		-0.42
						3	49847	2506.63	489.00	24.59	A1	0.421		-0.38
						4							damaged	
						5	45872	2360.86	450.00	23.16	A1	0.387		-0.41
					2	6	57737	2419.98	566.40	23.74	A1	0.489		-0.31
						7	56575	2428.13	555.00	23.82	A1	0.479		-0.32
						8							damaged	
						9	50968	2395.51	500.00	23.50	A1	0.431		-0.37
						10	37207	2538.23	365.00	24.90	A1	0.313		-0.50
					3	11	25484	2477.06	250.00	24.30	A1	0.213		-0.67
						12	37207	2485.22	365.00	24.38	A1	0.313		-0.50
						13	38736	2378.19	380.00	23.33	A1	0.326		-0.49
						14	34659	2354.74	340.00	23.10	A1	0.291		-0.54
						15	22426	2412.84	220.00	23.67	A1	0.186		-0.73
					Sample Mean							**0.347**		**-0.48**
					Sample Standard Deviation							**0.095**		**0.13**
					Coefficient of Variation							**0.273**		**-0.27**
					Y_c									**-0.72**
					Characteristic bond strength, f_{wk} (N/mm^2)									**0.19**

Table F.43: NHL 5 brick masonry bond strength calculations, 165 mm flow, outdoor cured (6 months)

Test No.	Mortar ID	Unit Type	PC/lime / sand Ratio	Curing	Sample No.	Joint No.	Applied Load (g)	Weight of Top Unit (g)	Applied Load, F_1 (N)	Weight of Top Unit, W (N)	Failure Mode	Bond Strength, f_{wi} (N/mm^2)	Notes	$\log_{10}$ of bond strength (Y_i)
44	B_CL90s_165_1M_T	Brick	0:1:3	External	1	1	6626	2430.17	65.00	23.84	A1	0.051		-1.29
						2	4383	2396.53	43.00	23.51	A1	0.032		-1.50
						3	5097	2546.38	50.00	24.98	A1	0.038		-1.42
						4	8665	2410.81	85.00	23.65	A1	0.068		-1.17
						5	8665	2390.42	85.00	23.45	A1	0.068		-1.17
					2	6	9684	2441.39	95.00	23.95	A1	0.077		-1.11
						7							damaged	
						8							damaged	
						9	8970	2501.53	88.00	24.54	A1	0.071		-1.15
						10	7441	2433.23	73.00	23.87	A1	0.058		-1.24
					3	11							damaged	
						12	8665	2445.46	85.00	23.99	A1	0.068		-1.17
						13	6626	2405.71	65.00	23.60	A1	0.051		-1.29
						14	8665	2589.19	85.00	25.40	A1	0.068		-1.17
						15	5505	2441.39	54.00	23.95	A1	0.041		-1.39
					Sample Mean							**0.058**		**-1.26**
					Sample Standard Deviation							**0.015**		**0.13**
					Coefficient of Variation							**0.259**		**-0.10**
					Y_c									**-1.50**
					Characteristic bond strength, f_{wk} (N/mm^2)									**0.03**

Table F.44: NHL CL90-s brick masonry bond strength calculations, 165 mm flow, outdoor cured (1 month)

Test No.	Mortar ID	Unit Type	PC/lime / sand Ratio	Curing	Sample No.	Joint No.	Applied Load (g)	Weight of Top Unit (g)	Applied Load, F_1 (N)	Weight of Top Unit, W (N)	Failure Mode	Bond Strength, f_{wi} (N/mm^2)	Notes	$\log_{10}$ of bond strength (Y_i)
45	B_CL90s_165_2M_T	Brick	0:1:3	External	1	1	14577	2391.44	143.00	23.46	A1	0.119		-0.92
						2	6116	2394.50	60.00	23.49	A1	0.046		-1.33
						3	7441	2400.61	73.00	23.55	A1	0.058		-1.24
						4	13761	2477.06	135.00	24.30	A1	0.112		-0.95
						5	9684	2488.28	95.00	24.41	A1	0.077		-1.11
					2	6							damaged	
						7							damaged	
						8	23649	2431.19	232.00	23.85	A1	0.197		-0.71
						9	12742	2404.69	125.00	23.59	A1	0.103		-0.99
						10	5505	2492.35	54.00	24.45	A1	0.041		-1.39
					3	11	8869	2499.49	87.00	24.52	A1	0.070		-1.15
						12	13660	2395.51	134.00	23.50	A1	0.111		-0.95
						13	9786	2432.21	96.00	23.86	A1	0.078		-1.11
						14	6626	2450.56	65.00	24.04	A1	0.051		-1.29
						15	12232	2512.74	120.00	24.65	A1	0.099		-1.01
					Sample Mean							**0.089**		**-1.09**
					Sample Standard Deviation							**0.042**		**0.19**
					Coefficient of Variation							**0.468**		**-0.18**
					Y_c									**-1.46**
					Characteristic bond strength, f_{wk} (N/mm^2)									**0.03**

Table F.45: NHL 3.5 CL90-s brick masonry bond strength calculations, 165 mm flow, outdoor cured (2 months)

Test No.	Mortar ID	Unit Type	PC/lime / sand Ratio	Curing	Sample No.	Joint No.	Applied Load (g)	Weight of Top Unit (g)	Applied Load, F_1 (N)	Weight of Top Unit, W (N)	Failure Mode	Bond Strength, f_{wi} (N/mm^2)	Notes	$\log_{10}$ of bond strength (Y_i)
46	B_CL90s_165_6M_T	Brick	0:1:3	External	1	1	8563	2441.39	84.00	23.95	A1	0.067		-1.17
						2	22936	2480.12	225.00	24.33	A1	0.191		-0.72
						3	17023	2532.11	167.00	24.84	A1	0.140		-0.85
						4							damaged	
						5	18858	2399.59	185.00	23.54	A1	0.156		-0.81
					2	6	15698	2386.34	154.00	23.41	A1	0.129		-0.89
						7							damaged	
						8							damaged	
						9	19368	2477.06	190.00	24.30	A1	0.160		-0.80
						10	18756	2548.42	184.00	25.00	A1	0.155		-0.81
					1	11	15596	2477.06	153.00	24.30	A1	0.128		-0.89
						12	24771	2385.32	243.00	23.40	A1	0.206		-0.69
						13	24975	2431.19	245.00	23.85	A1	0.208		-0.68
						14	23445	2400.61	230.00	23.55	A1	0.195		-0.71
						15	25994	2419.98	255.00	23.74	A1	0.217		-0.66
					Sample Mean							**0.163**		**-0.81**
					Sample Standard Deviation							**0.044**		**0.14**
					Coefficient of Variation							**0.268**		**-0.17**
					Y_c									**-1.08**
					Characteristic bond strength, f_{wk} (N/mm^2)									**0.08**

Table F.46: CL90-s brick masonry bond strength calculations, 165 mm flow, outdoor cured (6 months)

Test No.	Mortar ID	Unit Type	PC/lime / sand Ratio	Curing	Sample No.	Joint No.	Applied Load (g)	Weight of Top Unit (g)	Applied Load, F_1 (N)	Weight of Top Unit, W (N)	Failure Mode	Bond Strength, f_{wi} (N/mm^2)	Notes	$\log_{10}$ of bond strength (Y_i)
47	B_M6_170_1m_T	Brick	1:½:4	External	1	1	75739	2378.19	743.00	23.33	A1	0.644		-0.19
						2	77880	2500.51	764.00	24.53	A1	0.662		-0.18
						3	58919	2363.91	578.00	23.19	A1	0.499		-0.30
						4	87054	2430.17	854.00	23.84	A1	0.741		-0.13
						5	36086	2510.70	354.00	24.63	A1	0.303		-0.52
					2	6	39144	2477.06	384.00	24.30	A1	0.330		-0.48
						7							damaged	
						8	48930	2395.51	480.00	23.50	A1	0.414		-0.38
						9	69827	2433.23	685.00	23.87	A1	0.593		-0.23
						10	65138	2477.06	639.00	24.30	A1	0.553		-0.26
					3	11	59531	2589.19	584.00	25.40	A1	0.505		-0.30
						12	67278	2432.21	660.00	23.86	A1	0.571		-0.24
						13	79511	2408.77	780.00	23.63	A1	0.676		-0.17
						14	40775	2477.06	400.00	24.30	A1	0.344		-0.46
						15	56473	2354.74	554.00	23.10	A1	0.478		-0.32
					Sample Mean							**0.522**		**-0.30**
					Sample Standard Deviation							**0.137**		**0.12**
					Coefficient of Variation							**0.263**		**-0.41**
					Y_c									**-0.53**
					Characteristic bond strength, f_{wk} (N/mm^2)									**0.29**

Table F.47: M6 brick masonry bond strength calculations, 165 mm flow, outdoor cured (1 month)

Test No.	Mortar ID	Unit Type	PC/lime / sand Ratio	Curing	Sample No.	Joint No.	Applied Load (g)	Weight of Top Unit (g)	Applied Load, F_1 (N)	Weight of Top Unit, W (N)	Failure Mode	Bond Strength, f_{wi} (N/mm^2)	Notes	$\log_{10}$ of bond strength (Y_i)
48	B_M6_170_2m_T	Brick	1:½:4	External	1	1	90520	2446.48	888.00	24.00	A1	0.770		-0.11
						2	66259	2401.63	650.00	23.56	A1	0.562		-0.25
						3	76453	2431.19	750.00	23.85	A1	0.650		-0.19
						4	59633	2359.84	585.00	23.15	A1	0.505		-0.30
						5	86035	2410.81	844.00	23.65	A1	0.732		-0.14
					2	6	96840	2498.47	950.00	24.51	A1	0.825		-0.08
						7	83792	2410.81	822.00	23.65	A1	0.713		-0.15
						8	84913	2436.29	833.00	23.90	A1	0.722		-0.14
						9	55046	2407.75	540.00	23.62	A1	0.466		-0.33
						10							damaged	
					3	11	81549	2410.81	800.00	23.65	A1	0.693		-0.16
						12	55046	2400.61	540.00	23.55	A1	0.466		-0.33
						13	79307	2499.49	778.00	24.52	A1	0.674		-0.17
						14	89195	2544.34	875.00	24.96	A1	0.759		-0.12
						15	85627	2324.16	840.00	22.80	A1	0.728		-0.14
					Sample Mean							**0.662**		**-0.19**
					Sample Standard Deviation							**0.116**		**0.08**
					Coefficient of Variation							**0.176**		**-0.44**
					Y_c									**-0.34**
					Characteristic bond strength, f_{wk} (N/mm^2)									**0.45**

Table F.48: M6 brick masonry bond strength calculations, 165 mm flow, outdoor cured (2 months)

Test No.	Mortar ID	Unit Type	PC/lime / sand Ratio	Curing	Sample No.	Joint No.	Applied Load (g)	Weight of Top Unit (g)	Applied Load, F_1 (N)	Weight of Top Unit, W (N)	Failure Mode	Bond Strength, f_{wi} (N/mm^2)	Notes	$\log_{10}$ of bond strength (Y_i)
49	B_M6_170_6m_T	Brick	1:½:4	External	1	1	124567	2344.55	1222.00	23.00	A1	1.062		0.03
						2	99898	2434.25	980.00	23.88	A1	0.851		-0.07
						3	112334	2477.06	1102.00	24.30	A1	0.957		-0.02
						4	84913	2426.10	833.00	23.80	A1	0.722		-0.14
						5	116718	2422.02	1145.00	23.76	A1	0.995		0.00
					2	6	96330	2462.69	945.00	24.16	A1	0.820		-0.09
						7	96126	2385.32	943.00	23.40	A1	0.818		-0.09
						8	103976	2354.74	1020.00	23.10	A1	0.886		-0.05
						9	99898	2533.13	980.00	24.85	A1	0.851		-0.07
						10	96840	2477.06	950.00	24.30	A1	0.825		-0.08
					3	11	115087	2385.32	1129.00	23.40	A1	0.981		-0.01
						12	97859	2400.61	960.00	23.55	A1	0.833		-0.08
						13	122324	2430.17	1200.00	23.84	A1	1.043		0.02
						14	99898	2383.28	980.00	23.38	A1	0.851		-0.07
						15	98369	2440.37	965.00	23.94	A1	0.838		-0.08
					Sample Mean							**0.889**		**-0.05**
					Sample Standard Deviation							**0.096**		**0.05**
					Coefficient of Variation							**0.108**		**-0.87**
					Y_c									**-0.14**
					Characteristic bond strength, f_{wk} (N/mm^2)									**0.72**

Table F.49: M6 brick masonry bond strength calculations, 165 mm flow, outdoor cured (6 months)

Test No.	Mortar ID	Unit Type	PC/lime / sand Ratio	Curing	Sample No.	Joint No.	Applied Load (g)	Weight of Top Unit (g)	Applied Load, F_1 (N)	Weight of Top Unit, W (N)	Failure Mode	Bond Strength, f_{wi} (N/mm^2)	Notes	$\log_{10}$ of bond strength (Y_i)
50	B_NHL5_170_1m_T	Brick	0:1:3	External	1	1	25484	2385.32	250.00	23.40	A1	0.213		-0.67
						2	16820	2517.84	165.00	24.70	A1	0.138		-0.86
						3	23649	2534.15	232.00	24.86	A1	0.197		-0.71
						4	25994	2513.76	255.00	24.66	A1	0.217		-0.66
						5	32824	2385.32	322.00	23.40	A1	0.276		-0.56
					2	6	29969	2344.55	294.00	23.00	A1	0.251		-0.60
						7	26096	2431.19	256.00	23.85	A1	0.218		-0.66
						8	13354	2384.30	131.00	23.39	A1	0.109		-0.96
						9	15087	2429.15	148.00	23.83	A1	0.123		-0.91
						10							damaged	
					3	11	29256	2412.84	287.00	23.67	A1	0.245		-0.61
						12	16820	2497.45	165.00	24.50	A1	0.138		-0.86
						13	20897	2399.59	205.00	23.54	A1	0.173		-0.76
						14	26911	2477.06	264.00	24.30	A1	0.225		-0.65
						15	15698	2324.16	154.00	22.80	A1	0.129		-0.89
					Sample Mean							**0.189**		**-0.74**
					Sample Standard Deviation							**0.054**		**0.13**
					Coefficient of Variation							**0.285**		**-0.18**
					Y_c									**-0.99**
					Characteristic bond strength, f_{wk} (N/mm^2)									**0.10**

Table F.50: NHL 5 brick masonry bond strength calculations, 170 mm flow, outdoor cured (1 month)

Test No.	Mortar ID	Unit Type	PC/lime / sand Ratio	Curing	Sample No.	Joint No.	Applied Load (g)	Weight of Top Unit (g)	Applied Load, F_1 (N)	Weight of Top Unit, W (N)	Failure Mode	Bond Strength, f_{wi} (N/mm^2)	Notes	$\log_{10}$ of bond strength (Y_i)
51	B_NHL5_170_2m_T	Brick	0:1:3	External	1	1	43833	2410.81	430.00	23.65	A1	0.370		-0.43
						2	41794	2486.24	410.00	24.39	A1	0.352		-0.45
						3	38532	2385.32	378.00	23.40	A1	0.324		-0.49
						4	35168	2440.37	345.00	23.94	A1	0.296		-0.53
						5	37207	2299.69	365.00	22.56	A1	0.313		-0.50
					2	6	23853	2497.45	234.00	24.50	A1	0.199		-0.70
						7	31600	2593.27	310.00	25.44	A1	0.265		-0.58
						8	39755	2397.55	390.00	23.52	A1	0.335		-0.47
						9	25280	2417.94	248.00	23.72	A1	0.211		-0.68
						10	25280	2363.91	248.00	23.19	A1	0.211		-0.68
					3	11	26402	2506.63	259.00	24.59	A1	0.220		-0.66
						12	22120	2591.23	217.00	25.42	A1	0.184		-0.74
						13	33537	2579.00	329.00	25.30	A1	0.282		-0.55
						14	32824	2354.74	322.00	23.10	A1	0.276		-0.56
						15	37207	2405.71	365.00	23.60	A1	0.313		-0.50
					Sample Mean							**0.277**		**-0.57**
					Sample Standard Deviation							**0.060**		**0.10**
					Coefficient of Variation							**0.216**		**-0.17**
					Y_c									**-0.76**
					Characteristic bond strength, f_{wk} (N/mm^2)									**0.18**

Table F.51: NHL 5 brick masonry bond strength calculations, 170 mm flow, outdoor cured (2 months)

Test No.	Mortar ID	Unit Type	PC/lime / sand Ratio	Curing	Sample No.	Joint No.	Applied Load (g)	Weight of Top Unit (g)	Applied Load, F_1 (N)	Weight of Top Unit, W (N)	Failure Mode	Bond Strength, f_{wi} (N/mm^2)	Notes	$\log_{10}$ of bond strength (Y_i)
52	B_NHL5_170_6m_T	Brick	0:1:3	External	1	1	49439	2399.59	485.00	23.54	A1	0.418		-0.38
						2	43323	2431.19	425.00	23.85	A1	0.366		-0.44
						3	43833	2512.74	430.00	24.65	A1	0.370		-0.43
						4							damaged	
						5							damaged	
					2	6	44750	2472.99	439.00	24.26	A1	0.378		-0.42
						7	29052	2496.43	285.00	24.49	A1	0.243		-0.61
						8	44750	2441.39	439.00	23.95	A1	0.378		-0.42
						9	46177	2310.91	453.00	22.67	A1	0.390		-0.41
						10	53007	2405.71	520.00	23.60	A1	0.449		-0.35
					3	11							damaged	
						12	36493	2430.17	358.00	23.84	A1	0.307		-0.51
						13	45362	2388.38	445.00	23.43	A1	0.383		-0.42
						14	33129	2487.26	325.00	24.40	A1	0.278		-0.56
						15	26504	2441.39	260.00	23.95	A1	0.221		-0.66
					Sample Mean							**0.348**		**-0.47**
					Sample Standard Deviation							**0.070**		**0.10**
					Coefficient of Variation							**0.202**		**-0.21**
					Y_c									**-0.65**
					Characteristic bond strength, f_{wk} (N/mm^2)									**0.22**

Table F.52: NHL 5 brick masonry bond strength calculations, 170 mm flow, outdoor cured (6 months)

Test No.	Mortar ID	Unit Type	PC/lime / sand Ratio	Curing	Sample No.	Joint No.	Applied Load (g)	Weight of Top Unit (g)	Applied Load, F_1 (N)	Weight of Top Unit, W (N)	Failure Mode	Bond Strength, f_{wi} (N/mm^2)	Notes	$\log_{10}$ of bond strength (Y_i)
53	B_CL90s_170_1M_T	Brick	0:1:3	External	1	1	7747	2480.12	76.00	24.33	A1	0.060		-1.22
						2							damaged	
						3	8461	2403.67	83.00	23.58	A1	0.067		-1.18
						4							damaged	
						5	6014	2395.51	59.00	23.50	A1	0.046		-1.34
					2	6	10398	2390.42	102.00	23.45	A1	0.083		-1.08
						7	6626	2533.13	65.00	24.85	A1	0.051		-1.29
						8							damaged	
						9							damaged	
						10	9684	2366.97	95.00	23.22	A1	0.077		-1.11
					3	11	5607	2298.67	55.00	22.55	A1	0.042		-1.38
						12							damaged	
						13	7645	2413.86	75.00	23.68	A1	0.060		-1.23
						14	5607	2385.32	55.00	23.40	A1	0.042		-1.38
						15	8665	2424.06	85.00	23.78	A1	0.068		-1.17
					Sample Mean							**0.060**		**-1.24**
					Sample Standard Deviation							**0.014**		**0.11**
					Coefficient of Variation							**0.242**		**-0.09**
					Y_c									**-1.44**
					Characteristic bond strength, f_{wk} (N/mm^2)									**0.04**

Table F.53: CL90-s brick masonry bond strength calculations, 170 mm flow, outdoor cured (1 month)

Test No.	Mortar ID	Unit Type	PC/lime / sand Ratio	Curing	Sample No.	Joint No.	Applied Load (g)	Weight of Top Unit (g)	Applied Load, F_1 (N)	Weight of Top Unit, W (N)	Failure Mode	Bond Strength, f_{wi} (N/mm^2)	Notes	$\log_{10}$ of bond strength (Y_i)
54	B_CL90s_170_2M_T	Brick	0:1:3	External	1	1	12538	2477.06	123.00	24.30	A1	0.101		-0.99
						2							damaged	
						3	15698	2375.13	154.00	23.30	A1	0.129		-0.89
						4							damaged	
						5							damaged	
					2	6	10703	2436.29	105.00	23.90	A1	0.086		-1.07
						7	13456	2401.63	132.00	23.56	A1	0.109		-0.96
						8	14679	2388.38	144.00	23.43	A1	0.120		-0.92
						9	8665	2523.96	85.00	24.76	A1	0.068		-1.17
						10							damaged	
					3	11	7951	2364.93	78.00	23.20	A1	0.062		-1.21
						12							damaged	
						13	12742	2354.74	125.00	23.10	A1	0.103		-0.99
						14	13252	2579.00	130.00	25.30	A1	0.108		-0.97
						15	12640	2417.94	124.00	23.72	A1	0.102		-0.99
					Sample Mean							**0.099**		**-1.01**
					Sample Standard Deviation							**0.021**		**0.10**
					Coefficient of Variation							**0.213**		**-0.10**
					Y_c									**-1.21**
					Characteristic bond strength, f_{wk} (N/mm^2)									**0.06**

Table F.54: CL90-s brick masonry bond strength calculations, 170 mm flow, outdoor cured (2 months)

Test No.	Mortar ID	Unit Type	PC/lime / sand Ratio	Curing	Sample No.	Joint No.	Applied Load (g)	Weight of Top Unit (g)	Applied Load, F_1 (N)	Weight of Top Unit, W (N)	Failure Mode	Bond Strength, f_{wi} (N/mm^2)	Notes	$\log_{10}$ of bond strength (Y_i)
55	B_CL90s_170_6M_T	Brick	0:1:3	External	1	1	18858	2388.38	185.00	23.43	A1	0.156		-0.81
						2	12334	2404.69	121.00	23.59	A1	0.100		-1.00
						3							damaged	
						4	25994	2293.58	255.00	22.50	A1	0.217		-0.66
						5							damaged	
					2	6	16820	2399.59	165.00	23.54	A1	0.138		-0.86
						7	10601	2515.80	104.00	24.68	A1	0.085		-1.07
						8	8563	2538.23	84.00	24.90	A1	0.067		-1.17
						9	19062	2579.00	187.00	25.30	A1	0.157		-0.80
						10	17023	2486.24	167.00	24.39	A1	0.140		-0.85
					1	11							damaged	
						12	12742	2364.93	125.00	23.20	A1	0.103		-0.99
						13	25790	2410.81	253.00	23.65	A1	0.215		-0.67
						14	22936	2440.37	225.00	23.94	A1	0.191		-0.72
						15	26198	2430.17	257.00	23.84	A1	0.219		-0.66
					Sample Mean							**0.149**		**-0.86**
					Sample Standard Deviation							**0.053**		**0.17**
					Coefficient of Variation							**0.357**		**-0.20**
					Y_c									**-1.18**
					Characteristic bond strength, f_{wk} (N/mm^2)									**0.07**

Table F.55: CL90-s brick masonry bond strength calculations, 170 mm flow, outdoor cured (6 months)

Test No.	Mortar ID	Unit Type	PC/lime / sand Ratio	Curing	Sample No.	Joint No.	Applied Load (g)	Weight of Top Unit (g)	Applied Load, F_1 (N)	Weight of Top Unit, W (N)	Failure Mode	Bond Strength, f_{wi} (N/mm^2)	Notes	$\log_{10}$ of bond strength (Y_i)
56	S_bk_CL90s_165_1M_T	Broken Sandstone	0:1:3	Lab	1	1	4587	3445.30	45.00	33.80	A1	0.033		-1.48
						2	2548	3534.30	25.00	34.67	A1	0.015		-1.81
						3							damaged	
						4	5505	3444.60	54.00	33.79	A1	0.041		-1.39
						5	2446	3564.00	24.00	34.96	A1	0.014		-1.84
					2	6							damaged	
						7							damaged	
						8	5607	3565.70	55.00	34.98	A3	0.042		-1.38
						9	6014	3696.30	59.00	36.26	A1	0.045		-1.35
						10							damaged	
					3	11							damaged	
						12	6422	3498.90	63.00	34.32	A1	0.049		-1.31
						13							damaged	
						14	3364	3448.90	33.00	33.83	A1	0.022		-1.65
						15	4689	3454.76	46.00	33.89	A1	0.034		-1.47
					Sample Mean							**0.033**		**-1.52**
					Sample Standard Deviation							**0.013**		**0.20**
					Coefficient of Variation							**0.388**		**-0.13**
					Y_c									**-1.90**
					Characteristic bond strength, f_{wk} (N/mm^2)									**0.012**

Table F.56: CL90-s broken sandstone masonry bond strength calculations, 165 mm flow (1 month)

Test No.	Mortar ID	Unit Type	PC/lime / sand Ratio	Curing	Sample No.	Joint No.	Applied Load (g)	Weight of Top Unit (g)	Applied Load, F_1 (N)	Weight of Top Unit, W (N)	Failure Mode	Bond Strength, f_{wi} (N/mm^2)	Notes	$\log_{10}$ of bond strength (Y_i)
57	S_bk_CL90s_165_2M_T	Broken Sandstone	0:1:3	Lab	1	1	3296	3431.19	32.33	33.66	A1	0.022		-1.66
						2							damaged	
						3							damaged	
						4	5530	3489.30	54.25	34.23	A1	0.041		-1.39
						5	5782	3437.31	56.72	33.72	A1	0.043		-1.37
					2	6							damaged	
						7	8013	3502.55	78.61	34.36	A1	0.062		-1.21
						8	7136	3439.35	70.00	33.74	A3	0.055		-1.26
						9	5348	3424.06	52.46	33.59	A1	0.039		-1.40
						10	4973	3517.84	48.79	34.51	A1	0.036		-1.44
					3	11	6158	3546.40	60.41	34.79	A1	0.046		-1.33
						12							damaged	
						13	4774	3446.48	46.83	33.81	A1	0.034		-1.46
						14	6559	3455.66	64.34	33.90	A1	0.050		-1.30
						15							damaged	
					Sample Mean							**0.043**		**-1.38**
					Sample Standard Deviation							**0.011**		**0.13**
					Coefficient of Variation							**0.264**		**-0.09**
					Y_c									**-1.63**
					Characteristic bond strength, f_{wk} (N/mm^2)									**0.024**

Table F.57: CL90-s broken sandstone masonry bond strength calculations, 165 mm flow (2 months)

Test No.	Mortar ID	Unit Type	PC/lime / sand Ratio	Curing	Sample No.	Joint No.	Applied Load (g)	Weight of Top Unit (g)	Applied Load, F_1 (N)	Weight of Top Unit, W (N)	Failure Mode	Bond Strength, f_{wi} (N/mm^2)	Notes	$\log_{10}$ of bond strength (Y_i)
58	S_bk_CL90s_165_6M_T	Broken Sandstone	0:1:3	Lab	1	1	10296	3417.94	101.00	33.53	A1	0.082		-1.09
						2							damaged	
						3	5097	3531.09	50.00	34.64	A1	0.037		-1.43
						4							damaged	
						5	5607	3427.12	55.00	33.62	A1	0.042		-1.38
					2	6							damaged	
						7	8155	3447.50	80.00	33.82	A1	0.063		-1.20
						8							damaged	
						9	7339	3557.59	72.00	34.90	A1	0.056		-1.25
						10	4893	3530.07	48.00	34.63	A1	0.035		-1.45
					1	11	6978	3454.64	68.45	33.89	A3	0.053		-1.27
						12	8970	3447.50	88.00	33.82	A1	0.070		-1.15
						13	6728	3490.32	66.00	34.24	A1	0.051		-1.29
						14							damaged	
						15	9174	3507.65	90.00	34.41	A1	0.072		-1.14
					Sample Mean							**0.056**		**-1.27**
					Sample Standard Deviation							**0.016**		**0.12**
					Coefficient of Variation							**0.278**		**-0.10**
					Y_c									**-1.50**
					Characteristic bond strength, f_{wk} (N/mm^2)									**0.031**

Table F.58: CL90-s broken sandstone masonry bond strength calculations, 165 mm flow (6 months)

Test No.	Mortar ID	Unit Type	PC/lime / sand Ratio	Curing	Sample No.	Joint No.	Applied Load (g)	Weight of Top Unit (g)	Applied Load, F_1 (N)	Weight of Top Unit, W (N)	Failure Mode	Bond Strength, f_{wi} (N/mm^2)	Notes	$\log_{10}$ of bond strength (Y_i)
59	S_bk_NHL2_165_1M_T	Broken Sandstone	0:1:3	Lab	1	1	8914	3409.79	87.45	33.45	A1	0.070		-1.15
						2	10442	3520.90	102.44	34.54	A1	0.083		-1.08
						3							damaged	
						4							damaged	
						5	4651	3432.62	45.63	33.67	A1	0.033		-1.48
					2	6	5652	3460.75	55.45	33.95	A1	0.042		-1.38
						7	8636	3529.05	84.72	34.62	A3	0.068		-1.17
						8	6722	3460.75	65.94	33.95	A1	0.051		-1.29
						9	8180	3529.05	80.25	34.62	A1	0.064		-1.20
						10	10001	3554.54	98.11	34.87	A1	0.079		-1.10
					3	11							damaged	
						12	10734	3550.46	105.30	34.83	A1	0.086		-1.07
						13	7655	3438.33	75.10	33.73	A1	0.059		-1.23
						14	4643	3533.13	45.55	34.66	A1	0.033		-1.48
						15	8668	3390.42	85.03	33.26	A1	0.068		-1.17
					Sample Mean							**0.061**		**-1.23**
					Sample Standard Deviation							**0.018**		**0.14**
					Coefficient of Variation							**0.294**		**-0.12**
					Y_c									**-1.51**
					Characteristic bond strength, f_{wk} (N/mm^2)									**0.031**

Table F.59: NHL 2 broken sandstone masonry bond strength calculations, 165 mm flow (1 month)

Test No.	Mortar ID	Unit Type	PC/lime / sand Ratio	Curing	Sample No.	Joint No.	Applied Load (g)	Weight of Top Unit (g)	Applied Load, F_1 (N)	Weight of Top Unit, W (N)	Failure Mode	Bond Strength, f_{wi} (N/mm^2)	Notes	$\log_{10}$ of bond strength (Y_i)
60	S_bk_NHL2_165_2M_T	Broken Sandstone	0:1:3	Lab	1	1							damaged	
						2	12297	3531.09	120.63	34.64	A1	0.099		-1.00
						3	12641	3476.04	124.01	34.10	A1	0.102		-0.99
						4	8637	3426.10	84.73	33.61	A1	0.068		-1.17
						5	4980	3561.67	48.85	34.94	A1	0.036		-1.44
					2	6	11234	3421.00	110.21	33.56	A1	0.090		-1.05
						7							damaged	
						8	13259	3531.09	130.07	34.64	A3	0.107		-0.97
						9	9183	3482.16	90.09	34.16	A1	0.072		-1.14
						10							damaged	
					3	11							damaged	
						12	10703	3386.34	105.00	33.22	A1	0.085		-1.07
						13	12779	3392.46	125.36	33.28	A1	0.103		-0.99
						14	8793	3474.01	86.26	34.08	A1	0.069		-1.16
						15	9335	3430.17	91.58	33.65	A1	0.074		-1.13
					Sample Mean							**0.082**		**-1.10**
					Sample Standard Deviation							**0.021**		**0.14**
					Coefficient of Variation							**0.257**		**-0.12**
					Y_c									**-1.36**
					Characteristic bond strength, f_{wk} (N/mm^2)									**0.04**

Table F.60: NHL 2 broken sandstone masonry bond strength calculations, 165 mm flow (2 months)

Test No.	Mortar ID	Unit Type	PC/lime / sand Ratio	Curing	Sample No.	Joint No.	Applied Load (g)	Weight of Top Unit (g)	Applied Load, F_1 (N)	Weight of Top Unit, W (N)	Failure Mode	Bond Strength, f_{wi} (N/mm^2)	Notes	$\log_{10}$ of bond strength (Y_i)
61	S_bk_NHL2_165_6M_T	Broken Sandstone	0:1:3	Lab	1	1							damaged	
						2	14604	3517.84	143.27	34.51	A1	0.119		-0.93
						3	15875	3390.42	155.73	33.26	A1	0.130		-0.89
						4	6905	3433.23	67.74	33.68	A1	0.053		-1.28
						5	16754	3565.75	164.36	34.98	A1	0.137		-0.86
					2	6	9389	3467.89	92.11	34.02	A1	0.074		-1.13
						7	15761	3529.05	154.62	34.62	A1	0.129		-0.89
						8							damaged	
						9	14814	3433.03	145.33	33.68	A1	0.121		-0.92
						10	8417	3392.46	82.57	33.28	A1	0.066		-1.18
					3	11	10410	3439.35	102.12	33.74	A1	0.083		-1.08
						12							damaged	
						13	15529	3529.05	152.34	34.62	A1	0.127		-0.90
						14	7708	3484.20	75.62	34.18	A1	0.060		-1.22
						15	17352	3470.95	170.22	34.05	A1	0.142		-0.85
					Sample Mean							**0.103**		**-1.01**
					Sample Standard Deviation							**0.033**		**0.16**
					Coefficient of Variation							**0.323**		**-0.16**
					Y_c									**-1.31**
					Characteristic bond strength, f_{wk} (N/mm^2)									**0.049**

Table F.61: NHL 2 broken sandstone masonry bond strength calculations, 165 mm flow (6 months)

Test No.	Mortar ID	Unit Type	PC/lime / sand Ratio	Curing	Sample No.	Joint No.	Applied Load (g)	Weight of Top Unit (g)	Applied Load, F_1 (N)	Weight of Top Unit, W (N)	Failure Mode	Bond Strength, f_{wi} (N/mm^2)	Notes	$\log_{10}$ of bond strength (Y_i)
62	S_bk_CL90s_170_1M_T	Broken Sandstone	0:1:3	Lab	1	1	4645	3542.30	45.57	34.75	A1	0.033		-1.48
						2	3541	3393.48	34.74	33.29	A1	0.024		-1.62
						3							damaged	
						4	6661	3424.06	65.34	33.59	A1	0.051		-1.30
						5	4744	3491.34	46.54	34.25	A1	0.034		-1.47
					2	6	3539	3493.37	34.72	34.27	A1	0.024		-1.62
						7							damaged	
						8							damaged	
						9	5095	3453.62	49.98	33.88	A1	0.037		-1.43
						10	4396	3480.63	43.12	34.15	A1	0.031		-1.51
					3	11	5654	3450.56	55.47	33.85	A3	0.042		-1.38
						12	5445	3524.97	53.42	34.58	A1	0.040		-1.40
						13							damaged	
						14	3440	3421.00	33.75	33.56	A1	0.023		-1.64
						15	4705	3476.04	46.16	34.10	A1	0.034		-1.47
					Sample Mean							**0.034**		**-1.48**
					Sample Standard Deviation							**0.009**		**0.11**
					Coefficient of Variation							**0.251**		**-0.07**
					Y_c									**-1.69**
					Characteristic bond strength, f_{wk} (N/mm^2)									**0.020**

Table F.62: CL90-s broken sandstone masonry bond strength calculations, 170 mm flow (1 month)

Test No.	Mortar ID	Unit Type	PC/lime / sand Ratio	Curing	Sample No.	Joint No.	Applied Load (g)	Weight of Top Unit (g)	Applied Load, F_1 (N)	Weight of Top Unit, W (N)	Failure Mode	Bond Strength, f_{wi} (N/mm^2)	Notes	$\log_{10}$ of bond strength (Y_i)
63	S_bk_CL90s_170_2M_T	Broken Sandstone	0:1:3	Lab	1	1	6595	3415.90	64.70	33.51	A1	0.050		-1.30
						2	6968	3529.05	68.36	34.62	A1	0.053		-1.27
						3	9214	3476.04	90.39	34.10	A1	0.073		-1.14
						4	11239	3522.94	110.25	34.56	A1	0.090		-1.05
						5							damaged	
					2	6							damaged	
						7	3411	3443.43	33.46	33.78	A1	0.023		-1.64
						8	2556	3383.28	25.07	33.19	A3	0.015		-1.81
						9							damaged	
						10	8904	3485.22	87.35	34.19	A1	0.070		-1.16
					3	11	3723	3414.88	36.52	33.50	A3	0.025		-1.59
						12							damaged	
						13							damaged	
						14	6642	3527.01	65.16	34.60	A1	0.050		-1.30
						15	7017	3412.84	68.84	33.48	A1	0.054		-1.27
					Sample Mean							**0.050**		**-1.35**
					Sample Standard Deviation							**0.024**		**0.25**
					Coefficient of Variation							**0.471**		**-0.18**
					Y_c									**-1.83**
					Characteristic bond strength, f_{wk} (N/mm^2)									**0.015**

Table F.63: CL90-s broken sandstone masonry bond strength calculations, 170 mm flow (2 months)

Test No.	Mortar ID	Unit Type	PC/lime / sand Ratio	Curing	Sample No.	Joint No.	Applied Load (g)	Weight of Top Unit (g)	Applied Load, F_1 (N)	Weight of Top Unit, W (N)	Failure Mode	Bond Strength, f_{wi} (N/mm^2)	Notes	$\log_{10}$ of bond strength (Y_i)
64	S_bk_CL90s_170_6M_T	Broken Sandstone	0:1:3	Lab	1	1	6685	3518.86	65.58	34.52	A1	0.051		-1.29
						2	10430	3416.92	102.32	33.52	A1	0.083		-1.08
						3							damaged	
						4	8876	3427.12	87.07	33.62	A1	0.070		-1.16
						5							damaged	
					2	6	2522	3563.30	24.74	34.96	A1	0.015		-1.82
						7	4614	3491.34	45.26	34.25	A3	0.033		-1.48
						8							damaged	
						9	6651	3432.82	65.25	33.68	A1	0.051		-1.30
						10	10968	3460.75	107.60	33.95	A1	0.088		-1.06
					1	11	7752	3485.22	76.05	34.19	A3	0.060		-1.22
						12	8191	3466.87	80.35	34.01	A1	0.064		-1.20
						13	5954	3425.08	58.41	33.60	A1	0.045		-1.35
						14	10205	3425.08	100.11	33.60	A1	0.081		-1.09
						15	6966	3461.77	68.34	33.96	A1	0.053		-1.27
					Sample Mean							**0.058**		**-1.28**
					Sample Standard Deviation							**0.021**		**0.21**
					Coefficient of Variation							**0.369**		**-0.17**
					Y_c									**-1.68**
					Characteristic bond strength, f_{wk} (N/mm^2)									**0.021**

Table F.64: CL90-s broken sandstone masonry bond strength calculations, 170 mm flow (6 months)

Test No.	Mortar ID	Unit Type	PC/lime / sand Ratio	Curing	Sample No.	Joint No.	Applied Load (g)	Weight of Top Unit (g)	Applied Load, F_1 (N)	Weight of Top Unit, W (N)	Failure Mode	Bond Strength, f_{wi} (N/mm^2)	Notes	$\log_{10}$ of bond strength (Y_i)
65	S_bk_NHL2_170_1M_T	Broken Sandstone	0:1:3	Lab	1	1	9011	3521.92	88.40	34.55	A1	0.071		-1.15
						2	11990	3450.56	117.62	33.85	A1	0.096		-1.02
						3							damaged	
						4							damaged	
						5	12245	3517.84	120.12	34.51	A1	0.099		-1.01
					2	6	6688	3421.00	65.61	33.56	A1	0.051		-1.29
						7	7650	3380.22	75.05	33.16	A1	0.059		-1.23
						8	10767	3460.75	105.62	33.95	A1	0.086		-1.07
						9	9749	3529.05	95.64	34.62	A1	0.077		-1.11
						10	6831	3466.87	67.01	34.01	A1	0.052		-1.28
					3	11	6475	3522.94	63.52	34.56	A1	0.049		-1.31
						12	7696	3538.23	75.50	34.71	A1	0.059		-1.23
						13	4709	3366.97	46.20	33.03	A1	0.034		-1.47
						14	9801	3409.79	96.15	33.45	A1	0.078		-1.11
						15							damaged	
					Sample Mean							**0.068**		**-1.19**
					Sample Standard Deviation							**0.020**		**0.14**
					Coefficient of Variation							**0.298**		**-0.12**
					Y_c									**-1.45**
					Characteristic bond strength, f_{wk} (N/mm^2)									**0.035**

Table F.65: NHL 2 broken sandstone masonry bond strength calculations, 170 mm flow (1 month)

Test No.	Mortar ID	Unit Type	PC/lime / sand Ratio	Curing	Sample No.	Joint No.	Applied Load (g)	Weight of Top Unit (g)	Applied Load, F_1 (N)	Weight of Top Unit, W (N)	Failure Mode	Bond Strength, f_{wi} (N/mm^2)	Notes	$\log_{10}$ of bond strength (Y_i)
66	S_bk_NHL2_170_2M_T	Broken Sandstone	0:1:3	Lab	1	1	12687	3409.79	124.46	33.45	A1	0.102		-0.99
						2	14844	3428.13	145.62	33.63	A1	0.121		-0.92
						3							damaged	
						4	8121	3529.05	79.67	34.62	A1	0.063		-1.20
						5							damaged	
					2	6	5690	3461.77	55.82	33.96	A1	0.042		-1.37
						7	15979	3529.05	156.75	34.62	A3	0.131		-0.88
						8	9708	3425.08	95.24	33.60	A3	0.077		-1.11
						9	13773	3450.56	135.11	33.85	A1	0.112		-0.95
						10							damaged	
					3	11							damaged	
						12							damaged	
						13	10626	3482.16	104.24	34.16	A1	0.085		-1.07
						14	9748	3542.30	95.63	34.75	A1	0.077		-1.11
						15	14692	3390.42	144.13	33.26	A1	0.120		-0.92
					Sample Mean							**0.093**		**-1.05**
					Sample Standard Deviation							**0.029**		**0.15**
					Coefficient of Variation							**0.308**		**-0.14**
					Y_c									**-1.35**
					Characteristic bond strength, f_{wk} (N/mm^2)									**0.045**

Table F.66: NHL 2 broken sandstone masonry bond strength calculations, 170 mm flow (2 months)

Test No.	Mortar ID	Unit Type	PC/lime / sand Ratio	Curing	Sample No.	Joint No.	Applied Load (g)	Weight of Top Unit (g)	Applied Load, F_1 (N)	Weight of Top Unit, W (N)	Failure Mode	Bond Strength, f_{wi} (N/mm^2)	Notes	$\log_{10}$ of bond strength (Y_i)
67	S_bk_NHL2_170_6M_T	Broken Sandstone	0:1:3	Lab	1	1	13784	3540.27	135.22	34.73	A1	0.112		-0.95
						2	15965	3529.05	156.62	34.62	A1	0.130		-0.88
						3	16791	3416.92	164.72	33.52	A1	0.138		-0.38
						4	14307	3426.10	140.35	33.61	A1	0.116		-0.93
						5							damaged	-0.38
					2	6	14803	3482.16	145.22	34.16	A1	0.120		-0.38
						7	8943	3530.07	87.73	34.63	A1	0.070		-1.15
						8	15831	3449.54	155.30	33.84	A3	0.129		-0.89
						9	9710	3493.07	95.26	34.27	A1	0.077		-0.38
						10	15988	3534.15	156.85	34.67	A1	0.131		-0.88
					3	11							damaged	
						12	13479	3443.43	132.23	33.78	A1	0.109		-0.96
						13	13793	3410.81	135.31	33.46	A1	0.112		-0.95
						14							damaged	
						15	12771	3480.12	125.28	34.14	A1	0.103		-0.99
					Sample Mean							**0.112**		**-0.78**
					Sample Standard Deviation							**0.021**		**0.28**
					Coefficient of Variation							**0.186**		**-0.37**
					Y_c									**-1.32**
					Characteristic bond strength, f_{wk} (N/mm^2)									**0.047**

Table F.67: NHL 2 broken sandstone masonry bond strength calculations, 170 mm flow (6 months)

Test No.	Mortar ID	Unit Type	PC/lime / sand Ratio	Curing	Sample No.	Joint No.	Applied Load (g)	Weight of Top Unit (g)	Applied Load, F_1 (N)	Weight of Top Unit, W (N)	Failure Mode	Bond Strength, f_{wi} (N/mm^2)	Notes	$\log_{10}$ of bond strength (Y_i)
68	L_bk_CL90s_165_1M_T	Broken Limestone	0:1:3	Lab	1	1	6626	2583.08	65.00	25.34	A1	0.019		-1.73
						2	4383	2586.14	43.00	25.37	A1	0.031		-1.51
						3							damaged	
					2	4	8665	2696.23	85.00	26.45	A1	0.036		-1.44
						5	8665	2637.10	85.00	25.87	A1	0.022		-1.66
						6	9684	2630.99	95.00	25.81	A1	0.041		-1.39
					3	7	9684	2663.61	95.00	26.13	A1	0.033		-1.48
						8	9684	2688.07	95.00	26.37	A1	0.036		-1.44
						9	8970	2613.66	88.00	25.64	A1	0.039		-1.41
					4	10							damaged	
						11	9684	2662.59	95.00	26.12	A1	0.034		-1.47
						12	8665	2666.67	85.00	26.16	A1	0.025		-1.60
					5	13	6626	2621.81	65.00	25.72	A1	0.019		-1.72
						14	8665	2681.96	85.00	26.31	A1	0.015		-1.82
						15	5505	2695.21	54.00	26.44	A1	0.032		-1.49
					Sample Mean							**0.029**		**-1.55**
					Sample Standard Deviation							**0.008**		**0.14**
					Coefficient of Variation							**0.288**		**-0.09**
					Y_c									**-1.82**
					Characteristic bond strength, f_{wk} (N/mm^2)									**0.015**

Table F.68: CL90-s broken limestone masonry bond strength calculations, 165 mm flow (1 month)

Test No.	Mortar ID	Unit Type	PC/lime / sand Ratio	Curing	Sample No.	Joint No.	Applied Load (g)	Weight of Top Unit (g)	Applied Load, F_1 (N)	Weight of Top Unit, W (N)	Failure Mode	Bond Strength, f_{wi} (N/mm^2)	Notes	$\log_{10}$ of bond strength (Y_i)
69	L_bk_CL90s_165_2M_T	Broken Limestone	0:1:3	Lab	1	1	5470	2626.91	53.66	25.77	A1	0.066		-1.18
						2							damaged	
						3	7479	2662.59	73.37	26.12	A1	0.043		-1.37
					2	4	8688	2677.88	85.23	26.27	A1	0.055		-1.26
						5	9695	2627.93	95.11	25.78	A1	0.077		-1.11
						6	7519	2691.13	73.76	26.40	A1	0.058		-1.23
					3	7							damaged	
						8	5421	2682.98	53.18	26.32	A1	0.040		-1.39
						9	6386	2689.09	62.65	26.38	A1	0.049		-1.31
					4	10	5696	2619.78	55.88	25.70	A1	0.043		-1.37
						11	8942	2608.56	87.72	25.59	A1	0.071		-1.15
						12	4748	2666.67	46.58	26.16	A1	0.035		-1.46
					5	13	6768	2616.72	66.39	25.67	A1	0.052		-1.28
						14	6626	2645.26	65.00	25.95	A1	0.051		-1.30
						15	4673	2706.42	45.84	26.55	A1	0.034		-1.47
					Sample Mean							**0.052**		**-1.30**
					Sample Standard Deviation							**0.013**		**0.11**
					Coefficient of Variation							**0.259**		**-0.09**
					Y_c									**-1.51**
					Characteristic bond strength, f_{wk} (N/mm^2)									**0.031**

Table F.69: CL90-s broken limestone masonry bond strength calculations, 165 mm flow (2 months)

Test No.	Mortar ID	Unit Type	PC/lime / sand Ratio	Curing	Sample No.	Joint No.	Applied Load (g)	Weight of Top Unit (g)	Applied Load, F_1 (N)	Weight of Top Unit, W (N)	Failure Mode	Bond Strength, f_{wi} (N/mm^2)	Notes	$\log_{10}$ of bond strength (Y_i)
70	L_bk_CL90s_165_6M_T	Broken Limestone	0:1:3	Lab	1	1	6624	2618.76	64.98	25.69	A1	0.051		-1.30
						2	8948	2673.80	87.78	26.23	A1	0.071		-1.15
						3							damaged	
					2	4	9207	2687.05	90.32	26.36	A1	0.073		-1.14
						5	5698	2619.78	55.90	25.70	A1	0.043		-1.37
						6	7939	2633.03	77.88	25.83	A1	0.062		-1.21
					3	7	6017	2638.12	59.03	25.88	A1	0.045		-1.34
						8	9392	2685.02	92.14	26.34	A1	0.074		-1.13
						9							damaged	
					4	10							damaged	
						11	7108	2646.28	69.73	25.96	A1	0.055		-1.26
						12	8963	2617.74	87.93	25.68	A1	0.071		-1.15
					5	13	7274	2675.84	71.36	26.25	A1	0.056		-1.25
						14	6641	2706.42	65.15	26.55	A1	0.051		-1.29
						15	8823	2607.54	86.55	25.58	A1	0.070		-1.16
					Sample Mean							**0.060**		**-1.23**
					Sample Standard Deviation							**0.011**		**0.08**
					Coefficient of Variation							**0.189**		**-0.07**
					Y_c									**-1.39**
					Characteristic bond strength, f_{wk} (N/mm^2)									**0.041**

Table F.70: CL90-s broken limestone masonry bond strength calculations, 165 mm flow (6 months)

Test No.	Mortar ID	Unit Type	PC/lime / sand Ratio	Curing	Sample No.	Joint No.	Applied Load (g)	Weight of Top Unit (g)	Applied Load, F_1 (N)	Weight of Top Unit, W (N)	Failure Mode	Bond Strength, f_{wi} (N/mm^2)	Notes	$\log_{10}$ of bond strength (Y_i)
71	L_bk_NHL2_165_1M_T	Broken Limestone	0:1:3	Lab	1	1	4716	2633.03	46.26	25.83	A1	0.034		-1.46
						2	5283	2634.05	51.83	25.84	A1	0.039		-1.41
						3	3557	2661.57	34.89	26.11	A1	0.024		-1.61
					2	4							damaged	
						5	2512	2612.64	24.64	25.63	A1	0.015		-1.81
						6	4877	2651.38	47.84	26.01	A1	0.036		-1.45
					3	7	3760	2669.72	36.89	26.19	A1	0.026		-1.58
						8							damaged	
						9	4189	2642.20	41.09	25.92	A1	0.030		-1.53
					4	10	3113	2640.16	30.54	25.90	A1	0.021		-1.69
						11	3021	2655.45	29.64	26.05	A1	0.020		-1.70
						12	3725	2636.09	36.54	25.86	A1	0.026		-1.59
					5	13	4882	2686.03	47.89	26.35	A1	0.036		-1.45
						14	4346	2644.24	42.63	25.94	A1	0.031		-1.51
						15	3478	2638.12	34.12	25.88	A1	0.024		-1.63
					Sample Mean							**0.028**		**-1.57**
					Sample Standard Deviation							**0.007**		**0.12**
					Coefficient of Variation							**0.258**		**-0.08**
					Y_c									**-1.80**
					Characteristic bond strength, f_{wk} (N/mm^2)									**0.016**

Table F.71: NHL 2 broken limestone masonry bond strength calculations, 165 mm flow (1 month)

Test No.	Mortar ID	Unit Type	PC/lime / sand Ratio	Curing	Sample No.	Joint No.	Applied Load (g)	Weight of Top Unit (g)	Applied Load, F_1 (N)	Weight of Top Unit, W (N)	Failure Mode	Bond Strength, f_{wi} (N/mm^2)	Notes	$\log_{10}$ of bond strength (Y_i)
72	L_bk_NHL2_165_2M_T	Broken Limestone	0:1:3	Lab	1	1	5808	2686.03	56.98	26.35	A1	0.044		-1.36
						2	5955	2614.68	58.42	25.65	A1	0.045		-1.35
						3	4582	2636.09	44.95	25.86	A1	0.033		-1.48
					2	4	4140	2639.14	40.61	25.89	A1	0.029		-1.53
						5	6038	2629.97	59.23	25.80	A1	0.046		-1.34
						6	3984	2693.17	39.08	26.42	A1	0.028		-1.55
					3	7	5748	2662.59	56.39	26.12	A1	0.043		-1.36
						8	6716	2690.11	65.88	26.39	A1	0.051		-1.29
						9							damaged	
					4	10	6318	2618.76	61.98	25.69	A1	0.048		-1.32
						11	4802	2638.12	47.11	25.88	A1	0.035		-1.46
						12							damaged	
					5		5101	2681.96	50.04	26.31	A1	0.038		-1.42
						14	6863	2655.45	67.33	26.05	A1	0.053		-1.28
						15	5963	2634.05	58.50	25.84	A1	0.045		-1.35
					Sample Mean							**0.041**		**-1.39**
					Sample Standard Deviation							**0.008**		**0.09**
					Coefficient of Variation							**0.194**		**-0.06**
					Y_c									**-1.56**
					Characteristic bond strength, f_{wk} (N/mm^2)									**0.027**

Table F.72: NHL 2 broken limestone masonry bond strength calculations, 165 mm flow (2 months)

Test No.	Mortar ID	Unit Type	PC/lime / sand Ratio	Curing	Sample No.	Joint No.	Applied Load (g)	Weight of Top Unit (g)	Applied Load, F_1 (N)	Weight of Top Unit, W (N)	Failure Mode	Bond Strength, f_{wi} (N/mm^2)	Notes	$\log_{10}$ of bond strength (Y_i)
73	L_bk_NHL2_165_6M_T	Broken Limestone	0:1:3	Lab	1	1	9017	2616.72	88.46	25.67	A1	0.071		-1.15
						2							damaged	
						3							damaged	
					2	4	5317	2626.71	52.16	25.77	A1	0.039		-1.40
						5	4948	2686.03	48.54	26.35	A1	0.036		-1.44
						6	6391	2645.26	62.70	25.95	A1	0.049		-1.31
					3	7							damaged	
						8	5428	2636.09	53.25	25.86	A1	0.040		-1.39
						9	4698	2692.15	46.09	26.41	A1	0.034		-1.47
					4	10	6682	2685.02	65.55	26.34	A1	0.051		-1.29
						11	4778	2625.89	46.87	25.76	A1	0.035		-1.46
						12	9077	2640.16	89.05	25.90	A1	0.072		-1.14
					5	13	6004	2635.07	58.90	25.85	A1	0.045		-1.34
						14	7497	2687.05	73.55	26.36	A1	0.058		-1.24
						15	6104	2667.69	59.88	26.17	A1	0.046		-1.34
					Sample Mean							**0.048**		**-1.33**
					Sample Standard Deviation							**0.013**		**0.11**
					Coefficient of Variation							**0.270**		**-0.08**
					Y_c									**-1.54**
					Characteristic bond strength, f_{wk} (N/mm^2)									**0.029**

Table F.73: NHL 2 broken limestone masonry bond strength calculations, 165 mm flow (6 months)

Test No.	Mortar ID	Unit Type	PC/lime / sand Ratio	Curing	Sample No.	Joint No.	Applied Load (g)	Weight of Top Unit (g)	Applied Load, F_1 (N)	Weight of Top Unit, W (N)	Failure Mode	Bond Strength, f_{wi} (N/mm^2)	Notes	$\log_{10}$ of bond strength (Y_i)
74	L_bk_CL90s_170_1M_T	Broken Limestone	0:1:3	Lab	1	1	3680	2606.52	36.10	25.57	A1	0.025		-1.59
						2	4591	2645.26	45.04	25.95	A1	0.033		-1.48
						3	3941	2667.69	38.66	26.17	A1	0.028		-1.56
					2	4	4672	2671.76	45.83	26.21	A1	0.034		-1.47
						5							damaged	
						6	3297	2685.02	32.34	26.34	A1	0.022		-1.66
					3	7							damaged	
						8	3593	2654.43	35.25	26.04	A1	0.025		-1.61
						9	3631	2693.17	35.62	26.42	A1	0.025		-1.60
					4	10							damaged	
						11	3642	2606.52	35.73	25.57	A1	0.025		-1.60
						12	4660	2643.22	45.71	25.93	A1	0.034		-1.47
					5	13							damaged	
						14	4617	2617.74	45.29	25.68	A1	0.033		-1.48
						15	2599	2687.05	25.50	26.36	A1	0.016		-1.79
					Sample Mean							**0.027**		**-1.57**
					Sample Standard Deviation							**0.006**		**0.10**
					Coefficient of Variation							**0.211**		**-0.06**
					Y_c									**-1.76**
					Characteristic bond strength, f_{wk} (N/mm^2)									**0.017**

Table F.74: CL90-s broken limestone masonry bond strength calculations, 170 mm flow (1 month)

Test No.	Mortar ID	Unit Type	PC/lime / sand Ratio	Curing	Sample No.	Joint No.	Applied Load (g)	Weight of Top Unit (g)	Applied Load, F_1 (N)	Weight of Top Unit, W (N)	Failure Mode	Bond Strength, f_{wi} (N/mm^2)	Notes	$\log_{10}$ of bond strength (Y_i)
75	L_bk_CL90s_170_2M_T	Broken Limestone	0:1:3	Lab	1	1	4622	2624.87	45.34	25.75	A1	0.034		-1.47
						2	5643	2648.32	55.36	25.98	A1	0.042		-1.37
						3	6161	2636.09	60.44	25.86	A1	0.047		-1.33
					2	4	4625	2696.23	45.37	26.45	A1	0.034		-1.47
						5	4833	2671.76	47.41	26.21	A1	0.035		-1.45
						6	7048	2686.03	69.14	26.35	A1	0.054		-1.27
					3	7	5208	2617.74	51.09	25.68	A1	0.039		-1.41
						8							damaged	
						9	5048	2646.28	49.52	25.96	A1	0.037		-1.43
					4	10	5592	2633.03	54.86	25.83	A1	0.042		-1.38
						11	7392	2682.98	72.52	26.32	A1	0.057		-1.24
						12	3718	2643.22	36.47	25.93	A1	0.026		-1.59
					5	13	3433	2682.98	33.68	26.32	A1	0.023		-1.63
						14							damaged	
						15	5388	2674.82	52.86	26.24	A1	0.040		-1.40
					Sample Mean							**0.039**		**-1.42**
					Sample Standard Deviation							**0.010**		**0.11**
					Coefficient of Variation							**0.249**		**-0.08**
					Y_c									**-1.63**
					Characteristic bond strength, f_{wk} (N/mm^2)									**0.023**

Table F.75: CL90-s broken limestone masonry bond strength calculations, 170 mm flow (2 months)

Test No.	Mortar ID	Unit Type	PC/lime / sand Ratio	Curing	Sample No.	Joint No.	Applied Load (g)	Weight of Top Unit (g)	Applied Load, F_1 (N)	Weight of Top Unit, W (N)	Failure Mode	Bond Strength, f_{wi} (N/mm^2)	Notes	$\log_{10}$ of bond strength (Y_i)
76	L_bk_CL90s_170_6M_T	Broken Limestone	0:1:3	Lab	1	1	4497	2694.19	44.12	26.43	A1	0.032		-1.49
						2	7975	2688.07	78.23	26.37	A1	0.062		-1.21
						3	6221	2662.59	61.03	26.12	A1	0.047		-1.33
					2	4							damaged	
						5	3729	2613.66	36.58	25.64	A1	0.026		-1.59
						6							damaged	
					3	7	7962	2625.89	78.11	25.76	A1	0.062		-1.21
						8	4940	2693.17	48.46	26.42	A1	0.036		-1.44
						9	7148	2637.10	70.12	25.87	A1	0.055		-1.26
					4	10	5031	2629.97	49.35	25.80	A1	0.037		-1.43
						11							damaged	
						12	3423	2644.24	33.58	25.94	A1	0.023		-1.63
					5	13							damaged	
						14	6998	2651.38	68.65	26.01	A1	0.054		-1.27
						15	5151	2645.26	50.53	25.95	A1	0.038		-1.42
					Sample Mean							**0.043**		**-1.39**
					Sample Standard Deviation							**0.014**		**0.15**
					Coefficient of Variation							**0.322**		**-0.11**
					Y_c									**-1.67**
					Characteristic bond strength, f_{wk} (N/mm^2)									**0.021**

Table F.76: CL90-s broken limestone masonry bond strength calculations, 170 mm flow (6 months)

Test No.	Mortar ID	Unit Type	PC/lime / sand Ratio	Curing	Sample No.	Joint No.	Applied Load (g)	Weight of Top Unit (g)	Applied Load, F_1 (N)	Weight of Top Unit, W (N)	Failure Mode	Bond Strength, f_{wi} (N/mm^2)	Notes	$\log_{10}$ of bond strength (Y_i)
77	L_bk_NHL2_170_1M_T	Broken Limestone	0:1:3	Lab	1	1							damaged	
						2							damaged	
						3	5335	2682.98	52.34	26.32	A1	0.040		-1.40
					2	4	4065	2571.87	39.88	25.23	A1	0.029		-1.54
						5	4216	2666.67	41.36	26.16	A1	0.030		-1.52
						6	5313	2637.10	52.12	25.87	A1	0.039		-1.40
					3	7	4676	2648.32	45.87	25.98	A1	0.034		-1.47
						8	6106	2615.70	59.90	25.66	A1	0.046		-1.33
						9	7291	2676.86	71.52	26.26	A3	0.056		-1.25
					4	10	0						damaged	
						11	6127	2618.76	60.11	25.69	A1	0.046		-1.33
						12	3743	2651.38	36.72	26.01	A1	0.026		-1.59
					5	13	4032	2674.82	39.55	26.24	A1	0.028		-1.55
						14	5983	2662.59	58.69	26.12	A1	0.045		-1.35
						15	5650	2634.05	55.43	25.84	A1	0.042		-1.37
					Sample Mean							**0.039**		**-1.43**
					Sample Standard Deviation							**0.009**		**0.11**
					Coefficient of Variation							**0.241**		**-0.07**
					Y_c									**-1.63**
					Characteristic bond strength, f_{wk} (N/mm^2)									**0.024**

Table F.77: NHL 2 broken limestone masonry bond strength calculations, 170 mm flow (1 month)

Test No.	Mortar ID	Unit Type	PC/lime / sand Ratio	Curing	Sample No.	Joint No.	Applied Load (g)	Weight of Top Unit (g)	Applied Load, F_1 (N)	Weight of Top Unit, W (N)	Failure Mode	Bond Strength, f_{wi} (N/mm^2)	Notes	$\log_{10}$ of bond strength (Y_i)
78	L_bk_NHL2_170_2M_T	Broken Limestone	0:1:3	Lab	1	1	9851	2607.54	96.64	25.58	A1	0.078		-1.11
						2	8950	2673.80	87.80	26.23	A1	0.071		-1.15
						3	5347	2660.55	52.45	26.10	A1	0.040		-1.40
					2	4	6488	2634.05	63.65	25.84	A1	0.050		-1.31
						5							damaged	
						6	8527	2639.14	83.65	25.89	A1	0.067		-1.17
					3	7	8611	2651.38	84.47	26.01	A1	0.068		-1.17
						8	5473	2661.57	53.69	26.11	A1	0.041		-1.39
						9	10341	2687.05	101.45	26.36	A1	0.083		-1.08
					4	10							damaged	
						11							damaged	
						12	6242	2663.61	61.23	26.13	A1	0.047		-1.32
					5	13	7177	2646.28	70.41	25.96	A1	0.055		-1.26
						14	5990	2637.10	58.76	25.87	A1	0.045		-1.34
						15	5655	2627.93	55.48	25.78	A1	0.042		-1.37
					Sample Mean							**0.057**		**-1.26**
					Sample Standard Deviation							**0.015**		**0.11**
					Coefficient of Variation							**0.267**		**-0.09**
					Y_c									**-1.48**
					Characteristic bond strength, f_{wk} (N/mm^2)									**0.033**

Table F.78: NHL 2 broken limestone masonry bond strength calculations, 170 mm flow (2 months)

Test No.	Mortar ID	Unit Type	PC/lime / sand Ratio	Curing	Sample No.	Joint No.	Applied Load (g)	Weight of Top Unit (g)	Applied Load, F_1 (N)	Weight of Top Unit, W (N)	Failure Mode	Bond Strength, f_{wi} (N/mm^2)	Notes	$\log_{10}$ of bond strength (Y_i)
79	L_bk_NHL2_170_6M_T	Broken Limestone	0:1:3	Lab	1	1	8414	2633.03	82.54	25.83	A1	0.066		-1.18
						2	9314	2685.02	91.37	26.34	A1	0.074		-1.13
						3	8300	2661.57	81.42	26.11	A1	0.065		-0.38
					2	4	7791	2606.52	76.43	25.57	A1	0.061		-1.22
						5	6955	2687.05	68.23	26.36	A1	0.054		-0.38
						6	6417	2638.12	62.95	25.88	A1	0.049		-1.31
					3	7							damaged	
						8	5684	2659.53	55.76	26.09	A1	0.043		-1.37
						9	5862	2623.85	57.51	25.74	A1	0.044		-0.38
					4	10	9761	2681.96	95.76	26.31	A1	0.078		-1.11
						11	10402	2687.05	102.04	26.36	A1	0.083		-0.38
						12	7780	2617.74	76.32	25.68	A1	0.061		-1.22
					5	13	10612	2651.38	104.10	26.01	A1	0.085		-1.07
						14	8197	2617.74	80.41	25.68	A1	0.064		-1.19
						15	7265	2622.83	71.27	25.73	A1	0.056		-1.25
					Sample Mean							**0.063**		**-0.97**
					Sample Standard Deviation							**0.013**		**0.39**
					Coefficient of Variation							**0.213**		**-0.41**
					Y_c									**-1.73**
					Characteristic bond strength, f_{wk} (N/mm^2)									**0.019**

Table F.79: NHL 2 broken limestone masonry bond strength calculations, 170 mm flow (6 months)

Test No.	Mortar ID	Unit Type	PC/lime / sand Ratio	Curing	Sample No.	Joint No.	Applied Load (g)	Weight of Top Unit (g)	Applied Load, F_1 (N)	Weight of Top Unit, W (N)	Failure Mode	Bond Strength, f_{wi} (N/mm^2)	Notes	$\log_{10}$ of bond strength (Y_i)
80	L_cut_CL90s_165_1M_T	Cut Limestone	0:1:3	Lab	1	1	4383	3722.80	43.00	36.52	A1	0.031		-1.51
						2	2854	3718.30	28.00	36.48	A1	0.018		-1.75
						3	3364	3721.30	33.00	36.51	A1	0.022		-1.65
						4	3568	3722.80	35.00	36.52	A1	0.024		-1.62
						5							damaged	
					2	6							damaged	
						7	2854	3727.30	28.00	36.56	A1	0.018		-1.75
						8	2548	3721.40	25.00	36.51	A1	0.015		-1.82
						9							damaged	
						10	4587	3719.30	45.00	36.49	A1	0.033		-1.49
					3	11							damaged	
						12	4281	3721.80	42.00	36.51	A1	0.030		-1.52
						13							damaged	
						14							damaged	
						15	5607	3721.70	55.00	36.51	A1	0.041		-1.38
					Sample Mean							**0.026**		**-1.61**
					Sample Standard Deviation							**0.009**		**0.15**
					Coefficient of Variation							**0.333**		**-0.09**
					Y_c									**-1.89**
					Characteristic bond strength, f_{wk} (N/mm^2)									**0.013**

Table F.80: CL90-s cut limestone masonry bond strength calculations, 165 mm flow (1 month)

Test No.	Mortar ID	Unit Type	PC/lime / sand Ratio	Curing	Sample No.	Joint No.	Applied Load (g)	Weight of Top Unit (g)	Applied Load, F_1 (N)	Weight of Top Unit, W (N)	Failure Mode	Bond Strength, f_{wi} (N/mm^2)	Notes	$\log_{10}$ of bond strength (Y_i)
81	L_cut_CL90s_165_2M_T	Cut Limestone	0:1:3	Lab	1	1	5403	3723.70	53.00	36.53	A1	0.040		-1.40
						2	7034	3723.00	69.00	36.52	A1	0.054		-1.27
						3	6626	3721.90	65.00	36.51	A1	0.050		-1.30
						4							damaged	
						5							damaged	
					2	6	3568	3721.20	35.00	36.50	A1	0.024		-1.62
						7	1529	3719.80	15.00	36.49	A1	0.007		-2.19
						8							damaged	
						9	4077	3717.30	40.00	36.47	A1	0.028		-1.55
						10	2345	3719.00	23.00	36.48	A1	0.013		-1.87
					3	11	1631	3721.10	16.00	36.50	A1	0.007		-2.13
						12	8869	3722.00	87.00	36.51	A1	0.069		-1.16
						13	3772	3721.80	37.00	36.51	A1	0.026		-1.59
						14	3058	3721.00	30.00	36.50	A1	0.020		-1.71
						15	6422	3719.20	63.00	36.49	A1	0.048		-1.31
					Sample Mean							**0.032**		**-1.59**
					Sample Standard Deviation							**0.020**		**0.33**
					Coefficient of Variation							**0.621**		**-0.21**
					Y_c									**-2.23**
					Characteristic bond strength, f_{wk} (N/mm^2)									**0.006**

Table F.81: CL90-s cut limestone masonry bond strength calculations, 165 mm flow (2 months)

Test No.	Mortar ID	Unit Type	PC/lime / sand Ratio	Curing	Sample No.	Joint No.	Applied Load (g)	Weight of Top Unit (g)	Applied Load, F_1 (N)	Weight of Top Unit, W (N)	Failure Mode	Bond Strength, f_{wi} (N/mm^2)	Notes	$\log_{10}$ of bond strength (Y_i)
82	L_cut_CL90s_165_6M_T	Cut Limestone	0:1:3	Lab	1	1	7645	3722.10	75.00	36.51	A1	0.059		-1.23
						2							damaged	
						3	6626	3721.60	65.00	36.51	A1	0.050		-1.30
						4	4587	3723.80	45.00	36.53	A1	0.033		-1.49
						5							damaged	
					2	6	4383	3719.20	43.00	36.49	A1	0.031		-1.51
						7	3568	3721.40	35.00	36.51	A1	0.024		-1.62
						8	5607	3719.80	55.00	36.49	A1	0.041		-1.38
						9							damaged	
						10	5505	3720.00	54.00	36.49	A1	0.041		-1.39
					1	11	7441	3721.30	73.00	36.51	A1	0.057		-1.24
						12	8665	3725.80	85.00	36.55	A1	0.068		-1.17
						13	3466	3723.50	34.00	36.53	A1	0.023		-1.64
						14	7034	3721.00	69.00	36.50	A1	0.054		-1.27
						15	6626	3719.80	65.00	36.49	A1	0.050		-1.30
					Sample Mean							**0.044**		**-1.38**
					Sample Standard Deviation							**0.014**		**0.15**
					Coefficient of Variation							**0.326**		**-0.11**
					Y_c									**-1.67**
					Characteristic bond strength, f_{wk} (N/mm^2)									**0.021**

Table F.82: CL90-s cut limestone masonry bond strength calculations, 165 mm flow (6 months)

Test No.	Mortar ID	Unit Type	PC/lime / sand Ratio	Curing	Sample No.	Joint No.	Applied Load (g)	Weight of Top Unit (g)	Applied Load, F_1 (N)	Weight of Top Unit, W (N)	Failure Mode	Bond Strength, f_{wi} (N/mm^2)	Notes	$\log_{10}$ of bond strength (Y_i)
83	L_cut_NHL2_165_1M_T	Cut Limestone	0:1:3	Lab	1	1								
						2	3466	3722.00	34.00	36.51	A1	0.023		-1.64
						3							damaged	
						4	3976	3717.30	39.00	36.47	A1	0.027		-1.56
						5	3364	3723.60	33.00	36.53	A1	0.022		-1.65
					2	6							damaged	
						7	4587	3717.60	45.00	36.47	A1	0.033		-1.49
						8	3568	3719.00	35.00	36.48	A1	0.024		-1.62
						9	3772	3720.70	37.00	36.50	A1	0.026		-1.59
						10	5607	3722.90	55.00	36.52	A1	0.041		-1.38
					3	11	3772	3724.10	37.00	36.53	A1	0.026		-1.59
						12							damaged	
						13							damaged	
						14	2345	3715.80	23.00	36.45	A1	0.013		-1.87
						15	5810	3720.10	57.00	36.49	A1	0.043		-1.36
					Sample Mean							**0.028**		**-1.58**
					Sample Standard Deviation							**0.009**		**0.14**
					Coefficient of Variation							**0.322**		**-0.09**
					Y_c									**-1.85**
					Characteristic bond strength, f_{wk} (N/mm^2)									**0.014**

Table F.83: NHL 2 cut limestone masonry bond strength calculations, 165 mm flow (1 month)

Test No.	Mortar ID	Unit Type	PC/lime / sand Ratio	Curing	Sample No.	Joint No.	Applied Load (g)	Weight of Top Unit (g)	Applied Load, F_1 (N)	Weight of Top Unit, W (N)	Failure Mode	Bond Strength, f_{wi} (N/mm^2)	Notes	$\log_{10}$ of bond strength (Y_i)
84	L_cut_NHL2_165_2M_T	Cut Limestone	0:1:3	Lab	1	1	5607	3718.30	55.00	36.48	A1	0.041		-1.38
						2	8563	3719.60	84.00	36.49	A1	0.067		-1.18
						3							damaged	
						4	4587	3721.80	45.00	36.51	A1	0.033		-1.49
						5							damaged	
					2	6	3568	3720.70	35.00	36.50	A1	0.024		-1.62
						7	5505	3721.00	54.00	36.50	A1	0.041		-1.39
						8	7951	3719.70	78.00	36.49	A1	0.062		-1.21
						9							damaged	
						10	4587	3719.30	45.00	36.49	A1	0.033		-1.49
					3	11	7747	3718.00	76.00	36.47	A1	0.060		-1.22
						12	7645	3722.80	75.00	36.52	A1	0.059		-1.23
						13							damaged	
						14	7136	3721.10	70.00	36.50	A1	0.055		-1.26
						15	3568	3720.90	35.00	36.50	A1	0.024		-1.62
					Sample Mean							**0.045**		**-1.37**
					Sample Standard Deviation							**0.016**		**0.16**
					Coefficient of Variation							**0.348**		**-0.12**
					Y_c									**-1.69**
					Characteristic bond strength, f_{wk} (N/mm^2)									**0.021**

Table F.84: NHL 2 cut limestone masonry bond strength calculations, 165 mm flow (2 months)

Test No.	Mortar ID	Unit Type	PC/lime / sand Ratio	Curing	Sample No.	Joint No.	Applied Load (g)	Weight of Top Unit (g)	Applied Load, F_1 (N)	Weight of Top Unit, W (N)	Failure Mode	Bond Strength, f_{wi} (N/mm^2)	Notes	$\log_{10}$ of bond strength (Y_i)
85	L_cut_NHL2_165_6M_T	Cut Limestone	0:1:3	Lab	1	1							damaged	
						2							damaged	
						3	4383	3720.90	43.00	36.50	A1	0.031		-0.38
						4	10194	3719.20	100.00	36.49	A1	0.081		-1.09
						5	4485	3718.50	44.00	36.48	A1	0.032		-0.38
					2	6	5505	3719.40	54.00	36.49	A1	0.041		-1.39
						7	7645	3721.20	75.00	36.50	A1	0.059		-1.23
						8							damaged	
						9	5607	3721.70	55.00	36.51	A1	0.041		-0.38
						10	8869	3719.60	87.00	36.49	A1	0.069		-1.16
					3	11	7034	3720.30	69.00	36.50	A1	0.054		-0.38
						12							damaged	
						13	6626	3719.00	65.00	36.48	A1	0.050		-1.30
						14	7238	3719.30	71.00	36.49	A1	0.055		-1.26
						15	5810	3724.50	57.00	36.54	A1	0.043		-1.36
					Sample Mean							**0.051**		**-0.94**
					Sample Standard Deviation							**0.015**		**0.45**
					Coefficient of Variation							**0.303**		**-0.48**
					Y_c									**-1.80**
					Characteristic bond strength, f_{wk} (N/mm^2)									**0.016**

Table F.85: NHL 2 cut limestone masonry bond strength calculations, 165 mm flow (6 months)

Test No.	Mortar ID	Unit Type	PC/lime / sand Ratio	Curing	Sample No.	Joint No.	Applied Load (g)	Weight of Top Unit (g)	Applied Load, F_1 (N)	Weight of Top Unit, W (N)	Failure Mode	Bond Strength, f_{wi} (N/mm^2)	Notes	$\log_{10}$ of bond strength (Y_i)
86	L_cut_CL90s_170_1M_T	Cut Limestone	0:1:3	Lab	1	1	4485	3719.50	44.00	36.49	A1	0.032		-1.50
						2	3466	3711.50	34.00	36.41	A1	0.023		-1.64
						3							damaged	
						4	3976	3732.30	39.00	36.61	A1	0.027		-1.56
						5							damaged	
					2	6							damaged	
						7							damaged	
						8	2345	3731.90	23.00	36.61	A1	0.013		-1.87
						9	3772	3713.60	37.00	36.43	A1	0.026		-1.59
						10	5607	3733.60	55.00	36.63	A1	0.041		-1.38
					3	11	3772	3738.50	37.00	36.67	A1	0.026		-1.59
						12							damaged	
						13	3466	3719.40	34.00	36.49	A1	0.023		-1.64
						14	2345	3720.40	23.00	36.50	A1	0.013		-1.87
						15	3568	3722.70	35.00	36.52	A1	0.024		-1.62
					Sample Mean							**0.025**		**-1.63**
					Sample Standard Deviation							**0.008**		**0.15**
					Coefficient of Variation							**0.327**		**-0.09**
					Y_c									**-1.91**
					Characteristic bond strength, f_{wk} (N/mm^2)									**0.012**

Table F.86: CL90-s cut limestone masonry bond strength calculations, 170 mm flow (1 month)

Test No.	Mortar ID	Unit Type	PC/lime / sand Ratio	Curing	Sample No.	Joint No.	Applied Load (g)	Weight of Top Unit (g)	Applied Load, F_1 (N)	Weight of Top Unit, W (N)	Failure Mode	Bond Strength, f_{wi} (N/mm^2)	Notes	$\log_{10}$ of bond strength (Y_i)
87	L_cut_CL90s_170_2M_T	Cut Limestone	0:1:3	Lab	1	1	5505	3719.00	54.00	36.48	A1	0.041		-1.39
						2	4689	3722.20	46.00	36.51	A1	0.034		-1.47
						3	5199	3723.30	51.00	36.53	A1	0.038		-1.42
						4	3262	3718.30	32.00	36.48	A1	0.021		-1.67
						5	3670	3722.50	36.00	36.52	A1	0.025		-1.60
					2	6							damaged	
						7							damaged	
						8	4995	3720.30	49.00	36.50	A1	0.036		-1.44
						9	4587	3717.90	45.00	36.47	A1	0.033		-1.49
						10	4485	3721.40	44.00	36.51	A1	0.032		-1.50
					3	11	3262	3721.80	32.00	36.51	A1	0.021		-1.67
						12							damaged	
						13	7441	3720.60	73.00	36.50	A1	0.057		-1.24
						14	4383	3717.30	43.00	36.47	A1	0.031		-1.51
						15	4689	3720.00	46.00	36.49	A1	0.034		-1.47
					Sample Mean							**0.034**		**-1.49**
					Sample Standard Deviation							**0.010**		**0.12**
					Coefficient of Variation							**0.287**		**-0.08**
					Y_c									**-1.72**
					Characteristic bond strength, f_{wk} (N/mm^2)									**0.019**

Table F.87: CL90-s cut limestone masonry bond strength calculations, 170 mm flow (2 months)

Test No.	Mortar ID	Unit Type	PC/lime / sand Ratio	Curing	Sample No.	Joint No.	Applied Load (g)	Weight of Top Unit (g)	Applied Load, F_1 (N)	Weight of Top Unit, W (N)	Failure Mode	Bond Strength, f_{wi} (N/mm^2)	Notes	$\log_{10}$ of bond strength (Y_i)
88	L_cut_CL90s_170_6M_T	Cut Limestone	0:1:3	Lab	1	1	3364	3722.30	33.00	36.52	A1	0.022		-1.65
						2	5912	3721.80	58.00	36.51	A1	0.044		-1.36
						3	4995	3719.30	49.00	36.49	A1	0.036		-1.44
						4	5912	3722.40	58.00	36.52	A1	0.044		-1.36
						5							damaged	
					2	6	6626	3723.20	65.00	36.52	A1	0.050		-1.30
						7							damaged	
						8							damaged	
						9	3976	3719.80	39.00	36.49	A1	0.027		-1.56
						10							damaged	
					1	11	7951	3719.00	78.00	36.48	A1	0.062		-1.21
						12	6626	3728.20	65.00	36.57	A1	0.050		-1.30
						13							damaged	
						14	4485	3718.30	44.00	36.48	A1	0.032		-1.50
						15	5708	3719.00	56.00	36.48	A1	0.042		-1.37
					Sample Mean							**0.041**		**-1.40**
					Sample Standard Deviation							**0.012**		**0.13**
					Coefficient of Variation							**0.288**		**-0.10**
					Y_c									**-1.66**
					Characteristic bond strength, f_{wk} (N/mm^2)									**0.022**

Table F.88: CL90-s cut limestone masonry bond strength calculations, 170 mm flow (6 months)

Test No.	Mortar ID	Unit Type	PC/lime / sand Ratio	Curing	Sample No.	Joint No.	Applied Load (g)	Weight of Top Unit (g)	Applied Load, F_1 (N)	Weight of Top Unit, W (N)	Failure Mode	Bond Strength, f_{wi} (N/mm^2)	Notes	$\log_{10}$ of bond strength (Y_i)
89	L_cut_NHL2_170_1M_T	Cut Limestone	0:1:3	Lab	1	1	4485	3721.00	44.00	36.50	A1	0.032		-1.50
						2	5505	3723.40	54.00	36.53	A1	0.041		-0.81
						3							damaged	
						4							damaged	
						5	6626	3721.30	65.00	36.51	A1	0.050		-1.30
					2	6	3772	3719.00	37.00	36.48	A1	0.026		-1.59
						7	5607	3719.80	55.00	36.49	A1	0.041		-0.81
						8							damaged	
						9	3772	3722.90	37.00	36.52	A1	0.026		-0.81
						10	4383	3717.30	43.00	36.47	A1	0.031		-0.89
					3	11			37.00				damaged	
						12							damaged	
						13	3466	3722.30	34.00	36.52	A1	0.023		-0.89
						14	3466	3722.70	34.00	36.52	A1	0.023		-1.64
						15	5810	3720.10	57.00	36.49	A1	0.043		-1.36
					Sample Mean							**0.034**		**-1.16**
					Sample Standard Deviation							**0.010**		**0.35**
					Coefficient of Variation							**0.286**		**-0.30**
					Y_c									**-1.83**
					Characteristic bond strength, f_{wk} (N/mm^2)									**0.015**

Table F.89: NHL 2 cut limestone masonry bond strength calculations, 170 mm flow (1 month)

Test No.	Mortar ID	Unit Type	PC/lime / sand Ratio	Curing	Sample No.	Joint No.	Applied Load (g)	Weight of Top Unit (g)	Applied Load, F_1 (N)	Weight of Top Unit, W (N)	Failure Mode	Bond Strength, f_{wi} (N/mm^2)	Notes	$\log_{10}$ of bond strength (Y_i)
90	L_cut_NHL2_170_2M_T	Cut Limestone	0:1:3	Lab	1	1	9990	3718.00	98.00	36.47	A1	0.079		-1.10
						2	4587	3720.30	45.00	36.50	A1	0.033		-1.49
						3							damaged	
						4	7441	3722.40	73.00	36.52	A1	0.057		-1.24
						5							damaged	
					2	6	6830	3719.70	67.00	36.49	A1	0.052		-1.28
						7	6932	3720.40	68.00	36.50	A1	0.053		-1.28
						8	6218	3722.30	61.00	36.52	A1	0.047		-1.33
						9	5708	3719.20	56.00	36.49	A1	0.042		-1.37
						10	5199	3720.40	51.00	36.50	A1	0.038		-1.42
					3	11	8053	3721.30	79.00	36.51	A1	0.062		-1.20
						12	8665	3720.70	85.00	36.50	A1	0.068		-1.17
													damaged	
						14	2345	3724.30	23.00	36.54	A1	0.013		-1.87
						15							damaged	
					Sample Mean							**0.050**		**-1.34**
					Sample Standard Deviation							**0.018**		**0.21**
					Coefficient of Variation							**0.362**		**-0.15**
					Y_c									**-1.74**
					Characteristic bond strength, f_{wk} (N/mm^2)									**0.018**

Table F.90: NHL 2 cut limestone masonry bond strength calculations, 170 mm flow (2 months)

Test No.	Mortar ID	Unit Type	PC/lime / sand Ratio	Curing	Sample No.	Joint No.	Applied Load (g)	Weight of Top Unit (g)	Applied Load, F_1 (N)	Weight of Top Unit, W (N)	Failure Mode	Bond Strength, f_{wi} (N/mm^2)	Notes	$\log_{10}$ of bond strength (Y_i)
91	L_cut_NHL2_170_6M_T	Cut Limestone	0:1:3	Lab	1	1	4383	3724.80	43.00	36.54	A1	0.031		-1.51
						2	6626	3722.30	65.00	36.52	A1	0.050		-1.30
						3	6422	3719.30	63.00	36.49	A1	0.048		-1.31
						4	11213	3719.00	110.00	36.48	A1	0.090		-1.05
						5	4587	3719.80	45.00	36.49	A1	0.033		-1.49
					2	6							damaged	
						7							damaged	
						8	6524	3728.80	64.00	36.58	A1	0.049		-1.31
						9	7951	3717.30	78.00	36.47	A1	0.062		-1.21
						10	9684	3718.80	95.00	36.48	A1	0.076		-1.12
					3	11	5505	3719.50	54.00	36.49	A1	0.041		-1.39
						12							damaged	
						13	9174	3721.90	90.00	36.51	A1	0.072		-1.14
						14	8665	3722.70	85.00	36.52	A1	0.068		-1.17
						15	10398	3721.40	102.00	36.51	A1	0.083		-1.08
					Sample Mean							**0.059**		**-1.26**
					Sample Standard Deviation							**0.019**		**0.15**
					Coefficient of Variation							**0.331**		**-0.12**
					Y_c									**-1.55**
					Characteristic bond strength, f_{wk} (N/mm^2)									**0.028**

Table F.91: NHL 2 cut limestone masonry bond strength calculations, 170 mm flow (6 months)

APPENDIX G

MASONRY FLEXURAL STRENGTH RESULTS AND CALCULATIONS

(PARALLEL AND PERPENDICULAR TO BEDDING JOINTS)

Test no	Masonry ID		Unit Type	PC/ lime/ sand	Initial flow (mm)	Curing	Test age	Specimen Dims Length b (mm)	Width t_u (mm)	Height (mm)	Apparatus Dims l_1 (mm)	l_2 (mm)	Max load, F_c (kN)	Flexural strength, f_{xi} (N/mm^2)	Mean compressive strength, R_c (N/mm^2)	COV (%)	Characteristic compressive strength f_k (N/mm^2)
1	B_M6_165_1m_F1	A	Brick	0:1:3	165	lab	28	335	102.5	375	285	154	9.67	0.54	**0.49**	**12.79%**	**0.33**
2		B					days	335	102.5	375	285	154	8.78	0.49			
3		C						335	102.5	375	285	154	7.38	0.41			
4		D						335	102.5	375	285	154	7.99	0.45			
5		E						335	102.5	375	285	154	10.07	0.56			
6	B_M6_165_2m_F1	A	Brick	0:1:3	165	lab	56	335	102.5	375	285	154	10.03	0.56	**0.59**	**5.99%**	**0.39**
7		B					days	335	102.5	375	285	154	11.28	0.63			
8		C						335	102.5	375	285	154	9.85	0.55			
9		D						335	102.5	375	285	154	10.57	0.59			
10		E						335	102.5	375	285	154	11.11	0.62			
11	B_M6_165_6m_F1	A	Brick	0:1:3	165	lab	6	335	102.5	375	285	154	12.91	0.72	**0.67**	**10.33%**	**0.45**
12		B					mts.	335	102.5	375	285	154	11.93	0.67			
13		C						335	102.5	375	285	154	11.94	0.67			
14		D						335	102.5	375	285	154	10.03	0.56			
15		E						335	102.5	375	285	154	13.19	0.74			
16	B_M6_170_1m_F1	A	Brick	0:1:3	165	lab	28	335	102.5	375	285	154	11.64	0.65	**0.63**	**7.13%**	**0.42**
17		B					days	335	102.5	375	285	154	10.69	0.60			
18		C						335	102.5	375	285	154	10.21	0.57			
19		D						335	102.5	375	285	154	11.71	0.65			
20		E						335	102.5	375	285	154	12.16	0.68			
21	B_M6_170_2m_F1	A	Brick	0:1:3	165	lab	56	335	102.5	375	285	154	11.64	0.65	**0.68**	**12.54%**	**0.45**
22		B					days	335	102.5	375	285	154	12.18	0.68			
23		C						335	102.5	375	285	154	9.92	0.55			
24		D						335	102.5	375	285	154	13.43	0.75			
25		E						335	102.5	375	285	154	13.72	0.77			
26	B_M6_170_6m_F1	A	Brick	0:1:3	165	lab	6	335	102.5	375	285	154	12.72	0.71	**0.76**	**8.02%**	**0.51**
27		B					mts.	335	102.5	375	285	154	15.22	0.85			
28		C						335	102.5	375	285	154	12.48	0.70			
29		D						335	102.5	375	285	154	13.88	0.78			
30		E						335	102.5	375	285	154	13.76	0.77			

Table G.1: M6 brick masonry flexural strength (parallel to bedding joints)

Test no	Masonry ID		Unit Type	PC/ lime/ sand	Initial flow (mm)	Curing	Test age	Specimen Dims Length b (mm)	Width t_u (mm)	Height (mm)	Apparatus Dims l_1 (mm)	l_2 (mm)	Max load, F_c (kN)	Flexural strength, f_{xi} (N/mm^2)	Mean compressive strength, R_c (N/mm^2)	COV (%)	Characteristic compressive strength f_k (N/mm^2)
31	B_NHL5_165_1m_F1	A	Brick	0:1:3	165	lab	28	335	102.5	375	285	154	3.37	0.19	**0.22**	**9.97%**	**0.15**
32		B					days	335	102.5	375	285	154	4.03	0.23			
33		C						335	102.5	375	285	154	3.85	0.22			
34		D						335	102.5	375	285	154	4.46	0.25			
35		E						335	102.5	375	285	154	3.99	0.22			
36	B_NHL5_165_2m_F1	A	Brick	0:1:3	165	lab	56	335	102.5	375	285	154	6.34	0.35	**0.32**	**8.10%**	**0.21**
37		B					days	335	102.5	375	285	154	5.83	0.33			
38		C						335	102.5	375	285	154	damaged				
39		D						335	102.5	375	285	154	5.61	0.31			
40		E						335	102.5	375	285	154	5.22	0.29			
41	B_NHL5_165_6m_F1	A	Brick	0:1:3	165	lab	6	335	102.5	375	285	154	7.99	0.45	**0.43**	**6.20%**	**0.29**
42		B					mts.	335	102.5	375	285	154	7.81	0.44			
43		C						335	102.5	375	285	154	8.17	0.46			
44		D						335	102.5	375	285	154	7.61	0.43			
45		E						335	102.5	375	285	154	6.93	0.39			
46	B_NHL5_170_1m_F1	A	Brick	0:1:3	165	lab	28	335	102.5	375	285	154	4.39	0.25	**0.24**	**3.31%**	**0.16**
47		B					days	335	102.5	375	285	154	4.23	0.24			
48		C						335	102.5	375	285	154	4.14	0.23			
49		D						335	102.5	375	285	154	4.25	0.24			
50		E						335	102.5	375	285	154	4.50	0.25			
51	B_NHL5_170_2m_F1	A	Brick	0:1:3	165	lab	56	335	102.5	375	285	154	6.00	0.34	**0.35**	**5.01%**	**0.23**
52		B					days	335	102.5	375	285	154	6.13	0.34			
53		C						335	102.5	375	285	154	6.50	0.36			
54		D						335	102.5	375	285	154	6.70	0.37			
55		E						335	102.5	375	285	154	6.02	0.34			
56	B_NHL5_170_6m_F1	A	Brick	0:1:3	165	lab	6	335	102.5	375	285	154	9.06	0.51	**0.51**	**8.87%**	**0.34**
57		B					mts.	335	102.5	375	285	154	9.53	0.53			
58		C						335	102.5	375	285	154	8.33	0.47			
59		D						335	102.5	375	285	154	10.30	0.58			
60		E						335	102.5	375	285	154	8.45	0.47			

Table G.2: NHL 5 brick masonry flexural strength (parallel to bedding joints)

Test no	Masonry ID		Unit Type	PC/ lime/ sand	Initial flow (mm)	Curing	Test age	Specimen Dims Length b (mm)	Width t_u (mm)	Height (mm)	Apparatus Dims l_1 (mm)	l_2 (mm)	Max load, F_c (kN)	Flexural strength, f_{xi} (N/mm^2)	Mean compressive strength, R_c (N/mm^2)	COV (%)	Characteristic compressive strength f_k (N/mm^2)
61	B_NHL3.5_165_1m_F1	A	Brick	0:1:3	165	lab	28	335	102.5	375	285	154	2.99	0.17	**0.18**	**8.83%**	**0.12**
62		B					days	335	102.5	375	285	154	damaged				
63		C						335	102.5	375	285	154	3.67	0.21			
64		D						335	102.5	375	285	154	2.97	0.17			
65		E						335	102.5	375	285	154	3.30	0.18			
66	B_NHL3.5_165_2m_F1	A	Brick	0:1:3	165	lab	56	335	102.5	375	285	154	3.49	0.20	**0.20**	**7.62%**	**0.13**
67		B					days	335	102.5	375	285	154	3.62	0.20			
68		C						335	102.5	375	285	154	3.17	0.18			
69		D						335	102.5	375	285	154	3.74	0.21			
70		E						335	102.5	375	285	154	3.89	0.22			
71	B_NHL3.5_165_6m_F1	A	Brick	0:1:3	165	lab	6	335	102.5	375	285	154	5.95	0.33	**0.30**	**6.75%**	**0.20**
72		B					mts.	335	102.5	375	285	154	5.39	0.30			
73		C						335	102.5	375	285	154	5.28	0.30			
74		D						335	102.5	375	285	154	4.94	0.28			
75		E						335	102.5	375	285	154	5.30	0.30			
76	B_NHL3.5_170_1m_F1	A	Brick	0:1:3	165	lab	28	335	102.5	375	285	154	3.55	0.20	**0.19**	**4.81%**	**0.13**
77		B					days	335	102.5	375	285	154	3.13	0.18			
78		C						335	102.5	375	285	154	3.37	0.19			
79		D						335	102.5	375	285	154	3.47	0.19			
80		E						335	102.5	375	285	154	3.49	0.20			
81	B_NHL3.5_170_2m_F1	A	Brick	0:1:3	165	lab	56	335	102.5	375	285	154	3.92	0.22	**0.21**	**4.60%**	**0.14**
82		B					days	335	102.5	375	285	154	3.85	0.22			
83		C						335	102.5	375	285	154	3.51	0.20			
84		D						335	102.5	375	285	154	3.65	0.20			
85		E						335	102.5	375	285	154	3.87	0.22			
86	B_NHL3.5_170_6m_F1	A	Brick	0:1:3	165	lab	6	335	102.5	375	285	154	5.48	0.31	**0.30**	**5.63%**	**0.20**
87		B					mts.	335	102.5	375	285	154	5.41	0.30			
88		C						335	102.5	375	285	154	5.64	0.32			
89		D						335	102.5	375	285	154	5.48	0.31			
90		E						335	102.5	375	285	154	4.85	0.27			

Table G.3: NHL3. 5 brick masonry flexural strength (parallel to bedding joints)

Test no	Masonry ID		Unit Type	PC/ lime/ sand	Initial flow (mm)	Curing	Test age	Specimen Dims Length b (mm)	Width t_u (mm)	Height (mm)	Apparatus Dims l_1 (mm)	l_2 (mm)	Max load, F_c (kN)	Flexural strength, f_{xi} (N/mm^2)	Mean compressive strength, R_c (N/mm^2)	COV (%)	Characteristic compressive strength f_k (N/mm^2)
91	B_NHL3.5_165_1m_F1	A	Brick	0:1:2	165	lab	28	335	102.5	375	285	154	5.62	0.31	**0.30**	**11.52%**	**0.20**
92		B					days	335	102.5	375	285	154	6.14	0.34			
93		C						335	102.5	375	285	154	5.28	0.30			
94		D						335	102.5	375	285	154	5.37	0.30			
95		E						335	102.5	375	285	154	4.44	0.25			
96	B_NHL3.5_165_2m_F1	A	Brick	0:1:2	165	lab	56	335	102.5	375	285	154	6.90	0.39	**0.39**	**7.24%**	**0.26**
97		B					days	335	102.5	375	285	154	6.34	0.35			
98		C						335	102.5	375	285	154	7.38	0.41			
99		D						335	102.5	375	285	154	6.72	0.38			
100		E						335	102.5	375	285	154	7.59	0.42			
101	B_NHL3.5_165_6m_F1	A	Brick	0:1:2	165	lab	6	335	102.5	375	285	154	8.11	0.45	**0.45**	**2.59%**	**0.30**
102		B					mts.	335	102.5	375	285	154	8.08	0.45			
103		C						335	102.5	375	285	154	8.29	0.46			
104		D						335	102.5	375	285	154	8.10	0.45			
105		E						335	102.5	375	285	154	7.72	0.43			

Table G.4: NHL3. 5 brick masonry flexural strength (parallel to bedding joints) (mix ratio 0:1:2)

Test no	Masonry ID		Unit Type	PC/ lime/ sand	Initial flow (mm)	Curing	Test age	Specimen Dims Length b (mm)	Width t_u (mm)	Height (mm)	Apparatus Dims l_1 (mm)	l_2 (mm)	Max load, F_c (kN)	Flexural strength, f_{xi} (N/mm^2)	Mean compressive strength, R_c (N/mm^2)	COV (%)	Characteristic compressive strength f_k (N/mm^2)
106	B_NHL2_165_1m_F1	A	Brick	0:1:3	165	lab	28	335	102.5	375	285	154	1.49	0.08	**0.08**	**6.43%**	**0.05**
107		B					days	335	102.5	375	285	154	1.40	0.08			
108		C						335	102.5	375	285	154	1.29	0.07			
109		D						335	102.5	375	285	154	1.47	0.08			
110		E						335	102.5	375	285	154	1.52	0.09			
111	B_NHL2_165_2m_F1	A	Brick	0:1:3	165	lab	56	335	102.5	375	285	154	2.76	0.15	**0.14**	**13.16%**	**0.09**
112		B					days	335	102.5	375	285	154	2.81	0.16			
113		C						335	102.5	375	285	154	2.36	0.13			
114		D						335	102.5	375	285	154	2.60	0.15			
115		E						335	102.5	375	285	154	2.01	0.11			
116	B_NHL2_165_6m_F1	A	Brick	0:1:3	165	lab	6	335	102.5	375	285	154	3.53	0.20	**0.19**	**5.68%**	**0.13**
117		B					mts.	335	102.5	375	285	154	3.33	0.19			
118		C						335	102.5	375	285	154	3.15	0.18			
119		D						335	102.5	375	285	154	3.65	0.20			
120		E						335	102.5	375	285	154	3.35	0.19			
121	B_NHL2_170_1m_F1	A	Brick	0:1:3	165	lab	28	335	102.5	375	285	154	1.65	0.09	**0.09**	**21.02%**	**0.06**
122		B					days	335	102.5	375	285	154	damaged				
123		C						335	102.5	375	285	154	1.33	0.07			
124		D						335	102.5	375	285	154	2.02	0.11			
125		E						335	102.5	375	285	154	1.33	0.07			
126	B_NHL2_170_2m_F1	A	Brick	0:1:3	165	lab	56	335	102.5	375	285	154	3.03	0.17	**0.18**	**8.98%**	**0.12**
127		B					days	335	102.5	375	285	154	2.92	0.16			
128		C						335	102.5	375	285	154	3.35	0.19			
129		D						335	102.5	375	285	154	3.65	0.20			
130		E						335	102.5	375	285	154	3.17	0.18			
131	B_NHL2_170_6m_F1	A	Brick	0:1:3	165	lab	6	335	102.5	375	285	154	3.76	0.21	**0.21**	**6.13%**	**0.14**
132		B					mts.	335	102.5	375	285	154	3.83	0.21			
133		C						335	102.5	375	285	154	4.01	0.22			
134		D						335	102.5	375	285	154	3.82	0.21			
135		E						335	102.5	375	285	154	3.39	0.19			

Table G.5: NHL2 brick masonry flexural strength (parallel to bedding joints)

Test no	Masonry ID		Unit Type	PC/ lime/ sand	Initial flow (mm)	Curing	Test age	Specimen Dims Length b (mm)	Width t_u (mm)	Height (mm)	Apparatus Dims l_1 (mm)	l_2 (mm)	Max load, F_c (kN)	Flexural strength, f_{xi} (N/mm^2)	Mean compressive strength, R_c (N/mm^2)	COV (%)	Characteristic compressive strength f_k (N/mm^2)
136	B_CL90-s_165_1m_F1	A	Brick	0:1:3	165	lab	28	335	102.5	375	285	154	1.49	0.08	**0.08**	**6.43%**	**0.05**
137		B					days	335	102.5	375	285	154	1.40	0.08			
138		C						335	102.5	375	285	154	1.29	0.07			
139		D						335	102.5	375	285	154	1.47	0.08			
140		E						335	102.5	375	285	154	1.52	0.09			
141	B_CL90-s_165_2m_F1	A	Brick	0:1:3	165	lab	56	335	102.5	375	285	154	2.76	0.15	**0.14**	**13.16%**	**0.09**
142		B					days	335	102.5	375	285	154	2.81	0.16			
143		C						335	102.5	375	285	154	2.36	0.13			
144		D						335	102.5	375	285	154	2.60	0.15			
145		E						335	102.5	375	285	154	2.01	0.11			
146	B_CL90-s_165_6m_F1	A	Brick	0:1:3	165	lab	6	335	102.5	375	285	154	3.53	0.20	**0.19**	**5.68%**	**0.13**
147		B					mts.	335	102.5	375	285	154	3.33	0.19			
148		C						335	102.5	375	285	154	3.15	0.18			
149		D						335	102.5	375	285	154	3.65	0.20			
150		E						335	102.5	375	285	154	3.35	0.19			
151	B_CL90-s_170_1m_F1	A	Brick	0:1:3	165	lab	28	335	102.5	375	285	154	1.65	0.09	**0.09**	**21.02%**	**0.06**
152		B					days	335	102.5	375	285	154	damaged				
153		C						335	102.5	375	285	154	1.33	0.07			
154		D						335	102.5	375	285	154	2.02	0.11			
155		E						335	102.5	375	285	154	1.33	0.07			
156	B_CL90-s_170_2m_F1	A	Brick	0:1:3	165	lab	56	335	102.5	375	285	154	3.03	0.17	**0.18**	**8.98%**	**0.12**
157		B					days	335	102.5	375	285	154	2.92	0.16			
158		C						335	102.5	375	285	154	3.35	0.19			
159		D						335	102.5	375	285	154	3.65	0.20			
160		E						335	102.5	375	285	154	3.17	0.18			
161	B_CL90-s_170_6m_F1	A	Brick	0:1:3	165	lab	6	335	102.5	375	285	154	3.76	0.21	**0.21**	**6.13%**	**0.14**
162		B					mts.	335	102.5	375	285	154	3.83	0.21			
163		C						335	102.5	375	285	154	4.01	0.22			
164		D						335	102.5	375	285	154	3.82	0.21			
165		E						335	102.5	375	285	154	3.39	0.19			

Table G.6: NHL3. 5 brick masonry flexural strength (parallel to bedding joints)

Test no	Masonry ID		Unit Type	PC/ lime/ sand	Initial flow (mm)	Curing	Test age	Specimen Dims Length b (mm)	Width t_u (mm)	Height (mm)	Apparatus Dims l_1 (mm)	l_2 (mm)	Max load, F_c (kN)	Flexural strength, f_{xi} (N/mm^2)	Mean compressive strength, R_c (N/mm^2)	COV (%)	Characteristic compressive strength f_k (N/mm^2)
166	B_M6_165_1m_F2	A	Brick	0:1:3	165	lab	28	558	102.5	300	470	235	12.84	1.44	**1.50**	**2.95%**	**1.00**
167		B					days	558	102.5	300	470	235	13.19	1.48			
168		C						558	102.5	300	470	235	13.70	1.53			
169		D						558	102.5	300	470	235	13.53	1.51			
170		E						558	102.5	300	470	235	13.81	1.54			
171	B_M6_165_2m_F2	A	Brick	0:1:3	165	lab	56	558	102.5	300	470	235	15.39	1.72	**1.77**	**2.62%**	**1.18**
172		B					days	558	102.5	300	470	235	15.67	1.75			
173		C						558	102.5	300	470	235	15.97	1.79			
174		D						558	102.5	300	470	235	16.47	1.84			
175		E						558	102.5	300	470	235	15.64	1.75			
176	B_M6_165_6m_F2	A	Brick	0:1:3	165	lab	6	558	102.5	300	470	235	16.50	1.85	**1.90**	**2.78%**	**1.27**
177		B					mts.	558	102.5	300	470	235	17.56	1.96			
178		C						558	102.5	300	470	235	16.58	1.85			
179		D						558	102.5	300	470	235	17.37	1.94			
180		E						558	102.5	300	470	235	16.94	1.89			
181	B_M6_170_1m_F2	A	Brick	0:1:3	165	lab	28	558	102.5	300	470	235	15.42	1.72	**1.73**	**3.22%**	**1.15**
182		B					days	558	102.5	300	470	235	14.69	1.64			
183		C						558	102.5	300	470	235	15.49	1.73			
184		D						558	102.5	300	470	235	15.71	1.76			
185		E						558	102.5	300	470	235	16.04	1.79			
186	B_M6_170_2m_F2	A	Brick	0:1:3	165	lab	56	558	102.5	300	470	235	16.81	1.88	**1.85**	**14.90%**	**1.23**
187		B					days	558	102.5	300	470	235	16.48	1.84			
188		C						558	102.5	300	470	235	16.94	1.89			
189		D						558	102.5	300	470	235	12.79	1.43			
190		E						558	102.5	300	470	235	19.70	2.20			
191	B_M6_170_6m_F2	A	Brick	0:1:3	165	lab	6	558	102.5	300	470	235	18.88	2.11	**2.17**	**3.01%**	**1.45**
192		B					mts.	558	102.5	300	470	235	19.55	2.19			
193		C						558	102.5	300	470	235	18.72	2.09			
194		D						558	102.5	300	470	235	19.76	2.21			
195		E						558	102.5	300	470	235	20.10	2.25			

Table G.7: M6 brick masonry flexural strength (parallel to bedding joints)

Test no	Masonry ID		Unit Type	PC/ lime/ sand	Initial flow (mm)	Curing	Test age	Specimen Dims Length b (mm)	Width t_u (mm)	Height (mm)	Apparatus Dims l_1 (mm)	l_2 (mm)	Max load, F_c (kN)	Flexural strength, f_{xi} (N/mm^2)	Mean compressive strength, R_c (N/mm^2)	COV (%)	Characteristic compressive strength f_k (N/mm^2)
196	B_NHL5_165_1m_F2	A	Brick	0:1:3	165	lab	28	558	102.5	300	470	235	7.80	0.87	**1.05**	**9.94%**	**0.70**
197		B					days	558	102.5	300	470	235	9.49	1.06			
198		C						558	102.5	300	470	235	9.57	1.07			
199		D						558	102.5	300	470	235	9.90	1.11			
200		E						558	102.5	300	470	235	10.19	1.14			
201	B_NHL5_165_2m_F2	A	Brick	0:1:3	165	lab	56	558	102.5	300	470	235	11.09	1.24	**1.18**	**4.47%**	**0.79**
202		B					days	558	102.5	300	470	235	9.94	1.11			
203		C						558	102.5	300	470	235	10.90	1.22			
204		D						558	102.5	300	470	235	10.22	1.14			
205		E						558	102.5	300	470	235	10.60	1.19			
206	B_NHL5_165_6m_F2	A	Brick	0:1:3	165	lab	6	558	102.5	300	470	235	11.95	1.34	**1.32**	**5.34%**	**0.88**
207		B					mts.	558	102.5	300	470	235	12.11	1.35			
208		C						558	102.5	300	470	235	12.29	1.38			
209		D						558	102.5	300	470	235	10.70	1.20			
210		E						558	102.5	300	470	235	11.96	1.34			
211	B_NHL5_170_1m_F2	A	Brick	0:1:3	165	lab	28	558	102.5	300	470	235	9.82	1.10	**1.08**	**7.38%**	**0.72**
212		B					days	558	102.5	300	470	235	9.94	1.11			
213		C						558	102.5	300	470	235	9.06	1.01			
214		D						558	102.5	300	470	235	10.61	1.19			
215		E						558	102.5	300	470	235	8.85	0.99			
216	B_NHL5_170_2m_F2	A	Brick	0:1:3	165	lab	56	558	102.5	300	470	235	10.94	1.22	**1.23**	**10.99%**	**0.82**
217		B					days	558	102.5	300	470	235	10.61	1.19			
218		C						558	102.5	300	470	235	11.21	1.25			
219		D						558	102.5	300	470	235	12.79	1.43			
220		E						558	102.5	300	470	235	9.43	1.06			
221	B_NHL5_170_6m_F2	A	Brick	0:1:3	165	lab	6	558	102.5	300	470	235	13.91	1.56	**1.54**	**5.13%**	**1.03**
222		B					mts.	558	102.5	300	470	235	12.92	1.45			
223		C						558	102.5	300	470	235	13.98	1.56			
224		D						558	102.5	300	470	235	14.75	1.65			
225		E						558	102.5	300	470	235	13.28	1.49			

Table G.8: NHL 5 brick masonry flexural strength (perpendicular to bedding joints)

Test no	Masonry ID		Unit Type	PC/ lime/ sand	Initial flow (mm)	Curing	Test age	Specimen Dims Length b (mm)	Width t_u (mm)	Height (mm)	Apparatus Dims l_1 (mm)	l_2 (mm)	Max load, F_c (kN)	Flexural strength, f_{xi} (N/mm^2)	Mean compressive strength, R_c (N/mm^2)	COV (%)	Characteristic compressive strength f_k (N/mm^2)
226	B_NHL3.5_165_1m_F2	A	Brick	0:1:3	165	lab	28	558	102.5	300	470	235	6.59	0.74	**0.72**	**6.21%**	**0.48**
227		B					days	558	102.5	300	470	235	6.94	0.78			
228		C						558	102.5	300	470	235	6.10	0.68			
229		D						558	102.5	300	470	235	5.96	0.67			
230		E						558	102.5	300	470	235	6.60	0.74			
231	B_NHL3.5_165_2m_F2	A	Brick	0:1:3	165	lab	56	558	102.5	300	470	235	7.64	0.85	**0.88**	**6.76%**	**0.59**
232		B					days	558	102.5	300	470	235	7.26	0.81			
233		C						558	102.5	300	470	235	7.60	0.85			
234		D						558	102.5	300	470	235	8.32	0.93			
235		E						558	102.5	300	470	235	8.53	0.95			
236	B_NHL3.5_165_6m_F2	A	Brick	0:1:3	165	lab	6	558	102.5	300	470	235	8.53	0.95	**0.92**	**3.96%**	**0.61**
237		B					mts.	558	102.5	300	470	235	8.18	0.92			
238		C						558	102.5	300	470	235	7.69	0.86			
239		D						558	102.5	300	470	235	8.41	0.94			
240		E						558	102.5	300	470	235	8.32	0.93			
241	B_NHL3.5_170_1m_F2	A	Brick	0:1:3	165	lab	28	558	102.5	300	470	235	7.64	0.85	**0.80**	**8.55%**	**0.53**
242		B					days	558	102.5	300	470	235	7.18	0.80			
243		C						558	102.5	300	470	235	6.74	0.75			
244		D						558	102.5	300	470	235	6.37	0.71			
245		E						558	102.5	300	470	235	7.84	0.88			
246	B_NHL3.5_170_2m_F2	A	Brick	0:1:3	165	lab	56	558	102.5	300	470	235	8.43	0.94	**0.89**	**7.17%**	**0.59**
247		B					days	558	102.5	300	470	235	7.34	0.82			
248		C						558	102.5	300	470	235	8.54	0.96			
249		D						558	102.5	300	470	235	8.10	0.91			
250		E						558	102.5	300	470	235	7.38	0.83			
251	B_NHL3.5_170_6m_F2	A	Brick	0:1:3	165	lab	6	558	102.5	300	470	235	9.13	1.02	**1.00**	**13.08%**	**0.67**
252		B					mts.	558	102.5	300	470	235	10.09	1.13			
253		C						558	102.5	300	470	235	9.42	1.05			
254		D						558	102.5	300	470	235	6.97	0.78			
255		E						558	102.5	300	470	235	9.09	1.02			

Table G.9: NHL 3.5 brick masonry flexural strength (perpendicular to bedding joints)

Test no	Masonry ID		Unit Type	PC/ lime/ sand	Initial flow (mm)	Curing	Test age	Specimen Dims Length b (mm)	Width t_u (mm)	Height (mm)	Apparatus Dims l_1 (mm)	l_2 (mm)	Max load, F_c (kN)	Flexural strength, f_{xi} (N/mm^2)	Mean compressive strength, R_c (N/mm^2)	COV (%)	Characteristic compressive strength f_k (N/mm^2)
256	B_NHL3.5_170_1m_F2	A	Brick	0:1:2	165	lab	28	558	102.5	300	470	235	7.54	0.84	**0.87**	**6.47%**	**0.58**
257		B					days	558	102.5	300	470	235	7.61	0.85			
258		C						558	102.5	300	470	235	8.49	0.95			
259		D						558	102.5	300	470	235	7.20	0.81			
260		E						558	102.5	300	470	235	8.06	0.90			
261	B_NHL3.5_170_2m_F2	A	Brick	0:1:2	165	lab	56	558	102.5	300	470	235	12.23	1.37	**1.32**	**8.90%**	**0.88**
262		B					days	558	102.5	300	470	235	11.16	1.25			
263		C						558	102.5	300	470	235	10.41	1.16			
264		D						558	102.5	300	470	235	13.14	1.47			
265		E						558	102.5	300	470	235	12.07	1.35			
266	B_NHL3.5_170_6m_F2	A	Brick	0:1:2	165	lab	6	558	102.5	300	470	235	12.88	1.44	**1.43**	**2.18%**	**0.95**
267		B					mts.	558	102.5	300	470	235	12.47	1.40			
268		C						558	102.5	300	470	235	12.90	1.44			
269		D						558	102.5	300	470	235	12.54	1.40			
270		E						558	102.5	300	470	235	13.14	1.47			

Table G.10: NHL3. 5 brick masonry flexural strength (perpendicular to bedding joints) (mix ratio 0:1:2)

Test no	Masonry ID		Unit Type	PC/ lime/ sand	Initial flow (mm)	Curing	Test age	Specimen Dims Length b (mm)	Width t_u (mm)	Height (mm)	Apparatus Dims l_1 (mm)	l_2 (mm)	Max load, F_c (kN)	Flexural strength, f_{xi} (N/mm^2)	Mean compressive strength, R_c (N/mm^2)	COV (%)	Characteristic compressive strength f_k (N/mm^2)
271	B_NHL2_165_1m_F2	A	Brick	0:1:3	165	lab	28	558	102.5	300	470	235	3.96	0.44	**0.45**	**5.80%**	**0.30**
272		B					days	558	102.5	300	470	235	4.05	0.45			
273		C						558	102.5	300	470	235	4.33	0.48			
274		D						558	102.5	300	470	235	3.68	0.41			
275		E						558	102.5	300	470	235	4.10	0.46			
276	B_NHL2_165_2m_F2	A	Brick	0:1:3	165	lab	56	558	102.5	300	470	235	4.26	0.48	**0.47**	**12.14%**	**0.31**
277		B					days	558	102.5	300	470	235	4.41	0.49			
278		C						558	102.5	300	470	235	4.02	0.45			
279		D						558	102.5	300	470	235	4.86	0.54			
280		E						558	102.5	300	470	235	3.47	0.39			
281	B_NHL2_165_6m_F2	A	Brick	0:1:3	165	lab	6	558	102.5	300	470	235	4.96	0.56	**0.57**	**5.12%**	**0.38**
282		B					mts.	558	102.5	300	470	235	5.15	0.58			
283		C						558	102.5	300	470	235	5.12	0.57			
284		D						558	102.5	300	470	235	4.77	0.53			
285		E						558	102.5	300	470	235	5.48	0.61			
286	B_NHL2_170_1m_F2	A	Brick	0:1:3	165	lab	28	558	102.5	300	470	235	4.13	0.46	**0.46**	**9.76%**	**0.31**
287		B					days	558	102.5	300	470	235	4.18	0.47			
288		C						558	102.5	300	470	235	4.70	0.53			
289		D						558	102.5	300	470	235	3.96	0.44			
290		E						558	102.5	300	470	235	3.59	0.40			
291	B_NHL2_170_2m_F2	A	Brick	0:1:3	165	lab	56	558	102.5	300	470	235	5.04	0.56	**0.56**	**7.19%**	**0.37**
292		B					days	558	102.5	300	470	235	4.69	0.52			
293		C						558	102.5	300	470	235	5.34	0.60			
294		D						558	102.5	300	470	235	5.37	0.60			
295		E						558	102.5	300	470	235	4.60	0.51			
296	B_NHL2_170_6m_F2	A	Brick	0:1:3	165	lab	6	558	102.5	300	470	235	5.58	0.62	**0.61**	**3.23%**	**0.41**
297		B					mts.	558	102.5	300	470	235	5.60	0.63			
298		C						558	102.5	300	470	235	5.45	0.61			
299		D						558	102.5	300	470	235	5.48	0.61			
300		E						558	102.5	300	470	235	5.16	0.58			

Table G.11: NHL 2 brick masonry flexural strength (perpendicular to bedding joints)

Test no	Masonry ID		Unit Type	PC/ lime/ sand	Initial flow (mm)	Curing	Test age	Specimen Dims Length b (mm)	Width t_u (mm)	Height (mm)	Apparatus Dims l_1 (mm)	l_2 (mm)	Max load, F_c (kN)	Flexural strength, f_{xi} (N/mm^2)	Mean compressive strength, R_c (N/mm^2)	COV (%)	Characteristic compressive strength f_k (N/mm^2)
301	B_CL90-s_165_1m_F2	A	Brick	0:1:3	165	lab	28	558	102.5	300	470	235	1.27	0.14	**0.13**	**12.04%**	**0.08**
302		B					days	558	102.5	300	470	235	1.19	0.13			
303		C						558	102.5	300	470	235	1.22	0.14			
304		D						558	102.5	300	470	235	1.02	0.11			
305		E						558	102.5	300	470	235	0.96	0.11			
306	B_CL90-s_165_2m_F2	A	Brick	0:1:3	165	lab	56	558	102.5	300	470	235	1.58	0.18	**0.18**	**6.25%**	**0.12**
307		B					days	558	102.5	300	470	235	1.56	0.17			
308		C						558	102.5	300	470	235	1.78	0.20			
309		D						558	102.5	300	470	235	1.61	0.18			
310		E						558	102.5	300	470	235	1.52	0.17			
311	B_CL90-s_165_6m_F2	A	Brick	0:1:3	165	lab	6	558	102.5	300	470	235	2.19	0.25	**0.25**	**16.00%**	**0.17**
312		B					mts.	558	102.5	300	470	235	2.24	0.25			
313		C						558	102.5	300	470	235	2.02	0.23			
314		D						558	102.5	300	470	235	1.90	0.21			
315		E						558	102.5	300	470	235	2.83	0.32			
316	B_CL90-s_170_1m_F2	A	Brick	0:1:3	165	lab	28	558	102.5	300	470	235	1.01	0.11	**0.12**	**11.26%**	**0.08**
317		B					days	558	102.5	300	470	235	1.27	0.14			
318		C						558	102.5	300	470	235	0.95	0.11			
319		D						558	102.5	300	470	235	1.07	0.12			
320		E						558	102.5	300	470	235	1.06	0.12			
321	B_CL90-s_170_2m_F2	A	Brick	0:1:3	165	lab	56	558	102.5	300	470	235	1.93	0.22	**0.18**	**15.90%**	**0.12**
322		B					days	558	102.5	300	470	235	1.80	0.20			
323		C						558	102.5	300	470	235	1.59	0.18			
324		D						558	102.5	300	470	235	1.39	0.16			
325		E						558	102.5	300	470	235	1.33	0.15			
326	B_CL90-s_170_6m_F2	A	Brick	0:1:3	165	lab	6	558	102.5	300	470	235	2.19	0.25	**0.25**	**3.63%**	**0.17**
327		B					mts.	558	102.5	300	470	235	2.18	0.24			
328		C						558	102.5	300	470	235	2.29	0.26			
329		D						558	102.5	300	470	235	2.35	0.26			
330		E						558	102.5	300	470	235	2.16	0.24			

Table G.12: CL90-s brick masonry flexural strength (perpendicular to bedding joints)

APPENDIX H

MASONRY UNIT TEST RESULTS AND CALCULATIONS

Unit Type		Brick	
Unit length	(mm)	215	
Unit width	(mm)	102.5	
Unit height	(mm)	65	
Gross surface area	(mm^2)	22575	
Net loaded Area	(mm^2)	8700	
Loading rate	(N/mm^2)/sec	0.15	
			COV (%)
Mean compressive strength	(N/mm^2)	15.02	10.01
Mean modulus of elasticity	(N/mm^2)	1240.01	7.52
Mean flexural strength	(N/mm^2)	2.63	4.33%

Test no	Applied load, F_i (kN)	Compressive strength, R_{ci} (N/mm^2)	Change in Stress $\Delta\delta$ (N/mm^2)	Change in Strain $\Delta\varepsilon$	Elastic modulus, E_i (N/mm^2)	Applied load, F_i (kN)	Flexural strength, R_{fi} (N/mm^2)
1	149.99	17.24	3.98	0.0030	1338.72	753.07	2.82
2	117.89	13.55	4.52	0.0041	1104.21	704.67	2.64
3	141.11	16.22	5.41	0.0041	1314.84	707.04	2.65
4	130.50	15.00	5.00	0.0045	1120.23	670.08	2.51
5	143.46	16.49	5.50	0.0040	1358.46	701.89	2.63
6	125.89	14.47	4.82	0.0037	1298.36	671.25	2.52
7	108.32	11.71	4.15	0.0036	1149.73		
8	137.98	15.86	5.29	0.0042	1271.22		
9	132.33	15.21	5.07	0.0040	1260.25		
10	125.72	14.45	4.82	0.0041	1184.08		

Table H.1: Brick units compressive and flexural strength, and elastic modulus results and calculations

Unit Type		Limestone	
Unit length	(mm)	50	
Unit width	(mm)	50	
Unit height	(mm)	50	
Gross surface area	(mm^2)	2500	
Net loaded Area	(mm^2)	2500	
Loading rate	(N/mm^2)/sec	1	
			COV (%)
Mean compressive strength	(N/mm^2)	87.12	5.87%
Mean modulus of elasticity	(N/mm^2)	55015.62	7.83%
Mean flexural strength	(N/mm^2)	18.6	5.51%

Test no	Applied load, F_i (kN)	Compressive strength, R_{ci} (N/mm^2)	Change in Stress $\Delta\delta$ (N/mm^2)	Change in Strain $\Delta\varepsilon$	Elastic modulus, E_i (N/mm^2)	Applied load, F_i (kN)	Flexural strength, R_{fi} (N/mm^2)
1	215.00	90.71	28.67	0.0005	55203.40	4760.53	17.85
2	203.53	78.41	27.14	0.0005	55012.62	4653.73	17.45
3	206.38	82.55	27.52	0.0005	53515.02	4411.33	16.54
4	198.18	84.44	26.42	0.0006	45152.71	4936.59	18.51
5	189.70	82.54	25.29	0.0005	55142.88	4565.55	17.12
6	221.85	90.74	29.58	0.0005	54158.00	5135.47	19.26
7	224.50	89.80	29.93	0.0005	55964.74		
8	225.35	94.14	30.05	0.0005	61510.46		
9	205.88	92.18	27.45	0.0005	59852.62		
10	214.23	85.69	28.56	0.0005	54643.75		

Table H.2: Limestone units compressive and flexural strength, and elastic modulus results and calculations

Unit Type		Sandstone	
Unit length	(mm)	50	
Unit width	(mm)	50	
Unit height	(mm)	50	
Gross surface area	(mm^2)	2500	
Net loaded Area	(mm^2)	2500	
Loading rate	(N/mm^2)/sec	0.6	
			COV (%)
Mean compressive strength	(N/mm^2)	58.32	8.31%
Mean modulus of elasticity	(N/mm^2)	36582.72	10.27%
Mean flexural strength	(N/mm^2)	14.11	6.41%

Test no	Applied load, F_i (kN)	Compressive strength, R_{ci} (N/mm^2)	Change in Stress $\Delta\delta$ (N/mm^2)	Change in Strain $\Delta\varepsilon$	Elastic modulus, E_i (N/mm^2)	Applied load, F_i (kN)	Flexural strength, R_{fi} (N/mm^2)
1	155.75	57.42	20.77	0.0006	37333.97	3511.52	13.17
2	139.60	55.84	18.61	0.0005	35654.55	4110.81	15.42
3	142.13	56.85	18.95	0.0005	36425.10	3781.75	14.18
4	149.60	59.84	19.95	0.0006	35162.51	3957.87	14.842
5	141.63	56.65	18.88	0.0006	30512.75	3508.40	13.1565
6	149.60	59.84	19.95	0.0006	35851.66	3705.65	13.8962
7	149.70	59.88	19.96	0.0006	35985.87	-	-
8	146.10	58.44	19.48	0.0005	36452.80	-	-
9	172.48	68.99	23.00	0.0005	45849.85	-	-
10	98.63	49.45	13.15	0.0005	36598.14	-	-

Table H.3: Sandstone units compressive and flexural strength, and elastic modulus results and calculations